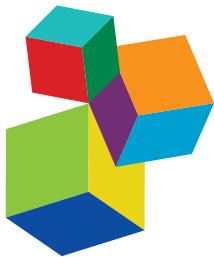


PROTEIN QUALITY CONTROLLING SYSTEMS IN PLANT RESPONSES TO ENVIRONMENTAL STRESSES

EDITED BY: Minghui Lu, Yule Liu, Jie Zhou, Hanjo A. Hellmann, Wei Wang
and Sophia Stone

PUBLISHED IN: Frontiers in Plant Science





Frontiers Copyright Statement

© Copyright 2007-2018 Frontiers Media SA. All rights reserved.

All content included on this site, such as text, graphics, logos, button icons, images, video/audio clips, downloads, data compilations and software, is the property of or is licensed to Frontiers Media SA ("Frontiers") or its licensees and/or subcontractors. The copyright in the text of individual articles is the property of their respective authors, subject to a license granted to Frontiers.

The compilation of articles constituting this e-book, wherever published, as well as the compilation of all other content on this site, is the exclusive property of Frontiers. For the conditions for downloading and copying of e-books from Frontiers' website, please see the Terms for Website Use. If purchasing Frontiers e-books from other websites or sources, the conditions of the website concerned apply.

Images and graphics not forming part of user-contributed materials may not be downloaded or copied without permission.

Individual articles may be downloaded and reproduced in accordance with the principles of the CC-BY licence subject to any copyright or other notices. They may not be re-sold as an e-book.

As author or other contributor you grant a CC-BY licence to others to reproduce your articles, including any graphics and third-party materials supplied by you, in accordance with the Conditions for Website Use and subject to any copyright notices which you include in connection with your articles and materials.

All copyright, and all rights therein, are protected by national and international copyright laws.

The above represents a summary only. For the full conditions see the Conditions for Authors and the Conditions for Website Use.

ISSN 1664-8714

ISBN 978-2-88945-558-4

DOI 10.3389/978-2-88945-558-4

About Frontiers

Frontiers is more than just an open-access publisher of scholarly articles: it is a pioneering approach to the world of academia, radically improving the way scholarly research is managed. The grand vision of Frontiers is a world where all people have an equal opportunity to seek, share and generate knowledge. Frontiers provides immediate and permanent online open access to all its publications, but this alone is not enough to realize our grand goals.

Frontiers Journal Series

The Frontiers Journal Series is a multi-tier and interdisciplinary set of open-access, online journals, promising a paradigm shift from the current review, selection and dissemination processes in academic publishing. All Frontiers journals are driven by researchers for researchers; therefore, they constitute a service to the scholarly community. At the same time, the Frontiers Journal Series operates on a revolutionary invention, the tiered publishing system, initially addressing specific communities of scholars, and gradually climbing up to broader public understanding, thus serving the interests of the lay society, too.

Dedication to Quality

Each Frontiers article is a landmark of the highest quality, thanks to genuinely collaborative interactions between authors and review editors, who include some of the world's best academicians. Research must be certified by peers before entering a stream of knowledge that may eventually reach the public - and shape society; therefore, Frontiers only applies the most rigorous and unbiased reviews.

Frontiers revolutionizes research publishing by freely delivering the most outstanding research, evaluated with no bias from both the academic and social point of view. By applying the most advanced information technologies, Frontiers is catapulting scholarly publishing into a new generation.

What are Frontiers Research Topics?

Frontiers Research Topics are very popular trademarks of the Frontiers Journals Series: they are collections of at least ten articles, all centered on a particular subject. With their unique mix of varied contributions from Original Research to Review Articles, Frontiers Research Topics unify the most influential researchers, the latest key findings and historical advances in a hot research area! Find out more on how to host your own Frontiers Research Topic or contribute to one as an author by contacting the Frontiers Editorial Office: researchtopics@frontiersin.org

PROTEIN QUALITY CONTROLLING SYSTEMS IN PLANT RESPONSES TO ENVIRONMENTAL STRESSES

Topic Editors:

Minghui Lu, Northwest A&F University, China

Yule Liu, Tsinghua University, China

Jie Zhou, Zhejiang University, China

Hanjo A. Hellmann, Washington State University, United States

Wei Wang, Henan Agricultural University, China

Sophia Stone, Dalhousie University, Canada

Environmental stress factors negatively affect plant growth by inducing proteins dysfunction. As coping strategies, plants have developed a comprehensive protein quality controlling system (PQCS) to keep proteins homeostasis. In this research topic of "Protein Quality Controlling Systems in Plant Responses to Environmental Stresses", some latest researches and opinions in this field, including heat shock proteins (HSPs), unfolded protein response (UPR), ubiquitin-proteasome system (UPS) and autophagy, were reported, aiming to provide novel insights for increasing crop production under environmental challenges.

Citation: Lu, M., Liu, Y., Zhou, J., Hellmann, H. A., Wang, W., Stone, S., eds. (2018). Protein Quality Controlling Systems in Plant Responses to Environmental Stresses. Lausanne: Frontiers Media. doi: 10.3389/978-2-88945-558-4

Table of Contents

- 05 Editorial: Protein Quality Controlling Systems in Plant Responses to Environmental Stresses**

Minghui Lu, Hanjo A. Hellmann, Yule Liu and Wei Wang

- 08 Responses of Plant Proteins to Heavy Metal Stress—A Review**

Md. Kamrul Hasan, Yuan Cheng, Mukesh K. Kanwar, Xian-Yao Chu, Golam J. Ahammed and Zhen-Yu Qi

SECTION 1

INVOLVEMENT OF HEAT SHOCK PROTEINS (HSPS) IN PLANT RESPONSE TO ENVIRONMENTAL STRESS

- 17 Genome-Wide Identification and Expression Profiling of Tomato Hsp20 Gene Family in Response to Biotic and Abiotic Stresses**

Jiahong Yu, Yuan Cheng, Kun Feng, Meiyi Ruan, Qingjing Ye, Rongqing Wang, Zhimiao Li, Guozhi Zhou, Zhuping Yao, Yuejian Yang and Hongjian Wan

- 38 The DnaJ Gene Family in Pepper (*Capsicum annuum L.*): Comprehensive Identification, Characterization and Expression Profiles**

FangFei Fan, Xian Yang, Yuan Cheng, Yunyan Kang and Xirong Chai

SECTION 2

INVOLVEMENT OF UNFOLDED PROTEIN RESPONSE (UPR) IN PLANT RESPONSE TO ENVIRONMENTAL STRESS

- 49 Endoplasmic Reticulum Stress Response in *Arabidopsis* Roots**

Yueh Cho and Kazue Kanehara

- 59 The Unfolded Protein Response Supports Plant Development and Defense as Well as Responses to Abiotic Stress**

Yan Bao and Stephen H. Howell

SECTION 3

INVOLVEMENT OF UBIQUITIN-PROTEASOME SYSTEM (UPS) IN PLANT RESPONSE TO ENVIRONMENTAL STRESS

- 65 The Banana Fruit SINA Ubiquitin Ligase MaSINA1 Regulates the Stability of MalCE1 to be Negatively Involved in Cold Stress Response**

Zhong-Qi Fan, Jian-Ye Chen, Jian-Fei Kuang, Wang-Jin Lu and Wei Shan

- 77 Overexpression of Hevea Brasiliensis HbICE1 Enhances Cold Tolerance in *Arabidopsis***

Hong-Mei Yuan, Ying Sheng, Wei-Jie Chen, Yu-Qing Lu, Xiao Tang, Mo Ou-Yang and Xi Huang

SECTION 4

INVOLVEMENT OF AUTOPHAGY PATHWAY IN PLANT RESPONSE TO ENVIRONMENTAL STRESS

- 94 Autophagy: An Important Biological Process That Protects Plants From Stressful Environments**

Wenyi Wang, Mengyun Xu, Guoping Wang and Gad Galili

- 98** *The AMP-Activated Protein Kinase KIN10 is Involved in the Regulation of Autophagy in Arabidopsis*
Liang Chen, Ze-Zhuo Su, Li Huang, Fan-Nv Xia, Hua Qi, Li-Juan Xie, Shi Xiao and Qin-Fang Chen
- 109** *TOR-Dependent and -Independent Pathways Regulate Autophagy in Arabidopsis Thaliana*
Yunting Pu, Xinjuan Luo and Diane C. Bassham
- 122** *Endocytosis of AtRGS1 is Regulated by the Autophagy Pathway After D-Glucose Stimulation*
Quanquan Yan, Jingchun Wang, Zheng Qing Fu and Wenli Chen
- 133** *Autophagy is Rapidly Induced by Salt Stress and is Required for Salt Tolerance in Arabidopsis*
Liming Luo, Pingping Zhang, Ruihai Zhu, Jing Fu, Jing Su, Jing Zheng, Ziyue Wang, Dan Wang and Qingqiu Gong

SECTION 5

PROTEOMIC STUDY OF PROTEIN QUALITY CONTROLLING SYSTEMS (PQCS) INPLANT RESPONSE TO ENVIRONMENTAL STRESS

- 146** *Proteomic and Physiological Analyses Reveal Putrescine Responses in Roots of Cucumber Stressed by NaCl*
Yinghui Yuan, Min Zhong, Sheng Shu, Nanshan Du, Jin Sun and Shirong Guo
- 165** *Comparative Proteomic Analysis Provides Insight Into the Key Proteins Involved in Cucumber (*Cucumis sativus L.*) Adventitious Root Emergence Under Waterlogging Stress*
Xuewen Xu, Jing Ji, Xiaotian Ma, Qiang Xu, Xiaohua Qi and Xuehao Chen
- 179** *Proteomic Analysis Reveals the Positive Roles of the Plant-Growth-Promoting Rhizobacterium NSY50 in the Response of Cucumber Roots to *Fusarium Oxysporum f. sp. Cucumerinum* Inoculation*
Nanshan Du, Lu Shi, Yinghui Yuan, Bin Li, Sheng Shu, Jin Sun and Shirong Guo
- 198** *Proteomic Analysis Reveals the Positive Effect of Exogenous Spermidine in Tomato Seedlings' Response to High-Temperature Stress*
Qinqin Sang, Xi Shan, Yahong An, Sheng Shu, Jin Sun and Shirong Guo



Editorial: Protein Quality Controlling Systems in Plant Responses to Environmental Stresses

Minghui Lu^{1*}, Hanjo A. Hellmann^{2*}, Yule Liu^{3*} and Wei Wang^{4*}

¹ College of Horticulture, Northwest A&F University, Shaanxi, China, ² School of Biological Sciences, Washington State University, Pullman, WA, United States, ³ MOE Key Laboratory of Bioinformatics, Center for Plant Biology, Tsinghua-Peking Joint Center for Life Sciences, School of Life Sciences, Tsinghua University, Beijing, China, ⁴ College of Life Sciences, State Key Lab of Wheat & Maize Crop Science, Henan Agricultural University, Zhengzhou, China

Keywords: plant, heat shock proteins, unfolded protein response, proteasome, autophagy, abiotic stress

Editorial on the Research Topic

Protein quality controlling systems in plant responses to environmental stresses

OPEN ACCESS

Edited and reviewed by:

Elison B. Blancaflor,
Noble Research Institute, LLC,
United States

*Correspondence:

Minghui Lu
xnjacklu@nwauaf.edu.cn
Hanjo A. Hellmann
hellmann@wsu.edu
Yule Liu
yuleliu@mail.tsinghua.edu.cn
Wei Wang
wangwei@henau.edu.cn

Specialty section:

This article was submitted to
Plant Cell Biology,
a section of the journal
Frontiers in Plant Science

Received: 29 May 2018

Accepted: 08 June 2018

Published: 29 June 2018

Citation:

Lu M, Hellmann HA, Liu Y and
Wang W (2018) Editorial: Protein
Quality Controlling Systems in Plant
Responses to Environmental Stresses.
Front. Plant Sci. 9:908.
doi: 10.3389/fpls.2018.00908

In nature, plants are routinely exposed to adverse environmental conditions, such as elevated temperature, drought, salinity, heavy metal, etc., which are among the main causes for declining crop productivity worldwide and lead to billions of dollars of annual losses (Dhankher and Foyer, 2018). These stressors negatively affect plant growth and development by inducing misfolding, denaturation, oxidation and aggregation of proteins. Evolutionarily, plants have developed a comprehensive protein quality controlling system (PQCS) to maintain protein homeostasis, mainly including heat shock proteins (HSPs), unfolded protein response (UPR), ubiquitin-proteasome system (UPS) and autophagy. This research topic aims to summarize and report novel findings on the identification, functional analysis, signal transduction, transcriptional and post-transcriptional regulation, and protein interaction of candidate components in the above systems.

HSPs are abundantly expressed under abiotic stress conditions, and function as molecular chaperones to promote proper protein folding and to prevent denatured proteins from self-aggregation (Reddy et al., 2016). Yu et al. identified 42 putative *SlHSP20* genes from tomato (*Solanum lycopersicum*), and found that their transcript levels were profusely induced by abiotic stresses such as heat, drought, salt, but also by the fungal pathogens *Botrytis cinerea*, and tomato spotted wilt virus (TSWV). In addition, a total of 76 putative *CaDnaj/HSP40* genes were identified in pepper (*Capsicum annuum* L.), and more than 80% of them responded to heat stress treatment (Fan et al.). These studies underscore the potential involvements of HSP genes in mediating the response of plants not only to elevated temperatures but also to a broader range of environmental stress conditions.

Endoplasmic reticulum (ER) is the major organelle for folding and assembling of secretory proteins. When plants are subjected to environmental stresses, the unfolded or misfolded proteins accumulate in the ER which is referred to as ER stress (Schröder and Kaufman, 2005), and which further activates UPR to enhance the operation of the ER protein-folding machinery (Duwi Fanata et al., 2013). Bao and Howell summarized in this research topic the latest progresses in UPR. The authors discuss recent findings that this pathway is not only associated with abiotic stress response, but is also required during normal vegetative and reproductive development. In addition, it fulfills critical roles in plant immunity, affecting bacterial and viral infections. Evidence that the UPR in multicellular organisms acts in a tissue specific manner comes from Cho and Kanehara. The authors measured expression of the immunoglobulin-binding protein gene *BiP3*, a marker for ER-stress. This gene was strongly up-regulated

after treatment with the ER-stress inducer tunicamycin (TM). Interestingly, *BiP3* expression in the plant was not uniformly increased but more tissue specific. For example, the mRNA abundance of *BiP3* was preferentially increased in the vascular tissues, and leaf hydathodes. In the root tip, high expression was specifically observed in the columella, and the epidermal cell layer of the elongation zone. These findings indicate that in response to TM, plants emphasize certain tissues and/or organs to maintain ER homeostasis.

When stressed protein repair or folding demands exceed the cellular capacities, protein degradation systems such as UPS and autophagy are activated to remove misfolded proteins (Liu and Howell, 2016). The UPS marks proteins for degradation by attaching polyubiquitin chains to target proteins, which in turn leads to their degradation via the 26S proteasome (Liu and Howell, 2016). But degradation of misfolded proteins is only one aspect of the UPS function. The pathway represents a central regulatory tool that affects most cellular processes in plants. For example, ICE1 (INDUCER OF CBF EXPRESSION 1) is involved in chilling and freezing tolerance by promoting expression of the *CBF3* (C-REPEAT-BINDING FACTOR 3) transcription factor, and other cold-responsive genes (Chinnusamy et al., 2003). However, after ICE1 facilitated a cold-shock response, it becomes ubiquitinated by the E3 ligase HOS1 (HIGH EXPRESSION OF OSMOTICALLY RESPONSIVE GENE 1) followed by proteasomal degradation (Dong et al., 2006).

In this research topic, Yuan et al. cloned *HbICE1* from rubber trees (*Hevea brasiliensis*) and showed that its overexpression in *Arabidopsis* enhances cold tolerance. Fan et al. reported the identification of MaSINA1 (SEVEN IN ABSENTIA1), an E3 ligase from banana (*Musa acuminata*), which interacts with MaICE1, and promotes its degradation. Consequently, the authors suggested that MaSINA1 functions as a negative regulator of cold stress response in banana.

While UPS is targeting single proteins for degradation, autophagy is active on a broader scale and responsible for the degradation of single proteins, as well as protein aggregates or even whole organelles (Zientara-Rytter and Sirkko, 2016). Autophagy is characterized by the *de novo* formation of a double membrane organelle (called autophagosome), to transport the targeted cargo components to the vacuole for degradation (Batoko et al., 2017). Autophagy-related proteins (ATGs) or their complexes recognize the target components by specific cargo receptors. In a review article, Wang et al. summarized the identification and functional characterization of three potential cargo receptors involved in plant abiotic stress, including NBR1 (NEIGHBOR OF BRCA1), TSPO (TRYPTOPHAN-RICH SENSORY PROTEIN), ATI1 (AUTOPHAGY INTERACTING PROTEIN1).

The timely degradation of misfolded proteins is important for the development of plant tolerance to abiotic stress. Luo et al. suggested that rapid protein turnover through autophagy is a prerequisite for the establishment of salt tolerance in *Arabidopsis*. They found that after salt treatment autophagosome formation is induced shortly, and the level of autophagy peaks within 30 min. Accordingly, within 3 h of salt treatment, accumulation of oxidized proteins is alleviated, and then contents of soluble

sugar and some compatible solutes such as proline are enhanced. However, these processes are not observed or kept at lower levels in mutants such as *atg2* or *atg7* that are defective in autophagy. The authors propose that autophagy under salt stress is a critical requirement for bulk protein turnover.

The TOR (TARGET OF RAPAMYCIN) protein kinase is a major controller of growth-related processes in all eukaryotes. Under favorable conditions, TOR positively regulates cell and organ growth but restrains autophagy processes (John et al., 2011). However, Pu et al. reported that the modulation of autophagy by TOR was stress-type dependent. They found that the overexpression of the TOR kinase inhibited autophagy activation by nutrient starvation, salt and osmotic stress, but not by oxidative or ER stress. A similar result was observed after the treatment with the auxin NAA (1-naphthaleneacetic acid), a phytohormone that upregulates TOR activity. Since NAA treatment was unable to overcome blocked autophagy induced by a TOR inhibitor, it was suggested that auxin acts upstream of TOR in the regulation of autophagy.

Chen et al. found that KIN10 (KINASE HOMOLOG 10), a plant ortholog of the mammalian AMPK (AMP-ACTIVATED PROTEIN KINASE), acts as a positive regulator of autophagy by affecting the phosphorylation of ATG1 proteins in *Arabidopsis*. In *KIN10* overexpression lines (*KIN10-OE*), the stress-induced formation of autophagosomes were accelerated. In addition, leaf senescence was delayed, while the tolerance to nutrient starvation, drought and hypoxia treatments was increased. Furthermore, carbon starvation (transfer of seedlings to continuous darkness) enhanced the level of phosphorylated ATG1a in *KIN10-OE* lines.

Another aspect of autophagy in this research topic was investigated by Yan et al. by studying the impact of autophagy and D-glucose on the endocytosis of RGS1 (REGULATOR OF G-PROTEIN SIGNALING 1). Under normal conditions, RGS1 interacts with and arrests the GTPase activity of the heterotrimeric G-protein subunit G α subunit (GPA1). However, D-glucose recruits WNK8 (WITH-NO-LYSING KINASE 8) to phosphorylate AtRGS1, which in turn causes its endocytosis. The endocytosis of RGS1 physically uncouples its inhibitory activity from GPA1, and then activates the G protein-mediated sugar signaling (Urano et al., 2012). Yan et al. reported that D-glucose induced RGS1 endocytosis is needed for the formation of autophagosomes likely by activating ATG8-phosphatidylethanolamine (PE) and ATG12/ATG5 conjugation systems. The autophagy pathway on the other hand is needed for RGS1 endocytosis as RGS1 remains associated with GPA1 in *atg2* and *atg5* autophagy mutants, even in the presence of D-glucose. The findings show a nice interplay between endocytic and autophagy pathways, and shed new light on sugar signaling in plant cells.

The development of plant tolerance to abiotic stress always requires the simultaneous participation of different PQCSs. Heavy metals negatively affect plant cell viability mainly by disturbing protein folding and stimulating protein aggregation. In the review article of Hasan et al. the authors summarized the recent advances on the involvement of PQCSs in plant tolerance to heavy metal stress, including ion detoxification

by phytochelatins and metallothioneins, reparation of damaged proteins by HSPs and UPR, degradation of denatured proteins by UPS and autophagy.

The proteomics study of Xu et al. provides us with new insights into the involvement of PQCS in establishing plant tolerance under adverse environmental conditions. Based on iTRAQ-quantitative proteomics approach, the authors compared the cucumber (*Cucumis sativus*) proteomes in adventitious roots under control and waterlogging conditions. They identified a total of 146 differentially regulated proteins (DRPs), of which 13 belonged to the categories of posttranslational modification, protein turnover and chaperones.

Polyamines such as putrescine (Put), spermidine (Spd) and spermine (Spm), are suggested to maintain the function and structure of cellular components in plant response to stress (Liu et al., 2015). After treatment with exogenous Put, Yuan et al. analyzed the DRPs of cucumber under salt stress by MALDI-TOF/TOF MS, and identified 62 DRPs, of which 15 functioned in protein metabolism, 15 in defense responses, 12 in carbohydrate metabolism, and 9 in amino acid metabolism. In a similar study in tomato with exogenous Spd, 67 DRPs were identified after high temperature treatment. The percentage of the identified proteins played roles in photosynthesis was 27%, followed by 24% of cell rescue, and defense. However, a significant amount was also related to protein synthesis, folding and degradation (22%) as well as energy and metabolism (13%) (Sang et al.).

The plant growth-promoting rhizobacterium (PGPR) can induce resistance against a broad spectrum of pathogens by simultaneously activating salicylic acid and jasmonate/ethylene-dependent signaling pathways (Niu et al., 2011). With a new potential strain NSY50, Du et al. investigated the mechanisms

of PGPR protecting cucumber from the attack of *Fusarium oxysporum* f. sp. *Cucumerinum* (FOC) by a proteomic approach. Among the 56 DRPs, 14 belonged to the protein metabolism category and two to the HSP70 family, which suggests a functional connection between the PGPR and PQCS under biotic stress.

With the unprecedented global climate changes, extreme weather conditions are more likely to occur, and which will severely impact plant growth and crop production. A better understanding of the mechanisms of how plants are able to cope with and alleviate environmental stresses is essential for crop breeders to develop efficient strategies for maintaining our current agricultural productivity and to secure a sustainable agriculture. The research topic summarized here may provide some novel insights that can help to address these eminent challenges and to further increase crop production and secure yield in the upcoming decades.

AUTHOR CONTRIBUTIONS

ML prepared the first draft of this editorial. HH, YL, and WW revised it. All authors listed approved it for publication.

ACKNOWLEDGMENTS

We thank Prof. Jie Zhou (Zhejiang University, China) and Prof. Sophia Stone (Dalhousie University, Canada) for their outstanding contribution to the edit of manuscripts submitted to this Research Topic. ML is thankful to the support from the National Natural Science Foundation of China (Grant No. 31572114).

REFERENCES

- Batoko, H., Dagdas, Y., Baluska, F., and Sirk, A. (2017). Understanding and exploiting autophagy signaling in plants. *Essays Biochem.* 61, 675–685. doi: 10.1042/EBC20170034
- Chinnusamy, V., Ohta, M., Kanrar, S., Lee, B. H., Hong, X., Agarwal, M., et al. (2003). ICE1: a regulator of cold-induced transcriptome and freezing tolerance in *Arabidopsis*. *Genes Dev.* 17, 1043–1054. doi: 10.1101/gad.1077503
- Dhankher, O. P., and Foyer, C. H. (2018). Climate resilient crops for improving global food security and safety. *Plant Cell Environ.* 41, 877–884. doi: 10.1111/pce.13207
- Dong, C. H., Agarwal, M., Zhang, Y., Xie, Q., and Zhu, J. K. (2006). The negative regulator of plant cold responses, HOS1, is a RING E3 ligase that mediates the ubiquitination and degradation of ICE1. *Proc. Natl. Acad. Sci. U.S.A.* 103, 8281–8286. doi: 10.1073/pnas.0602874103
- Duwi Fanata, W. I., Lee, S. Y., and Lee, K. O. (2013). The unfolded protein response in plants: a fundamental adaptive cellular response to internal and external stresses. *J. Proteomics.* 93, 356–368. doi: 10.1016/j.jprot.2013.04.023
- John, F., Roffler, S., Wicker, T., and Ringli, C. (2011). Plant TOR signaling components. *Plant Signal Behav.* 6, 1700–1705. doi: 10.4161/psb.6.11.17662
- Liu, J. H., Wang, W., Wu, H., Gong, X., and Moriguchi, T. (2015). Polyamines function in stress tolerance: from synthesis to regulation. *Front. Plant Sci.* 6:827. doi: 10.3389/fpls.2015.00827
- Liu, J. X., and Howell, S. H. (2016). Managing the protein folding demands in the endoplasmic reticulum of plants. *New Phytol.* 211, 418–428. doi: 10.1111/nph.13915
- Niu, D. D., Liu, H. X., Jiang, C. H., Wang, Y. P., Wang, Q. Y., Jin, H. L., et al. (2011). The plant growth-promoting rhizobacterium *Bacillus cereus* AR156 induces systemic resistance in *Arabidopsis thaliana* by simultaneously activating salicylate- and jasmonate/ethylene-dependent signaling pathways. *Mol. Plant Microbe Interact.* 24, 533–542. doi: 10.1094/MPMI-09-10-0213
- Reddy, P. S., Chakradhar, T., Reddy, R. A., Nitnavare, R. B., Mahanty, S., and Reddy, M. K. (2016). “Role of heat shock proteins in improving heat stress tolerance in crop plants,” in *Heat shock Proteins and Plants*, Vol. 10 eds A. A. A. Asea, S. K. Calderwood, and P. Kaur (Cham: Springer; International Publishing), 283–307.
- Schröder, M., and Kaufman, R. J. (2005). ER stress and the unfolded protein response. *Mutat. Res. Fund. Mol. Mech. Mutagen.* 569, 29–63. doi: 10.1016/j.mrfmmm.2004.06.056
- Urano, D., Phan, N., Jones, J. C., Yang, J., Huang, J., Grigston, J., et al. (2012). Endocytosis of the seven-transmembrane RGS1 protein activates G-protein-coupled signalling in *Arabidopsis*. *Nat. Cell Biol.* 14, 1079–1088. doi: 10.1038/ncb2568
- Zientara-Rytter, K., and Sirk, A. (2016). To deliver or to degrade - an interplay of the ubiquitin-proteasome system, autophagy and vesicular transport in plants. *FEBS J.* 283, 3534–3555. doi: 10.1111/febs.13712
- Conflict of Interest Statement:** The authors declare that the research was conducted in the absence of any commercial or financial relationships that could be construed as a potential conflict of interest.
- Copyright © 2018 Lu, Hellmann, Liu and Wang. This is an open-access article distributed under the terms of the Creative Commons Attribution License (CC BY). The use, distribution or reproduction in other forums is permitted, provided the original author(s) and the copyright owner(s) are credited and that the original publication in this journal is cited, in accordance with accepted academic practice. No use, distribution or reproduction is permitted which does not comply with these terms.**



Responses of Plant Proteins to Heavy Metal Stress—A Review

Md. Kamrul Hasan^{1,2†}, Yuan Cheng^{3†}, Mukesh K. Kanwar^{1†}, Xian-Yao Chu⁴, Golam J. Ahammed^{1*} and Zhen-Yu Qi^{5*}

¹ Department of Horticulture, Zhejiang University, Hangzhou, China, ² Department of Agricultural Chemistry, Sylhet Agricultural University, Sylhet, Bangladesh, ³ State Key Laboratory Breeding Base for Zhejiang Sustainable Pest and Disease Control, Institute of Vegetables, Zhejiang Academy of Agricultural Sciences, Hangzhou, China, ⁴ Zhejiang Institute of Geological Survey, Geological Research Center for Agricultural Applications, China Geological Survey, Beijing, China, ⁵ Agricultural Experiment Station, Zhejiang University, Hangzhou, China

OPEN ACCESS

Edited by:

Minghui Lu,
Northwest A&F University, China

Reviewed by:

Shabir Hussain Wani,
Michigan State University,
United States
Liang Xu,
Nanjing Agricultural University, China

*Correspondence:

Golam J. Ahammed
ahammed@zju.edu.cn
Zhen-Yu Qi
qizhenyu@zju.edu.cn

[†]These authors have contributed
equally to this work.

Specialty section:

This article was submitted to
Plant Cell Biology,
a section of the journal
Frontiers in Plant Science

Received: 30 May 2017

Accepted: 11 August 2017

Published: 05 September 2017

Citation:

Hasan MK, Cheng Y, Kanwar MK,
Chu X-Y, Ahammed GJ and Qi Z-Y
(2017) Responses of Plant Proteins to
Heavy Metal Stress—A Review.
Front. Plant Sci. 8:1492.
doi: 10.3389/fpls.2017.01492

Plants respond to environmental pollutants such as heavy metal(s) by triggering the expression of genes that encode proteins involved in stress response. Toxic metal ions profoundly affect the cellular protein homeostasis by interfering with the folding process and aggregation of nascent or non-native proteins leading to decreased cell viability. However, plants possess a range of ubiquitous cellular surveillance systems that enable them to efficiently detoxify heavy metals toward enhanced tolerance to metal stress. As proteins constitute the major workhorses of living cells, the chelation of metal ions in cytosol with phytochelatins and metallothioneins followed by compartmentalization of metals in the vacuoles as well as the repair of stress-damaged proteins or removal and degradation of proteins that fail to achieve their native conformations are critical for plant tolerance to heavy metal stress. In this review, we provide a broad overview of recent advances in cellular protein research with regards to heavy metal tolerance in plants. We also discuss how plants maintain functional and healthy proteomes for survival under such capricious surroundings.

Keywords: heavy metals, phytochelatins, metallothioneins, protein quality control system, ubiquitin proteasome system, autophagy

INTRODUCTION

Proteins are functionally versatile macromolecules that constitute the major workhorses of living cells. They function in cellular signaling, regulation, catalysis, intra and inter cellular movement of nutrients and other molecules, membrane fusion, structural support and protection (Amm et al., 2014). The function of a protein is basically determined by its structure, which is acquired following ribosomal synthesis of its amino acid chain. In addition, the conformation of a protein largely depends on the physical and chemical conditions of the protein environment as affected by extreme temperatures, reactive molecules, heavy metal (HM) ions and other stresses that not only disrupt the folding process of a newly synthesized protein, but also induce the mis-folding of already existing proteins (Goldberg, 2003; Amm et al., 2014; Zhou et al., 2016).

Over the last several decades, the emission of pollutants into the environment has been increased tremendously due to rapid industrialization, urbanization and excessive usage of agricultural amendments. Being sessile, plants are routinely confronted by a wide array of biotic and/or abiotic stresses including HM stress (Al-Whaibi, 2011). HMs are thought to obstruct the biological

functions of a protein by altering the native conformation through binding on it (Hossain and Komatsu, 2013). For example, in yeast, methyl-mercury (MeHg) strongly inhibits L-glutamine: D-fructose-6-phosphate aminotransferase, and overexpression of this enzyme confers tolerance to MeHg (Naganuma et al., 2000). Similarly, cadmium (Cd) can inhibit the activity of thiol transferase leading to oxidative damage, possibly by binding to cysteine residues in its active sites. In *Brassica juncea*, Cd-dependent changes in beta carbonic anhydrase result in the enhancement of photorespiration which may protect photosystem from oxidation (D'Alessandro et al., 2013). The modifications caused by Cd disrupt the stabilizing interactions associated with changes in the tertiary structure and cause loss of promising functions of that protein (Chrestensen et al., 2000). Fallout dysfunction of protein stimulates the danger of protein aggregation.

The biosynthesis of metal binding cysteine rich peptides that function to immobilize, sequester and detoxify the metal ions is thought to be the central for detoxification of HMs (Clemens, 2006; Viehweger, 2014). Nonetheless, under extreme conditions, metal ions profoundly affect cellular protein homeostasis by interfering with their folding process and stimulate aggregation of nascent or non-native proteins, leading to the endoplasmic reticulum (ER) stress and a decreased cell viability. To restrict the aggregation as well as to mend them is-folded proteins, cells initiate different quality control systems that fine-tune protein homeostasis. In the center of the system, a typical set of proteins, called heat shock proteins (HSPs; Amm et al., 2014), function as surveillance mechanisms, which are preferentially expressed under stress to maintain functional and healthy proteomes. In contrast, the damaged proteins that fail to achieve their native conformations are subjected to degradation through the ubiquitinproteasome process (UPS), called as ER-associated degradation (ERAD) or through autophagy to minimize the accumulation of misfolded proteins in cells (Liu and Howell, 2016). Although a significant progress has been made in our understanding of protein quality control systems, information on plant system, especially pertaining to HMs stress still remain scanty. In this review, we aim to provide a better insight into the protein quality control system in plants with regards to heavy metal tolerance. We also discuss how plants try to ensure functional and healthy proteomes under HM stress.

HEAVY METALS (HMs) DETOXIFICATION

Toxic metal ions at cellular level, evoke oxidative stress by generating reactive oxygen species (ROS; Li et al., 2016a). They promote DNA damage and/or impair DNA repair mechanisms, impede membrane functional integrity, nutrient homeostasis and perturb protein function and activity (Tamás et al., 2014). On the other hand, plant cells have evolved a myriad of adaptive mechanisms to manage excess metal ions and utilize detoxification mechanisms to prevent their participations in unwanted toxic reactions. In the first line of defense, plants utilize strategies that prevent or reduce uptake by restricting metal ions to the apoplast through binding them to the cell wall or to cellular

exudates, or by inhibiting long distance transport (Manara, 2012; Hasan et al., 2015). In contrast, when present at elevated concentrations, cells activate a complex network of storage and detoxification strategies, such as chelation of metal ions with phytochelatins and metallothioneins in the cytosol, trafficking, and sequestration into the vacuole by vacuolar transporters (Figure 1; Zhao and Chengcui, 2011).

Phytochelatins: Structure, Regulation and Function in Heavy-Metal Stress Tolerance

In order to reduce or prevent damage caused by HMs, plants synthesize small cysteine-rich oligomers, called Phytochelatins (PCs) at the very beginning of metal stress (Ashraf et al., 2010; Pochodlo and Aristilde, 2017). Notably, PC syntheses play the most crucial role in mediating plant tolerance to HMs (Clemens, 2006; Emamverdian et al., 2015). It has been well documented that the biosynthesis of PCs can be regulated at post-translational level by metal(oid)s in many plant species. However, the over-expression of phytochelatin synthase (PCS) gene in plants does not always result in an enhanced tolerance to HM stress. For instance, over expression of *AtPCS1* in *Arabidopsis*, paradoxically shows hypersensitivity toward Cd and Zn; although, PCs production is increased by 2.1-folds, when compared with wild type plants (Lee et al., 2003). In reality, excess PCs levels in mutant plants accelerate accumulation of HMs like Cd without improving plant tolerance (Pomponi et al., 2006; Furini, 2012). This phenomenon possibly indicates some additional roles of PCs in plant cells, such as their involvement in essential metal ion homeostasis, antioxidant mechanisms, and sulfur metabolism (Furini, 2012). Therefore, prevention of the free circulation of toxic metal inside the cytosol exhibits a potential mechanism for dealing with HM-induced toxicity (Hasan et al., 2016).

The mechanism of HMs detoxification is not only limited to the chelation, but also involves accumulation and stabilization of HM in the vacuole through formation of high molecular weight (HMW) complexes with PCs (Figure 1; Jabeen et al., 2009; Furini, 2012). Generally, sequestration of metal ions is a strategy adopted by organisms to ameliorate toxicity. The arrested metal ions are transported from cytosol to the vacuole for sequestration via transporters. vacuolar sequestration is the vital mechanism to HM homeostasis in plants, which is directly driven by ATP-dependent vacuolar pumps (V-ATPase and V-PPase) and a set of tonoplast transporters (Sharma et al., 2016). RNA-Seq and *de novo* transcriptome analysis showed that different candidate genes that encode heavy metal ATPases (HMAs), ABC transporter, zinc iron permeases (ZIPs) and natural resistance-associated macrophage proteins (NRAMPs) are involved in metal transport and cellular detoxification (Xu et al., 2015; Sharma et al., 2016). A classic example of such protein in Cd uptake in *A. thaliana* is the Fe (II) transporter iron-regulated transporter 1 (IRT1) belonging to the ZIP family (Connolly et al., 2002). Furthermore, NRAMPs members such as NRAMP5 is recognized as an important transporter for Mn acquisition and major pathway of Cd entry into rice roots, which

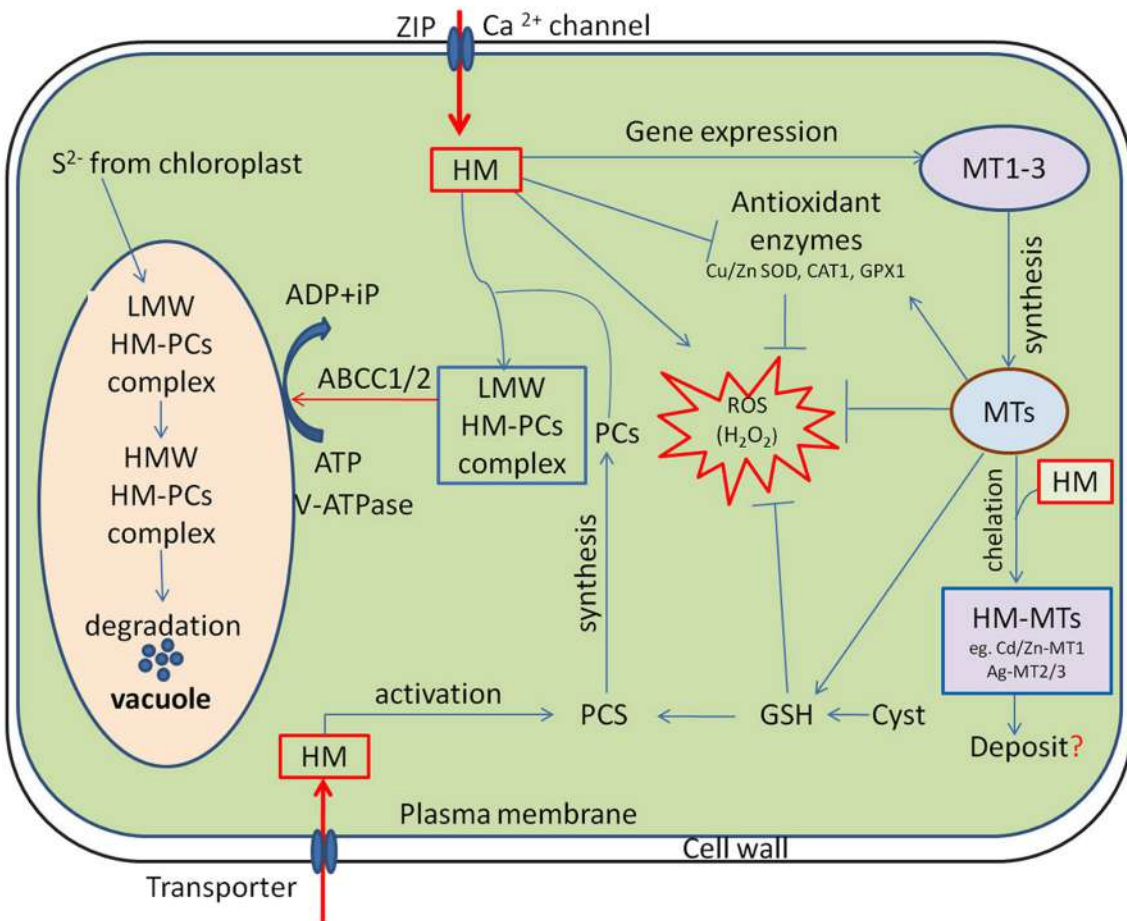


FIGURE 1 | Cellular functions of phytochelatins (PCs) and metallothioneins (MTs) in heavy metal (HM) detoxification. HM activates phytochelatin synthase (PCS) and MTs expression, subsequently the low molecular weight (LMW) HM-PC and HM-MTs complexes are formed in the cytosol. The LMW HM-PCs complexes are consequently transported through tonoplast to vacuole by ATP-binding-cassette and V-ATPase transporter (ABCC1/2). Following compartmentalization, LMW complexes further integrate HM and sulfide (S^{2-} , generated by the chloroplasts) to finally form high molecular weight (HMW) HM-PCs complexes. MTs regulates cellular redox homeostasis independently and also by stimulating antioxidant system and stabilizing relatively high cellular GSH concentrations. “→” indicates “Positive regulation” and “-|” represents “Inhibition”, whereas “?” is a “speculation.”

is localized at the distal side of exodermis and endodermis of the plasma membrane of cells (Clemens and Ma, 2016). Interestingly, another transporter HMA2 localized in the plasma membrane of pericycle cells is thought to transport Cd from the apoplast to the symplast to facilitate translocation via the phloem in rice, whereas HMA3 in the tonoplast sequesters Cd into vacuoles by serving as primary pump (Clemens and Ma, 2016; Sharma et al., 2016). The HM transporter 1 (HMT1) was first identified in 1995 in the yeast *S. pombe*, as a vacuolar PC transporter required for Cd tolerance (Mendoza-Cózatl et al., 2011). The *HMT1* gene encodes ATP-binding cassette (ABC) membrane transport proteins; therefore, both *HMT1* and ATP are required for the translocation of LMW PC-Cd complexes into the vacuole (Figure 1; Cobbett and Goldsbrough, 2002). In progression, two ABCC subfamily members of ABC transporters, *ABCC1* and *ABCC2* were also identified as additional vacuolar metal-PC

complex transporter in *S. pombe* and *Arabidopsis* (Mendoza-Cózatl et al., 2010; Park et al., 2012). Using double mutants, Song et al. (2014) demonstrated that vacuolar sequestration by *ABCC1* and *ABCC2* is necessary for complete detoxification of Arsenic (As) and Cd in *Arabidopsis*. Interestingly, they also reported that the addition of necessary metal ions, such as zinc (Zn), copper (Cu), manganese (Mn) and iron(Fe) to the transport assay further enhances PC₂ transport efficiency in barley vacuoles, suggesting that PCs might contribute to both the homeostasis of essential metals and detoxification of non-essential toxic metal(lloid)s in plants (Song et al., 2014). Although the mechanism how the transporters regulate the sequestration of metal-PCs conjugates to vacuoles is not clear. Very recent, Zhang et al. (2017), for the first time provided evidence that phosphorylation-mediated regulation of *ABCC1* activity is required for vacuolar sequestration of As. They found

that Ser⁸⁴⁶ phosphorylation is required for the As resistance function of ABCC1 in *Arabidopsis*.

Metallothioneins (MTs): Structure, Regulation and Functions in HM Tolerance

Alike PCs, MTs are also naturally-occurring intracellular cysteine-rich major metal-binding proteins, which are used by cells to immobilize, sequester, and detoxify metal ions (Capdevila and Atrian, 2011). Although plant MTs have been discovered over last three decades, the precise physiological functions of MTs have not yet been fully elucidated (Liu et al., 2015a). The proposed roles of MTs include (a) participation in maintaining the homeostasis of essential transition metal ions, (b) sequestration of toxic HMs, and (c) protection against intracellular oxidative damage induced by stress (Hossain et al., 2012a).

Transition metals such as Cu, Fe, Mn and Zn are essential for all organisms because they play critical roles in a variety of physiological processes. For example, Cu is required for photosynthesis, respiration, ethylene perception, ROS metabolism and cell walls in plants (Burkhead et al., 2009; Peñarrubia et al., 2010). A number of studies suggested the involvement of plant MTs in the participation of metal ion homeostasis, especially for Cu, during both vegetative growth and senescence. For example, Benatti et al. (2014) demonstrated that the MTs deficient mutants accumulate 45% and 30% less Cu in shoot and root, compared to the WT, while there are no obvious differences in the life cycle between WT and quad-MT mutant plants under various growth conditions. Again, at early vegetative stage, there is no significant difference in Cu uptake in leaves of 4-week-old WT and MT-deficient mutants. However, the concentration of Cu remains twice in leaves of 12-week-old MT-deficient plants compared to leaves of WT. In contrast, the Cu concentration in seeds of MT-deficient plants was less than half compared to the seeds of WT (Benatti et al., 2014). All these results suggest that MTs are not required to complete life cycle, but are important for essential ions homeostasis and distribution in plants.

In general, sequestration of intracellular HMs in eukaryotes also involves binding of HMs with cytosolic cysteine-rich MTs peptides as well as compartmentalization (Sácký et al., 2014). The combination of low kinetic stability and high thermodynamic is the main features of metal-MT complexes, which bind the metals very firmly, while a part of the metal ions is easily exchanged for other proteins (Maret, 2000). Transgenic plants overexpressing MTs genes have been scored for enhanced metal tolerance and they demonstrate modified metal accumulation or distribution strategies (Gu et al., 2015; Liu et al., 2015a; Tomas et al., 2015). In plants, vacuole is considered as the final destination of detoxification of HMs. Although the chelation of metal ions by MTs is well documented, a little is known about the mechanisms of transport of metals-MT complex from the cytoplasm to the vacuole (Yang et al., 2011). Surprisingly, in *ThMT3* (*hispida* metallothionein-like ThMT3) transgenic material, the expression of four genes (*GLR1*, *GTT2*, *GSH1*, and *YCF1*) which aid

transport of HMs from the cytoplasm to the vacuole is not induced by Cd, Zn, or Cu stress (Yang et al., 2011). These results advocate that metals are not transported into vacuoles, and that *ThMT3* may only regulate HMs accumulation in the cytoplasm.

The biologic functions of MTs have been a perplexing topic ever since their discovery. Many studies have suggested that in addition to the chelation or metal ion homeostasis, MTs play an important role in cellular redox homeostasis under diverse stress conditions (Kang, 2006). Abiotic stresses like HMs induce excessive accumulation of ROS in plants, and cause damages to the cellular macromolecules such as proteins, leading to metabolic and physiological disorders in cells or even cell death (Hasan et al., 2016). Interestingly, MTs have been proposed as an alternative tool by which plants protect themselves from stress-induced oxidative damage (Figure 1; Hassinen et al., 2011; Ansarypour and Shahpuri, 2017). Although many reports have indicated the roles of MTs in abiotic stress tolerance as ROS scavengers, the mechanisms through which MTs mediate ROS homeostasis remain unclear (Hassinen et al., 2011). It has been proposed that during ROS scavenging, metals are released from MTs and ROS moiety is bounded to the Cys residues of the same. A number of studies have also advocated that the released metals might be involved in the initiation of signaling cascade required for ROS scavenging (Hassinen et al., 2011). For example, normal cellular functioning requires Zn mobilization and its transfer from one location to another or from one Zn-binding site to another. The released Zn from MT mobilized by an oxidative reaction may either constitute a general pathway by which Zn is distributed in the cell or be restricted to conditions of oxidative stress, where Zn is essential for antioxidant defense systems (Kang, 2006), suggesting an important role of MTs in ROS homeostasis and protection of cellular macromolecules from stress-induced ROS. Additionally, the different classes of MTs have distinct tissue-specific expression patterns in plants. As example, GUS reporter constructs explored that *MT1a* and *MT2b* are expressed in the phloem, whereas *MT2a* and *MT3* in the mesophyll cells of young leaves and in root tips (Hassinen et al., 2011). Likewise, Liu et al. (2015a) also demonstrated that *OsMT2c* gene encoding for type 2 MT expressed in the roots, leaf sheathes, and leaves of rice, whereas its weak expression was observed in seeds. Considering their diversified role and tissue specific expression, recently Irvine et al. (2017) showed an excellent effort to develop a low-cost MT-biosensor that can dramatically increase the signal associated with a metal of interest. Such a simple sensor technology could be potentially used in environmental monitoring specially in the areas with the metal contamination problems.

REPAIRING OF DAMAGED PROTEINS

Proteins are the primary targets of HMs. They either form a complex with functional side chain groups of proteins or displace essential ions from metallo proteins, leading to impairment of

physiological functions (Tamás et al., 2014). In addition, HMs interfere with the native confirmations of proteins by inhibiting folding process of nascent or non-native proteins that manifest both in a quantitative deficiency of the affected proteins and in the formation of proteotoxic aggregates (Bierkens, 2000; Tamás et al., 2014). Interestingly, plants inherently respond to stress by triggering the activation of the genes involved in cell survival and/or death in contaminated environments (Hossain et al., 2013). As a part of this plant response ubiquitously involves a set of genes, commonly termed as stress genes, are induced to synthesize a group of proteins called HSPs (Gupta et al., 2010). In stress conditions, the induced synthesis of HSPs plays a significant role in maintaining the cellular homeostasis by assisting accurate folding of nascent and stress accumulated misfolded proteins, preventing protein aggregation or by promoting selective degradation of misfolded or denatured proteins (Hüttner et al., 2012; Park and Seo, 2015).

In fact, HSPs functions as molecular chaperones; proteins which are involved in “house-keeping” inside the cell (Sørensen et al., 2003). Several classes of HSP have been identified in plants (**Table 1**) and the HSP proteins having molecular weights ranging from 10 to 200 KD are characterized as chaperones which participate in the induction of the signal in stress conditions (Schöfl et al., 1999). For example, in endoplasmic reticulum (ER) all the nascent polypeptides, firstly, are stabilized by chaperones (HSP40 and HSP70-like proteins) such as ERdj3 and binding protein (BiP) before they are properly modified and folded, which prevents aggregation and helps their proper folding (**Figure 2**; Howell, 2013).

Role of HSPs in Plant Tolerance to HM Stress

HM stress often causes disturbance to the cellular homeostasis by inactivating essential enzymes and by suppressing proteins functioning (Hossain et al., 2012b). Hence, the induction of HSPs proteins is thought-out as a critical protective, eco-physiologically adaptive and genetically conserved response of organisms to the environmental anxiety. Thus, they accomplish a key function in the hostility of stress by re-establishing normal protein conformation and cellular homeostasis (Rhee et al., 2009). Among the major categories of HSPs, HSP70 family members have extensively been studied. Functional characterization of HSP70 revealed that HSP70 is accumulated in response to environmental stressors in a wide range of plant species (Gupta et al., 2010). The specific members of this family are localized into the cytosol, mitochondria and endoplasmic reticulum(ER) and are constitutively expressed as well as regulated to maintain cellular homeostasis. An example to cite, the 70-KDa heat shock cognates(HSC70) are constitutively expressed in cells and often assist in the folding of *de novo* synthesized polypeptides and import or translocations of precursor proteins (Wang et al., 2004).

The recent advancements in proteomics research have enabled us to identify the functional genes or proteins involved in the responses of plants to HM stress at molecular levels (Ahsan et al., 2009). Transcript analysis in many plant species showed

that HSP70 is highly expressed under a variety of metal stress (**Table 1**). Although many studies showed that the over-expression of HSP70 genes is positively correlated with the acquisition of tolerance to various stresses, including HMs, but the cellular mechanisms of HSP70 function under stress situation are not completely understood (Wang et al., 2004). HSP70 chaperones, together with their co-chaperones like DnaJ, make a set of prominent cellular machines to prevent accumulation of newly synthesized proteins as aggregates and ensure the proper folding of protein during their transfer to the destination (Al-Whaibi, 2011; Park and Seo, 2015). In transportation of precursor protein, the HSC70 is essential for cell-to-cell transport through interaction with the plasmodesmatal translocation pathway (Aoki et al., 2002). The induction of HSP70 not only limits the proteotoxic symptoms of metal ions, but also helps the sequestration and detoxification of these ions by MTs (Haap et al., 2016). While the entire mechanism of HSPs-induced metal detoxification via MT has yet to be explored, only few studies pointed out that HSP60 might participate in protein folding and aggregation of many other proteins that are transported to organelles such as mitochondria and chloroplasts (Al-Whaibi, 2011). With our increasing understanding of the proteome, it is becoming clear that HSP60 is essential for cellular functions both at normal or stress environments, including metal stress (**Table 1**). Interestingly, proteomics analysis also revealed that the induction HSP60 chaperones prevents the denaturation of proteins even in the presence of metal ions in the cytoplasm (Sarry et al., 2006; Rodríguez-Celma et al., 2010). Similarly, a good number of studies showed the induction of HSP90 family proteins by different metals in many plant species (**Table 1**) which play a major role in protein folding and regulating signal-transduction networks, cell-cycle control, protein degradation and protein trafficking (Pratt and Toft, 2003; Al-Whaibi, 2011). Interestingly, they have also been found in association with several other intercellular proteins, including calmodulin, actin, tubulin and some other receptors and signaling kinases (Wang et al., 2004; Gupta et al., 2010; Park and Seo, 2015). The multiple sites of localization and high accumulation in combination with other intercellular proteins lead to the suggestion that these polypeptides perform a general mode of cellular activities (Prasad et al., 2010). This family of proteins might provide genetic buffering and contribute to the evolutionary adaptation of plant both in normal and stressful conditions (Wang et al., 2004). By contrast, there is no substantial evidence implicating HSP100/Clp proteins in HMs tolerance in plants (Agarwal et al., 2003). Recently, few studies reported that many members of this family are induced in response to metal treatments (**Table 1**), and they accomplish house keeping functions necessary for cellular homeostasis (Lee et al., 2006).

Most of the members of sHSPs are strongly inducible and some are also constitutively expressed under environmental stress conditions. One of the featured functions of this family of protein is the degradation of the proteins not suitable for folding (Gupta et al., 2010). Similar to other HSPs, sHSPs also function as molecular chaperones, however, the important characteristic that distinguishes sHSPs from other chaperone classes, such as DnaK or ClpB/DnaK is that their activity is independent of ATP (Sun

TABLE 1 | Five major classes of heat shock proteins (HSPs) that are induced in response to heavy metal stress in plants.

HSP classes	Members	Plant species	Metals	References
HSPs70	HSP70	<i>Populus trichocarpa</i> , <i>Lycopersicon peruvianum L.</i> , <i>Glycine max</i> , <i>Arabidopsis thaliana</i> , <i>Populus tremula</i> × <i>P. alba</i> , <i>Populus tremula</i> , <i>Populus nigra</i>	Cd	Lomaglio et al., 2015 Neumann et al., 1994 Hossain et al., 2012b Sarry et al., 2006 Durand et al., 2010 Kieffer et al., 2008
		<i>Elodea canadensis Michx</i> <i>Conocephalum conicum</i> <i>Lemna minor</i>	Cd Pb Cd, Pb, Cu Cu Cd, Pb, Cr, Zn	Lomaglio et al., 2015 Sergio et al., 2007 Basile et al., 2013 Basile et al., 2015
		<i>Oriza sativa</i>	As	Chakrabarty et al., 2009; Rai et al., 2015
		<i>Suaeda salsa</i>	Hg	Liu et al., 2013
	HSP 70, BiP	<i>Populus alba L</i>	Cu, Zn	Lingua et al., 2012
	HSP70	<i>Oriza sativa</i> , <i>Suaeda salsa</i>	Ag	Chen et al., 2012; Liu et al., 2013
	HSP68	<i>Solanum lycopersicum</i>	Cd	Rodríguez-Celma et al., 2010
	BiP	<i>Oriza sativa</i>	Cu,	Ahsan et al., 2007a
	BiP	<i>Oriza sativa</i>	Cd	Ahsan et al., 2007b
	HSP 70	<i>Enteromorpha intestinalis</i>	Cu	Lewis et al., 2001
HSPs 70A	HSPs 70A	<i>Chlamydomonas acidophila</i>	Fe, Zn	Spijkerman et al., 2007
	HSP70	<i>Oryza sativa L.</i>	Cr	Dubey et al., 2010
	HSC70	<i>Phytolacca Americana</i>	Cd	Zhao et al., 2011
	HSC70-2	<i>Raphanus sativus</i>	Cr	Xie et al., 2015
HSPs 60	cpn60 ²	<i>Oriza sativa</i>	Hg	Chen et al., 2012
	HSP60, Cpn60-B	<i>Solanum lycopersicum</i>	Cd	Rodríguez-Celma et al., 2010
	HSP60	<i>Arabidopsis thaliana</i>	Cd	Sarry et al., 2006
	HSP60	<i>Chlamydomonas acidophila</i>	Fe, Zn	Spijkerman et al., 2007
HSPs 90	HSP90-1	<i>Lemna gibba</i>	Cu	Akhtar et al., 2005
	HSP90-1	<i>Arabidopsis thaliana</i>	As	Haralampidis et al., 2002
	HSP81-2	<i>Oryza sativa L.</i>	Cu	Song et al., 2013
	HSP82	<i>S. cerevisiae</i>	As, Cu, Cd	Sanchez et al., 1992
	HSP81.2, 81.3, 81.4, 88.1 & 89.1	<i>Arabidopsis thaliana</i>	Cu, Cd, Pb, As	Milioni and Hatzopoulos, 1997
	HSP90-1	<i>Solanum lycopersicum</i>	Cr, As	Goupil et al., 2009
	HSP82	<i>Oryza sativa</i>	As	Chakrabarty et al., 2009
	HSP81-1	<i>Oryza sativa</i>	Cd	Oono et al., 2016
HSPs 100	HSP104	<i>S. cerevisiae</i>	As, Cu, Cd	Sanchez et al., 1992
	HSP101	<i>Oryza sativa L.</i> ,	As	Agarwal et al., 2003
	ClpB-C	<i>Oryza sativa L.</i>	Cans, Cu, Co	Singh et al., 2012
	ClpB-C	<i>Arabidopsis thaliana</i>	As	Mishra and Grover, 2014
sHSPs	HSP17	<i>Lycopersicon peruvianum L</i> ,	Cd	Neumann et al., 1994
	HSP17	<i>Populus alba L</i>	Cu, Zn	Lingua et al., 2012
	HSP21	<i>Arabidopsis thaliana</i>	Cd	Zhao et al., 2009
	HSP20, HSP23p	<i>Kandelia candel</i>	Cd	Weng et al., 2013
	HSP26.13p	<i>Chenopodium album</i>	Ni, Cd, Cu	Haq et al., 2013
	HSP17	<i>Armeria maritime</i>	Cu	Neumann et al., 1995

(Continued)

TABLE 1 | Continued

HSP classes	Members	Plant species	Metals	References
HSP17		<i>Silene vulgaris, Lycopersicon peruvianum</i>	Hg, Cu, Cd,	Wollgiehn and Neumann, 1999
HSP24		<i>Capsicum annuum L</i>	Zn	Zhu et al., 2013
HSP22		<i>Chlamydomonas acidophila</i>	Cu	Spijkerman et al., 2007
HSP17.4		<i>Oryza sativa L.</i>	Fe, Zn	Dubey et al., 2010
HSP20, HSP21, HSP22		<i>Raphanus sativus</i>	Cr	Xie et al., 2015
HSP23		<i>Glycine max</i>	Cr	Zhen et al., 2007
HSP23.9		<i>Oryza sativa</i>	Al	Chakrabarty et al., 2009
HSP17.4, HSP17.5		<i>Tamarix hispida</i>	As	Gao et al., 2012
HSP18.3		<i>Oryza sativa</i>	Cu, Cd, Zn	Rai et al., 2015

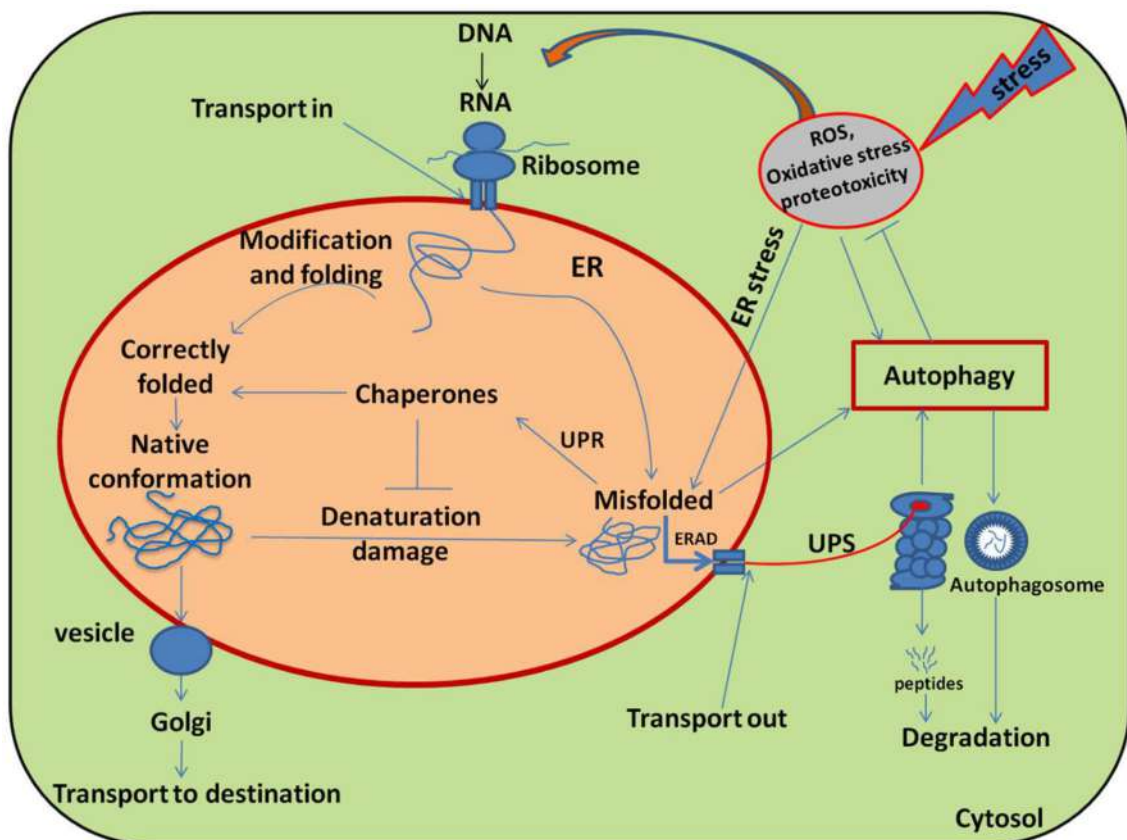


FIGURE 2 | Schematic diagram illustrating the main pathways and regulation of protein folding and modification in the endoplasmic reticulum (ER). Many newly synthesized proteins are translocated into the ER, where proteins folded into their native three dimensional structures with the help of chaperones. The correctly folded proteins are then transported to the Golgi complex, followed by delivery to the destination where they eventually function. While exposure of plants to stress causes oxidative stress by generating over ride of ROS and stimulating the misfolding of proteins. The incorrectly folded proteins are then detected by quality control system, which stimulates another pathway called unfolded protein response (UPR). The terminally misfolded proteins are then eliminated through the endoplasmic reticulum associated degradation (ERAD) pathway, where they initially ubiquitinated and then degraded in the cytoplasm by proteasome system (UPS) or subjected to autophagy. Adopted from Dobson (2003) with modifications.

et al., 2002; Mogk and Bukau, 2017). sHSPs maintain denatured proteins in a folding-competent state and allow subsequent ATP-dependent disaggregation through the HSP70/90 chaperone system, thereby facilitating their subsequent refolding (Wang

et al., 2004). Recently, it has been shown that BAG3 protein acts as a modulator, brings the chaperone families together into a complex and coordinates the potentiality of Hsp22 and Hsp70 to refold the denatured proteins (Rauch et al., 2017). Additionally,

this family of HSPs is also involved in signaling similar to their counterparts, where they become phosphorylated by stress-kinases, and increase the amount of reduced glutathione in the cytoplasm (Arrigo, 1998). A number of studies suggest a strong correlation between sHSP accumulation and plant tolerance, particularly to HMs stress (Table 1; Wang et al., 2004). In *Arabidopsis*, 13 different sHsps have been identified in distinct cellular compartments, which probably function as mediators of molecular adaptation to stress conditions and are unique to plants. The differential regulation of chloroplastic i.e., Cp-sHSPs or HSP26.13p in *C. album* plays a dual role in protecting the plant from heat and metals like Ni, Cu, and Cd stress (Haq et al., 2013).

Notably, most of HSPs are activated early in the cascade of cellular events following toxic exposure even below the lethal dose and thus, considered as strong biomarkers for environmental pollution (Bierkens et al., 1998). The excessive accumulation of ROS at cellular level is a common consequence of abiotic stress such as HMs. Interestingly, the high HSP levels protect plants against abiotic stresses not only by preventing irreversible protein aggregation, but also by promoting cellular redox homeostasis through stimulating antioxidant systems (Mu et al., 2013). Recently, Cai et al. (2017) revealed that HSPs-induced metal tolerance in plants has a strong correlation with melatonin (N-acetyl-5-methoxy tryptamine) biosynthesis, which is regulated by heat-shock factor A1a (HsfA1a). Therefore, all the above presented results suggest that the inducible HSPs are important and beneficial for fitness in normal, as well as under capricious environment. As a part of protein quality control system, HSPs play a major role in maintaining the functionality of cellular machinery under environmental stress. Therefore, research on the functional and structural aspects, cross-talk with other chaperones and relationship between different HSP expressions along with the physiological stress response should be expanded to better understand their functions.

Heavy Metals-Induced ER Stress

In cells, both recently synthesized and preexisting polypeptides are at constant risk of misfolding and aggregation. It has been estimated that one-third of recently synthesized proteins are misfolded under ambient conditions (Schubert et al., 2000). In addition, cells continuously face environmental challenges such as mutations, heat, active oxygen radicals and HM ions, which not only disrupt protein folding but also cause the misfolding of already folded protein, (Amm et al., 2014). The disruption of proper functioning of the ER is particularly relevant under stress conditions, whereas the demand for secreted proteins exceeds its working capacity and disrupts normal functioning of ER, termed as ER stress (Schröder and Kaufman, 2005). A number of studies have shown that HMs and metalloids inhibit refolding of chemically denatured proteins *in vitro*, obstruct protein folding *in vivo* and stimulate aggregation of nascent proteins in living cells (Sharma et al., 2011; Jacobson et al., 2012). For example, Cr has been shown to trigger oxidative protein damage and protein aggregation in yeast by enhancing mRNA mistranslation (Sumner et al., 2005; Holland et al., 2007). Likewise, Cd has also been shown to cause the widespread aggregation of nascent protein and ER stress in yeast

(Gardarin et al., 2010), whilst the mechanistic details of protein misfolding in the ER and cytoplasm remain to be elucidated (Tamás et al., 2014). But somehow, this could be related to metal-induced structural alteration of ER. Recently, Karmous et al. (2015) demonstrated that Cu treatment in embryonic cells of *Phaseolus vulgaris* results in prevalently swollen cisternae of smooth endoplasmic reticulum and vesicles with electron-dense contents. Although this phenomenon is often not well recognizable, it robustly inhibits cellular homeostasis. While the toxicity of metals, like Cd, As, Pb, Hg, and Cr is unquestionable and their interference with protein folding in living cells is well-documented, the potency of accumulation of misfolded and aggregated proteins appears to be different (Tamás et al., 2014). In yeast cells, the accumulations of aggregated proteins occur in the order As>Cd>Cr upon exposure of equi-toxic concentrations of these metals (Jacobson et al., 2012). The *in vivo* potency of these environmental threats to prompt protein aggregation possibly depends on the efficiency of their cellular uptake/transport and their distinct modes of biological action (Tamás et al., 2014). Under such circumstances, a coordinated adaptive program called the unfolded protein response (UPR) is commonly initiated.

The UPR is a homeostatic response to alleviate ER stress through transcriptional and translational events. The induction of UPR has three aims; initially to restore the normal function of the cell by halting production of secreted and membrane proteins, removal of misfolded proteins through ER-associated degradation (ERAD) systems, and activation of the signaling pathways that lead to increased production of molecular chaperones involved in protein folding. If these cell-sparing activities are not achieved within a certain time span or the disruption is prolonged, then the UPR aims toward programmed cell death (PCD) which is called apoptosis (Deng et al., 2013; Liu and Howell, 2016). The UPR is a sensitive surveillance mechanism that monitors the ER loading capacity. If persistently misfolded proteins exceed the ER loading capacity, cellular communication between the ER and nucleus occurs for ER homeostasis, leading to the transcriptional activation that up-regulates the cellular chaperones (Brandizzi et al., 2014). Recently, it has been reported as two arm process in plants, where proteolytic processing of membrane-associated bZIP TFs and RNA splicing factor inositol-requiring enzyme-1 (IRE1) act as transducers in ER stress or UPR signaling pathway. Structural details of bZIP TFs, bZIP17, bZIP28 and IRE1/bZIP60 and their underlying principles of mobilization in response to ER stress suggest that the UPR signaling pathway is assisted by these factors in order to protect plants from ER stress (Deng et al., 2013; Sun et al., 2013; Yang et al., 2014). This UPR transcriptional activation enhances the production of molecular chaperones such as binding protein (BiP) and glucose-regulated protein 94 (GRP94), involved in increased ER protein-folding potentiality (Yoshida et al., 1998). The molecular chaperones binding proteins (BiP) are the master regulatory elements of these quality control systems and a classical marker of UPR activation (Malhotra and Kaufman, 2007). For example, Xu et al. (2013) demonstrated that heterologous expression of *AtBiP2* protein in BY-2 act as a negative regulator of Cd-induced ER stress and

PCD. Recently, Guan et al. (2015) also showed that ER chaperone binding protein *BiP* acts as a positive regulator in Cd stress tolerance. To explore the mechanism, the author also examined the transcript level of *GSH* gene in *LcBiP*-overexpressed tobacco. Interestingly, the transcript levels of the *GSH* and the ER stress marker gene are not induced, meaning that BiP may enhance the folding capacity of *GSH* in the ER in plants. In contrast, proteins that fail to achieve their native conformation and aggregate in ER are eliminated through the ERAD pathway *via* a series of tightly coupled steps that include substrate recognition, targeting of terminally misfolded proteins, retro-translocations, and ubiquitin-dependent proteasomal destruction (Liu and Howell, 2016). Liu et al. (2015b) discover a plant-specific component of ERAD system in *Arabidopsis*. They uncovered that EBS7 (methanesulfonate-mutagenized brassinosteroid insensitive 1 suppressor 7) interacts with the ER membrane-anchored ubiquitin ligase AtHrd1a, one of the central components of the *Arabidopsis* ERAD machinery, whose mutation destabilizes AtHrd1a to reduce polyubiquitination. Similarly, very recently, Liu et al. (2016) demonstrated that α 1, 6-linked mannose is necessary for luminal N-glycoproteins degradation via ERAD system in yeast where Htm1p-Pdi1p complex acts as a folding-sensitive mannosidase for catalyzing the first committed step. Thus, any defects in this sophisticated ERAD machinery system raise death and life issues of cells survival, especially under stressed environments. For instance, Van Hoewyk (2016) demonstrated that *Arabidopsis* HRD1 and SEL1L mutant plants showed decreased tolerance to selenate (Se) stress. As-Se toxicity causes both oxidative stress and protein misfolding due to the substitution of a cysteine to Se-cysteine (Van Hoewyk, 2013), whereas selenium enhances Cd tolerance in tomato plants (Li et al., 2016b). Actually, this is an alternative adaptive mechanism, involved in actively controlled and precise degradation of cellular components, and selective elimination of harmful, unwanted or damaged cells in eukaryotes (Tuzhikov et al., 2011; Brandizzi et al., 2014). Such selective suicide or PCD is paradoxically a crucial event which eventually provides survival benefits for the whole organism under extreme environmental conditions like HMs stress (Yakimova et al., 2007; Adamakis et al., 2011). However, the details of involved mechanisms are still obscure and remain to be further disclosed.

DEGRADATION OF METAL-INDUCED DENATURED PROTEINS

Much of plant physiological processes, growth and development are controlled by the selective degradation of unwanted misfolded or damaged proteins in order to maintain cellular homeostasis. In plants, protein degradation or proteolysis occurs either by ubiquitin proteosome system (UPS) or by autophagosomes induction (Liu and Howell, 2016). The UPS is a fundamental, highly regulated multistep enzymatic cascade that tightly controls the cellular protein homeostasis. It is a very rapid and effective method for a precise degradation of an unwanted protein at a particular time, whereas most of the times a protein is degraded only in response to a specific

cellular signal or event (Pines and Lindon, 2005). The recent progress in molecular genetics revealed that like a tip of iceberg, UPS components regulate critical processes in plants (Sadanandom et al., 2012). It has been found that over 6% of *Arabidopsis* protein-coding genes are dedicated to the UPS (Vierstra, 2009). In eukaryotic cells proteins that destined to degrade, firstly, labeled by ubiquitin and then the ubiquitylated protein digested to small peptides by the large proteolytic complex, the 26S proteasome (Goldberg, 2003). Ubiquitylation is an energy dependent key regulatory process, which is executed by three different E1-E2-E3 enzymes conjugation cascade (Maupin-Furlow, 2013). In the first step of this cascade, ubiquitin is covalently conjugated to ubiquitin-activating enzyme (E1) in an ATP-dependent reaction, and then this activated ubiquitin is transferred from E1 to E2 (or Ub-conjugating enzyme) by transesterification. Finally, E3 (ubiquitin ligase) catalyzes the transfer of the ubiquitin from the E2 enzyme to a lysine residue on the target protein. After initial polyubiquitination, this step is repeated to form polyubiquitinated chains on the target protein and designated for degradation by the 26S proteasome (Ruschak et al., 2011; Sadanandom et al., 2012). Upon delivery, the deubiquitinating enzymes remove the polyubiquitin chain before unfolding, import and proteolysis of targeted substrates (Hartmann-Petersen et al., 2003).

On the other hand, autophagy is a biological self-destruction process, by which eukaryotic cells maintain their cellular homeostasis by turning over damaged proteins or organelles into the vacuole during developmental transitions and under stress conditions (Liu and Bassham, 2012; Wen-Xing, 2012). Upon the induction of an autophagic pathway, the cytoplasmic components that designate to degradation, are surrounded by a double membrane structure, called autophagosomes (Figure 2). The autophagosome then delivers its cargo materials to the vacuole, where the outer membrane of the autophagosome initially fuses with the vacuole membrane, after which the cargo materials are degraded by vacuolar hydrolases in the vacuole and recycled (Yang et al., 2016). There are four different types of autophagy detailed out in eukaryotes, including microautophagy, macroautophagy, chaperone-mediated autophagy and organelle-specific autophagy (Liu and Bassham, 2012). Out of these, microautophagy and macroautophagy (hereafter referred as autophagy), have been shown to occur in plants (Han et al., 2011).

UPS-Dependent Proteasome Activity and Metals Stress

Extreme environmental conditions such as HMs pollution often adversely affect proteins quality by increasing free radicals that encourage denaturation and damage, thus causing the misfolding of proteins. Cells under stress, need to prevent further damage by initiating defense machinery to repair the damaged proteins or remove them when irreparable. In such circumstances, the UPS plays a crucial role in plant response and adaptation to changing environmental conditions (Stone, 2014). The UPS, functions both in cytoplasm and nucleus, responsible to modulate the levels of regulatory proteins and to remove most abnormal peptides and short-lived cellular regulators which may accumulate following

exposure to abiotic stress (Lyzenga and Stone, 2012). The significant role of the UPS in the cellular response to HM stress has been recognized few years ago and is evident to increased expression of polyubiquitin genes (Genschik et al., 1992; Jungmann et al., 1993). It is believed that the expression of polyubiquitin genes under stress conditions is one of the important indications that the UPS is involved in regulation of plant HMs stress tolerance (Sun and Callis, 1997; Chai and Zhang, 1998). The genome-wide transcription analysis of rice plants showed that low concentrations of Cd treatment induces polyubiquitin expression both in root and shoot (Oono et al., 2016). In contrast, elevated metal concentrations induce the disruption of proteasomal activity, resulting in the accumulation of abnormal proteins in the cytosol, which alter cellular protein homeostasis and thereby activating apoptosis (Yu et al., 2011). For instance, proteome analysis in different plant species has shown that ubiquitin activity can significantly be reduced by Cd, Co, Cu, Cr, Hg, Ni and Pb at 100 μ M but not by Al and Zn, whereas low concentrations can induce 26S proteasome activity (Aina et al., 2007; Pena et al., 2007, 2008). Although Co, Cu, Cr, Hg, Ni, and Pb induce accumulation of ubiquitin conjugated proteins, the abundance of 20S core protein in UPS system is not changed (Pena et al., 2008). In contrast, Karmous et al. (2014) showed that Cu treatment (200 μ M) has a strong effect on UPS pathway and can inhibit about 88% of the 20S proteasome activity in the cotyledons of germinating bean seeds. This implies that the effect of HMs on proteolytic system can not be generalized; however, the functional impairment-induced decrease in proteases activities appears to be a common aspect of metal toxicity in plant.

In extreme environments, over-expression of genes involved in UPS cascade, enhances tolerance to multiple stresses without any adverse effects on growth and development in plants (Guo et al., 2008). For example, Lim et al. (2014) showed the E3 or ubiquitin ligase enzyme is an important regulator for the removal of aberrant proteins under metal stress. In addition, the heterogeneous expression of rice E3 ligase enzyme synthesis RING domain *OsHIR1 gene* in *Arabidopsis* has been found to be decreased with As and Cd accumulation in both root and shoot (Dametto et al., 2015). Although the mechanism is not clear, it could probably be regulated by its substrate protein, since the OsHIR1 protein positively interacts with the OsTIP4;1 related to As and Cd uptake. Therefore, the development of strategies to reduce metal uptake and translocation as well as to improve cellular protein homeostasis with the ubiquitin/proteasome 26S system in plants seems to be a promising approach to ensure crop yield and food safety.

Autophagy in Metal Stress Responses

Autophagy has shown to be involved in the adaptation of plants to a wide range of drastic environmental stresses such as nutrient starvation, oxidative stress, heat stress, drought, salt, and pathogen invasion (Han et al., 2011; Wang et al., 2015; Xu et al., 2016; Yang et al., 2016). However, its pivotal roles in plants, particularly in HMs stress and adaptive responses, have perhaps not received the attention they deserve and thus remains elusive (Chiarelli and Roccheri, 2012; Pérez-Martín et al.,

2015). Fascinatingly, in recent years scientists begun to explore, the involvement of autophagy in plant toward metal tolerance and the mechanism of adaptation is the same as in human and yeast. Firstly, Zhang and Chen (2010), afterwards, Zheng et al. (2012) demonstrated that autophagy is induced in metal treated plants. In progression, the expression profile analysis in tobacco seedlings after five different HMs (Cu, Ni, Zn, Cd and Mn) treatments showed that among the 30 ATGs genes, 18 ATGs genes are upregulated by more than two folds by at least one HM. They also explored that among the 18 ATGs, 11 ATGs are commonly up-regulated in seedlings by all five metals, and the expression is more sensitive to Zn treatment than others. Recently, Abd-Alla et al. (2016) for the first time demonstrated that Ag-NPs treatments result in the induction of autophagy in root nodules of *Rhizobium leguminosarum* as a mechanism of detoxification and surveillance. Taken together, recent studies explored the involvement of autophagy as a sophisticated regulator of surveillance under HMs stress, nevertheless, the mechanisms, especially how metals regulate autophagy, still remain to be elucidated in the future (Zhou et al., 2015).

Interestingly, the cellular sites of ROS production and signaling are thought to be primary targets of autophagy, which leads to either survival or death of cells (Scherz-Shouval and Lazar, 2007; Minibayeva et al., 2012). It has now been undoubtedly established that ROS can function as specific second messengers in signaling cascade. Environmental toxicants, like HMs are known to be strong inducers of oxidative stress due to excessive accumulation of ROS that alter the cellular homeostasis. In general excess accumulation of ROS causes many types of cellular injuries including damage to proteins, lipids and DNA, whereas some of which can result in apoptotic cell death and autophagy (Farah et al., 2016). Several lines of evidence suggest that metal-induced intracellular ROS production function in the signal transduction pathways, leading to induction of autophagy (Zhang and Chen, 2010; Pérez-Martín et al., 2015; Farah et al., 2016). Although an extensive number of studies showed that oxidative stress stimulates the autophagic induction to relieve the plants from oxidative damage, but the mechanistic information still remain limited. Very recently, Yang et al. (2016) put forward an excellent effort to open-up the mechanism for activation of autophagy. They demonstrated that unfolded proteins accumulation in the ER is a trigger for autophagy under conditions that cause ER stress. They showed that the reduction of unfolded proteins accumulation by PBA or TUDCA addition or BiP over-expression inhibits the autophagy in *Arabidopsis*. Whereas, the introduction of the constitutively unfolded proteins zeolin or CPY* activates the UPR and autophagy via IRE1b (inositol-requiring enzyme 1b) dependent manner. But how the ER stress activating these signaling cascades remains to be further revealed.

In addition to their core function, autophagic induction has also been shown to be involved in the regulation of metal uptake. For instance, Li et al. (2015) showed that induction of autophagy with mono-ubiquitination under Fe excess condition affects the functional activity and stability of exogenous *Malus xiaojinensis* iron-regulated transporter (MxIRT1) in yeast, thereby preventing Fe uptake via this root transporter. They

also showed that in Fe led conditions, the transcript levels of ATG8 and ATG8-PE protein significantly increased, which resulted in enhanced MxIRT1 degradation, while the inhibition of autophagic initiation has opposite effects. Therefore, the development of strategies to regulate metal uptake by promoting autophagy under excess metal conditions could have potential implication in increased or even safe food production. However such kind of assumption in plant is still a matter of speculation and thus requires further extensive investigation.

CONCLUDING REMARKS AND FUTURE PERSPECTIVES

The present review outlines the impact of HM stress on cellular protein homeostasis and illustrates the diverse mechanistic approach that operates inside cells to regulate quality control systems toward functional and healthy proteomes. Proteins are major workhorse of cells and directly involved in plant stress response. HMs can trigger the cellular pathways that are broadly classified as death and survival signals. As surveillance mechanism, the ubiquitous plants response to HM stress is the chelation of toxic ions in the cytosol by cysteine rich peptides such as PCs and MTs, compartmentalization of metals in the vacuole by tonoplast located transporters, and the process that involves repair of stress-damaged proteins. In-depth review of recent research works revealed that MTs are not only required to complete the plants life cycle, but also play significant roles in ionic homeostasis and distribution in plants as well as cleanup of ROS and sequestration of metals as that of PCs (Benatti et al., 2014; Tomas et al., 2016). Whilst in extreme conditions metals profoundly affect cellular protein homeostasis by interfering with the folding process, they also stimulate aggregation of nascent or non-native proteins leading to ER stress and decreased cell viability. However, there is a typical set of proteins, called stress

proteins or HSPs proteins, which are preferentially expressed under stress. HSPs restrict aggregation of nascent or non-native proteins but trigger repair of misfolded proteins. In contrast, the damaged proteins which fail to achieve their native conformations, are removed from ER by the activation of ERAD machinery of ERQC system, leading to proteasomal (UPS) or autophagic degradation.

Recent advances in protein research, summarized herein, show that as core degradation process of misfolded or damaged polypeptides, the over-expression of E3 enzyme in UPS pathway and the autophagic induction with mono-ubiquitination prevent metal accumulation in plants (Dametto et al., 2015; Li et al., 2015). However, we are still far away from the complete understanding of the mechanism of subsequent signaling cascades that regulate metal accumulation. The development of strategies to reduce metal uptake and translocation by manipulating cellular protein quality control system in plants seems to be a promising approach that can potentially ensure increased yield as well as food safety.

AUTHOR CONTRIBUTIONS

MH and GA conceived the idea and designed the outlines of the article. MH, YC, MK and GA wrote the article. GA, XC, and ZQ revised the article.

ACKNOWLEDGMENTS

Research in the authors' laboratories is supported by grants from the National Key Research and Development Program of China (2016YFD0201001), the Geological Exploration Foundation of Zhejiang Province, China (2014002-02) and the National Natural Science Foundation of China (31401877, 31550110201, 31772294), and the China Postdoctoral Science Foundation (517000-X91608, 2015M580515).

REFERENCES

- Abd-Alla, M. H., Nafady, N. A., and Khalaf, D. M. (2016). Assessment of silver nanoparticles contamination on faba bean-*Rhizobium leguminosarum* bv. *viciae*-Glomus aggregatum symbiosis: implications for induction of autophagy process in root nodule. *Agri. Ecosys. Env.* 218, 163–177. doi: 10.1016/j.agee.2015.11.022
- Adamakis, I. D. S., Panteris, E., and Eleftheriou, E. P. (2011). The fatal effect of tungsten on *Pisum sativum* L. root cells: indications for endoplasmic reticulum stress-induced programmed cell death. *Planta* 234, 21–34. doi: 10.1007/s00425-011-1372-5
- Agarwal, M., Sahi, C., Katiyar-Agarwal, S., Agarwal, S., Young, T., Gallie, D. R., et al. (2003). Molecular characterization of rice hsp101: complementation of yeast hsp104 mutation by disaggregation of protein granules and differential expression in indica and japonica rice types. *Plant Mol. Biol.* 51, 543–553. doi: 10.1023/A:1022324920316
- Ahsan, N., Lee, D. G., Lee, S. H., Kang, K. Y., Lee, J. J., Kim, P. J., et al. (2007a). Excess copper induced physiological and proteomic changes in germinating rice seeds. *Chemosphere* 67, 1182–1193. doi: 10.1016/j.chemosphere.2006.10.075
- Ahsan, N., Lee, S. H., Lee, D. G., Lee, H., Lee, S. W., Bahk, J. D., et al. (2007b). Physiological and protein profiles alteration of germinating rice seedlings exposed to acute cadmium toxicity. *C. R. Biol.* 330, 735–746. doi: 10.1016/j.crvi.2007.08.001
- Ahsan, N., Renaut, J., and Komatsu, S. (2009). Recent developments in the application of proteomics to the analysis of plant responses to heavy metals. *Proteom.* 9, 2602–2621. doi: 10.1002/pmic.200800935
- Aina, R., Labra, M., Fumagalli, P., Vannini, C., Marsoni, M., Cucchi, U., et al. (2007). Thiol-peptide level and proteomic changes in response to cadmium toxicity in *Oryza sativa* L. roots. *Environ. Exp. Bot.* 59, 381–392. doi: 10.1016/j.envexpbot.2006.04.010
- Akhtar, T. A., Lampi, M. A., and Greenberg, B. M. (2005). Identification of six differentially expressed genes in response to copper exposure in the aquatic plant *Lemna gibba* (duckweed). *Environ. Toxicol. Chem.* 24, 1705–1715. doi: 10.1897/04-352R.1
- Al-Whaibi, M. H. (2011). Plant heat-shock proteins: a mini review. *J. King Saud Univ.-Sci.* 23, 139–150. doi: 10.1016/j.jksus.2010.06.022
- Amm, I., Sommer, T., and Wolf, D. H. (2014). Protein quality control and elimination of protein waste: the role of the ubiquitin–proteasome system. *Biochim. Biophys. AcaBBA. Molecul. Cell Res.* 1843, 182–196. doi: 10.1016/j.bbamcr.2013.06.031
- Ansarypour, Z., and Shahpiri, A. (2017). Heterologous expression of a rice metallothionein isoform (OsMTI-1b) in *Saccharomyces cerevisiae* enhances

- cadmium, hydrogen peroxide and ethanol tolerance. *Braz. J. Microbio.* 48, 537–543. doi: 10.1016/j.bjm.2016.10.024
- Aoki, K., Kragler, F., Xoconostle-Cázares, B., and Lucas, W. J. (2002). A subclass of plant heat shock cognate 70 chaperones carries a motif that facilitates trafficking through plasmodesmata. *Proc. Natl. Acad. Sci. U.S.A.* 99, 16342–16347. doi: 10.1073/pnas.252427999
- Arrigo, A. P. (1998). Small stress proteins: chaperones that act as regulators of intracellular redox state and programmed cell death. *Biol. Chem.* 379, 19–26.
- Ashraf, M., Qztürk, M. A., and Ahmad, M. S. A. (2010). *Plant Adaptation and Phytoremediation*. New York, NY: Springer.
- Basile, A., Sorbo, S., Cardi, M., Lentini, M., Castiglia, D., Cianciullo, P., et al. (2015). Effects of heavy metals on ultrastructure and Hsp70 induction in *Lemna minor* L. exposed to water along the Sarno River, Italy. *Ecotoxicol. Environ. Saf.* 114, 93–101. doi: 10.1016/j.ecoenv.2015.01.009
- Basile, A., Sorbo, S., Conte, B., Cardi, M., and Esposito, S. (2013). Ultrastructural changes and Heat Shock Proteins 70 induced by atmospheric pollution are similar to the effects observed under *in vitro* heavy metals stress in *Conocephalum conicum* (Marchantiophyta-Bryophyta). *Environ. Pollut.* 182, 209–216. doi: 10.1016/j.envpol.2013.07.014
- Benatti, R. M., Yookongkaew, N., Meetam, M., Guo, W. J., Punyasuk, N., AbuQamar, S., et al. (2014). Metallothionein deficiency impacts copper accumulation and redistribution in leaves and seeds of *Arabidopsis*. *New Phyto.* 202, 940–951. doi: 10.1111/nph.12718
- Bierkens, J. G. (2000). Applications and pitfalls of stress-proteins in biomonitoring. *Toxicology* 153, 61–72. doi: 10.1016/S0300-483X(00)00304-8
- Bierkens, J., Maes, J., and Vander Plaetse, F. (1998). Dose-dependent induction of heat shock protein 70 synthesis in *Raphidocelis subcapitata* following exposure to different classes of environmental pollutants. *Environ. Pollut.* 101, 91–97. doi: 10.1016/S0269-7491(98)00010-4
- Brandizzi, F., Frigerio, L., Howell, S. H., and Schäfer, P. (2014). Endoplasmic reticulum—shape and function in stress translation. *Front. Plant Sci.* 5:425. doi: 10.3389/fpls.2014.00425
- Burkhead, J. L., Gogolin Reynolds, K. A., Abdel-Ghany, S. E., Cohu, C. M., and Pilon, M. (2009). Copper homeostasis. *New Phyto.* 182, 799–816. doi: 10.1111/j.1469-8137.2009.02846.x
- Cai, S. Y., Zhang, Y., Xu, Y. P., Qi, Z. Y., Li, M. Q., Ahammed, G. J., et al. (2017). HsfA1a upregulates melatonin biosynthesis to confer cadmium tolerance in tomato plants. *J. Pineal. Res.* 62:e12387. doi: 10.1111/jpi.12387
- Capdevila, M., and Atrian, S. (2011). Metallothionein protein evolution: a miniassay. *J. Biol. Inorg. Chem.* 16, 977–989. doi: 10.1007/s00775-011-0798-3
- Chai, T., and Zhang, Y. (1998). Expression analysis of polyubiquitin genes from bean in response to heavy metals. *Acta Bot. Sini.* 41, 1052–1057.
- Chakrabarty, D., Trivedi, P. K., Misra, P., Tiwari, M., Shri, M., Shukla, D., et al. (2009). Comparative transcriptome analysis of arsenate and arsenite stresses in rice seedlings. *Chemosphere* 74, 688–702. doi: 10.1016/j.chemosphere.2008.09.082
- Chen, Y. A., Chi, W. C., Huang, T. L., Lin, C. Y., Quynh Nguyen, T. T., Hsiung, Y. C., et al. (2012). Mercury-induced biochemical and proteomic changes in rice roots. *Plant Physiol. Biochem.* 55, 23–32. doi: 10.1016/j.plaphy.2012.03.008
- Chiarelli, R., and Roccheri, M. C. (2012). Heavy metals and metalloids as autophagy inducing agents: focus on cadmium and arsenic. *Cells* 1, 597–616. doi: 10.3390/cells1030597
- Chrestensen, C. A., Starke, D. W., and Mieyal, J. J. (2000). Acute cadmium exposure inactivates thioltransferase (Glutaredoxin), inhibits intracellular reduction of protein-glutathionyl-mixed disulfides, and initiates apoptosis. *J. Biol. Chem.* 275, 26556–26565. doi: 10.1074/jbc.M004097200
- Clemens, S. (2006). Evolution and function of phytochelatin synthases. *J. Plant Physiol.* 163, 319–332. doi: 10.1016/j.jplph.2005.11.010
- Clemens, S., and Ma, J. F. (2016). Toxic heavy metal and metalloid accumulation in crop plants and foods. *Annu. Rev. Plant Biol.* 67, 489–512. doi: 10.1146/annurev-arplant-043015-112301
- Cobbett, C., and Goldsbrough, P. (2002). Phytochelatins and metallothioneins: roles in heavy metal detoxification and homeostasis. *Ann. Rev. Plant Biol.* 53, 159–182. doi: 10.1146/annurev.arplant.53.100301.135154
- Connolly, E. L., Fett, J. P., and Guerinot, M. L. (2002). Expression of the IRT1 metal transporter is controlled by metals at the levels of transcript and protein accumulation. *Plant Cell* 14, 1347–1357. doi: 10.1105/tpc.001263
- D'Alessandro, A., Taamalli, M., Gevi, F., Timperio, A. M., Zolla, L., and Ghnaya, T. (2013). Cadmium stress responses in *Brassica juncea*: hints from proteomics and metabolomics. *J. Proteom. Res.* 12, 4979–4997. doi: 10.1021/pr400793e
- Dametto, A., Buffon, G., Dos Reis Blasi, É. A., and Sperotto, R. A. (2015). Ubiquitination pathway as a target to develop abiotic stress tolerance in rice. *Plant Signal. Behav.* 10:e1057369. doi: 10.1080/15592324.2015.1057369
- Deng, Y., Srivastava, R., and Howell, S. H. (2013). Endoplasmic reticulum (ER) stress response and its physiological roles in plants. *Int. J. Mol. Sci.* 14, 8188–8212. doi: 10.3390/ijms14048188
- Dobson, C. M. (2003). Protein folding and misfolding. *Nature*, 426, 884–890. doi: 10.1038/nature02261
- Dubey, S., Misra, P., Dwivedi, S., Chatterjee, S., Bag, S. K., Mantri, S., et al. (2010). Transcriptomic and metabolomic shifts in rice roots in response to Cr (VI) stress. *BMC Genom.* 11:648. doi: 10.1186/1471-2164-11-648
- Durand, T. C., Sergeant, K., Planchon, S., Carpin, S., Label, P., Morabito, D., et al. (2010). Acute metal stress in *Populus tremula x P. alba* (717-1B4 genotype): leaf and cambial proteome changes induced by cadmium²⁺. *Proteomics* 10, 349–368. doi: 10.1002/pmic.200900484
- Emamverdian, A., Ding, Y., Mokhberdorran, F., and Xie, Y. (2015). Heavy metal stress and some mechanisms of plant defense response. *Sci. World J.* 2015: 756120. doi: 10.1155/2015/756120
- Farah, M. A., Ali, M. A., Chen, S. M., Li, Y., Al-Hemaid, F. M., Abou-Tarboush, F. M., et al. (2016). Silver nanoparticles synthesized from *Adenium obesum* leaf extract induced DNA damage, apoptosis and autophagy via generation of reactive oxygen species. *Colloids Surf. B. Biointerfaces* 141, 158–169. doi: 10.1016/j.colsurfb.2016.01.027
- Furini, A. (2012). *Plants and Heavy Metals*. Netherlands: Springer.
- Gao, C., Jiang, B., Wang, Y., Liu, G., and Yang, C. (2012). Overexpression of a heat shock protein (ThHSP18. 3) from *Tamarix hispida* confers stress tolerance to yeast. *Mol. Biol. Rep.* 39, 4889–4897. doi: 10.1007/s11033-011-1284-2
- Gardarin, A., Chédin, S., Lagniel, G., Aude, J. C., Godat, E., Catty, P., et al. (2010). Endoplasmic reticulum is a major target of cadmium toxicity in yeast. *Mol. Microbiol.* 76, 1034–1048. doi: 10.1111/j.1365-2958.2010.07166.x
- Genschik, P., Parmentier, Y., Durr, A., Marbach, J., Criqui, M. C., Jamet, E., et al. (1992). Ubiquitin genes are differentially regulated in protoplast-derived cultures of *Nicotiana sylvestris* and in response to various stresses. *Plant Mol. Biol.* 20, 897–910. doi: 10.1007/BF00027161
- Goldberg, A. L. (2003). Protein degradation and protection against misfolded or damaged proteins. *Nature* 426, 895–899. doi: 10.1038/nature02263
- Goupil, P., Souguir, D., Ferjani, E., Faure, O., Hitmi, A., and Ledoigt, G. (2009). Expression of stress-related genes in tomato plants exposed to arsenic and chromium in nutrient solution. *J. Plant Physiol.* 166, 1446–1452. doi: 10.1016/j.jplph.2009.01.015
- Gu, C. S., Liu, L. Q., Deng, Y. M., Zhu, X. D., Huang, S. Z., and Lu, X. Q. (2015). The heterologous expression of the *Iris lactea* var. chinensis type 2 metallothionein IIIMT2b gene enhances copper tolerance in *Arabidopsis thaliana*. *Bull. Environ. Contam. Toxicol.* 94, 247–253. doi: 10.1007/s00128-014-1444-x
- Guan, C., Jin, C., Ji, J., Wang, G., and Li, X. (2015). LcBiP, a endoplasmic reticulum chaperone binding protein gene from *Lycium chinense*, confers cadmium tolerance in transgenic tobacco. *Biotech. Prog.* 31, 358–368. doi: 10.1002/btpr.2046
- Guo, Q., Zhang, J., Gao, Q., Xing, S., Li, F., and Wang, W. (2008). Drought tolerance through overexpression of monoubiquitin in transgenic tobacco. *J. Plant Physiol.* 165, 1745–1755. doi: 10.1016/j.jplph.2007.10.002
- Gupta, S. C., Sharma, A., Mishra, M., Mishra, R. K., and Chowdhuri, D. K. (2010). Heat shock proteins in toxicology: how close and how far? *Life Sci.* 86, 377–384. doi: 10.1016/j.lfs.2009.12.015
- Haap, T., Schwarz, S., and Köhler, H. R. (2016). Metallothionein and Hsp70 trade-off against one another in *Daphnia magna* cross-tolerance to cadmium and heat stress. *Aquat. Toxicol.* 170, 112–119. doi: 10.1016/j.aquatox.2015.11.008
- Han, S., Yu, B., Wang, Y., and Liu, Y. (2011). Role of plant autophagy in stress response. *Pro. Cell 2*, 784–791. doi: 10.1007/s13238-011-1104-4
- Haq, N. U., Raza, S., Luthe, D. S., Heckathorn, S. A., and Shakeel, S. N. (2013). A dual role for the chloroplast small heat shock protein of *Chenopodium album* including protection from both heat and metal stress. *Plant Mol. Biol. Rep.* 31, 398–408. doi: 10.1007/s11105-012-0516-5

- Haralampidis, K., Milioni, D., Rigas, S., and Hatzopoulos, P. (2002). Combinatorial Interaction of Cis Elements Specifies the Expression of the *Arabidopsis* AtHsp90-1Gene. *Plant Physiol.* 129, 1138–1149. doi: 10.1104/pp.004044
- Hartmann-Petersen, R., Seeger, M., and Gordon, C. (2003). Transferring substrates to the 26S proteasome. *Trends Biochem. Sci.* 28, 26–31. doi: 10.1016/S0968-0004(02)00002-6
- Hasan, M., Ahammed, G. J., Yin, L., Shi, K., Xia, X., Zhou, Y., et al. (2015). Melatonin mitigates cadmium phytotoxicity through modulation of phytochelatins biosynthesis, vacuolar sequestration, and antioxidant potential in *Solanum lycopersicum* L. *Front. Plant Sci.* 6:601. doi: 10.3389/fpls.2015.00601
- Hasan, M. K., Liu, C., Wang, F., Ahammed, G. J., Zhou, J., Xu, M. X., et al. (2016). Glutathione-mediated regulation of nitric oxide, S-nitrosothiol and redox homeostasis confers cadmium tolerance by inducing transcription factors and stress response genes in tomato. *Chemosphere* 161, 536–545. doi: 10.1016/j.chemosphere.2016.07.053
- Hassinen, V. H., Tervahauta, A. I., Schat, H., and Kärenlampi, S. O. (2011). Plant metallothioneins–metal chelators with ROS scavenging activity? *Plant Biol.* 13, 225–232. doi: 10.1111/j.1438-8677.2010.00398.x
- Holland, S., Lodwig, E., Sideri, T., Reader, T., Clarke, I., Gkargkas, K., et al. (2007). Application of the comprehensive set of heterozygous yeast deletion mutants to elucidate the molecular basis of cellular chromium toxicity. *Genome Biol.* 8, R268. doi: 10.1186/gb-2007-8-12-r268
- Hossain, M. A., Piyatida, P., da Silva, J. A. T., and Fujita, M. (2012a). Molecular mechanism of heavy metal toxicity and tolerance in plants: central role of glutathione in detoxification of reactive oxygen species and methylglyoxal and in heavy metal chelation. *J. Bot.* 2012:872875. doi: 10.1155/2012/872875
- Hossain, Z., Khatoon, A., and Komatsu, S. (2013). Soybean proteomics for unraveling abiotic stress response mechanism. *J. Proteom Res.* 12, 4670–4684. doi: 10.1021/pr400604b
- Hossain, Z., and Komatsu, S. (2013). Contribution of proteomic studies towards understanding plant heavy metal stress response. *Front. Plant Sci.* 3:310. doi: 10.3389/fpls.2012.00310
- Hossain, Z., Makino, T., and Komatsu, S. (2012b). Proteomic study of β-aminobutyric acid-mediated cadmium stress alleviation in soybean. *J. Proteom.* 75, 4151–4164. doi: 10.1016/j.jprot.2012.05.037
- Howell, S. H. (2013). Endoplasmic reticulum stress responses in plants. *Ann. Rev. Plant Biol.* 64, 477–499. doi: 10.1146/annurev-arplant-050312-120053
- Hüttner, S., Veit, C., Schoberer, J., Grass, J., and Strasser, R. (2012). Unraveling the function of *Arabidopsis thaliana* OS9 in the endoplasmic reticulum-associated degradation of glycoproteins. *Plant. Mol. Biol.* 79, 21–33. doi: 10.1007/s11103-012-9891-4
- Irvine, G. W., Tan, S. N., and Stillman, M. J. (2017). A simple metallothionein-based biosensor for enhanced detection of arsenic and mercury. *Biosensors* 7:14. doi: 10.3390/bios7010014
- Jabeen, R., Ahmad, A., and Iqbal, M. (2009). Phytoremediation of heavy metals: physiological and molecular mechanisms. *Bot. Rev.* 75, 339–364. doi: 10.1007/s12229-009-9036-x
- Jacobson, T., Navarrete, C., Sharma, S. K., Sideri, T. C., Ibstedt, S., Priya, S., et al. (2012). Arsenite interferes with protein folding and triggers formation of protein aggregates in yeast. *J. Cell Sci.* 125, 5073–5083. doi: 10.1242/jcs.107029
- Jungmann, J., Reins-H., Schobert, C., and Jentsch, S. (1993). Resistance to cadmium mediated by ubiquitin dependent proteolysis. *Nature* 361, 369–371. doi: 10.1038/361369a0
- Kang, Y. J. (2006). Metallothionein redox cycle and function. *Exp. Biol. Med.* 231, 1459–1467. doi: 10.1177/153537020623100903
- Karmous, I., Bellani, L. M., Chaoui, A., El Ferjani, E., and Muccifora, S. (2015). Effects of copper on reserve mobilization in embryo of *Phaseolus vulgaris* L. *Environ. Sci. Poll. Res.* 22, 10159–10165. doi: 10.1007/s11356-015-4208-1
- Karmous, I., Chaoui, A., Jaouani, K., Sheehan, D., El Ferjani, E., Scoccianti, V., et al. (2014). Role of the ubiquitin-proteasome pathway and some peptidases during seed germination and copper stress in bean cotyledons. *Plant Physiol. Biochem.* 76, 77–85. doi: 10.1016/j.plaphy.2013.12.025
- Kieffer, P., Dommes, J., Hoffmann, L., Hausman, J. F., and Renault, J. (2008). Quantitative changes in protein expression of cadmium-exposed poplar plants. *Proteomics* 8, 2514–2530. doi: 10.1002/pmic.200701110
- Lee, S., Moon, J. S., Ko, T.-S., Petros, D., Goldsbrough, P. B., and Korban, S. S. (2003). Overexpression of *Arabidopsis* phytochelatin synthase paradoxically leads to hypersensitivity to cadmium stress. *Plant Physiol.* 131, 656–663. doi: 10.1104/pp.014118
- Lee, U., Rioflorido, I., Hong, S. W., Larkindale, J., Waters, E. R., and Vierling, E. (2006). The *Arabidopsis* ClpB/ Hsp100 family of proteins: chaperones for stress and chloroplast development. *Plant J.* 49, 115–127. doi: 10.1111/j.1365-313X.2006.02940.x
- Lewis, S., Donkin, M. E., and Depledge, M. H. (2001). Hsp70 expression in *Enteromorpha intestinalis* (Chlorophyta) exposed to environmental stressors. *Aquat. Toxicol.* 51, 277–291. doi: 10.1016/S0166-445X(00)01119-3
- Li, M., Ahammed, G. J., Li, C., Bao, X., Yu, J., Huang, C., et al. (2016a). Brassinosteroid ameliorates zinc oxide nanoparticles-induced oxidative stress by improving antioxidant potential and redox homeostasis in tomato seedling. *Front. Plant Sci.* 7:615. doi: 10.3389/fpls.2016.00615
- Li, M.-Q., Hasan, M. K., Li, C.-X., Ahammed, G. J., Xia, X.-J., Shi, K., et al. (2016b). Melatonin mediates selenium-induced tolerance to cadmium stress in tomato plants. *J. Pineal. Res.* 61, 291–302. doi: 10.1111/jpi.12346
- Li, S., Zhang, X., Zhang, X. Y., Xiao, W., Berry, J. O., Li, P., et al. (2015). Expression of *Malus xiaojinensis* IRT1 (MxIRT1) protein in transgenic yeast cells leads to degradation through autophagy in the presence of excessive iron. *Yeast* 32, 499–517. doi: 10.1002/yea.3075
- Lim, S. D., Hwang, J. G., Han, A. R., Park, Y. C., Lee, C., Ok, Y. S., et al. (2014). Positive regulation of rice RING E3 ligase OsHIL1 in arsenic and cadmium uptakes. *Plant Mol. Biol.* 85, 365–379. doi: 10.1007/s11103-014-0190-0
- Lingua, G., Bona, E., Todeschini, V., Cattaneo, C., Marsano, F., Berta, G., et al. (2012). Effects of heavy metals and *arbuscular mycorrhiza* on the leaf proteome of a selected poplar clone: a time course analysis. *PLoS ONE* 7:e38662. doi: 10.1371/journal.pone.0038662
- Liu, J., Shi, X., Qian, M., Zheng, L., Lian, C., Xia, Y., et al. (2015a). Copper-induced hydrogen peroxide upregulation of a metallothionein gene, OsMT2c, from *Oryza sativa* L. confers copper tolerance in *Arabidopsis thaliana*. *J. Hazard Mater.* 294, 99–108. doi: 10.1016/j.jhazmat.2015.03.060
- Liu, J. X., and Howell, S. H. (2016). Managing the protein folding demands in the endoplasmic reticulum of plants. *New Phytol.* 211, 418–428. doi: 10.1111/nph.13915
- Liu, X., Wu, H., Ji, C., Wei, L., Zhao, J., and Yu, J. (2013). An integrated proteomic and metabolomic study on the chronic effects of mercury in *Suaeda salsa* under an environmentally relevant salinity. *PLoS ONE* 8:e64041. doi: 10.1371/journal.pone.0064041
- Liu, Y., and Bassham, D. C. (2012). Autophagy: pathways for self-eating in plant cells. *Ann. Rev. Plant Biol.* 63, 215–237. doi: 10.1146/annurev-arplant-042811-105441
- Liu, Y. C., Fujimori, D. G., and Weissman, J. S. (2016). Htm1p–Pd1p is a folding-sensitive mannosidase that marks N-glycoproteins for ER-associated protein degradation. *Proc. Natl. Acad. Sci. U.S.A.* 113, E4015–E4024. doi: 10.1073/pnas.1608795113
- Liu, Y., Zhang, C., Wang, D., Su, W., Liu, L., Wang, M., et al. (2015b). EBS7 is a plant-specific component of a highly conserved endoplasmic reticulum-associated degradation system in *Arabidopsis*. *Proc. Natl. Acad. Sci. U.S.A.* 112, 12205–12210. doi: 10.1073/pnas.1511724112
- Lomaglio, T., Rocco, M., Trupiano, D., De Zio, E., Grosso, A., Marra, M., et al. (2015). Effect of short-term cadmium stress on *Populus nigra* L. detached leaves. *J. Plant Physiol.* 182, 40–48. doi: 10.1016/j.jplph.2015.04.007
- Lyzenga, W. J., and Stone, S. L. (2012). Abiotic stress tolerance mediated by protein ubiquitination. *J. Exp. Bot.* 63, 599–616. doi: 10.1093/jxb/err310
- Malhotra, J. D., and Kaufman, R. J. (2007). Endoplasmic reticulum stress and oxidative stress: a vicious cycle or a double-edged sword? *Antioxid. Redox Signal.* 9, 2277–2294. doi: 10.1089/ars.2007.1782
- Manara, A. (2012). “Plant responses to heavy metal toxicity,” in *Plants and Heavy Metals*, ed A. Furini (Springer), 27–53.
- Maret, W. (2000). The function of zinc metallothionein: a link between cellular zinc and redox state. *J. Nutr.* 130, 1455S–1458S.
- Maupin-Furlow, J. A. (2013). Ubiquitin-like proteins and their roles in archaea. *Trends Microbiol.* 21, 31–38. doi: 10.1016/j.tim.2012.09.006
- Mendoza-Cózatl, D. G., Jobe, T. O., Hauser, F., and Schroeder, J. I. (2011). Long-distance transport, vacuolar sequestration, tolerance, and transcriptional responses induced by cadmium and arsenic. *Curr. Opin. Plant Biol.* 14, 554–562. doi: 10.1016/j.pbi.2011.07.004

- Mendoza-Cózatl, D. G., Zhai, Z., Jobe, T. O., Akmakjian, G. Z., Song, W. Y., Limbo, O., et al. (2010). Tonoplast-localized Abc2 transporter mediates phytochelatin accumulation in vacuoles and confers cadmium tolerance. *J. Biol. Chem.* 285, 40416–40426. doi: 10.1074/jbc.M110.155408
- Milioni, D., and Hatzopoulos, P. (1997). Genomic organization of hsp90 gene family in *Arabidopsis*. *Plant Mol. Biol.* 35, 955–961. doi: 10.1023/A:1005874521528
- Minibayeva, F., Dmitrieva, S., Ponomareva, A., and Ryabovol, V. (2012). Oxidative stress-induced autophagy in plants: the role of mitochondria. *Plant Physiol. Biochem.* 59, 11–19. doi: 10.1016/j.plaphy.2012.02.013
- Mishra, R. C., and Grover, A. (2014). Intergenic sequence between *Arabidopsis* ClpB-C/Hsp100 and choline kinase genes functions as a heat inducible bidirectional promoter. *Plant Physiol.* 166, 1646–1658. doi: 10.1104/pp.114.250787
- Mogk, A., and Bukau, B. (2017). Role of sHsps in organizing cytosolic protein aggregation and disaggregation. *Cell Stress Chaperones* 22, 493–502. doi: 10.1007/s12192-017-0762-4
- Mu, C., Zhang, S., Yu, G., Chen, N., Li, X., and Liu, H. (2013). Overexpression of small heat shock protein LimHSP16.45 in *Arabidopsis* enhances tolerance to abiotic stresses. *PLoS ONE* 8:e82264. doi: 10.1371/journal.pone.0082264
- Naganuma, A., Miura, N., Kaneko, S., Mishina, T., Hosoya, S., Miyairi, S., et al. (2000). GFAT as a target molecule of methylmercury toxicity in *Saccharomyces cerevisiae*. *FASEB J.* 14, 968–972.
- Neumann, D., Lichtenberger, O., Günther, D., Tschiessch, K., and Nover, L. (1994). Heat-shock proteins induce heavy-metal tolerance in higher plants. *Planta* 194, 360–367. doi: 10.1007/BF00197536
- Neumann, D., Zur Nieden, U., Lichtenberger, O., and Leopold, I. (1995). How does *Armeria maritima* tolerate high heavy metal concentrations? *J. Plant Physiol.* 146, 704–717. doi: 10.1016/S0176-1617(11)81937-1
- Oono, Y., Yazawa, T., Kanamori, H., Sasaki, H., Mori, S., Handa, H., et al. (2016). Genome-wide transcriptome analysis of cadmium stress in rice. *BioMed Res. Int.* 2016:9739505. doi: 10.1155/2016/9739505
- Park, C. J., and Seo, Y. S. (2015). Heat Shock Proteins: A review of the molecular chaperones for plant immunity. *Plant Pathol. J.* 31, 323–333. doi: 10.5423/PPJ.RW.08.2015.0150
- Park, J., Song, W. Y., Ko, D., Eom, Y., Hansen, T. H., Schiller, M., et al. (2012). The phytochelatin transporters AtABCC1 and AtABCC2 mediate tolerance to cadmium and mercury. *Plant J.* 69, 278–288. doi: 10.1111/j.1365-313X.2011.04789.x
- Pena, L. B., Pasquini, L. A., Tomaro, M. L., and Gallego, S. M. (2007). 20S proteasome and accumulation of oxidized and ubiquitinated proteins in maize leaves subjected to cadmium stress. *Phytochemistry* 68, 1139–1146. doi: 10.1016/j.phytochem.2007.02.022
- Pena, L. B., Zawoznik, M. S., Tomaro, M. L., and Gallego, S. M. (2008). Heavy metals effects on proteolytic system in sunflower leaves. *Chemosphere* 72, 741–746. doi: 10.1016/j.chemosphere.2008.03.024
- Peñarrubia, L., Andrés-Colás, N., Moreno, J., and Puig, S. (2010). Regulation of copper transport in *Arabidopsis thaliana*: a biochemical oscillator? *JBIC J. Biol. Inorg. Chem.* 15, 29.
- Pérez-Martín, M., Blaby-Haas, C. E., Pérez-Pérez, M. E., Andrés-Garrido, A., Blaby, I. K., Merchant, S. S., et al. (2015). Activation of autophagy by metals in *Chlamydomonas reinhardtii*. *Eukaryot. Cell.* 14, 964–973. doi: 10.1128/EC.00081-15
- Pines, J., and Lindon, C. (2005). Proteolysis: anytime, anywhere? *Nature Cell Biol.* 7, 731–735. doi: 10.1038/ncb0805-731
- Pochodyo, A. L., and Aristilde, L. (2017). Molecular dynamics of stability and structures in phytochelatin complexes with Zn, Cu, Fe, Mg, and Ca: Implications for metal detoxification. *Environ. Chem. Lett.* 1–6. doi: 10.1007/s10311-017-0609-3
- Pomponi, M., Censi, V., Di Girolamo, V., De Paolis, A., Di Toppi, L. S., Aromolo, R., et al. (2006). Overexpression of *Arabidopsis* phytochelatin synthase in tobacco plants enhances Cd²⁺ tolerance and accumulation but not translocation to the shoot. *Planta* 223, 180–190. doi: 10.1007/s00425-005-0073-3
- Prasad, B. D., Goel, S., and Krishna, P. (2010). *In silico* identification of carboxylate clamp type tetratricopeptide repeat proteins in *Arabidopsis* and rice as putative co-chaperones of Hsp90/Hsp70. *PLoS ONE* 5:e12761. doi: 10.1371/journal.pone.0012761
- Pratt, W. B., and Toft, D. O. (2003). Regulation of signaling protein function and trafficking by the hsp90/hsp70-based chaperone machinery. *Exp. Biol. Med.* 228, 111–133. doi: 10.1177/153537020322800201
- Rai, A., Bhardwaj, A., Misra, P., Bag, S. K., Adhikari, B., Tripathi, R. D., et al. (2015). Comparative transcriptional profiling of contrasting rice genotypes shows expression differences during arsenic stress. *Plant Genome* 8:2. doi: 10.3835/plantgenome2014.09.0054
- Rauch, J. N., Tse, E., Freilich, R., Mok, S. A., Makley, L. N., Southworth, D. R., et al. (2017). BAG3 Is a modular, scaffolding protein that physically links heat shock protein 70 (Hsp70) to the small heat shock proteins. *J. Mol. Biol.* 429, 128–141. doi: 10.1016/j.jmb.2016.11.013
- Rhee, J. S., Raisuddin, S., Lee, K. W., Seo, J. S., Ki, J. S., Kim, I. C., et al. (2009). Heat shock protein (Hsp) gene responses of the intertidal copepod *Tigriopus japonicus* to environmental toxicants. *Comp. Biochem. Physiol. C Toxicol. Pharmacol.* 149, 104–112. doi: 10.1016/j.cbpc.2008.07.009
- Rodríguez-Celma, J., Rellán-Álvarez, R., Abadía, A., Abadía, J., and López-Millán, A.-F. (2010). Changes induced by two levels of cadmium toxicity in the 2-DE protein profile of tomato roots. *J. Proteom.* 73, 1694–1706. doi: 10.1016/j.jprot.2010.05.001
- Ruschak, A. M., Slassi, M., Kay, L. E., and Schimmer, A. D. (2011). Novel proteasome inhibitors to overcome bortezomib resistance. *J. Nat. Can. Inst.* 103, 1007–1017. doi: 10.1093/jnci/djr160
- Sácký, J., Leonhardt, T., Borovička, J., Gryndler, M., Briksí, A., and Kotrba, P. (2014). Intracellular sequestration of zinc, cadmium and silver in *Hebeloma mesophaeum* and characterization of its metallothionein genes. *Fungal Genet. Biol.* 67, 3–14. doi: 10.1016/j.fgb.2014.03.003
- Sadanandom, A., Bailey, M., Ewan, R., Lee, J., and Nelis, S. (2012). The ubiquitin-proteasome system: central modifier of plant signalling. *New Phytol.* 196, 13–28. doi: 10.1111/j.1469-8137.2012.04266.x
- Sanchez, Y., Taulien, J., Borkovich, K. A., and Lindquist, S. (1992). Hsp104 is required for tolerance to many forms of stress. *EMBO J.* 11, 2357.
- Sarry, J. E., Kuhn, L., Ducruix, C., Lafaye, A., Junot, C., Hugouvieux, V., Jourdain, A., et al. (2006). The early responses of *Arabidopsis thaliana* cells to cadmium exposure explored by protein and metabolite profiling analyses. *Proteomics* 6, 2180–2198. doi: 10.1002/pmic.200500543
- Scherz-Shouval, R., and Lazar, Z. (2007). ROS, mitochondria and the regulation of autophagy. *Trends Cell Biol.* 17, 422–427. doi: 10.1016/j.tcb.2007.07.009
- Schröder, M., and Kaufman, R. J. (2005). ER stress and the unfolded protein response. *Mutat. Res./Fund. Mol. Mechan. Mutagen.* 569, 29–63. doi: 10.1016/j.mrfmmm.2004.06.056
- Schubert, U., Anton, L. C., Gibbs, J., Norbury, C. C., Yewdell, J. W., and Bennink, J. R. (2000). Rapid degradation of a large fraction of newly synthesized proteins by proteasomes. *Nature* 404, 770–774. doi: 10.1038/3508096
- Schöffl, F., Prandl, R., and Reindl, A. (1999). “Molecular responses to heat stress,” in *Molecular Responses to Cold, Drought, Heat and Salt Stress in Higher Plants*, eds K. Shinozaki, and K. R. G. Yamaguchi-Shinozaki (Austin, TX: Landes Co.), 81–98.
- Sergio, E., Cobianchi, R. C., Sorbo, S., Conte, B., and Basile, A. (2007). Ultrastructural alterations and HSP 70 induction in *Elodea canadensis* exposed to heavy metals. *Caryologia* 60, 115–120.
- Sharma, S. K., Goloubinoff, P., and Christen, P. (2011). “Non-native Proteins as Newly-Identified Targets of Heavy Metals and Metalloids,” in *Cellular Effects of Heavy Metals*, ed G. Banfalvi (Springer), 263–274.
- Sharma, S. S., Dietz, K. J., and Mimura, T. (2016). Vacuolar compartmentalization as indispensable component of heavy metal detoxification in plants. *Plant Cell Environ.* 39, 1112–1126. doi: 10.1111/pce.12706
- Singh, A., Mittal, D., Lavania, D., Agarwal, M., Mishra, R. C., and Grover, A. (2012). OsHsfA2c and OsHsfB4b are involved in the transcriptional regulation of cytoplasmic OsClpB (Hsp100) gene in rice (*Oryza sativa* L.). *Cell Stress Chaperones* 17, 243–254. doi: 10.1007/s12192-011-0303-5
- Song, W. Y., Mendoza-Cozatl, D. G., Lee, Y., Schroeder, J. I., Ahn, S. N., Lee, H. S., et al. (2014). Phytochelatin–metal (loid) transport into vacuoles shows different

- substrate preferences in barley and *Arabidopsis*. *Plant Cell Env.* 37, 1192–1201. doi: 10.1111/pce.12227
- Song, Y., Cui, J., Zhang, H., Wang, G., Zhao, F. J., and Shen, Z. (2013). Proteomic analysis of copper stress responses in the roots of two rice (*Oryza sativa* L.) varieties differing in Cu tolerance. *Plant Soil* 366, 647–658.
- Sørensen, J. G., Kristensen, T. N., and Loeschke, V. (2003). The evolutionary and ecological role of heat shock proteins. *Ecol. Lett.* 6, 1025–1037. doi: 10.1046/j.1461-0248.2003.00528.x
- Spijkerman, E., Barua, D., Gerloff-Elias, A., Kern, J., Gaedke, U., and Heckathorn, S. A. (2007). Stress responses and metal tolerance of *Chlamydomonas acidophila* in metal-enriched lake water and artificial medium. *Extremophiles* 11, 551–562. doi: 10.1007/s00792-007-0067-0
- Stone, S. L. (2014). The role of ubiquitin and the 26S proteasome in plant abiotic stress signaling. *Front. Plant Sci.* 5:135. doi: 10.3389/fpls.2014.00135
- Sumner, E. R., Shanmuganathan, A., Sideri, T. C., Willetts, S. A., Houghton, J. E., and Avery, S. V. (2005). Oxidative protein damage causes chromium toxicity in yeast. *Microbiology* 151, 1939–1948. doi: 10.1099/mic.0.27945-0
- Sun, C. W., and Callis, J. (1997). Independent modulation of *Arabidopsis thaliana* polyubiquitin mRNAs in different organs and in response to environmental changes. *Plant J.* 11, 1017–1027. doi: 10.1046/j.1365-313X.1997.1105.1017.x
- Sun, L., Lu, S. J., Zhang, S. S., Zhou, S. F., Sun, L., and Liu, J. X. (2013). The lumen-facing domain is important for the biological function and organelle-to-organelle movement of bZIP28 during ER stress in *Arabidopsis*. *Mol. Plant* 6, 1605–1611. doi: 10.1093/mp/sst059
- Sun, W., Motangu, M. V., and Verbruggen, N. (2002). Small heat shock proteins and stress tolerance in plants. *Biochim. Biophys. Acta* 1577, 1–9. doi: 10.1016/S0167-4781(02)00417-7
- Tamás, M. J., Sharma, S. K., Ibstedt, S., Jacobson, T., and Christen, P. (2014). Heavy metals and metalloids as a cause for protein misfolding and aggregation. *Biomolecules* 4, 252–267. doi: 10.3390/biom4010252
- Tomas, M., Pagani, M. A., Andreo, C. S., Capdevila, M., Atrian, S., and Bofill, R. (2015). Sunflower metallothionein family characterisation. Study of the Zn (II)- and Cd (II)-binding abilities of the HaMT1 and HaMT2 isoforms. *J. Inorg. Biochem.* 148, 35–48. doi: 10.1016/j.jinorgbio.2015.02.016
- Tomas, M., Tinti, A., Bofill, R., Capdevila, M., Atrian, S., and Torreggiani, A. (2016). Comparative Raman study of four plant metallothionein isoforms: insights into their Zn (II) clusters and protein conformations. *J. Inorg. Biochem.* 156, 55–63. doi: 10.1016/j.jinorgbio.2015.12.027
- Tuzhikov, A. I., Vartapetian, B. B., Vartapetian, A. B., and Chichkova, N. V. (2011). “Abiotic stress-induced programmed cell death in plants: a phytase connection,” in *Biochemistry, Genetics, and Molecular Biology, Abiotic Stress Response in Plants - Physiological, Biochemical and Genetic Perspectives*, eds A. Shanker and B. Venkateswarlu (InTech), 183–196. doi: 10.5772/23785
- Van Hoewyk, D. (2013). A tale of two toxicities: malformed selenoproteins and oxidative stress both contribute to selenium stress in plants. *Ann. Bot.* 112, 965–972. doi: 10.1093/aob/mct163
- Van Hoewyk, D. (2016). Defects in endoplasmic reticulum-associated degradation (ERAD) increase selenate sensitivity in *Arabidopsis*. *Plant Signal. Behav.* doi: 10.1080/15592324.2016.1171451
- Viehweger, K. (2014). How plants cope with heavy metals. *Bot. Stud.* 55:35. doi: 10.1186/1999-3110-55-35
- Vierstra, R. D. (2009). The ubiquitin–26S proteasome system at the nexus of plant biology. *Nat. Rev. Mol. Cell Biol.* 10, 385–397. doi: 10.1038/nrm2688
- Wang, W., Vinocur, B., Shoseyov, O., and Altman, A. (2004). Role of plant heat-shock proteins and molecular chaperones in the abiotic stress response. *Trends Plant Sci.* 9, 244–252. doi: 10.1016/j.tplants.2004.03.006
- Wang, Y., Cai, S. Y., Yin, L. L., Shi, K., Xia, X. J., Zhou, Y. H., et al. (2015). Tomato HsfA1a plays a critical role in plant drought tolerance by activating ATG genes and inducing autophagy. *Autophagy* 11, 2033–2047. doi: 10.1080/15548627.2015.1098798
- Weng, Z. X., Wang, L. X., Tan, F. L., Huang, L., Xing, J. H., Chen, S. P., et al. (2013). Proteomic and physiological analyses reveal detoxification and antioxidation induced by Cd stress in *Kandelia candel* roots. *Trees* 27, 583–595. doi: 10.1007/s00468-012-0811-7
- Wen-Xing, D., (2012). Autophagy in toxicology: defense against xenobiotics. *J. Drug. Metab. Toxicol.* 3:e108. doi: 10.4172/2157-7609.1000e108
- Wollgiehn, R., and Neumann, D. (1999). Metal stress response and tolerance of cultured cells from *Silene vulgaris* and *Lycopersicon peruvianum*: role of heat stress proteins. *J. Plant Physiol.* 154, 547–553. doi: 10.1016/S0176-1617(99)80296-X
- Xie, Y., Ye, S., Wang, Y., Xu, L., Zhu, X., Yang, J., et al. (2015). Transcriptome-based gene profiling provides novel insights into the characteristics of radish root response to Cr stress with next-generation sequencing. *Front. Plant Sci.* 6:202. doi: 10.3389/fpls.2015.00202
- Xu, H., Xu, W., Xi, H., Ma, W., He, Z., and Ma, M. (2013). The ER luminal binding protein (BiP) alleviates Cd²⁺-induced programmed cell death through endoplasmic reticulum stress–cell death signaling pathway in tobacco cells. *J. Physiol.* 170, 1434–1441. doi: 10.1016/j.jplph.2013.05.017
- Xu, L., Wang, Y., Liu, W., Wang, J., Zhu, X., Zhang, K., et al. (2015). *In vivo* sequencing of root transcriptome reveals complex cadmium-responsive regulatory networks in radish (*Raphanus sativus* L.). *Plant. Sci.* 236, 313–323. doi: 10.1016/j.plantsci.2015.04.015
- Xu, W., Cai, S. Y., Zhang, Y., Wang, Y., Ahammed, G. J., Xia, X. J., et al. (2016). Melatonin enhances thermotolerance by promoting cellular protein protection in tomato plants. *J. Pineal. Res.* doi: 10.1111/jpi.12359
- Yakimova, E. T., Kapchina-Toteva, V. M., and Woltering, E. J. (2007). Signal transduction events in aluminum-induced cell death in tomato suspension cells. *J. Physiol.* 164, 702–708. doi: 10.1016/j.jplph.2006.03.018
- Yang, J., Wang, Y., Liu, G., Yang, C., and Li, C. (2011). *Tamarix hispida* metallothionein-like ThMT3, a reactive oxygen species scavenger, increases tolerance against Cd²⁺, Zn²⁺, Cu²⁺, and NaCl in transgenic yeast. *Molec. Biol. Rep.* 38, 1567–1574. doi: 10.1007/s11033-010-0265-1
- Yang, X., Srivastava, R., Howell, S. H., and Bassham, D. C. (2016). Activation of autophagy by unfolded proteins during endoplasmic reticulum stress. *Plant J.* 85, 83–95. doi: 10.1111/tpj.13091
- Yang, Z. T., Lu, S. J., Wang, M. J., Bi, D. L., Sun, L., Zhou, S. F., et al. (2014). A plasma membrane-tethered transcription factor, NAC062/ANAC062/NTL6, mediates the unfolded protein response in *Arabidopsis*. *Plant J.* 79, 1033–1043. doi: 10.1111/tpj.12604
- Yoshida, H., Haze, K., Yanagi, H., Yura, T., and Mori, K. (1998). Identification of the cis-acting endoplasmic reticulum stress response element responsible for transcriptional induction of mammalian glucose-regulated proteins. Involvement of basic leucine zipper transcription factors. *J. Biol. Chem.* 273, 33741–33749. doi: 10.1074/jbc.273.50.33741
- Yu, X., Ponce, R. A., and Faustman, E. M. (2011). “Metals induced disruption of ubiquitin proteasome system, activation of stress signaling and apoptosis,” in *Cellular Effects of Heavy Metals*, ed G. Banfalvi (Springer), 291–311.
- Zhang, J., Hwang, J. U., Song, W. Y., Martinolia, E., and Lee, Y. (2017). Identification of amino acid residues important for the arsenic resistance function of *Arabidopsis* ABCC1. *FEBS Lett.* 591, 656–666. doi: 10.1002/1873-3468.12576
- Zhang, W., and Chen, W. (2010). “Autophagy induction upon reactive oxygen species in Cd-stressed *Arabidopsis thaliana*,” in *Proceedings SPIE 7568, Imaging, Manipulation, and Analysis of Biomolecules, Cells, and Tissues VIII* (San Francisco, CA). doi: 10.1117/12.841394
- Zhao, C. R., Ikka, T., Sawaki, Y., Kobayashi, Y., Suzuki, Y., Hibino, T., et al. (2009). Comparative transcriptomic characterization of aluminum, sodiumchloride, cadmiumand copper rhizotoxicities in *Arabidopsis thaliana*. *BMC Plant Biol.* 9:32. doi: 10.1186/1471-2229-9-32
- Zhao, L., Sun, Y. L., Cui, S. X., Chen, M., Yang, H. M., Liu, H. M., et al. (2011). Cd-induced changes in leaf proteome of the hyperaccumulator plant *Phytolacca americana*. *Chemosphere* 85, 56–66. doi: 10.1016/j.chemosphere.2011.06.029
- Zhao, Y., and Chengcai, C. (2011). “Towards understanding plant response to heavy metal stress,” in *AbioticStress in Plants - Mechanisms and Adaptations*, ed A. Shanker (Rijeka: Tech Europe), 59–78.
- Zhen, Y., Qi, J. L., Wang, S. S., Su, J., Xu, G. H., Zhang, M. S., et al. (2007). Comparative proteome analysis of differentially expressed proteins induced by Al toxicity in soybean. *Physiol. Planta.* 131, 542–554. doi: 10.1111/j.1399-3054.2007.00979.x
- Zheng, L., Peer, T., Seybold, V., and Lütz-Meindl, U. (2012). Pb-induced ultrastructural alterations and subcellular localization of Pb in two species of *Lespedeza* by TEM-coupled electron energy loss spectroscopy. *Environ. Exp. Bot.* 77, 196–206. doi: 10.1016/j.envexpbot.2011.11.018

- Zhou, S., Okekeogbu, I., Sangireddy, S., Ye, Z., Li, H., Bhatti, S., et al. (2016). Proteome modification in tomato plants upon long-term aluminum treatment. *J. Proteom. Res.* 15, 1670–1684. doi: 10.1021/acs.jproteome.6b00128
- Zhou, X. M., Zhao, P., Wang, W., Zou, J., Cheng, T. H., Peng, X. B., et al. (2015). A comprehensive, genome-wide analysis of autophagy-related genes identified in tobacco suggests a central role of autophagy in plant response to various environmental cues. *DNA Res.* 22, 245–257. doi: 10.1093/dnares/dsv012
- Zhu, W., Lu, M., Gong, Z., and Chen, R. (2013). Cloning and expression of a small heat shock protein gene CaHSP24 from pepper under abiotic stress. *African J. Biotech.* 10, 4968–4976.

Conflict of Interest Statement: The authors declare that the research was conducted in the absence of any commercial or financial relationships that could be construed as a potential conflict of interest.

Copyright © 2017 Hasan, Cheng, Kanwar, Chu, Ahammed and Qi. This is an open-access article distributed under the terms of the Creative Commons Attribution License (CC BY). The use, distribution or reproduction in other forums is permitted, provided the original author(s) or licensor are credited and that the original publication in this journal is cited, in accordance with accepted academic practice. No use, distribution or reproduction is permitted which does not comply with these terms.



Genome-Wide Identification and Expression Profiling of Tomato *Hsp20* Gene Family in Response to Biotic and Abiotic Stresses

Jiahong Yu^{1,2†}, Yuan Cheng^{1†}, Kun Feng¹, Meiyi Ruan¹, Qingjing Ye¹, Rongqing Wang¹, Zhimiao Li¹, Guozhi Zhou¹, Zhuping Yao¹, Yuejian Yang¹ and Hongjian Wan^{1*}

¹ State Key Laboratory Breeding Base for Zhejiang Sustainable Pest and Disease Control, Institute of Vegetables, Zhejiang Academy of Agricultural Sciences, Hangzhou, China, ² College of Chemistry and Life Science, Zhejiang Normal University, Jinhua, China

OPEN ACCESS

Edited by:

Jie Zhou,
Zhejiang University, China

Reviewed by:

Chu-Yu Ye,
Zhejiang University, China
Jianfei Kuang,
South China Agricultural University,
China

*Correspondence:

Hongjian Wan
wanhongjian@sina.com

[†]These authors have contributed
equally to this work.

Specialty section:

This article was submitted to
Plant Biotic Interactions,
a section of the journal
Frontiers in Plant Science

Received: 12 June 2016

Accepted: 02 August 2016

Published: 17 August 2016

Citation:

Yu J, Cheng Y, Feng K, Ruan M, Ye Q, Wang R, Li Z, Zhou G, Yao Z, Yang Y and Wan H (2016) Genome-Wide Identification and Expression Profiling of Tomato *Hsp20* Gene Family in Response to Biotic and Abiotic Stresses. *Front. Plant Sci.* 7:1215.
doi: 10.3389/fpls.2016.01215

The *Hsp20* genes are involved in the response of plants to environment stresses including heat shock and also play a vital role in plant growth and development. They represent the most abundant small heat shock proteins (sHsps) in plants, but little is known about this family in tomato (*Solanum lycopersicum*), an important vegetable crop in the world. Here, we characterized heat shock protein 20 (*SlHsp20*) gene family in tomato through integration of gene structure, chromosome location, phylogenetic relationship, and expression profile. Using bioinformatics-based methods, we identified at least 42 putative *SlHsp20* genes in tomato. Sequence analysis revealed that most of *SlHsp20* genes possessed no intron or a relatively short intron in length. Chromosome mapping indicated that inter-arm and intra-chromosome duplication events contributed remarkably to the expansion of *SlHsp20* genes. Phylogenetic tree of *Hsp20* genes from tomato and other plant species revealed that *SlHsp20* genes were grouped into 13 subfamilies, indicating that these genes may have a common ancestor that generated diverse subfamilies prior to the mono-dicot split. In addition, expression analysis using RNA-seq in various tissues and developmental stages of cultivated tomato and the wild relative *Solanum pimpinellifolium* revealed that most of these genes (83%) were expressed in at least one stage from at least one genotype. Out of 42 genes, 4 genes were expressed constitutively in almost all the tissues analyzed, implying that these genes might have specific housekeeping function in tomato cell under normal growth conditions. Two *SlHsp20* genes displayed differential expression levels between cultivated tomato and *S. pimpinellifolium* in vegetative (leaf and root) and reproductive organs (floral bud and flower), suggesting inter-species diversification for functional specialization during the process of domestication. Based on genome-wide microarray analysis, we showed that the transcript levels of *SlHsp20* genes could be induced profusely by abiotic and biotic stresses such as heat, drought, salt, *Botrytis cinerea*,

and Tomato Spotted Wilt Virus (TSWV), indicating their potential roles in mediating the response of tomato plants to environment stresses. In conclusion, these results provide valuable information for elucidating the evolutionary relationship of *Hsp20* gene family and functional characterization of the *SlHsp20* gene family in the future.

Keywords: heat shock protein 20, gene organization, phylogenetic relationship, expression profile, abiotic and biotic stresses

INTRODUCTION

Plants live in a complex environment, where multiple biotic and abiotic stresses may seriously restrict their growth and development (Cramer et al., 2011). In the recent years, due to unprecedented global warming caused by various factors, high temperature has appeared as one of the most severe abiotic stresses around the world. To survive and acclimatize under the adverse environment conditions, plants have established self-defense mechanisms during the course of long-term evolution. Heat shock proteins (Hsps), acknowledged as evolutionarily conserved ubiquitous proteins in all organisms, were first discovered in *Drosophila melanogaster* in response to the elevated temperature stress (Ritossa, 1962; Neta-Sharir et al., 2005; Cashikar et al., 2006). Previous studies have shown that high temperature as well as other environmental cues (cold, salinity, drought, heavy metals, anoxia, pathogens, etc.) could induce the occurrence of Hsps (Lindquist and Craig, 1988; Wang et al., 2003). In addition, the Hsps were also found to be associated with plant growth and development, such as embryogenesis, seed germination, and fruit maturation (Neta-Sharir et al., 2005).

According to sequence homology and molecular weight, Hsps in eukaryotes can be grouped into six families such as Hsp110, Hsp90, Hsp70, Hsp60, small heat shock protein (sHsp) of 15–42 kDa (or Hsp20) and ubiquitin (Carper et al., 1987; Sarkar et al., 2009). Out of these six groups of Hsps, sHsps are the most primary and abundant proteins under thermal stimulation in many species (Vierling et al., 1989; Vierling, 1991). Notably, among eukaryotes, the higher plants possessed more quantities of *Hsp20s* (Vierling, 1991). As *Hsp20* is encoded by a multigene family, it is considered as the most ample and complicated member in Hsps (Vierling, 1991). The characteristic feature of *Hsp20* is the presence of a carboxyl-terminal conserved domain of 80–100 amino acid residues, which can be defined as the α -crystallin domain (ACD). This highly conserved ACD, which is flanked by a short carboxyl-terminal extension and a variable amino-terminal domain, is believed to comprise two hydrophobic β -sheet motifs that are separated by a hydrophilic α -helical region of variable length (de Jong et al., 1998). Moreover, the *Hsp20* gene family also exhibits extensive sequence variability and evolutionary divergence, which is remarkably different from other families of Hsps (Basha et al., 2012).

An earlier study showed that Hsp20 proteins in eukaryotes, which are collectively known as molecular chaperones, function as multimeric complexes ranging from 8 to 24 or more subunits (Van Montfort et al., 2002). These chaperons can selectively

bind to partially folded or denatured proteins in an ATP-independent manner, which can prevent proteins from the irreversible aggregation and facilitate them folding properly (Lee and Vierling, 2000; Sun et al., 2002; Van Montfort et al., 2002). Recent studies revealed that these chaperones were important for disease resistance triggered by resistance (R) proteins and played a fundamental role in plant immunity (Boter et al., 2007; Shirasu, 2009).

To date, the *Hsp20* gene families have been investigated in several plant species, including *Arabidopsis*, rice, soybean, pepper, and *Populus trichocarpa* (Scharf et al., 2001; Waters et al., 2008; Ouyang et al., 2009; Sarkar et al., 2009; Lopes-Caitar et al., 2013; Guo et al., 2015). In addition, some key features of *Hsp20* and biologic function of several *Hsp20* genes had been identified (Nautiyal and Shono, 2010; Goyal et al., 2012; Huther et al., 2013; Mahesh et al., 2013; Arce et al., 2015; Zhang et al., 2016). Although the availability of the tomato whole-genome sequence provides valuable resources for getting into an in-depth understanding of *Hsp20s* (Sato et al., 2012), little information is available on the integrated *Hsp20* family at whole genomic level in tomato.

In the current paper, the members of *SlHsp20* gene family in tomato were identified using a bioinformatics method and characterized by integration of sequence features, chromosome location, phylogenetic relationship, evolutionary origin, and expression patterns. These results provide valuable information that can be implicated in elucidating the evolutionary relationship of *Hsp20* gene family in higher plants and functional characterization of the *SlHsp20* gene family in the future.

MATERIALS AND METHODS

Retrieval and Identification of *Hsp20* Genes in Tomato

In this paper, the predicted *SlHsp20* genes were identified as follows: firstly, the tomato genome sequences were downloaded from the database Sol Genomics Network (SGN, Release 2.5, <http://solgenomics.net/>) and used to set up a local database by the software “DNATOOLS.” Secondly, the Hidden Markov Model (HMM) profile of *Hsp20* domain (PF00011) from Pfam (<http://pfam.sanger.ac.uk/>) was employed to search against the local database using BlastP method ($e < 1e-5$). Furthermore, *Hsp20* candidates with incomplete *Hsp20* domain might be missed using HMM profile. Name search using the word “*hsp20*” as a keyword also applied to retrieve in SGN database. The redundant sequences were manually removed. Finally, all these predicted genes were examined for the *Hsp20* domain in

SMART (<http://smart.embl-heidelberg.de/smart/batch.pl>), Pfam and InterProScan (<http://www.ebi.ac.uk/interpro/>), and those without the common Hsp20 domain were excluded.

Sequence Analysis and Structural Characterization

Information of candidate *SlHsp20* genes was obtained via searching the SGN database (<http://solgenomics.net/search/locus>), including chromosome locations, intron numbers, genomic sequences, coding sequences (CDS), and amino acid sequences. Intron-exon structure was determined by alignment of genome DNA and full-length cDNA sequence using Gene Structure Display Server 2.0 (<http://gsds.cbi.pku.edu.cn/>) (Hu et al., 2015). Molecular weight, theoretical isoelectric point (theoretical pI), and instability index (II; with the value >40 classified as unstable) of *SlHsp20* proteins were analyzed by using ProtParam tool (<http://web.expasy.org/protparam/>).

The putative protein sequences were subjected to MEME program (<http://meme-suite.org/tools/meme>) to investigate conserved motifs with the following parameters: site distribution—any number of repetitions, number of motifs—10, the motif width between 6 and 200.

Phylogenetic Analysis

To illuminate evolutionary relationship of *Hsp20* gene family, the representative *Hsp20* genes from *Arabidopsis*, rice, soybean, bluebunch wheatgrass, barley, common wheat, Eurasian aspen, together with *SlHsp20* genes from tomato, were selected for constructing phylogenetic tree (Ouyang et al., 2009; Sarkar et al., 2009; Lopes-Caitar et al., 2013). Multiple sequence alignment of *Hsp20* proteins was conducted using ClustalX 1.83. An unrooted Neighbor-joining phylogenetic tree was constructed using MEGA 7.0 software with default settings (Kumar et al., 2016). The bootstrap test was performed by 1000 replications.

Four Online tools were employed to predict subcellular localization, including, Predotar (<https://urgi.versailles.inra.fr/Tools/Predotar>), Wolf Psort (http://www.genscript.com/psort/wolf_psorth.html), TargetP (<http://www.cbs.dtu.dk/services/TargetP/>), and MultiLoc (<http://abi.inf.uni-tuebingen.de/Services/MultiLoc2>). The prediction of signal peptide and transmembrane domain was performed with SMART program (<http://smart.embl-heidelberg.de/smart/batch.pl>).

Chromosome Localization and Gene Duplication

Chromosome mapping of the candidate *SlHsp20* genes was viewed using the software MapDraw V2.1 (Liu and Meng, 2003). Tandem duplication and segmental duplication were also further investigated. The former was confirmed with the following criteria: (1) an array of two or more *SlHsp20* genes within a range of 100 kb distance; (2) the alignment had a coverage rate more than 70% of the longer gene; (3) and the identity of the aligned region was no less than 70% (Li et al., 2010; Huang et al., 2012; Wei et al., 2016). The latter was identified based on Plant Genome Duplication Database (PGDD, <http://chibba.agtec.uga.edu/duplication/index/locus>).

Tissue-Specific Expression Analysis

In this study, RNA-seq data from Tomato Functional Genomics Database (TFGD, <http://ted.bti.cornell.edu/cgi-bin/TFGD/digital/home.cgi>) were used to investigate expression patterns of putative *SlHsp20* genes in different tissues of cultivated tomato (*Solanum lycopersicum*) and the wild relative (*Solanum pimpinellifolium*). Different tissues in cultivated tomato included leaves, roots, flower buds, fully opened flowers, 1 cm, 2 cm, 3 cm, mature green, breaker, and breaker+10 fruits. In the wild species (*S. pimpinellifolium*), nine tissues and organs were selected for analysis, including leaves, whole root, hypocotyl, cotyledons, flower buds 10 days before anthesis or younger, flowers at anthesis, 10 days post anthesis (DPA) fruit, 20 DPA fruit and breaker stage ripening fruit. Digital gene expression analysis of the putative *SlHsp20* gene family was performed using software MultiExperiment Viewer (MeV) (Howe et al., 2010).

Expression Profile of *SlHsp20* Genes under Different Stress Conditions

To get insight into the expression profiles of the *SlHsp20* gene family under different environmental stresses, microarray analysis was performed. Whole genome microarray data for diverse environment stresses such as heat, drought, salt, *Botrytis cinerea*, and Tomato Spotted Wilt Virus (TSWV) was downloaded from database TFGD (<http://ted.bti.cornell.edu/>). The array platforms for microarray data included TOM2 oligo array and Affymetrix genome array. For TOM2 oligo array, the probe sets of the *SlHsp20* genes were identified through BlastN analysis in the database “TOM2 oligo sequences.” For Affymetrix genome array, Probe Match tool in NetAffx Analysis Center (<http://www.affymetrix.com>) was used to obtain probe sequences. Average value was considered for *SlHsp20* genes that had more than one probe set. The expression values of *SlHsp20* genes that were up- or down-regulated more than two-fold with $P < 0.05$ were considered as differently expressed.

RESULTS

Identification of *Hsp20* Family Members in Tomato

Name search and HMM analysis showed a total of 42 candidate *SlHsp20* genes, four of which were identified to contain incomplete *Hsp20* domains. For convenience, the *SlHsp20* genes were named according to their molecular weight in our study. Details on gene name, locus name, chromosome location, open reading frame (ORF) length, intron number, protein length, molecular weight, isoelectric point (pI), and instability index were listed in Table 1.

The four *SlHsp20* genes with incomplete *Hsp20* domain encoded truncated proteins (67–129 aa) and could be non-functional or pseudogenes. Therefore, these *SlHsp20* genes were excluded in phylogenetic tree construction. Molecular weight of the remaining predicted *SlHsp20* genes ranged from 15.2 to 49.3 kDa, except for *SlHsp11.9* and *SlHsp14.5*.

TABLE 1 | Features of *SlHsp20* genes in tomato.

Name	SGN locus	Chromosome location	ORF (bp)	Introns	Protein length	Molecular weight (kD)	Point	Index	Domain
SlHsp11.9	Solyc00g053740	Chr0:13824977–13825669	324	3	107	11.9	6.25	25.61	
SlHsp25.7A	Solyc01g009200	Chr 1:3241560–3240198	699	1	232	25.7	5.86	44.14	Transmembrane domain
SlHsp23.8A	Solyc01g009220	Chr 1:3247795–3246119	642	1	213	23.8	9.48	36.33	Transmembrane domain
SlHsp17.3A	Solyc01g017030	Chr 1:23550205–23554512	462	4	153	17.3	8.99	39.67	
SlHsp14.5	Solyc01g017790	Chr 1:25432286–25427746	390	5	129	14.5	6.94	34.03	
SlHsp15.8	Solyc01g018070	Chr 1:27398962–27394648	429	4	142	15.8	5.1	29.41	Transmembrane domain
SlHsp49.3	Solyc01g096960	Chr 1:87963575–87961920	1277	1	441	49.3	8.73	35.27	Transmembrane domain
SlHsp39.4	Solyc01g096980	Chr 1:87968194–87971404	1047	2	348	39.4	9.11	53.1	
SlHsp21.6A	Solyc01g102960	Chr 1:91610881–91611760	570	0	189	21.6	7.89	53.22	Signal peptide
SlHsp15.7	Solyc02g080410	Chr 2:44640649–44639813	414	1	137	15.7	4.91	44.72	
SlHsp15.6	Solyc02g093600	Chr 2:54402405–54403349	411	1	136	15.6	7.65	42.53	
SlHsp26.2	Solyc03g082420	Chr 3:45899828–45898742	708	1	236	26.2	7.84	34.18	
SlHsp23.7	Solyc03g113180	Chr 3:63421266–63422260	630	1	209	23.7	4.96	60.11	
SlHsp21.5A	Solyc03g113930	Chr 3:63978540–63979106	567	0	188	21.5	6.93	50.33	Signal peptide
SlHsp16.1A	Solyc03g123540	Chr 3:70366718–70367347	435	1	144	16.1	8.4	62.05	
SlHsp16.1B	Solyc04g014480	Chr 4:4722700–4724263	438	1	145	16.1	6.97	49.27	
SlHsp37.0	Solyc04g071490	Chr 4:58477607–58478832	978	1	325	37.0	5.83	36.54	Transmembrane domain
SlHsp17.9	Solyc04g072250	Chr 4:59249315–59251089	492	1	163	17.9	5.47	40.33	
SlHsp25.7B	Solyc05g014280	Chr 5:8089580–8092146	666	2	221	25.7	9.31	45.74	
SlHsp17.7A	Solyc06g076520	Chr 6:47546790–47547254	627	0	154	17.7	5.84	51.74	
SlHsp17.6A	Solyc06g076540	Chr 6:47551057–47551521	465	0	154	17.6	5.82	47.21	
SlHsp17.6B	Solyc06g076560	Chr 6:47559714–47560178	465	0	154	17.6	5.84	50.91	
SlHsp17.6C	Solyc06g076570	Chr 6:47564101–47564565	465	0	154	17.6	5.57	46.42	
SlHsp9.1	Solyc07g045610	Chr 7:58755057–58754174	237	1	78	9.1	5.17	23.22	
SlHsp26.5	Solyc07g055720	Chr 7:63655500–63657426	717	5	238	26.5	9.42	60.7	
SlHsp21.6B	Solyc07g064020	Chr 7:66320971–66322805	567	1	188	21.6	5.64	37.37	
SlHsp17.3B	Solyc08g062340	Chr 8:50913795–50913023	468	0	155	17.3	6.75	35.61	
SlHsp17.6D	Solyc08g062450	Chr 8:51109016–51109492	477	0	158	17.6	6.32	36.62	
SlHsp23.8B	Solyc08g078700	Chr 8:62469844–62471072	633	1	210	23.8	6.45	60.54	
SlHsp21.5B	Solyc08g078710	Chr 8:62472773–62473878	591	1	196	21.5	8.37	55.57	
SlHsp18.2	Solyc08g078720	Chr 8:62475339–62476959	507	1	168	18.2	5.06	34.01	
SlHsp26.8	Solyc09g007140	Chr 9:769674–771056	711	1	236	26.8	5.23	47.91	Transmembrane domain
SlHsp24.5	Solyc09g011710	Chr 9:4976527–4978000	627	1	208	24.5	7.15	59.67	
SlHsp15.2	Solyc09g015000	Chr 9:7427223–7428264	405	1	134	15.2	8.86	57.81	
SlHsp17.7B	Solyc09g015020	Chr 9:7440133–7440597	465	0	154	17.7	5.84	55.8	
SlHsp7.8	Solyc09g059210	Chr 9:53755532–53755735	204	0	67	7.8	4.69	48.31	
SlHsp15.5	Solyc10g076880	Chr 10:59862547–59863282	420	1	139	15.5	9.21	11.34	
SlHsp27.1	Solyc10g086680	Chr 10:65453568–65452864	705	0	234	27.1	9.48	37.94	
SlHsp21.5C	Solyc11g020330	Chr 11:10856316–10856888	573	0	190	21.5	5.75	39.6	Signal peptide
SlHsp27.5	Solyc11g071560	Chr 11:54984205–54985643	744	1	247	27.5	6.04	44.67	Transmembrane domain
SlHsp9.0	Solyc12g042830	Chr 12:39616918–39617157	240	0	79	9.0	4.53	38.02	
SlHsp27.2	Solyc12g056560	Chr 12:62506816–62507722	723	1	240	27.2	8.71	37.27	Transmembrane domain

that were less than 15 kDa. Molecular weights of these *SlHsp20* proteins had a large variation. Isoelectric points ranged from 4.53 (*SlHsp9.0*) to 9.8 (*SlHsp23.8A*), and protein length ranged from 67 (*SlHsp7.8*) to 441 aa (*SlHsp49.3*). The instability index indicates that 18 of the predicted *SlHsp20* proteins were deemed to be stable proteins, while others were unstable.

Gene Structure of the *SlHsp20* Genes

Structure and phases of introns/exons were determined by alignment of genomic DNA and full-length cDNA sequences of *SlHsp20* genes (**Supplementary Figure S1**). This information was available on Sol Genomics Network (**Supplementary Table S1**). It was found that among the total 42 *SlHsp20* genes, 13(30.95%) were noted to be intronless, while 22

genes (52.38%) had one intron, and only 7(16.67%) had two or more introns. Based on the number of introns, we divided the genes into three patterns (pattern one has no intron, pattern two has one intron, and pattern three has more than one) (Ouyang et al., 2009). It was evident that most *SlHsp20* genes belonged to pattern 1 and 2. Additionally, a relatively short intron length was found in *SlHsp20* proteins in tomato, which was similar to the results reported on sHsp20 proteins in rice (Sarkar et al., 2009).

Using the MEME tool, 10 putative conserved motifs (motif 1 to motif 10) in *SlHsp20* gene family were identified (**Supplementary Table S2**). The lengths of these conserved motifs varied from 15 to 57 aa ($P < 0.0001$). Details of all the putative motifs are outlined in **Table 2**. Among the 10 motifs, motif 2 appeared in all putative *SlHsp20* genes, except for *SlHsp15.5*. Based on the analysis of Pfam, the full sequences of motif 1, 2, 3, 4, 5, and 8 were corresponding to the region of conserved ACD. We also found that motif 1 was in the C-terminal regions, while motif 6 appeared in the N-terminal regions generally. In addition, motif 9 was also distributed in the C-terminal regions of several genes. Notably, four *SlHsp20* genes (*SlHsp11.9*, *SlHsp17.3A*, *SlHsp14.5*, and *SlHsp15.8*) present similar patterns of motif distribution. Also, the same scenario was found in other four *SlHsp20* genes (*SlHsp17.6C*, *SlHsp17.7A*, *SlHsp17.6B*, and *SlHsp17.6A*) on chromosome 6. These results suggest that these genes may have relatively high conservation. Nevertheless, the functions of these highly conserved amino acid motifs still remain elusive.

It was reported that highly conserved ACD domain might be associated with the formation of multimeric complexes that are crucial for the chaperone activity of *Hsp20* genes (Waters et al., 1996; Sun et al., 2002). In the current paper, in line with a previous report (Waters et al., 1996), the highly conserved ACD in *SlHsp20* proteins was divided into two parts (consensus I and consensus II) based on multiple sequence alignment (**Figure 1**). These two conserved regions were separated by a hydrophilic domain with variable length and characterized by residue Pro-X (14)-Gly-Val-Leu and Pro-X (14)-X-Val/Leu/Ile-Val/Leu/Ile, respectively (Caspers et al., 1995). Intriguingly, consensus I matched well with the motif 1 located on carboxyl terminal presumed by MEME.

TABLE 2 | List of the putative motifs of *SlHsp20* proteins.

Motif	Width	Sequence
1	41	WHRMERSCGKFMRRFLPENANMDQIKASMENGVLTVTPK
2	15	DLPGYKKEDIKVQVE
3	57	GRLVITGQPHQLDNFWGVTSFKVVTLPARIDQLRTNAILTFHG CLHVHPFAQQNL
4	21	CAFANTRIDWKETPEAHVFKV
5	29	WCRFQKDFQLPDNCNMDKISAKFENGILY
6	15	MDRVLRLISGERNVEE
7	57	TPVKPTAQQPQPKQAHKDQDSTRNETMGSAESSNTQKGDN FPPRTTYPTTQAAPRK
8	29	DVQVWDVGPPADWVKINVRATNDSFEVYA
9	21	YEDFVPTSEWVQEQQADYLLI
10	21	FDPFSIDVFDPFRELGFPGTN

Phylogenetic Analysis of *SlHsp20* Gene Family

An unrooted N-J phylogenetic tree was constructed from a complete alignment of amino acid sequences of Hsp20 proteins in tomato and other seven plant species (**Figure 2**). All these Hsp20 proteins were grouped into 17 distinct subfamilies. However, the *SlHsp20* proteins were distributed into 13 out of 17 subfamilies, including previously identified subfamilies like CI, CII, CIII, P, Px, ER, and MI (Waters et al., 1996), recently defined CV, CVI, CVII, CIX, and CXI subfamilies (Siddique et al., 2008; Sarkar et al., 2009) and a new subfamily, CXII, identified by *in silico* prediction of subcellular localization (**Supplementary Table S3**). Besides, we also found two orphan *SlHsp20* genes in tomato that lack homologs genes in all seven organisms. The *SlHsp20* genes from 13 subfamilies were distributed to a variety of cellular organelles: 29 were nucleo-cytoplasmic (C) *SlHsp20* genes (9 subfamilies), 3 were endoplasmic reticulum (ER) genes, 2 were plastidial (P) genes, and 1 each for mitochondrial (M) and peroxisomal (Px) genes.

Notably, all three *SlHsp20* genes belonging to ER subfamily have a signal peptide in the N-terminal region, which was consistent with the result showed by Lopes-Caitar et al. (2013) (**Table 1**). The signal peptides were reported to play a positive role in facilitating the process of protein synthesis via guiding the proteins into rough endoplasmic reticulum (Bauvois, 2012). Moreover, eight *SlHsp20* genes, one from CVI subfamily and seven from CXII, had a transmembrane domain in the C-terminal region (**Table 1**).

We also found a close relationship between intron pattern and phylogenetic classification (**Supplementary Figure S1**). The result showed that the CI, CII, and ER subfamilies lacked introns. All the CVII members had more than one intron, indicating a particular phylogenetic status (Ouyang et al., 2009). The CIII, CV, CVI, CXI, MI, and Px subfamilies, together with most members of the CXII subfamily, had one intron, which may indicate a close phylogenetic relationship. In addition, gene structure may provide clues for evolutionary relationship of *SlHsp20* family.

Chromosomal Localization and Gene Duplication

Out of the 42 predicted *SlHsp20* genes, 41 are randomly distributed across the 12 tomato chromosomes, except for the *SlHsp11.9* (**Figure 3**). Majority of the *SlHsp20* genes were located on the distal ends of the chromosomes and mainly on the lower arms. A maximum number of eight predicted *SlHsp20* genes scattered in three clusters, were present on chromosome 1.

We further performed chromosome mapping to determine the gene duplication of *SlHsp20* genes on the 12 tomato chromosomes. As shown in **Figure 3**, two groups of *SlHsp20* genes (*SlHsp49.3/SlHsp39.4* and *SlHsp17.7A/SlHsp17.6A/SlHsp17.6B/SlHsp17.6C*) can be identified as tandem duplication genes (**Supplementary Table S4**). One group (*SlHsp49.3* and *SlHsp39.4*) was from the CXII subfamily and located on chromosome 1. The other (*SlHsp17.7A*, *SlHsp17.6A*, *SlHsp17.6B*, and *SlHsp17.6C*) was from one branch of CI subfamily and juxtaposed compactly on chromosome 6, implying that the

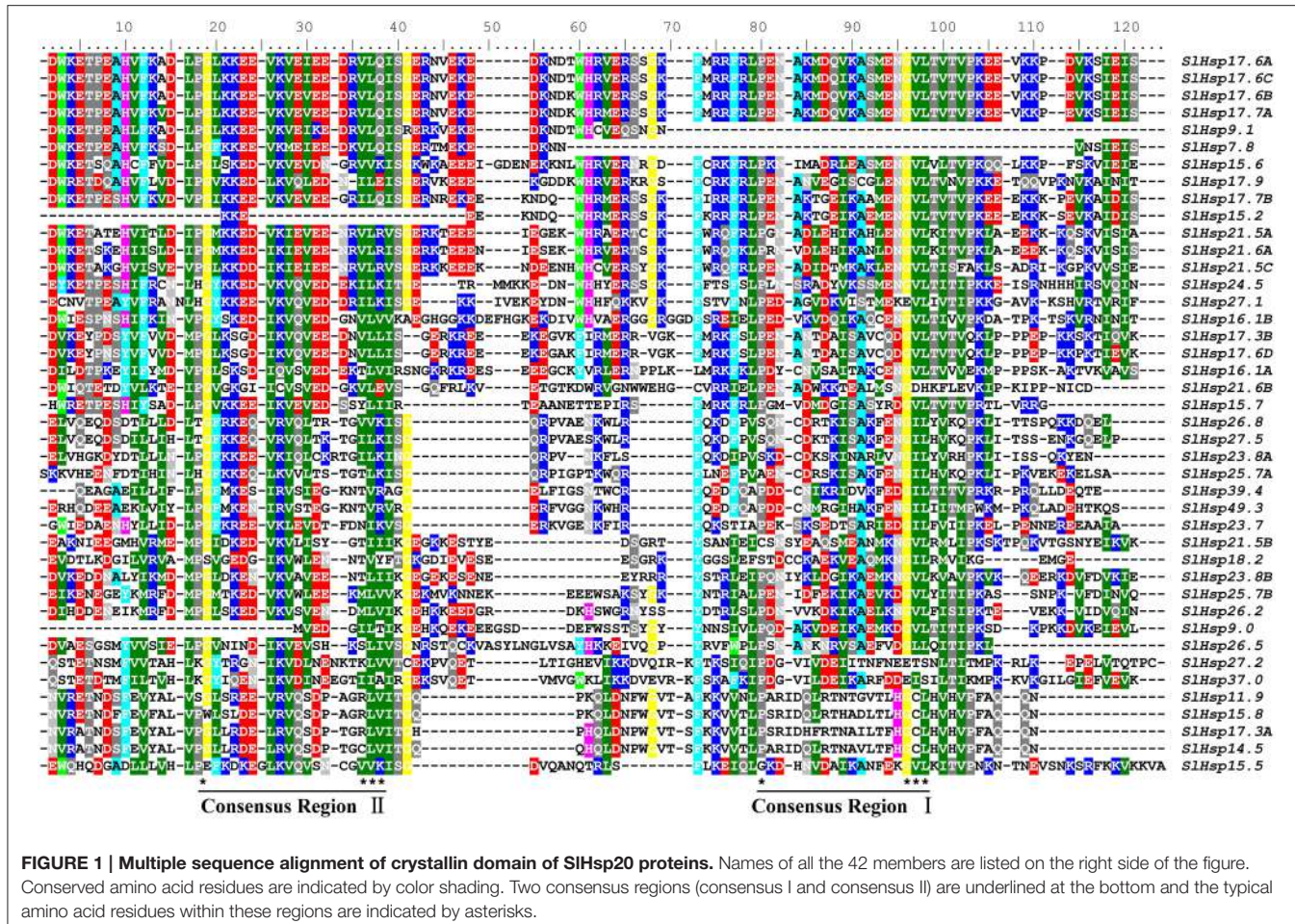


FIGURE 1 | Multiple sequence alignment of crystallin domain of SlHsp20 proteins. Names of all the 42 members are listed on the right side of the figure. Conserved amino acid residues are indicated by color shading. Two consensus regions (consensus I and consensus II) are underlined at the bottom and the typical amino acid residues within these regions are indicated by asterisks (*).

high density of *SlHsp20* genes on this chromosome was mainly due to the tandem duplication events. The chromosome location of tandemed genes showed that these four pairs of *SlHsp20* genes (*SlHsp49.3/SlHsp39.4*, *SlHsp17.7A/SlHsp17.6A*, *SlHsp17.6A/SlHsp17.6B*, *SlHsp17.6B/SlHsp17.6C*) was intervened by no more than one gene and was close in distance on the chromosomes (approximately 4.6, 3.8, 8.2, and 3.9 kb) (Supplementary Table S5).

On the other hand, three segmental duplication groups were found to scatter in seven chromosomes (Figure 3; Supplementary Table S6). A duplicated segment of the *SlHsp37.0* region on the distal part of chromosome 4 was present on the same location of chromosome 12, where *SlHsp27.2* was located. *SlHsp25.7A* on chromosome 1 also showed synteny to *SlHsp27.5* localized on a duplicated segment of chromosome 11. In addition, three *SlHsp20* genes (*SlHsp17.7A*, *SlHsp24.5*, and *SlHsp27.1*) regions showed segmental duplication and were present on chromosome 6, 9, and 10, respectively.

Genome-Wide Expression Analysis of *SlHsp20* Genes

In silico expression patterns of the putative *SlHsp20* genes at different tissues and development stages of tomato cultivar

Heinz and the wild species *S. pimpinellifolium* were analyzed (Figure 4). It showed that most of the genes (83.3%) were expressed in at least one stage (tissue) from at least one genotype. Fourteen genes (*SlHsp17.7A*, *SlHsp17.6B*, *SlHsp17.6C*, *SlHsp24.5*, *SlHsp18.2*, *SlHsp16.1A*, *SlHsp17.7B*, *SlHsp17.6A*, *SlHsp25.7B*, *SlHsp15.2*, *SlHsp21.6A*, *SlHsp17.6D*, *SlHsp16.1B*, *SlHsp23.8B*) were expressed constitutively in all the stages analyzed, whereas the transcripts of 12 genes (*SlHsp23.8A*, *SlHsp17.3A*, *SlHsp17.9*, *SlHsp9.1*, *SlHsp39.4*, *SlHsp37.0*, *SlHsp21.5B*, *SlHsp11.9*, *SlHsp14.5*, *SlHsp15.8*, *SlHsp7.8*, and *SlHsp15.5*) were at almost undetectable levels. Among these genes, *SlHsp17.6B* had the highest expression level in the 30 DPA fruit.

When the expression patterns of *SlHsp20* genes in vegetative organs (leaf and root) and reproductive organs (flower bud and flower) were compared between the 2 tomato genotype, 17 genes were either highly-induced (3) or barely expressed (14) (Figure 4). Conversely, two genes (*SlHsp25.7B* and *SlHsp17.6A*) displayed significantly differential expression in the various genotypes. Further, seven genes exhibited varied expression in vegetative and reproductive organs of tomato cultivar Heinz, while only two of them expressed differentially in *S. pimpinellifolium*. Notably, expression of seven genes was restricted to the leaf (*SlHsp26.5*) and root (*SlHsp23.7*, *SlHsp49.3*,

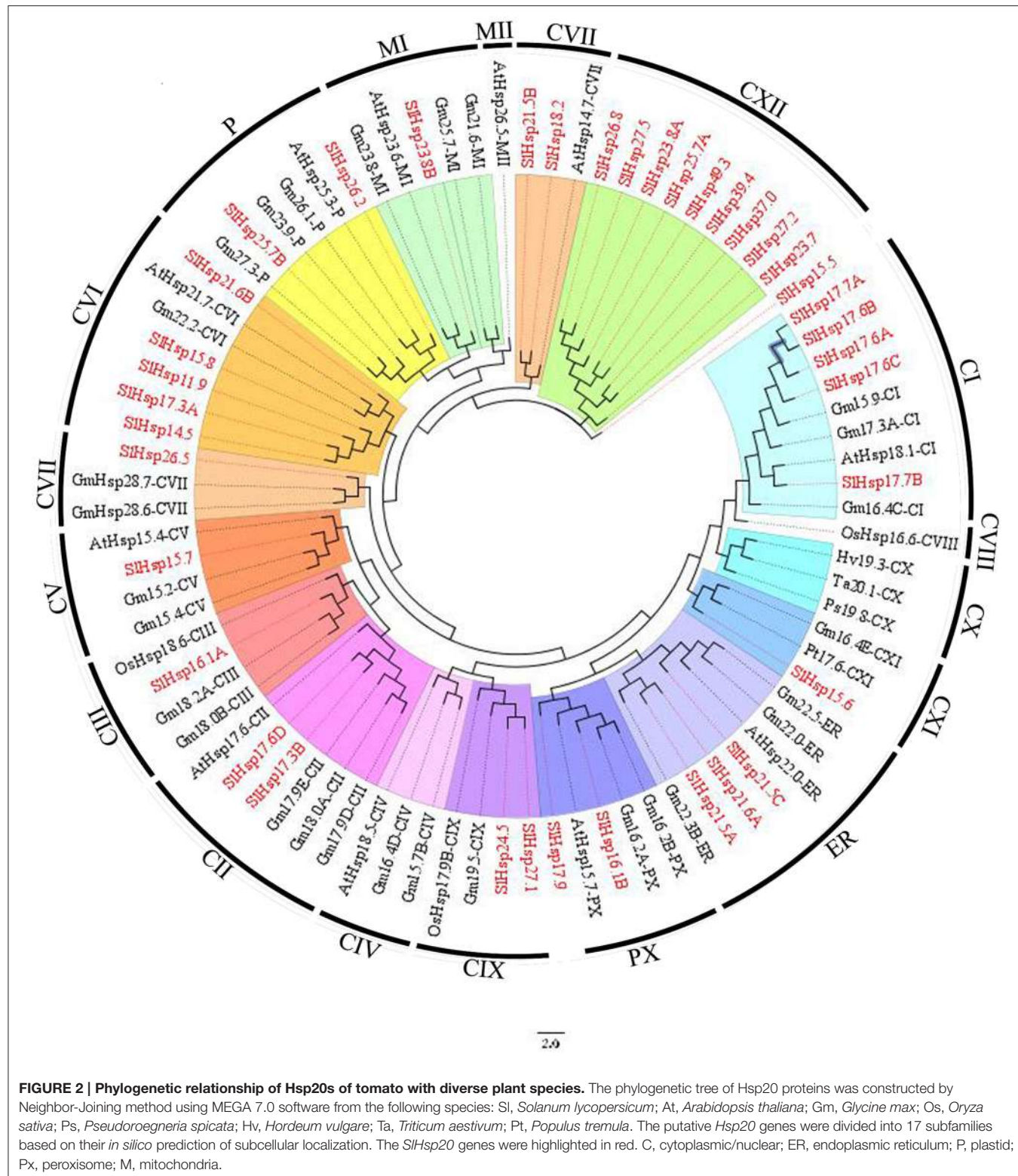
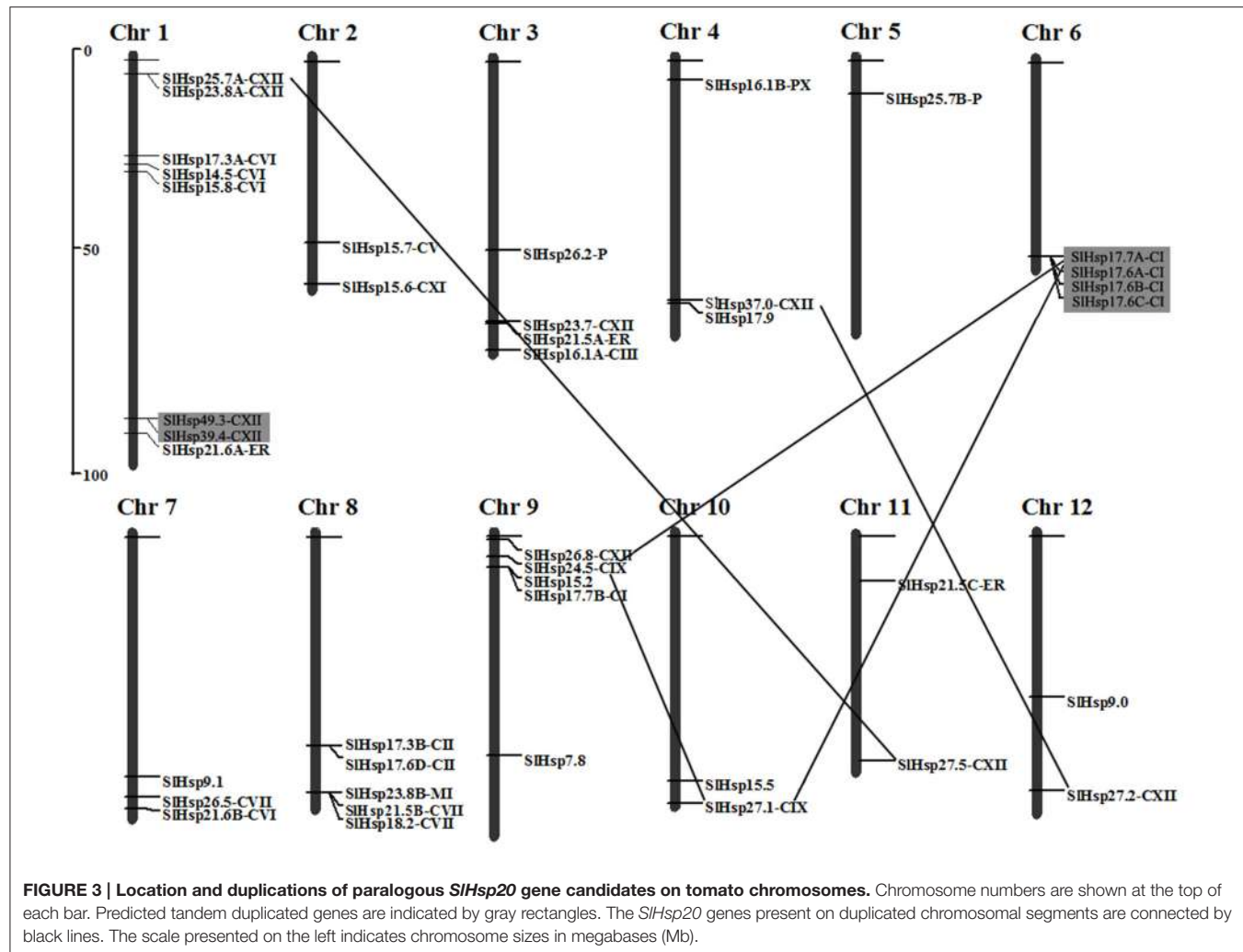


FIGURE 2 | Phylogenetic relationship of Hsp20s of tomato with diverse plant species. The phylogenetic tree of Hsp20 proteins was constructed by Neighbor-Joining method using MEGA 7.0 software from the following species: *Sl*, *Solanum lycopersicum*; *At*, *Arabidopsis thaliana*; *Gm*, *Glycine max*; *Os*, *Oryza sativa*; *Ps*, *Pseudoroegneria spicata*; *Hv*, *Hordeum vulgare*; *Ta*, *Triticum aestivum*; *Pt*, *Populus tremula*. The putative Hsp20 genes were divided into 17 subfamilies based on their *in silico* prediction of subcellular localization. The *SlHsp20* genes were highlighted in red. C, cytoplasmic/nuclear; ER, endoplasmic reticulum; P, plastid; Px, peroxisome; M, mitochondria.

SlHsp25.7, *SlHsp26.8*, *SlHsp27.5*, and *SlHsp15.5*) in Heniz, and only one gene was noted to root (*SlHsp7.8*) in *S. pimpinellifolium*. It indicates that these genes are regulated in a tissue-specific manner.

Expression levels of *SlHsp20* genes at breaker stage fruits were higher than that in other development stages in both genotypes. In tomato cultivar Heniz, expression of several *SlHsp20* genes (*SlHsp25.7B*, *SlHsp26.2*, *SlHsp21.5A*, *SlHsp21.5C*, and *SlHsp15.6*)



was not almost detected in young tomato fruits (1 cm-, 2 cm-, 3 cm-, and MG fruit), but a distinct expression was observed in the breaker fruits (Figure 4A). In *S. pimpinellifolium*, two *SlHsp20* genes, *SlHsp17.9*, and *SlHsp15.6*, were only expressed in 20 DPA and 33 DPA fruits (Figure 4B). Furthermore, expression of three *SlHsp20* genes (*SlHsp23.8A*, *SlHsp23.7*, and *SlHsp39.4*) derived from CXII subfamily showed tissue specificity in hypocotyl. Besides, by analyzing the expression profiles of tandem and segmental duplication of *SlHsp20* genes in two genotypes, we found that two groups of tandemly *SlHsp20* genes (*SlHsp49.3/SlHsp39.4*; *SlHsp17.7A/SlHsp17.6A/SlHsp17.6B/SlHsp17.6C*) displayed a more similar expression pattern, while difference in expression was observed for *SlHsp20* genes (*SlHsp27.1/SlHsp17.7A/SlHsp24.5; SlHsp37.0/SlHsp27.2*) in segmental duplication regions.

Expression Profiles of *SlHsp20* Genes Induced by Different Biotic and Abiotic Stresses

To further explore the expression profiles of *SlHsp20* genes under various abiotic and biotic stresses, microarray analysis were

performed (Figure 5). In the present paper, five tomato microarray data sets, belonging to two array platforms (TOM2 oligo array and Affymetrix genome array), were obtained from Tomato Functional Genomics Database (TFGD, <http://ted.bti.cornell.edu/>). A total of 24 probes (57%) corresponding to *SlHsp20* genes were identified, while five probes (LE17D07, LE26P10, LE26F10, LE13N06, Les.4004.1.S1_a_at) showed cross-reactivity with 12 *SlHsp20* genes (Supplementary Table S7).

Microarray-based expression analysis of tomato under various abiotic stresses revealed that expression of most of the *SlHsp20* genes were highly variable (Figures 5A–C). Expression of 13 of all tested *SlHsp20* genes, especially *SlHsp25.7B*, *SlHsp15.2*, *SlHsp21.5C*, and *SlHsp16.1B*, was drastically enhanced in resistant and susceptible tomato plants under high temperature condition, except for *SlHsp15.7* that was down-regulated in susceptible plants in response to heat stress (Figure 5A). Half of the analyzed *SlHsp20* genes in susceptible plants showed a higher expression level than those in tolerant plants. Under salt treatment condition, 12 *SlHsp20* genes displayed highly elevated expression, whereas *SlHsp15.7* was shown to be significantly down-regulated

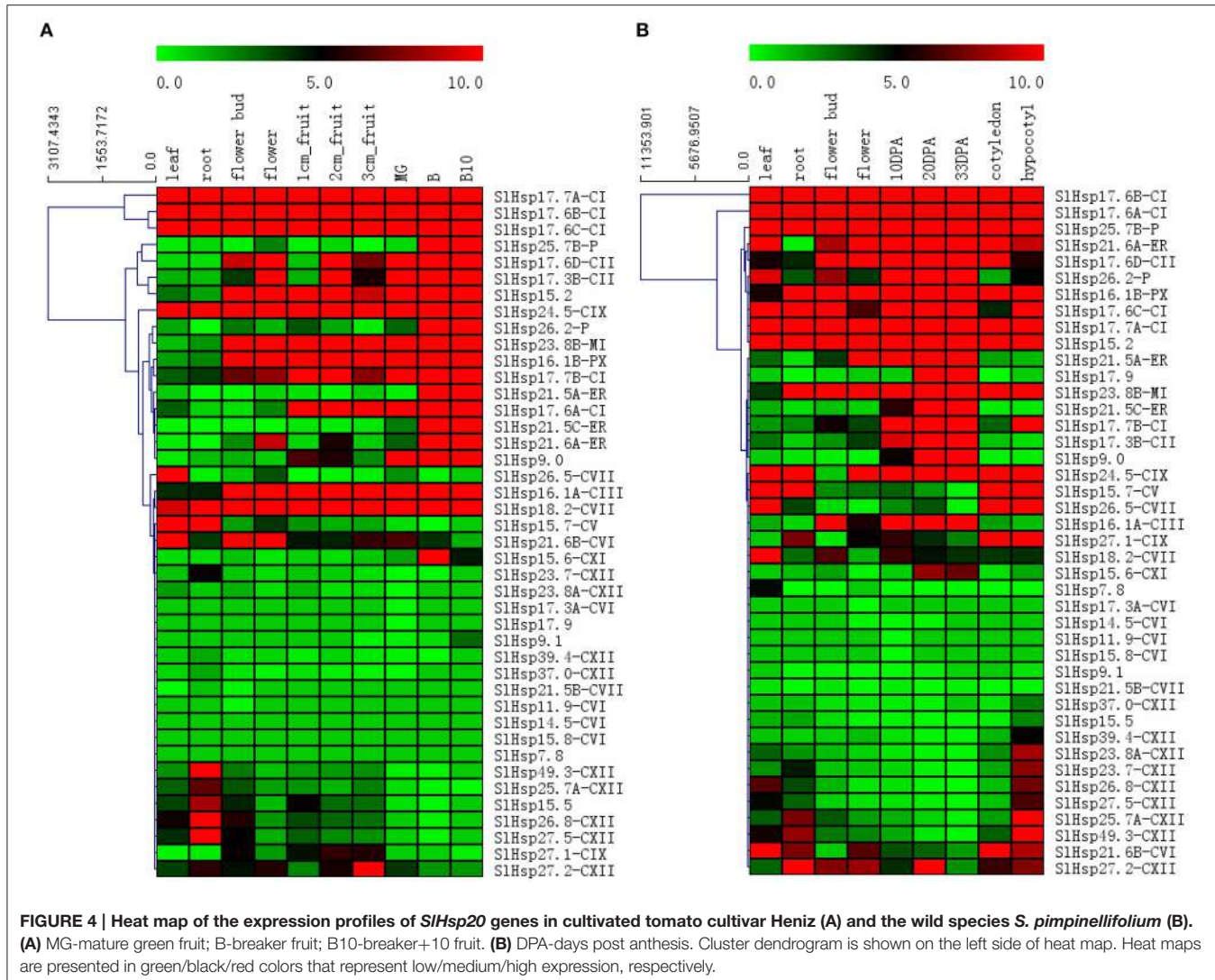


FIGURE 4 | Heat map of the expression profiles of *SlHsp20* genes in cultivated tomato cultivar Heniz (A) and the wild species *S. pimpinellifolium* (B). (A) MG-mature green fruit; B-breaker fruit; B10-breaker+10 fruit. (B) DPA-days post anthesis. Cluster dendrogram is shown on the left side of heat map. Heat maps are presented in green/black/red colors that represent low/medium/high expression, respectively.

(Figure 5B). PI365967, a more salt-tolerant tomato genotype, showed relatively more responsive genes compared to tomato cultivar Moneymaker. Under drought stress condition, transcript levels of 10 and 4 *SlHsp20* genes were up-regulated and down-regulated in drought-tolerant tomato lines (IL2-5 and IL9-1) and drought-sensitive cultivar M82, respectively (Figure 5C). Among these genes, *SlHsp26.5* showed a drastic enhancement of the transcript level (more than 16 fold) in three tested tomato genotypes. The expression of *SlHsp26.2* was dramatically up-regulated in M82 (a drought-sensitive cultivar), which was much higher (four times) than that in IL2-5 and IL9-1.

Invoked by wound and the invasion of *B. cinerea*, transcript levels of three genes (*SlHsp15.7*, *SlHsp23.8B*, and *SlHsp16.1B*) were remained unaltered, up- and down-regulated levels, respectively, in all tested samples (Figure 5D). In mature green fruit, most of the *SlHsp20* genes displayed a stronger expression in wounded fruits than that in fruits of wound-inoculated with *B. cinerea*. In red ripe fruit, however, the expression patterns of *SlHsp20* genes showed a reverse pattern between

the wounded and wound-inoculated with *B. cinerea* fruits. Interestingly, seven genes (*SlHsp17.6D*, *SlHsp17.7A*, *SlHsp17.6A*, *SlHsp17.6B*, *SlHsp17.6C*, *SlHsp9.1*, and *SlHsp26.2*) displayed differential expression between mature green- and red ripe fruits. In addition, under TSWV infection condition, three *SlHsp20* genes (*SlHsp11.9*, *SlHsp17.6D*, and *SlHsp27.1*) were up-regulated in tomato roots, three genes (*SlHsp15.2*, *SlHsp17.7B*, and *SlHsp15.7*) were down-regulated, and expression of the remaining genes remained unchanged (Figure 5E). In shoots of tomato, almost half *SlHsp20* genes were enhanced, six genes were reduced and expression levels of the remaining six genes were unaltered.

DISCUSSION

Identification and Phylogenetic Relationship of *SlHsp20* Gene Family

Using *in silico* methods to search for *Hsp20* genes in the *S. lycopersicum* genome, at least 42 putative *SlHsp20* genes were

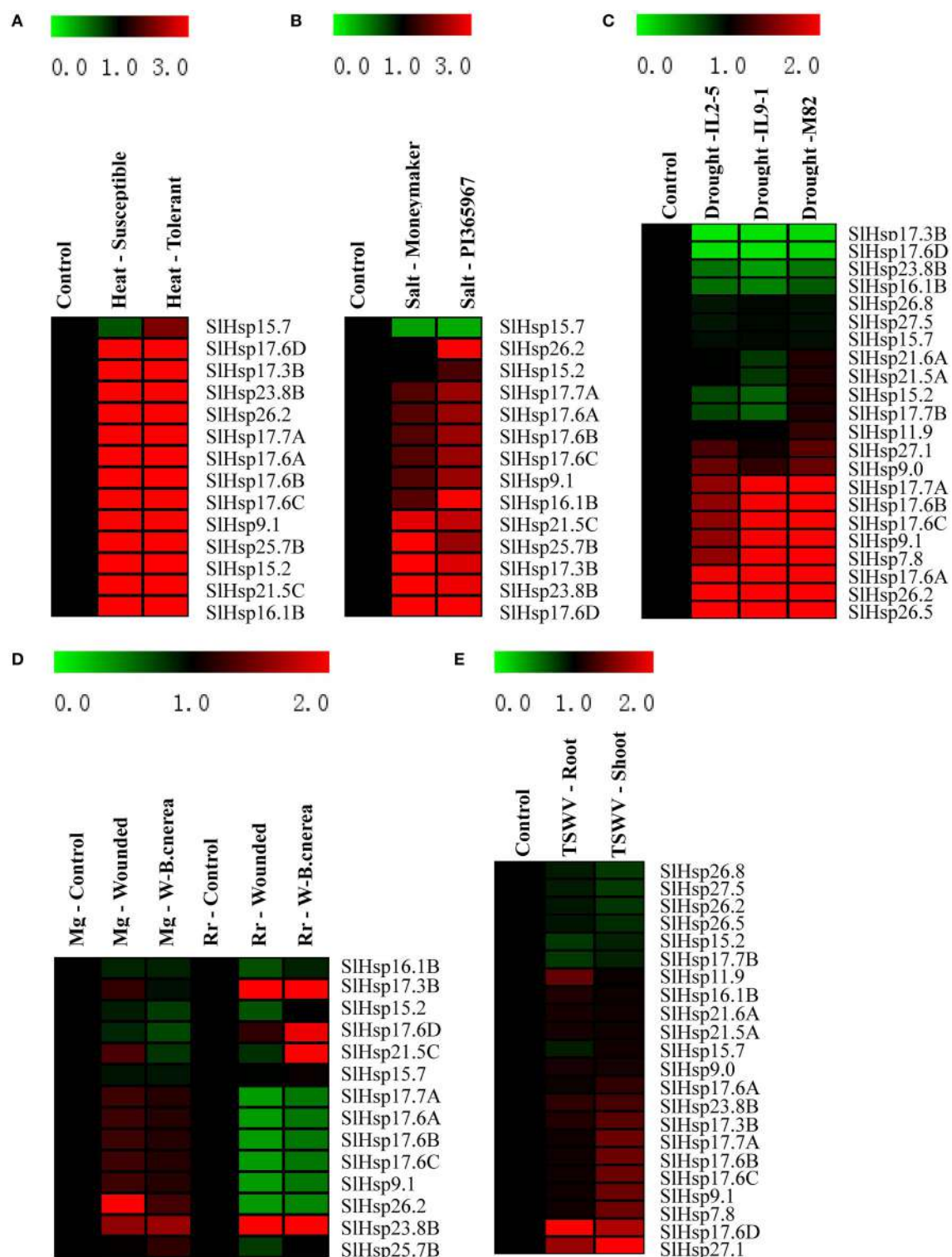


FIGURE 5 | Expression profiles of *SlHsp20* genes under various biotic and abiotic stresses conditions. Blocks with colors represent decreased (green) or increased (red) transcript levels relative to the respective control. **(A)** Expression profiles of *SlHsp20* genes in tolerant and susceptible tomatoes under heat stress condition. **(B)** Expression profiles of *SlHsp20* genes under salt stress in a wild tomato genotype “PI365967” (salt-tolerant) and cultivated tomato var. moneymaker (salt-sensitive). **(C)** Expression profiles of *SlHsp20* genes under drought stress condition in two drought-tolerant lines (IL2-5 and IL9-1) and a drought-sensitive cultivar (M82). **(D)** Expression profiles of *SlHsp20* genes infected by wound and wound-inoculated with *Botrytis cinerea* in mature green (Mg) and red fruits (Rr). **(E)** Expression profiles of *SlHsp20* genes in tomato leaves and roots infected by tomato spotted wilt virus (TSWV).

identified (**Table 1**). Among them, four predicted *SlHsp20* genes were excluded in the phylogenetic tree construction due to incomplete Hsp20 domain. Previously, *Hsp20* gene family in *Arabidopsis* was categorized into 12 subfamilies (CI, CII, CIII, CIV, CV, CVI, CVII, MI, MII, P, ER, and Px) (Scharf et al., 2001; Siddique et al., 2008). Likewise, four novel nucleocytoplasmic subfamilies (CVIII, CIX, CX, and CXI) were also reported on *OsHsp20* genes in rice (Sarkar et al., 2009). In the present paper, to reveal phylogenetic relationship of *Hsp20* genes, *Hsp20* genes from seven plant species, together with *Hsp20* genes from tomato, were used to construct phylogenetic tree (**Figure 2**). The results showed that *Hsp20* genes from the tested plant species could be grouped into 17 subfamilies, according to the method described previously (Scharf et al., 2001; Siddique et al., 2008; Sarkar et al., 2009). The *Hsp20* genes from tomato were grouped into 13 out of 17 subfamilies. A novel subfamily, CXII, was identified using *in silico* localization prediction, which was composed of 9 *Hsp20* genes from tomato (**Supplementary Table S3**). No *SlHsp20* genes were grouped into the remaining four subfamilies (CIV, CVIII, CX, and MII subfamilies). Previous study showed that CIV and MII subfamilies may play an important role in response to various stress conditions and were developmentally regulated (Siddique et al., 2008). Members of CVIII subfamily could be heat-induced and CX subfamily might be involved in specific housekeeping functions under normal growth conditions (Sarkar et al., 2009). Similarly, several subfamilies of the *Hsp20* genes in pepper also lacks, including CIV, CV, CVIII, CIX, CX, and CXI subfamilies. (Guo et al., 2015). Furthermore, the CIV and CVII subfamilies in rice *Hsp20* family were absent (Sarkar et al., 2009). Thus, we were tempting to speculate that gene gain and gene loss events were occurred widely in plant species. The lack of subfamilies exists not only in tomato, but also in other species. It also revealed a wide range of genetic diversity in dicotyledons and monocotyledons.

Furthermore, we also found that most of *Hsp20* genes (69.0%) were clustered into nine nucleocytoplasmic subfamilies, which also had been described in *Arabidopsis* and rice (Scharf et al., 2001; Sarkar et al., 2009). Among these subfamilies, CXII was the largest subfamily with nine members. Therefore, we speculated that cytoplasm, as a site mainly for proteins to be synthesized, could be the primary place for *Hsp20* interacting with denatured proteins to avoid them from inappropriate aggregation and degradation (Lopes-Caitar et al., 2013). In addition, most subfamilies included *Hsp20* genes from multiple plant species and formed a mixture of groups, suggested that diversification of *SlHsp20* subfamilies predated the divergence of these species from the ancestral species.

Organization of *SlHsp20* Genes

It was reported that gene organization played a vital role in the evolution of multigene family (Xu et al., 2012). Our results showed that *SlHsp20* genes of CI, CII, and ER subfamilies had no intron (pattern one) (**Supplementary Figure S1**). Members of CIII, CV, CIX, MI, and PX subfamilies as well as most members of CXII subfamily had one intron (pattern two). Furthermore, these *SlHsp20* genes within the same subfamily shared a similar motif arrangement (**Supplementary Table S2**). This correlation

between motif arrangement, intron numbers and phylogeny can be served as an additional support to their classification.

The results also showed that most of *SlHsp20* genes had no intron or one intron and the length of introns of *SlHsp20* genes with one intron is relatively short. This is concurrent with the result reported previously by the researcher that plants were prone to retain more genes with no intron or a short intron (Mattick and Gagen, 2001). In addition, the instability index of most proteins was equal or greater than 40, signifying that *SlHsp20* proteins can be identified as unstable proteins (**Table 1**). The instability is also considered as a common trait of stress-activated proteins and thus sheds a brilliant light on the rapid induction of the *Hsp20* genes (Rao et al., 2008).

Evolution of the *SlHsp20* Gene Family

Previous research reported that *Hsp20* proteins were ubiquitous from single-celled creatures including bacteria to higher organisms like human (Kim et al., 1998; Waters et al., 2008; Li et al., 2009). It implied that *Hsp20* proteins may have evolved in early stages of the life's history which predated to the divergence of the three domains of life (Eukarya, Bacteria, and Archaea). However, the formation of individual *Hsp20* subfamilies was various. There were no *Hsp20* subfamilies but only cytosolic sHsps in the green algae and then CI, CII, and P subfamilies appeared in mosses (Waters and Vierling, 1999a,b). The process generated gene families attribute to gene duplication, gene loss, and recombination (including gene conversion) (Nei and Rooney, 2005; Flagel and Wendel, 2009). The sHsps might had undergone duplication events early in the history of land plant (Waters, 2013).

Gene duplication was reported as one of the primary forces that drive the evolution processes of genetic systems and genomes (Moore and Purugganan, 2003). In this paper, chromosome mapping showed that 41 *SlHsp20* genes were located unevenly on 12 tomato chromosomes (**Figure 3**). The localization of most of the *SlHsp20* genes was on the terminal regions of the chromosomes, which might contribute to the occurrence of duplication events in tomato *Hsp20* gene family.

In our study, a total of 12 *SlHsp20* genes were demonstrated to be involved in gene duplication, including tandem duplication and segmental duplication (**Figure 3**). Two tandem duplication events (*SlHsp49.3/SlHsp39.4* and *SlHsp17.7A/SlHsp17.6A/SlHsp17.6B/SlHsp17.6C*) and three segmental duplication events (*SlHsp25.7A/SlHsp27.5*, *SlHsp17.7A/SlHsp24.5/SlHsp27.1*, and *SlHsp37.0/SlHsp27.2*) were observed in CI, CIX, and CXII subfamilies. Intriguingly, *SlHsp17.7A* on chromosome 6 was shown to participate in both tandem and segmental events. It shared a duplicated region with *SlHsp27.1* at the similar position on chromosome 10 and *SlHsp24.5* on the upper arm of chromosome 9, while *SlHsp27.1* and *SlHsp24.5* had no tandem duplicated genes in their surrounding region. Comparative analysis revealed that sequence similarity between *SlHsp17.7A* and *SlHsp27.1* was lower than that between *SlHsp17.7A* and *SlHsp17.6A*, suggesting that segmental duplication event predated the tandem duplication event in the *SlHsp17.7A* cluster, and the tandemly organized genes close to *SlHsp27.1* might be lost after the segmental duplication event

(**Supplementary Tables S5, S6**). Similar scenario was observed for *SlHsp17.7A* and *SlHsp24.5*. Together, these results indicated that both tandem duplication and segmental duplication made significant contributions to the expansion of the *SlHsp20* gene family in tomato.

Expression Patterns of *SlHsp20* Genes in Different Tissues

Based on RNA-Seq atlas, a spatio-temporal regulation of *SlHsp20* gene family was observed in various tissues and development stages. Under normal growth conditions, a high or preferential expression of 11 *SlHsp20* genes was found, which showed tissue- and development-specific expression in leaf, root, hypocotyl, and breaker fruit (**Figure 4**). All these tissue- and development-preferential expressed genes may play a critical role in growth and development of tomato and their functions still deserve further investigation. In addition, the expression behavior of some *SlHsp20* genes differed in various tissues and development stages, indicating that the *SlHsp20* proteins may play diverse functional roles. We also found that four genes (*SlHsp17.7A*, *SlHsp17.6B*, *SlHsp17.6C*, and *SlHsp24.5*) were highly expressed in all the investigated tissues, implying that they might be implicated in specific housekeeping activity of tomato cell under normal growth conditions. In vegetative and reproductive organs, two *SlHsp20* genes (*SlHsp25.7B* and *SlHsp17.6A*) displayed differential expression levels between cultivated tomato and the wild relative *S. pimpinellifolium*, which indicated that inter-species divergence of gene expression was occurred and it might lead to functional specialization.

Expression Patterns of *SlHsp20* Genes under Abiotic and Biotic Stresses

Under various stress conditions, it's evident that the *SlHsp20* genes were induced to a larger extent when tomato suffered from abiotic stresses, including heat, salt, and drought treatments (**Figure 5**). Furthermore, we found that the heat stress inducibility of *SlHsp20* genes in susceptible plants was stronger than that in tolerant plants, which also had been demonstrated in *CaHsp20* genes (Guo et al., 2015). This finding indicated that a more efficient mechanism might have been built in the tolerant plants so that fewer *Hsp20* genes were sufficient to reduce the damage from heat shock.

Previous research had reported that the duplicated genes were easier for increasing the diversity of gene expression than single-copy genes (Gu et al., 2004). Here, we found that expression patterns of two groups of the tandemly duplicated genes were highly similar, which reflected that these *SlHsp20* genes might share similar induction mechanisms and network (Ouyang et al., 2009). Actually, compared with tandem duplications, *SlHsp20* genes in segmental duplicated group showed a more differential expression behavior. For example, the different expression between *SlHsp37.0-CXII* and *SlHsp27.2-CXII* suggested that segmentally duplicated genes may also exhibit divergent expression patterns (Waters, 2013). Earlier study revealed that distantly related duplicate

genes may exist functional redundancy and have more chances to acclimatize than the single-copy genes (Gu et al., 2003). Thus, the duplicated *SlHsp20* genes might go through crucial diversification after duplication events, which eventually caused neo-functionalization (Ouyang et al., 2009). It was also reported as a means for the retention of those duplicated genes in a genome (Force et al., 1999).

CONCLUSIONS

In the current study, 42 putative *SlHsp20* genes were identified in tomato. Subsequently, characterization of *SlHsp20* genes was performed through integration of comprehensive sequence, genome organization and expression profile analysis among different tissues and under different stresses (heat, drought, salt, TSWV, and *B. cinerea*) by using RNA-seq and microarray atlas. This study provided a comprehensive understanding of the *SlHsp20* gene family in tomato and made a basis for working out the functional roles of the *Hsp20* genes in the Solanaceae family in the future.

AUTHOR CONTRIBUTIONS

Conceived and designed the experiments: HW and YY. Performed the experiments: JY, YC, MR, QY, RW, ZL, GZ, and ZY. Analyzed the data: JY, YC, and KF. Wrote the paper: JY and YC. All authors have read and approved the manuscript.

ACKNOWLEDGMENTS

Research is supported by the National Natural Science Foundation of China (31301774, 31272156, and 31071800), Zhejiang Provincial Natural Science Foundation of China (Q15C150010) and Young Talent Cultivation Project of Zhejiang Academy of Agricultural Sciences (2015R23R08E07, 2015R23R08E09), State Key Laboratory Breeding Base for Zhejiang Sustainable Pest and Disease Control (No. 2010DS700124-KF1518), Public Agricultural Technology Research in Zhejiang (2016C32101, 2015C32049), and Technological System of Ordinary Vegetable Industry (CARS-25-G-16).

SUPPLEMENTARY MATERIAL

The Supplementary Material for this article can be found online at: <http://journal.frontiersin.org/article/10.3389/fpls.2016.01215>

Supplementary Figure S1 | Intron/exon configurations of *SlHsp20* genes.

The numbers (0, 1, 2) represented introns phases, which indicated three different splicing patterns.

Supplementary Table S1 | Genomic sequences, coding sequences and amino acid sequences of *SlHsp20* genes.

Supplementary Table S2 | Organization of putative motifs in *SlHsp20* proteins. Ten putative motifs are represented by numbered color boxes. Names of all the proteins were indicated on the left side.

- Supplementary Table S3 | Predicted subcellular location of *SlHsp20* genes.**
- Supplementary Table S4 | Homology matrixes of predicted tandem *SlHsp20* gene sequences.**
- Supplementary Table S5 | Tandemly duplicated *SlHsp20* genes.**

REFERENCES

- Arce, D. P., Krsticevic, F. J., Bertolaccini, M. R., Ezpeleta, J., Ponce, S. D., and Tapia, E. (2015). “Analysis of small heat shock protein gene family expression (RNA-Seq) during the tomato fruit maturation,” in *IFMBE Proceedings*, ed A. Braidot (Berlin: Springer International Publishing), 679–682.
- Basha, E., O’Neill, H., and Vierling, E. (2012). Small heat shock proteins and α -crystallins: dynamic proteins with flexible functions. *Trends Biochem. Sci.* 37, 106–117. doi: 10.1016/j.tibs.2011.11.005
- Bauvois, B. (2012). New facets of matrix metalloproteinases MMP-2 and MMP-9 as cell surface transducers: outside-in signaling and relationship to tumor progression. *Biochim. Biophys. Acta Rev. Cancer* 1825, 29–36. doi: 10.1016/j.bbcan.2011.10.001
- Botter, M., Amigues, B., Peart, J., Breuer, C., Kadota, Y., Casais, C., et al. (2007). Structural and functional analysis of SGT1 reveals that its interaction with HSP90 is required for the accumulation of Rx, an R protein involved in plant immunity. *Plant Cell* 19, 3791–3804. doi: 10.1105/tpc.107.050427
- Carper, S. W., Duffy, J. J., and Gerner, E. W. (1987). Heat shock proteins in thermotolerance and other cellular processes. *Cancer Res.* 47, 5249–5255.
- Cashikar, A. G., Duennwald, M., and Lindquist, S. L. (2006). A chaperone pathway in protein disaggregation. *J. Biol. Chem.* 281, 8996. doi: 10.1074/jbc.M502854200
- Caspers, G. J., Leunissen, J. A. M., and de Jong, W. W. (1995). The expanding small heat-shock protein family, and structure predictions of the conserved “ α -crystallin domain.” *J. Mol. Evol.* 40, 238–248. doi: 10.1007/BF00163229
- Cramer, G. R., Urano, K., Delrot, S., Pezzotti, M., and Shinozaki, K. (2011). Effects of abiotic stress on plants: a systems biology perspective. *BMC Plant Biol.* 11:163. doi: 10.1186/1471-2229-11-163
- de Jong, W. W., Caspers, G. J., and Leunissen, J. A. M. (1998). Genealogy of the α -crystallin-small heat-shock protein superfamily. *Int. J. Biol. Macromol.* 22, 151–162. doi: 10.1016/S0141-8130(98)00013-0
- Flagel, L. E., and Wendel, J. F. (2009). Gene duplication and evolutionary novelty in plants. *New Phytol.* 183, 557–564. doi: 10.1111/j.1469-8137.2009.02923.x
- Force, A., Lynch, M., Pickett, F. B., Amores, A., Yan, Y. L., and Postlethwait, J. (1999). Preservation of duplicate genes by complementary, degenerative mutations. *Genetics* 151, 1531–1545.
- Goyal, R. K., Kumar, V., Shukla, V., Mattoo, R., Liu, Y., Chung, S. H., et al. (2012). Features of a unique intronless cluster of class I small heat shock protein genes in tandem with box C/D snoRNA genes on chromosome 6 in tomato (*Solanum lycopersicum*). *Planta* 235, 453–471. doi: 10.1007/s00425-011-1518-5
- Gu, Z., Rifkin, S. A., White, K. P., and Li, W. H. (2004). Duplicate genes increase gene expression diversity within and between species. *Nat. Genet.* 36, 577–579. doi: 10.1038/ng1355
- Gu, Z., Steinmetz, L. M., Gu, X., Scharfe, C., Davis, R. W., and Li, W. H. (2003). Role of duplicate genes in genetic robustness against null mutations. *Nature* 421, 63–66. doi: 10.1038/nature01198
- Guo, M., Liu, J. H., Lu, J. P., Zhai, Y. F., Wang, H., Gong, Z. H., et al. (2015). Genome-wide analysis of the *CaHsp20* gene family in pepper: comprehensive sequence and expression profile analysis under heat stress. *Front. Plant Sci.* 6:806. doi: 10.3389/fpls.2015.00806
- Howe, E., Holton, K., Nair, S., Schlauch, D., Sinha, R., and Quackenbush, J. (2010). “Mev: multiexperiment viewer,” in *Biomedical Informatics for Cancer Research*, ed M. F. Ochs (New York, NY: Springer US), 267–277.
- Hu, B., Jin, J., Guo, A. Y., Zhang, H., Luo, J., and Gao, G. (2015). GSDS 2.0: an upgraded gene feature visualization server. *Bioinformatics* 31, 1296–1297. doi: 10.1093/bioinformatics/btu817
- Huang, S., Gao, Y., Liu, J., Peng, X., Niu, X., Fei, Z., et al. (2012). Genome-wide analysis of WRKY transcription factors in *Solanum lycopersicum*. *Mol. Genet. Genomics* 287, 495–513. doi: 10.1007/s00438-012-0696-6
- Huther, C. M., Ramm, A., Rombaldi, C. V., and Bacarin, M. A. (2013). Physiological response to heat stress of tomato ‘Micro-Tom’ plants expressing high and low levels of mitochondrial sHSP23. 6 protein. *Plant Growth Regul.* 70, 175–185. doi: 10.1007/s10725-013-9790-y
- Kim, K. K., Kim, R., and Kim, S. H. (1998). Crystal structure of a small heat-shock protein. *Nature* 394, 595–599. doi: 10.1038/29106
- Kumar, S., Stecher, G., and Tamura, K. (2016). MEGA7: molecular evolutionary genetics analysis version 7.0 for bigger datasets. *Mol. Biol. Evol.* 33, 1870–1874. doi: 10.1093/molbev/msw054
- Lee, G. J., and Vierling, E. (2000). A small heat shock protein cooperates with heat shock protein 70 systems to reactivate a heat-denatured protein. *Plant Physiol.* 122, 189–198. doi: 10.1104/pp.122.1.189
- Li, X., Cheng, Y., Ma, W., Zhao, Y., Jiang, H., and Zhang, M. (2010). Identification and characterization of NBS-encoding disease resistance genes in *Lotus japonicus*. *Plant Syst. Evol.* 289, 101–110. doi: 10.1007/s00606-010-0331-0
- Li, Z. W., Li, X., Yu, Q. Y., Xiang, Z. H., Kishino, H., and Zhang, Z. (2009). The small heat shock protein (sHSP) genes in the silkworm, *Bombyx mori*, and comparative analysis with other insect sHSP genes. *BMC Evol. Biol.* 9:215. doi: 10.1186/1471-2148-9-215
- Lindquist, S., and Craig, E. A. (1988). The heat-shock proteins. *Annu. Rev. Genet.* 22, 631–677. doi: 10.1146/annurev.ge.22.120188.003215
- Liu, R. H., and Meng, J. L. (2003). MapDraw: a microsoft excel macro for drawing genetic linkage maps based on given genetic linkage data. *Hereditas (Beijing)* 25, 317–321. doi: 10.3321/j.issn:0253-9772.2003.03.019
- Lopes-Caitar, V. S., de Carvalho, M. C., Darben, L. M., Kuwahara, M. K., Nepomuceno, A. L., Dias, W. P., et al. (2013). Genome-wide analysis of the *Hsp20* gene family in soybean: comprehensive sequence, genomic organization and expression profile analysis under abiotic and biotic stresses. *BMC genomics* 14:577. doi: 10.1186/1471-2164-14-577
- Mahesh, U., Mamidala, P., Rapolu, S., Aragao, F. J., Souza, M. T., Rao, P. J. M., et al. (2013). Constitutive overexpression of small *HSP24.4* gene in transgenic tomato conferring tolerance to high-temperature stress. *Mol. Breeding* 32, 687–697. doi: 10.1007/s11032-013-9901-5
- Mattick, J. S., and Gagen, M. J. (2001). The evolution of controlled multitasked gene networks: the role of introns and other noncoding RNAs in the development of complex organisms. *Mol. Biol. Evol.* 18, 1611–1630. doi: 10.1093/oxfordjournals.molbev.a003951
- Moore, R. C., and Purugganan, M. D. (2003). The early stages of duplicate gene evolution. *Proc. Natl. Acad. Sci. U.S.A.* 100, 15682–15687. doi: 10.1073/pnas.2 535513100
- Nautiyal, P. C., and Shono, M. (2010). Analysis of the role of mitochondrial and endoplasmic reticulum localized small heat shock proteins in tomato. *Biol. Plant* 54, 715–719. doi: 10.1007/s10535-010-0127-7
- Nei, M., and Rooney, A. P. (2005). Concerted and birth-and-death evolution of multigene families. *Annu. Rev. Genet.* 39, 121–152. doi: 10.1146/annurev.genet.39.073003.112240
- Neta-Sharir, I., Isaacson, T., Lurie, S., and Weiss, D. (2005). Dual role for tomato heat shock protein 21: protecting photosystem II from oxidative stress and promoting color changes during fruit maturation. *Plant Cell* 17, 1829–1838. doi: 10.1105/tpc.105.031914
- Ouyang, Y., Chen, J., Xie, W., Wang, L., and Zhang, Q. (2009). Comprehensive sequence and expression profile analysis of *Hsp20* gene family in rice. *Plant Mol. Biol.* 70, 341–357. doi: 10.1007/s11103-009-9477-y
- Rao, P. K., Roxas, B. A., and Li, Q. (2008). Determination of global protein turnover in stressed mycobacterium cells using hybrid-linear ion trap-fourier transform mass spectrometry. *Anal. Chem.* 80, 396–406. doi: 10.1021/ac701690d
- Ritossa, F. (1962). A new puffing pattern induced by temperature shock and DNP in *Drosophila*. *Experientia* 18, 571–573. doi: 10.1007/BF02172188
- Sarkar, N. K., Kim, Y. K., and Grover, A. (2009). Rice sHsp genes: genomic organization and expression profiling under stress and development. *BMC Genomics* 10:393. doi: 10.1186/1471-2164-10-393

- Sato, S., Tabata, S., Hirakawa, H., Asamizu, E., Shirasawa, K., Isobe, S., et al. (2012). The tomato genome sequence provides insights into fleshy fruit evolution. *Nature* 485, 635–641. doi: 10.1038/nature11119.
- Scharf, K. D., Siddique, M., and Vierling, E. (2001). The expanding family of *Arabidopsis thaliana* small heat stress proteins and a new family of proteins containing α -crystallin domains (Acd proteins). *Cell Stress Chaperones* 6, 225–237.
- Shirasu, K. (2009). The HSP90-SGT1 chaperone complex for NLR immune sensors. *Annu. Rev. Plant Biol.* 60, 139–164. doi: 10.1146/annurev.arplant.59.032607.092906
- Siddique, M., Gernhard, S., von Koskull-Döring, P., Vierling, E., and Scharf, K. D. (2008). The plant sHSP superfamily: five new members in *Arabidopsis thaliana* with unexpected properties. *Cell Stress Chaperones* 13, 183–197. doi: 10.1007/s12192-008-0032-6
- Sun, W., Van Montagu, M., and Verbruggen, N. (2002). Small heat shock proteins and stress tolerance in plants. *Biochim. Biophys. Acta* 1577, 1–9. doi: 10.1016/S0167-4781(02)00417-7
- Van Montfort, R., Slingsby, C., and Vierling, E. (2002). Structure and function of the small heat shock protein/alpha-crystallin family of molecular chaperones. *Adv. Protein Chem.* 59, 105–156. doi: 10.1016/S0065-3233(01)59004-X
- Vierling, E. (1991). The roles of heat shock proteins in plants. *Annu. Rev. Plant Biol.* 42, 579–620. doi: 10.1146/annurev.pp.42.060191.003051
- Vierling, E., Harris, L. M., and Chen, Q. (1989). The major low-molecular-weight heat shock protein in chloroplasts shows antigenic conservation among diverse higher plant species. *Mol. Cell. Biol.* 9, 461–468. doi: 10.1128/MCB.9.2.461
- Wang, W., Vinocur, B., and Altman, A. (2003). Plant responses to drought, salinity and extreme temperatures: towards genetic engineering for stress tolerance. *Planta* 218, 1–14. doi: 10.1007/s00425-003-1105-5
- Waters, E. R. (2013). The evolution, function, structure, and expression of the plant sHSPs. *J. Exp. Bot.* 64, 391–403. doi: 10.1093/jxb/ers355
- Waters, E. R., Aevermann, B. D., and Sanders-Reed, Z. (2008). Comparative analysis of the small heat shock proteins in three angiosperm genomes identifies new subfamilies and reveals diverse evolutionary patterns. *Cell Stress Chaperones* 13, 127–142. doi: 10.1007/s12192-008-0023-7
- Waters, E. R., Lee, G. J., and Vierling, E. (1996). Evolution, structure and function of the small heat shock proteins in plants. *J. Exp. Bot.* 47, 325–338. doi: 10.1093/jxb/47.3.325
- Waters, E. R., and Vierling, E. (1999a). The diversification of plant cytosolic small heat shock proteins preceded the divergence of mosses. *Mol. Biol. Evol.* 16, 127–139. doi: 10.1093/oxfordjournals.molbev.a026033
- Waters, E. R., and Vierling, E. (1999b). Chloroplast small heat shock proteins: evidence for atypical evolution of an organelle-localized protein. *Proc. Natl. Acad. Sci. U.S.A.* 96, 14394–14399. doi: 10.1073/pnas.96.25.14394
- Wei, Y., Wan, H., Wu, Z., Wang, R., Ruan, M., Ye, Q., et al. (2016). A comprehensive analysis of carotenoid cleavage dioxygenases genes in *Solanum lycopersicum*. *Plant Mol. Biol. Rep.* 34, 512–523. doi: 10.1007/s11105-015-0943-1
- Xu, G., Guo, C., Shan, H., and Kong, H. (2012). Divergence of duplicate genes in exon-intron structure. *Proc. Natl. Acad. Sci. U.S.A.* 109, 1187–1192. doi: 10.1073/pnas.1109047109
- Zhang, J., Chen, H., Wang, H., Li, B., Yi, Y., Kong, F., et al. (2016). Constitutive expression of a tomato small heat shock protein gene *LeHSP21* improves tolerance to high-temperature stress by enhancing antioxidation capacity in tobacco. *Plant Mol. Biol. Rep.* 34, 399–409. doi: 10.1007/s11105-015-0925-3

Conflict of Interest Statement: The authors declare that the research was conducted in the absence of any commercial or financial relationships that could be construed as a potential conflict of interest.

The reviewer CY and handling Editor declared their shared affiliation, and the handling Editor states that the process nevertheless met the standards of a fair and objective review.

Copyright © 2016 Yu, Cheng, Feng, Ruan, Ye, Wang, Li, Zhou, Yao, Yang and Wan. This is an open-access article distributed under the terms of the Creative Commons Attribution License (CC BY). The use, distribution or reproduction in other forums is permitted, provided the original author(s) or licensor are credited and that the original publication in this journal is cited, in accordance with accepted academic practice. No use, distribution or reproduction is permitted which does not comply with these terms.



The DnaJ Gene Family in Pepper (*Capsicum annuum L.*): Comprehensive Identification, Characterization and Expression Profiles

FangFei Fan^{1†}, Xian Yang^{1†}, Yuan Cheng², Yunyan Kang^{1*} and Xirong Chai¹

¹ College of Horticulture, South China Agricultural University, Guangzhou, China, ² State key Laboratory Breeding Base for Zhejiang Sustainable Pest and Disease Control, Institute of Vegetables, Zhejiang Academy of Agricultural Sciences, Hangzhou, China

OPEN ACCESS

Edited by:

Jie Zhou,
Zhejiang University, China

Reviewed by:

Sergey Morozov,
Moscow State University, Russia

Hao Li,
Northwest A&F University, China

*Correspondence:

Yunyan Kang
kangyunyan@scau.edu.cn

[†]These authors have contributed
equally to this work.

Specialty section:

This article was submitted to
Plant Cell Biology,
a section of the journal
Frontiers in Plant Science

Received: 21 January 2017

Accepted: 13 April 2017

Published: 01 May 2017

Citation:

Fan F, Yang X, Cheng Y, Kang Y and
Chai X (2017) The DnaJ Gene Family
in Pepper (*Capsicum annuum L.*):
Comprehensive Identification,
Characterization and Expression
Profiles. *Front. Plant Sci.* 8:689.
doi: 10.3389/fpls.2017.00689

The DnaJ proteins which function as molecular chaperone played critical roles in plant growth and development and response to heat stress (HS) and also called heat shock protein 40 based on molecular weight. However, little was reported on this gene family in pepper. Recently, the release of the whole pepper genome provided an opportunity for identifying putative DnaJ homologous. In this study, a total of 76 putative pepper *DnaJ* genes (CaDnaJ01 to CaDnaJ76) were identified using bioinformatics methods and classified into five groups by the presence of the complete three domains (J-domain, zinc finger domain, and C-terminal domain). Chromosome mapping suggested that segmental duplication and tandem duplication were occurred in evolution. The multiple stress-related *cis*-elements were found in the promoter region of these *CaDnaJ* genes, which indicated that the *CaDnaJs* might be involved in the process of responding to complex stress conditions. In addition, expression profiles based on RNA-seq showed that the 47 *CaDnaJs* were expressed in at least one tissue tested. The result implied that they could be involved in the process of pepper growth and development. qRT-PCR analysis found that 80.60% (54/67) *CaDnaJs* were induced by HS, indicated that they could participated in pepper response to high temperature treatments. In conclusion, all these results would provide a comprehensive basis for further analyzing the function of *CaDnaJ* members and be also significant for elucidating the evolutionary relationship in pepper.

Keywords: DnaJ, heat shock protein 40, chromosomal localization, stress-related *cis*-elements, expression patterns

INTRODUCTION

With the increase of global warming, high temperature has become one of the most vital abiotic stresses on crop plants (Glazebrook, 1999). Pepper (*Capsicum annuum L.*) which originated in the tropical regions of Latin America had been widely cultivated around the world as an important vegetable crop nowadays and is sensitive to high temperature during plant growth and development, especially in reproductive stage (Guo et al., 2014). The optimum temperature

of growing pepper is 20–30°C. Over 32°C can bring about serious effects on pollination and fertilization, and results in blossom and fruit dropping which can cause a significant reduction of pepper fruit yield and quality.

In the long-term evolution, plants have evolved a complicated response mechanism to respond to heat stress (HS). Previous researches had reported that heat shock response (HSR) was induced in many plant species under HS condition (Vierling, 1991). Among them, a great deal of ubiquitous and evolutionary-conserved proteins was identified as heat shock proteins (Hsps), one of the main products of the HSR (Vierling, 1991). The Hsp was first discovered in *Drosophila melanogaster* in response to HS (Ritossa, 1962). In the following years, more Hsps were identified in other plants (Agarwal et al., 2002; Sarkar et al., 2009; Lopes-Caitar et al., 2013; Mulaudzi-Masuku et al., 2015). According to approximate molecular weight and sequence homology, the Hsps were classified into five families, including the Hsp100, Hsp90, Hsp70, Hsp60 and small Hsps (Wang et al., 2004; Kotak et al., 2007; Gupta et al., 2010).

The Hsp40, one of the important plant Hsps, was first identified in *Escherichia coli*, generally existed in organisms as 41 kDa Hsps (Georgopoulos et al., 1980; Bukau and Horwich, 1998; Craig et al., 2006). The Hsp40s, also known as DnaJ proteins or J-proteins, generally consisted of the J-domain, a proximal G/F-domain, a distal zinc finger (CxxCxGxG) domain, and followed by less conserved C-terminal sequences (Caplan et al., 1993; Silver and Way, 1993). The characteristic feature of the J-proteins was the presence of evolutionarily conserved J-domain which located nearby the N-terminus and composed of approximately 70 amino acids residues (Cyr et al., 1992). The invariant tripeptide (HPD) was the hallmark of J-domain. It stimulated the ATPase activity of Hsp70 and was crucial for keeping J-protein's function (Kampinga and Craig, 2010). Previously, Cheetham and Caplan (1998) attempted to separate these proteins into three groups. Group I J-proteins were characterized by the J-domain, G/F-domain, and zinc finger domain. Group II would have the J-domain plus either a G/F-domain or zinc finger domain. Group III J-proteins only comprised the J-domain (Ohtsuka and Hata, 2000).

In recent years, it has been found that plant DnaJ proteins played important roles in response to both biotic and abiotic stresses, such as pest, pathogenic bacterium, drought, salt, and heat. In 2007, a J-domain virulence effector of *Pseudomonas syringae* remolded host chloroplasts when responded to pathogen (Jelenska et al., 2007). The researchers reported that over-expression of tomato (*Solanum lycopersicum*) chloroplast-targeted J-protein, *LeCDJ1*, facilitated heat tolerance in transgenic tomatoes (Kong et al., 2014a) and further found that it also played important role in maintaining photosystem II under chilling stress (Kong et al., 2014b). Subsequently, the study has also demonstrated that this gene could enhance tolerance to drought stress and resistance to *P. solanacearum* in transgenic tobacco (Wang et al., 2014). In addition, Xia et al. (2014) reported that a putative J-proteins ortholog from *Nicotiana tabacum* could be involved in drought stress response and its over-expression enhanced drought tolerance possibly through regulating expression of stress-responsive genes.

Up to now, many J-proteins in organisms were identified, such as *Arabidopsis thaliana* (89) (Miernyk, 2001), yeast (22) (Walsh et al., 2004) and human (41) (Craig et al., 2006). Despite ongoing efforts to characterize the members of J-protein from other organisms (Sarkar et al., 2009; Kong et al., 2014a,b; Xia et al., 2014), none of its from pepper has been identified at the genomic level. Fortunately, the pepper whole genomic sequences were completely available (Kim et al., 2014; Qin et al., 2014), which provided an opportunity for identifying candidate J-protein genes at the genomic level. In the present work, the J-protein gene family members were identified in pepper through bioinformatics method and analyzed by integration of gene structure, conserved motifs, chromosomal localization, *cis*-element and expression patterns.

MATERIALS AND METHODS

Genome-Wide Identification of *CaDnaJ* Genes in Pepper

The genomic sequences of pepper downloaded from the Pepper Genome Database (PGD¹) (Kim et al., 2014) were used to build the local database on the software BioEdit 7.0. The Hidden Markov Model (HMM) profile of J-domain (PF00226) downloaded from the Pfam protein family database² was used as query sequence to search against putative pepper J-protein genes with *e*-value <10⁻⁵. Subsequently, each of all putative pepper J-protein genes was used to identify the presence of J-domain on Pfam³. The protein sequences of identified pepper J-protein gene family members were analyzed with EXPASY PROTOPARAM⁴ to obtain molecular weight and theoretical isoelectric point (pI).

Multiple Alignment and Chromosomal Location

In this paper, the J-proteins in pepper were classified based on structural features. In each class, the full amino acid sequences of pepper J-proteins were aligned using the software Clustal X 2.01 (Larkin et al., 2007). Each of the J-protein genes was mapped on chromosomes using MapDraw2.1 (Liu and Meng, 2003) based on information in PGD. Two duplication events, tandem duplication and segmental duplication, were also further elaborated. For tandem duplication, three criteria were adopted. Firstly, two or more pepper *DnaJ* genes were arrayed within a range of 100 kb distance. Secondly, the multiple alignments of these *DnaJ* genes had a high coverage rate of the longer gene (more than 70%). Thirdly, the identity of the aligned region in these *DnaJ* genes was also more than 70% (Li et al., 2009; Huang et al., 2012; Wei et al., 2016). The segmental duplication was investigated according to Plant Genome Duplication Database (PGDD⁵).

¹<http://peppergenome.snu.ac.kr/>

²<http://pfam.xfam.org/family/PF00226.29>

³<http://pfam.xfam.org/>

⁴<http://www.expasy.org/tools/protparam.html>

⁵<http://chibba.agtec.uga.edu/duplication/>

Promoters Analysis of Pepper *CaDnaJ* Genes

The upstream regions (1.5 kb) of the *DnaJ* gene sequences were downloaded from PGD, and were used to search for regulating factor such as gibberellins (GA), abscisic acid (ABA), salicylic acid (SA), ethylene, drought, salt and heat.

Tissue-Specific Expression of *CaDnaJ* Genes Based on RNA-Seq

In this paper, RNA-seq data reported by previous researchers (Kim et al., 2014) were used to investigate expression patterns of putative *CaDnaJ* genes in pepper. Different tissues were selected: root, stem, leaf and pericarp at 6 days post-anthesis (DPA), 16 DPA, 25 DPA, respectively, and mature green (MG), breaker (B), 5 days post-breaker (B5), B10. RPKM (Reads Per Kilo bases per Million mapped Reads) values of *CaDnaJ* genes were log₂-transformed (Wei et al., 2012). Heat maps of *CaDnaJ* genes in different tissues were performed using software MultiExperiment Viewer (MeV) (Howe et al., 2010).

Plant Materials and Heat Stress Treatment

A hot pepper hybrid (*zhejiao 3#*), which developed by Zhejiang Academy of Agricultural Sciences, was selected in the experiments. Seeds were sterilized for 5 min using 10% hypochlorous acid solution and washed three times using distilled water. These seeds were further placed in water-saturated filter paper to germinate, then cultivated in Hoagland solution in a growth chamber which was maintained at a 16 h light at 26°C and 8 h dark at 19°C. At the stage of 6–8 true leaves, plants were treated with 42°C for 4 h and plants grown at 25°C were used as the control group. Young leaves were collected and immediately frozen with liquid nitrogen for total RNA extraction. Each treatment was conducted with three biological replicates, and samples from five plants were collected for each replicate.

RNA Extraction and qRT-PCR Analysis

Total RNA was extracted using Total RNA kit (Tiangen Biotech, Beijing, China) and reverse-transcribed using FastQuant RT Kit (Tiangen Biotech, Beijing, China), the operational procedure followed the manufacturer's procedure.

For quantitative RT-PCR analysis, we amplified PCR products in triplicate using 2 × Taq Master Mix (Vazyme, Nanjing, China) in 20 μL qRT-PCR reactions. PCR was performed using the ABI step-one plus 96-well real-time PCR Detection System (Bio-Rad) and cycling conditions consisted of denaturation at 94°C for 5 min, followed by 33 cycles of denaturation at 94°C for 30 s, annealing at 55°C for 30 s and extension at 72°C for 30 s. The *UBI* gene was used as an internal control (Wan et al., 2011). Gene-specific primers were designed and used for amplification as described in **Supplementary Table S1**. Analysis of relative gene expression data was performed using the $2^{-\Delta\Delta Ct}$ method (Livak and Schmittgen, 2001).

RESULTS

Genome-Wide Identification of *CaDnaJ* Genes in Pepper

A total of 85 putative sequences of pepper *DnaJ* genes were gotten from PGD by HMM search. Among them, nine sequences without a complete J-domain (CA03g32700, CA06g22620, CA00g87730, CA12g09540, CA02g21540, CA05g10320, CA11g03100, CA06g00080, and CA05g07590) were removed. The remaining 76 genes were assigned as pepper *DnaJ* genes. As a matter of convenience, the 76 *DnaJ* proteins were named as *CaDnaJ01* to *CaDnaJ76* according to their location on chromosome (**Table 1**).

The length of *CaDnaJ* proteins ranged from 130 (*CaDnaJ23*) to 1272 (*CaDnaJ45*) amino acids, and the predicted molecular weights were between 15.597 kDa (*CaDnaJ59*) and 157.85 kDa (*CaDnaJ25*). The *CaDnaJs* shared a conserved J-domain comprised about 70 amino acids, in which *CaDnaJ57* owned the shortest J-domain with 39 amino acids, while J-domain of *CaDnaJ25* was the longest (84 amino acids). The predicted pI-values of *CaDnaJ* proteins ranged from 4.56 (*CaDnaJ74*) to 9.87 (*CaDnaJ24*), indicating acidic and alkaline proteins. Besides, it was also found that 25 (32.89%) of the total 76 *CaDnaJ* genes had no introns, 11 genes (14.47%) had a single intron, while only *CaDnaJ03* had 11 introns (**Table 1**).

Classification and Sequence Alignment of *CaDnaJ* Genes

The *CaDnaJ* protein usually contains conserved J-domain, zinc finger domain, and uncharacterized C-terminal domain (Cheetham and Caplan, 1998). According to the presence of the complete three domains, the *CaDnaJ* genes were classified into five groups (A, B, C, D, and E), including 9, 8, 53, 1 and 5 members, respectively. Group A *CaDnaJ* proteins are characterized by the J-domain, zinc finger domain and a less conserved C-terminal. The difference between Group A and B was lack of the zinc finger domain. Group C *CaDnaJ* proteins only comprised the J-domain, otherwise, Group D would both have the J-domain and zinc finger domain. Group E contains a *CaDnaJ* protein lacked of HPD motif, which have been described as J-like proteins (Walsh et al., 2004).

Based on the classification above, sequence alignment of *CaDnaJ* genes was performed separately (**Supplementary Table S2**). It was found that nine members in group A possessed a conserved HPD motif in J-domain and two zinc finger domains (CxxCxGxG). Eight members in group B were lack of the zinc finger domain but owned conserved HPD motif in J-domain. The largest group (group C) which included 53 members only consisted of complete J-domain. Group D which contained merely one member (*CaDnaJ36*) had both the conserved HPD motif and zinc finger domain. The last group (group E), which comprised five members, held the least conservation among five groups. All the members in group E possessed J-domains lacked of HPD motif.

TABLE 1 | The list of *CaDnaJ* members identified in pepper.

Gene name	Locus name	Location	Chr.	Group ^a	Size(aa)	MW(Da)	PI	Introns
CaDnaJ01	CA01g16030	97618202–97621808	1	C	574	64187.51	8.54	5
CaDnaJ02	CA01g17770	143624907–143627243	1	C	778	32485.78	6.35	0
CaDnaJ03	CA01g18690	156550800–156555986	1	A	300	32485.78	6.35	11
CaDnaJ04	CA01g22020	169879103–169880683	1	C	526	58220.93	8.34	0
CaDnaJ05	CA01g25030	203653187–203656231	1	C	1014	113869.47	5.73	0
CaDnaJ06	CA01g27370	222188570–222189529	1	C	288	32533.02	8.65	1
CaDnaJ07	CA01g30060	252896608–252899637	1	C	968	110547.4	8.45	2
CaDnaJ08	CA02g03340	46401318–46404099	2	C	469	51784.11	7.97	3
CaDnaJ09	CA02g06030	81542166–81542741	2	C	184	20655.63	8.95	1
CaDnaJ10	CA02g07560	109106142–109111419	2	C	505	57920.91	8.19	4
CaDnaJ11	CA02g15460	144816870–144819496	2	B	352	38501.82	9.17	2
CaDnaJ12	CA03g00750	1443148–1444782	3	C	180	21530.33	9.49	1
CaDnaJ13	CA03g08730	28341344–28342355	3	C	249	28757.26	5.52	1
CaDnaJ14	CA03g19380	212945408–212947600	3	C	730	81652.23	9.02	0
CaDnaJ15	CA03g24080	228862136–228863317	3	C	393	43430.55	9.85	0
CaDnaJ16	CA03g25800	235233410–235241868	3	C	785	59082.25	7.21	9
CaDnaJ17	CA03g31950	249441998–249454817	3	A	421	45593.07	9.23	7
CaDnaJ18	CA03g37040	257676539–257678405	3	C	215	23745.93	5.02	5
CaDnaJ19	CA04g03850	11909825–11910715	4	A	286	31473.8	8.86	1
CaDnaJ20	CA04g12150	170393420–170395215	4	C	209	23712.34	5.97	2
CaDnaJ21	CA04g16150	205132799–205133939	4	C	347	37710.14	8.68	2
CaDnaJ22	CA04g16480	205935059–205935586	4	C	175	20694.67	9.97	0
CaDnaJ23	CA04g19270	214481447–214481839	4	E	130	15006.93	9.52	0
CaDnaJ24	CA04g21880	219689981–219690469	4	C	162	17672.7	9.87	0
CaDnaJ25	CA05g00380	478405–487668	5	C	1432	157852.71	8.6	10
CaDnaJ26	CA05g03820	10149653–10153690	5	A	417	46743.88	6.12	5
CaDnaJ27	CA05g09770	104367131–104370250	5	C	212	23288.3	5.32	5
CaDnaJ28	CA05g10040	111541112–111547755	5	E	258	28711.63	8.68	1
CaDnaJ29	CA05g11830	157117370–157119724	5	C	784	88043.88	7.08	0
CaDnaJ30	CA05g12050	165924883–165925699	5	C	183	20601.3	9.21	2
CaDnaJ31	CA05g17350	225414158–225414685	5	C	175	20366.33	9.6	0
CaDnaJ32	CA05g18040	227747673–227748459	5	C	233	27032.68	6.54	1
CaDnaJ33	CA05g19550	231614733–231618044	5	A	419	46582.74	6.01	4
CaDnaJ34	CA06g00330	381222–387261	6	B	345	39132.52	6.35	9
CaDnaJ35	CA06g19300	218954099–218961832	6	B	345	38203.22	9.11	1
CaDnaJ36	CA06g27020	234692516–234693273	6	D	216	24361.61	9.77	1
CaDnaJ37	CA07g03000	13658626–13660185	7	E	519	57652.71	5.32	0
CaDnaJ38	CA07g04780	39783049–39785325	7	C	758	84482.15	8.38	0
CaDnaJ39	CA07g14410	212076067–212082495	7	B	345	37215.12	9.17	2
CaDnaJ40	CA07g14580	212629401–212635278	7	C	295	33432.67	5.6	8
CaDnaJ41	CA07g20780	230038893–230039930	7	C	138	15577.42	9.69	1
CaDnaJ42	CA07g20790	230043861–230044460	7	C	199	16176.37	8.87	0
CaDnaJ43	CA07g21520	231469760–231475634	7	C	562	64225.13	8.53	8
CaDnaJ44	CA08g04550	83124279–83126597	8	C	772	86114.31	8.13	0
CaDnaJ45	CA08g04600	84686555–84694315	8	C	1272	140416.01	6.06	7
CaDnaJ46	CA08g06460	119037486–119039876	8	B	323	35771.63	8.74	2
CaDnaJ47	CA08g09710	127054669–127056621	8	C	650	74087.37	8.35	0
CaDnaJ48	CA08g11000	129804829–129805596	8	C	255	28904.03	9.37	0
CaDnaJ49	CA08g11250	130268529–130271774	8	C	1081	120431.12	8.59	0
CaDnaJ50	CA08g12000	131886063–131888726	8	C	268	29611.44	6.97	6
CaDnaJ51	CA08g12400	132522159–132523390	8	C	169	19029.27	5.96	4
CaDnaJ52	CA08g15850	138087951–138093573	8	A	447	48202.89	9.29	6
CaDnaJ53	CA08g16300	138809830–138812058	8	E	742	81179.23	8.8	0

(Continued)

TABLE 1 | Continued

Gene name	Locus name	Location	Chr.	Group ^a	Size(aa)	MW(Da)	pI	Introns
CaDnaJ54	CA08g16570	139457347–139458186	8	C	279	31836.41	7.73	0
CaDnaJ55	CA09g01340	2706279–2712890	9	C	666	74144.61	5.07	10
CaDnaJ56	CA09g02890	7558262–7563055	9	C	437	48590.89	6.07	7
CaDnaJ57	CA09g10060	137889893–137892146	9	C	524	57233.33	9.24	4
CaDnaJ58	CA09g11550	183732592–183739583	9	B	344	37544.53	9.23	2
CaDnaJ59	CA10g18490	226999515–226999919	10	C	134	15596.59	9.45	0
CaDnaJ60	CA10g20680	230815988–230820272	10	C	285	32803.76	5.92	7
CaDnaJ61	CA10g21560	232003695–232006477	10	C	303	34356.11	7.71	2
CaDnaJ62	CA11g00780	1313193–1320773	11	C	414	45782.29	5.93	10
CaDnaJ63	CA11g05830	31452436–31455481	11	B	309	34460.23	9.18	1
CaDnaJ64	CA11g10010	113882240–113883699	11	B	355	39775.51	7.59	2
CaDnaJ65	CA11g15800	246441094–246443635	11	A	420	46685.7	5.96	5
CaDnaJ66	CA11g15990	246907971–246916099	11	C	249	29550.83	9.42	8
CaDnaJ67	CA12g07660	35330989–35333794	12	A	420	46676.65	6.17	5
CaDnaJ68	CA12g15900	210077200–210078225	12	C	341	38582.29	8.38	0
CaDnaJ69	CA12g16980	217402887–217403441	12	C	184	20599.06	4.81	0
CaDnaJ70	CA12g18310	225521850–225529944	12	C	366	41110.67	5.41	8
CaDnaJ71	CA12g21480	233476472–233477521	12	C	349	40840.83	7.63	0
CaDnaJ72	CA00g32600			A	421	47162.33	7	6
CaDnaJ73	CA00g54170			E	711	77402.78	5.83	0
CaDnaJ74	CA00g57050			C	193	22938.37	4.56	4
CaDnaJ75	CA00g75210			C	771	86305.23	9.37	0
CaDnaJ76	CA00g93240			C	570	62812.03	4.95	7

^aGroup A are characterized by the J-domain, zinc finger domain and a less conserved C-terminal; Group B are characterized by the J-domain and a less conserved C-terminal; Group C only comprised the J-domain; Group D would both have the J-domain and zinc finger domain; Group E was described as J-like proteins contained a J-protein lacked of HPD motif. MW, Molecular weight; pI, isoelectric points.

Chromosomal Location and Gene Duplication

All these *CaDnaJ* genes (9 members in group A, 8 members in group B, 53 members in group C, 1 members in group D and 5 members in group E) in pepper were unevenly distributed on 12 chromosomes (**Figure 1**). Among them, eleven and nine genes were located on chromosome 8 and 5, respectively. Seven genes on each of chromosome 1, 3, 7, six genes on chromosome 4, five genes on each of chromosome 11 and 12, four genes on each of chromosome 2, 9, three genes on each of chromosome 6 and 10.

We further analyzed the gene duplication of *CaDnaJ* genes in pepper. As shown in **Figure 1**, one tandem duplication event (*CaDnaJ41/CaDnaJ42*) was identified on chromosome 7. The chromosome location of this pair of *CaDnaJ* genes was close in distance and was inserted by less than one gene. In addition, two segmental duplication events were detected. *CaDnaJ04* on chromosome 1 presented synteny to *CaDnaJ44* localized on a duplicated segment of chromosome 8. Similar scenario was observed for *CaDnaJ19* on chromosome 4 and *CaDnaJ67* on chromosome 12. These results suggested that these duplication events made contributions to expansion of pepper *CaDnaJ* gene family.

Analysis of Stress-Related *cis*-Elements in Pepper *CaDnaJ* Promoters

The upstream regions (1.5 kb) of the *CaDnaJ* sequences were searched for regulating factor on different stress conditions. The

stress-related *cis*-elements were not found in the promoter region of two *CaDnaJ* genes (*CaDnaJ26* and *27*), and the rest of 74 *CaDnaJ* genes possessed multiple *cis*-elements. Among them, the *CaDnaJ 28* and *50* possessed the maximum types of stress-related *cis*-elements (10). On the contrary, only two types of stress-related *cis*-elements were held on *CaDnaJ10*. Besides, *CaDnaJ 34* has the most stress-related *cis*-elements (23), including twelve methyl jasmonic acid (MeJA) related, six drought and indoleacetic acid (IAA) related, four ABA related and one GA related (**Figure 2** and **Supplementary Table S3**).

To further explore the possible regulation mechanism of *CaDnaJ* genes to HS, the heat stress responsiveness elements (HSEs) were also searched in the promoter region of all these *CaDnaJ* genes. The result showed that 66.21% (49 out of 74) *CaDnaJ* genes have HSEs in the promoter regions. The maximum numbers of HSEs (6) were identified in *CaDnaJ25* and *CaDnaJ28*. Only one HSEs was found in fifteen *CaDnaJ* genes (*CaDnaJ01, 03, 04, 08, 22, 33, 37, 39, 41, 42, 47, 52, 55, 68, and 72*). In addition, other stress-related *cis*-elements were also detected. There were 107 TC-rich repeats in 55 genes, 99 MBS in 49 genes, 33 LTR in 26 genes, 79 TCA-element in 47 genes, 36 TGA-element in 27 genes, 87 GARE-motif in 49 genes, 138 CGTCA-motif in 41 genes, 37 ERE in 27 genes and 55 ABRE in 28 genes.

Expression Patterns of *CaDnaJ* Genes in Different Tissues

Based on RNA-seq data of different pepper tissue (root, stem, leaf, and pericarp) published previously (Kim et al., 2014), expression

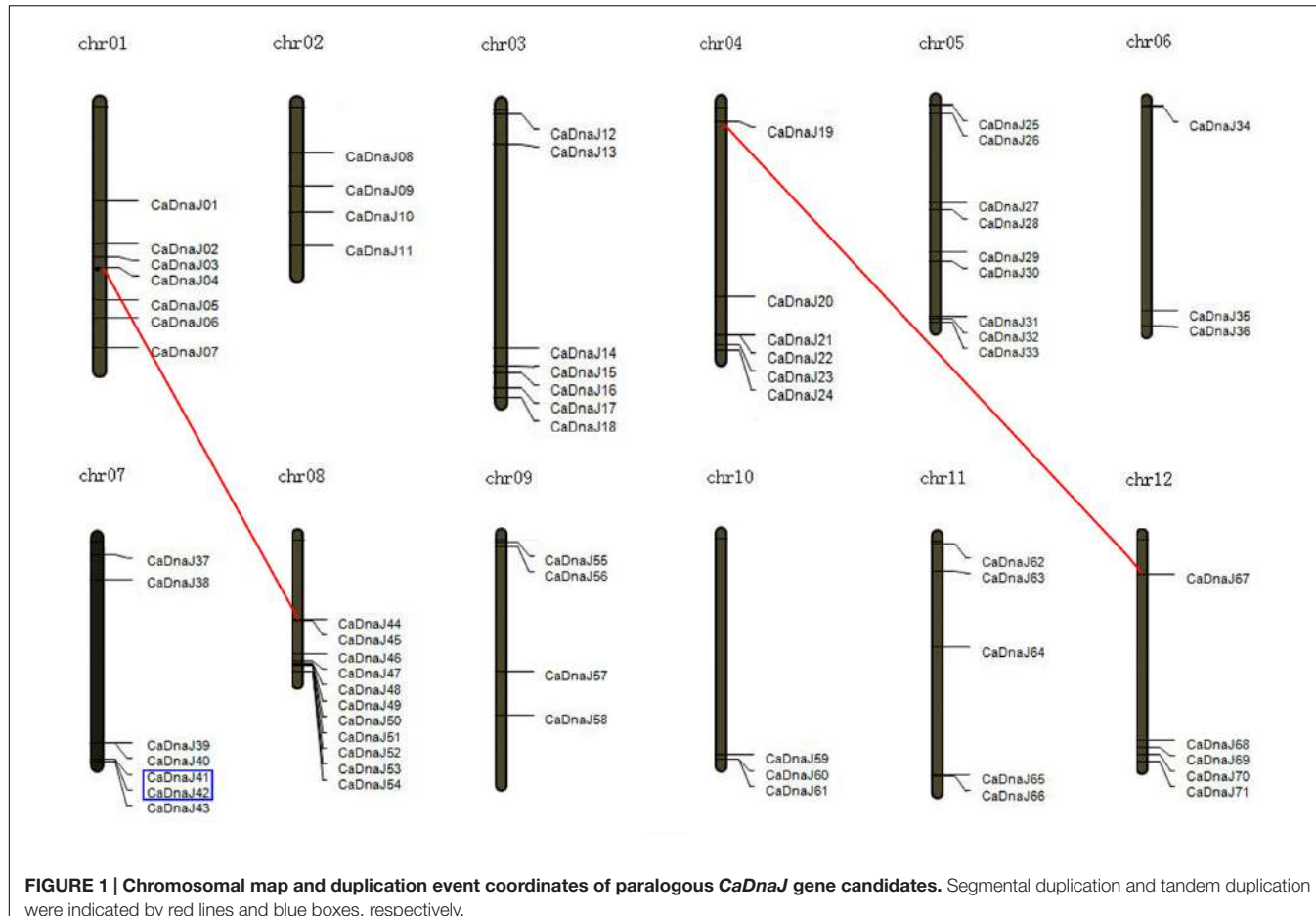


FIGURE 1 | Chromosomal map and duplication event coordinates of paralogous *CaDnaJ* gene candidates. Segmental duplication and tandem duplication were indicated by red lines and blue boxes, respectively.

profiles of *CaDnaJ* genes were revealed (Figure 3). A total of seven different stages of pericarp [6 DPA, 16 DPA, 25 DPA, MG, breaker (B), 5 days post-breaker (B5), B10] were selected for expression analysis in the present study. As shown in Figure 3, 29 out of 76 *CaDnaJ* genes were barely expressed in the tested tissues, including *CaDnaJ01, 03, 05, 09, 12, 14, 15, 16, 19, 22, 26, 29, 30, 38, 39, 48, 49, 51, 57, 58, 59, 63, 64, 65, 67, 69, 71, 72 and 75*. The left 47 *CaDnaJ* genes could be detected at least in one tissue. Ten genes (*CaDnaJ06, 08, 21, 27, 28, 47, 50, 55, 56 and 76*) were expressed in all tested tissues. Of them, four genes (*CaDnaJ06, 21, 28 and 76*) were expressed at relatively high levels. Besides, tissue-specific expression was also found in some *CaDnaJ* genes. The *CaDnaJ66* was specifically expressed in leaf, *CaDnaJ07* and *13* were specifically expressed in root. During the stage of pericarp development, the expression of *CaDnaJ02* was significantly up-regulated, while *CaDnaJ74* and *CaDnaJ45* was obviously down-regulated.

Expression Patterns of *CaDnaJ* Genes in Response to Heat Treatments

To gain more insight into the role of *CaDnaJ* genes under HS condition, expression profiles of *CaDnaJ* genes in pepper response to high temperature based on qRT-PCR technique were performed. In this study, a total of 67 *CaDnaJ* genes were used

to design successfully specific primers for expression analysis. As shown in Figure 4, expression of these tested *CaDnaJ* genes was significantly changed under high temperature stress treatments. Expression levels of five *CaDnaJ* genes (*CaDnaJ4, 50, 59, 63, and 72*) were down-regulated, and 49 *CaDnaJ* genes were up-regulated. For the remaining 13 *CaDnaJ* genes (*CaDnaJ1, 17, 27, 31, 43, 48, 49, 53, 54, 58, 60, 73 and 75*), no difference was observed. Notably, among the *CaDnaJ* genes up-regulated, the expression levels of 71.4% (35/49) were increased to three folds. In total, expression of most of *CaDnaJ* genes was significantly altered under HS, indicating that the *CaDnaJ* genes were involved in plants response to high temperature stress.

DISCUSSION

As an important vegetable crop all over the world, pepper is deeply loved by a large population since its major ingredient in cuisines, essential vitamins and other healthy nutrients (Kim et al., 2014). High temperature has become one of the important environmental stresses and affected seriously the growth and development in pepper. The DnaJs, one of the significant Hsps, was produced in the process of plant responding to HS. Up to now, functional identification of DnaJ has been reported in

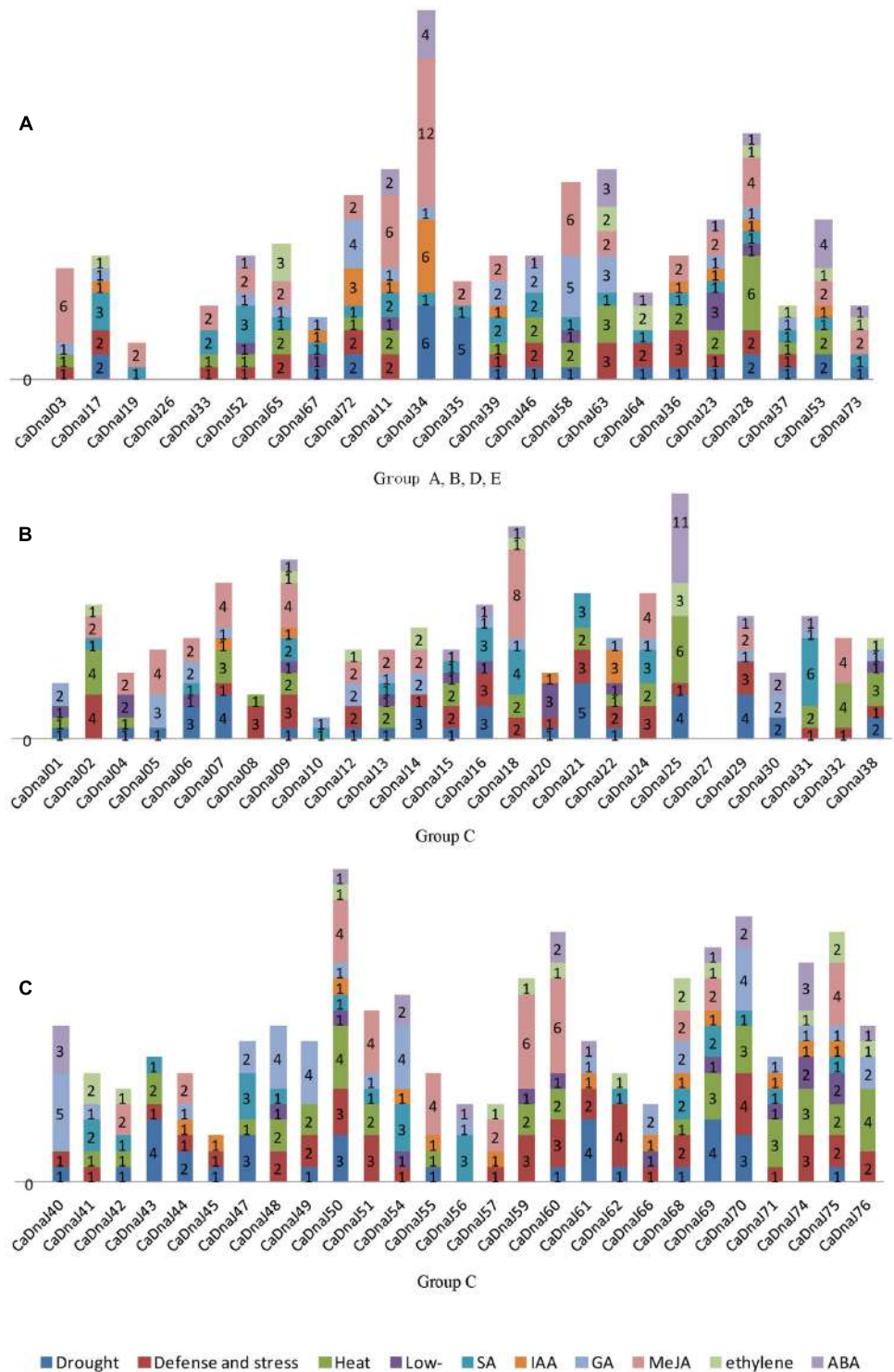


FIGURE 2 | Predicted cis-elements in the promoter regions of *CaDnaJ* genes. Promoter sequences (~1500 bp) for 74 *CaDnaJ* genes (promoter regions of *CaDnaJ26* and 27 were absent) are analyzed. The names of the promoters of *CaDnaJ* genes are shown on the bottom of the figure. Different cis-elements with the common functions are marked with same color. **(A)** Predicted cis-elements in the promoter regions of group A, B, D, E. **(B)** Predicted cis-elements in the promoter regions of group C (26 of 53 *CaDnaJs*). **(C)** Predicted cis-elements in the promoter regions of group C (27 of 53 *CaDnaJs*).

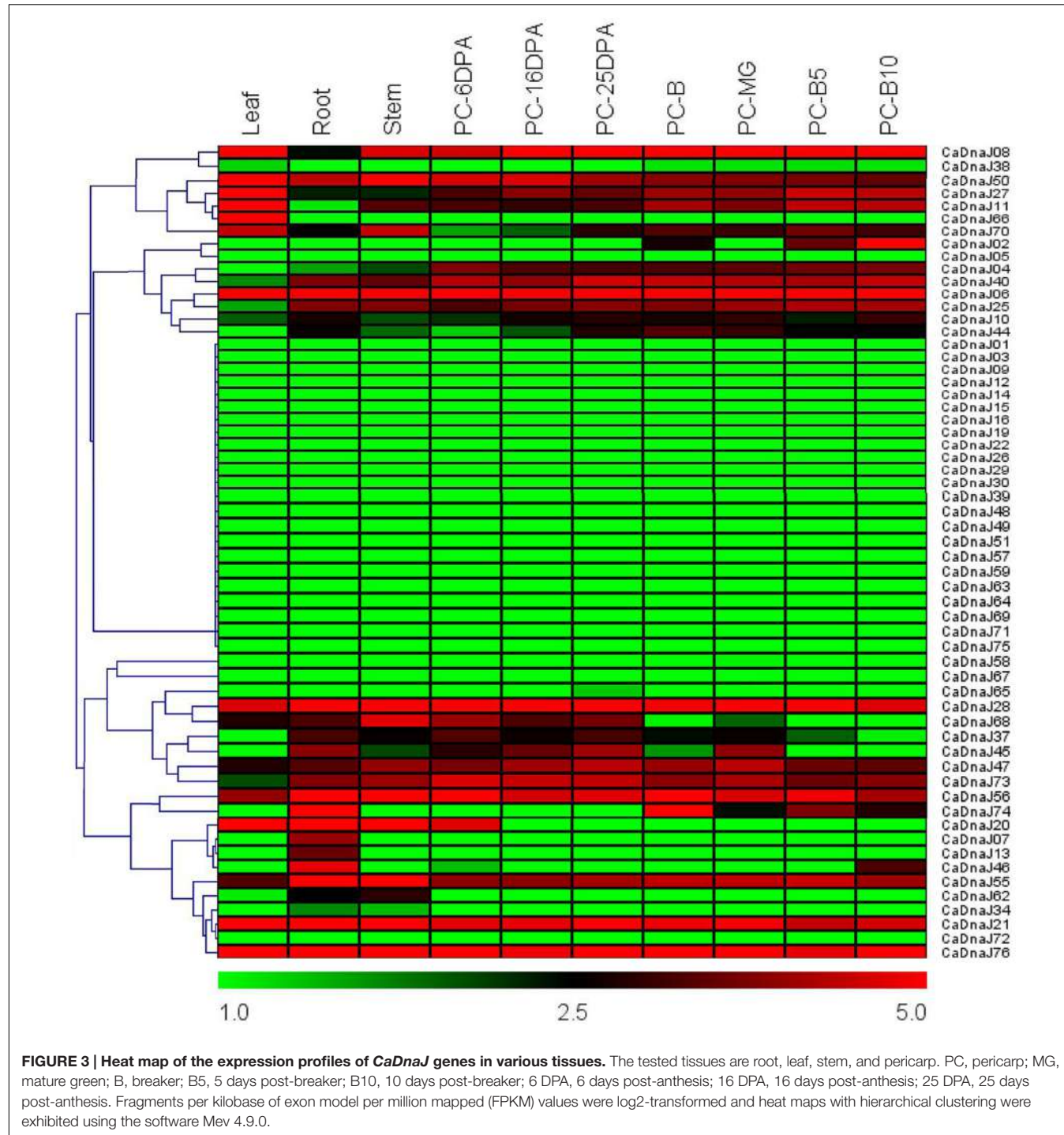


FIGURE 3 | Heat map of the expression profiles of *CaDnaJ* genes in various tissues. The tested tissues are root, leaf, stem, and pericarp. PC, pericarp; MG, mature green; B, breaker; B5, 5 days post-breaker; B10, 10 days post-breaker; 6 DPA, 6 days post-anthesis; 16 DPA, 16 days post-anthesis; 25 DPA, 25 days post-anthesis. Fragments per kilobase of exon model per million mapped (FPKM) values were log2-transformed and heat maps with hierarchical clustering were exhibited using the software Mev 4.9.0.

many plant species (Miernyk, 2001; Qiu et al., 2006; Bekh-Ochir et al., 2013; Fristedt et al., 2014; Kong et al., 2014a,b). At the whole genome level, it has been found that *Arabidopsis* has 89 members and encoded multiple gene family (Miernyk, 2001). Recently, the whole pepper genome has released and provided an opportunity for identifying putative DnaJ homologous. In the current paper, a systematic analysis of *CaDnaJ* gene family was performed using bioinformatics methods, which focused on gene

structure, chromosomal localization, stress-related *cis*-elements, and expression profiles in different tissues. The results would be significant for further analyzing the function of *CaDnaJ* members and illuminating the evolutionary relationship in pepper.

Since the first DnaJ proteins were isolated from *E. Coli* as 41 kDa Hsps (Georgopoulos et al., 1980), many DnaJ proteins have been subsequently reported in other life species (Bukau and Horwich, 1998; Miernyk, 2001; Walsh et al., 2004; Craig et al.,

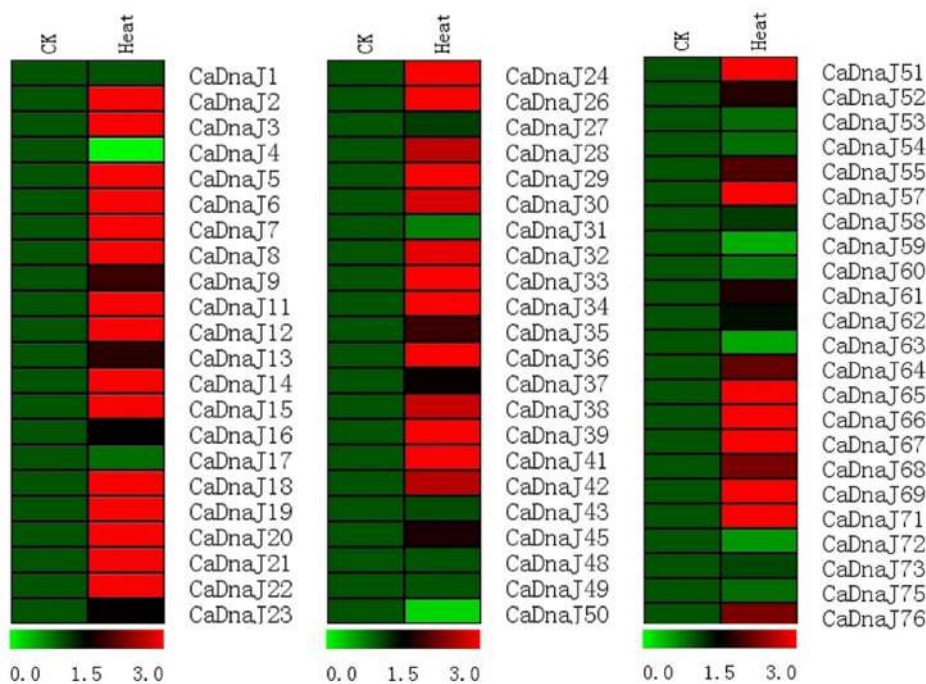


FIGURE 4 | Gene expression profiles of *CaDnaJ* genes in response to heat stress treatment. The expression levels of these *CaDnaJs* under high temperature stress treatment were tested using qRT-PCR. Green, black, and red elements indicate low, regular, and high signal intensity, respectively.

2006). Generally, DnaJ proteins contained one to four domains (J-domain, G/F-domain, zinc finger domains and less conserved C-terminal) (Silver and Way, 1993). Initially, the DnaJ proteins were classified into three groups (A, B, C) based on domain composition (Cheetham and Caplan, 1998; Miernyk, 2001). In this study, more complex structure of DnaJ genes was observed in pepper. For example, the HPD tripeptide which was crucial for J-domain function (Kampinga and Craig, 2010) was not found in *CaDnaJ23, 28, 37, 53* and *73*. Therefore, given the high diversity of *CaDnaJ* genes, a more systematic classification was proposed in our study. A total of 76 *CaDnaJ* genes were classified into five groups (A, B, C, D and E). Group A was characterized by the J-domain, zinc finger domains and a less conserved C-terminal. Group B were lack of the zinc finger domains but contained the J-domain and a less conserved C-terminal. Group C only comprised the J-domain. Group D would both have the J-domain and zinc finger domains but lack of C-terminal, and group E which have been described as J-like proteins with the J-domain lack of HPD motif (Table 1 and Supplementary Table S2).

It was reported that gene duplication was become one of the primary evolution forces during the processes of genetic systems and genomes (Moore and Purugganan, 2003). In our study, chromosome location showed that all these *CaDnaJ* genes were mapped unevenly on 12 pepper chromosomes (Figure 1). Six of them were involved in gene duplication, including tandem duplication and segmental duplication (Figure 1). One tandem duplication event (*CaDnaJ41/CaDnaJ42*) and two segmental duplication events (*CaDnaJ04/CaDnaJ44*, and *CaDnaJ19/CaDnaJ67*) were observed. These results indicated

that both tandem duplication and segmental duplication played role in expansion of the *CaDnaJ* gene family in pepper.

It has been demonstrated that *cis*-elements participated in responding multiple abiotic and biotic stresses. For instance, several *cis*-elements, such as ABRE, DRE, CRT, SARE and SURE, had been identified for responding to ABA, dehydration, cold, SA, and sulfur, respectively (Sakuma et al., 2002; Maruyama-Nakashita et al., 2005; Shi et al., 2010; Osakabe et al., 2014; Feng et al., 2016). In this paper, we identified *cis*-elements in the promoter regions of *CaDnaJ* genes using the PlantCARE server (Lescot et al., 2002). Two major groups of *cis*-elements were observed, including stress-responsive and hormone-responsive. The former contained HSE, LTR, and TC-rich *cis*-elements, which was responsive to heat, low-temperature, and defense, respectively. The latter was composed of TCA-element, TGA-element, GARE-motif, CGTCA-motif, ABRE and ERE, which was responsive to SA, IAA, GA, MeJA, ABA and ethylene, respectively (Figure 2 and Supplementary Table S3). These results implied that *CaDnaJ* genes could be involved in the process of plant respond to multiple stresses. Especially, one of the most important *cis*-element, HSEs, which kept AAAAATTTTC as the core sequence, accounted for 13.64% of all the *cis*-elements. As we all known that the expression of Hsp was controlled by heat shock transcription factors that bind to HSEs in the promoter region of the Hsp genes (Hancock et al., 2009). A total of 49 (66.21%) *CaDnaJ* genes have HSEs in the promoter region. Thus, the results will contribute to further understand the vital function role of *CaDnaJ* genes under HS condition in the further.

To obtain more insights into the expression profiles of *CaDnaJ* genes in different tissues, RNA-seq data were acquired from leaf, root, stem and different stage of pericarp (Kim et al., 2014). Based on RNA-seq, we found that all these *CaDnaJ* genes exhibited three different expression patterns: (1) barely expression or too low expression level to detect; (2) constitutive expression; (3) tissue-specific expression patterns. The expression of these *CaDnaJ* genes differed in tissues tested, indicating that the *CaDnaJ* proteins may play different functional roles. Expression of some *CaDnaJ* genes showed tissue- and development-specific in root, stem, leaf and pericarp, suggested that they may participated in growth and development of pepper. In addition, we also found that 10 genes (*CaDnaJ06*, 08, 21, 27, 28, 47, 50, 55, 56 and 76) were highly expressed in all the tested tissues, implying that they might be involved in specific housekeeping action under normal growth conditions in pepper (Figure 3).

It has been known that plant growth and development were frequently affected by biotic and abiotic stresses under natural conditions (Xia et al., 2014). Previous researchers had reported that the DnaJ protein was involved in plant response to heat and drought stresses (Xia et al., 2014; Wang et al., 2015). To further comprehend the putative roles of *CaDnaJ* genes in pepper response to HS, expressions patterns of *CaDnaJ* genes under HS treatment conditions were analyzed by qRT-PCR. Expression analysis revealed that most *CaDnaJ* genes were changed in response to HS (Figure 4). Among them, almost half of these *CaDnaJ* genes were up-regulated for three folds. We also found that there are multiple types and numbers of *cis*-elements in these *CaDnaJs* promoter, which is reported to involved in abiotic stresses (Feng et al., 2016), including TC-rich, HSEs, MBS motif. All these results suggested that these *CaDnaJ* genes could involved in plant response to HS.

REFERENCES

- Agarwal, M., Katiyar-Agarwal, S., and Grover, A. (2002). Plant Hsp100 proteins: structure, function and regulation. *Plant Sci.* 163, 397–405.
- Bekh-Ochir, D., Shimada, S., Yamagami, A., Kanda, S., Ogawa, K., Nakazawa, M., et al. (2013). A novel mitochondrial DnaJ/Hsp40 family protein BIL2 promotes plant growth and resistance against environmental stress in brassinosteroid signaling. *Planta* 237, 1509–1525. doi: 10.1007/s00425-013-1859-3
- Bukau, B., and Horwich, A. L. (1998). The Hsp70 and Hsp60 chaperone machines. *Cell* 92, 351–366.
- Caplan, A. J., Cyr, D. M., and Douglas, M. G. (1993). Eukaryotic homologues of *Escherichia coli* DnaJ: a diverse protein family that functions with Hsp70 stress proteins. *Mol. Biol. Cell* 4, 555–563.
- Cheetham, M. E., and Caplan, A. J. (1998). Structure, function and evolution of DnaJ: conservation and adaptation of chaperone function. *Cell Stress Chaperones* 3, 28–36.
- Craig, E. A., Huang, P., Aron, R., and Andrew, A. (2006). The diverse roles of J-proteins, the obligate Hsp70 co-chaperone. *Rev. Physiol. Biochem. Pharmacol.* 156, 1–21.
- Cyr, D. M., Lu, X., and Douglas, M. G. (1992). Regulation of Hsp70 function by a eukaryotic DnaJ homolog. *J. Biol. Chem.* 267, 20927–20931.
- Feng, K., Yu, J., Cheng, Y., Ruan, M., Wang, R., Ye, Q., et al. (2016). The SOD gene family in tomato: identification, phylogenetic relationships, and expression patterns. *Front. Plant Sci.* 7:1279. doi: 10.3389/fpls.2016.01279
- Fristedt, R., Williams-Carrie, R., Merchant, S. S., and Barkan, A. (2014). A thylakoid membrane protein harboring a DnaJ-type zinc finger domain is required for photosystem I accumulation in plants. *J. Biol. Chem.* 289, 30657–30667. doi: 10.1074/jbc.M114.587758
- Georgopoulos, C. P., Lundquist-Heil, A., Yochem, J., and Feiss, M. (1980). Identification of the *E. coli* DnaJ gene product. *Mol. Gen. Genet.* 178, 583–588. doi: 10.1007/BF00337864
- Glazebrook, J. (1999). Genes controlling expression of defense responses in *Arabidopsis*. *Curr. Opin. Plant Biol.* 2, 280–286. doi: 10.1016/S1369-5266(99)80050-8
- Guo, M., Yin, Y. X., Ji, J. J., Ma, B. P., Lu, M. H., and Gong, Z. H. (2014). Cloning and expression analysis of heat-shock transcription factor gene *CaHsfA2* from pepper (*Capsicum annuum* L.). *Genet. Mol. Res.* 13, 1865–1875. doi: 10.4238/2014.March.17.14
- Gupta, S. C., Sharma, A., Mishra, M., Mishra, R. K., and Chowdhuri, D. K. (2010). Heat shock proteins in toxicology: how close and how far? *Life Sci.* 86, 377–384. doi: 10.1016/j.lfs.2009.12.015
- Hancock, M. K., Xia, M., Frey, E. S., Sakamuru, S., and Bi, K. (2009). HTS-compatible β-lactamase transcriptional reporter gene assay for interrogating the heat shock response pathway. *Curr. Chem. Genomics* 3, 1–6. doi: 10.2174/1875397300903010001
- Howe, E., Holton, K., Nair, S., Schlauch, D., Sinha, R., and Quackenbush, J. (2010). “Mev: multi experiment viewer,” in *Biomedical Informatics for Cancer Research*, ed. M. F. Ochs (New York, NY: Springer), 267–277.
- Huang, S., Gao, Y., Liu, J., Peng, X., Niu, X., Fei, Z., et al. (2012). Genome-wide analysis of WRKY transcription factors in *Solanum lycopersicum*. *Mol. Genet. Genomics* 287, 495–513. doi: 10.1007/s00438-012-0696-6
- Jelenska, J., Yao, N., Vinatzer, B. A., Wright, C. M., Brodsky, J. L., and Greenberg, J. T. (2007). A J domain virulence effector of *Pseudomonas syringae* remodels host chloroplasts and suppresses defenses. *Curr. Biol.* 17, 499–508. doi: 10.1016/j.cub.2007.02.028

AUTHOR CONTRIBUTIONS

Conceived and designed the experiments: FF and YK. Performed the experiments: XY, XC, and YC. Analyzed the data: FF and YK. Wrote the paper: FF. All authors have read and approved the manuscript.

ACKNOWLEDGMENTS

The research is supported by National Natural Science Foundation of China (No. 31301767), Foundation for Distinguished Young Talents in Higher Education of Guangdong, China (No. YQ2015028), and Modern agricultural industry technology system construction of Guangdong, China (No. 2016LM1109).

SUPPLEMENTARY MATERIAL

The Supplementary Material for this article can be found online at: <http://journal.frontiersin.org/article/10.3389/fpls.2017.00689/full#supplementary-material>

TABLE S1 | Specific primer for qRT-PCR of each *CaDnaJ* gene.

TABLE S2 | Multiple sequence alignment of the pepper *CaDnaJs*. The sequences of 76 *CaDnaJs* were aligned according to the classification. Names of all the 76 members are showed on the left side of the figure. Conserved amino acid residues are highlighted in black. The sequences which boxed in red rectangle represented the conserved HPD motif, and sequences in yellow rectangle were zinc finger domains.

TABLE S3 | Stress-related *cis*-elements in pepper *CaDnaJ* promoters.

- Kampinga, H. H., and Craig, E. A. (2010). The HSP70 chaperone machinery: J proteins as drivers of functional specificity. *Nat. Rev. Mol. Cell Biol.* 11, 579–592. doi: 10.1038/nrm2941
- Kim, S., Park, M., Yeom, S. I., Kim, Y. M., Lee, J. M., Lee, H. A., et al. (2014). Genome sequence of the hot pepper provides insights into the evolution of pungency in *Capsicum* species. *Nat. Genet.* 46, 270–278. doi: 10.1038/ng.2877
- Kong, F., Deng, Y., Wang, G., Wang, J., Liang, X., and Meng, Q. (2014a). LeCDJ1, a chloroplast DnaJ protein, facilitates heat tolerance in transgenic tomatoes. *J. Integr. Plant Biol.* 56, 63–74. doi: 10.1111/jipb.12119
- Kong, F., Deng, Y., Zhou, B., Wang, G., Wang, Y., and Meng, Q. (2014b). A chloroplast-targeted DnaJ protein contributes to maintenance of photosystem II under chilling stress. *J. Exp. Bot.* 65, 143–158. doi: 10.1093/jxb/ert357
- Kotak, S., Larkindale, J., Lee, U., von Koskull-Doring, P., Vierling, E., and Scharf, K. D. (2007). Complexity of the heat stress response in plants. *Curr. Opin. Plant Biol.* 10, 310–316. doi: 10.1016/j.pbi.2007.04.011
- Larkin, M. A., Blackshields, G., Brown, N. P., Chenna, R., McGettigan, P. A., McWilliam, H., et al. (2007). Clustal W and Clustal X version 2.0. *Bioinformatics* 23, 2947–2948. doi: 10.1093/bioinformatics/btm404
- Lescot, M., Déhais, P., Thijss, G., Marchal, K., Moreau, Y., Van de Peer, Y., et al. (2002). PlantCARE, a database of plant *cis*-acting regulatory elements and a portal to tools for in silico analysis of promoter sequences. *Nucleic Acids Res.* 30, 325–327. doi: 10.1093/nar/30.1.325
- Li, Z. W., Li, X., Yu, Q. Y., Xiang, Z. H., Kishino, H., and Zhang, Z. (2009). The small heat shock protein (sHSP) genes in the silkworm, *Bombyx mori*, and comparative analysis with other insects HSP genes. *BMC Evol. Biol.* 9:215. doi: 10.1186/1471-2148-9-215
- Liu, R. H., and Meng, J. L. (2003). MapDraw: a Microsoft excel macro for drawing genetic linkage maps based on given genetic linkage data. *Hereditas* 25, 317–321.
- Livak, K. J., and Schmittgen, T. D. (2001). Analysis of relative gene expression data using real-time quantitative PCR and the $2^{-\Delta\Delta Ct}$ method. *Methods* 25, 402–408. doi: 10.1006/meth.2001.1262
- Lopes-Caitar, V. S., de Carvalho, M. C., Darben, L. M., Kuwahara, M. K., Nepomuceno, A. L., Dias, W. P., et al. (2013). Genome-wide analysis of the *Hsp20* gene family in soybean: comprehensive sequence, genomic organization and expression profile analysis under abiotic and biotic stresses. *BMC Genomics* 14:577. doi: 10.1186/1471-2164-14-577
- Maruyama-Nakashita, A., Nakamura, Y., Watanabe-Takahashi, A., Inoue, E., Yamaya, T., and Takahashi, H. (2005). Identification of a novel *cis*-acting element conferring sulfur deficiency response in *Arabidopsis* roots. *Plant J.* 42, 305–314. doi: 10.1111/j.1365-313X.2005.02363.x
- Miernyk, J. A. (2001). The J-domain proteins of *Arabidopsis thaliana*: an unexpectedly large and diverse family of chaperones. *Cell Stress Chaperones* 6, 209–218.
- Moore, R. C., and Purugganan, M. D. (2003). The early stages of duplicate gene evolution. *Proc. Natl. Acad. Sci. U.S.A.* 100, 15682–15687. doi: 10.1073/pnas.2535513100
- Mulaudzi-Masuku, T., Mutepe, R. D., Mukhoro, O. C., Faro, A., and Ndimba, B. (2015). Identification and characterization of a heat-inducible *Hsp70* gene from *Sorghum bicolor* which confers tolerance to thermal stress. *Cell Stress Chaperones* 20, 793–804. doi: 10.1007/s12192-015-0591-2
- Ohtsuka, K., and Hata, M. (2000). Mammalian HSP40/DNAJ homologs: cloning of novel cDNAs and a proposal for their classification and nomenclature. *Cell Stress Chaperones* 5, 98–112.
- Osakabe, Y., Yamaguchi-Shinozaki, K., Shinozaki, K., and Tran, L. S. P. (2014). ABA control of plant macroelement membrane transport systems in response to water deficit and high salinity. *New Phytol.* 202, 35–49. doi: 10.1111/nph.12613
- Qin, C., Yu, C., Shen, Y., Fang, X., Chen, L., Min, J., et al. (2014). Whole-genome sequencing of cultivated and wild peppers provides insights into *Capsicum* domestication and specialization. *Proc. Natl. Acad. Sci. U.S.A.* 111, 5135–5140. doi: 10.1073/pnas.1400975111
- Qiu, X. B., Shao, Y. M., Miao, S., and Wang, L. (2006). The diversity of the DnaJ/Hsp40 family, the crucial partners for Hsp70 chaperones. *Cell. Mol. Life Sci.* 63, 2560–2570. doi: 10.1007/s00018-006-6192-6
- Ritossa, F. (1962). A new puffing pattern induced by temperature shock and DNP in *Drosophila*. *Experientia* 18, 571–573. doi: 10.1007/BF02172188
- Sakuma, Y., Liu, Q., Dubouzet, J. G., Abe, H., Shinozaki, K., and Yamaguchi-Shinozaki, K. (2002). DNA-binding specificity of the ERF/AP2 domain of *Arabidopsis* DREBs, transcription factors involved in dehydration-and cold-inducible gene expression. *Biochem. Biophys. Res. Commun.* 290, 998–1009. doi: 10.1006/bbrc.2001.6299
- Sarkar, N. K., Kim, Y. K., and Grover, A. (2009). Rice sHsp genes: genomic organization and expression profiling under stress and development. *BMC Genomics* 10:393. doi: 10.1186/1471-2164-10-393
- Shi, Z., Maximova, S. N., Liu, Y., Verica, J., and Guiltinan, M. J. (2010). Functional analysis of the *Theobroma cacao NP1* gene in *Arabidopsis*. *BMC Plant Biol.* 10:248. doi: 10.1186/1471-2229-10-248
- Silver, P. A., and Way, J. C. (1993). Eukaryotic DnaJ homologs and the specificity of Hsp70 activity. *Cell* 74, 5–6.
- Vierling, E. (1991). The roles of heat shock proteins in plants. *Annu. Rev. Plant Biol.* 42, 579–620. doi: 10.1146/annurev.pp.42.060191.003051
- Walsh, P., Bursac, D., Law, Y. C., Cyr, D., and Lithgow, T. (2004). The J-protein family: modulating protein assembly, disassembly and translocation. *EMBO Rep.* 5, 567–571. doi: 10.1038/sj.emboj.7400172
- Wan, H., Yuan, W., Ruan, M., Ye, Q., Wang, R., Li, Z., et al. (2011). Identification of reference genes for reverse transcription quantitative real-time PCR normalization in pepper (*Capsicum annuum* L.). *Biochem. Biophys. Res. Commun.* 416, 24–30. doi: 10.1016/j.bbrc.2011.10.105
- Wang, G. D., Cai, G. H., Kong, F. Y., Deng, Y. S., Ma, N. N., and Meng, Q. W. (2014). Overexpression of tomato chloroplast-targeted DnaJ protein enhances tolerance to drought stress and resistance to *Pseudomonas solanacearum* in transgenic tobacco. *Plant Physiol. Biochem.* 82, 95–104. doi: 10.1016/j.plaphy.2014.05.011
- Wang, G. D., Kong, F. Y., Zhang, S., Meng, X., Wang, Y., and Meng, Q. W. (2015). A tomato chloroplast-targeted DnaJ protein protects Rubisco activity under heat stress. *J. Exp. Bot.* 66, 3027–3040. doi: 10.1093/jxb/erv102
- Wang, W., Vinocur, B., Shoseyov, O., and Altman, A. (2004). Role of plant heat-shock proteins and molecular chaperones in the abiotic stress response. *Trends Plant Sci.* 9, 244–252. doi: 10.1016/j.tplants.2004.03.006
- Wei, K. F., Chen, J., Chen, Y. F., Wu, L. J., and Xie, D. X. (2012). Molecular phylogenetic and expression analysis of the complete WRKY transcription factor family in maize. *DNA Res.* 19, 153–164. doi: 10.1093/dnares/dsr048
- Wei, Y., Wan, H., Wu, Z., Wang, R., Ruan, M., Ye, Q., et al. (2016). A comprehensive analysis of carotenoid cleavage dioxygenases genes in *Solanum lycopersicum*. *Plant Mol. Biol. Rep.* 34, 512–523. doi: 10.1007/s11105-015-0943-1
- Xia, Z., Zhang, X., Li, J., Su, X., and Liu, J. (2014). Overexpression of a tobacco J-domain protein enhances drought tolerance in transgenic *Arabidopsis*. *Plant Physiol. Biochem.* 83, 100–106. doi: 10.1016/j.plaphy.2014.07.023

Conflict of Interest Statement: The authors declare that the research was conducted in the absence of any commercial or financial relationships that could be construed as a potential conflict of interest.

Copyright © 2017 Fan, Yang, Cheng, Kang and Chai. This is an open-access article distributed under the terms of the Creative Commons Attribution License (CC BY). The use, distribution or reproduction in other forums is permitted, provided the original author(s) or licensor are credited and that the original publication in this journal is cited, in accordance with accepted academic practice. No use, distribution or reproduction is permitted which does not comply with these terms.



Endoplasmic Reticulum Stress Response in *Arabidopsis* Roots

Yueh Cho^{1,2,3} and Kazue Kanehara^{1,2,4,5*}

¹ Institute of Plant and Microbial Biology, Academia Sinica, Taipei, Taiwan, ² Molecular and Biological Agricultural Sciences Program, Taiwan International Graduate Program, Academia Sinica and National Chung-Hsing University, Taipei, Taiwan,

³ Graduate Institute of Biotechnology, National Chung-Hsing University, Taichung, Taiwan, ⁴ Biotechnology Center, National Chung-Hsing University, Taichung, Taiwan, ⁵ Muroran Institute of Technology, Muroran, Japan

Roots are the frontier of plant body to perceive underground environmental change. Endoplasmic reticulum (ER) stress response represents circumvention of cellular stress caused by various environmental changes; however, a limited number of studies are available on the ER stress responses in roots. Here, we report the tunicamycin (TM)-induced ER stress response in *Arabidopsis* roots by monitoring expression patterns of immunoglobulin-binding protein 3 (BiP3), a representative marker for the response. Roots promptly responded to the TM-induced ER stress through the induction of similar sets of ER stress-responsive genes. However, not all cells responded uniformly to the TM-induced ER stress in roots, as BiP3 was highly expressed in root tips, an outer layer in elongation zone, and an inner layer in mature zone of roots. We suggest that ER stress response in roots has tissue specificity.

OPEN ACCESS

Edited by:

Hanjo A. Hellmann,
Washington State University, USA

Reviewed by:

Alessandro Vitale,
National Research Council, Italy
Zhaojun Ding,
Shandong University, China

*Correspondence:

Kazue Kanehara
kanehara@gate.sinica.edu.tw

Specialty section:

This article was submitted to
Plant Cell Biology,
a section of the journal
Frontiers in Plant Science

Received: 11 August 2016

Accepted: 24 January 2017

Published: 01 March 2017

Citation:

Cho Y and Kanehara K (2017)
Endoplasmic Reticulum Stress Response in *Arabidopsis* Roots.

Front. Plant Sci. 8:144.
doi: 10.3389/fpls.2017.00144

INTRODUCTION

Roots are the frontier of plant body to perceive underground environmental change. In response to environmental stimuli, a crucial set of molecular processes is induced that maintains cellular homeostasis and thus circumvents fatal defects caused by the stresses. Among various organelles involved in the cellular homeostasis, the ER plays a decisive role in protein folding and secretion.

The ER is the gateway for the eukaryotic protein secretory pathway. Secretory proteins are translocated into the ER and enter protein-folding cycles to fold and assemble themselves (Anelli and Sitia, 2008). Only properly folded proteins are allowed to leave the ER by a surveillance system, collectively termed the ER quality control. The ER quality control is well-conserved molecular mechanisms among eukaryotic cells including animals, yeasts and plants (Iwata and Koizumi, 2005, 2012; Howell, 2013). When aberrant proteins are accumulated in the ER, the ER quality control recognizes these aberrant proteins and responds to maintain the ER homeostasis using multiple strategies such as UPR and ER-associated degradation (ERAD) (Kanehara et al., 2007; Walter and Ron, 2011; Ruggiano et al., 2014). The ER membrane-localized ribonuclease inositol-requiring enzyme 1 (IRE1) is one of major signal transducers in the UPR. The IRE1 senses protein-folding status in the ER and transmits signals into the nuclei by catalyzing unconventional cytoplasmic splicing of *bZIP60* mRNA in plants (*XBP1* in mammals and *HAC1* in yeasts) followed by activation of UPR target genes including a molecular chaperone BiP (Nagashima et al., 2011; Walter and Ron, 2011). BiP is one of the most abundant chaperones in the ER lumen and is thought to bind nascent

Abbreviations: ER stress, endoplasmic reticulum stress; TM, tunicamycin; BiP, immunoglobulin-binding protein; UPR, unfolded protein response.

peptides to prevent protein aggregation. BiPs belong to the heat shock protein 70 family that binds ATP and operates in conjunction with J-domain-containing proteins (J proteins) (Fewell et al., 2001). Arabidopsis genome encodes three *BiP* genes, *BiP1* (At5g28540), *BiP2* (At5g42020), and *BiP3* (At1g09080) (Noh et al., 2003). *BiP1* and *BiP2* encode ubiquitously expressed proteins whose amino acid sequences are 99% identical to each other. *BiP3* encodes a less conserved protein, whose expression is limited under ER stress conditions in young seedlings (Noh et al., 2003). BiPs are also master regulators of the ER stress response in Arabidopsis (Srivastava et al., 2013). Recent studies showed that *BiP3* functions in pollen development and female gametogenesis (Maruyama et al., 2014, 2015).

Extensive studies across different model organisms have revealed details of molecular mechanisms underlying the ER stress response. In plant research, however, ER stress response is an emerging subject despite its high relevance to general plant stress response studies (Liu and Howell, 2010). In addition to the conserved molecular mechanisms, recent studies have suggested that plants may have plant-specific ER stress responses, involving heterotrimeric G proteins and phosphoinositide signaling (Wang et al., 2007; Chen and Brandizzi, 2012; Kanehara et al., 2015b). Our understanding about the molecular mechanisms of the ER stress response in plants has been based mostly on the studies using whole Arabidopsis seedlings. Because root biomass is marginal to the total seedling biomass, effect of root-specific changes may be diluted to be non-measurable in the whole seedling sample even if the root and shoot differentially responds to the ER stress. In fact, previous studies explored ER stress responses in roots of various plant species. For example, the tissue-specific transcriptional regulation of soybean *BiPs*, *gsBiP6* and *gsBiP9* in transgenic *Nicotiana tabacum* plants was reported using *gsBiPs* promoter-GUS chimeric reporter genes (Buzeli et al., 2002). In roots of *Pisum sativum*, the expression levels of *BiP-D*, *bZIP28*, and *bZIP60* were elevated during tungsten treatment, which is known to affect plant growth (Adamakis et al., 2011). In addition, rice *OsBiPs* and its co-chaperones, *OsERdj5*, were transcriptionally upregulated under the ER stress conditions in roots of rice seedlings (Ohta et al., 2013). However, little is known about a detailed molecular mechanism of ER stress response in roots despite that root is an important organ to perceive environmental stresses. Although tissue specificity of the UPR in plants has been investigated in the gametophyte development (Maruyama et al., 2010, 2014; Deng et al., 2013), it remains elusive whether an individual cells of multicellular organisms responds uniformly or differentially to the ER stress caused by external environmental stresses. The Arabidopsis root is an excellent model to investigate tissue type- and cell type-specific response *in vivo* because it is a transparent organ and each tissue/cell type has been characterized well.

In an effort to explore the ER stress response in the plant root system and address tissue-specific response in an intact multicellular organism, current study investigated ER stress response in Arabidopsis roots. To monitor the ER stress responses, a well-described UPR gene *BiP3* has been employed because of the extremely low expression under non-stress condition but acute induction upon ER stress (Noh et al., 2003;

Srivastava et al., 2013; Cho et al., 2015). Based on the time-course observation of stable transgenic plant expressing the *ProBiP3:BiP3-GUS-HDEL* or *ProBiP3:mRFP*, we found that *BiP3* was differentially expressed in root under the ER stress condition: the root tip including columella, outer layers in elongation zone and inner layers in mature zone were highly responsive to the ER stress. Our results suggest that the ER stress response has tissue-type and cell-type specificity and not all cells may respond uniformly to the ER stress in the Arabidopsis roots.

MATERIALS AND METHODS

Plant Materials and Growth Condition

Arabidopsis plants (Columbia-0 ecotype) were grown under continuous light at 22°C. Murashige and Skoog (MS) media was used at half-strength concentration for plant culture (Murashige and Skoog, 1962). Seeds of *bip3-1* (SALK_024133) were obtained from Nottingham Arabidopsis Stock Centre (NASC). Homozygous T-DNA mutant plants were isolated by PCR-based genotyping with the specific primers (KK200/KK201, LB1.3/KK201). Position of T-DNA insertion was determined by sequencing to be located within the protein coding sequence of *BiP3* (Figure 3A). For TM treatment, seedlings were immersed in liquid MS media containing 5 µg/ml TM for indicated time. For detection of aggregated proteins, seedlings were immersed in liquid MS media containing 10 mM MG-132 for 16 h. DMSO was used as negative controls for both TM and MG-132 treatments.

Sequence Alignment of BiPs

The amino acid sequences of three *BiP* isoforms were adopted from TAIR database (protein accession numbers: *BiP1*: 1009129411, *BiP2*: 1009134007, and *BiP3*: 5019479994). A multiple alignment of the protein sequences for BiPs was assembled using ClustalW¹ and BoxShade².

Plasmid Vector Construction and Plant Transformation

A 4 kbp fragment of the genomic sequence for *BiP3* was amplified by PCR with oligonucleotide primers KK131 and KK132, and cloned into the pENTR/D-TOPO plasmid vector (Invitrogen, Carlsbad, CA, USA) to obtain pCC38. To create the GUS reporter construct (*ProBiP3:BiP3-GUS-HDEL*), *SmaI* site was inserted at the position immediately before the ER retention sequence HDEL of *BiP3* by PCR-based site directed mutagenesis with primer KK152 (Sawano and Miyawaki, 2000). Then, a GUS cassette was inserted into the *SmaI* site to produce pCC71, which was recombined to a pBGW destination vector by use of LR Clonase (Karimi et al., 2005). The resulting pCC67 was transformed into wild-type (WT) plants via Agrobacterium GV3101-mediated gene transformation. Twenty-four transformed plants were selected by spraying 0.1% Basta solution to the seedlings on soil. The T1 seeds were screened by Basta, and the resistant plants

¹<http://clustalw.ddbj.nig.ac.jp/>

²http://www.ch.embnet.org/software/BOX_form.html

harboring *ProBiP3:BiP3-GUS-HDEL* were selected by PCR-based genotyping with primers (KK98/KK200). *ProBiP3:BiP3-GUS-HDEL* line No. 17 was selected as a representative line for observation. For the fluorescent reporter construct (*ProBiP3:mRFP*), the 0.9 kbp promoter region of *BiP3* was amplified with primers KK131 and KK172, and cloned into pENTR/D-TOPO plasmid vector (Invitrogen, Carlsbad, CA, USA) to obtain pCC76. This was recombined into a destination vector pGWB653 (Nakamura et al., 2010) by use of LR Clonase and the resulting plasmid pCC79 was transformed into WT plants via Agrobacterium GV3101-mediated gene transformation. Then, 16 plants were selected by spraying 0.1% Basta solution to the seedling on soil. The T2 seeds were screened by Basta, and the resistant plants harboring *ProBiP3:mRFP* were selected by PCR-based genotyping with primers (KK202/KK133). *ProBiP3: mRFP* line No. 11 was selected as a representative line and used for observation by confocal laser-scanning microscopy.

The sequence of primers used were listed in Supplementary Table S1.

Quantitative RT-PCR (qRT-PCR)

Quantitative RT-PCR analysis was performed as previously described using total RNA was isolated from 7-day-old seedlings (Lin et al., 2015). The means and standard deviations of $\Delta\Delta CT$ were calculated from three independent biological replicates for whole seedlings. Six independent biological replicates were used for roots. The primers used for qRT-PCR are listed in Supplementary Table S1.

Histochemical GUS Staining

Gus staining was performed as previously described by Kanehara et al. (2015a). Briefly, seedling samples were immersed in GUS staining solution (10 mM EDTA, 5 mM potassium ferricyanide, 5 mM potassium ferrocyanide, 0.1% [w/v] Triton

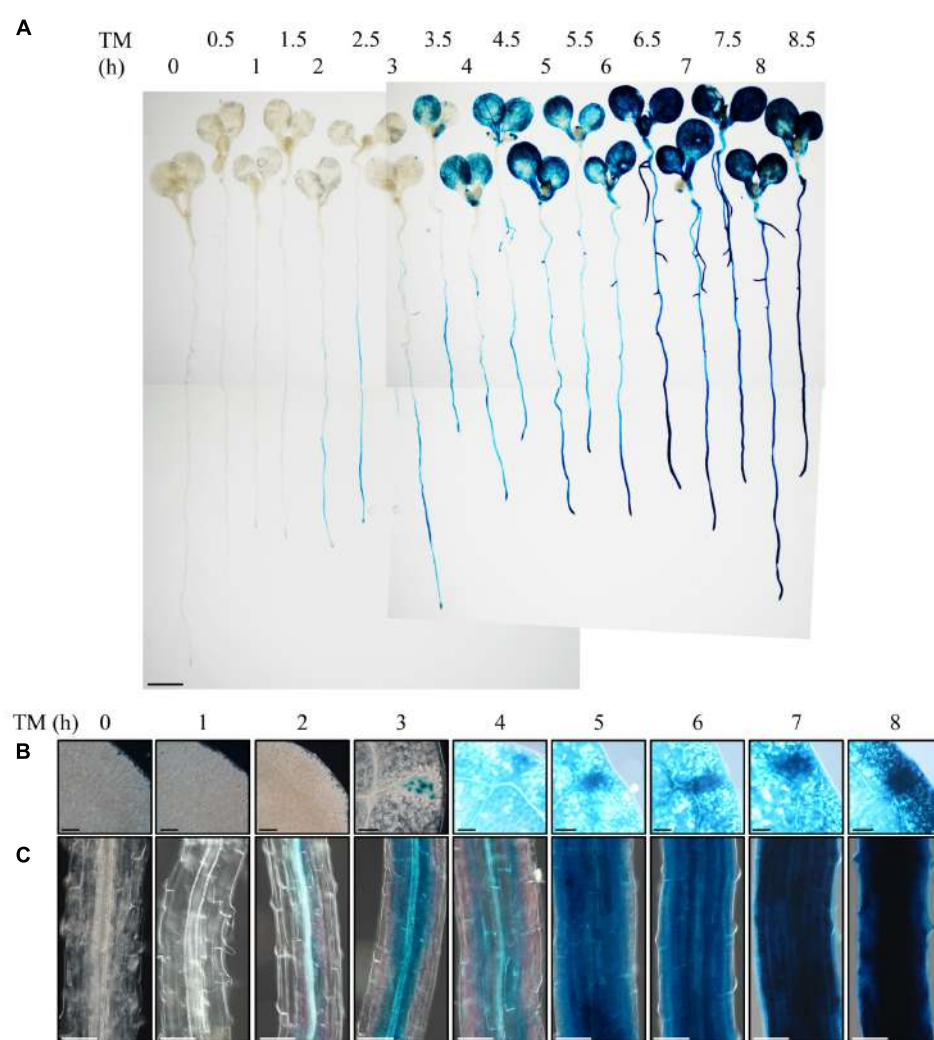
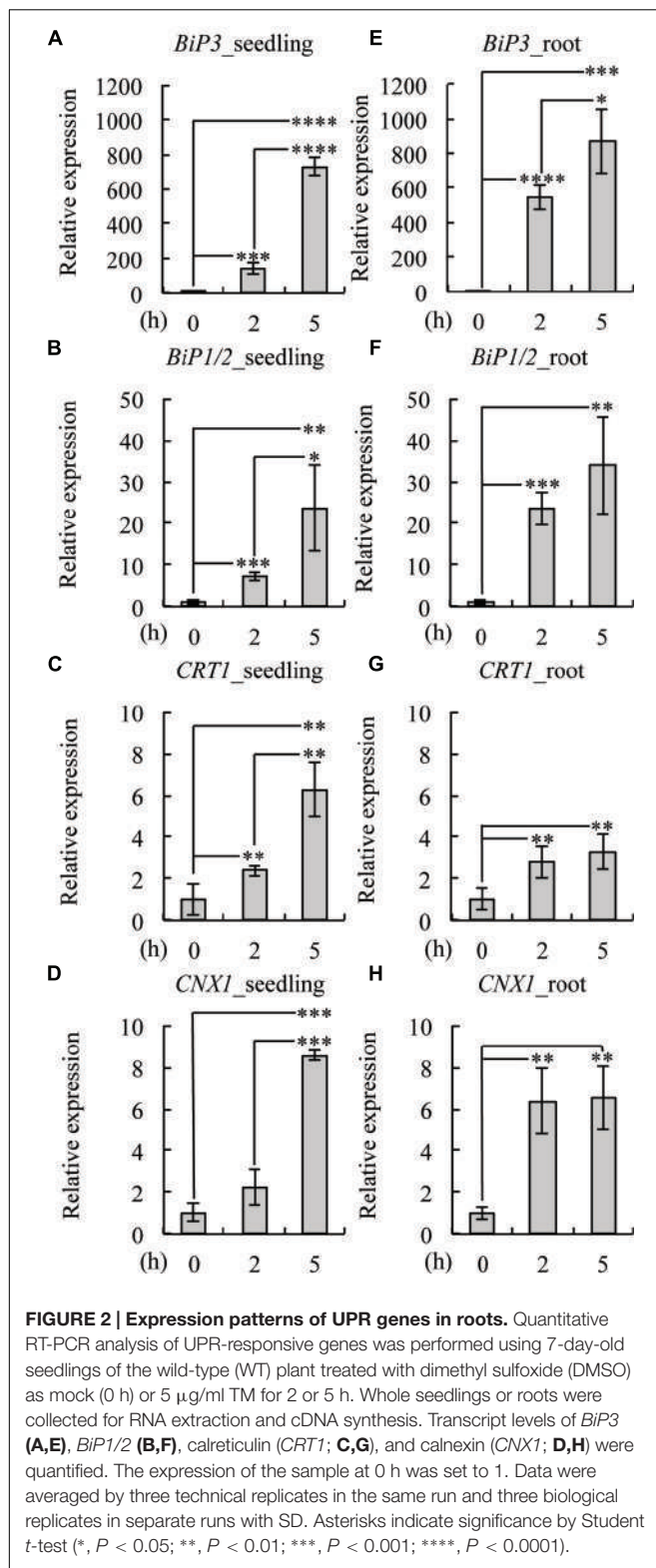
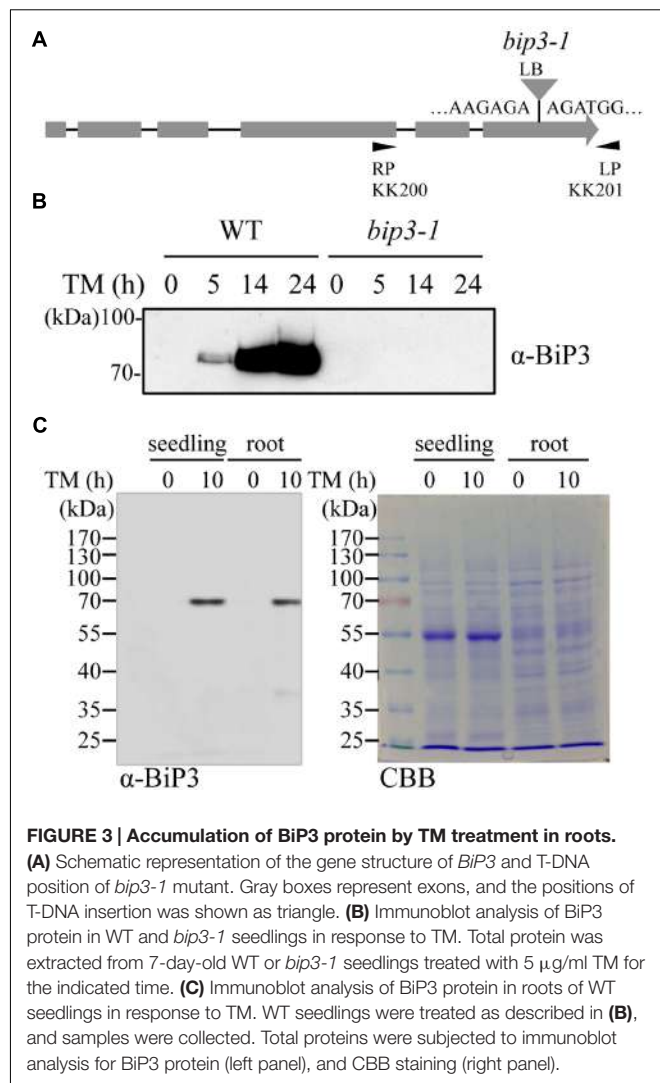


FIGURE 1 | Observation of the ER stress response in root with the *BiP3-GUS* reporter system. Seven-day-old seedlings of *ProBiP3:BiP3-GUS* were treated with 5 μ g/ml TM for time indicated and GUS staining was performed. **(A)** Whole seedlings or magnified view of the cotyledon **(B)**, and the maturation zone of roots **(C)**. Scale bars: 1 mm **(A)**; 100 μ m **(B,C)**.



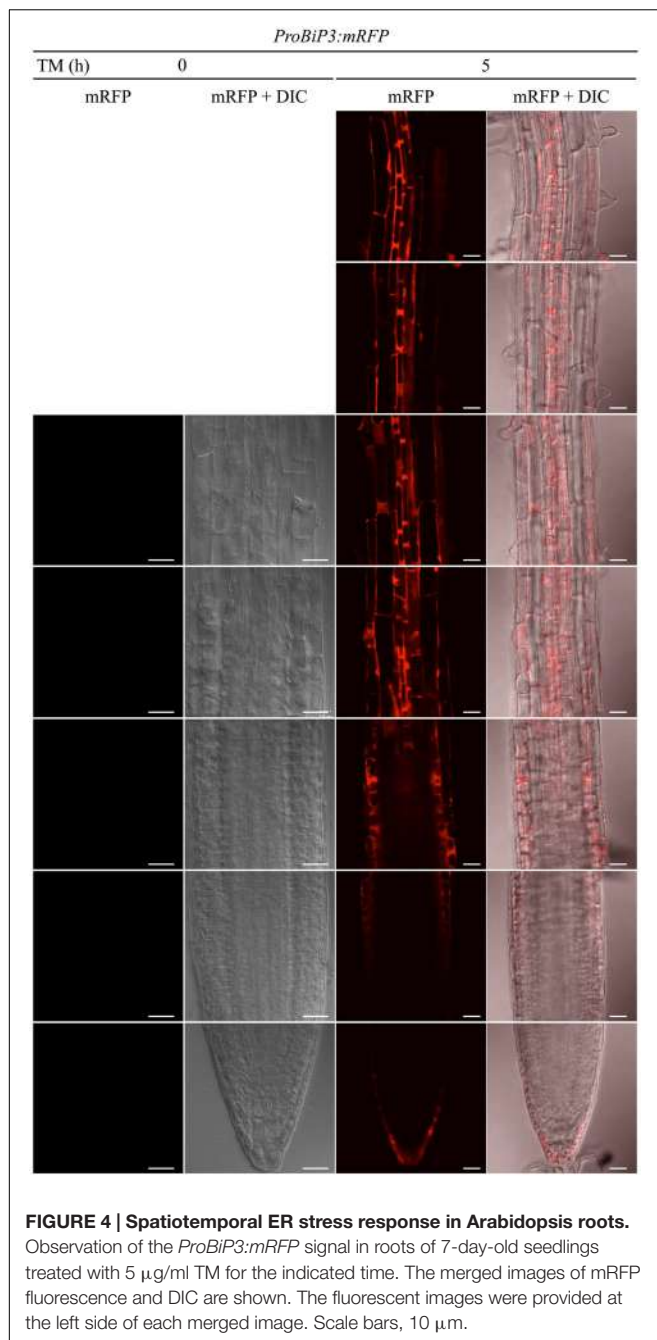
X-100, and 0.5 mg/ml X-Gluc [5-bromo-4-chloro-3-indolyl-β-D-glucuronide] in 100 mM phosphate buffer), and incubated at 37°C. Then, the reaction was stopped by replacing the solution with 70% ethanol. For colored tissues, pigments were removed



by immersing the tissue in 6:1 (v:v) ethanol : acetic acid. The images were obtained using a stereomicroscope (Zeiss Stemi 2000) equipped with a Nikon D7000 camera and an upright microscope (Zeiss Axio Imager A2) equipped with a Canon EOS 500D camera.

Preparation of Anti-BiP3 Antibody and Immunoblotting

To avoid a cross-reaction with BiP1 and BiP2, which show high amino acid similarity to BiP3, a polypeptide consisting of the C-terminal 19 amino acid residues of BiP3, VYEKTEGENEDDDGDDHDE, was synthesized and used to raise an anti-BiP3 polyclonal antibody in rabbits (LTK BioLaboratories, Taoyuan, Taiwan). For immunoblotting, total cell lysate from seedlings or roots was extracted in a lysis buffer [50 mM Tris-HCl (pH6.8), 2% SDS, 10 mM β-mercaptoethanol, 1% v/v protease inhibitor cocktail (Sigma)]. Protein samples were separated by 10% acrylamide SDS-PAGE and transferred to a polyvinylidene difluoride membrane for immunoblotting with



rabbit polyclonal anti-BiP3 antibodies; 1:2,000, followed by goat anti-rabbit IgG peroxidase conjugates (Santa Cruz); 1:10,000. BiP3 proteins were visualized by use of chemiluminescence detection reagent (SuperSignal West Pico, Pierce) and Image Quant LAS4000 (GE Healthcare). SDS-PAGE gel was also stained with 0.1% Coomassie Brilliant Blue for 1 h at room temperature.

Confocal Laser-Scanning Microscopy

Fluorescence of mRFP in seedlings of *ProBiP3:mRFP* was observed under a microscope (LSM 510 Meta; Carl Zeiss) equipped with Objectives C-Apochromat 40×/1.2-numerical

aperture (NA) and C-Apochromat 63×/1.2-NA. Images were captured using an LSM 510 v3.2 confocal microscope (Carl Zeiss) with filter (543-nm laser, band-pass 560–615 nm). Cell boundaries were visualized by differential interference contrast (DIC) images.

Detection of Aggregated Protein

Aggregated proteins were stained by Proteostat® Aggresome Detection Kit (Enzo: ENZ-51035) according to manufacturer's instruction with a slight modification. Briefly, seedlings after the chemical treatments were fixed in 4% paraformaldehyde in the assay buffer (Proteostat® Aggresome Detection Kit, Enzo) for 30 min at room temperature, which was then washed by phosphate-buffered saline (PBS) three times. Seedlings were transferred into a permeabilizing solution (0.5% Triton X-100, 3 mM EDTA, pH 8) for 30 min. After washing with PBS buffer, seedlings were incubated with Proteostat® dye (Proteostat® Aggresome Detection Kit, Enzo) at 1:5000 dilution for 1 h in the dark.

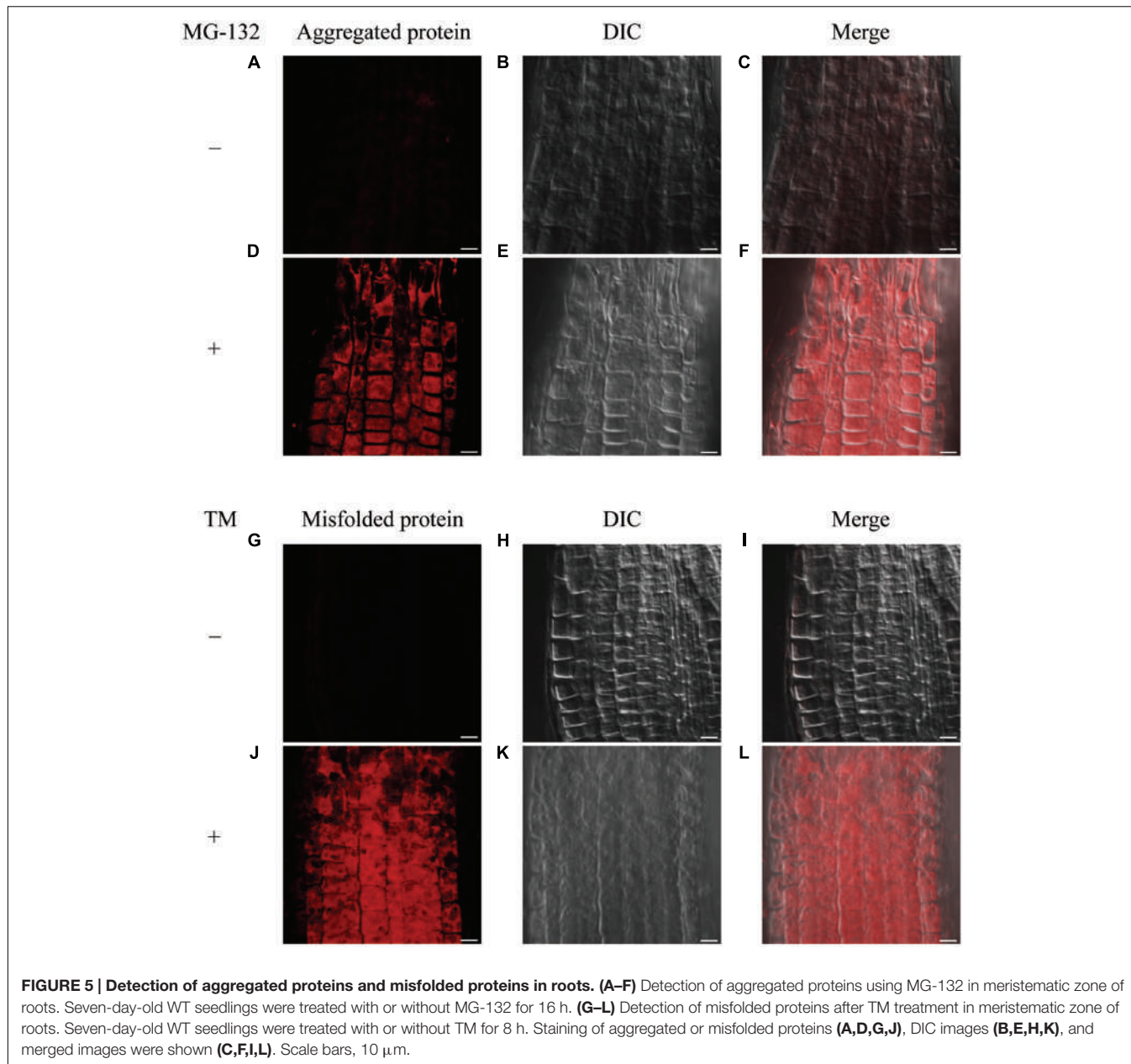
Immunolocalization Analysis of BiP3 and Aggregated Proteins

After chemical treatments, seedlings were fixed in 4% paraformaldehyde (Merck) in PBS for 90 min with vacuum dry. To break down cell walls, the seedlings were incubated with 1.5% Driselase (Sigma) in PBS at 37°C for 50 min. For plasma membrane penetration, the samples were incubated with a PBS solution containing 3% IGEPAL CA-630 (Sigma) and 10% DMSO for 30 min at room temperature. To decrease non-specific binding, samples were blocked in PBS containing 3% BSA for 3 h at room temperature. After overnight incubation with anti-BiP3 antibodies (1:100) at 4°C, samples were washed with PBS six times, and incubated with secondary antibody, goat anti-rabbit Alexa Fluor 488 (1:1,000, Life Technologies) for 3 h at room temperature. To detect aggregated proteins, samples were incubated with Proteostat® dye (Proteostat® Aggresome Detection Kit, Enzo; 1:5000) for 1 h at room temperature. After three times washing by PBS, samples were mounted in a drop of 9:1 (v/v) glycerol: PBS, and observed under a microscope (LSM 510 Meta; Carl Zeiss) equipped with objectives C-Apochromat 40×/1.2-NA and C-Apochromat 63×/1.2-NA. Images were captured using an LSM 510 v3.2 confocal microscope (Carl Zeiss) with filter (488-nm laser, band-pass 505–530 nm) for BiP3, and with filter (543-nm laser, band-pass 560–615 nm) for aggregated proteins. Cell boundaries were visualized by DIC images.

RESULTS

Observation of the ER Stress Response in Roots via the BiP3-GUS Reporter System

To observe the ER stress response in roots of intact plants, we employed *Arabidopsis BiP3* gene as a reporter. *BiP3* is a widely



used marker gene for the ER stress response, whose expression is extremely low at either RNA or protein levels under non-stress conditions but is highly up-regulated upon the ER stress in *Arabidopsis* young seedlings (Noh et al., 2003; Cho et al., 2015). We established a transgenic *Arabidopsis* plant that stably expresses BiP3-GUS fusion protein containing the ER retention signal (HDEL) for ER localization, which is driven by the own promoter (*ProBiP3:BiP3-GUS-HDEL* in WT background). We treated 7-day-old seedlings of the *ProBiP3:BiP3-GUS-HDEL* plants with TM for 0 to 8.5 h and observed the expression of GUS reporter by histochemical staining (Figure 1A). TM inhibits protein N-glycosylation and thus induces ER stress (Helenius and Aebi, 2004). As can be seen, GUS staining emerged

after 2-h treatment mainly at vascular bundles in roots and root tip but no staining in leaves (Figures 1A,C). At 3 h, an obvious staining appeared first in hydathodes of leaves (Figures 1A,B), which was extended to the entire cotyledons at 4 h (Figures 1A,B). In roots, the GUS expression was enhanced from the vasculature to the outer layer by extending the duration of TM treatment (Figure 1C). Despite the exogenous chemical treatment by TM, the first GUS expression was detected in the root vasculatures, an innermost tissue. This observation suggests that roots respond to TM treatment more rapidly than leaves, and that the vasculatures and root tips are the initial sites of TM-induced ER stress response in *Arabidopsis* roots.

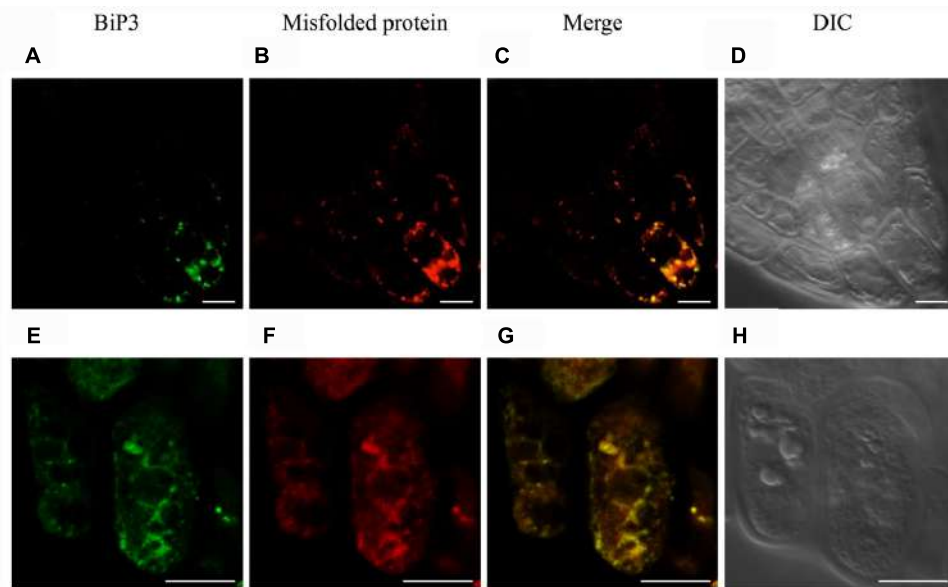


FIGURE 6 | Immunofluorescence analysis of BiP3 and colocalization with misfolded proteins in roots. Four-day-old WT seedlings were treated with TM for 24 h. BiP3 localization detected by anti-BiP3 antibodies (**A,E**), misfolded proteins detected by Aggresome dye ProteoStat® (**B,F**), merged images (**C,G**), and DIC images (**D,H**). Scale bars, 10 μm.

Expression Patterns of UPR Genes in Roots

To investigate whether the same set of UPR genes is induced by TM treatment in roots, we treated 7-day-old WT seedlings with TM and compared the gene expression of *BiP3*, *BiP1/2*, *CALRETICULIN* (*CRT1*: At1g56340), and *CALNEXIN* (*CNX1*: At5g61790) at 2 and 5 h after the TM treatment by qRT-PCR (Figure 2). The expression of all of these genes was induced both in the whole seedlings (Figures 2A–D) and roots (Figures 2E–H) upon TM treatment. These data suggest that a similar set of UPR genes was induced by TM treatment in roots as compared to the whole seedlings. Notably, however, some minor difference was observed including higher fold increase in *BiP3*, *BiP1/2* and *CNX1* at 2 h (Figures 2A,B,D,E,F,H). These results are consistent with the GUS reporter assay (Figure 1), in which roots robustly responded upon TM treatment.

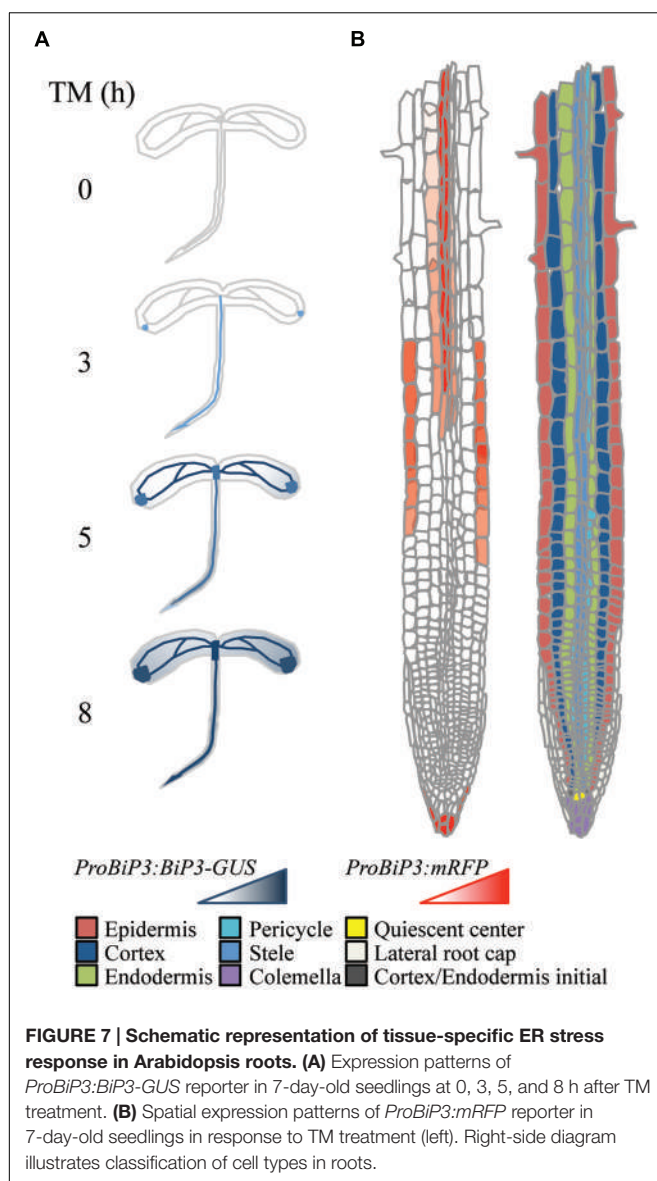
Accumulation of BiP3 Protein by TM Treatment

To detect endogenous BiP3 protein in WT plants, we produced polyclonal anti-BiP3 antibodies against a synthetic peptide corresponding to 19 amino acid residues at C-terminus of BiP3 protein because of low sequence similarity of this region with those in BiP1 and BiP2 (Supplementary Figure S1). To examine the specificity of the antibodies, we extracted total protein from 7-day-old seedlings of the WT and the *bip3-1* mutant (Figure 3A) treated with TM for 5, 14, and 24 h, then performed immunoblot analysis. The *bip3-1* mutant was previously reported as a null mutant (Maruyama et al., 2010). As shown in Figure 3B, a specific band at approximately 75 kDa was detected at 5 h after TM treatment in the WT, whose intensity was further increased

at 14 h and 24 h. Because these bands were not detected in TM-treated *bip3-1* mutant, the result indicated that anti-BiP3 antibodies we raised recognized BiP3 specifically. We detected BiP3 in roots as well as in the whole seedlings treated with TM for 10 h (Figure 3C). Thus, both roots and whole seedlings accumulate endogenous BiP3 in response to TM treatment.

Spatiotemporal ER Stress Response in Arabidopsis Roots

Next, to observe spatiotemporal ER stress responses in intact Arabidopsis roots, we established a transgenic Arabidopsis plant that stably expresses a fluorescent mRFP protein under endogenous *BiP3* promoter (*ProBiP3:mRFP*) in the WT background. The mRFP protein was expected to localize at cytoplasm. No mRFP signals were observed in roots without the TM treatment (at 0 h in Figure 4). Time-course observation of the *ProBiP3:mRFP* plants up to 5 h after TM treatment showed that fluorescent signal first appeared at 3.5 h (Figure 4 and Supplementary Figure S2). At 5-h treatment, obvious signals were detected into the three regions, a root tip in the meristematic zone, an outer layer in the elongation zone and an inner layer in the mature zone (Figure 4). This pattern became more obvious at 8-h treatment (Supplementary Figure S3). At 24 h after TM treatment, fluorescent mRFP signals were strongly detected at inner layers including stele in the mature zone, columella and lateral root cap of the root tip (Supplementary Figure S3) in the meristematic zone. Since we cannot exclude a possibility that time-dependent changes and cell type-specific features of BiP3 detection might in part reflect the kinetics of TM uptake by intact plantlets, we compared mRFP signals of the *ProBiP3:mRFP* plants treated with dithiothreitol (DTT),



another known ER stress inducer. As shown in **Supplementary Figure S4**, the patterns with DTT treatment were similar to those with TM at 5- and 8-h treatments although the intensity of signal was slightly lower than that with TM. These localizations are in agreement with the result of GUS staining (**Figure 1**) at the early time point after TM treatment. Nevertheless, the other cell did not show the mRFP signal at 24 h, suggesting that specific cells may respond to the ER stress in *Arabidopsis* roots.

Distribution of Misfolded Protein via Detection of Aggresome in *Arabidopsis* Roots

It has been known that the accumulation of misfolded protein in the ER triggers the ER stress response. To investigate the distribution of misfolded protein in *Arabidopsis* roots under

ER stress conditions, we first tested detection of an aggresome by use of a commercially available aggresome detection kit (Proteostat® Aggresome Detection Kit, Enzo), which was previously reported to detect aggresome formed by adding proteasome inhibitor MG-132 in mammalian cells as well as plant cultured cells (Kothawala et al., 2012; Nakajima and Suzuki, 2013). When we treated 7-day-old WT seedlings with MG-132 for 16 h, signals for aggregation were detected in root epidermis cells (**Figures 5D–F** and **Supplementary Figures S5A–C**), but not in the cells with mock treatment (**Figures 5A–C**). This result indicates that the assay works for the intact *Arabidopsis* roots. Next, we treated 7-day-old WT seedlings with TM to examine whether this assay detects misfolded proteins under the ER stress condition. As can be seen in (**Figures 5J–L** and **Supplementary Figures S5D–F**), the signals were detected in root epidermal cells treated with TM, but not without the treatment (**Figures 5G–I**). Hence, the assay can be used for the detection of misfolded proteins in *Arabidopsis* roots.

Localization of BiP3 and Misfolded Proteins under the ER Stress Condition

To observe a possible co-localization of misfolded protein and BiP3 under the ER stress in *Arabidopsis* roots, we performed immunofluorescence analysis using anti-BiP3 antibodies and fluorescent-labeled secondary antibodies with the above-mentioned assay to detect misfolded proteins. When the seedlings were treated with TM for 24 h, BiP3 and misfolded proteins co-localized well at columella in root tips (**Figures 6C,G** and **Supplementary Figure S6**), indicating the co-localization of ER stress response represented by BiP3 and misfolded protein accumulation.

DISCUSSION

Current study explored ER stress response in roots of *Arabidopsis*. *BiP3* was more rapidly and intensively induced in root tissues compared to leaves (**Figure 1**). Indeed, the induction of *BiP3* was more significant in roots for not only *BiP3* but also *BiP1/2* after 2 h of TM treatment (**Figure 2**). This rapid up-regulation was also found for *CNX1* (**Figure 2**). Between 2 h and 5 h after TM treatment, the relative fold changes of UPR genes expression were less significant in roots than whole seedlings. Moreover, high abundance in *BiP3* proteins was detected in roots after 10 h of ER stress treatment (**Figure 3C**). Of note, no obvious morphological changes were found in roots during the short-term TM treatment (**Figure 4** and **Supplementary Figure S2**), while the long-term TM treatment is known to cause the root growth defect (Cho et al., 2015; Kanehara et al., 2015b).

Interestingly, *BiP3* was not ubiquitously expressed among different tissues in young seedlings under the ER stress condition. Our GUS reporter assay revealed that *BiP3* is primarily expressed in vascular tissues and apical meristem in roots as well as hydathodes in leaves (**Figure 1**). This observation in roots was further elaborated by *BiP3* promoter reporter assay with mRFP, which not only supports the result of GUS staining but

also detailed the location of *BiP3* expression at root tips in the meristematic zone, the outer layer in the elongation zone and the inner layer in the mature zone (**Figure 4**). In addition, the co-localization of misfolded proteins and *BiP3* was observed in the root tip (**Figure 6**). Although hydathodes, root caps, and root apical meristems are known for their secretory activity, root hair cells that are another highly secretory cells did not show a high *BiP3* expression to the TM-induced ER stress in our observation (Battey et al., 1996; Tsugeki and Fedoroff, 1999; Komarnitsky et al., 2000; Pilot et al., 2004; Preuss et al., 2004; Cole et al., 2014). This suggests that cell-type specific responses do not simply reflect different secretory activity of individual cell types.

Taken together these observations, we propose a schematic model in which a specific response to ER stress is suggested based on the reporter assay of *BiP3* following TM treatment at tissue (**Figure 7A**) or cellular (**Figure 7B**) levels. Molecular mechanisms on the ER stress response have been extensively studied in unicellular models; however, how individual tissues or cells are orchestrated in intact multicellular organisms is an enigma to date. This specific response to TM may correspond to the differential strategy or priority of ER stress response among different tissues, whose mechanistic details await future investigation based on our current study. In conclusion, we suggest that ER stress response in roots has tissue specificity.

AUTHOR CONTRIBUTIONS

KK conceived the research and designed the experiments; YC performed the experiments and analyzed the data; YC and KK wrote the manuscripts; both authors commented on the manuscript and approved the contents.

FUNDING

This study was financially supported by the grants from Institute of Plant and Microbial Biology, Academia Sinica to KK and the JSPS KAKENHI (grant no. 16K07388) to KK.

REFERENCES

- Adamakis, I. D. S., Panteris, E., and Eleftheriou, E. P. (2011). The fatal effect of tungsten on *Pisum sativum* L. root cells: indications for endoplasmic reticulum stress-induced programmed cell death. *Planta* 234, 21–34. doi: 10.1007/s00425-011-1372-5
- Anelli, T., and Sitia, R. (2008). Protein quality control in the early secretory pathway. *EMBO J.* 27, 315–327. doi: 10.1038/sj.emboj.7601974
- Battey, N., Carroll, A., Vankesteren, R., Taylor, A., and Brownlee, C. (1996). The measurement of exocytosis in plant cells. *J. Exp. Bot.* 47, 717–728. doi: 10.1093/jxb/47.6.717
- Buzeli, R. A. A., Cascardo, J. C. M., Rodrigues, L. A. Z., Andrade, M. O., Almeida, R. S., Loureiro, M. E., et al. (2002). Tissue-specific regulation of BiP genes: a cis-acting regulatory domain is required for BiP promoter activity in plant meristems. *Plant Mol. Biol.* 50, 757–771. doi: 10.1023/A:1019994721545
- Chen, Y., and Brandizzi, F. (2012). AtIRE1A/AtIRE1B and AGB1 independently control two essential unfolded protein response pathways in *Arabidopsis*. *Plant J.* 69, 266–277. doi: 10.1111/j.1365-313X.2011.04788.x
- Cho, Y., Yu, C. Y., Iwasa, T., and Kanehara, K. (2015). Heterotrimeric G protein subunits differentially respond to endoplasmic reticulum stress in *Arabidopsis*. *Plant Signal. Behav.* 10:e1061162. doi: 10.1080/15592324.2015.1061162
- Cole, R. A., McInally, S. A., and Fowler, J. E. (2014). Developmentally distinct activities of the exocyst enable rapid cell elongation and determine meristem size during primary root growth in *Arabidopsis*. *BMC Plant Biol.* 14:1594. doi: 10.1186/s12870-014-0386-0
- Deng, Y., Srivastava, R., and Howell, S. H. (2013). Protein kinase and ribonuclease domains of IRE1 confer stress tolerance, vegetative growth, and reproductive development in *Arabidopsis*. *Proc. Natl. Acad. Sci. U.S.A.* 110, 19633–19638. doi: 10.1073/pnas.1314749110
- Fewell, S. W., Travers, K. J., Weissman, J. S., and Brodsky, J. L. (2001). The action of molecular chaperones in the early secretory pathway. *Annu. Rev. Genet.* 35, 149–191. doi: 10.1146/annurev.genet.35.102401.090313

ACKNOWLEDGMENTS

We thank Chia-En Chen (Institute of Plant and Microbial Biology, Academia Sinica, Taiwan) for technical assistances and Dr. Tsuyoshi Nakagawa (Shimane University) for providing Gateway binary vector pGWB653 that contains the *bar* gene, which was identified by Meiji Seika Kaisha, Ltd.

SUPPLEMENTARY MATERIAL

The Supplementary Material for this article can be found online at: <http://journal.frontiersin.org/article/10.3389/fpls.2017.00144/full#supplementary-material>

FIGURE S1 | Multiple alignment of amino acid sequences of the BiPs. The carboxyl-terminal sequences used to raise *BiP3*-specific antibodies are underlined.

FIGURE S2 | Spatiotemporal ER stress response in *Arabidopsis* roots. Observation of the *ProBiP3:mRFP* signal in roots of 7-day-old seedlings treated with 5 µg/ml TM for the indicated time. The merged images of mRFP fluorescence and DIC are shown. Scale bars, 10 µm.

FIGURE S3 | Spatiotemporal ER stress response in *Arabidopsis* roots. Observation of the *ProBiP3:mRFP* signal in roots of 7-day-old seedlings treated with 5 µg/ml TM for the time indicated. Merged images of mRFP fluorescence and DIC are shown. The fluorescent images were provided at the left side of each merged image. Scale bars, 10 µm.

FIGURE S4 | Spatiotemporal ER stress response in *Arabidopsis* roots treated with DTT. Observation of the *ProBiP3:mRFP* signal in roots of 7-day-old seedlings treated with 5 µg/ml TM or 2 mM dithiothreitol (DTT) for the time indicated. Merged images of mRFP fluorescence and DIC are shown. The fluorescent images were provided at the left side of each merged image. Scale bars, 10 µm.

FIGURE S5 | Detection of aggregated proteins and misfolded proteins in roots. **(A–C)** Detection of aggregated proteins using MG-132 in roots. Seven-day-old WT seedlings were treated with MG-132 for 16 h. **(D–F)** Detection of misfolded proteins after TM treatment in roots. Seven-day-old WT seedlings were treated with TM for 8 h. Staining of aggregated or misfolded proteins **(A,D)**, DIC images **(B,E)**, and merged images **(C,F)**. Scale bars, 10 µm.

FIGURE S6 | Immunofluorescence analysis of *BiP3* and colocalization with misfolded proteins in roots. Four-day-old WT seedlings were treated with TM for 24 h. *BiP3* localization detected by anti-*BiP3* antibodies **(A)**, misfolded proteins detected by Aggresome dye ProteoStat® **(B)**, merged image **(C)**, and DIC image **(D)**. Scale bars, 10 µm.

- Helenius, A., and Aebi, M. (2004). Roles of N-linked glycans in the endoplasmic reticulum. *Annu. Rev. Biochem.* 73, 1019–1049. doi: 10.1146/annurev.biochem.73.011303.073752
- Howell, S. H. (2013). Endoplasmic reticulum stress responses in plants. *Annu. Rev. Plant Biol.* 64, 477–499. doi: 10.1146/annurev-aplant-050312-120053
- Iwata, Y., and Koizumi, N. (2005). An *Arabidopsis* transcription factor, AtbZIP60, regulates the endoplasmic reticulum stress response in a manner unique to plants. *Proc. Natl. Acad. Sci. U.S.A.* 102, 5280–5285. doi: 10.1073/pnas.0408941102
- Iwata, Y., and Koizumi, N. (2012). Plant transducers of the endoplasmic reticulum unfolded protein response. *Trends Plant Sci.* 17, 720–727. doi: 10.1016/j.tplants.2012.06.014
- Kanehara, K., Cho, Y., Lin, Y. C., Chen, C. E., Yu, C. Y., and Nakamura, Y. (2015a). *Arabidopsis* DOK1 encodes a functional dolichol kinase involved in reproduction. *Plant J.* 81, 292–303. doi: 10.1111/tpj.12727
- Kanehara, K., Kawaguchi, S., and Ng, D. T. (2007). The EDEM and Yos9p families of lectin-like ERAD factors. *Semin. Cell Dev. Biol.* 18, 743–750. doi: 10.1016/j.semcd.2007.09.007
- Kanehara, K., Yu, C. Y., Cho, Y., Cheong, W. F., Torta, F., Shui, G., et al. (2015b). *Arabidopsis* AtPLC2 is a primary phosphoinositide-specific phospholipase C in phosphoinositide metabolism and the endoplasmic reticulum stress response. *PLoS Genet.* 11:e1005511. doi: 10.1371/journal.pgen.1005511
- Karimi, M., De Meyer, B., and Hilson, P. (2005). Modular cloning in plant cells. *Trends Plant Sci.* 10, 103–105. doi: 10.1016/j.tplants.2005.01.008
- Komarnytsky, S., Borisjuk, N. V., Borisjuk, L. G., Alam, M. Z., and Raskin, I. (2000). Production of recombinant proteins in tobacco guttation fluid. *Plant Physiol.* 124, 927–933. doi: 10.1104/pp.124.3.927
- Kothawala, A., Kilpatrick, K., Novoa, J. A., and Segatori, L. (2012). Quantitative analysis of alpha-synuclein solubility in living cells using split GFP complementation. *PLoS ONE* 7:e43505. doi: 10.1371/journal.pone.0043505
- Lin, Y. C., Liu, Y. C., and Nakamura, Y. (2015). The choline/ethanolamine kinase family in *Arabidopsis*: essential role of CEK4 in phospholipid biosynthesis and embryo development. *Plant Cell* 27, 1497–1511. doi: 10.1105/tpc.15.00207
- Liu, J. X., and Howell, S. H. (2010). Endoplasmic reticulum protein quality control and its relationship to environmental stress responses in plants. *Plant Cell* 22, 2930–2942. doi: 10.1105/tpc.110.078154
- Maruyama, D., Endo, T., and Nishikawa, S. (2010). BiP-mediated polar nuclei fusion is essential for the regulation of endosperm nuclei proliferation in *Arabidopsis thaliana*. *Proc. Natl. Acad. Sci. U.S.A.* 107, 1684–1689. doi: 10.1073/pnas.0905795107
- Maruyama, D., Endo, T., and Nishikawa, S. (2015). BiP3 supports the early stages of female gametogenesis in the absence of BiP1 and BiP2 in *Arabidopsis thaliana*. *Plant Signal. Behav.* 10:e1035853. doi: 10.1080/15592324.2015.1035853
- Maruyama, D., Sugiyama, T., Endo, T., and Nishikawa, S. (2014). Multiple BiP genes of *Arabidopsis thaliana* are required for male gametogenesis and pollen competitiveness. *Plant Cell Physiol.* 55, 801–810. doi: 10.1093/pcp/pcu018
- Murashige, T., and Skoog, F. (1962). A revised medium for rapid growth and bio assays with tobacco tissue cultures. *Physiol. Plant.* 15, 473–497. doi: 10.1111/j.1399-3054.1962.tb08052.x
- Nagashima, Y., Mishiba, K., Suzuki, E., Shimada, Y., Iwata, Y., and Koizumi, N. (2011). *Arabidopsis* IRE1 catalyses unconventional splicing of bZIP60 mRNA to produce the active transcription factor. *Sci. Rep.* 1:29. doi: 10.1038/srep00029
- Nakajima, Y., and Suzuki, S. (2013). Environmental stresses induce misfolded protein aggregation in plant cells in a microtubule-dependent manner. *Int. J. Mol. Sci.* 14, 7771–7783. doi: 10.3390/ijms1404771
- Nakamura, S., Mano, S., Tanaka, Y., Ohnishi, M., Nakamori, C., Araki, M., et al. (2010). Gateway binary vectors with the bialaphos resistance gene, bar, as a selection marker for plant transformation. *Biosci. Biotechnol. Biochem.* 74, 1315–1319. doi: 10.1271/bbb.100184
- Noh, S. J., Kwon, C. S., Oh, D. H., Moon, J. S., and Chung, W. I. (2003). Expression of an evolutionarily distinct novel BiP gene during the unfolded protein response in *Arabidopsis thaliana*. *Gene* 311, 81–91. doi: 10.1016/S0378-1119(03)00559-6
- Ohta, M., Wakasa, Y., Takahashi, H., Hayashi, S., Kudo, K., and Takaiwa, F. (2013). Analysis of rice ER-resident J-proteins reveals diversity and functional differentiation of the ER-resident Hsp70 system in plants. *J. Exp. Bot.* 64, 5429–5441. doi: 10.1093/jxb/ert312
- Pilot, G., Stranksy, H., Bushey, D. F., Pratelli, R., Ludewig, U., Wingate, V. P. M., et al. (2004). Overexpression of glutamine dumper1 leads to hypersecretion of glutamine from hydathodes of *Arabidopsis* leaves. *Plant Cell* 16, 1827–1840. doi: 10.1105/tpc.021642
- Preuss, M. L., Serna, J., Falbel, T. G., Bednarek, S. Y., and Nielsen, E. (2004). The *Arabidopsis* Rab GTPase RabA4b localizes to the tips of growing root hair cells. *Plant Cell* 16, 1589–1603. doi: 10.1105/tpc.021634
- Ruggiano, A., Foresti, O., and Carvalho, P. (2014). ER-associated degradation: protein quality control and beyond. *J. Cell Biol.* 204, 869–879. doi: 10.1083/jcb.201312042
- Sawano, A., and Miyawaki, A. (2000). Directed evolution of green fluorescent protein by a new versatile PCR strategy for site-directed and semi-random mutagenesis. *Nucleic Acids Res.* 28:E78. doi: 10.1093/nar/28.16.e78
- Srivastava, R., Deng, Y., Shah, S., Rao, A. G., and Howell, S. H. (2013). BINDING PROTEIN is a master regulator of the endoplasmic reticulum stress sensor/transducer bZIP28 in *Arabidopsis*. *Plant Cell* 25, 1416–1429. doi: 10.1105/tpc.113.110684
- Tsugeki, R., and Fedoroff, N. V. (1999). Genetic ablation of root cap cells in *Arabidopsis*. *Proc. Natl. Acad. Sci. U.S.A.* 96, 12941–12946. doi: 10.1073/pnas.96.22.12941
- Walter, P., and Ron, D. (2011). The unfolded protein response: from stress pathway to homeostatic regulation. *Science* 334, 1081–1086. doi: 10.1126/science.1209038
- Wang, S., Narendra, S., and Fedoroff, N. (2007). Heterotrimeric G protein signaling in the *Arabidopsis* unfolded protein response. *Proc. Natl. Acad. Sci. U.S.A.* 104, 3817–3822. doi: 10.1073/pnas.0611735104

Conflict of Interest Statement: The authors declare that the research was conducted in the absence of any commercial or financial relationships that could be construed as a potential conflict of interest.

Copyright © 2017 Cho and Kanehara. This is an open-access article distributed under the terms of the Creative Commons Attribution License (CC BY). The use, distribution or reproduction in other forums is permitted, provided the original author(s) or licensor are credited and that the original publication in this journal is cited, in accordance with accepted academic practice. No use, distribution or reproduction is permitted which does not comply with these terms.



The Unfolded Protein Response Supports Plant Development and Defense as well as Responses to Abiotic Stress

Yan Bao and Stephen H. Howell*

Plant Sciences Institute and the Department of Genetics, Development and Cell Biology, Iowa State University, Ames, IA, USA

OPEN ACCESS

Edited by:

Minghui Lu,
Northwest A&F University, China

Reviewed by:

Richard Strasser,
University of Natural Resources
and Life Sciences, Vienna, Austria
Nozomu Koizumi,
Osaka Prefecture University, Japan

***Correspondence:**

Stephen H. Howell
shh@iastate.edu

Specialty section:

This article was submitted to
Plant Cell Biology,
a section of the journal
Frontiers in Plant Science

Received: 08 December 2016

Accepted: 27 February 2017

Published: 15 March 2017

Citation:

Bao Y and Howell SH (2017)
*The Unfolded Protein Response
Supports Plant Development
and Defense as well as Responses
to Abiotic Stress.*
Front. Plant Sci. 8:344.
doi: 10.3389/fpls.2017.00344

The unfolded protein response (UPR) is a stress response conserved in eukaryotic organisms and activated by the accumulation of misfolded proteins in the endoplasmic reticulum (ER). Adverse environmental conditions disrupt protein folding in the ER and trigger the UPR. Recently, it was found that the UPR can be elicited in the course of plant development and defense. During vegetative plant development, the UPR is involved in normal root growth and development, the effect of which can be largely attributed to the influence of the UPR on plant hormone biology. The UPR also functions in plant reproductive development by protecting male gametophyte development from heat stress. In terms of defense, the UPR has been implicated in virus and microbial defense. Viral defense represents a double edge sword in that various virus infections activate the UPR, however, in a number of cases, the UPR actually supports viral infections. The UPR also plays a role in plant immunity to bacterial infections, again through the action of plant hormones in regulating basal immunity responses.

Keywords: protein folding, ER (endoplasmic reticulum) stress, IRE1, bZIP28, regulated-IRE1 dependent RNA decay (RID), auxin, brassinosteroid, plant virus

INTRODUCTION

The unfolded protein response (UPR) is widely regarded as a stress response which is activated by stress conditions in the endoplasmic reticulum (ER) (Hartl and Hayer-Hartl, 2009; Gardner et al., 2013). ER stress is brought about by a variety of different conditions that can lead to the accumulation of misfolded or unfolded proteins in the ER (Duwi Fanata et al., 2013). These conditions include abiotic stresses, such as high temperature, salt stress or biotic agents, such as viral or bacterial pathogens. The UPR is also activated under protein synthesis overload conditions when the need for protein folding simply cannot meet demands (Liu and Howell, 2010b, 2016; Körner et al., 2015).

Stress conditions in the ER are communicated to the nucleus via the UPR signaling pathway. There are two arms to this pathway in plants (Howell, 2013a) (Figure 1). One arm is mediated by RNA splicing factor, IRE1, an ER transmembrane protein with its N-terminus facing the ER lumen and its C-terminus, bearing both its protein kinase and ribonuclease domains, facing the cytosol. The luminal domain of IRE1 senses the protein status in the ER. The primary target of IRE1 in plants is bZIP60 mRNA which is spliced in response to stress (Deng et al., 2011). In *Arabidopsis*, IRE1's cleavage of bZIP60 mRNA results in the excision of a 23 base-pair intron

(Deng et al., 2011; Nagashima et al., 2011). The unspliced form of bZIP60 mRNA encodes a membrane-anchored transcription factor, however, splicing causes a frame shift eliminating the transmembrane domain, yielding a form of bZIP60 (bZIP60s) targeted to the nucleus (Deng et al., 2011). Under normal growth conditions, the unspliced form of bZIP60 (bZIP60u) is transcribed and translated (Iwata et al., 2008; Nagashima et al., 2011), but it is not yet clear what its function might be.

Beside its splicing function, IRE1 also attacks other mRNAs in response to stress in a process called regulated-IRE1 dependent RNA decay (RIDD) (Hollien and Weissman, 2006; Hollien et al., 2009). Studies by Mishiba et al. (2013) showed that RIDD in *Arabidopsis* largely targets mRNAs encoding secretory pathway proteins. Thus, IRE1 is a major factor shaping the stress transcriptome, upregulating genes by promoting the production of a potent transcription factor (bZIP60s) and by degrading other transcripts through RIDD (Mishiba et al., 2013).

The other arm of the ER stress signaling pathway is mediated by ER membrane-associated transcription factors, bZIP17 and bZIP28 (Figure 1). Under unstressed conditions, these factors are retained in the ER by their association with binding protein (BiP). In response to stress, when misfolded proteins accumulate in the ER, BiP is competed away and dissociates from bZIP28 (Srivastava et al., 2013). Once liberated, the factors relocate from the ER to the Golgi, where they are cleaved by two Golgi-resident proteases, Site-1 and Site-2 protease (S1P and S2P) (Liu et al., 2007a; Che et al., 2010). Cleavage by S2P in the Golgi membrane releases the cytosolic-facing components of bZIP17/bZIP28 from the Golgi allowing for their transport into the nucleus to upregulate the expression of stress response genes (Liu et al., 2007a,b; Liu and Howell, 2010a).

THE UPR IN VEGETATIVE DEVELOPMENT

The UPR has been extensively studied in the context of ER stress, although recently more attention has been paid to the role of the UPR in plant development and defense. The UPR has been found to play roles in both vegetative and reproductive development. Vegetative development studies have focused on root development, and under normal growth conditions, root growth is inhibited in *ire1a ire1b* double mutants that knock out both IRE1 isoforms in *Arabidopsis* (Chen and Brandizzi, 2012). *IRE1a* and *IRE1b* have overlapping functions, however, the extent of overlap has not been fully resolved (Nagashima et al., 2011; Chen and Brandizzi, 2013; Howell, 2013b). In some studies *IRE1b* appears to be more active in response to ER stress agents (Deng et al., 2011), while *IRE1a* is reported to play a more prominent role in certain biotic stress responses (Moreno et al., 2012).

IRE1 is a multifunctional protein with ribonuclease and protein kinase domains, and IRE1b has been dissected with site-specific mutations in an effort to learn which of its functional domains is required for normal root growth (Figure 2A). One of the site-specific mutations knocks out the ribonuclease activity of IRE1b (N820A) while two other affect activities associated with the protein kinase domain (Deng et al., 2013). Of the latter two, one blocks the catalytic activity of the protein kinase (D628A), while the other double mutant prevents nucleotide binding (D608N, K610N), which is required for activating the ribonuclease activity of IRE1b. In complementation experiments with these site-specific IRE1b mutations, it was found that neither the mutation in the ribonuclease domain (N820A) or the nucleotide binding domain (D608N, K610N) could restore normal root growth in an *ire1a ire1b* double mutant (Deng et al., 2013). However, the mutation in catalytic site of the protein kinase domain (D628A) complemented root growth in the *ire1a ire1b* mutant, meaning that the ribonuclease function of IRE1 is necessary for normal root growth, but that the catalytic activity of IRE1's protein kinase is dispensable.

The principal target of IRE1's RNA splicing activity is bZIP60 mRNA, and so it is curious that the short root phenotype is not observed in *bzip60* single or *bzip28 bzip60* and *bzip17 bzip60* double mutants. This finding argues that the impact of

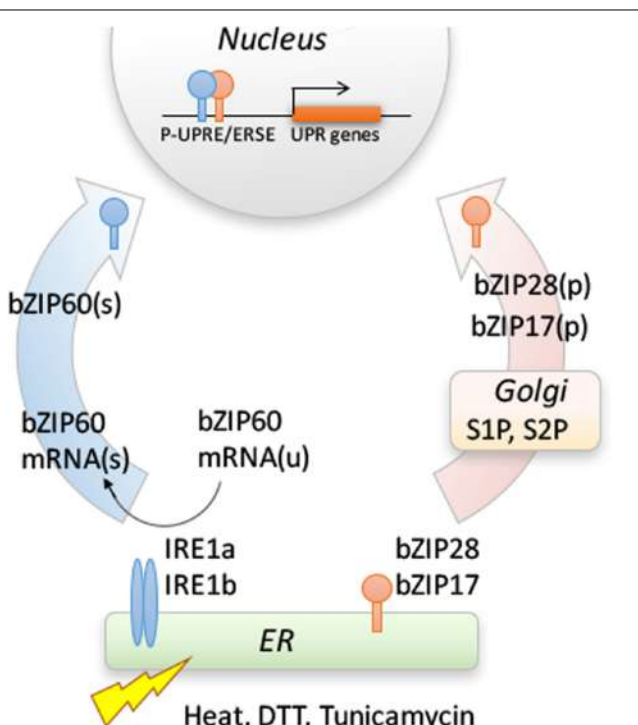
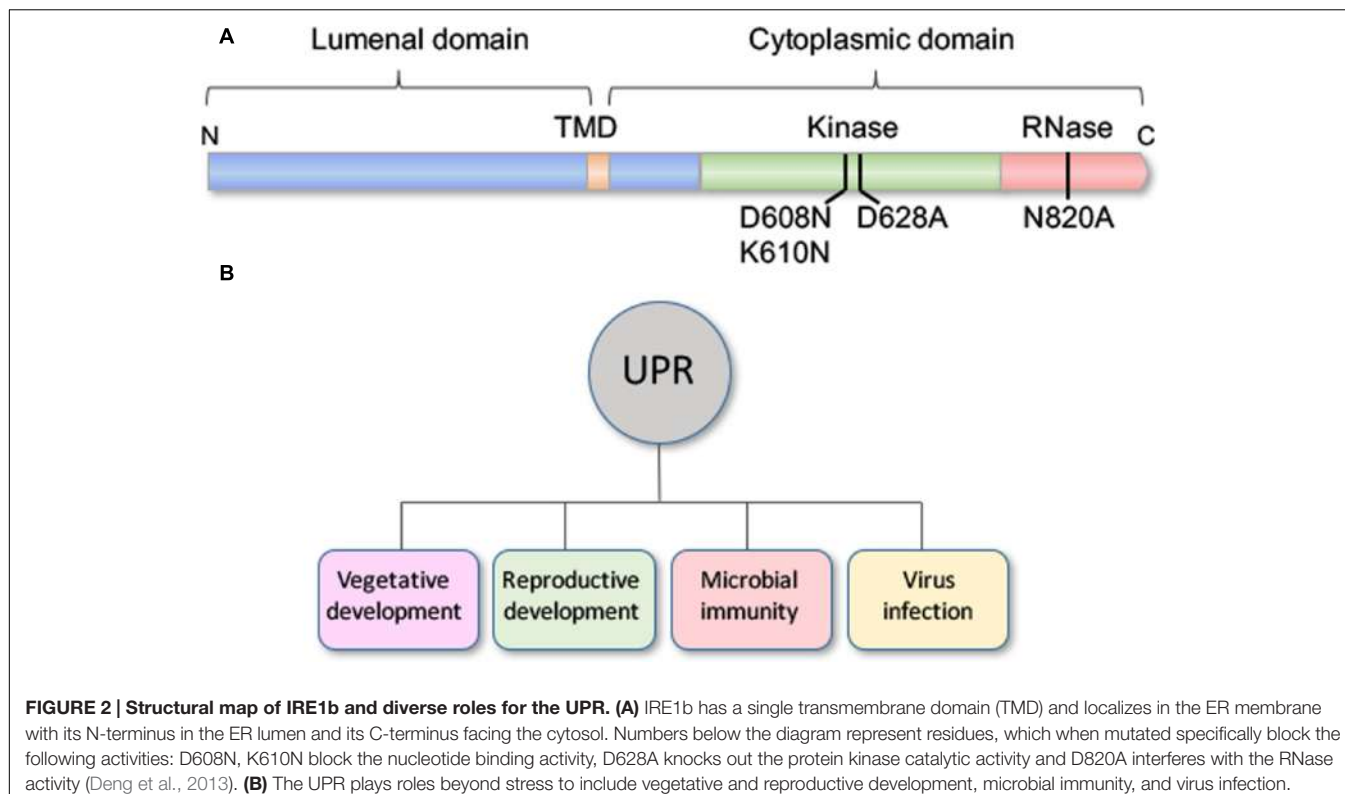


FIGURE 1 | Two branches of UPR signaling pathway in plants. One branch involves the dual protein kinase and ribonuclease, IRE1, which splices bZIP60 mRNA when activated. The other branch is mediated by two ER membrane-anchored transcription factors, bZIP17 and bZIP28. Different stresses interfere with protein folding in the ER, leading to an accumulation of unfolded or misfolded proteins in the ER, activating the UPR. The splicing of bZIP60(u) mRNA introduces a frameshift, such that the resultant spliced form bZIP60(s) mRNA is translated into a transcription factor targeted to the nucleus. ER stress also provokes the mobilization of the membrane-anchored transcription factors from ER to Golgi, where they are processed to bZIP17(p) and bZIP28(p) by Golgi resident S1P and S2P proteases, releasing their cytosolic transcription factor domains. The factors from both branches are targeted to the nucleus, and either homodimerize or heterodimerize to bind to the promoters and regulate the expression of stress response genes. Based on Howell (2013b).



IRE1 on root development is dependent on the ribonuclease activity of IRE1, but independent of its principal RNA splicing target bZIP60 mRNA (Deng et al., 2013). The only ribonuclease activity of IRE1 that is known to be independent of bZIP60 is its RIDD activity, the promiscuous ribonuclease activity of IRE1 in attacking other mRNAs encoding secretory proteins (Mishiba et al., 2013). Interestingly, the short root phenotype of *ire1a ire1b* is also observed in *bzip28 ire1b* seedlings, implying that the two branches of the UPR signaling pathway coordinately influence root development (Deng et al., 2013).

THE UPR IN PLANT HORMONE BIOLOGY

The UPR is reported to play an unsuspected role in hormone biology, which may explain the influence of the UPR on vegetative growth and development. Chen et al. (2014) recently examined the possible relationship between the UPR and auxin regulation in *Arabidopsis*. They found, quite unexpectedly, that ER stress down-regulates the expression of genes encoding ER- and PM-localized auxin efflux transporters (PIN-formed or PIN proteins) and the auxin receptors TIR1/AFBs. The extent of down-regulation was modest, and the mechanism by which this happens is unclear. It does not require IRE1, which eliminates the possibility that RIDD might be involved in the down-regulation. One consequence of the down-regulation of auxin receptors TIR1/AFBs was the possible stabilization of AUX/IAA proteins. Chen et al. (2014) analyzed the levels

DII-VENUS, a fluorescently tagged AUX/IAA surrogate that contains the degron responsible for auxin-induced TIR1/AFB-mediated protein degradation. They found that the levels of DII-VENUS increased in response to ER stress suggesting that under stress, auxin responsive genes may remain repressed (or otherwise controlled) by AUX/IAA in the presence of auxin.

On the other hand, Chen et al. (2014) also reported that activation of UPR requires certain auxin regulators and ER-localized PINs, such as PIN5 and PIN6. They found that in response to ER stress, loss-of-function *pin5*, *pin6* and even *abf1* mutants showed reduced expression of some common UPR biomarker genes, such as *BIP1* and *PROTEIN DISULFIDE ISOMERASE6* (*PDI6*). Again, the effect was modest and there was no clear explanation for this phenomenon, although the authors speculated that the mutants might affect organellar distribution of free auxin, which might influence ER stress responses in some undefined way.

The UPR has also been implicated in brassinosteroid (BR)-mediated responses. The relationship appears to involve the membrane-associated transcription factors, bZIP17 and bZIP28, and not the RNA splicing arm of the UPR signaling pathway. The relationship was uncovered in mutants of *S2P*, a gene encoding a Golgi-resident protease that processes bZIP17 and bZIP28 when mobilized by ER stress (Che et al., 2010). Mutants in *S2P* have a short root phenotype, which can be overcome by expressing a preprocessed form of bZIP17 (bZIP17 Δ C) or bZIP28 (bZIP28 Δ C). The relationship of this phenomenon to BR signaling derives from the fact that high levels of a BR agonist,

brassinolide (BL), inhibit root growth in WT seedlings, but not in *s2p* mutants and that the root growth inhibition by BL in WT can be overcome by expressing bZIP17ΔC or bZIP28ΔC.

Che et al. (2010) also found that bZIP17ΔC or bZIP28ΔC assists in activating BR responses in *bri1-5* mutants. The BR receptor in *bri1-5* mutants is functional, but defective in trafficking to the cell surface. Thus, the expression of bZIP17ΔC or bZIP28ΔC likely aids the BR receptor in *bri1-5* in trafficking, but not in other aspects of BR signaling. That notion was reinforced by the finding that bZIP17ΔC or bZIP28ΔC expression did not rescue *bri1-6* and *det2* mutants, defective respectively in BR perception and synthesis. Nonetheless, to show that bZIP17ΔC or bZIP28ΔC expression helped to make the BR receptor in *bri1-5* operational, the authors demonstrated that the expression of either of the two bZIPΔCs partially restored BES1 dephosphorylation (a measure of BR signaling by the BRI1 receptor) and the upregulation of BR-induced genes in response to BL.

THE UPR IN REPRODUCTIVE DEVELOPMENT

Recently, it was shown that the UPR also plays a role in protecting plant reproductive development from elevated temperature. Plants are vulnerable to heat stress during the reproductive phase in their life cycle, and Deng et al. (2016) showed the RNA splicing arm of the UPR guides *Arabidopsis* reproductive development in such a way so as to protect it from elevated temperature. The authors found that the double *ire1a ire1b* mutant and a mutant in the immediate downstream target, bZIP60, were sterile at elevated temperature. Through, reciprocal crosses it was revealed that the temperature sensitive sterility was a male trait and impacted pollen production. The defect was also found to be sporophytic in nature, and at elevated temperature it affected the structure of the tapetum, which is ER-rich nurse tissue for the developing male gametophyte. The tapetum contributes materials for the formation of the pollen wall and coat, and it was observed that the defect dramatically affected the proper deposition of the pollen coat.

In another study, Deng et al. (2013) dissected IRE1b as described in the previous section with the intent of finding out what IRE1 activities protect male gametophyte development. Using site-specific IRE1b mutants in complementation experiments, the authors demonstrated that, both kinase and RNase functions of IRE1 are required to promote and protect male reproductive development. Deng et al. (2016) further found that bZIP60, the downstream target of IRE1, is also required for temperature protection of male gametophyte production. IRE1 splices bZIP60 mRNA to make an active transcription factor, and there were major expression changes in genes that likely contribute to pollen wall/coat construction, such as small cysteine rich pollen coat proteins. Quite surprisingly, the expression of SEC31A, a protein involved in COPII vesicle formation, restored fertility of *ire1a ire1b* at elevated temperature. SEC31A is the gene most highly dependent on *IRE1a IRE1b* function during ER stress in vegetative tissue. The basis for

SEC31A's fertility restoration activity in *ire1a ire1b* mutants at elevated temperature is not known, but it is speculated that its contribution to ER to Golgi trafficking may compensate for other defects in the double mutant (Deng et al., 2016).

The role of the UPR in normal plant development was unsuspected because the UPR is thought to be quiescent under normal conditions and is only activated by stress. Does the unspliced form of bZIP60 produced under normal conditions, but upregulated in response to stress, have some function that we are not aware of? On the other hand, the UPR may have a low level of activity under "normal" conditions, sufficient to play a supporting role in plant development. What activates IRE1 under these conditions is not known, although it is speculated that the heavy demand for protein synthesis and/or secretion during development may activate the UPR.

THE UPR AND MICROBIAL IMMUNITY

The UPR is also reported to play roles in bacterial immunity. Tateda et al. (2008) found that when *Nicotiana benthamiana* was inoculated with a non-host pathogen, *Pseudomonas cichorii*, and a host-specific pathogen, *Pseudomonas syringae*, the non-host pathogen led to the upregulation in expression of bZIP60, while the host-specific pathogen did not. The authors silenced *N. benthamiana* bZIP60 using virus induced gene silencing (VIGS) and found that the plants became more susceptible to the non-host pathogen. Therefore, the authors conclude that the UPR, and more specifically the expression of bZIP60, is an important component of immunity to host pathogens.

Likewise, Moreno et al. (2012) reported that the UPR confers bacterial immunity to *Arabidopsis*. In their analysis, they observed that *ire1a ire1b* double mutants and a mutant in their downstream target, *bzip60*, were more susceptible to *P. syringae* avrRpt2. In addition, the mutants were less able to establish systemic acquired resistance (SAR) to the bacteria when treated with salicylic acid (SA), the only plant hormone which is known to induce UPR in *Arabidopsis* (Nagashima et al., 2014). A signature of SAR in *Arabidopsis* is the secretion of Pathogenesis Related Protein 1 (PR1), and low levels of secreted PR1 were found in SA-treated *ire1a ire1b* double mutants and also in the *ire1a* single mutant. From this, Moreno et al. (2012) argued that IRE1-bZIP60 branch of UPR is involved in SA-mediated plant immune responses and that mutants compromised in the UPR are more susceptible to bacterial pathogens.

THE UPR AND VIRUS INFECTIONS

The UPR also plays a significant role in plant virus infection and immunity (Ye et al., 2011). However, the role of UPR is a double edge sword in that on the one hand the UPR appears to bolster plant immunity, but on the other hand the UPR assists in virus infection. Tobacco mosaic virus (TMV) and the tobacco N-gene is a classic case of virus resistance in plants, which appears to involve the UPR in strengthening plant immunity. The N-gene was identified and cloned by Dinesh-Kumar et al. (1995) as

a resistance R gene. During N-mediated defense, a number of genes characteristic of the UPR are upregulated including protein disulfide isomerase, ERp57 and P5, calreticulin 3, glucose-regulated protein 78 (GRP78) and BiP5 (Caplan et al., 2009). To determine whether the upregulation of these genes in tobacco was of consequence to TMV infection, VIGS was used to suppress their expression. Silencing of these genes did, indeed, result in a loss of virus containment in inoculated leaves but did not fully prevent the programmed cell death caused by the virus (Caplan et al., 2009). Thus, this observation implicates the UPR in bolstering N-mediated TMV immunity.

However, there are far more examples for how the UPR supports viral infection. ER membrane expansion is an integral part of the UPR, and *Brome mosaic virus* (BMV), *Tobacco etch virus* (TEV), *Cowpea mosaic virus* (CPMV), *Red clover necrotic mosaic virus* (RCNMV), *Grapevine fan leaf virus* (GFLV), and *Potato virus X* (PVX) are all known to induce proliferation and invaginations of the ER (Ritzenthaler et al., 1995; Schaad et al., 1997; Carette et al., 2002; Lee and Ahlquist, 2003; Lee et al., 2003; Turner et al., 2004). The ER membranes serve as a scaffold for plant virus replication and movement complexes and/or they support virion maturation (Verchot, 2016).

Infection of *N. benthamiana* plants with *potato virus X* (PVX) induces a number of genes associated with the UPR including BIP, PDI, calreticulin (CRT) and calmodulin (CAM) (Ye et al., 2011). The viral component responsible for the activation has been traced to the triple gene block protein 3, TGBp3, a viral membrane movement protein. TGBp3 delivered on its own by a *tobacco mosaic virus* vector will also upregulate UPR-related factors. Not only does PVX upregulate the UPR, but the UPR helps to support PVX infection. This was revealed by silencing *N. benthamiana* bZIP60 and finding that the silencing inhibits virus replication in protoplasts and delays virus systemic accumulation in plants.

The UPR also supports *turnip mosaic virus* (TuMV) infections demonstrated by the fact that double *ire1a ire1b* mutant suppresses TuMV symptoms in *Arabidopsis*. Since the major splicing target for IRE1a and IRE1b is bZIP60 mRNA, Zhang et al. (2015) reported that a knockout in bZIP60 also suppressed viral symptoms and that the suppression of symptoms in the bZIP60 knockout could be overcome by the transgenic expression of an activated form of bZIP60. They further showed that bZIP60 is spliced in response to virus infection and that a viral membrane protein, 6K2, on its own could elicit bZIP60 mRNA splicing in a *N. benthamiana* transient expression system (Zhang et al., 2015).

How could it be that TGBp3 in PVX and 6K2 in TuMV elicit the UPR? There is precedence for the expression of certain

proteins causing ER stress. In *Arabidopsis* chronically misfolded forms of carboxypeptidase Y, CPY* (Finger et al., 1993) and zeolin, a fusion between two storage proteins, zein and phaseolin (Mainieri et al., 2004) produce ER-stress induced autophagy (autophagy that can be reversed by chemical chaperones) (Yang et al., 2016). Thus, TGBp3 in PVX and 6K2 in TuMV may be interpreted by the ERQC system as chronically misfolded proteins or they may interfere with the folding of other proteins.

The virulence determinant in *soybean mosaic virus* (SMV), a potyvirus, also elicits UPR in its host, but appears to do so by a different mode (Luan et al., 2016). The virulence factor in the potyvirus is the P3 protein, which is involved in a variety of functions including viral replication, movement and pathogenesis. Luan et al. (2016) showed that SMV P3 interacts with soybean translation elongation factor 1A (eEF1A). Using VIGs, the authors knocked down the expression of eEF1A, which reduced the ability of the plants to induce ER stress and rendered the plants more resistant to SMV.

CONCLUSION

The UPR, which has been long associated with stress, also functions during normal development, defense and viral infection (Figure 2B). The conditions that elicit the response and the consequence of its induction are current subjects of investigation.

AUTHOR CONTRIBUTIONS

All authors listed, have made substantial, direct and intellectual contribution to the work, and approved it for publication.

FUNDING

YB was supported by a grant from the National Science Foundation IOS 1353867. SH was funded by the Plant Sciences Institute at Iowa State University.

ACKNOWLEDGMENT

We acknowledge Diane C. Bassham for reviewing the article and providing suggestions.

REFERENCES

- Caplan, J. L., Zhu, X., Mamillapalli, P., Marathe, R., Anandalakshmi, R., and Dinesh-Kumar, S. P. (2009). Induced ER chaperones regulate a receptor-like kinase to mediate antiviral innate immune response in plants. *Cell Host Microbe* 6, 457–469. doi: 10.1016/j.chom.2009.10.005
- Carette, J. E., Gühl, K., Wellink, J., and Van Kammen, A. (2002). Coalescence of the sites of cowpea mosaic virus RNA replication into a cytopathic structure. *J. Virol.* 76, 6235–6243. doi: 10.1128/JVI.76.12.6235-6243.2002
- Che, P., Bussell, J. D., Zhou, W., Estavillo, G. M., Pogson, B. J., and Smith, S. M. (2010). Signaling from the endoplasmic reticulum activates brassinosteroid signaling and promotes acclimation to stress in *Arabidopsis*. *Sci. Signal.* 3:ra69. doi: 10.1126/scisignal.2001140
- Chen, Y., Aung, K., Rolcik, J., Walicki, K., Friml, J., and Brandizzi, F. (2014). Inter-regulation of the unfolded protein response and auxin signaling. *Plant J.* 77, 97–107. doi: 10.1111/tpj.12373
- Chen, Y., and Brandizzi, F. (2012). AtIRE1A/AtIRE1B and AGB1 independently control two essential unfolded protein response pathways

- in *Arabidopsis*. *Plant J.* 69, 266–277. doi: 10.1111/j.1365-313X.2011.04788.x
- Chen, Y., and Brandizzi, F. (2013). IRE1: ER stress sensor and cell fate executor. *Trends Cell Biol.* 23, 547–555. doi: 10.1016/j.tcb.2013.06.005
- Deng, Y., Humbert, S., Liu, J., Srivastava, R., Rothstein, S., and Howell, S. H. (2011). Heat induces the splicing by IRE1 of a mRNA encoding a transcription factor involved in the unfolded protein response in *Arabidopsis*. *Proc. Natl. Acad. Sci. U.S.A.* 108, 7247–7252. doi: 10.1073/pnas.1102117108
- Deng, Y., Srivastava, R., and Howell, S. H. (2013). Protein kinase and ribonuclease domains of IRE1 confer stress tolerance, vegetative growth, and reproductive development in *Arabidopsis*. *Proc. Natl. Acad. Sci. U.S.A.* 110, 19633–19638. doi: 10.1073/pnas.1314749110
- Deng, Y., Srivastava, R., Quilichini, T. D., Dong, H., Bao, Y., Horner, H. T., et al. (2016). IRE1, a component of the unfolded protein response signaling pathway, protects pollen development in *Arabidopsis* from heat stress. *Plant J.* 88, 193–204. doi: 10.1111/tpj.13239
- Dinesh-Kumar, S. P., Whitham, S., Choi, D., Hehl, R., Corr, C., and Baker, B. (1995). Transposon tagging of tobacco mosaic virus resistance gene N: its possible role in the TMV-N-mediated signal transduction pathway. *Proc. Natl. Acad. Sci. U.S.A.* 92, 4175–4180. doi: 10.1073/pnas.92.10.4175
- Duwi Fanata, W. I., Lee, S. Y., and Lee, K. O. (2013). The unfolded protein response in plants: a fundamental adaptive cellular response to internal and external stresses. *J Proteomics* 93, 356–368. doi: 10.1016/j.jprot.2013.04.023
- Finger, A., Knop, M., and Wolf, D. H. (1993). Analysis of two mutated vacuolar proteins reveals a degradation pathway in the endoplasmic reticulum or a related compartment of yeast. *Eur. J. Biochem.* 218, 565–574. doi: 10.1111/j.1432-1033.1993.tb18410.x
- Gardner, B. M., Pincus, D., Gotthardt, K., Gallagher, C. M., and Walter, P. (2013). Endoplasmic reticulum stress sensing in the unfolded protein response. *Cold Spring Harb. Perspect. Biol.* 5:a013169. doi: 10.1101/csphperspect.a013169
- Hartl, F. U., and Hayer-Hartl, M. (2009). Converging concepts of protein folding *in vitro* and *in vivo*. *Nat. Struct. Mol. Biol.* 16, 574–581. doi: 10.1038/nsmb.1591
- Hollien, J., Lin, J. H., Li, H., Stevens, N., Walter, P., and Weissman, J. S. (2009). Regulated Ire1-dependent decay of messenger RNAs in mammalian cells. *J. Cell Biol.* 186, 323–331. doi: 10.1083/jcb.200903014
- Hollien, J., and Weissman, J. S. (2006). Decay of endoplasmic reticulum-localized mRNAs during the unfolded protein response. *Science* 313, 104–107. doi: 10.1126/science.1129631
- Howell, S. H. (2013a). Endoplasmic reticulum stress responses in plants. *Annu. Rev. Plant Biol.* 64, 477–499. doi: 10.1146/annurev-arplant-050312-120053
- Howell, S. H. (2013b). ER stress responses in plants. *Ann. Rev. Plant Biol.* 64, 477–499. doi: 10.1146/annurev-arplant-050312-120053
- Iwata, Y., Fedoroff, N. V., and Koizumi, N. (2008). *Arabidopsis* bZIP60 is a proteolysis-activated transcription factor involved in the endoplasmic reticulum stress response. *Plant Cell* 20, 3107–3121. doi: 10.1105/tpc.108.061002
- Körner, C. J., Du, X., Vollmer, M. E., and Pajerowska-Mukhtar, K. M. (2015). Endoplasmic reticulum stress signaling in plant immunity—at the crossroad of life and death. *Int. J. Mol. Sci.* 16, 26582–26598. doi: 10.3390/ijms16112596
- Lee, A. H., Iwakoshi, N. N., and Glimcher, L. H. (2003). XBP-1 regulates a subset of endoplasmic reticulum resident chaperone genes in the unfolded protein response. *Mol. Cell. Biol.* 23, 7448–7459. doi: 10.1128/MCB.23.21.7448-7459.2003
- Lee, W. M., and Ahlquist, P. (2003). Membrane synthesis, specific lipid requirements, and localized lipid composition changes associated with a positive-strand RNA virus RNA replication protein. *J. Virol.* 77, 12819–12828. doi: 10.1128/JVI.77.23.12819-12828.2003
- Liu, J. X., and Howell, S. H. (2010a). bZIP28 and NF-Y transcription factors are activated by ER stress and assemble into a transcriptional complex to regulate stress response genes in *Arabidopsis*. *Plant Cell* 22, 782–796. doi: 10.1105/tpc.109.072173
- Liu, J. X., and Howell, S. H. (2010b). Endoplasmic reticulum protein quality control and its relationship to environmental stress responses in plants. *Plant Cell* 22, 2930–2942. doi: 10.1105/tpc.110.078154
- Liu, J. X., and Howell, S. H. (2016). Managing the protein folding demands in the endoplasmic reticulum of plants. *New Phytol.* 211, 418–428. doi: 10.1111/nph.13915
- Liu, J. X., Srivastava, R., Che, P., and Howell, S. H. (2007a). An endoplasmic reticulum stress response in *Arabidopsis* is mediated by proteolytic processing and nuclear relocation of a membrane-associated transcription factor, bZIP28. *Plant Cell* 19, 4111–4119. doi: 10.1105/tpc.106.050021
- Liu, J. X., Srivastava, R., Che, P., and Howell, S. H. (2007b). Salt stress responses in *Arabidopsis* utilize a signal transduction pathway related to endoplasmic reticulum stress signaling. *Plant J.* 51, 897–909. doi: 10.1111/j.1365-313X.2007.03195.x
- Luan, H., Shine, M. B., Cui, X., Chen, X., Ma, N., Kachroo, P., et al. (2016). The potyviral P3 protein targets eukaryotic elongation factor 1A to promote the unfolded protein response and viral pathogenesis. *Plant Physiol.* 172, 221–234. doi: 10.1104/pp.16.00505
- Mainieri, D., Rossi, M., Archinti, M., Bellucci, M., De Marchis, F., Vavassori, S., et al. (2004). Zeolin. A new recombinant storage protein constructed using maize gamma-zein and bean phaseolin. *Plant Physiol.* 136, 3447–3456. doi: 10.1104/pp.104.046409
- Mishiba, K., Nagashima, Y., Suzuki, E., Hayashi, N., Ogata, Y., Shimada, Y., et al. (2013). Defects in IRE1 enhance cell death and fail to degrade mRNAs encoding secretory pathway proteins in the *Arabidopsis* unfolded protein response. *Proc. Natl. Acad. Sci. U.S.A.* 110, 5713–5718. doi: 10.1073/pnas.1219047110
- Moreno, A. A., Mukhtar, M. S., Blanco, F., Boatwright, J. L., Moreno, I., Jordan, M. R., et al. (2012). IRE1/bZIP60-mediated unfolded protein response plays distinct roles in plant immunity and abiotic stress responses. *PLoS ONE* 7:e31944. doi: 10.1371/journal.pone.0031944
- Nagashima, Y., Iwata, Y., Ashida, M., Mishiba, K., and Koizumi, N. (2014). Exogenous salicylic acid activates two signaling arms of the unfolded protein response in *Arabidopsis*. *Plant Cell Physiol.* 55, 1772–1778. doi: 10.1093/pcp/pcu108
- Nagashima, Y., Mishiba, K., Suzuki, E., Shimada, Y., Iwata, Y., and Koizumi, N. (2011). *Arabidopsis* IRE1 catalyzes unconventional splicing of bZIP60 mRNA to produce the active transcription factor. *Sci. Rep.* 1:29. doi: 10.1038/srep00029
- Ritzenthaler, C., Pinck, M., and Pinck, L. (1995). Grapevine fanleaf nepovirus P38 putative movement protein is not transiently expressed and is a stable final maturation product *in vivo*. *J. Gen. Virol.* 76 (Pt 4), 907–915. doi: 10.1099/0022-1317-76-4-907
- Schaad, M. C., Jensen, P. E., and Carrington, J. C. (1997). Formation of plant RNA virus replication complexes on membranes: role of an endoplasmic reticulum-targeted viral protein. *EMBO J.* 16, 4049–4059. doi: 10.1093/emboj/16.13.4049
- Srivastava, R., Deng, Y., Shah, S., Rao, A. G., and Howell, S. H. (2013). BINDING PROTEIN IS a master regulator of the endoplasmic reticulum stress sensor/transducer bZIP28 in *Arabidopsis*. *Plant Cell* 25, 1416–1429. doi: 10.1105/tpc.113.110684
- Tateda, C., Ozaki, R., Onodera, Y., Takahashi, Y., Yamaguchi, K., Berberich, T., et al. (2008). NtbZIP60, an endoplasmic reticulum-localized transcription factor, plays a role in the defense response against bacterial pathogens in *Nicotiana tabacum*. *J. Plant Res.* 121, 603–611. doi: 10.1007/s10265-008-0185-5
- Turner, K. A., Sit, T. L., Callaway, A. S., Allen, N. S., and Lommel, S. A. (2004). Red clover necrotic mosaic virus replication proteins accumulate at the endoplasmic reticulum. *Virology* 320, 276–290. doi: 10.1016/j.virol.2003.12.006
- Verchot, J. (2016). How does the stressed out ER find relief during virus infection? *Curr. Opin. Virol.* 17, 74–79. doi: 10.1016/j.coviro.2016.01.018
- Yang, X., Srivastava, R., Howell, S. H., and Bassham, D. C. (2016). Activation of autophagy by unfolded proteins during endoplasmic reticulum stress. *Plant J.* 85, 83–95. doi: 10.1111/tpj.13091
- Ye, C., Dickman, M. B., Whitham, S. A., Payton, M., and Verchot, J. (2011). The unfolded protein response is triggered by a plant viral movement protein. *Plant Physiol.* 156, 741–755. doi: 10.1104/pp.111.174110
- Zhang, L., Chen, H., Brandizzi, F., Verchot, J., and Wang, A. (2015). The UPR branch IRE1-bZIP60 in plants plays an essential role in viral infection and is complementary to the only UPR pathway in yeast. *PLoS Genet.* 11:e1005164. doi: 10.1371/journal.pgen.1005164

Conflict of Interest Statement: The authors declare that the research was conducted in the absence of any commercial or financial relationships that could be construed as a potential conflict of interest.

Copyright © 2017 Bao and Howell. This is an open-access article distributed under the terms of the Creative Commons Attribution License (CC BY). The use, distribution or reproduction in other forums is permitted, provided the original author(s) or licensor are credited and that the original publication in this journal is cited, in accordance with accepted academic practice. No use, distribution or reproduction is permitted which does not comply with these terms.



The Banana Fruit SINA Ubiquitin Ligase MaSINA1 Regulates the Stability of MalCE1 to be Negatively Involved in Cold Stress Response

Zhong-Qi Fan, Jian-Ye Chen, Jian-Fei Kuang, Wang-Jin Lu and Wei Shan ^{*}

State Key Laboratory for Conservation and Utilization of Subtropical Agro-Bioresources/Guangdong Provincial Key Laboratory of Post-harvest Science of Fruits and Vegetables, College of Horticulture, South China Agricultural University, Guangzhou, China

OPEN ACCESS

Edited by:

Hanjo A. Hellmann,
Washington State University,
United States

Reviewed by:

Xiaosa Xu,
Cold Spring Harbor Laboratory,
United States
Caiji Gao,
South China Normal University, China

***Correspondence:**

Wei Shan
shanwei@scau.edu.cn

Specialty section:

This article was submitted to
Plant Cell Biology,
a section of the journal
Frontiers in Plant Science

Received: 19 January 2017

Accepted: 26 May 2017

Published: 12 June 2017

Citation:

Fan Z-Q, Chen J-Y, Kuang J-F,
Lu W-J and Shan W (2017)
The Banana Fruit SINA Ubiquitin
Ligase MaSINA1 Regulates
the Stability of MalCE1 to be
Negatively Involved in Cold Stress
Response. *Front. Plant Sci.* 8:995.
doi: 10.3389/fpls.2017.00995

The regulation of ICE1 protein stability is important to ensure effective cold stress response, and is extensively studied in *Arabidopsis*. Currently, how ICE1 stability in fruits under cold stress is controlled remains largely unknown. Here, we reported the possible involvement of a SEVEN IN ABSENTIA (SINA) ubiquitin ligase MaSINA1 from banana fruit in affecting MalCE1 stability. MaSINA1 was identified based on a yeast two-hybrid screening using MalCE1 as bait. Further yeast two-hybrid, pull-down, bimolecular fluorescence complementation (BiFC) and co-immunoprecipitation (CoIP) assays confirmed that MaSINA1 interacted with MalCE1. The expression of MaSINA1 was repressed by cold stress. Subcellular localization analysis in tobacco leaves showed that MaSINA1 was localized predominantly in the nucleus. *In vitro* ubiquitination assay showed that MaSINA1 possessed E3 ubiquitin ligase activity. More importantly, *in vitro* and semi-*in vivo* experiments indicated that MaSINA1 can ubiquitinate MalCE1 for the 26S proteasome-dependent degradation, and therefore suppressed the transcriptional activation of MalCE1 to MaNAC1, an important regulator of cold stress response of banana fruit. Collectively, our data reveal a mechanism in banana fruit for control of the stability of ICE1 and for the negative regulation of cold stress response by a SINA E3 ligase via the ubiquitin proteasome system.

Keywords: banana fruit, cold stress, E3 ligase, ICE1, ubiquitination

INTRODUCTION

Banana (*Musa acuminata*) is one of the most popular fruit crops worldwide (Paul et al., 2016; Shan et al., 2016). As a typical climacteric fruit, bananas have a very limited shelf-life due to rapid softening (Han et al., 2016). Practically, low temperature storage is an effective technology to maintain post-harvest banana fruit qualities and to extend its shelf-life. However, being tropical fruits, banana fruit are highly sensitive to cold stress, and storage at low temperatures (<13°C) results generally in peel browning and failure of ripening, causing severe post-harvest losses (Chen et al., 2008), which restricts the application of low temperature storage during transportation of banana fruit.

Cold stress is one of the major abiotic stresses limiting plant growth and development, productivity, product quality, post-harvest life and geographic distribution (Knight and Knight, 2012; Shan et al., 2014; Jammehmadi et al., 2015). To overcome this constraint, plants have developed sophisticated responses at the physiological and biochemical levels (Hu et al., 2013; Huang et al., 2015; Jia et al., 2016). Over the last decades, enormous progress has been achieved in the identification of important components involving in the cold signaling network, among which the INDUCER OF CBF EXPRESSION (ICE)-CREPEAT BINDING FACTOR/DRE BINDING FACTOR-COLD REGULATED (ICE-CBF-COR) transcriptional cascade is pretty well understood (Medina et al., 2011; Zhou et al., 2011; Wisniewski et al., 2014; Shi et al., 2015). In this pathway, *CBFs* are induced rapidly by cold stress, and in turn activate downstream *COR* genes to increase plant cold tolerance. ICEs encode MYC-type bHLH transcription factors (TFs) that can activate *CBFs* gene expression via binding to their promoters (Chinnusamy et al., 2003; Shi et al., 2015).

It is well-known that ICE-CBF-COR pathway is positively or negatively controlled by many important regulators at transcriptional, post-transcriptional, and post-translational levels. Among these regulators, CAMTA3 (calmodulin-binding transcription activator 3) (Doherty et al., 2009), SIZ1 (for SAP and Miz1) (Miura et al., 2007) and OST1 (OPEN STOMATA 1) (Ding et al., 2015) are positive regulators, while MYB15 (Agarwal et al., 2006), HOS1 (HIGH EXPRESSION OF OSMOTICALLY RESPONSIVE GENES1) (Lee et al., 2001; Dong et al., 2006; Jung et al., 2014) EIN3 (ethylene insensitive 3) (Shi et al., 2012) and JA ZIM-domain 1/4 (JAZ1/4) (Hu et al., 2013) function as negative regulators of ICE-CBF-COR pathway. For example, HOS1 ubiquitinates and degrades ICE1 protein via the 26S proteasome pathway, indicating that HOS1 attenuates cold responses by triggering ICE1 degradation through the ubiquitin-proteasome system (UPS) (Lee et al., 2001; Dong et al., 2006; Jung et al., 2014). On the contrary, a small ubiquitin-related modifier (SUMO) E3 ligase, SIZ1 sumoylates ICE1, antagonizing the polyubiquitination of ICE1 to facilitate its stability, thus causes enhanced cold tolerance (Miura et al., 2007). More recently, the protein kinase OST1 is also shown to phosphorylate ICE1 to enhance its stability and transcriptional activity, resulting in increased cold tolerance (Ding et al., 2015). These findings suggest that the regulation of ICE1 protein stability is important to ensure effective cold stress response. Although the UPS-mediated protein degradation is an important post-translational regulatory mechanism for controlling the abundance of key regulators, and has emerged as an integral player in plant response and adaptation to environmental stresses, its involvement in regulating ICE1 stability in relation to cold stress response of economical fruits, such as bananas, needs to be investigated.

Giving the increasing demand of cold storage and the cold sensitivity of banana fruit, we are aiming at the molecular mechanism(s) of the cold response in banana fruit, which will contributes to genetic improving cold tolerance, fruit quality and storage potential. Our previous studies have shown that two banana fruit MYC2 proteins act together with ICE1, which

is related to the methyl jasmonate (MeJA)-induced chilling tolerance (Zhao et al., 2013). In addition, a cold-responsive NAC (NAM, ATAF1/2, and CUC2) TF MaNAC1, is a novel direct target of MaICE1 and may be associated with cold stress through interacting with MaCBF1 (Shan et al., 2014). Nevertheless, the factors controlling ICE1 protein stability associated with cold stress response of banana fruit are far from being clearly elucidated. In this study, we report that a SEVEN IN ABSENTIA (SINA) E3 ligase MaSINA1 interacts with and ubiquitinates MaICE1, leading to the degradation of MaICE1 and the attenuation of its transcriptional activity. Our study thus reveals that MaSINA1 may negatively regulate cold stress response of banana fruit via controlling MaICE1 stability.

MATERIALS AND METHODS

Plant Materials and Treatments

Pre-climacteric banana (*M. acuminata*, AAA group, cv. Cavendish) fruit at 75–80% maturation (about 12 weeks after anthesis) were harvested from a local commercial plantation near Guangzhou, China. Each banana hand was cut into individual fingers. Banana fruit of uniform weight, shape and maturity, and free of visual defects, were used for this study. For cold stress, fruit were stored immediately at 7°C for 5 days, while for control, fruit were directly stored at 22°C. Samples were taken at 0, 6, and 12 h and 1, 3, and 5 days of storage. Banana peel was collected, frozen in liquid nitrogen and stored at –80°C for further use.

Tobacco (*Nicotiana benthamiana*) plants were planted in a growth chamber of 22°C under long day conditions (16-h light/8-h dark), and 4- to 6-week-old plants were selected for analysis.

Yeast Two-Hybrid (Y2H) Screening/Assay

Yeast two-hybrid screening/assay was performed using the Matchmaker™ Gold yeast two-hybrid system (Clontech, Cat. No. 630489) following the User Manual. Briefly, to screen the interacting proteins, the coding sequence of *MaICE1* was cloned into pGK7 vector to fuse with the DNA-binding domain (DBD) as bait, and transformed into yeast strain Gold Y2H by the lithium acetate method. The cDNA library (2.0×10^9 cfu/ml) was generated by TAKARA BIOTECHNOLOGY (DALIAN) CO., LTD using poly (A)⁺ mRNAs extracted from banana fruit that were stored under cold stress, fusing to pGADT7 with activation domain (AD) and was transformed into Gold Y2H carrying the MaICE1 bait. The transformed cells (approximately 6.0×10^6 cfu) were placed on DDO medium (minimal media double dropouts, SD medium with -Leu/-Trp), and positive clones among the transformants were identified by scoring growth on QDO medium (minimal media quadruple dropouts, SD medium with -Leu/-Trp/-Ade/-His). Plasmids of positive clones was extracted from the yeast cells using a TIANprep yeast plasmid DNA kit (Tiangen) and then transformed into *Escherichia coli* for sequencing.

To confirm the MaSINA1-MaICE1 interaction, the coding sequences of *MaSINA1* and *MaICE1* were inserted into pGKBT7 or pGADT7 vector as bait and prey, respectively, and were co-transformed into Gold Y2H. Yeast cells were grown on DDO medium for 3 days, then transformed colonies were plated onto QDO medium, as well as QDO media containing 4 mg mL⁻¹ X- α -Gal (α -Gal) for blue color development, to verify the possible interaction between MaSINA1 and MaICE1 according to their growth status and the activity of α -galactosidase. Primers used for Y2H assay are listed in Supplementary Table 1.

Bimolecular Fluorescence Complementation (BiFC) Analysis

To create constructs for BiFC assay, the coding sequence of MaICE1 or MaSINA1 fusing with YNE or YCE, was cloned into the pEAQ-HT vector (Sainsbury et al., 2009). The resulting constructs were then introduced into the *Agrobacterium tumefaciens* strain GV3101, and co-infiltrated into the abaxial side of 4- to 6-week-old tobacco (*N. benthamiana*) leaves using a 1-mL needless syringe as described previously (Fan et al., 2016). Infected tissues were analyzed at 48 h after infiltration. YFP fluorescence was captured using the Confocal Spectral Microscope Imaging System (Leica TCS SP5), with an argon blue laser at 488 nm, a beam splitter for excitation at 500 nm, and a spectral detector set between 515 and 540 nm. Primers used for generating the constructs are listed in Supplementary Table 1.

In Vitro GST Pull-Down Assay

The full-length cDNA of *MaSINA1* was cloned into the pMAL-c2X expression vector (New England Biolabs) (primers are listed in Supplementary Table 1). The maltose binding protein (MBP)-tagged MaSINA1 fusion protein was expressed in *BM* Rosetta (DE3) and purified by affinity chromatography using amylose resin (New England Biolabs, Cat. No. E8021S) according to the manufacturer's instructions. GST-MaICE1 protein was obtained as described previously (Shan et al., 2014). *In vitro* GST pull-down assay was performed as described previously with minor modifications (Liu et al., 2013). Briefly, GST or GST-MaICE1 recombinant protein was incubated with 30 μ L of Glutathione resin in 1× PBS buffer for 2 h at 4°C, the binding reaction was washed three times with 1× PBS buffer and then the MBP-MaSINA1 recombinant protein was added and incubated for an additional 2 h at 4°C. The beads were washed five times with wash buffer (1× PBS, 0.1% Triton X-100), following the elution by boiling with SDS loading buffer, separated by 10% SDS-PAGE, and subjected to western blotting analysis using the anti-MBP antibody (Abcam, Cat. No. ab9084) and the anti-GST antibody (Abcam, Cat. No. ab9085) respectively, with secondary goat anti-rabbit IgG peroxidase antibody (Thermo Scientific, Cat. No. 32460). Detection was carried out using the chemiluminescent substrate SuperSignal West Pico (Thermo Scientific, Cat. No. 34080) for horse-radish peroxidase and imaged on a ChemiDoc™ MP Imaging System (Bio-Rad Laboratories).

Semi-In Vivo Coimmunoprecipitation (CoIP) and Ubiquitination Assays

To create MaSINA1-His and MaICE1-GFP constructs, full-length *MaSINA1* or *MaICE1* was inserted into pEAQ-HT-His and pEAQ-HT-GFP vectors (primers are listed in Supplementary Table 1), respectively (Sainsbury et al., 2009; Peyret and Lomonossoff, 2013), and were introduced into *A. tumefaciens* strain GV3101, following co-infiltrated into the abaxial side of 4- to 6-wk-old tobacco leaves using a 1-mL needleless syringe. After 36 h of infiltration, 10 μ M MG132 (Merck, Cat. No. 474790) was injected into tobacco leaves to prevent protein degradation. After 36 h, tobacco leaves were harvested and the protein was extracted as described by Han et al. (2016) and Ye et al. (2016), as well as the following CoIP assay. A 10 μ L volume of anti-GFP antibody (Abcam, Cat. No. ab290) was added to 1 mL of cell lysates. Then, binding was gently shaken at 4°C for 4 h, and 50 μ L of protein A agarose beads (Roche, Cat. No. 11134515001) was added. After 3 h of incubation at 4°C, the precipitated samples were washed, separated by SDS-PAGE and then performed western blotting analysis as described above using 4000-fold diluted anti-His antibody (Abcam, Cat. No. ab9108) and anti-GFP antibody (Abcam, Cat. No. ab290) respectively, for CoIP assay, and anti-ubiquitin antibody (Sigma-Aldrich, Cat. No. U119) for examining the ubiquitination of MaICE1.

Gene Isolation, Sequence and Expression Analysis

Frozen banana peel was ground in liquid nitrogen using a mortar and pestle. Total RNA was extracted using the hot borate method of Wan and Wilkins (1994), and the extract was treated with DNase I digestion using an RNase-free kit (Promega, Cat. No. M6101). The DNA-free total RNA was used as template for reverse-transcription PCR. The first-strand cDNA of the product was applied to PCR amplification. Quantitative real-time PCR (qRT-PCR) was carried out on a Bio-Rad CFX96 Real-Time PCR System using the GoTaq® qPCR Master Mix Kit (Promega, Cat. No. A600A) following the manufacturer's instructions. *MaACT1* was used as the reference gene to normalize the gene expression levels (Chen et al., 2011). Primers for gene isolation and qRT-PCR are listed in Supplementary Table 1.

Alignments were carried out on ClustalX (version 1.83) and GeneDoc software, and a phylogenetic tree was constructed using the Neighbor-Joining method in the MEGA5 program.

Subcellular Localization Assay

The complete Open Reading Frame (ORF) of *MaSINA1* was amplified and inserted into the pEAQ-GFP vector (primers are listed in Supplementary Table 1). The MaSINA1-GFP plasmid was electroporated into the *A. tumefaciens* strain GV3101, and injected into the abaxial side of 4- to 6-week-old tobacco leaves as described above. pEAQ-GFP was employed as the positive control. After 48 h of infiltration, GFP signal was visualized with a fluorescence microscope (Zeiss Axioskop 2 Plus) with a beam splitter for excitation at 500 nm.

Promoter Isolation and Activity Analysis

Genomic DNA of banana leaves was extracted using the DNeasy Plant Mini Kit (Qiagen, Cat. No. 69104). The *MaSINA1* promoter region was amplified by PCR using the specific primers listed in Supplementary Table 1. Conserved *cis*-element motifs in the promoter were predicted using Plant-CARE¹ database. The PCR product was inserted into the pGreenII 0800-LUC double reporter vector (Hellens et al., 2005) to fuse it with the Firefly luciferase (LUC) reporter gene (*MaSINA1* pro-LUC). A Renilla luciferase (REN) driven by the 35S promoter at the same vector was used as an internal control. The construct CaMV35S-REN/*MaSINA1* pro-LUC was infiltrated into tobacco leaf protoplasts by polyethylene glycol (PEG) methods as described previously (Shan et al., 2014; Fan et al., 2016).

The promoter activity was assayed according to Fan et al. (2016). The transformed protoplasts were incubated at room temperature (22°C) or cold (7°C). After 36 h, LUC and REN activities were measured on the Luminoskan Ascent Microplate Luminometer (Thermo) using the dual luciferase assay kits (Promega, Cat. No. E1910), with a 5-s delay and 15-s integrated measurements. The promoter activity is indicated by LUC/REN ratio. At least six assay repeats were included for each.

In Vitro Ubiquitination Assay

The ubiquitination assay was generally conducted as described by Cheng et al. (2012). For E3 ubiquitin ligase activity assay of *MaSINA1*, 500 ng MBP-*MaSINA1* recombinant protein was incubated for 2 h in the presence or absence of 50 ng of human E1 (Boston Biochem, Cat. No. E305), 250 ng of human E2 (Boston Biochem, Cat. No. E2-622), 2 mg of ubiquitin (Boston Biochem, Cat. No. u-100sc). The reaction products were subjected to western blotting using anti-MBP (Abcam, Cat. No. ab9084) and anti-Ub antibodies (Sigma-Aldrich, Cat. No. U119). For the *in vitro* *MaSINA1*-mediated MaICE1 ubiquitination assay, MBP-*MaSINA1* and GST-MaICE1 proteins were coincubated as described above. The reaction products were analyzed using the anti-GST, -MBP and -Ub antibody, respectively.

Semi-In Vivo Cell-Free Proteasomal Degradation Assay

To construct pEAQ-MaICE1-GFP-LUC, firstly the coding region of firefly LUC was amplified from pGreenII 0800-LUC as template, and inserted into pEAQ-GFP, generating pEAQ-LUC-GFP. Then the full length of *MaICE1* was cloned into pEAQ-LUC-GFP to fuse in frame with LUC and GFP to give rise to pEAQ-MaICE1-LUC-GFP. The full-length cDNA of *MaSINA1* without the stop codon was cloned into pEAQ vector, generating pEAQ-*MaSINA1*. The specific primers used for construction these vectors are shown in Supplementary Table 1. The constructs were electroporated into the *A. tumefaciens* strain GV3101, growing in YEP medium (1% peptone, 1% yeast extract, and 0.5% NaCl) supplemented with 100 mg/L kanamycin and 10 mg/L rifampin overnight at 28°C. Cells were centrifuged, resuspended to OD₆₀₀ = 0.6 in infiltration buffer [10 mM MgCl₂,

10 mM MES (pH 5.6), 100 μM acetosyringone]. After 4 h of incubation at room temperature, equal volumes (1:1) of different combinations of the strain harboring each construct were mixed and co-infiltrated into tobacco leaves as described above.

The cell free proteasomal degradation assay was performed as described previously (García-Cano et al., 2014). For MG132 treatment, 10 μM MG132 or distilled water, was injected into tobacco leaves, respectively. After 4 h of injection, leaves were harvested and ground into fine powder in liquid nitrogen. Total protein extracts from 12.5 mg of fresh leaf weight, prepared by bead-beating the tissue in 25 μL of degradation/DNase digestion buffer [10 mM Tris-HCl (pH 7.6), 0.5 mM CaCl₂, 10 mM MgCl₂, 5 mM DTT, 5 mM ATP, and 1× plant protease inhibitor mixture (Sigma-Aldrich)], were incubated at room temperature for 30 min in a final reaction volume of 120 μL. The protein concentration was determined using the Bradford reagent (Bio-Rad Laboratories). Reactions were terminated by boiling in SDS sample buffer, and subjected to SDS-PAGE followed by western blotting using anti-GFP antibody (Abcam, Cat. No. ab290), as described above. Putative Rubisco large chains (~55 kDa) was adopted as the loading control (Huang et al., 2013). LUC activity was also measured using the dual luciferase assay kit, as described above.

Semi-In Vivo Analysis of MaICE1 Transactivational Activity

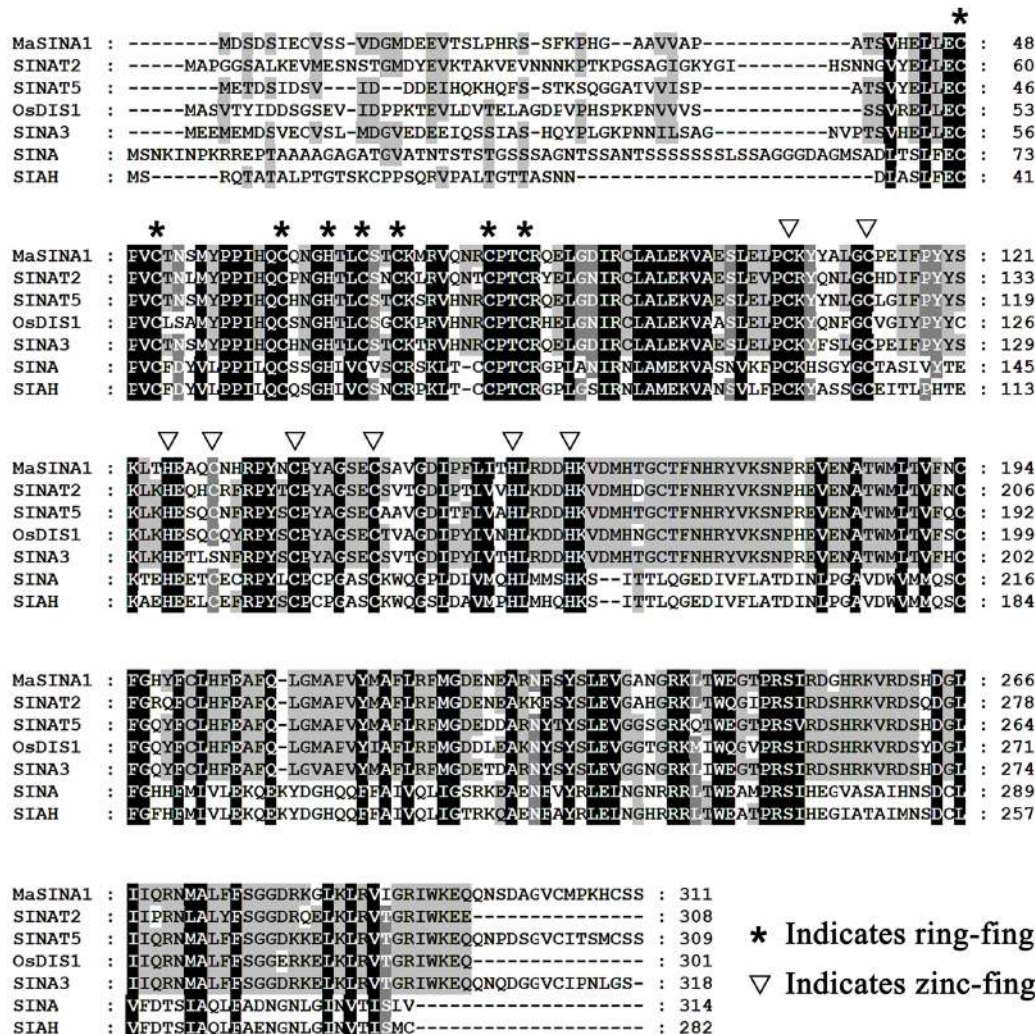
This transient expression assay was performed in tobacco leaves as described above. The *MaNAC1* promoter was cloned into the pGreenII 0800-LUC double reporter vector, while MaICE1 or *MaSINA1*, was cloned into the pEAQ vector as effectors (Primers are listed in Supplementary Table 1). The LUC and REN activity were recorded as described above. The *trans*-activation ability of MaICE1 to the *MaNAC1* promoter is indicated by the LUC/REN ratio. The experiments were repeated at least six times, yielding similar results.

RESULTS

MaSINA1 Physically Interacts with MaICE1

In our previous study, ICE1-CBF pathway is acknowledged to be involved in cold tolerance of banana fruit (Peng et al., 2013; Zhao et al., 2013; Shan et al., 2014). In *Arabidopsis*, it has been well documented that ICE1 protein stability is vital for cold tolerance (Miura et al., 2011; Ding et al., 2015). To gain a deeper insight into regulators that will affect ICE1 stability of banana fruit, we screened a banana fruit cold stress-related cDNA library using MaICE1 as the bait. Among the eight candidate interacting proteins of MaICE1, one of the promising interactors (GSMUA_Achr9G05880_001; XP_009416451) was particularly interesting because it encodes a SEVEN IN ABSENTIA (SINA) ubiquitin ligase (termed *MaSINA1*), and it was studied further. The deduced protein of this gene contains conserved RING finger and zinc finger motifs, and has high sequence identity (85%) with *Arabidopsis* SINAT5 (Xie et al., 2002) (Figure 1), which

¹<http://bioinformatics.psb.ugent.be/webtools/plantcare/html/>



* Indicates ring-finger

▽ Indicates zinc-finger

FIGURE 1 | Multiple alignment of MaSINA1 and other SINA family proteins including *Arabidopsis* SINAT2 and SINAT5, rice OsDIS1, tomato SINA3, *Drosophila* SINA and human SIAH. The amino acid residues that are highly conserved among the examined proteins are shaded. The conserved ring-finger and zinc-finger motifs are indicated by asterisks and triangles, respectively.

was identified as a homolog of *Drosophila* SINA (Carthew and Rubin, 1990). The interaction between MaSINA1 and MaICE1 was further examined by yeast two-hybrid assay. As shown in **Figure 2A**, positive α-galactosidase activity confirmed the interaction between MaSINA1 and MaICE1. Then *in vitro* GST pull-down assay was performed to further confirm the interaction between MaSINA1 and MaICE1. The results showed that MBP-MaSINA1 protein was pulled down by GST-MaICE1 (**Figure 2B**), also supporting that MaSINA1 interacts with MaICE1.

Subsequently, we used BiFC to determine where MaSINA1-MaICE1 complex formation occurs within the plant cell. For this assay, MaSINA1 and MaICE1 were fused with the C-terminal half and N-terminal half of the YFP, respectively. Both constructs were then transiently expressed in tobacco (*N. benthamiana*) leaves. Reconstituted YFP fluorescence was captured in the nucleus of the tobacco leave cells when MaSINA1-YC was coexpressed with

MaICE1-YN, but not with the control combinations (**Figure 2C**), revealing that MaSINA1 interacts with MaICE1 in the nucleus.

To further validate this interaction in the plant cell, CoIP assay was performed in tobacco leaves expressing MaICE1-GFP and MaSINA1-His. The protein extraction was immunoprecipitated with the anti-GFP antibody, the immunoprecipitated protein complex was analyzed by western blotting using anti-GFP and anti-His antibodies. As shown in **Figure 2D**, the MaSINA1-His protein was only detected in the immunoprecipitated complex from the leaf tissue expressing MaSINA1-His and MaICE1-GFP. No MaSINA1-His protein was appeared in the immunoprecipitated complex from the leaf tissue expressing MaSINA1-His with the vector control (empty-GFP) (**Figure 2D**). These results together clearly demonstrate that MaSINA1 directly interacts with MaICE1.

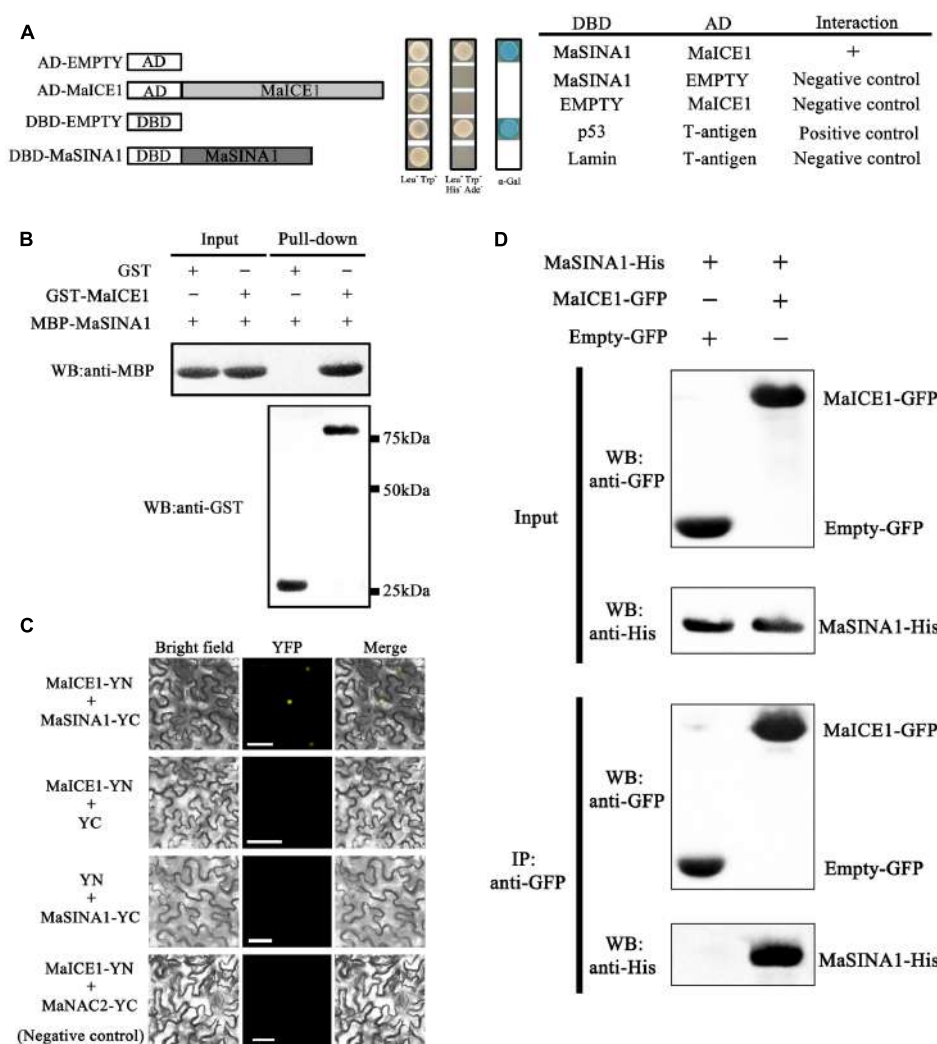


FIGURE 2 | MaSINA1 interacts with MaICE1 *in vitro* and semi-*in vivo*. **(A)** Yeast two-hybrid assay for the interaction between MaSINA1 and MaICE1. The coding regions of MaSINA1 and MaICE1 were fused with DBD and AD vectors, respectively, as indicated, and co-transformed into the yeast strain Gold Y2H. The ability of yeast cells to grow on synthetic medium lacking tryptophan, leucine, histidine, and adenine but containing 125 μM Aureobasidin A, and to turn blue in the presence of the chromogenic substrate X-α-Gal, was scored as a positive interaction. **(B)** *In vitro* GST pull-down analysis of MaSINA1–MaICE1 interaction. MBP-MaSINA1 protein was incubated with GST-MaICE1 or GST, the bounded proteins were then detected by western blotting assays using the anti-His antibody and anti-GST antibody, respectively. **(C)** BiFC in tobacco leaf epidermal cells showing the interaction between MaSINA1 and MaICE1 in living cells. MaSINA1 fused with the C-terminus of YFP and MaICE1 fused with the N-terminus of YFP, were co-transfected into tobacco leaves and visualized using confocal microscopy. Expressions of MaSINA1 or MaICE1 alone, and MaICE1 with MaNAC2 were used as negative controls. YFP-fluorescence of YFP; Merge-digital merge of bright field and fluorescent images. The length of the bar indicated in the photographs is 30 μm. **(D)** CoIP assay showing the interaction between MaSINA1 with MaICE1. Tobacco leaves co-expressing MaICE1-GFP and MaSINA1-His, or empty-GFP and MaSINA1-His, was used to immunoprecipitate with the anti-GFP antibody, and the immunoblot was probed with the anti-GFP and anti-His antibody, respectively. These assays were conducted three biological repeats, yielding similar results.

Molecular Characterization of MaSINA1

Unlike *MaICE1* expressed constitutively in the banana fruit under cold stress (Zhao et al., 2013), qRT-PCR analysis showed that *MaSINA1* was down-regulated by cold stress. Compared with the expression of *MaSINA1* in control fruit, the expression of *MaSINA1* in the fruit directly stored at 7°C (cold stress) decreased at 6 h, and was ~14% of control on day 5 (Figure 3A).

To better understand the *MaSINA1* expression in response to cold stress, *MaSINA1* promoter with 1059 bp length was isolated

from the genome of *M. acuminata*. Based on the Plant-CARE database, one low-temperature responsive element, CCGAC, termed LTRECOREATCOR15 was found in the *MaSINA1* promoter at -573 bp to -577 bp from the initiation codon (Supplementary Figure 1), indicating that *MaSINA1* promoter might be cold-responsive. Furthermore, a transient assay using the dual luciferase reporter system in tobacco leaf protoplasts showed that *MaSINA1* promoter activity was inhibited by cold stress (Figure 3B). These results indicate that *MaSINA1* is repressed by cold.

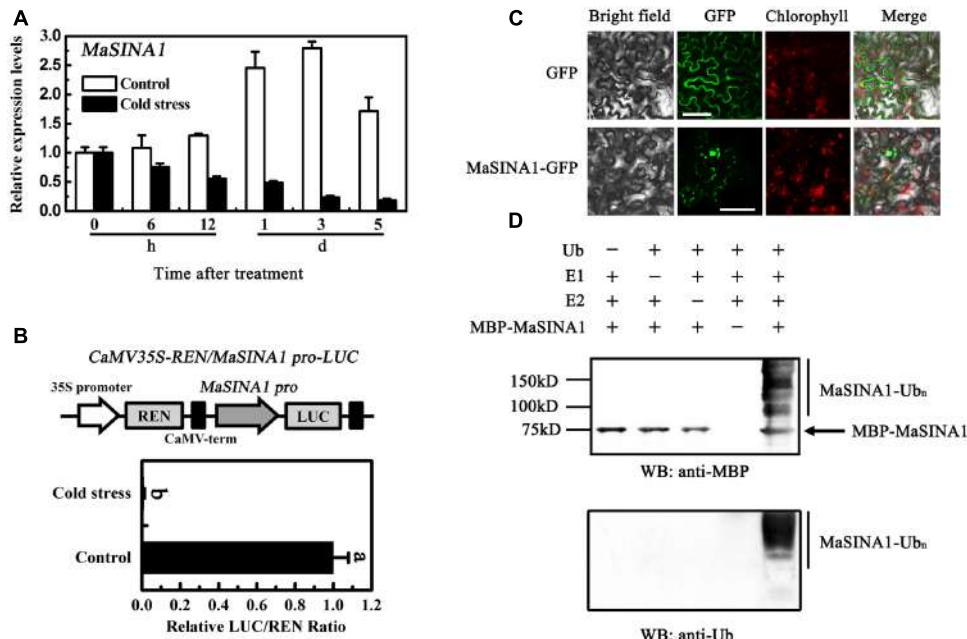


FIGURE 3 | Molecular characterization of MaSINA1. **(A)** Expression of MaSINA1 during cold storage. For cold stress, fruit were directly stored at 7°C, whereas for non-cold stress control, fruit were directly stored at 22°C. Expression level at different time points was expressed as a ratio relative to the harvest time (0 days of non-cold stress control), which was set at 1. Each value represents the means of three biological replicates, and vertical bars indicate the SE. **(B)** MaSINA1 promoter activity in response to cold stress. The dual luciferase reporter vector containing MaSINA1 promoter (CaMV35S-REN/MaSINA1 pro-LUC) was transiently transformed into tobacco leaf protoplasts using a modified PEG method and test for cold stress (7°C) induction. After incubation for 36 h, LUC and REN luciferase activities were assayed, and the promoter activity is indicated by the ratio of LUC to REN. Each value represents the means of six biological replicates, and vertical bars represent the SE. Different letters above bars indicate significant difference at the 5% level by Student's *t*-test. **(C)** Subcellular localization of MaSINA1 in tobacco leaves. MaSINA1 fused with the GFP or GFP positive control were infiltrated into tobacco leaves via *Agrobacterium tumefaciens* strain GV3101. After 48 h of the infiltration, GFP fluorescence was visualized using a fluorescence microscope. Red colors represent chlorophyll autofluorescent signals. Bars, 30 μm. **(D)** E3 ubiquitin ligase activity of MaSINA1. Recombinant MBP-MaSINA1 fusion protein was incubated in the presence or absence of E1, E2, and/or ubiquitin. The reactions were analyzed with immunoblots using anti-MBP and anti-ubiquitin antibodies. E3 ubiquitin ligase activity of MBP-MaSINA1 was only detected in the presence of E1, E2, and ubiquitin.

To investigate the subcellular location of MaSINA1, we fused the GFP with MaSINA1 protein, and transient expressed it in tobacco leaves. The GFP fluorescence of MaSINA1 fusion protein was localized predominantly in the nucleus, and some in the cytoplasm and plasma membrane (Figure 3C), which is similar with the localization of SINAT5 in *Arabidopsis* (Xie et al., 2002) and OsDIS1 in rice (Ning et al., 2011).

Previous studies showed that many RING motif-containing proteins possess E3 ubiquitin ligase activity (Stone et al., 2005). MaSINA1 contains a C3HC4-type RING finger motif at the N terminus with conserved Cys and His residues (Figure 1). To test whether MaSINA1 is a functional E3 ligase enzyme, we produced MaSINA1 in *E. coli* as a fusion with the MBP tag and purified the tagged protein (Supplementary Figure 2). Human E1, E2 and ubiquitin were used for the *in vitro* E3 ubiquitin ligase activity assay. Ubiquitination activity was detected using anti-MBP antibody and anti-ubiquitin antibody. As shown in Figure 3D, self-ubiquitination of MaSINA1 (polyubiquitinated smear ladders) was observed when Ub, E1, and E2 were present (Figure 3D, lane 5), but not in any negative controls that missed any one of the necessary components for the reaction (Figure 3D, lanes 1–4). Thus, MaSINA1 functions as an E3 ubiquitin ligase.

MaSINA1 Targets MaICE1 for Ubiquitination Degradation

As MaSINA1 interacts with MaICE1 (Figure 1), and MaSINA1 functions as an E3 ubiquitin ligase, we sought to investigate whether MaICE1 protein could be ubiquitinated by MaSINA1, an *in vitro* ubiquitination assay was also carried out using MaICE1 protein as a substrate. Recombinant GST-MaICE1 and MBP-MaSINA1 proteins were co-incubated in the presence or absence of Ub, E1, and E2 at 30°C for 2 h. The reaction mixture was analyzed by immunoblotting using anti-GST antibody. Co-incubation of GST-MaICE1 and MBP-MaSINA1 in the presence of Ub, E1, and E2 gave rise to a high-molecular-mass band, while lacking of Ub, E1, or E2 in the reaction mixture abolished the ubiquitinated band (Figure 4A), suggesting that MaSINA1 is a ubiquitin ligase capable of ubiquitinating MaICE1. The ubiquitination of MaICE1 by MaSINA1 was further confirmed *in planta*. MaICE1-GFP and MaSINA1-His constructs were co-expressed in *N. benthamiana* leaves. After immunoprecipitation with the anti-GFP antibody matrix, the immunoprecipitated complex was verified by Western blotting using the anti-ubiquitin antibody. As shown in Figure 4B, a smear banding representing the polyubiquitinated

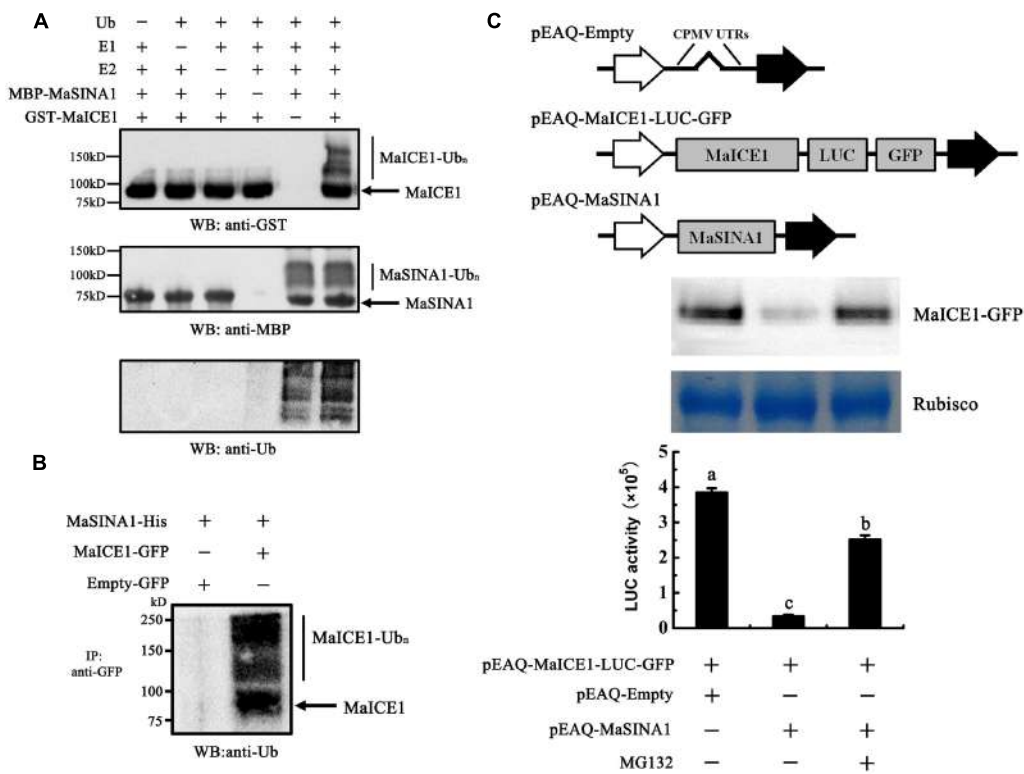


FIGURE 4 | Ubiquitination of MaICE1 and degradation of MaICE1 in tobacco leaves by MaSINA1. **(A)** *In vitro* ubiquitination of MaICE1 by MaSINA1. Recombinant MBP-MaSINA1 protein was co-incubated with GST-MaICE1 protein in the presence or absence of Ub, human E1, and human E2 at 30°C for 2 h. The reaction mixture was analyzed by immunoblotting with the anti-GST, anti-MBP, and anti-ubiquitin antibody, respectively. Ubiquitination results in a heterogeneous collection of higher-molecular mass proteins that were detected using these antibodies. **(B)** Semi-*in vivo* ubiquitination of MaICE1 by MaSINA1. Tobacco leaves co-expressing MaICE1-GFP and MaSINA1-His, or empty-GFP and MaSINA1-His, was used to immunoprecipitate with the anti-GFP antibody, and the immunoblot was probed with the anti-ubiquitin antibody. **(C)** Proteasome-mediated degradation assay of MaICE1 in plant cells. Up panel, Western blot analysis of MaICE1 degradation in the tobacco cell-free system. As indicated, MaICE1 fused with GFP and LUC was expressed alone or co-expressed with MaSINA1 in tobacco leaves in the presence or absence of MG132. The resulting protein extracts were analyzed using an anti-GFP antibody. Putative Rubisco large chains (~55 kDa) was adopted as the loading control for total protein. Bottom panel, LUC activity in each sample used in Western blot analysis. Each value represents the mean \pm SE of six biological replicates. Different letters above bars indicate a statistical difference at the 5% level compared with the empty.

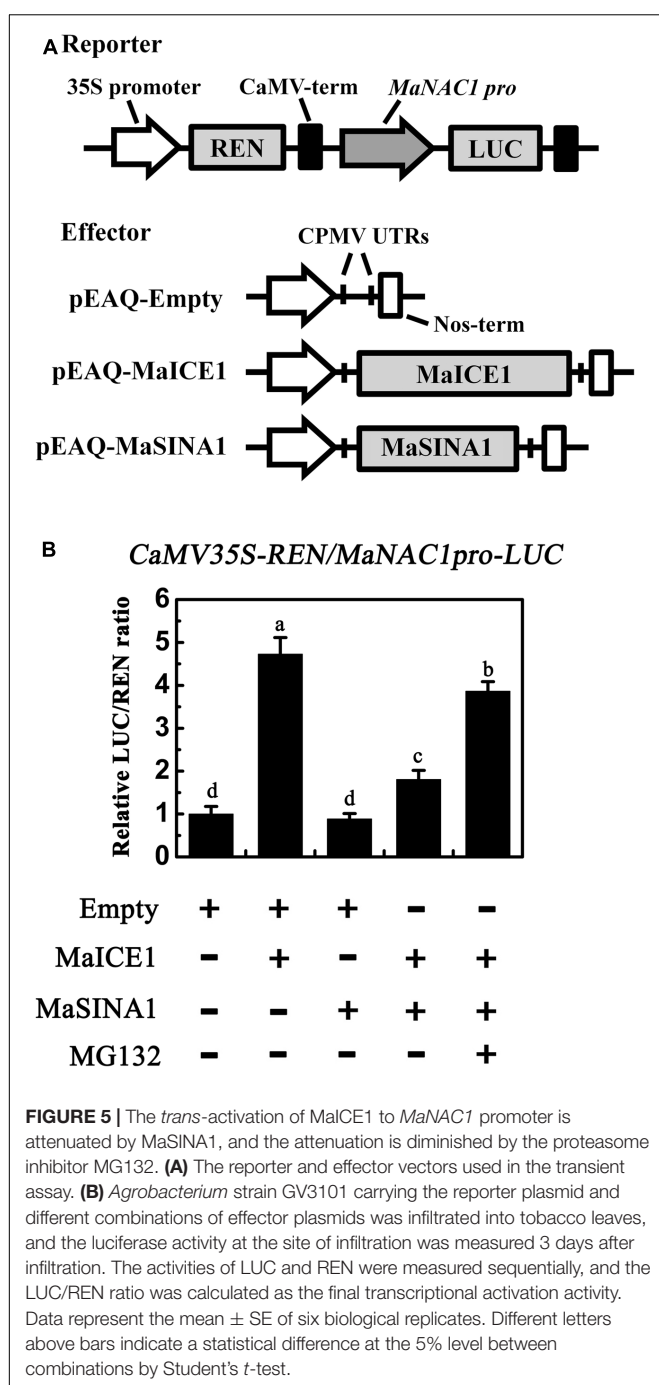
MaICE1 protein was detected by the anti-ubiquitin antibody in the anti-GFP-immunoprecipitated complex from the co-expression of MaICE1-GFP and MaSINA1-His, but not in the immunoprecipitated complex from the co-expression of empty-GFP and MaSINA1-His control (Figure 4B). Together, these data reveal that MaSINA1 is able to ubiquitinate MaICE1.

To test whether MaSINA1 can promote MaICE1 degradation through ubiquitination, the stability of MaICE1 protein in plant cells was next examined using a cell free proteasome degradation assay. The *MaICE1* fused to a GFP and a LUC tag was inserted into pEAQ vector (Figure 4C). Total proteins were extracted from tobacco leaves transiently co-expressing GFP- and LUC-tagged MaICE1 and/or MaSINA1, and the stability of MaICE1-GFP was tested by western blotting with anti-GFP antibody. As shown in Figure 4C, MaICE1 amounts declined substantially in the presence of MaSINA1, whereas without MaSINA1, MaICE1 remained relatively stable. This MaSINA1-mediated destabilization of MaICE1 most likely occurred by proteasome degradation pathway, because it was inhibited by MG132, a known selective inhibitor of proteasomal activity

(Yang et al., 2004). Quantification of LUC activity also showed that expression of MaSINA1 protein resulted in the degradation of MaICE1 protein, while in the presence of MG132, the degradation of MaICE1 was eliminated (Figure 4C). Together, these findings strongly demonstrate that MaSINA1 and MaICE1 form a protein module by which MaSINA1 ubiquitinates and controls the steady protein level of MaICE1.

MaSINA1 Attenuates the Trans-activation of MaICE1 to MaNAC1

Our previous study showed that MaICE1 bound specifically to the MYC recognition sequence in the *MaNAC1* promoter and positively regulated *MaNAC1* expression, which is an important transcriptional regulator of cold stress response of banana fruit (Shan et al., 2014). The result that MaSINA1 targets MaICE1 for ubiquitination degradation led us to investigate whether or not MaSINA1 interferes with *trans*-activation of *MaNAC1* by MaICE1. To this end, we performed transient expression assays using the dual-luciferase reporter system. In this experiment, the *MaNAC1* promoter-driven



LUC (*MaNAC1* pro-LUC) and CaMV35S promoter-driven REN (CaMV35S-REN; as an internal control) were constructed in the same vector, together with an effector plasmid expressing MaICE1 or MaSINA1 (Figure 5A), and expressed in the tobacco leaves. The *in vivo* transcriptional activity of MaICE1 was reflected by the LUC/REN ratio. Compared with the control that was co-transfected with the empty construct, co-expression of MaICE1 with *MaNAC1* Pro-LUC significantly increased the LUC/REN ratio, while this increase was abolished when MaSINA1 was co-expressed (Figure 5B), indicating that

MaSINA1 attenuates the *trans*-activation of MaICE1 to *MaNAC1*. Importantly, in the presence of MG132, the attenuation of MaSINA1 on MaICE1 transcriptional activation of *MaNAC1* was diminished (Figure 5B). These data indicate that MaSINA1 might act as a negative regulator of cold stress response of banana fruit via controlling the stability and *trans*-activation of MaICE1.

DISCUSSION

Cold storage is effectively applied to maintain the post-harvest qualities and extend the shelf life of many horticultural fruits and vegetables. However, tropical and subtropical fruits, like bananas, are easily susceptible to chilling injury, resulting in quality deterioration and substantial losses, which significantly shortens storage life (Chen et al., 2008; Zhao et al., 2013; Shan et al., 2014). Thus, revealing the molecular mechanism(s) of the cold response in banana fruit is important for the genetic improvement of cold tolerance and improving fruit quality and storage potential. Currently, the most well-known cold signaling pathway is ICE-CBF-COR cascade (Ding et al., 2015; Shi et al., 2015). Accordingly, we also previously found that ICE-CBF pathway is positively involved in cold stress response of banana fruit (Zhao et al., 2013; Shan et al., 2014). However, regulators that act upstream in this cascade have not been identified. In this study, we sought to identify a SINA ubiquitin ligase MaSINA1 from banana fruit, and show that MaSINA1 controls MaICE1 protein stability via the UPS.

The UPS serves as a versatile post-translational modification, and has been implicated in almost all aspects of growth and development, as well as in responses to biotic and abiotic stress in plants (Lyzenga and Stone, 2012; Stone, 2014; Sharma et al., 2016). Specificity of the UPS is controlled mainly by the substrate-recruiting E3 ubiquitin ligases, and consequently, a large number of E3 ligases, have been isolated and shown to be involved in plant stress responses by modulating the abundance of key downstream stress-responsive TFs (Lyzenga and Stone, 2012; Stone, 2014; Sharma et al., 2016). However, only a few ubiquitin ligases such as HOS1, CONSTITUTIVE PHOTOMORPHOGENIC 1 (COP1), carboxyl terminus of Hsc70-interacting protein (CHIP) and *Arabidopsis* F-box protein 7 (FBP7), have been implicated in cold stress response (Barrero-Gil and Salinas, 2013). *Arabidopsis* HOS1 was the first RING-type E3 ubiquitin ligase to act as a negative regulator of cold responses (Jung et al., 2014). Under normal growth conditions, HOS1 did not affect the nuclear localization and the abundance of GFP-ICE1, while HOS1 can interact with and ubiquitinate ICE1 for degradation under cold stress (Dong et al., 2006). Consistent with a role in mediating ICE1 degradation, overexpression of HOS1 results in reduced expression of cold-responsive genes and increased sensitivity to cold stress (Lee et al., 2001), suggesting HOS1 functions to attenuate stress signaling. Strangely, no interaction was found between banana fruit MaHOS1 and MaICE1 (data not shown). Indeed in the present work, another RING-type E3 termed MaSINA1 was identified from banana fruit. MaSINA1 showed high sequence similarity to *Arabidopsis* SINAT5 (Figure 1), and was repressed by cold

stress (**Figure 3**). We also found that MaSINA1 interacted with and ubiquitinated MaICE1 and promoted MaICE1 degradation via the UPS (**Figures 2, 4**). In addition, we demonstrated that MaSINA1 attenuated the *trans*-activation of MaICE1 to MaNAC1 (**Figure 5**). Based on these results, it could be speculated that MaSINA1 negatively regulates cold stress response of banana fruit by promoting the ubiquitination-mediated degradation of MaICE1 protein. To the best of our knowledge, it is the first report that except HOS1, another novel E3 ubiquitin ligase controls ICE1 protein stability in fruits. Previously, we also showed that unlike *Arabidopsis* ICE1, cold-induced phosphorylation of MaICE1 might not be necessary for its transcriptional activity, but could enhance its *trans*-activation ability (Shan et al., 2014). The present data also reveal that the regulators of controlling ICE1 stability via UPS during cold stress response might be different in banana fruit and *Arabidopsis*. However, whether MaICE1 stability controlled by MaSINA1 is cold-dependent or -independent needs to be elucidated. In addition, it should be pointed out that ubiquitination is a reversible post-translational modification and de-ubiquitination enzymes (ubiquitin proteases) are also involved in modulating protein function (Barrero-Gil and Salinas, 2013). Therefore, the participation of ubiquitin proteases in plant responses to cold stress will be a subject of future research.

Besides ubiquitination, protein phosphorylation and sumoylation also play an important role in the regulation of ICE1 activity under cold stress (Chinnusamy et al., 2007; Barrero-Gil and Salinas, 2013). In contrast with HOS1, SIZ1 mediates sumoylation of ICE1, which reduces the polyubiquitination of ICE1 to enhance its stability (Miura et al., 2007). Although a very earlier research hypothesized that cold stress induces phosphorylation of ICE1 (Chinnusamy et al., 2007), until recently, the hypothesis is confirmed by Ding et al. (2015). They found that under cold stress, OST1 (OPEN STOMATA 1), a well-known Ser/Thr protein kinase in ABA signaling, phosphorylates ICE1 to antagonize the degradation of ICE1 mediated by HOS1. More interestingly, the OST1 protein also competes with HOS1 to bind to ICE1, thus releasing ICE1 from the HOS1-ICE1 complex. Thus, the dual role of OST1 contributes to the enhancement of ICE1 stability (Ding et al., 2015). Our previous study also indicated that the *trans*-activation ability of MaICE1 is enhanced by MaICE1 phosphorylation. Given that ICE1 protein stability

is regulated by various post-translational modifications, it is of interest to find out how these modifications are coordinately balanced to maintain ICE1 homeostasis in response to cold stress.

CONCLUSION

In summary, a banana fruit SINA ubiquitin ligase MaSINA1 was identified. MaSINA1 can ubiquitinate MaICE1 for the 26S proteasome-dependent degradation, and therefore suppresses the transcriptional activation of MaICE1. Our findings reveal a novel mechanism in banana fruit for control of the stability of ICE1 and for the negative regulation of cold stress response by a SINA E3 ligase.

AUTHOR CONTRIBUTIONS

J-YC, W-JL, and WS designed the research. Z-QF, and WS performed the experiments. Z-QF, J-YC, J-FK, W-JL, and WS wrote the manuscript.

FUNDING

This work was supported in part by the National Key Research and Development Program (grant no. 2016YFD0400103) and the China Agriculture Research System (grant no. CARS-32-09).

ACKNOWLEDGMENT

We thank Professor George P. Lomonosoff (Department of Biological Chemistry, John Innes Centre, Norwich Research Park) for the generous gift of pEAQ series vectors.

SUPPLEMENTARY MATERIAL

The Supplementary Material for this article can be found online at: <http://journal.frontiersin.org/article/10.3389/fpls.2017.00995/full#supplementary-material>

REFERENCES

- Agarwal, M., Hao, Y., Kapoor, A., Dong, C. H., Fujii, H., Zheng, X., et al. (2006). A R2R3 type MYB transcription factor is involved in the cold regulation of CBF genes and in acquired freezing tolerance. *J. Biol. Chem.* 281, 37636–37645. doi: 10.1074/jbc.M605895200
- Barrero-Gil, J., and Salinas, J. (2013). Post-translational regulation of cold acclimation response. *Plant Sci.* 205–206, 48–54. doi: 10.1016/j.plantsci.2013.01.008
- Carthew, R. W., and Rubin, G. M. (1990). *Seven in absentia*, a gene required for specification of R7 cell fate in the *Drosophila* eye. *Cell* 63, 561–577. doi: 10.1016/0092-8674(90)90452-K
- Chen, J. Y., He, L. H., Jiang, Y. M., Wang, Y., Joyce, D. C., Ji, Z. L., et al. (2008). Role of phenylalanine ammonia-lyase in heat pretreatment-induced chilling tolerance in banana fruit. *Physiol. Plant.* 132, 318–328. doi: 10.1111/j.1399-3054.2007.01013.x
- Chen, L., Zhong, H. Y., Kuang, J. F., Li, J. G., Chen, J. Y., and Lu, W. J. (2011). Validation of reference genes for RT-qPCR studies of gene expression in banana fruit under different experimental conditions. *Planta* 234, 377–390. doi: 10.1007/s00425-011-1410-3
- Cheng, M. C., Hsieh, E. J., Chen, J. H., Chen, H. Y., and Lin, T. P. (2012). *Arabidopsis* RGLG2, functioning as a RING E3 ligase, interacts with AtERF53 and negatively regulates the plant drought stress response. *Plant Physiol.* 158, 363–375. doi: 10.1104/pp.111.189738
- Chinnusamy, V., Ohta, M., Kanrar, S., Lee, B. H., Hong, X., Agarwal, M., et al. (2003). ICE1: a regulator of cold-induced transcriptome and freezing tolerance in *Arabidopsis*. *Genes Dev.* 17, 1043–1054. doi: 10.1101/gad.1077503

- Chinnusamy, V., Zhu, J., and Zhu, J. K. (2007). Cold stress regulation of gene expression in plants. *Trends Plant Sci.* 12, 444–451. doi: 10.1016/j.tplants.2007.07.002
- Ding, Y., Li, H., Zhang, X., Xie, Q., Gong, Z., and Yang, S. (2015). OST1 kinase modulates freezing tolerance by enhancing ICE1 stability in *Arabidopsis*. *Dev. Cell* 32, 278–289. doi: 10.1016/j.devcel.2014.12.023
- Doherty, C. J., Van Buskirk, H. A., Myers, S. J., and Thomashow, M. F. (2009). Roles for *Arabidopsis* CAMTA transcription factors in cold-regulated gene expression and freezing tolerance. *Plant Cell* 21, 972–984. doi: 10.1105/tpc.108.063958
- Dong, C. H., Agarwal, M., Zhang, Y., Xie, Q., and Zhu, J. K. (2006). The negative regulator of plant cold responses, HOS1, is a RING E3 ligase that mediates the ubiquitination and degradation of ICE1. *Proc. Natl. Acad. Sci. U.S.A.* 103, 8281–8286. doi: 10.1073/pnas.0602874103
- Fan, Z. Q., Kuang, J. F., Fu, C. C., Shan, W., Han, Y. C., Xiao, Y. Y., et al. (2016). The banana transcriptional repressor MaDEAR1 negatively regulates cell wall-modifying genes involved in fruit ripening. *Front. Plant Sci.* 7:1021. doi: 10.3389/fpls.2016.01021
- García-Cano, E., Zaltsman, A., and Citovsky, V. (2014). Assaying proteasomal degradation in a cell-free system in plants. *J. Vis. Exp.* 85:51293. doi: 10.3791/51293
- Han, Y. C., Kuang, J. F., Chen, J. Y., Liu, X. C., Xiao, Y. Y., Fu, C. C., et al. (2016). Banana transcription factor MaERF11 recruits histone deacetylase MaHDA1 and represses the expression of MaACO1 and expansins during fruit ripening. *Plant Physiol.* 171, 1070–1084. doi: 10.1104/pp.16.00301
- Hellens, R., Allan, A., Friel, E., Bolitho, K., Grafton, K., Templeton, M., et al. (2005). Transient expression vectors for functional genomics, quantification of promoter activity and RNA silencing in plants. *Plant Methods* 1:13. doi: 10.1186/1746-4811-1-13
- Hu, Y., Jiang, L., Wang, F., and Yu, D. (2013). Jasmonate regulates the inducer of CBF expression-C-repeat binding factor/DRE binding factor1 cascade and freezing tolerance in *Arabidopsis*. *Plant Cell* 25, 2907–2924. doi: 10.1105/tpc.113.112631
- Huang, W., Miao, M., Kud, J., Niu, X., Ouyang, B., Zhang, J., et al. (2013). SINAC1, a stress-related transcription factor, is fine-tuned on both the transcriptional and the post-translational level. *New Phytol.* 197, 1214–1224. doi: 10.1111/nph.12096
- Huang, X. S., Zhang, Q., Zhu, D., Fu, X., Wang, M., Zhang, Q., et al. (2015). ICE1 of *Poncirus trifoliata* functions in cold tolerance by modulating polyamine levels through interacting with arginine decarboxylase. *J. Exp. Bot.* 66, 3259–3274. doi: 10.1093/jxb/erv138
- Jamrohammadi, M., Zolla, L., and Rinalducci, S. (2015). Low temperature tolerance in plants: changes at the protein level. *Phytochemistry* 117, 76–89. doi: 10.1016/j.phytochem.2015.06.003
- Jia, Y., Ding, Y., Shi, Y., Zhang, X., Gong, Z., and Yang, S. (2016). The cbfs triple mutants reveal the essential functions of CBFs in cold acclimation and allow the definition of CBF regulons in *Arabidopsis*. *New Phytol.* 212, 345–353. doi: 10.1111/nph.14088
- Jung, J. H., Lee, H. J., Park, M. J., and Park, C. M. (2014). Beyond ubiquitination: proteolytic and nonproteolytic roles of HOS1. *Trends Plant Sci.* 19, 538–545. doi: 10.1016/j.tplants.2014.03.012
- Knight, M. R., and Knight, H. (2012). Low-temperature perception leading to gene expression and cold tolerance in higher plants. *New Phytol.* 195, 737–751. doi: 10.1111/j.1469-8137.2012.04239.x
- Lee, H., Xiong, L., Gong, Z., Ishitani, M., Stevenson, B., and Zhu, J. K. (2001). The *Arabidopsis* HOS1 gene negatively regulates cold signal transduction and encodes a RING finger protein that displays cold-regulated nucleocytoplasmic partitioning. *Genes Dev.* 15, 912–924. doi: 10.1101/gad.866801
- Liu, X., Chen, C. Y., Wang, K. C., Luo, M., Tai, R., Yuan, L., et al. (2013). PHYTOCHROME INTERACTING FACTOR3 associates with the histone deacetylase HDA15 in repression of chlorophyll biosynthesis and photosynthesis in etiolated *Arabidopsis* seedlings. *Plant Cell* 25, 1258–1273. doi: 10.1105/tpc.113.109710
- Lyzenga, W. J., and Stone, S. L. (2012). Abiotic stress tolerance mediated by protein ubiquitination. *J. Exp. Bot.* 63, 599–616. doi: 10.1093/jxb/err310
- Medina, J., Catalá, R., and Salinas, J. (2011). The CBFs: three *Arabidopsis* transcription factors to cold acclimate. *Plant Sci.* 180, 3–11. doi: 10.1016/j.plantsci.2010.06.019
- Miura, K., Jin, J. B., Lee, J., Yoo, C. Y., Stirm, V., Miura, T., et al. (2007). SIZ1-mediated sumoylation of ICE1 controls CBF3/DREB1A expression and freezing tolerance in *Arabidopsis*. *Plant Cell* 19, 1403–1414. doi: 10.1105/tpc.106.048397
- Miura, K., Ohta, M., Nakazawa, M., Ono, M., and Hasegawa, P. M. (2011). ICE1 Ser403 is necessary for protein stabilization and regulation of cold signaling and tolerance. *Plant J.* 67, 269–279. doi: 10.1111/j.1365-313X.2011.04589.x
- Ning, Y., Jantsaruyarat, C., Zhao, Q., Zhang, H., Chen, S., Liu, J., et al. (2011). The SINA E3 ligase OsDIS1 negatively regulates drought response in rice. *Plant Physiol.* 157, 242–255. doi: 10.1104/pp.111.180893
- Paul, J. Y., Khanna, H., Kleidon, J., Hoang, P., Geijssels, J., Daniells, J., et al. (2016). Golden bananas in the field: elevated fruit pro-vitamin A from the expression of a single banana transgene. *Plant Biotechnol. J.* 15, 520–532. doi: 10.1111/pbi.12650
- Peng, H. H., Shan, W., Kuang, J. F., Lu, W. J., and Chen, J. Y. (2013). Molecular characterization of cold-responsive basic helix-loop-helix transcription factors MabHLHs that interact with MaICE1 in banana fruit. *Planta* 238, 937–953. doi: 10.1007/s00425-013-1944-7
- Peyret, H., and Lomonosoff, G. P. (2013). The pEAQ vector series: the easy and quick way to produce recombinant proteins in plants. *Plant Mol. Biol.* 83, 51–58. doi: 10.1007/s11103-013-0036-1
- Sainsbury, F., Thuenemann, E. C., and Lomonosoff, G. P. (2009). pEAQ: versatile expression vectors for easy and quick transient expression of heterologous proteins in plants. *Plant Biotechnol. J.* 7, 682–693. doi: 10.1111/j.1467-7652.2009.00434.x
- Shan, W., Chen, J. Y., Kuang, J. F., and Lu, W. J. (2016). Banana fruit NAC transcription factor MaNAC5 cooperates with MaWRKYs to enhance the expression of pathogenesis-related genes against *Colletotrichum musae*. *Mol. Plant Pathol.* 17, 330–338. doi: 10.1111/mpp.12281
- Shan, W., Kuang, J. F., Lu, W. J., and Chen, J. Y. (2014). Banana fruit NAC transcription factor MaNAC1 is a direct target of MaICE1 and involved in cold stress through interacting with MaCBF1. *Plant Cell Environ.* 37, 2116–2127. doi: 10.1111/pce.12303
- Sharma, B., Joshi, D., Yadav, P. K., Gupta, A. K., and Bhatt, T. K. (2016). Role of ubiquitin-mediated degradation system in Plant Biology. *Front. Plant Sci.* 7:806. doi: 10.3389/fpls.2016.00806
- Shi, Y., Ding, Y., and Yang, S. (2015). Cold signal transduction and its interplay with phytohormones during cold acclimation. *Plant Cell Physiol.* 56, 7–15. doi: 10.1093/pcp/pcu115
- Shi, Y., Tian, S., Hou, L., Huang, X., Zhang, X., Guo, H., et al. (2012). Ethylene signaling negatively regulates freezing tolerance by repressing expression of CBF and type-A ARR genes in *Arabidopsis*. *Plant Cell* 24, 2578–2595. doi: 10.1105/tpc.112.098640
- Stone, S. L. (2014). The role of ubiquitin and the 26S proteasome in plant abiotic stress signaling. *Front. Plant Sci.* 5:135. doi: 10.3389/fpls.2016.00806
- Stone, S. L., Hauksdottir, H., Troy, A., Herschleb, J., Kraft, E., and Callis, J. (2005). Functional analysis of the RING-type ubiquitin ligase family of *Arabidopsis*. *Plant Physiol.* 137, 13–30. doi: 10.1104/pp.104.052423
- Wan, C. Y., and Wilkins, T. A. (1994). A modified hot borate method significantly enhances the yield of high-quality RNA from cotton (*Gossypium hirsutum* L.). *Anal. Biochem.* 223, 7–12. doi: 10.1006/abio.1994.1538
- Wisniewski, M., Nassuth, A., Teulieres, C., Marque, C., Rowland, J., Cao, P. B., et al. (2014). Genomics of cold hardiness in woody plants. *Crit. Rev. Plant Sci.* 33, 92–124. doi: 10.1080/07352689.2014.870408
- Xie, Q., Guo, H. S., Dallman, G., Fang, S., Weissman, A. M., and Chua, N. H. (2002). SINAT5 promotes ubiquitin-related degradation of NAC1 to attenuate auxin signals. *Nature* 419, 167–170. doi: 10.1038/nature00998
- Yang, P., Fu, H., Walker, J., Papa, C. M., Smalle, J., Ju, Y. M., et al. (2004). Purification of the *Arabidopsis* 26 S proteasome: biochemical and molecular analyses revealed the presence of multiple isoforms. *J. Biol. Chem.* 279, 6401–6413. doi: 10.1074/jbc.M311977200
- Ye, Y. J., Xiao, Y. Y., Han, Y. C., Shan, W., Fan, Z. Q., Xu, Q. G., et al. (2016). Banana fruit VQ motif-containing protein5 represses cold-responsive transcription

- factor MaWRKY26 involved in the regulation of JA biosynthetic genes. *Sci. Rep.* 6:23632. doi: 10.1038/srep23632
- Zhao, M. L., Wang, J. N., Shan, W., Fan, J. G., Kuang, J. F., Wu, K. Q., et al. (2013). Induction of jasmonate signalling regulators MaMYC2s and their physical interactions with MaICE1 in methyl jasmonate-induced chilling tolerance in banana fruit. *Plant Cell Environ.* 36, 30–51. doi: 10.1111/j.1365-3040.2012.02551.x
- Zhou, M. Q., Shen, C., Wu, L. H., Tang, K. X., and Lin, J. (2011). CBF-dependent signaling pathway: a key responder to low temperature stress in plants. *Crit. Rev. Biotechnol.* 31, 186–192. doi: 10.3109/07388551.2010.505910

Conflict of Interest Statement: The authors declare that the research was conducted in the absence of any commercial or financial relationships that could be construed as a potential conflict of interest.

Copyright © 2017 Fan, Chen, Kuang, Lu and Shan. This is an open-access article distributed under the terms of the Creative Commons Attribution License (CC BY). The use, distribution or reproduction in other forums is permitted, provided the original author(s) or licensor are credited and that the original publication in this journal is cited, in accordance with accepted academic practice. No use, distribution or reproduction is permitted which does not comply with these terms.



Overexpression of *Hevea brasiliensis* *HbICE1* Enhances Cold Tolerance in *Arabidopsis*

Hong-Mei Yuan^{1*}, Ying Sheng², Wei-Jie Chen¹, Yu-Qing Lu¹, Xiao Tang¹, Mo Ou-Yang¹ and Xi Huang^{1*}

¹ Hainan Key Laboratory for Sustainable Utilization of Tropical Bioresources, Institute of Tropical Agriculture and Forestry, Hainan University, Haikou, China, ² State Key Laboratory of Hybrid Rice, College of Life Sciences, Wuhan University, Wuhan, China

OPEN ACCESS

Edited by:

Jie Zhou,
Zhejiang University, China

Reviewed by:

Abidur Rahman,
Iwate University, Japan
Ren Maozhi,
Chongqing University, China

*Correspondence:

Hong-Mei Yuan
yuanhongmei@hainu.edu.cn
Xi Huang
xihuang@hainu.edu.cn

Specialty section:

This article was submitted to
Plant Cell Biology,
a section of the journal
Frontiers in Plant Science

Received: 05 April 2017

Accepted: 07 August 2017

Published: 22 August 2017

Citation:

Yuan H-M, Sheng Y, Chen W-J, Lu Y-Q, Tang X, Ou-Yang M and Huang X (2017) Overexpression of *Hevea brasiliensis* *HbICE1* Enhances Cold Tolerance in *Arabidopsis*. *Front. Plant Sci.* 8:1462.
doi: 10.3389/fpls.2017.01462

Rubber trees (*Hevea brasiliensis*) were successfully introduced to south China in the 1950s on a large-scale; however, due to the climate, are prone to cold injury during the winter season. Increased cold tolerance is therefore an important goal, yet the mechanism underlying rubber tree responses to cold stress remains unclear. This study carried out functional characterization of *HbICE1* (Inducer of CBF Expression 1) from *H. brasiliensis*. A nucleic protein with typical features of ICEs, *HbICE1* was able to bind to MYC recognition sites and had strong transactivation activity. *HbICE1* was constitutively expressed in all tested tissues, with highest levels in the bark, and was up-regulated when subjected to various stresses including cold, dehydration, salinity and wounding. When overexpressed in *Arabidopsis*, 35S::*HbICE1* plants showed enhanced cold resistance with increased proline content, reduced malondialdehyde (MDA) metabolism and electrolyte leakage, and decreased reactive oxygen species (ROS) accumulation. Expression of the cold responsive genes (*COR15A*, *COR47*, *RD29A*, and *KIN1*) was also significantly promoted in 35S::*HbICE1* compared to wild-type plants under cold stress. Differentially expressed genes (DEGs) analysis showed that cold treatment changed genes expression profiles involved in many biological processes and phytohormones perception and transduction. Ethylene, JA, ABA, as well as ICE-CBF signaling pathways might work synergistically to cope with cold tolerance in rubber tree. Taken together, these findings suggest that *HbICE1* is a member of the *ICE* gene family and a positive regulator of cold tolerance in *H. brasiliensis*.

Keywords: *hevea brasiliensis*, *ICE1*, cold stress, CBF pathway, bHLH, reactive oxygen species

INTRODUCTION

Cold stress is one of the most devastating environmental factors adversely affecting plant growth and development, significantly constraining geographic distribution and agricultural productivity. Cold stress interferes with various physiological and biochemical processes via direct inhibition of metabolic reactions and indirect induction of osmotic, oxidative and other stresses. *Hevea brasiliensis*, with its high rate of production and superior rubber quality, is the sole commercial source of natural rubber. A perennial tropical tree species originating from the Amazonian forests of Brazil, rubber trees were traditionally planted within a restricted region between 15° north and 15° south latitudes. Though rubber trees were successfully introduced to south China in the 1950s

on a large-scale, they are prone to cold injury during the winter season. Cold stress not only affects rubber production, but also threatens the survival of rubber trees in China. Increased cold tolerance is therefore a major aim of rubber tree breeding programs.

Plants have evolved various physiological, biochemical and molecular strategies aimed at adaptation to adverse situations (Nakashima et al., 2009; Thomashow, 2010; Theocharis et al., 2012). In the past decade, significant progress has been made in deciphering the key components of the cold signaling pathway in the model plants *Arabidopsis* and other species (Wisniewski et al., 2014; Shi Y. et al., 2015). In *Arabidopsis*, three *C-repeat-binding factors* (*CBFs*), *CBF1*, *CBF2*, and *CBF3*, have been functionally characterized (Jaglo-Ottosen et al., 1998; Medina et al., 1999). Under low temperatures, cold stress rapidly and transiently induces *CBF* expression, stimulating expression of *cold-responsive* (*COR*) genes by binding to *C-repeat* binding factor (*CRT*)/dehydration-responsive element (*DRE*) *cis*-elements in the promoters of *COR* genes, thereby increasing accumulation of proline and total sugar and protecting membranes and proteins from damage (Stockinger et al., 1997; Liu et al., 1998; Thomashow, 1999; Chinnusamy et al., 2007; Maruyama et al., 2012; Shi Y. et al., 2015). *ICE1* (inducer of *CBF* expression 1), a constitutively expressed MYC-like bHLH transcriptional activator, also functions during cold acclimation by inducing *CBF* expression via binding of MYC recognition elements in *CBF* promoters (Chinnusamy et al., 2003, 2010; Fursova et al., 2009). The mutant *ice1* was found to exhibit reduced plant tolerance to chilling and freezing stresses due to repression of *AtCBF3* expression and subsequent decreases in expression of various downstream *COR* genes (Chinnusamy et al., 2003; Fursova et al., 2009). In contrast, plants overexpressing either *AtICE1* or *AtICE2* display improved freezing tolerance via enhanced *AtCBF3* and *AtCBF1* expression (Chinnusamy et al., 2003; Fursova et al., 2009). Thus, the ICE-CBF-COR transcriptional regulatory cascade is a well-established plant response to cold stress (Chinnusamy et al., 2007; Shi Y. et al., 2015). Cold acclimation, which is thought to enhance freezing tolerance after exposure to low temperatures (Thomashow, 1999), is one of the major mechanisms of plant adaptation to cold stress. But whether cold acclimation can affect the cold resistance of rubber tree has not been reported so far. Besides transcriptional regulation of ICE gene, several important components have been found to regulate cold acclimation by modulating ICE-CBF pathway at posttranslational levels. The small ubiquitin-related modifier (SUMO) E3 ligase, SIZ1 (SAP and Miz 1) and the RING finger E3 ligase HOS1 (high expression of osmotically responsive genes1) have been shown to modify *ICE1* posttranslationally and function in the ICE-CBF/DREB1 signaling pathway (Dong et al., 2006; Miura et al., 2007). Recent reports further suggest that *ICE1* is also regulated by various other factors such as jasmonate signaling proteins JAZ 1/4 (JASMONATE ZIM-DOMAIN 1/4), which inhibit *ICE1*

Abbreviations: GFP, green fluorescent protein; *ICE1*, Inducer of CBF Expression 1; MDA, malondialdehyde; qRT-PCR, quantitative real-time PCR; ROS, reactive oxygen species.

transcriptional activity (Hu et al., 2013). Moreover, Ding et al. (2015) discovered that the protein kinase OST1 (open stomata 1), a key component in ABA signaling, interacts with and phosphorylates *ICE1* protein under cold stress, stabilizing and activating *ICE1* and thereby enhancing plant tolerance to freezing temperatures. *ICE1* is also degraded by the E3 ligase HOS1 (high expression of osmotically responsive gene 1)-mediated 26S-proteasome pathway (Dong et al., 2006). More recently, Huang X. S. et al. (2015) reported that *ICE1* from *Poncirus trifoliata* functions in cold tolerance by altering polyamine accumulation via interaction with arginine decarboxylase. *ICE1* is therefore not only a central component in cold signaling, but also serves as a convergence point, integrating signals to regulate cold tolerance in plants.

Studies on cold stress in rubber trees were mainly focused on changes in physiological parameters and alleviating injury after cold stress, the major components of cold signaling of rubber tree were nearly unidentified except *HbCBF1* and the molecular mechanisms underlying how rubber tree responses to cold stress were still very poorly understood (Cheng et al., 2015). In this study, the *H. brasiliensis* *ICE1* (*HbICE1*) gene was cloned and functionally characterized for its role in cold tolerance, revealing its location in the nucleus and ability to bind to MYC recognition sites. Overexpression of 35S::*HbICE1* in *Arabidopsis* enhanced cold resistance probably due to increased proline level, reduced MDA content and electrolyte leakage, and decreased reactive oxygen species (ROS) accumulation under cold stress. Furthermore, the cold responsive genes (*COR15A*, *COR47*, *RD29A*, and *KIN1*) were significantly activated in overexpressing plants compared to the wild-type (WT) under cold conditions. Taken together, these data suggest that *HbICE1* is a functional member of the *ICE* gene family, playing a positive role in cold resistance in *H. brasiliensis*.

MATERIALS AND METHODS

Plant Material and Treatments

Reyan 7-33-97 rubber trees (*H. brasiliensis*) cultivated at the experimental plantation of Hainan University, Hainan Province, China, were used in this study. The plants were pruned annually. To examine tissue-specific expression of *HbICE1*, samples from six tissues (the latex, leaves, stem, bark, stamen and pistil) were collected for RNA extraction from 17-year-old mature trees tapped for the previous two years. To determine expression of *HbICE1* in response to NaCl and dehydration treatment, four batches of 12 seedlings per treatment were selected. Three batches were treated with 200 mM NaCl or 10% polyethylene glycol (PEG), and one with ddH₂O then the leaves collected for RNA isolation. For cold treatment, seedlings were transferred to a culture room at 4°C under a 12 h light/12 h dark cycle with 80% humidity for 1, 3, 6, 12, or 24 h then the leaves collected for RNA isolation. For wounding treatment, leaves of 5-year-old mature virgin (untapped) trees were wounded with a hemostat then the leaves collected for RNA extraction.

To generate 35S::GFP-*HbICE1* transgenic *Arabidopsis* plants, the coding region of *HbICE1* was amplified using primers 5'-gaattcATGCTTGATACCGACTGGTATGATA-3' and 5'-gaattcT

CACATCATTCCATGAAAGCCAGCT-3'. The coding sequence fragment was then subcloned into the *ECOR1* site of the pEGAD vector and the recombinant plasmid introduced into *Arabidopsis* ecotype *Col-0* via *Agrobacterium tumefaciens* (GV3101)-mediated transformation using the floral dip method (Clough and Bent, 1998). *Arabidopsis* plants were sown in vermiculite in pots at 23°C under 16 h light/8 h dark conditions with 75% humidity and a light intensity of 150 mmol m⁻² s⁻¹.

To determine cold tolerance of the transgenic plants, a cold treatment assay was performed as described previously with slight modifications (Ding et al., 2015). Fourteen-day-old seedlings cultivated in 1/2 MS medium at 23°C were transferred to 4°C for 2 days then exposed to -8°C for 4 h and subsequently returned to normal conditions. Survival rates were measured after 7 days. To determine cold tolerance of the rubber tree seedlings, seedlings with or without cold acclimation (1 day at 4°C) were exposed to -16°C for 0.5 and 1 h and subsequently returned to normal conditions. The freezing treatment experiment was performed in triplicate. For *Arabidopsis*, T3 or T4 homozygous transgenic plants were used in this study.

Isolation and Bioinformatics Analysis of HbICE1

The CDS of HbICE1 was predicted using Bioedit software (<http://www.mbio.ncsu.edu/BioEdit/bioedit.html>) and confirmed using BLASTP on the NCBI BLAST server (<http://blast.ncbi.nlm.nih.gov/Blast.cgi>). The detailed *In silico* cloning procedure was carried out as previously described (Hong et al., 2015). Molecular weights (MW) and isoelectric points (pI) were predicted using ExPASy (<http://www.expasy.org/tools>), nuclear localization signals were predicted using the online server (<http://www.predictprotein.org/>), and protein secondary domains were predicted with a Motif scan (http://myhits.isb-sib.ch/cgi-bin/motif_scan). Sequence alignment was performed using DNAMAN software and a phylogenetic tree constructed using MEGA 5.1 software.

Subcellular Localization of HbICE1

The full-length CDS of HbICE1 was fused to the C terminus of the green fluorescent protein (GFP) of the pEGAD vector, driven by the 35S promoter. GFP in the roots of homozygote transgenic *Arabidopsis* 35S::GFP-HbICE1 plants was examined using confocal microscopy (excitation and emission: 488 and 515 nm, respectively; 22°C).

Transcriptional Activation Assay and MYCR-Binding Assay of HbICE1

For the transcriptional activation assay, the open reading frame (ORF) of HbICE1 was amplified by PCR using primers P1 (cgGAATCCatcgttataccgactggta) and P2 (aaCTGCAGcatcattccatgaaaggccag). The coding sequence fragment was then subcloned into the *EcoRI* and *PstI* restriction sites of the pGBKT7 vector, giving pGBKT7-HbICE1. The recombinant vector pGBKT7-HbICE1, as well as pGBKT7-53+pGADT7-T (positive control) and pGBKT7 (negative control), were transformed into yeast strain AH109 according to the manufacturer's instructions (Clontech, PT4084-1).

The transformed yeast was placed on plates containing SD/-Trp-Leu/X-α-Gal/Aureobasidin A, SD/-Trp-Leu, SD/-Trp, SD/-Trp-His or SD/-Trp-His-Ade medium then incubated at 28°C for 3–4 days for analysis of transformant growth.

To investigate whether HbICE1 was able to bind to the MYC recognition sequence, a yeast one-hybrid experiment (Y1H) was performed according to the manufacturer's instructions (Clontech). The ORF of HbICE1 was fused to the pGADT7 vector digested with *EcoRI* to create pGADT7-HbICE1. A 66-bp DNA fragment containing triple tandem repeats of the sequence containing the MYC recognition sequence (CACATG) was inserted into the pHIS2 vector, generating the recombinant vector pHIS2-MYCR. pHIS2-MYCR was then transformed into yeast strain Y187 on plates containing SD/-Trp, SD/-Trp/-His or SD/-Trp/-His/10mM 3-AT medium to verify autoactivation of pHIS2-MYCR. Both pGADT7-HbICE1 and pHIS2-MYCR were subsequently co-transformed into Y187 to verify the DNA sequence MYCR and HbICE1 protein interactions. The transformed yeast strains were placed on plates containing SD/-Trp/-Leu, SD/-Trp/-Leu/-His, or SD/-Trp/-Leu/-His/10mM 3-AT medium then incubated at 28°C for 3–4 days for analysis of transformant growth.

RNA Extraction and Quantitative Real-Time PCR

Hevea RNA was extracted from leaves of *H. brasiliensis* as described previously (Xia et al., 2011). *Arabidopsis* RNA was extracted using Trizol reagent (Invitrogen, Carlsbad, CA, USA) according to the instruction manual. All RNA samples were treated with RNase-free DNase I (Promega, Madison, WI, USA) to digest genomic DNA. The concentration and quality of DNaseI-treated total RNA was determined by spectrophotometry and agarose gel electrophoresis. As a template for first-strand cDNA synthesis, 2 µg DNase I-treated RNA was used according to the manufacturer's instructions (RevertAid First Stand cDNA Synthesis kit; Fermentas, Vilnius, Lithuania). Quantitative real-time PCR (qRT-PCR) was carried out using ABI-7500 Real-Time PCR apparatus with SYBR Green I dye (Takara, Tokyo, Japan) as follows: 95°C for 3 min followed by 40 cycles of 95°C for 20 s, 58°C for 15 s and 72°C for 20 s. The efficiency of each primer pair was evaluated prior to PCR using the primers listed in Table S1. Relative levels were calculated as 2^{-ΔΔCT}. Each biological sample was performed with three technical repetitions, and data analysis carried out using three independent biological replicates. The whole process from plant material treatment, RNA extraction, cDNA synthesis to qRT-PCR was repeated three times per treatment as three independent biological replicates. Values were statistically analyzed by ANOVA or the Student's *t*-test.

Analysis of Malondialdehyde (MDA) and Proline Contents, and Electrolyte Leakage

Three-week-old seedlings of transgenic 35S::HbICE1 and WT *Arabidopsis* were subjected to cold stress treatment then leaves harvested to determine MDA and proline contents, and the degree of electrolyte leakage. Proline accumulation was determined as described previously (Shi H. T. et al., 2012). Briefly, 0.25 g leaf samples were harvested and extracted in 3%

sulfosalicylic acid then centrifuged at 12,000 × g for 10 min. The supernatant (2 mL) was incubated with 2 mL ninhydrin reagent [2.5% (w/v) ninhydrin, 60% (v/v) glacial acetic acid, and 40% 6M phosphoric acid] and 2 mL glacial acetic acid at 100°C for 40 min, and the reaction terminated in an ice bath. MDA levels were measured using the thio-barbituric acid (TBA) method as described previously (Cai et al., 2015). Electrolyte leakage was measured as described previously (Lin et al., 2012). Eight leaves from transgenic and WT plants treated with and without cold treatment were placed in a bottle with 40 mL ddH₂O₂, shaken at 120 rpm for 3 h then conductivity (C1) measured using an ion leakage meter. Conductivity (C2) was measured after boiling the leaves for 30 min and shaking for 1 h. Electrolyte leakage was calculated as (C1/C2) × 100%.

Screening of Differentially Expressed Genes (Degs) Based on RNA-Seq

Total RNA was isolated from the rubber tree seedlings treated at 4°C for 3 and 12 h, including three biological repeats for each condition. RNA-Seq was performed by the Beijing Genomics Institute (Shenzhen, China). Oligo (dT) magnetic beads were used to select mRNA with polyA tail, followed by DNase I reaction to remove DNA probe. The purified mRNA was used reverse transcription to double-strand cDNA (dscDNA) by N6

random primer. End of dscDNA was repaired with phosphate at 5' end and stickiness "A" at 3' end, then ligated and with adaptor. Two specific primers of adaptor were used to amplify the ligation product. The PCR product was denatured by heat and the single strand DNA was cyclized by splint oligo and DNA ligase. The prepared library was sequenced by (Illumina HiSeqTM 2000).

Clean reads were mapped to the *hevea* contigs assembly using SOAPaligner/soap2 mismatches; no more than 2 bases were allowed in the alignment. The number of clean reads for each gene was calculated and then normalized to Reads Per Kb per Million reads (RPKM), which associates the read number with the gene expression levels. Further, deep analysis were performed based on DEGs, including Gene Ontology (GO) enrichment analysis, KEGG pathway enrichment analysis, cluster analysis, protein-protein interaction network analysis and finding transcription factor.

RESULTS

Cloning and Bioinformatics Analysis of *HbICE1*

Plant *ICE1*-like genes play a critical role in cold tolerance in a number of different plants; however, the *ICE1* gene has yet to be identified in *H. brasiliensis*. To clone the *HbICE1* gene

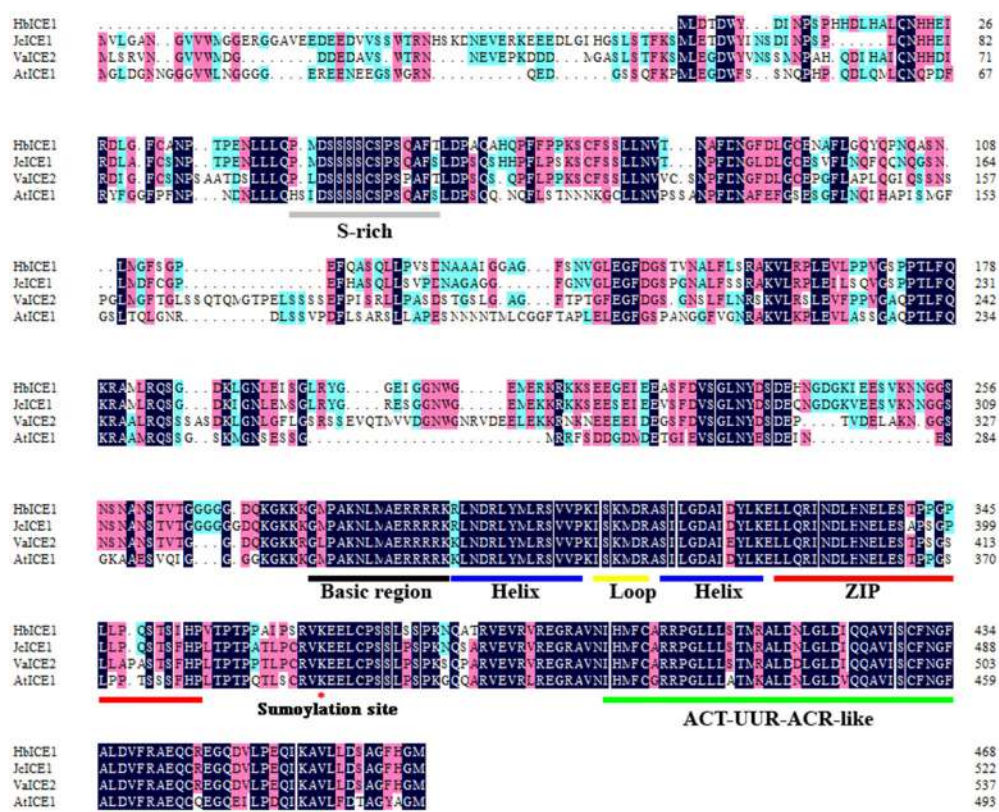


FIGURE 1 | Amino acid sequence alignment of HbICE1 and ICEs from other plant species. Sequences and accession numbers are as follows: *Jatropha curcas* (NP_001306848.1), *Vitis amurensis* (AGP04218.1) and *Arabidopsis thaliana* (NP_189309.2). Blue and pink backgrounds indicate identical and similar residues, respectively. The S-rich motif, basic-helix-loop-helix-leucine zipper (bHLH-ZIP) region, ACT-UUR-ACR-like domain, and sumoylation site are labeled.

from *H. brasiliensis*, the *A. thaliana* ICE1 protein sequence was used as a query sequence in a blast search against the *Hevea* EST and nucleotide database. The matching sequence with the lowest *E*-value was subsequently selected as a backbone for further *insilico* assembly of full-length cDNA. The predicted full-length HbICE1 cDNA contained an ORF of 1410 bps, as validated by PCR amplification and sequencing. The predicted ORF encoded a protein of 469 amino acid residues with an estimated MW of 51 kDa and a pI of 5.30. Multiple alignments of HbICE1 and ICE1 proteins from other plants indicated that the C terminus of all ICE1 proteins tested was highly conserved, whereas the N terminus varied (Figure 1). Furthermore, HbICE1 contained a MYC-like basic helix-loop-helix (bHLH) domain, a serine-rich region (S-rich), a zipper region (ZIP) and an ACT-UUT-ACR like domain, all of which are typical features of ICE proteins (Figure 1). A phylogenetic tree was reconstructed using the deduced amino acid sequence of HbICE1 and other plant ICEs, revealing that HbICE1 is most closely related to JcICE1 of *Jatropha curcas* (Figure 2).

HbICE1 Is Nuclear-Localized and Has Transactivation Activity in Yeast

As a possible transcriptional factor, HbICE1 should be located in the nucleus for transcription regulation. To verify this, we created a construct expressing the GFP-HbICE1 fusion protein by fusing GFP in-frame to the 5' end of the HbICE1 ORF under control of the cauliflower mosaic virus 35S promoter then transforming the construct into WT *Arabidopsis* using the floral dip method. Following selection by Basta resistance, independent transgenic lines were selected for verification by genomic PCR and qRT-PCR analysis. QRT-PCR data revealed high expression of *HbICE1* in six lines (L1, L2, L3, L6, L9, and L10), three of which (L1, L3, and L6) showing highest

transcript levels were selected for further analysis (Figure 3A). Roots of homozygote 35S::GFP-HbICE1 plants were examined using confocal microscopy revealing exclusive expression of the GFP-HbICE1 protein in the nucleus (Figure 3B). This finding confirmed that HbICE1 is a nuclear protein, consistent with a previous report suggesting that *Arabidopsis* ICE1 is a transcription factor (Chinnusamy et al., 2003).

Next, we assayed transactivation activity of HbICE1, another important feature of transcription factors. As shown in Figure 4A, yeast transformed with both pGBT7-53 and pGADT7-T (CK+) grew well on SD/-Trp-Leu and SD/-Trp-Leu/X- α -Gal/Aureobasidin A medium. Moreover, while yeast cells transformed with pGBT7-HbICE1 grew well on SD/-Trp medium, they grew normally on SD/-Trp-His-Ade medium, exhibiting fairly strong β -galactosidase activity. In contrast, yeast cells transformed with the negative control (pGBT7) did not grow on SD/-Trp-His medium (Figure 4A). These results further confirm that HbICE1 has transcriptional activation activity.

Since *Arabidopsis* ICE1 can bind to the MYC-recognition element (Chinnusamy et al., 2003), we also explored whether HbICE1 could bind to a sequence containing the MYC recognition element using a yeast one hybrid (Y1H) assay. As shown in Figure 4B, yeast cells co-transformed with pHIS2-MYCR and pGADT7-HbICE1 grew as well as those containing the positive control (p53HIS2+pGAD-Rec2-53) on SD/-Trp-Leu-His medium with and without 10 mM 3-AT. In contrast, cells co-transformed with the negative control (pHIS2MYCR+pGADT7) did not grow under this condition, further suggesting that HbICE1 binds to MYC recognition sites, activating the transcription of report genes in yeast.

Analysis of HbICE1 Expression Patterns

To investigate tissue-specific expression of *HbICE1*, *HbICE1* expression in the latex, leaves, stem, bark, stamen and pistil was examined by qRT-PCR. *HbICE1* was universally expressed in all tissues tested with the highest expression in bark (Figure 5A). We also examined expression profiles of *HbICE1* under various abiotic stresses including cold, dehydration, wounding, and salinity. *HbICE1* was significantly induced at 3 h after cold treatment, but expression decreased to a low level at 24 h (Figure 5B). Under dehydration, *HbICE1* mRNA was markedly induced by nearly 4.5-fold at 6 h then quickly returned to the normal level at 12 h post treatment (Figure 5C). After wounding treatment, the *HbICE1* transcripts showed strong induction at 1 and 3 h (Figure 5D), while under salt stress, expression was induced 3 h after treatment (Figure 5E). These results indicate that *HbICE1* expression is regulated during plant responses to multiple abiotic stresses.

Over-Expression of HbICE1 in *Arabidopsis* Increases Cold Tolerance

To further determine the role of *HbICE1* in cold tolerance, *HbICE1*-overexpressing lines and WT plants were subjected to freezing treatment. As shown in Figure 6A, *HbICE1*-overexpressing lines displayed less freezing damage and increased survival rate compared with the WT after 1-week recovery. The survival rate of WT plants was only 2.8%, significantly lower than

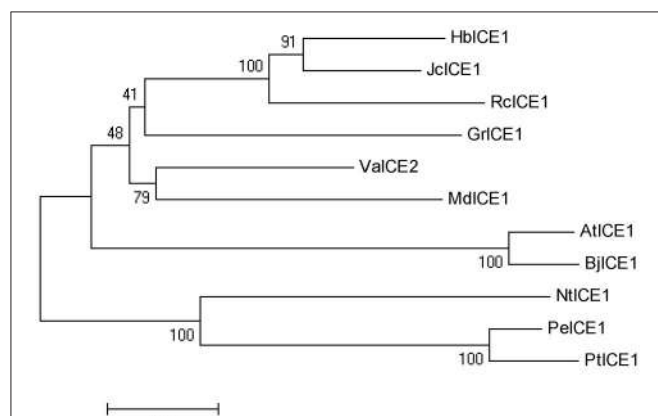
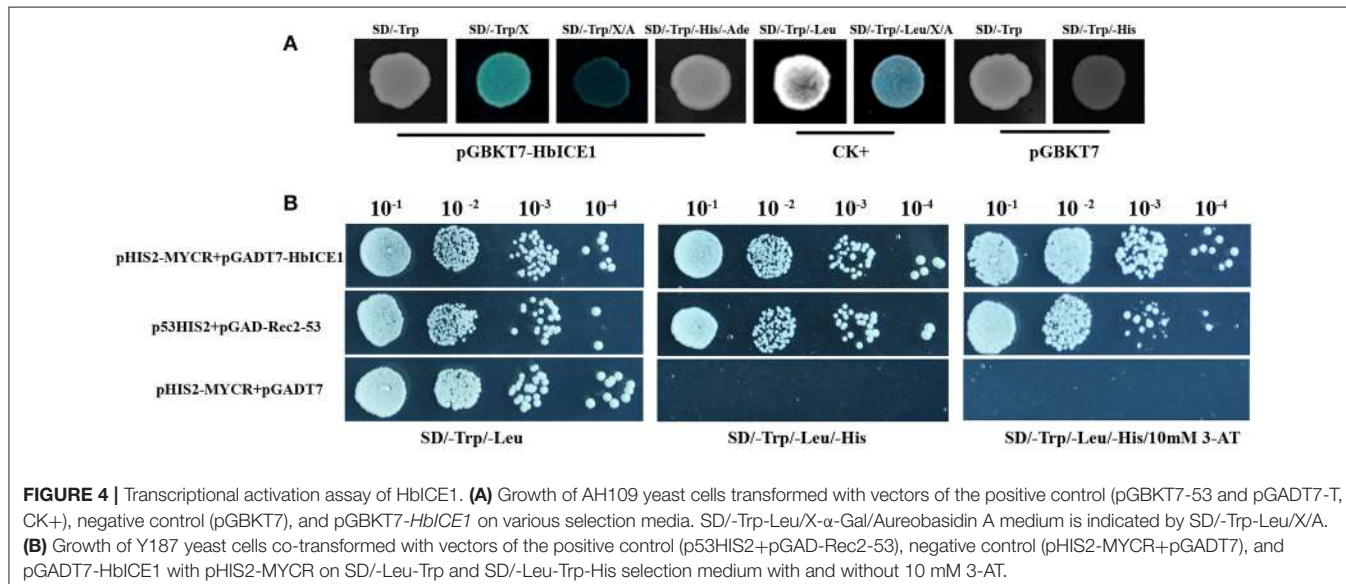
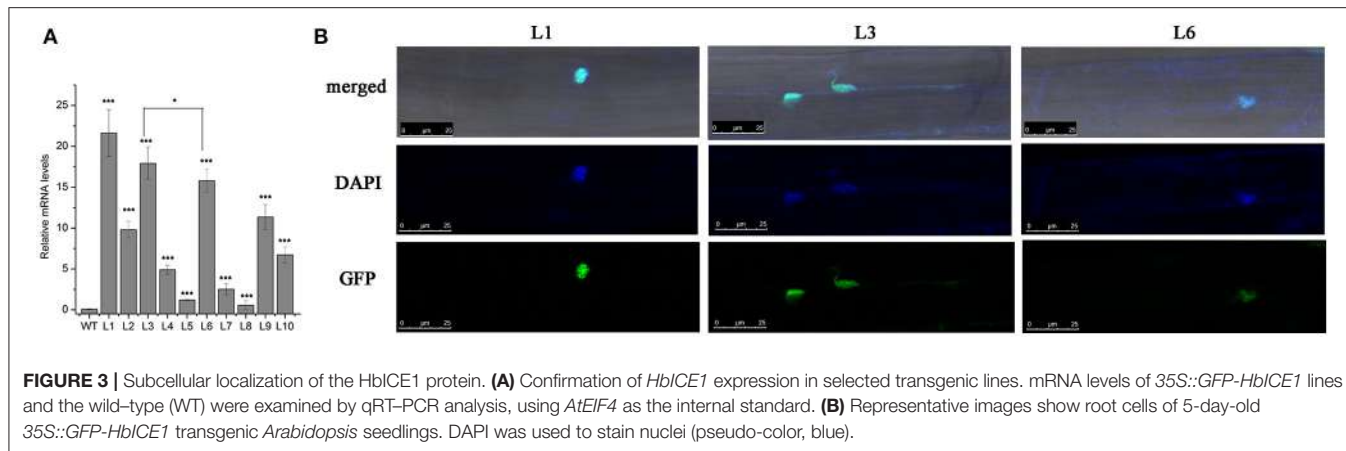


FIGURE 2 | Phylogenetic analysis of HbICE1 and ICEs from other plant species. The neighbor-joining method was used to construct the tree. GenBank accessions of the predicted ICE protein sequences used are as follows: JcICE1 (NP_001306848.1), ValICE1 (AGP04218.1), AtICE1 (NP_189309.2), RclICE1 (XP_015570780.1), GrlICE1 (XP_012489464.1), MdICE1 (XP_008379053.1), PeICE1 (XP_011040262.1), PtICE1 (XP_002318166.1), NtICE1 (XP_009625133.1) and BjICE1 (AEB97375.2).



that of the transgenic lines (77.1% for L1, 55.6% for L3, and 22.2% for L6; **Figure 6B**), suggesting that overexpression of *HbICE1* conferred cold tolerance in transgenic *Arabidopsis*.

Over-Expression of *HbICE1* Affects Proline Content, Electrolyte Leakage, MDA Metabolism and H₂O₂ Accumulation under Cold Stress

Many physiological parameters such as proline content, electrolyte leakage, MDA metabolism and ROS accumulation are known indicators of tolerance to a wide variety of abiotic stresses (Feng et al., 2012; Xu et al., 2014; Cai et al., 2015; Huang X. S. et al., 2015). Thus, these physiological parameters were subsequently examined in *HbICE1*-overexpressing lines under cold stress. Proline accumulation is considered an adaptive response to various kinds of environmental stress, conferring stress tolerance by promoting osmotic adjustment, protecting membranes and proteins, and inhibiting ROS production. Under

normal growth conditions, the proline content of the *HbICE1*-overexpressing lines was similar to that of the WT. However, after 24 and 48 h at 0°C, levels were significantly higher in the transgenic lines compared to the WT. At 48 h after treatment, proline levels were 2-fold higher in the transgenic compared to the WT plants (**Figure 7A**).

Electrolyte leakage is another reliable indicator of cell membrane damage during the plant stress response (Feng et al., 2012; Huang X. et al., 2015; Cheng et al., 2016). Under normal growth conditions, the transgenic lines and WT plants showed similar levels of electrolyte leakage ranging from 13 to 15%. However, during cold treatment, electrolyte leakage was considerably less in the transgenic lines compared to the WT, suggesting a reduction in cell membrane damage in the *HbICE1*-overexpressing lines (**Figure 7B**), and therefore, improved cold tolerance. MDA is also an important index of plant oxidative stress and cell injury in response to stress conditions. While no significant differences in MDA content were observed between transgenic lines and WT plants under normal conditions, lower

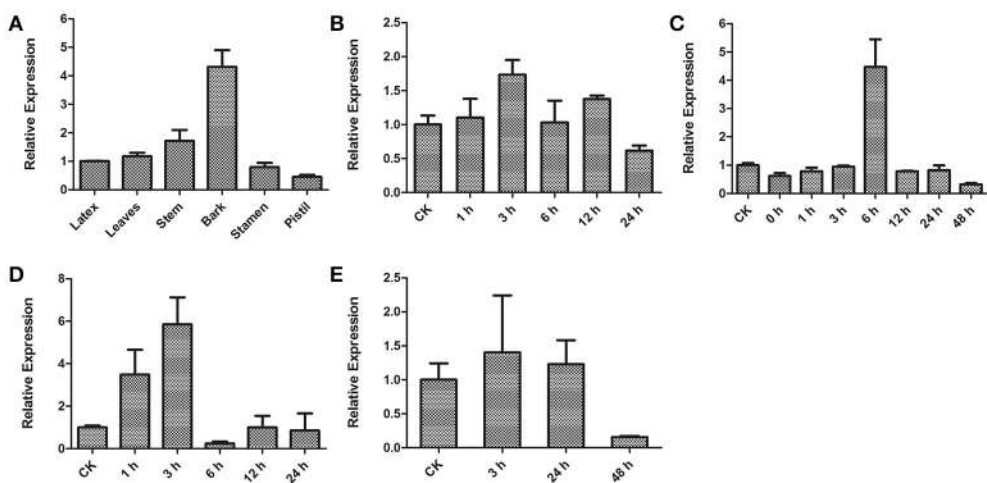


FIGURE 5 | Transcription patterns of *HbICE1* determined by qRT-PCR. **(A)** Differential expression of *HbICE1* in various tissues (the latex, leaves, stem, bark, stamen and pistil). Time-course expression patterns of *HbICE1* in response to different biotic and abiotic stresses: cold **(B)**, dehydration **(C)**, wounding **(D)**, and salt stress **(E)**.

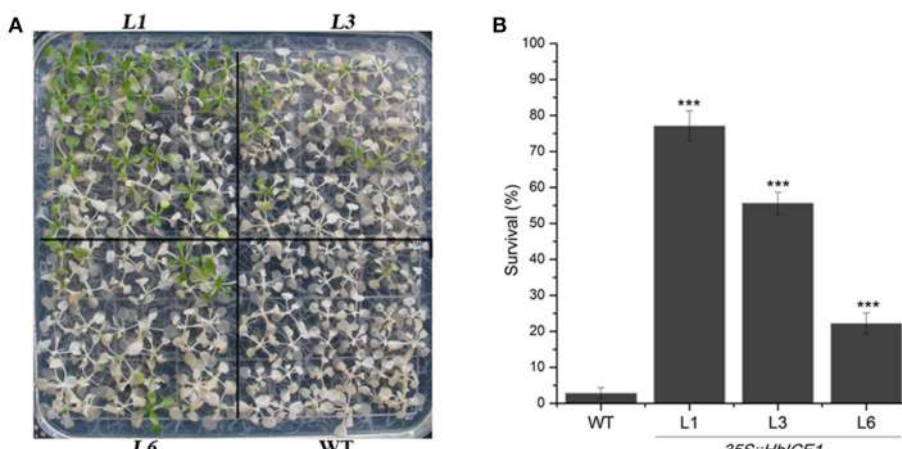


FIGURE 6 | Overexpression of *HbICE1* confers enhanced cold tolerance in *Arabidopsis*. Freezing phenotypes **(A)** and survival rates **(B)** of transgenic lines L1, L3, and L6 and the WT. Two-week-old *Arabidopsis* plants were transferred to 4°C for 2 days, exposed to -8°C for 4 h then returned to normal conditions. Photographs were taken before and after 7-d recovery. In **(B)**, data represent the means of three replicates ± SD. Asterisks indicate significant differences compared with the WT under the same treatment condition (**P < 0.005, student's t-test).

values were observed in the transgenic compared to WT plants after cold treatment (**Figure 7C**).

ROS-induced oxidative damage is associated with much of the stress-induced damage that occurs at the cellular level (Chinnusamy et al., 2007). Stress-induced ROS production results in degradation of polyunsaturated lipids, resulting in formation of MDA. In other words, the reduction in MDA content in the transgenic plants might reflect a decrease in ROS accumulation under cold stress. We therefore assayed ROS accumulation in the 35S::*HbICE1* plants using DAB staining. As expected, stronger staining was observed in the WT plants compared with the transgenic plants under cold conditions (**Figure 7D**), suggesting higher levels of damage in the WT. Taken together, these findings suggest that the increased cold tolerance of 35S::*HbICE1* plants is the result of increased

proline accumulation, reduced electrolyte leakage and MDA metabolism, and a decrease in H₂O₂ accumulation under cold conditions.

***HbICE1* Positively Regulates Cold-Responsive Gene Expression under Cold Conditions**

To further elucidate the molecular mechanism of the 35S::*HbICE1* plant response to cold stress, we examined transcript levels of cold-responsive genes using qRT-PCR. These cold response genes (*COR15A*, *COR47*, *KIN1*, and *RD29A*), which contain DRE or related motifs, are downstream target genes of CBF (Stockinger et al., 1997). Under normal conditions, expression levels of *COR15A*, *COR47*, *KIN1*, and *RD29A* were

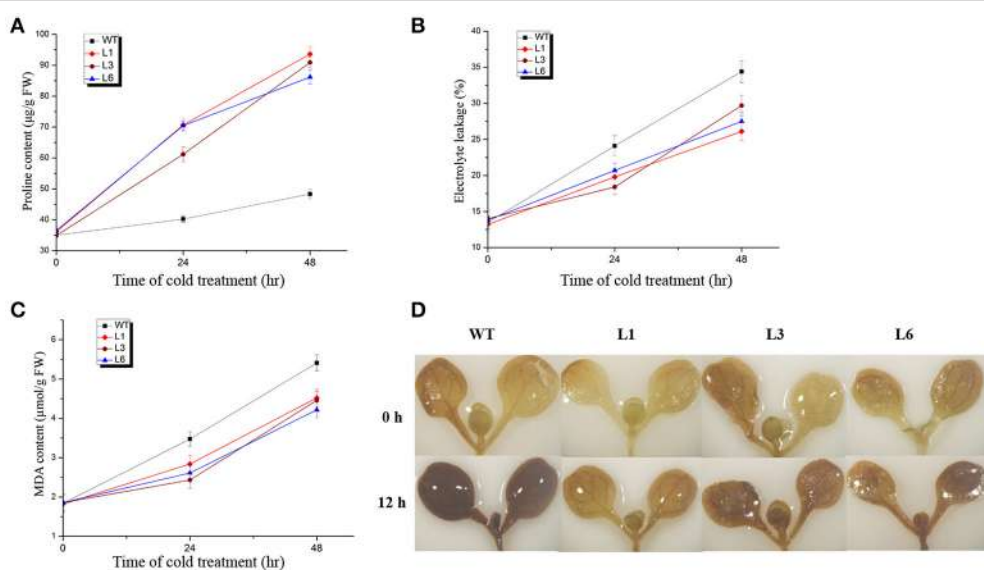


FIGURE 7 | Changes in physiological parameters of 35S::GFP-HbICE1 lines and wild-type (WT) plants under cold stress. Three-week-old *Arabidopsis* plants were grown at 0°C for the time indicated then leaves collected to determine the free proline content (A), electrolyte leakage (B) and MDA content (C). In (A–C), data represent the mean \pm SD ($n = 3$). (D) DAB staining of 6-day-old *Arabidopsis* plants with and without cold treatment.

relatively low in both the transgenic and WT plants. In contrast, after cold exposure for 12 h, expression levels of all tested genes were significantly up-regulated in all three 35S::HbICE1 lines compared with the WT (Figures 8A–D), suggesting that overexpression of HbICE1 positively regulates cold-responsive gene expression, thereby contributing to improved cold tolerance.

Analysis of Differentially Expressed Genes (DEGs) Based on RNA-Seq of Rubber Tree in Response to Cold Stress

In order to gain a global view of transcript expression in rubber tree in response to cold stress, RNA-Seq was used to analyze the differentially expressed genes, generating 24,108,424 raw sequencing reads and 24,050,817 clean reads after filtering low quality (Table S2). 96.50% reads of the control samples matched to a unique or multiple genomic locus, whereas 96.60% of the 3 h cold treatment sample and 96.16% of 12 h cold treatment matched, respectively (Table S3). A total of 8077 genes showed differential expression (low false discovery rate [FDR] < 0.001 and P -value < 0.05), including 4096 genes at 3 h (1389 up-regulated, 2707 down-regulated) and 6060 genes at 12 h (3188 up-regulated, 2872 down-regulated) after cold treatment (Figure 9, Tables S4, S5). More DEGs appeared at 12 h than at 3 h after treatment. All the DEGs could be categorized into three main clusters, e.g., biological process, cellular component and molecular function according to GO classification. In the cluster of “biological process,” 17 GO terms were significantly enriched, of which the GO terms “metabolic process,” “single-organism process,” “cellular process,” “location,” “response to stimulus”

were most evidently enriched (Figure S1), suggesting that these biological processes were responsive to cold stress in rubber tree.

Pathways Enrichment Analysis of DEGs

To further reveal the biological functions of cold responsive genes in rubber tree, pathway enrichment analysis of DEGs based on KEGG database were performed, generating a scatter plot of the top 20 of KEGG enrichment (Figure 10). Most DEGs were enriched in “metabolic pathway” and “biosynthesis of secondary metabolites.” Interestingly, “plant-pathogen interaction,” and “plant hormone signal transduction” pathways were also significantly enriched. Noteworthy, the DEGs enriched in “plant hormone signal transduction” pathway showed most differentially expression in both samples, suggesting that phytohormones involved in the perception and transduction of cold induced signaling in rubber tree. In total, 50 DEGs associated with biosynthesis and/or signal transduction of the phytohormones, including 13 genes related with auxin, 13 genes related with ethylene, 9 genes related with gibberellin (GA), 9 genes related with jasmonic acid (JA), 4 genes related with abscisic acid (ABA) and 2 genes related with cytokinin (CK) (Table 1). Interestingly, ABA 8'-hydroxylase 2 (scaffold0153_318575), ABSCISIC ACID-INSENSITIVE 5-like protein 2 isoform X1 (scaffold0430_516715), and two ABA receptors (scaffold2344_2623, scaffold0748_467762), were down-regulated by cold treatment at both 3 h and 12 h. Furthermore, 12 ethylene-responsive transcription factors (ERFs) showed differential expression, of which nine ERFs (scaffold0359_512732, scaffold0636_609282, scaffold0668_410096, scaffold0668_421116, scaffold0770_505198, scaffold0770_519202, scaffold0782_27868,

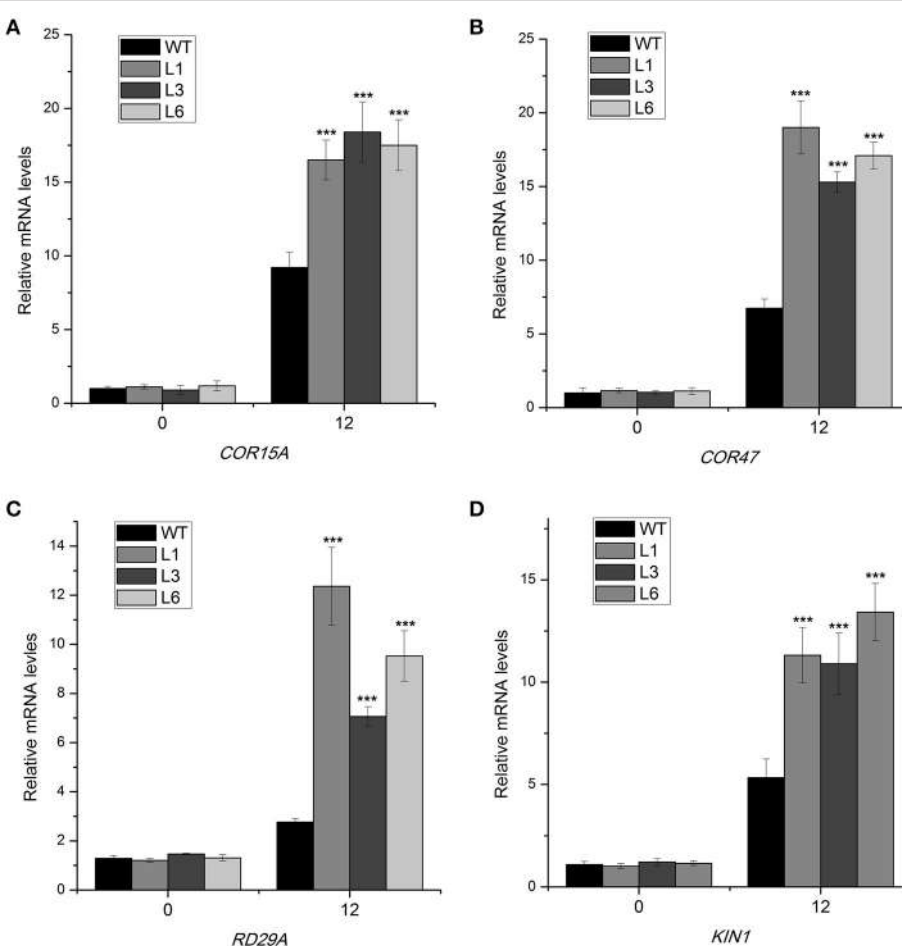


FIGURE 8 | Expression of cold-responsive genes in *HbICE1*-overexpressing lines subjected to cold stress. Expression of *COR15A* (A), *COR47* (B), *RD29A* (C), and *KIN1* (D) in wild-type (WT) and *HbICE1*-overexpressing lines under normal and cold conditions assayed by quantitative real-time PCR, using *AtEIF4* as the internal standard. Data represent means of three replicates \pm SE, and asterisks indicate significant differences at *** P < 0.005 (Student's *t*-test).

scaffold1267_104008, scaffold2594_1826) were up-regulated and three ERFs (scaffold0024_3294824, scaffold0447_369296, scaffold1195_120325) were down-regulated at 12 h after cold treatment. Additionally, four genes related with JA biosynthesis, two encoding allene oxide cyclase (AOC, scaffold1038_209563, scaffold1142_120639), one encoding 12-oxophytodienoate reductase (OPR, scaffold0150_641) and one encoding latex allene oxide synthase (AOS, scaffold1632_19091), were up regulated at 12 h after cold treatment. Furthermore, three *JAZ* genes and one *MYC2* were also significantly up-regulated, strongly suggesting that JA signaling pathway involved in cold response of rubber tree.

Identification of Transcription Factors (TFs) in Response to Cold Stress

Numerous families of transcription factors (TFs) are known to play crucial roles in signal transduction and regulation when plants are subjected with various abiotic stresses, including the AP2/EREBP, MYB, MYC, WRKY, NAC, and bHLH families (Agarwal and Jha, 2010; Liu et al., 2014).

In the current study, 105 putative TFs were found to be exhibited differential expression in response to the cold treatment, of which those encoding AP2/EREBP domain-containing proteins constituted the largest group (22.8%), followed by MYB proteins (16.2%), WRKY proteins (8.6%), NAC proteins (5.7%), C2H2 proteins (4.7%), bHLHs (3.8%) (Table 2). The largest group of the cold-mediated TFs belonged to the AP2/EREBP family and was composed of 24 members. Of these, two genes (scaffold0997_153922, scaffold1276_47774) were annotated as CBF/ DREB genes, which have been shown to play important roles in cold acclimation leading to freezing tolerance (Nakashima et al., 2009). In addition, four members (scaffold0103_29681, scaffold0749_398268, scaffold0914_54940, scaffold1218_8594) of bHLH family were found to be exhibited differential expression in response to the cold treatment. Of those, the expression of an ICE1-like TF (scaffold1218_8594) was observed to up-regulated by cold treatment. Our results therefore indicated that the ICE-CBF pathway is conserved in rubber tree responses to the cold stress. Among the differentially expressed C2H2 TFs, all of the four members (scaffold0248_1439020,

scaffold0540_449380, scaffold0760_285386, scaffold0827_2391, scaffold2824_5887) were up-regulated by cold treatment. We also noticed that the cold stress mediated the expression of TFs in the WRKY (scaffold0378_852023, scaffold0447_61208, scaffold0447_61719, scaffold0653_241031, scaffold0800_278767, scaffold0821_417450, scaffold0844_76279) family. The roles of members of these families in cold tolerance have been well established in numerous plants (Chinnusamy et al., 2010).

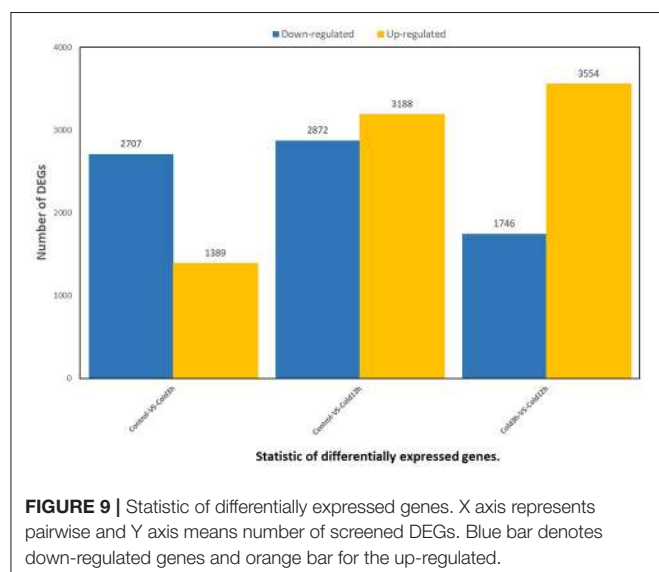


FIGURE 9 | Statistic of differentially expressed genes. X axis represents pairwise and Y axis means number of screened DEGs. Blue bar denotes down-regulated genes and orange bar for the up-regulated.

DISCUSSION

Cold is the major environmental abiotic stress adversely affecting the growth and geographical distribution of plants. *Hevea brasiliensis* is native to tropical rainforests in the Amazonian basin, but was expanded to sub-optimal environments worldwide in the late 1970s, prominently northeast India, southern China, highland and coastal areas of Vietnam, and southern Brazil. Cold stress has therefore become a limiting factor not only of rubber production, but also survival of rubber trees. Chilling temperatures (0–15°C) interfere with a number of metabolic and physiological processes such as chloroplast and mitochondria integrity, plastid membrane composition and photosynthetic electron transport, resulting in leaf wilt and lesions, bark breakdown and latex leakage, root system withering and frostbite, and ultimately cell death. Increased cold tolerance is therefore a major aim of rubber tree breeding programs.

As an upstream regulator, ICE1 plays a key role in cold signaling pathways in a wide range of plant species such as *Arabidopsis* (Shi Y. et al., 2012; Lang and Zhu, 2015), wheat, rice, *Phalaenopsis aphrodite*, *Trifoliate orange*, banana and grapevine (Badawi et al., 2008; Nakamura et al., 2011; Peng et al., 2013, 2014; Xu et al., 2014; Huang X. S. et al., 2015). It is therefore reasonable to expect that ICE1 homologs also play a key role in cold tolerance in *H. brasiliensis*. Characterization and functional analysis of the ICE1 gene in rubber trees is therefore a significant step in determining its cold signaling pathway.

Multiple sequence alignments indicate that HbICE1 shares typical ICE1 protein domains with other plant species such as the MYC-like basic helix-loop-helix (bHLH) domain, serine-rich

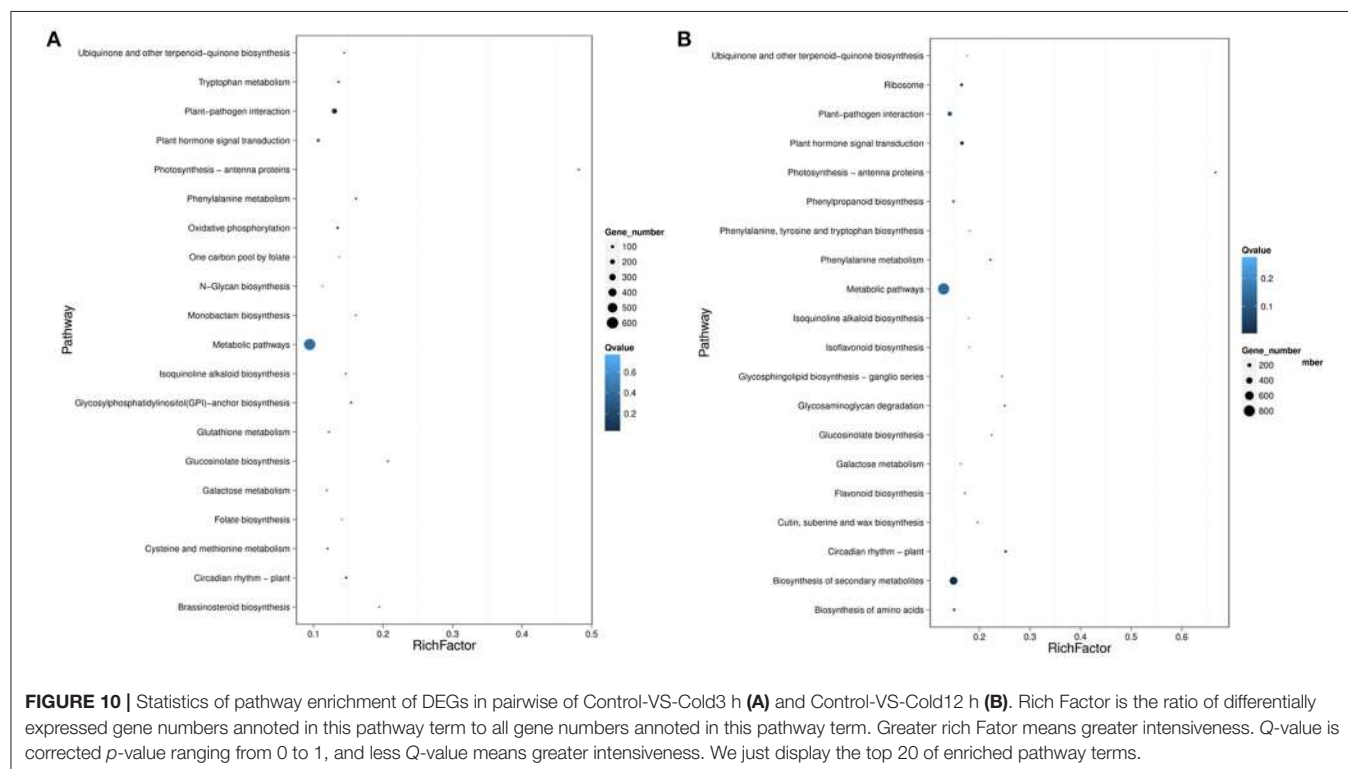


FIGURE 10 | Statistics of pathway enrichment of DEGs in pairwise of Control-VS-Cold3 h (**A**) and Control-VS-Cold12 h (**B**). Rich Factor is the ratio of differentially expressed gene numbers annotated in this pathway term to all gene numbers annotated in this pathway term. Greater rich Factor means greater intensiveness. Q-value is corrected *p*-value ranging from 0 to 1, and less Q-value means greater intensiveness. We just display the top 20 of enriched pathway terms.

TABLE 1 | Hormone-related genes that were differentially expressed during the cold treatment.

	Expression levels (log2ratio[cold/control])		Annotation
	Control-vs.-Cold 3 h	Control-vs.-Cold 12 h	
AUXIN			
scaffold0198_1391731	-1.7	1.4	Auxin-responsive protein IAA27-like [Jatropha curcas]
scaffold0369_43127	-1.0	-1.8	Auxin-induced protein X10A like [Vitis vinifera]
scaffold0425_327131	0.7	2.5	Auxin-binding protein ABP19a like [Ricinus communis]
scaffold0475_945027	2.6	2.2	Auxin-induced protein 6B like [Vitis vinifera]
scaffold0548_182005	-2.5	1.4	Auxin-responsive protein IAA14 like [Jatropha curcas]
scaffold0933_193093	2.0	2.2	Auxin-binding protein ABP20 like [Populus trichocarpa]
scaffold4789_3384	1.8	1.5	Auxin-responsive protein IAA29 [Jatropha curcas]
scaffold0064_497215	-0.1	1.2	Auxin-responsive protein IAA1 [Jatropha curcas]
scaffold0239_815404	0.3	1.5	Auxin-responsive protein IAA16-like [Populus euphratica]
scaffold0319_1118315	0.4	1.5	Auxin-induced protein AUX28 [Ricinus communis]
scaffold0375_663805	-0.6	-2.0	Auxin response factor 1-like [Populus euphratica]
scaffold1315_157576	0.1	1.3	Auxin-responsive protein IAA9 [Jatropha curcas]
scaffold1418_119368	-0.4	-1.2	Auxin signaling F-BOX 2-like [Jatropha curcas]
ETHYLENE			
scaffold0024_3294824	1.5	-1.7	Ethylene-responsive transcription factor CRF2-like [Jatropha curcas]
scaffold0359_512732	5.1	9.3	Ethylene-responsive transcription factor ERF109-like [Jatropha curcas]
scaffold0447_369296	-2.2	-1.4	Ethylene-responsive transcription factor ERF023 [Jatropha curcas]
scaffold0636_609282	-1.4	1.3	Ethylene-responsive transcription factor ERF113 [Ricinus communis]
scaffold0668_410096	3.2	2.2	Ethylene-responsive transcription factor 5-like [Jatropha curcas]
scaffold0668_421116	5.3	3.2	Ethylene-responsive transcription factor 5-like [Jatropha curcas]
scaffold0770_505198	4.8	3.0	Ethylene-responsive transcription factor 5-like [Jatropha curcas]
scaffold0770_519202	2.6	2.0	Ethylene-responsive transcription factor 5-like [Jatropha curcas]
scaffold0782_27868	1.9	4.4	Ethylene-responsive transcription factor ERF061 [Jatropha curcas]
scaffold0838_409025	-1.3	-1.1	Ethylene receptor 2 [Ricinus communis]
scaffold1195_120325	2.5	-1.5	Ethylene-responsive transcription factor ERF017 [Jatropha curcas]
scaffold1267_104008	1.1	1.1	Ethylene-responsive transcription factor RAP2-7 isoform X3 [Ricinus communis]
scaffold2594_1826	-7.0	1.6	Ethylene-responsive transcription factor ERF010-like [Jatropha curcas]
ABSCISIC ACID			
scaffold0153_318575	-2.7	-1.3	Abscisic acid 8'-hydroxylase 2 [Ricinus communis]
scaffold0430_516715	-1.1	-1.1	Abscisic acid-insensitive 5-like protein 2 isoform X1 [Ricinus communis]
scaffold0748_467762	-1.3	-1.3	Abscisic acid receptor PYR1 [Ricinus communis]
scaffold2344_2623	-1.0	-1.6	Abscisic acid receptor PYL2 [Ricinus communis]
GIBBERELLIN			
scaffold0017_768934	-2.4	1.1	Gibberellin-regulated protein 14 isoform X3 [Jatropha curcas]
scaffold0194_369390	-1.3	-1.1	Gibberellin 20 oxidase 1-B like [Ricinus communis]
scaffold0291_1331456	1.3	1.3	Gibberellin 20 oxidase 1 [Ricinus communis]
scaffold0441_414170	0.6	2.2	Gibberellin 20 oxidase 2 like [Ricinus communis]
scaffold0801_379002	1.9	1.8	Gibberellin 20 oxidase 1 like [Populus trichocarpa]
scaffold0831_491806	1.6	-1.8	Feruloyl CoA ortho-hydroxylase 2 like [Populus euphratica]
scaffold1101_43630	3.9	2.1	Chitin-inducible gibberellin-responsive protein 1-like isoform X2 [Jatropha curcas]
scaffold1293_148625	2.5	1.2	Chitin-inducible gibberellin-responsive protein 1-like isoform X1 [Jatropha curcas]
scaffold2517_27680	-1.8	-2.1	Probable carboxylesterase 18 [Jatropha curcas]
CYTOKININ			
scaffold0045_49663	2.2	1.1	UDP-glycosyltransferase 76C3 like [Citrus clementina]
scaffold0199_1250120	-3.2	-1.3	Cytokinin hydroxylase like [Jatropha curcas]

(Continued)

TABLE 1 | Continued

	Expression levels (log2ratio[cold/control])		Annotation
	Control-vs.-Cold 3 h	Control-vs.-Cold 12 h	
JASMONIC ACID			
scaffold0015_736848	4.7	8.4	Protein TIFY 10A like JAZ2 [<i>Hevea brasiliensis</i>]
scaffold0026_2677018	0.1	1.0	Protein TIFY 3B like JAZ11 [<i>Hevea brasiliensis</i>]
scaffold0103_29681	-1.2	1.5	Transcription factor MYC4 like [<i>Hevea brasiliensis</i>]
scaffold0150_641	1.0	1.7	12-oxophytodienoate reductase 3 like [<i>Hevea brasiliensis</i>]
scaffold0762_419876	-0.9	1.4	Protein TIFY 3B like JAZ11 [<i>Hevea brasiliensis</i>]
scaffold0914_54940	1.2	1.2	Transcription factor bHLH35 isoform X2 [<i>Jatropha curcas</i>]
scaffold1038_209563	1.9	3.2	Allene oxide cyclase 3, chloroplastic-like [<i>Populus euphratica</i>]
scaffold1632_19091	-1.6	1.6	Latex allene oxide synthase [<i>Hevea brasiliensis</i>]

region (S-rich), zipper region (ZIP) and ACT-UUT-ACR-like domain; however, it possesses a varied N terminus (**Figure 1**). A potential sumoylation site, which is reportedly crucial for AtICE1 activation and stability (Miura et al., 2007), was also found in HbICE1 (**Figure 1**), suggesting that HbICE1 activity is mediated by the SUMO E3 ligase. Furthermore, HbICE1 was confirmed as being nuclear localized, and able to bind to the MYC-recognition element. These observations imply that HbICE1 is a novel putative ICE1 homolog.

Expression profiles revealed that, like *AtICE1*, *HbICE1* is expressed constitutively in all tissues (Chinnusamy et al., 2003). Furthermore, *HbICE1* was induced by multiple abiotic stresses including cold, dehydration, wound and salinity (**Figure 5**). *HbICE1* was only slightly induced by cold, consistent with a previous report suggesting that cold stress induces little transcriptional alteration, instead resulting in posttranslational modification of ICE1 to active the CBF pathway (Chinnusamy et al., 2003; Ding et al., 2015). Upregulation of *HbICE1* following dehydration was consistent with previous reports in *P. trifoliata* and *Pyrus ussuriensis* (Huang X. et al., 2015; Huang X. S. et al., 2015), but differs from *AtICE1*, which is not triggered by dehydration (Chinnusamy et al., 2003). This disparity between *HbICE1* and *AtICE1* might be attributed to the inherent differences between plant species.

Cold acclimation is one of the major mechanisms for plant to adapt to cold stress (Thomashow, 1999). Indeed, cold acclimation was found to enhance freezing tolerance rubber tree after exposure to low temperature (**Figure S2**). The electrolyte leakage was less in the cold-acclimated (CA) rubber trees to the nonacclimated (NA) rubber tree, and CA rubber trees experienced less cold stress-induced H₂O₂ accumulation compared to the NA plants, suggesting an enhanced membrane integrity and the lower cold stress-induced H₂O₂ accumulation in the CA rubber tree seedlings to NA plants. Overexpression of *HbICE1* in *Arabidopsis* enhanced cold tolerance only after cold acclimation (**Figure 6**), indicating that other co-factors associated with cold acclimation are essential for *HbICE1*-mediated cold tolerance. Similar results were reported for wheat ICE genes (Badawi et al., 2008), where overexpression of *TaICE87* or *TaICE41* in *Arabidopsis* enhanced freezing tolerance only after cold acclimation (Badawi et al., 2008). These results

suggest that other co-factors induced by cold acclimation are essential for HbICE1-mediated cold tolerance. Previous reports also confirmed this hypothesis. Chinnusamy et al. (2003) showed that cold-induced modification of the AtICE1 protein or a transcriptional cofactor is necessary for AtICE1-induced activation of CBF expression. Furthermore, Miura et al. (2007) showed that SIZ1 (SAP and Miz1), mediates sumoylation of ICE1, which reduces the polyubiquitination of ICE1 to enhance its stability. A potential sumoylation site was also found in HbICE1 protein (**Figure 1**), suggesting that HbICE1 activity could be regulated by sumoylation via the SUMO E3 ligase.

Physiological parameters such as electrolyte leakage and contents of MDA, chlorophyll and proline are closely related to cold tolerance under the regulation of COR, which is triggered by the ICE transcription factor (Badawi et al., 2008; Peng et al., 2014; Xu et al., 2014; Liu et al., 2017). In many plant species, overexpression of ICE1 is sufficient to alter physiological parameters and enhance cold tolerance (Feng et al., 2013; Huang X. et al., 2015). In our study, the *HbICE1ox* transgenic lines showed improved survival rates and freezing tolerance as a result reduced electrolyte leakage and MDA metabolism, and increased proline accumulation (**Figure 7**), suggesting that *HbICE1* plays a positive regulatory role in the response to cold stress. These findings suggest that the ICE-CBF-COR transcriptional cascade, which influences the freezing tolerance capacity of plants, exists not only in *Arabidopsis* but other species such as *H. brasiliensis*.

H₂O₂ is often associated with biotic and abiotic stresses (Yuan and Huang, 2016; Cao et al., 2017; Lu et al., 2017; Yuan et al., 2017). Our study further suggests that the 35S::*HbICE1* plants experienced less cold stress-induced H₂O₂ accumulation compared to the WT, despite similar contents under normal conditions. Consistency with the decrease in MDA content and electrolyte leakage under cold stress, these data imply that enhanced membrane integrity and decreased levels of lipid peroxidation caused the lower cold stress-induced H₂O₂ accumulation in the transgenic compared to WT plants.

Transcription factors families such as AP2/EREBP, MYB, WRKY, C2H2, NAC, and bHLH are well known to be involved in stress tolerance in plants (Chinnusamy et al., 2010), but how they work synergistically to cope with cold tolerance requires

TABLE 2 | Differential expression transcription factor (TF) in response to the cold treatment.

Gene ID	Expression levels (log2ratio[cold/control])		Annotation
	Control-vs.-Cold 3 h	Control-vs.-Cold 12 h	
AP2-EREBP 24			
scaffold0009_198930	1.4	-1.2	Ethylene-responsive transcription factor ERF034 like [Populus euphratica]
scaffold0024_3294824	1.5	-1.7	Ethylene-responsive transcription factor CRF2 like [Jatropha curcas]
scaffold0093_1433865	1.7	1.4	Ethylene-responsive transcription factor 4 like [Hevea brasiliensis]
scaffold0319_822155	4.0	3.1	Ethylene-responsive transcription factor 9 like [Hevea brasiliensis]
scaffold0342_1158497	2.3	1.6	Ethylene-responsive transcription factor 4 like [Hevea brasiliensis]
scaffold0359_512732	5.1	9.3	Ethylene-responsive transcription factor ERF109 like [Jatropha curcas]
scaffold0426_862663	4.2	1.8	Ethylene-responsive transcription factor ERF105 like [Hevea brasiliensis]
scaffold0426_899695	2.8	1.9	Ethylene-responsive transcription factor 5 like [Hevea brasiliensis]
scaffold0426_906054	1.6	1.5	Ethylene-responsive transcription factor 2 like [Jatropha curcas]
scaffold0447_369296	-2.2	-1.4	Ethylene-responsive transcription factor ERF023 like [Jatropha curcas]
scaffold0557_665510	1.3	1.6	Pathogenesis-related genes transcriptional activator PTI5 like [Ricinus communis]
scaffold0566_721951	1.2	2.4	Ethylene-responsive transcription factor RAP2-3 like [Hevea brasiliensis]
scaffold0636_609282	-1.4	1.3	Ethylene-responsive transcription factor ERF113 like [Ricinus communis]
scaffold0668_410096	3.2	2.2	Ethylene-responsive transcription factor 6 like [Jatropha curcas]
scaffold0668_421116	5.3	3.2	Ethylene-responsive transcription factor 6 like [Jatropha curcas]
scaffold0668_444732	2.6	3.6	Ethylene-responsive transcription factor 1A like [Hevea brasiliensis]
scaffold0770_505198	4.8	3.0	Ethylene-responsive transcription factor 6 like [Jatropha curcas]
scaffold0770_519202	2.6	2.0	Ethylene-responsive transcription factor 6 like [Jatropha curcas]
scaffold0782_27868	1.9	4.4	Ethylene-responsive transcription factor ERF061 like [Jatropha curcas]
scaffold0997_153922	5.0	6.7	Dehydration-responsive element-binding protein 1D like [Hevea brasiliensis]
scaffold1195_120325	2.5	-1.5	Ethylene-responsive transcription factor ERF017 like [Jatropha curcas]
scaffold1267_104008	1.1	1.1	Ethylene-responsive transcription factor RAP2-7 like [Ricinus communis]
scaffold1276_47774	2.2	2.6	Dehydration-responsive element-binding protein 2C like [Ricinus communis]
scaffold2594_1826	-7.0	-7.0	Ethylene-responsive transcription factor ERF010 like [Jatropha curcas]
BES1			
scaffold1038_185360	7.0	7.1	Beta-amylase 7 like protein BZR1 homolog 4 [Ricinus communis]
bHLH			
scaffold0103_29681	-1.2	1.5	Transcription factor MYC4 like [Hevea brasiliensis]
scaffold0749_398268	1.1	1.1	Transcription factor bHLH130 like transcription factor bHLH130-like [Jatropha curcas]
scaffold0914_54940	1.2	1.2	Transcription factor bHLH35 like [Jatropha curcas]
scaffold1218_85940	1.7	1.1	Transcription factor ICE1 like [Jatropha curcas]
BSD			
scaffold0565_438757	-1.1	-1.7	Uncharacterized protein LOC105630818 [Jatropha curcas]
C2C2-CO-like			
scaffold1446_82920	-1.1	-2.1	Zinc finger protein CONSTANS-LIKE 16 like [Ricinus communis]
C2C2-GATA			
scaffold0801_483822	-3.7	-3.6	GATA transcription factor 9 like [Jatropha curcas]
C2H2			
scaffold0248_1439020	3.6	3.1	Zinc finger protein ZAT10 like [Jatropha curcas]
scaffold0540_449380	5.2	4.8	Zinc finger protein ZAT10 like [Jatropha curcas]
scaffold0760_285386	2.4	4.0	Zinc finger protein ZAT12 like [Jatropha curcas]
scaffold0827_2391	3.2	2.6	Zinc finger protein ZAT10 like [Vitis vinifera]
scaffold2824_5887	2.3	1.7	Zinc finger protein ZAT10 like [Jatropha curcas]
C3H			
scaffold1776_58662	3.2	1.4	Zinc finger CCCH domain-containing protein 29 like [Jatropha curcas]
scaffold2028_37706	-1.6	-2.8	Splicing factor U2af small subunit A like [Jatropha curcas]
CAMTA			
scaffold0824_240435	1.1	-1.2	Calmodulin-binding transcription activator 4 like [Jatropha curcas]

(Continued)

TABLE 2 | Continued

Gene ID	Expression levels (log2Ratio[Cold / Control])		Annotation
	Control-vs.-Cold 3 h	Control-vs.-Cold 12 h	
CPP			
scaffold0649_61663	-1.5	-1.1	Protein tesmin/TSO1-like CXC 5 like [Jatropha curcas]
E2F-DP			
scaffold0190_833611	1.2	1.7	E2F transcription factor-like E2FE like [Ricinus communis]
G2-LIKE			
scaffold0064_1337771	1.5	1.2	Transcription factor BOA like uncharacterized protein LOC105641987 [Jatropha curcas]
scaffold0745_414068	-1.2	-1.2	Myb family transcription factor APL like [Jatropha curcas]
GRAS			
scaffold0781_525657	2.9	1.6	Scarecrow-like protein 33 like [Jatropha curcas]
scaffold1101_43630	3.9	2.1	Chitin-inducible gibberellin-responsive protein 1 like [Jatropha curcas]
scaffold1293_148625	2.5	1.2	Chitin-inducible gibberellin-responsive protein 1 like [Jatropha curcas]
scaffold3316_7246	-1.0	-2.2	Scarecrow-like protein 4 like scarecrow-like protein 4 [Jatropha curcas]
HSF			
scaffold0887_230318	-1.2	-1.6	Heat stress transcription factor B-3 like [Jatropha curcas]
LIM			
scaffold0024_1661357	-1.6	-1.1	Protein DA1 like protein DA1 isoform X1 [Jatropha curcas]
scaffold0430_259601	1.1	-1.7	Pollen-specific protein SF3 like [Jatropha curcas]
scaffold1673_9405	-2.5	-1.3	Pollen-specific protein SF3 like LIM domain-containing protein WLIM [Ricinus communis]
LOB			
scaffold0387_385506	-1.2	-1.4	LOB domain-containing protein 15 like [Ricinus communis]
scaffold0540_479077	-1.7	1.5	LOB domain-containing protein 38 like [Jatropha curcas]
scaffold0814_192853	-1.4	-2.7	LOB domain-containing protein 41 like [Jatropha curcas]
MADS			
scaffold0048_1495608	-11.8	-11.8	Developmental protein SEPALLATA 2 like [Jatropha curcas]
scaffold0824_196540	-1.1	-3.2	Agamous-like MADS-box protein AGL31 like [Betula platyphylla]
scaffold1181_25280	-1.6	-1.6	Agamous-like MADS-box protein AGL80 like [Jatropha curcas]
mTERF			
scaffold0077_598827	3.4	3.1	Uncharacterized protein LOC105641042 [Jatropha curcas]
scaffold0128_170927	-1.1	-1.3	Uncharacterized protein LOC8276547 isoform X1 [Ricinus communis]
scaffold0475_493935	-2.1	-2.3	Uncharacterized protein LOC105646130 [Jatropha curcas]
scaffold0794_215338	1.9	1.8	Conserved hypothetical protein [Ricinus communis]
MYB			
scaffold0037_481747	-1.7	-1.5	Myb-related protein 306 like [Jatropha curcas]
scaffold0064_1337771	1.5	1.2	Transcription factor BOA like [Jatropha curcas]
scaffold0167_1341204	6.8	3.4	Myb-related protein Myb4 like [Populus trichocarpa]
scaffold0214_973719	3.4	1.6	Protein RADIALIS-like 3 like [Populus trichocarpa]
scaffold0269_286149	1.1	1.1	Transcription factor MYB44 like [Jatropha curcas]
scaffold0393_760883	-1.4	-1.2	Myb-related protein 306 like [Ricinus communis]
scaffold0561_805801	-1.6	-1.0	Transcription factor MYB44 like [Jatropha curcas]
scaffold0745_414068	-1.2	-1.2	Myb family transcription factor APL like [Jatropha curcas]
scaffold0753_56980	-1.8	-1.1	Protein ODORANT1 like [Jatropha curcas]
scaffold0778_340533	2.0	1.4	Transcription factor RADIALIS like [Jatropha curcas]
scaffold0802_328595	1.8	2.6	Transcription factor TRY like [Populus euphratica]
scaffold0823_390156	5.6	5.2	Transcription factor RADIALIS like [Ricinus communis]
scaffold0926_151816	4.2	3.4	Transcription factor MYB44 like [Ricinus communis]
scaffold1291_85884	2.0	2.2	Transcription factor MYB44 like [Jatropha curcas]
scaffold1503_36079	1.2	1.3	Transcription factor MYB44 like [Jatropha curcas]

(Continued)

TABLE 2 | Continued

Gene ID	Expression levels (log2ratio[cold/control])		Annotation
	Control-vs.-Cold 3 h	Control-vs.-Cold 12 h	
scaffold1604_48495	-2.0	-2.3	Protein ODORANT1 like protein ODORANT1 [Ricinus communis]
scaffold1881_19273	1.4	1.0	Transcription factor TT2 like [Eucalyptus grandis]
NAC			
scaffold0026_552629	-2.2	-1.0	NAC domain-containing protein 4 like [Jatropha curcas]
scaffold0026_564790	1.5	1.3	Protein FEZ like NAC domain-containing protein 89-like [Jatropha curcas]
scaffold0035_3053255	1.0	-1.1	NAC domain-containing protein 21/22 like [Manihot esculenta]
scaffold0807_44819	-2.6	-1.6	NAC transcription factor ONAC010 like [Ricinus communis]
scaffold0920_383574	3.0	2.2	NAC domain-containing protein 21/22 like [Manihot esculenta]
scaffold0926_71752	1.3	1.9	NAC domain-containing protein 100 like [Manihot esculenta]
SBP			
scaffold0896_63610	-1.3	-1.2	Squamosa promoter-binding-like protein 14 like [Jatropha curcas]
SRS			
scaffold1019_30037	-1.7	-3.1	Protein LATERAL ROOT PRIMORDIUM 1 like [Jatropha curcas]
TIG			
scaffold0824_240435	1.1	-1.2	Calmodulin-binding transcription activator 4 like [Jatropha curcas]
Trihelix			
scaffold0020_47233	-4.3	-3.5	Stress response protein NST1 [Jatropha curcas]
scaffold0442_841604	7.8	7.9	Trihelix transcription factor ASIL2-like [Jatropha curcas]
scaffold0626_598319	-1.9	1.5	Trihelix transcription factor ASIL1 [Jatropha curcas]
scaffold0753_500194	-1.8	-1.7	Stress response protein NST1 [Jatropha curcas]
VARL			
scaffold0194_575669	-1.0	-1.8	Histone-lysine N-methyltransferase ATX4 like [Jatropha curcas]
WRKY			
scaffold0189_35635	-4.9	-1.4	Probable WRKY transcription factor 11 like [Ricinus communis]
scaffold0378_852023	1.1	1.2	Probable WRKY transcription factor 70 like [Jatropha curcas]
scaffold0447_61208	4.2	2.0	Probable WRKY transcription factor 46 like [Populus trichocarpa]
scaffold0447_61719	4.2	2.0	Probable WRKY transcription factor 30 like [Populus trichocarpa]
scaffold0653_241031	3.7	2.3	Probable WRKY transcription factor 70 like [Jatropha curcas]
scaffold0800_278767	1.6	1.8	Probable WRKY transcription factor 27 like [Jatropha curcas]
scaffold0821_417450	3.4	1.2	Probable WRKY transcription factor 41 like [Populus trichocarpa]
scaffold0844_76279	3.3	1.1	Probable WRKY transcription factor 40 like [Populus trichocarpa]
scaffold3570_2572	-1.5	-1.9	Probable WRKY transcription factor 49 like [Jatropha curcas]
zF-HD			
scaffold0375_556816	2.0	2.3	Zinc-finger homeodomain protein 4 like [Populus euphratica]
scaffold0682_603876	1.5	1.7	Zinc-finger homeodomain protein 4 like [Populus euphratica]
scaffold0853_204606	-2.3	-1.1	Zinc-finger homeodomain protein 11 like [Ricinus communis]
scaffold1106_14241	1.4	1.7	Zinc-finger homeodomain protein 5 like [Ricinus communis]

determination. In this work, two genes (scaffold0997_153922, scaffold1276_47774) annotated as CBF/DREB and one ICE1 member of bHLH family (scaffold1218_8594) were up-regulated by cold treatment (**Table 2**), indicating that ICE-CBF pathway is conserved in rubber tree responses to the cold stress. The phytohormones auxin, ABA, JA, and ethylene are known to play important roles in the regulation of plant growth and abiotic stress responses (Shi Y. et al., 2015). In current study, the DGEs data suggested that many phytohormones related genes were responsive to cold treatment in rubber tree. ABA integrates various stress signals and modulates stress responses, but whether it is involved in cold responses is still debated (Tuteja, 2007). It has been suggested that plant's response to the cold stress

may be ABA-independent, but increasing evidences of contrary were reported (Lang et al., 1994; Wang et al., 2015). We noticed that ABA 8'-hydroxylase, a key enzyme in ABA catabolism, was down-regulated by cold treatment. Down-regulation of the ABA 8'-hydroxylase gene implies that catabolism of ABA might be attenuated in rubber tree under cold stress, which is consistent with the previous report that ABA levels increase slightly in response to low temperature (Lang et al., 1994). In addition, we detected the decreased expression of ABA receptor PYR1 and PYL2 (**Table 1**), how ABA mediated signaling is involved in the cold responses of rubber tree remains further investigation. Ethylene has been well documented in the cold stress response (Shi Y. et al., 2012, 2015). In our study, the expression of *ERFs*

was significantly regulated by cold treatment. JA was recently reported to significantly enhance plant freezing tolerance with or without cold acclimation, (Hu et al., 2013). We observed the increased expression of several key genes for JA biosynthesis, including *OPR* (scaffold0150_641), *AOS* (scaffold1038_209563) and *AOC* (scaffold1632_19091), and several essential genes (e.g., *JAZs* and *MYC*) in JA signaling pathways at 12 h after cold treatment, strongly suggesting that cold stress triggers JA biosynthesis and responses in rubber tree, which is consistent with the study of *A. thaliana* (Hu et al., 2013). JA was therefore proposed to be a positive regulator of cold responses in rubber tree.

In conclusion, a novel ICE-like transcription factor, designated HbICE1, was isolated from *H. brasiliensis* and functionally characterized. This nuclei protein, which has typical features of ICE proteins, was found to have transactivation activity via binding to MYC recognition sites. 35S::HbICE1 plants showed enhanced cold resistance via increased proline content, a reduction in MDA metabolism and electrolyte leakage, and a decrease in ROS accumulation, promoting expression of the cold-responsive genes. These findings suggest that *HbICE1* is a member of the *ICE* gene family and positive regulator of cold tolerance. Differentially expressed genes (DEGs) analysis showed that cold treatment changed genes expression profiles involved in many biological processes and phytohormones perception and transduction. Ethylene, JA, ABA, as well as ICE-CBF signaling pathways might work synergistically to cope with cold tolerance in rubber tree. These findings will help elucidate the cold signaling network in *H. brasiliensis*, ultimately aiding breeding programs aimed at improving cold stress tolerance.

AUTHOR CONTRIBUTIONS

HY conceived and directed this study, designed and performed the experiments, analyzed the data, wrote and revised the

REFERENCES

- Agarwal, P. K., and Jha, B. (2010). Transcription factors in plants and ABA dependent and independent abiotic stress signalling. *Biol. Plant.* 54, 201–212. doi: 10.1007/s10535-010-0038-7
- Badawi, M., Reddy, Y. V., Agharbaoui, Z., Tominaga, Y., Danyluk, J., Sarhan, F., et al. (2008). Structure and functional analysis of wheat ICE (inducer of CBF expression) genes. *Plant Cell Physiol.* 49, 1237–1249. doi: 10.1093/pcp/pcn100
- Cai, W., Liu, W., Wang, W. S., Fu, Z. W., Han, T. T., and Lu, Y. T. (2015). Overexpression of rat neurons nitric oxide synthase in rice enhances drought and salt tolerance. *PLoS ONE* 10:e0131599. doi: 10.1371/journal.pone.0131599
- Cao, Y., Zhai, J., Wang, Q., Yuan, H., and Huang, X. (2017). Function of Hevea brasiliensis NAC1 in dehydration-induced laticifer differentiation and latex biosynthesis. *Planta* 245, 31–44. doi: 10.1007/s00425-016-2589-0
- Cheng, H., Cai, H., Fu, H., An, Z., Fang, J., Hu, Y., et al. (2015). Functional characterization of Hevea brasiliensis CRT/DRE binding factor 1 gene revealed regulation potential in the cbf pathway of tropical perennial tree. *PLoS ONE* 10:e0137634. doi: 10.1371/journal.pone.0137634
- Cheng, H., Chen, X., Zhu, J., and Huang, H. (2016). Overexpression of a Hevea brasiliensis ErbB-3 binding protein 1 gene increases drought tolerance and organ size in Arabidopsis. *Front. Plant Sci.* 7:1703. doi: 10.3389/fpls.2016.01703
- Chinnusamy, V., Ohta, M., Kanrar, S., Lee, B. H., Hong, X., Agarwal, M., et al. (2003). ICE1: a regulator of cold-induced transcriptome and freezing tolerance in Arabidopsis. *Genes Dev.* 17, 1043–1054. doi: 10.1101/gad.1077503
- Chinnusamy, V., Zhu, J. K., and Sunkar, R. (2010). Gene regulation during cold stress acclimation in plants. *Methods Mol. Biol.* 639, 39–55. doi: 10.1007/978-1-60761-702-0_3
- Chinnusamy, V., Zhu, J., and Zhu, J. K. (2007). Cold stress regulation of gene expression in plants. *Trends Plant Sci.* 12, 444–451. doi: 10.1016/j.tplants.2007.07.002
- Clough, S. J., and Bent, A. F. (1998). Floral dip: a simplified method for Agrobacterium-mediated transformation of *Arabidopsis thaliana*. *Plant J.* 16, 735–743. doi: 10.1046/j.1365-313x.1998.00343.x
- Ding, Y., Li, H., Zhang, X., Xie, Q., Gong, Z., and Yang, S. (2015). OST1 kinase modulates freezing tolerance by enhancing ICE1 stability in *Arabidopsis*. *Dev. Cell* 32, 278–289. doi: 10.1016/j.devcel.2014.12.023
- Dong, C. H., Agarwal, M., Zhang, Y., Xie, Q., and Zhu, J. K. (2006). The negative regulator of plant cold responses, HOS1, is a RING E3 ligase that mediates the ubiquitination and degradation of ICE1. *Proc. Natl. Acad. Sci. U.S.A.* 103, 8281–8286. doi: 10.1073/pnas.0602874103
- Feng, H. L., Ma, N. N., Meng, X., Zhang, S., Wang, J. R., Chai, S., et al. (2013). A novel tomato MYC-type ICE1-like transcription factor, SLICE1a, confers cold, osmotic and salt tolerance in transgenic tobacco. *Plant Physiol. Biochem.* 73, 309–320. doi: 10.1016/j.plaphy.2013.09.014
- Feng, X. M., Zhao, Q., Zhao, L. L., Qiao, Y., Xie, X. B., Li, H. F., et al. (2012). The cold-induced basic helix-loop-helix transcription factor gene MdCIBHL1 encodes an ICE-like protein in apple. *BMC Plant Biol.* 12:22. doi: 10.1186/1471-2229-12-22

manuscript; YS, YL, MO, XT, and WC performed the experiments, analyzed the data; XH revised the manuscript. All authors have read and approved the final version submitted.

ACKNOWLEDGMENTS

This work was supported by the National Natural Science Foundation of China [grant number 31560197, 31260170], the Hainan Education Department Foundation [grant number Hnky2015-4], Hainan University Youth Foundation (hdkyxj201703) and the Startup Funding of Hainan University [grant number kyqd1437].

SUPPLEMENTARY MATERIAL

The Supplementary Material for this article can be found online at: <http://journal.frontiersin.org/article/10.3389/fpls.2017.01462/full#supplementary-material>

Figure S1 | GO functional classification on DEGs in pairwise of Control-vs.-Cold 3 h (**A**) and Control-vs.-Cold12 h (**B**). X axis means number of DEGs (the number is presented by its square root value). Y axis represents GO terms. All GO terms are grouped in to three ontologies: blue is for biological process, brown is for cellular component and orange is for molecular function.

Figure S2 | Electrolyte leakage (**A**) and DAB staining (**B**) of the rubber tree seedlings with indicated freezing temperatures. Seedlings were treated at -16°C for 0.5 h or 1 h for nonacclimated (NA) and cold-acclimated (CA) plants (CA; 1 day at 4°C). Error bars show SD from three replicates. (**P < 0.01, ***P < 0.005, student's t-test).

Table S1 | List of the primers used for qRT-PCR.

Table S2 | Summary of sequencing data for each sample.

Table S3 | Alignment statistics of reads align to reference genome.

Table S4 | Differentially Expressed Genes (using Noiseq) in pairwise of Control-VS-Cold 3 h.

Table S5 | Differentially Expressed Genes (using Noiseq) in pairwise of Control-VS-Cold 12 h.

- Fursova, O. V., Pogorelko, G. V., and Tarasov, V. A. (2009). Identification of ICE2, a gene involved in cold acclimation which determines freezing tolerance in *Arabidopsis thaliana*. *Gene* 429, 98–103. doi: 10.1016/j.gene.2008.10.016
- Hong, H., Xiao, H., Yuan, H., Zhai, J., and Huang, X. (2015). Cloning and characterisation of JAZ gene family in Hevea brasiliensis. *Plant Biol.* 17, 618–624. doi: 10.1111/plb.12288
- Hu, Y., Jiang, L., Wang, F., and Yu, D. (2013). Jasmonate regulates the inducer of cbf expression-C-repeat binding factor/DRE binding factor1 cascade and freezing tolerance in Arabidopsis. *Plant Cell* 25, 2907–2924. doi: 10.1105/tpc.113.112631
- Huang, X., Li, K., Jin, C., and Zhang, S. (2015). ICE1 of *Pyrus ussuriensis* functions in cold tolerance by enhancing PuDREBs transcriptional levels through interacting with PuHHP1. *Sci. Rep.* 5:17620. doi: 10.1038/srep17620
- Huang, X. S., Zhang, Q., Zhu, D., Fu, X., Wang, M., Moriguchi, T., et al. (2015). ICE1 of Poncirus trifoliata functions in cold tolerance by modulating polyamine levels through interacting with arginine decarboxylase. *J. Exp. Bot.* 66, 3259–3274. doi: 10.1093/jxb/erv138
- Jaglo-Ottosen, K. R., Gilmour, S. J., Zarka, D. G., Schabenberger, O., and Thomashow, M. F. (1998). Arabidopsis CBF1 overexpression induces COR genes and enhances freezing tolerance. *Science* 280, 104–106. doi: 10.1126/science.280.5360.104
- Lang, V., Mantyla, E., Welin, B., Sundberg, B., and Palva, E. T. (1994). Alterations in water status, endogenous abscisic acid content, and expression of rab18 gene during the development of freezing tolerance in *Arabidopsis thaliana*. *Plant Physiol.* 104, 1341–1349. doi: 10.1104/pp.104.4.1341
- Lang, Z., and Zhu, J. (2015). OST1 phosphorylates ICE1 to enhance plant cold tolerance. *Sci. China Life Sci.* 58, 317–318. doi: 10.1007/s11427-015-4822-7
- Lin, A., Wang, Y., Tang, J., Xue, P., Li, C., Liu, L., et al. (2012). Nitric oxide and protein S-nitrosylation are integral to hydrogen peroxide-induced leaf cell death in rice. *Plant Physiol.* 158, 451–464. doi: 10.1104/pp.111.184531
- Liu, J. H., Peng, T., and Dai, W. (2014). Critical cis-acting elements and interacting transcription factors: key players associated with abiotic stress responses in plants. *Plant Mol. Biol. Rep.* 32, 303–317. doi: 10.1007/s11105-013-0667-z
- Liu, Q., Kasuga, M., Sakuma, Y., Abe, H., Miura, S., Yamaguchi-Shinozaki, K., et al. (1998). Two transcription factors, DREB1 and DREB2, with an EREBP/AP2 DNA binding domain separate two cellular signal transduction pathways in drought- and low-temperature-responsive gene expression, respectively, in Arabidopsis. *Plant Cell* 10, 1391–1406. doi: 10.1105/tpc.10.8.1391
- Liu, Z., Jia, Y., Ding, Y., Shi, Y., Li, Z., Guo, Y., et al. (2017). Plasma membrane CRPK1-mediated phosphorylation of 14-3-3 proteins induces their nuclear import to fine-tune CBF signaling during cold response. *Mol. Cell* 66, 117–128.e115. doi: 10.1016/j.molcel.2017.02.016
- Lu, X., Zhou, X., Cao, Y., Zhou, M., McNeil, D., Liang, S., et al. (2017). RNA-seq analysis of cold and drought responsive transcriptomes of zea mays ssp. *mexicana* L. *Front. Plant Sci.* 8:136. doi: 10.3389/fpls.2017.00136
- Maruyama, K., Todaka, D., Mizoi, J., Yoshida, T., Kidokoro, S., Matsukura, S., et al. (2012). Identification of cis-acting promoter elements in cold- and dehydration-induced transcriptional pathways in Arabidopsis, rice, and soybean. *DNA Res.* 19, 37–49. doi: 10.1093/dnaresearch/dsr040
- Medina, J., Bargues, M., Terol, J., Perez-Alonso, M., and Salinas, J. (1999). The Arabidopsis CBF gene family is composed of three genes encoding AP2 domain-containing proteins whose expression is regulated by low temperature but not by abscisic acid or dehydration. *Plant Physiol.* 119, 463–470. doi: 10.1104/pp.119.2.463
- Miura, K., Jin, J. B., Lee, J., Yoo, C. Y., Stirm, V., Miura, T., et al. (2007). SIZ1-mediated sumoylation of ICE1 controls CBF3/DREB1A expression and freezing tolerance in Arabidopsis. *Plant Cell* 19, 1403–1414. doi: 10.1105/tpc.106.048397
- Nakamura, J., Yuasa, T., Huong, T. T., Harano, K., Tanaka, S., Iwata, T., et al. (2011). Rice homologs of inducer of CBF expression (OsICE) are involved in cold acclimation. *Plant Biotechnol.* 28, 303–309. doi: 10.5511/plantbiotechnology.11.0421a
- Nakashima, K., Ito, Y., and Yamaguchi-Shinozaki, K. (2009). Transcriptional regulatory networks in response to abiotic stresses in Arabidopsis and grasses. *Plant Physiol.* 149, 88–95. doi: 10.1104/pp.108.129791
- Peng, H. H., Shan, W., Kuang, J. F., Lu, W. J., and Chen, J. Y. (2013). Molecular characterization of cold-responsive basic helix-loop-helix transcription factors MabHLHs that interact with MaICE1 in banana fruit. *Planta* 238, 937–953. doi: 10.1007/s00425-013-1944-7
- Peng, P. H., Lin, C. H., Tsai, H. W., and Lin, T. Y. (2014). Cold response in phalaenopsis aphrodite and characterization of PaCBF1 and PaICE1. *Plant Cell Physiol.* 55, 1623–1635. doi: 10.1093/pcp/pcu093
- Shi, H. T., Li, R. J., Cai, W., Liu, W., Wang, C. L., and Lu, Y. T. (2012). Increasing nitric oxide content in *Arabidopsis thaliana* by expressing rat neuronal nitric oxide synthase resulted in enhanced stress tolerance. *Plant Cell Physiol.* 53, 344–357. doi: 10.1093/pcp/pcr181
- Shi, Y., Ding, Y., and Yang, S. (2015). Cold signal transduction and its interplay with phytohormones during cold acclimation. *Plant Cell Physiol.* 56, 7–15. doi: 10.1093/pcp/pcu115
- Shi, Y., Tian, S., Hou, L., Huang, X., Zhang, X., Guo, H., et al. (2012). Ethylene signaling negatively regulates freezing tolerance by repressing expression of CBF and type-A ARR genes in Arabidopsis. *Plant Cell* 24, 2578–2595. doi: 10.1105/tpc.112.098640
- Stockinger, E. J., Gilmour, S. J., and Thomashow, M. F. (1997). *Arabidopsis thaliana* CBF1 encodes an AP2 domain-containing transcriptional activator that binds to the C-repeat/DRE, a cis-acting DNA regulatory element that stimulates transcription in response to low temperature and water deficit. *Proc. Natl. Acad. Sci. U.S.A.* 94, 1035–1040. doi: 10.1073/pnas.94.3.1035
- Theocharis, A., Clement, C., and Barka, E. A. (2012). Physiological and molecular changes in plants grown at low temperatures. *Planta* 235, 1091–1105. doi: 10.1007/s00425-012-1641-y
- Thomashow, M. F. (1999). PLANT COLD ACCLIMATION: freezing tolerance genes and regulatory mechanisms. *Annu. Rev. Plant Physiol. Plant Mol. Biol.* 50, 571–599. doi: 10.1146/annurev.arplant.50.1.571
- Thomashow, M. F. (2010). Molecular basis of plant cold acclimation: insights gained from studying the CBF cold response pathway. *Plant Physiol.* 154, 571–577. doi: 10.1104/pp.110.161794
- Tuteja, N. (2007). Abscisic acid and abiotic stress signaling. *Plant Signal. Behav.* 2, 135–138. doi: 10.4161/psb.2.3.4156
- Wang, M., Zhang, X., and Liu, J. H. (2015). Deep sequencing-based characterization of transcriptome of trifoliate orange (*Poncirus trifoliata* (L.) Raf.) in response to cold stress. *BMC Genomics* 16:555. doi: 10.1186/s12864-015-1629-7
- Wisniewski, M., Nassuth, A., Teulieres, C., Marque, C., Rowland, J., Cao, P. B., et al. (2014). Genomics of cold hardiness in woody plants. *CRC. Crit. Rev. Plant Sci.* 33, 92–124. doi: 10.1080/07352689.2014.870408
- Xia, Z., Xu, H., Zhai, J., Li, D., Luo, H., He, C., et al. (2011). RNA-Seq analysis and de novo transcriptome assembly of Hevea brasiliensis. *Plant Mol. Biol.* 77, 299–308. doi: 10.1007/s11103-011-9811-z
- Xu, W., Jiao, Y., Li, R., Zhang, N., Xiao, D., Ding, X., et al. (2014). Chinese wild-growing *Vitis amurensis* ICE1 and ICE2 encode MYC-type bHLH transcription activators that regulate cold tolerance in Arabidopsis. *PLoS ONE* 9:e102303. doi: 10.1371/journal.pone.0102303
- Yuan, H. M., and Huang, X. (2016). Inhibition of root meristem growth by cadmium involves nitric oxide-mediated repression of auxin accumulation and signalling in Arabidopsis. *Plant Cell Environ.* 39, 120–135. doi: 10.1111/pce.12597
- Yuan, H. M., Liu, W. C., and Lu, Y. T. (2017). CATALASE2 Coordinates SA-mediated repression of both auxin accumulation and JA biosynthesis in plant defenses. *Cell Host Microbe* 21, 143–155. doi: 10.1016/j.chom.2017.01.007
- Conflict of Interest Statement:** The authors declare that the research was conducted in the absence of any commercial or financial relationships that could be construed as a potential conflict of interest.
- Copyright © 2017 Yuan, Sheng, Chen, Lu, Tang, Ou-Yang and Huang. This is an open-access article distributed under the terms of the Creative Commons Attribution License (CC BY). The use, distribution or reproduction in other forums is permitted, provided the original author(s) or licensor are credited and that the original publication in this journal is cited, in accordance with accepted academic practice. No use, distribution or reproduction is permitted which does not comply with these terms.



Autophagy: An Important Biological Process That Protects Plants from Stressful Environments

Wenyi Wang^{1,2}, Mengyun Xu², Guoping Wang^{2*} and Gad Galili^{1*}

¹ Department of Plant Science, Weizmann Institute of Science, Rehovot, Israel, ² College of Horticulture, South China Agricultural University, Guangzhou, China

Keywords: autophagy, protein degradation, abiotic stress, nbr1, TPSO, ATI1

Plants are sessile organisms that cannot escape from stressful environments, such as drought, high salinity, high temperature, and shortage of essential minerals in the soil. Hence, plants have evolved processes that protect them from these harmful conditions. One of these major processes is autophagy (which means, “self-eating”), a mechanism that destroys specific compounds that participate in efficient growth and requires extensive energy input and on the other hand stimulates biological processes that protect from the stress. Autophagy can be either a bulk process, turning over bulk amounts of various components in response to major stresses, such as serious accumulation of damaging compounds in the soil, or a selective process turning over specific components in response to specific and/or relatively minor environmental cues, such as minor shortage of rain and/or non-significant shortage of minerals in the soil (Han et al., 2011; Avin-Wittenberg et al., 2012; Liu and Bassham, 2012; Michaeli et al., 2016).

OPEN ACCESS

Edited by:

Minghui Lu,
Northwest A&F University, China

Reviewed by:

Shi Xiao,
Sun Yat-sen University, China
Xiaohong Zhuang,
The Chinese University of Hong Kong,
Hong Kong

*Correspondence:

Guoping Wang
gpwang@scau.edu.cn
Gad Galili
gad.galili@weizmann.ac.il

Specialty section:

This article was submitted to
Plant Cell Biology,
a section of the journal
Frontiers in Plant Science

Received: 01 November 2016

Accepted: 19 December 2016

Published: 11 January 2017

Citation:

Wang W, Xu M, Wang G and Galili G (2017) Autophagy: An Important Biological Process That Protects Plants from Stressful Environments. *Front. Plant Sci.* 7:2030.
doi: 10.3389/fpls.2016.02030

THE AUTOPHAGY-RELATED GENES (ATGs) INVOLVED IN ABIOTIC STRESS IN PLANTS

The identification of autophagy-related genes (ATGs) was an important milestone in the understanding of the mechanism of autophagy. Thus far, over 30 ATGs have been identified in *Arabidopsis*, rice, tobacco, and pepper based on comprehensive, genome-wide analysis (Xia et al., 2011; Zhou et al., 2015; Zhai et al., 2016). ATGs can be divided into three categories with respect to their function: (i) ATG1-ATG13 comprising the kinase complex, an upstream regulator that initiates autophagosome formation (Suttangkakul et al., 2011); (ii) The ATG9 and ATG6/vps30 complexes involved in vacuolar protein sorting in which ATG9 interacts with ATG2 and ATG18, boosting phagophore expansion. This operates via diverse shuttling of endomembranes, such as those of the endoplasmic reticulum (ER), Golgi, and mitochondria (Tooze and Yoshimori, 2010; Yang and Klionsky, 2010; Kang et al., 2011). The ATG6/vps30 complex recruited by ATG14, which localizes to the pre-autophagosomal structure (PAS) as well as the vacuolar membrane, to generate the autophagosomes (Tooze and Yoshimori, 2010); (iii) ubiquitin like conjugation systems (ATG5-ATG12 complex and ATG8-PE complex), which is essential for autophagosome formation. The ATG8-PE complex has been proven to recruit the cytoplasmic cargo to ensure autophagosome maturation and closure, and it is subsequently transported to the vacuole for degradation (Bassham, 2007; Michaeli et al., 2016). Most of complexes participating in each selective autophagy process have been identified in yeast and animal systems. However, it is still in infancy in plants (Michaeli et al., 2016).

Among the ATG genes, ATG8 is the central protein involved in autophagy and also a marker for the autophagosome (Shpilka et al., 2011). It has been shown to participate in various processes, such as diverse intracellular trafficking, post-mitotic Golgi reassembly, cargo receptor recognition, conjugation to phosphatidylethanolamine, etc. (Kwon and Park, 2008; Tooze and Yoshimori, 2010; Yang and Klionsky, 2010). Moreover, ATG8 plays an important role in the sensitivity of plants

to abiotic stresses. There are nine isoforms of ATG8 in *Arabidopsis* (ATG8a to ATG8i). The over-expression of AtATG8f led transgenic *Arabidopsis* plants to be more sensitive to mild salt and/or osmotic stress. This kind of sensitivity was accompanied by the modification of root architecture (Sláviková et al., 2005). Furthermore, the overexpression of *SiATG8a* improved the tolerance to nitrogen starvation and drought stress in transgenic *Arabidopsis* plants (Li et al., 2015).

The other ATGs also play critical roles in the stress response, especially the response to carbon and nitrogen starvation (Han et al., 2011). Two classical autophagy-related mutants, *atg5* and *atg7*, showed hypersensitivity to carbon and nitrogen starvation (Phillips et al., 2008; Yoshimoto et al., 2009). Autophagy-defective RNAi-AtATG18a plants displayed enhanced sensitivity to salt, drought and methyl viologen treatments compared with wild-type plants (Xiong et al., 2007; Liu et al., 2009). Moreover, *atg13* double-knockout (*atg13a atg13b*) and *atg11* knockout plants also showed a classical *atg* mutant phenotype, which exhibited increased sensitivity to carbon and nitrogen starvation (Suttangkakul et al., 2011). Rice *Osatg10b* mutants were sensitive to treatments with high salt (250 mM) and methyl viologen (MV) (Shin et al., 2009). Additionally, a series of autophagy-deficient mutants, such as *atg2-1*, *atg5-1*, *atg7-3*, *atg10-1*, were hypersensitive to submergence stress (Chen et al., 2015).

NBR1-MEDIATED SELECTIVE AUTOPHAGY MAKES THE HIGHLY UBIQUITINATED SOLUBLE PROTEINS PRONE TO AGGREGATION DURING ABIOTIC STRESSES

Out of a number of autophagy cargo receptors, the cargo receptor NBR1 (NEIGHBOR OF BRCA1 GENE 1) is one of the critical components of the autophagy process. NBR1 was identified in yeast, mammals and plants (Johansen and Lamark, 2011). NBR1 was the first selective cargo receptor, which was found to be responsible for sequestration of ubiquitinated proteins to the vacuole for their degradation inside this organelle. However, the involvement of the cargo receptors in autophagy is poorly understood. Recently, functional homologs of NBR1 proteins were identified in *Arabidopsis* (AtNBR1) and tobacco (JOKA2) plants (Svenning et al., 2011; Zientara-Rytter et al., 2011).

The *Arabidopsis* NBR1 is a homolog of the mammalian autophagic adaptor NBR1, with an ubiquitin-association domain binds selectively to six of the nine *Arabidopsis* ATG8 protein isoforms. The *nbr1* mutant exhibits sensitivity to a spectrum of abiotic stresses, similar to the autophagy-deficient *atg5* and *atg7* mutants, but had no obvious effect on the response to carbon starvation and resistance to a necrotrophic fungal pathogen. This indicates that AtNBR1 participates in the response to abiotic stress (Zhou et al., 2013). Under high heat conditions, an insoluble highly ubiquitinated detergent-resistant protein was shown to be prone to aggregation, thereby enabling recognition by NBR1 and its subsequent transport to the vacuole for degradation. Moreover, Rubisco activase and a number of catalases are linked to the response of plants to a wide variety

of abiotic stresses and these enzymes accumulated in the *nbr1* mutant (Zhou et al., 2014). These findings suggest that NBR1-mediated selective autophagy pathway plays a critical role during abiotic stresses (Figure 1).

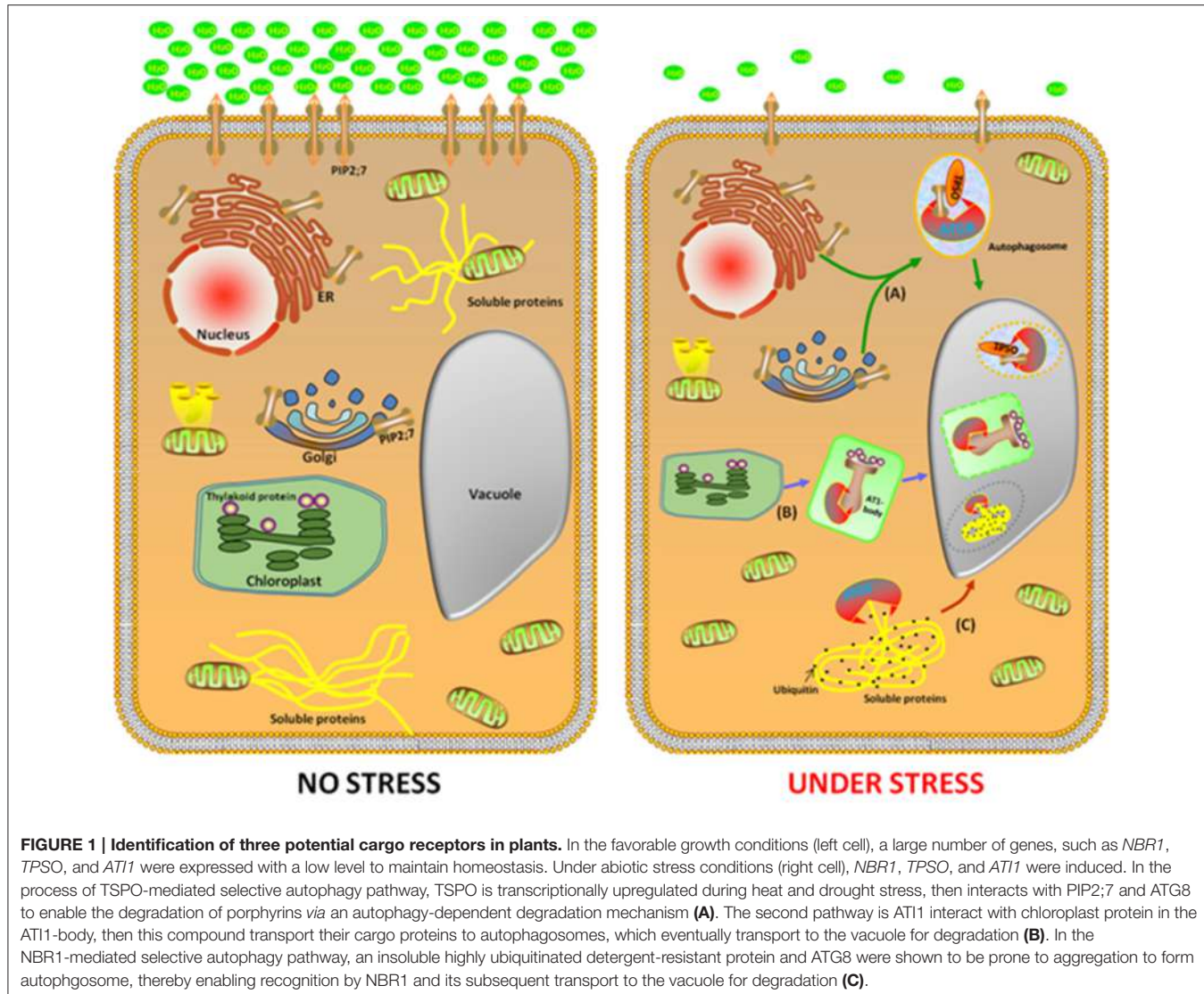
ABIOTIC STRESS-INDUCED TSPO-RELATED PROTEIN REDUCES AQUAPORIN PIP2;7 THROUGH AUTOPHAGIC DEGRADATION

To decipher the involvement of autophagy in abiotic stress in plants, the identification of the cargo receptor in the process of autophagy is crucial. This is because of the following reasons (i) under normal conditions, autophagy maintains a basal level for homeostasis; (ii) under abiotic stress, cargo receptors are active to remove the damaged or unwanted materials or to recycle the materials for providing anabolic substrates and metabolites to the cells. In plants, one of the critical processes of autophagy is the transport of the unnecessary components to the vacuole for degradation, which is a selective process requiring the cargos.

To minimize the effects of abiotic stresses, plants have developed a sophisticated protein quality control system that maintains the protein homeostasis. When subjected to abiotic stresses, such as heat and drought, the earliest response is inhibition of protein synthesis and increase in protein folding and processing. Recently a new *Arabidopsis* cargo receptor was identified and was named TRYPTOPHAN-RICH SENSORY PROTEIN (TSPO). It is a multi-stress regulator that is transiently induced by abiotic stress and is originally described as a heme-binding protein, which interacts with ATG8 to enable the degradation of porphyrins via an autophagy-dependent degradation mechanism (Vanhee et al., 2011). Moreover, TSPO interacts intracellularly with the plasma membrane aquaporin PIP2;7 (PLASMA MEMBRANE INTRINSIC PROTEIN 2;7) and downregulates it in the cell. The coexpression of TSPO and PIP2;7 led to decreased levels of PIP2;7 in the plasma membrane and abolished the membrane water permeability mediated by the overexpression of PIP2;7 in transgenic seedlings. Furthermore, ABA treatment activates TSPO and triggers the degradation of PIP2;7 through the autophagic pathway. These findings suggest that TSPO acts as a selective plant-specific autophagy cargo receptor during abiotic stress (Hachez et al., 2014). Remarkably, the autophagy-mediated reduction in the quantity of PIP2;7 modulates the osmotic water permeability of membranes, which is important during heat and drought stress (Figure 1).

AT1, A STRESS-ASSOCIATED PROTEIN ASSEMBLES INTO DIFFERENT TYPES OF NOVEL BODIES ASSOCIATED WITH EITHER ER OR PLASTIDS

With the aim of elucidating the biological processes in plants that are associated with selective autophagy in plants, our lab identified a number of plant-specific ATG8f binding proteins based on a yeast two-hybrid analysis. One of these



proteins, named “Autophagy Interacting Protein 1” (ATI1), was further subjected to detailed studies. When grown under regular, non-stress conditions, ATI1 was partially associated with the endoplasmic reticulum(ER) membrane. Furthermore, upon exposure of the plants to carbon or nitrogen starvation, ATI1 was assembled into two different types of novel bodies that were associated with either the ER or the plastids (Honig et al., 2012).

When the plants were exposed to carbon or nitrogen starvation, ATI1 was incorporated into novel bodies that were either moved along the ER network, or localized inside the plastids. These novel bodies were then transported into the central vacuole in which their contents were apparently being turned over inside the plastids (Figure 1). Interestingly, the seedlings of the over-expressing ATI1 plants germinated faster and showed increased tolerance to carbon starvation and salt stress, whereas the plants with suppressed expression of ATI1 showed reduced tolerance to carbon starvation and salt stress,

indicating that the biological processes using ATI1 confer faster growth and increased stress tolerance to the germinating seedlings (Michaeli et al., 2014).

The above results imply the ATI1 is a multifunctional protein, which is associated with ER-to-vacuole and plastid-to-vacuole trafficking by ATG8-mediated selective autophagy. Moreover, ATI1 is also involved in an autophagic system that promotes the seedling organization under abiotic stress conditions.

CONCLUDING REMARKS

Despite the identification of three potential cargo receptors in plants, a detailed understanding of these cargos is imperative. The questions that need to be addressed are whether there are links between the different cargo-mediated autophagy pathways, the mechanisms for the recognition and delivery of the misfolded and damaged proteins and organelles, and how the cargos are trafficked. We believe that with an in-depth

research on the involvement of autophagy in abiotic stress, particularly in crop plants, it is possible to open new avenues for the enhancement of stress tolerance by using genetic and/or genetic engineering approaches, ultimately leading to enhanced production.

REFERENCES

- Avin-Wittenberg, T., Honig, A., and Galili, G. (2012). Variations on a theme: plant autophagy in comparison to yeast and mammals. *Protoplasma* 249, 285–299. doi: 10.1007/s00709-011-0296-z
- Bassham, D. C. (2007). Plant autophagy—more than a starvation response. *Curr. Opin. Plant Biol.* 10, 587–593. doi: 10.1016/j.pbi.2007.06.006
- Chen, L., Liao, B., Qi, H., Xie, L. J., Huang, L., Tan, W. J., et al. (2015). Autophagy contributes to regulation of the hypoxia response during submergence in *Arabidopsis thaliana*. *Autophagy* 11, 2233–2246. doi: 10.1080/15548627.2015.1112483
- Hachez, C., Veljanovski, V., Reinhardt, H., Guillaumot, D., Vanhee, C., Chaumont, F., et al. (2014). The *Arabidopsis* abiotic stress-induced TSPO-related protein reduces cell-surface expression of the aquaporin PIP2; 7 through protein-protein interactions and autophagic degradation. *Plant Cell* 26, 4974–4990. doi: 10.1105/tpc.114.134080
- Han, S., Yu, B., Wang, Y., and Liu, Y. (2011). Role of plant autophagy in stress response. *Protein Cell* 2, 784–791. doi: 10.1007/s13238-011-1104-4
- Honig, A., Avin-Wittenberg, T., Ufaz, S., and Galili, G. (2012). A new type of compartment, defined by plant-specific ATG8-interacting proteins, is induced upon exposure of *Arabidopsis* plants to carbon starvation. *Plant Cell* 24, 288–303. doi: 10.1105/tpc.111.093112
- Johansen, T., and Lamark, T. (2011). Selective autophagy mediated by autophagic adapter proteins. *Autophagy* 7, 279–296. doi: 10.4161/auto.7.3.14487
- Kang, R., Zeh, H. J., Lotze, M. T., and Tang, D. (2011). The Beclin 1 network regulates autophagy and apoptosis. *Cell Death Dif.* 18, 571–580. doi: 10.1038/cdd.2010.191
- Kwon, S. I., and Park, O. K. (2008). Autophagy in plants. *J. Plant Biol.* 51, 313–320. doi: 10.1007/BF03036132
- Li, W. W., Chen, M., Zhong, L., Liu, J. M., Xu, Z. S., Li, L. C., et al. (2015). Overexpression of the autophagy-related gene *SiATG8a* from foxtail millet (*Setaria italica* L.) confers tolerance to both nitrogen starvation and drought stress in *Arabidopsis*. *Biochem. Biophys. Res. Commun.* 468, 800–806. doi: 10.1016/j.bbrc.2015.11.035
- Liu, Y., and Bassham, D. C. (2012). Autophagy: pathways for self-eating in plant cells. *Annu. Rev. Plant Biol.* 63, 215–237. doi: 10.1146/annurev-arplant-042811-105441
- Liu, Y., Xiong, Y., and Bassham, D. C. (2009). Autophagy is required for tolerance of drought and salt stress in plants. *Autophagy* 5, 954–963. doi: 10.4161/auto.5.7.9290
- Michaeli, S., Galili, G., Genschik, P., Fernie, A. R., and Avin-Wittenberg, T. (2016). Autophagy in plants—what's new on the menu? *Trends Plant Sci.* 21, 134–144. doi: 10.1016/j.tplants.2015.10.008
- Michaeli, S., Honig, A., Levanony, H., Peled-Zehavi, H., and Galili, G. (2014). *Arabidopsis* ATG8-INTERACTING PROTEIN1 is involved in autophagy-dependent vesicular trafficking of plastid proteins to the vacuole. *Plant Cell* 26, 4084–4101. doi: 10.1105/tpc.114.129999
- Phillips, A. R., Suttangkakul, A., and Vierstra, R. D. (2008). The ATG12-conjugating enzyme ATG10 is essential for autophagic vesicle formation in *Arabidopsis thaliana*. *Genetics* 178, 1339–1353. doi: 10.1534/genetics.107.086199
- Shin, J. H., Yoshimoto, K., Ohsumi, Y., Jeon, J. S., and An, G. (2009). OsATG10b, an autophagosome component, is needed for cell survival against oxidative stresses in rice. *Mol. Cells* 27, 67–74. doi: 10.1007/s10059-009-0006-2
- Shpilka, T., Weidberg, H., Pietrokovski, S., and Elazar, Z. (2011). Atg8: an autophagy-related ubiquitin-like protein family. *Genome Biol.* 12:1. doi: 10.1186/gb-2011-12-7-226
- Slávíková, S., Shy, G., Yao, Y., Glzman, R., Levanony, H., Pietrokovski, S., et al. (2005). The autophagy-associated Atg8 gene family operates both under favourable growth conditions and under starvation stresses in *Arabidopsis* plants. *J. Exp. Bot.* 56, 2839–2849. doi: 10.1093/jxb/eri276
- Suttangkakul, A., Li, F., Chung, T., and Vierstra, R. D. (2011). The ATG1/ATG13 protein kinase complex is both a regulator and a target of autophagic recycling in *Arabidopsis*. *Plant Cell* 23, 3761–3779. doi: 10.1105/tpc.111.090993
- Svenning, S., Lamark, T., Krause, K., and Johansen, T. (2011). Plant NBR1 is a selective autophagy substrate and a functional hybrid of the mammalian autophagic adapters NBR1 and p62/SQSTM1. *Autophagy* 7, 993–1010. doi: 10.4161/auto.7.9.16389
- Toozé, S. A., and Yoshimori, T. (2010). The origin of the autophagosomal membrane. *Nat. Cell Biol.* 12, 831–835. doi: 10.1038/ncb0910-831
- Vanhee, C., Zapotoczny, G., Masquelier, D., Ghislain, M., and Batoko, H. (2011). The *Arabidopsis* multistress regulator TSPO is a heme binding membrane protein and a potential scavenger of porphyrins via an autophagy-dependent degradation mechanism. *Plant Cell* 23, 785–805. doi: 10.1105/tpc.110.081570
- Xia, K., Liu, T., Ouyang, J., Wang, R., Fan, T., and Zhang, M. (2011). Genome-wide identification, classification, and expression analysis of autophagy-associated gene homologues in rice (*Oryza sativa* L.). *DNA Res.* 18, 363–377. doi: 10.1093/dnares/dsr024
- Xiong, Y., Contento, A. L., Nguyen, P. Q., and Bassham, D. C. (2007). Degradation of oxidized proteins by autophagy during oxidative stress in *Arabidopsis*. *Plant Physiol.* 143, 291–299. doi: 10.1104/pp.106.092106
- Yang, Z., and Klionsky, D. J. (2010). Eaten alive: a history of macroautophagy. *Nat. Cell Biol.* 12, 814–822. doi: 10.1038/ncb0910-814
- Yoshimoto, K., Jikumaru, Y., Kamiya, Y., Kusano, M., Consonni, C., Panstruga, R., et al. (2009). Autophagy negatively regulates cell death by controlling NPR1-dependent salicylic acid signaling during senescence and the innate immune response in *Arabidopsis*. *Plant Cell* 21, 2914–2927. doi: 10.1105/tpc.109.068635
- Zhai, Y., Guo, M., Wang, H., Lu, J., Liu, J., Zhang, C., et al. (2016). Autophagy, a conserved mechanism for protein degradation, responds to heat, and other abiotic stresses in *Capsicum annuum* L. *Front. Plant Sci.* 7:131. doi: 10.3389/fpls.2016.00131
- Zhou, J., Wang, J., Cheng, Y., Chi, Y. J., Fan, B., Yu, J. Q., et al. (2013). NBR1-mediated selective autophagy targets insoluble ubiquitinated protein aggregates in plant stress responses. *PLoS Genet.* 9:e1003196. doi: 10.1371/journal.pgen.1003196
- Zhou, J., Zhang, Y., Qi, J., Chi, Y., Fan, B., Yu, J. Q., et al. (2014). E3 ubiquitin ligase CHIP and NBR1-mediated selective autophagy protect additively against proteotoxicity in plant stress responses. *PLoS Genet.* 10:e1004116. doi: 10.1371/journal.pgen.1004116
- Zhou, X. M., Zhao, P., Wang, W., Zou, J., Cheng, T. H., Peng, X. B., et al. (2015). A comprehensive, genome-wide analysis of autophagy-related genes identified in tobacco suggests a central role of autophagy in plant response to various environmental cues. *DNA Res.* 22, 245–257. doi: 10.1093/dnares/dsv012
- Zientara-Rytter, K., Lukomska, J., Moniuszko, G., Gwozdecki, R., Surowiecki, P., Lewandowska, M., et al. (2011). Identification and functional analysis of Joka2, a tobacco member of the family of selective autophagy cargo receptors. *Autophagy* 7, 1145–1158. doi: 10.4161/auto.7.10.16617

AUTHOR CONTRIBUTIONS

WW and GG conceived and designed the project, and wrote the manuscript. MX and GW helped with figure revision. The manuscript was approved by all other authors.



The AMP-Activated Protein Kinase KIN10 Is Involved in the Regulation of Autophagy in *Arabidopsis*

Liang Chen^{1,2}, Ze-Zhuo Su¹, Li Huang¹, Fan-Nv Xia¹, Hua Qi¹, Li-Juan Xie¹, Shi Xiao^{1*} and Qin-Fang Chen^{1*}

¹ State Key Laboratory of Biocontrol and Guangdong Provincial Key Laboratory of Plant Resources, School of Life Sciences, Sun Yat-sen University, Guangzhou, China, ² College of Life Sciences, South China Agricultural University, Guangzhou, China

OPEN ACCESS

Edited by:

Minghui Lu,

Northwest A&F University, China

Reviewed by:

Taijoon Chung,

Pusan National University,

South Korea

Martin Dickman,

Texas A&M University, United States

*Correspondence:

Shi Xiao

xiaoshi3@mail.sysu.edu.cn

Qin-Fang Chen

chenqf3@mail.sysu.edu.cn

Specialty section:

This article was submitted to

Plant Cell Biology,

a section of the journal

Frontiers in Plant Science

Received: 30 December 2016

Accepted: 26 June 2017

Published: 10 July 2017

Citation:

Chen L, Su Z-Z, Huang L, Xia F-N, Qi H, Xie L-J, Xiao S and Chen Q-F (2017) The AMP-Activated Protein Kinase KIN10 Is Involved in the Regulation of Autophagy in *Arabidopsis*. *Front. Plant Sci.* 8:1201. doi: 10.3389/fpls.2017.01201

Autophagy is a highly conserved system in eukaryotes for the bulk degradation and recycling of intracellular components. Autophagy is involved in many physiological processes including development, senescence, and responses to abiotic and biotic stress. The adenosine 5'-monophosphate (AMP)-activated protein kinase AMPK positively regulates autophagy in mammals; however, the potential function of AMPK in plant autophagy remains largely unknown. Here, we identified KIN10, a plant ortholog of the mammalian AMPK, as a positive regulator of plant autophagy and showed that it acts by affecting the phosphorylation of ATG1 (AUTOPHAGY-RELATED GENE 1) proteins in *Arabidopsis*. Transgenic *Arabidopsis* lines overexpressing *KIN10* (*KIN10-OE*) showed delays in leaf senescence, and increased tolerance to nutrient starvation, these phenotypes required a functional autophagy pathway. Consistent with KIN10 having a potential role in autophagy, the nutrient starvation-induced formation of autophagosomes and cleavage of GFP-ATG8e were accelerated in the *KIN10-OE* lines compared to the wild type. Moreover, the *KIN10-OE* lines were less sensitive to drought and hypoxia treatments, compared with wild type. Carbon starvation enhanced the level of phosphorylated YFP-ATG1a in the *KIN10-OE* lines compared to that of wild type. Together, these findings suggest that KIN10 is involved in positive regulation of autophagy, possibly by affecting the phosphorylation of ATG1s in *Arabidopsis*.

Keywords: ATG1, AMPK, autophagy, KIN10, phosphorylation

INTRODUCTION

Autophagy is the process of degradation and recycling of cytoplasmic organelles, proteins, and macromolecules, and is highly conserved among eukaryotes. Autophagy is activated by a variety of stress factors, such as nutrient deprivation, hypoxia, reactive oxygen species, and infection by pathogen (Kroemer et al., 2010; Han et al., 2011). Autophagy plays an essential role in the maintenance of cellular homeostasis under changing nutrient conditions. Among the three types of autophagy, macroautophagy (hereafter referred to as autophagy) is the predominant form (Klionsky, 2007). During autophagy, double-membrane vesicles, called autophagosomes, are formed from the expanding membranes of preautophagosomal structures; these autophagosomes sequester the enclosed components and deliver them to the lysosome/vacuole for degradation.

The serine/threonine protein kinase ULK1(Unc-51-like kinases 1, mammalian homologs of ATG1) activates autophagy in response to developmental cues or stress signals by initiating autophagosome formation (Mizushima, 2010; Wirth et al., 2013; Wong et al., 2013). In mammalian cells, ULK1 activity is directly controlled by the target of rapamycin (TOR) and the AMP-dependent protein kinase (AMPK) (Kim et al., 2011; Shang and Wang, 2011; Alers et al., 2012). Under nutrient-rich conditions, the activated TOR kinase disrupts the ULK1-ATG13 complex by phosphorylating the ATG13 subunit, and thereby inhibits autophagy. However, under nutrient starvation conditions, AMPK directly phosphorylates ULK1 at the Ser 317 and Ser 777 residues, subsequently activating autophagy (Kim et al., 2011). Alternatively, AMPK may activate autophagy by inhibiting TORC1 (TOR complex 1) activity (Gwinn et al., 2008; Lee et al., 2010). ULK1 may also be involved in the termination of autophagy. Specifically, ULK1 represses AMPK activity through a negative regulatory feedback loop (Löffler et al., 2011). Similarly, another study suggests that the KLHL20-mediated ubiquitination and degradation of ULK1 contributes to the termination of autophagy (Liu et al., 2016).

In plants, the Snf1-related kinase 1 (SnRK1), a homolog of the yeast Snf1 and mammalian AMPK, is a highly conserved energy sensor and is activated under energy deprivation (Polge and Thomas, 2007; Baena-González and Sheen, 2008; Emanuelle et al., 2015). SnRK1 is composed of one catalytic α subunit (KIN10 and 11 in *Arabidopsis*) and two regulatory subunits, β and γ (Polge and Thomas, 2007; Emanuelle et al., 2015). Overexpression of *KIN10* delays flowering and leaf senescence in *Arabidopsis*, suggesting that KIN10 play a positive role in the regulation of growth and development as well as energy signaling (Baena-González et al., 2007). Although Snf1/AMPK likely promotes autophagy by directly activating ATG1/ULK1 in yeast and animals, the role of SnRK1 in plant autophagy is not well characterized.

Our study demonstrated that *Arabidopsis* KIN10 is a positive regulator of autophagy. Under nutrient starvation, transgenic plants overexpressing *KIN10* (*KIN10-OE*) showed enhanced autophagosome formation and increased tolerance to nutrient deprivations. Furthermore, the level of starvation-induced phosphorylation of ATG1 increased in the *KIN10-OE* lines, suggesting that KIN10 is likely involved in positive regulation of autophagy, possibly by affecting the phosphorylation of ATG1 proteins.

MATERIALS AND METHODS

Plant Materials, Growth Conditions, and Treatments

The *KIN10* overexpression lines (*OE-1* and *OE-2*) and *KIN10* RNAi lines (*RNAi-1* and *RNAi-7*) used in this study were in the *Arabidopsis* Landsberg *erecta* (*Ler*) background (Baena-González et al., 2007). The autophagy-related mutants *atg5-1* and *atg7-3* (Thompson et al., 2005; Lai et al., 2011; Chen et al., 2015; Col-0 ecotype) were backcrossed twice to the *Ler* wild-type plants to obtain *atg5-L* and *atg7-L* plants. The *atg5-L* and *atg7-L* mutants

were further crossed to the *OE-1* line to generate *OE-1 atg5-L* and *OE-1 atg7-L* lines. Transgenic lines expressing GFP-ATG8e and YFP-ATG1a, driven by the CaMV 35S promoter, have been previously described (Xiao et al., 2010; Suttangkakul et al., 2011). All *Arabidopsis* seeds were surface-sterilized with 20% bleach containing 0.1% Tween-20 for 20 min, and then washed 5 times with sterile water. Seeds were sown on Murashige and Skoog (MS) medium, followed by cold treatment in the dark for 3 days. Seven days after germination, seedlings were transplanted into soil and grown in a plant growth room with a 16-h-light/8-h-dark cycle at 22°C.

For the carbon starvation treatment, 7-day-old MS-grown seedlings or 4-week-old soil-grown plants were transferred to continuous darkness for the indicated duration followed by recovery under normal growth conditions for 7 days. Samples were collected or photographed at the indicated time points. To calculate the survival rate after darkness, at least 18 plants per genotype were dark-treated followed by a 7-day recovery. The number of surviving plants, where survival is defined as the capability to produce new leaves, was recorded. For the nitrogen starvation treatment, 7-day-old seedlings grown on MS medium were transferred to solid MS or nitrogen-deficient solid MS medium and grown for 5 days. Chlorophyll contents were measured and calculated after the recovery.

RNA Extraction and Quantitative Reverse-Transcription PCR Analysis

Total RNA extraction and quantitative reverse-transcription PCR (qRT-PCR) analysis were performed as previously described (Chen et al., 2015). Briefly, the isolated RNA was reverse transcribed using the PrimeScript RT Reagent Kit with gDNA Eraser (Takara, RR047A) following the manufacturer's instructions. The qPCR was carried out using SYBR Green master mix (Takara, RR420A) on a StepOne Plus real-time PCR system (Applied Biosystems). The conditions for the qPCR were: initial denaturation at 95°C for 5 min followed by 40 cycles of PCR (denaturing at 95°C for 10 s, annealing at 55°C for 15 s, and extension at 72°C for 30 s). Three experimental replicates were used for each reaction. ACTIN2 was used as the reference gene. Gene-specific primers used for the qPCR analysis are listed in Supplementary Table S1.

Laser Scanning Confocal Microscopy

The stable transgenic lines expressing a GFP-ATG8e fusion protein were used to monitor autophagosome formation (Xiao et al., 2010). Seven-day-old GFP-ATG8e seedlings grown in MS solid medium were transferred to MS medium or MS medium lacking sugars (MS-C) under darkness for the indicated times. After treatment, the primary root cells were observed using an LSM 780 NLO laser scanning confocal microscope (Carl Zeiss).

Western Blot Analysis

Total protein extraction was performed as previously described (Chen et al., 2015). Briefly, 4-week-old plant leaves or 7-day-old whole seedling were ground in liquid nitrogen and homogenized in ice-cold extraction buffer (50 mM sodium phosphate, pH

7.0, 200 mM NaCl, 10 mM MgCl₂, 0.2% β-mercaptoethanol and 10% glycerol) supplemented with protease inhibitor cocktail (Roche, 04693132001). Total homogenates were placed on ice for 30 min, and then centrifuged for 30 min at 11,000 g. The supernatant was transferred to a new microfuge tube for SDS-PAGE electrophoresis.

For immunoblot analysis, total proteins were subjected to SDS-PAGE and electrophoretically transferred to a Hybond-C membrane (Amersham, 10600016). Anti-GFP antibodies were used to detect GFP as previously described (Chen et al., 2015). YFP was detected with rabbit anti-GFP polyclonal antibodies (Abcam, ab290).

Phosphatase Treatment

Phosphatase treatment was performed according to Suttangkakul et al. (2011) with minor modification. Seven-day-old YFP-ATG1a and YFP-ATG1a/KIN10-OE seedling were homogenized in ice-cold protein extraction buffer supplemented with 1 mM phenylmethylsulfonyl fluoride and protease inhibitor cocktail (Roche). Samples were placed on ice for 30 min, and then centrifuged for 30 min at 11,000 g. The supernatant was incubated with λ protein phosphatase (New England Biolabs) with or without addition of phosphatase inhibitor PhosSTOP (Roche) for 30 min at 30°C. 2 × SDS-PAGE sample buffer was added to the total sample and heated to 95°C for 5 min.

Statistical Analysis

Data are reported as means ± SD of three independent experiments unless otherwise indicated. The significance of the differences between groups was determined by a two-tailed Student's *t*-test. *P*-values < 0.05 or < 0.01 were considered significant.

Accession Numbers

Sequence data from this article can be found in the Arabidopsis Genome Initiative or GenBank databases under the following accession numbers: KIN10 (At3g01090), ATG1a (At3g61960), ATG1b (At3g53930), ATG1c (At2g37840), ATG2 (At3g19190), ATG5 (At5g17290), ATG6 (At3g61710), ATG7 (At5g45900), ATG8a (At4g21980), ATG8e (At2g45170), ATG9 (At2g31260), ATG10 (At3g07525), ATG13a (At3g49590), ATG13b (At3g18770), ATG18a (At3g62770), and PI3K (At1g60490).

RESULTS

Transgenic Plants Overexpressing KIN10 Showed Delayed Leaf Senescence and Enhanced Tolerance to Nutrient Starvation

The KIN10 overexpression lines (OE-1 and OE-2) showed delayed leaf senescence (Baena-González et al., 2007). To examine the potential role of *Arabidopsis* KIN10 in autophagy, we further examined the response of the KIN10-OE lines and KIN10 RNA interference lines (RNAi-1 and RNAi-7) to naturally induced senescence and nutrient deficiency.

The RNA and protein level of KIN10 in the KIN10-OE and KIN10-RNAi lines were first confirmed by qRT-PCR and western blot analyses (Supplementary Figure S1). Under normal growth conditions, both KIN10-OE lines displayed slower growth and delayed natural senescence compared to the wild type, while the KIN10-RNAi lines showed similar phenotypes to the wild-type plants (Figure 1A). The level of chlorophyll in the leaves of 6-week-old KIN10-OE lines was much higher than that of the wild type (Figure 1B).

The KIN10-OE lines showed enhanced tolerance to carbon starvation induced by constant darkness for 7 days followed by a 7-day recovery, while the KIN10-RNAi lines appeared similar to the wild-type plants after this treatment (Figures 1C,D). For the nitrogen deficiency treatment, 7-day-old MS-grown seedlings were transferred to MS or MS-N solid medium for 5 days. The cotyledons of the wild-type plants and KIN10-RNAi lines were significantly yellowed as indicated by the reduced chlorophyll contents (Figures 1E,F). In contrast, the KIN10-OE lines were more resistant to nitrogen deficiency and had significantly higher chlorophyll levels compared to that of the wild type (Figures 1E,F). These findings suggest that overexpression of KIN10 can delay natural senescence and improves tolerance to carbon and nitrogen starvation.

The Enhanced Tolerance of the KIN10-OE Lines to Nutrient Starvation Is Dependent on a Functional Autophagy Pathway

Given that the KIN10-overexpression lines showed delayed leaf senescence and enhanced tolerance to nutrient starvation (Figures 1, 2), and that the autophagy-deficient mutants had the opposite phenotype (Baena-González et al., 2007; Li and Vierstra, 2012), we used these plants to further assess the genetic connection between KIN10 and the autophagy pathway. The *atg5-L* and *atg7-L* mutants (*atg5* and *atg7* mutants in the Ler background) were crossed to KIN10-OE-1 (OE-1) to generate OE-1 *atg5-L* and OE-1 *atg7-L* lines. We then tested the tolerance of the 4-week-old wild-type, OE-1, OE-1 *atg5-L*, OE-1 *atg7-L*, *atg5-L*, and *atg7-L* plants to carbon starvation. Compared to the wild-type plants, the OE-1 plants showed enhanced tolerance and the *atg5-L* and *atg7-L* plants showed decreased tolerance to carbon starvation. Interestingly, the OE-1 *atg5-L* and OE-1 *atg7-L* lines displayed similar sensitivities to carbon starvation to that of the *atg5-L* and *atg7-L* mutants (Figure 2A). In addition, the enhanced resistance of the OE-1 line to nitrogen deficiency was attenuated by the loss-of-function of ATG5 and ATG7 (Figure 2B). The enhanced tolerance to starvation in the OE-1 line was further supported by the higher survival rates (Figure 2C) and higher relative chlorophyll contents (Figure 2D) in this line. Together, these results indicate that the enhanced tolerance to nutrient starvation in the KIN10-OE lines is dependent on a functional autophagy pathway. The evidence that the autophagy-associated phenotypes in the KIN10-OEs were primarily recovered by the autophagy deficient mutants, suggesting that autophagy acts downstream of KIN10 to affect

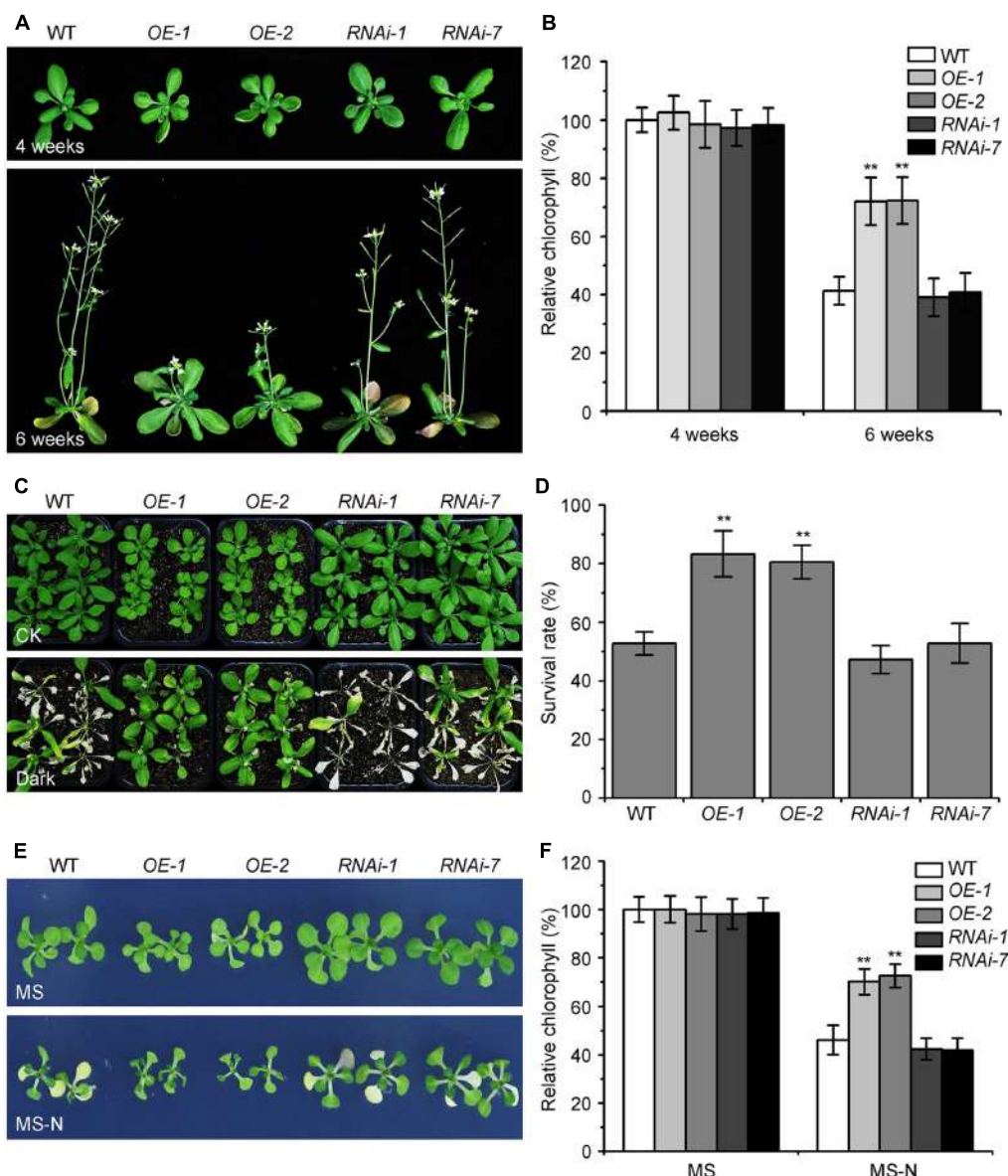


FIGURE 1 | Overexpression of *KIN10* delays senescence and enhances tolerance to nutrient starvation in *Arabidopsis*. **(A)** Naturally induced senescence of the wild type (WT) and the *KIN10*-OE (OE-1 and OE-2) and *KIN10*-RNAi lines (RNAi-1 and RNAi-7). Photos were taken at 4 and 6 weeks after germination. **(B)** Relative chlorophyll contents in the leaves of 4- and 6-week-old WT, OE-1, OE-2, RNAi-1, and RNAi-7 plants. The data are means \pm SD ($n = 3$) calculated from three biological replicates. For each experiment, a population of 14 plants was recorded per genotype. ** $P < 0.01$ by Student's *t*-test. **(C)** Phenotypes of the WT, OE-1, OE-2, RNAi-1, and RNAi-7 plants after carbon starvation. Four-week-old WT, OE-1, OE-2, RNAi-1, and RNAi-7 plants grown under normal growth conditions were transferred to constant darkness for 7 days and photos were taken after a 7-day recovery. **(D)** Survival rates of the WT, OE-1, OE-2, RNAi-1, and RNAi-7 plants described in **(C)**. The data are means \pm SD ($n = 3$) calculated from three biological replicates. For each biological replicate, a population of 18 plants was recorded per genotype. ** $P < 0.01$ by Student's *t*-test. **(E)** Phenotypes of the WT, OE-1, OE-2, RNAi-1, and RNAi-7 plants after nitrogen starvation. One-week-old WT, OE-1, OE-2, RNAi-1, RNAi-7 seedlings grown on MS solid medium were transferred to MS or MS-N solid medium and photos were taken after 5 days of treatment. **(F)** Relative chlorophyll contents of the WT, OE-1, OE-2, RNAi-1, and RNAi-7 seedlings described in **(E)**. The data are means \pm SD ($n = 3$) calculated from three biological replicates. For each biological replicate, a population of 20 plants was recorded per genotype. ** $P < 0.01$ by Student's *t*-test.

plant growth and stress responses. Given that *KIN10* is a well-known master regulator in energy signaling in *Arabidopsis*, we therefore proposed that it governs a cellular switch between plant growth and stress responses by modulating various downstream signaling pathways, including autophagy.

The *KIN10*-OE Lines Are Tolerant to Drought and Submergence

The autophagy-defective mutants are hypersensitive to abiotic stresses such as drought and submergence (Liu et al., 2009; Chen et al., 2015). To further assess the role of *KIN10* in

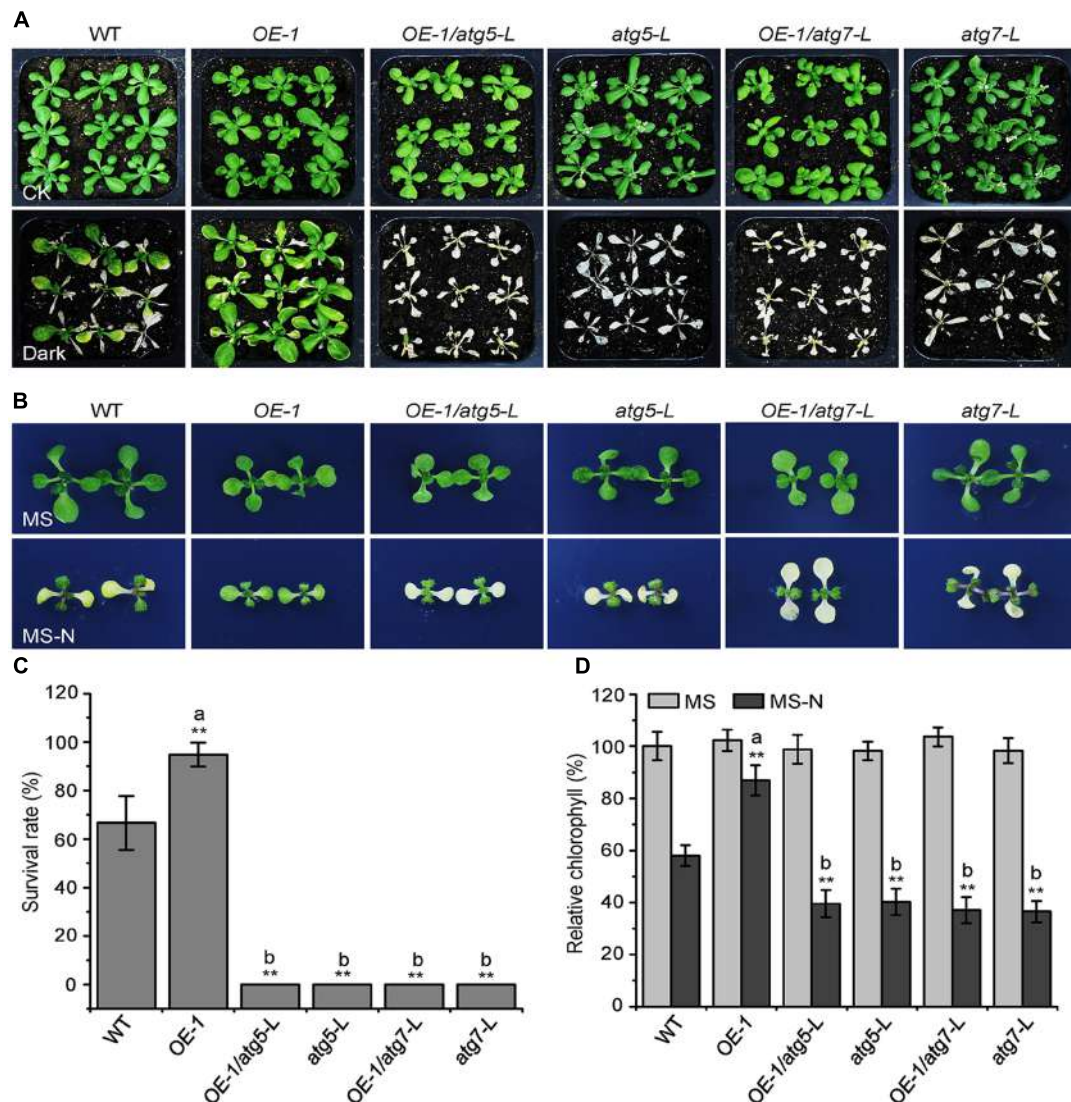


FIGURE 2 | The enhanced tolerance of the *KIN10-OE* lines to nutrient starvation is dependent on a functional autophagy pathway. **(A)** Phenotypes of the wild type (WT), OE-1, OE-1/atg5-L, atg5-L, OE-1/atg7-L, and atg7-L plants after carbon starvation. Four-week-old WT, OE1, OE-1/atg5-L, atg5-L, OE-1/atg7-L, and atg7-L plants grown under normal conditions were transferred to constant darkness for 7 days and photographs were taken after 7 days of dark treatment. **(B)** Phenotypes of the WT, OE-1, OE-1/atg5-L, atg5-L, OE-1/atg7-L, and atg7-L plants after nitrogen starvation. One-week-old WT, OE-1, OE-1/atg5-L, atg5-L, OE-1/atg7-L, and atg7-L seedlings grown on solid MS medium were transferred to MS or MS-N solid medium and photos were taken after 5 days of treatment. **(C)** Survival rate of the WT, OE-1, OE-1/atg5-L, atg5-L, OE-1/atg7-L, and atg7-L plants described in **(A)**. The data are means \pm SD ($n = 3$) calculated from three biological replicates. For each biological replicate, a population of 18 plants was recorded per genotype. $^{**}P < 0.01$ by Student's *t*-test. **(D)** Relative chlorophyll levels in the leaves of the WT, OE-1, OE-1/atg5-L, atg5-L, OE-1/atg7-L, and atg7-L seedlings described in **(B)**. The data are means \pm SD ($n = 3$) calculated from three biological replicates. For each biological replicate, five technical replicates (each replicate was pooled with 20 seedlings) were measured per genotype. $^{**}P < 0.01$ by Student's *t*-test. “a” indicates values that are significantly higher than that of the WT; “b” indicates values that are significantly lower than that of the WT.

autophagy-related stress responses, the wild-type (*Ler*), the *KIN10-OE* lines (*OE-1* and *OE-2*), and the *KIN10-RNAi* lines (*RNAi-1* and *RNAi-7*) were subjected to drought and submergence treatments. As shown in Figure 3, no significant differences were observed between the wild type and the *KIN10-OE* or *KIN10-RNAi* lines under normal growth conditions. However, after a 14-day drought treatment, the leaves of the wild type and the *KIN10-RNAi* lines turned yellow and wilted, while the leaves of the *KIN10-OE* lines remained green

and turgid (Figure 3A). After a 4-day recovery by rehydration, the survival rates of the *KIN10-OE* lines were significantly higher than those of the wild type and the *KIN10-RNAi* lines (Figure 3B). In addition, the *KIN10-OE* lines were much more tolerant than the wild type and the *KIN10-RNAi* plants to a 6-day submergence in water (under light conditions) followed by a 6-day recovery (Figure 3C), which was supported by the improved survival rates of the *KIN10-OE* lines compared to the wild-type plants after submergence (Figure 3D).

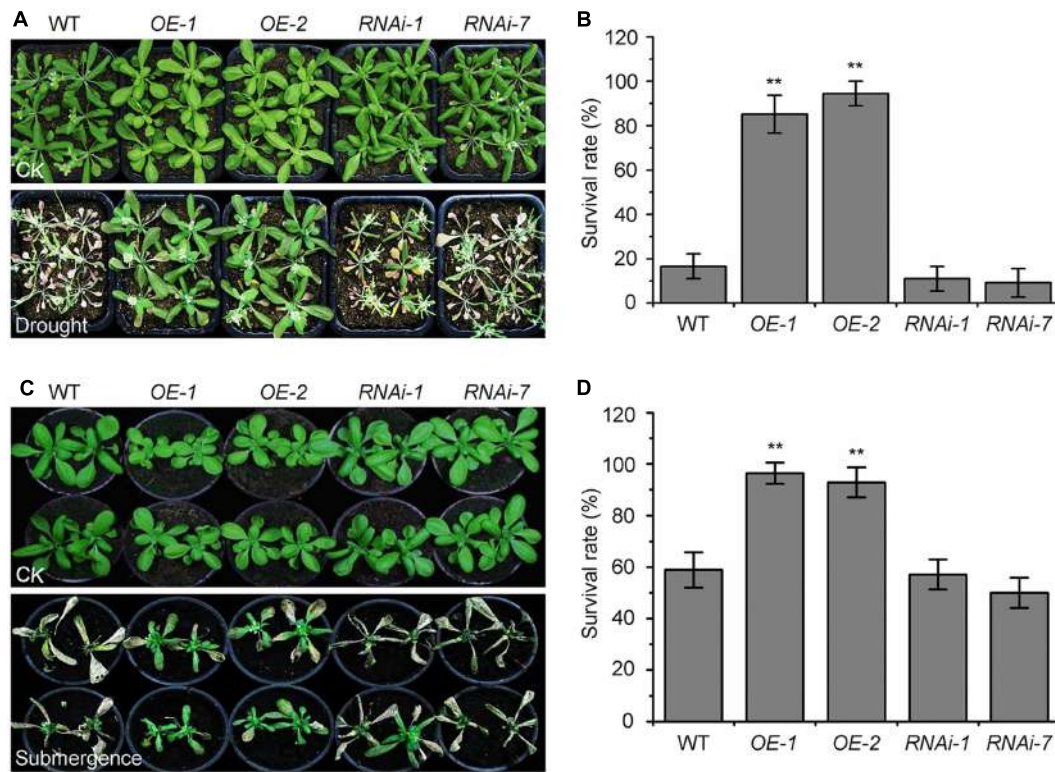


FIGURE 3 | Overexpression of *KIN10* enhances tolerance to drought and submergence. **(A)** Phenotypes of the wild type (WT), OE-1, OE-2, RNAi-1, and RNAi-7 plants after drought stress. WT, OE-1, OE-2, RNAi-1, and RNAi-7 plants were grown under normal growth conditions for 3 weeks and then water was withheld for a 14-day drought treatment. Photos were taken after a 4-day recovery. **(B)** Survival rates of the WT, OE-1, OE-2, RNAi-1, and RNAi-7 plants described in **(A)** after re-watering for 4 days. The data are means \pm SD ($n = 3$) calculated from three biological replicates. For each biological replicate, a population of 18 plants was recorded per genotype. ** $P < 0.01$ by Student's *t*-test. **(C)** Phenotypes of the WT, OE-1, OE-2, RNAi-1, and RNAi-7 plants after the submergence treatment. Four-week-old WT, OE-1, OE-2, RNAi-1, and RNAi-7 plants were submerged for 6 days and photos were taken after a 6-day recovery. **(D)** Survival rates of the WT, OE-1, OE-2, RNAi-1, and RNAi-7 plants described in **(C)** after the 6-day recovery. The data are means \pm SD ($n = 3$) calculated from three biological replicates. For each biological replicate, a population of 18 plants was recorded per genotype. ** $P < 0.01$ by Student's *t*-test.

Overexpression of *KIN10* Activates the Formation of Autophagosomes

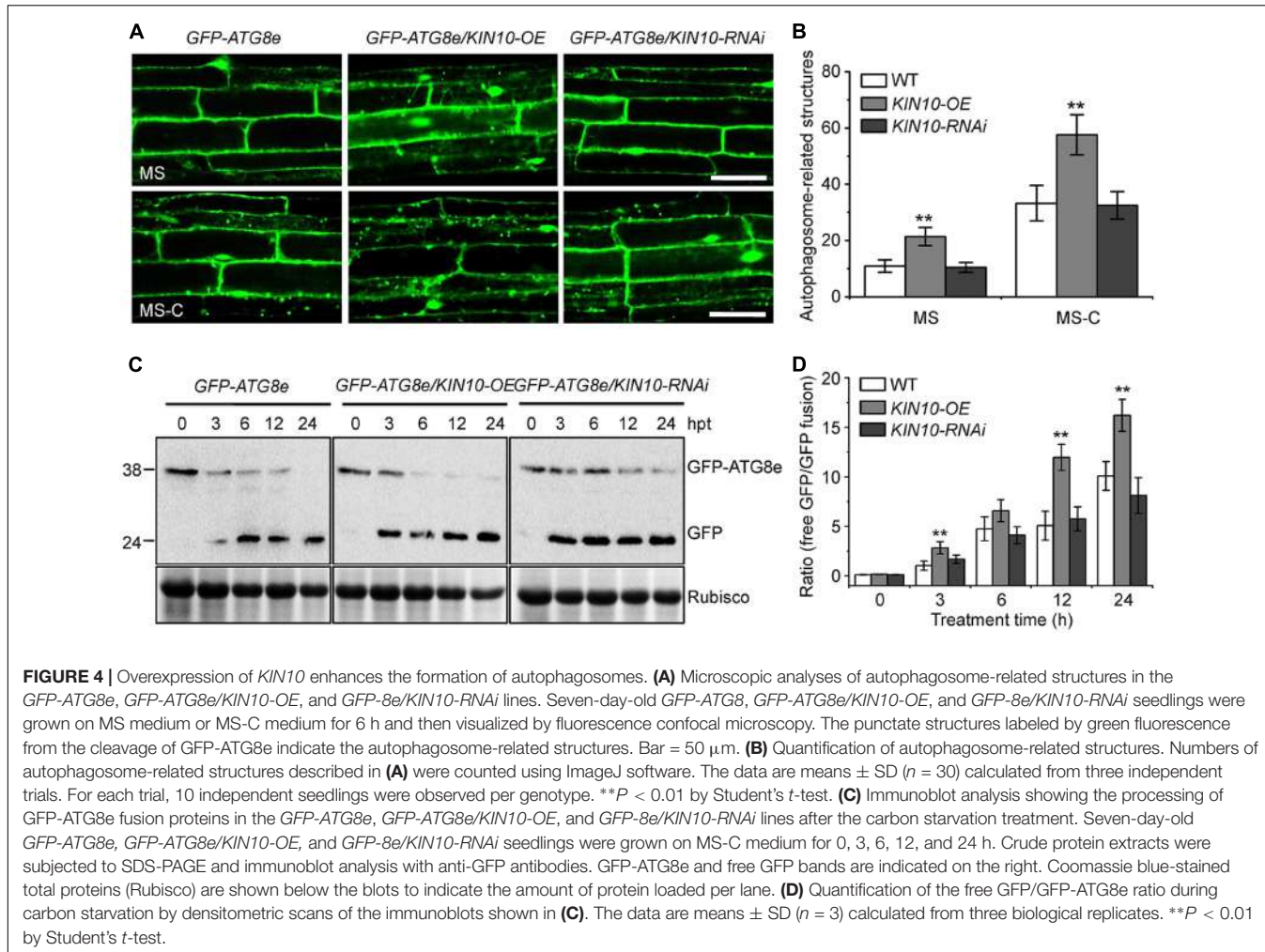
To examine the potential involvement of *KIN10* in regulating autophagosome formation, we first tested the abundance of ATG transcripts (*ATG2*, *ATG5*, *ATG7*, *ATG8a*, *ATG10*, and *ATG18a*) in the wild type, *KIN10*-OE lines (OE-1 and OE-2), and the *KIN10*-RNAi lines (RNAi-1 and RNAi-7). qRT-PCR analyses showed no significant changes in the expression levels of *ATG7*, *ATG10*, and *ATG18a* among the wild type, *KIN10*-OE lines, or the *KIN10*-RNAi lines, while the expression of *ATG2*, *ATG5*, and *ATG8a* was slightly upregulated in the *KIN10*-OE lines in comparison to the wild type (Supplementary Figure S2).

To further investigate the role of *KIN10* in the induction of autophagy, we examined autophagosome formation in the wild type, *KIN10*-OE and *KIN10*-RNAi lines using green fluorescent protein (GFP)-tagged ATG8e (Xiao et al., 2010). Seven-day-old GFP-ATG8e (wild-type background), GFP-ATG8e/*KIN10*-OE and GFP-ATG8e/*KIN10*-RNAi seedlings were transferred to solid MS medium (MS) or MS-C under darkness for 6 h, and the GFP fluorescence of root cells was subsequently observed using confocal microscopy. As shown in Figure 4, under both MS

and MS-C conditions, the numbers of GFP-ATG8e labeled punctate structures significantly increased in the *KIN10*-OE lines in comparison to the wild type and the *KIN10*-RNAi lines (Figures 4A,B). Upon nutrient starvation, the GFP-ATG8e fusion protein is degraded to release a free, relatively stable GFP, and the accumulation of GFP signals reflects the level of induction of autophagy (Li et al., 2014; Klionsky et al., 2016). As shown in Figure 4C, the degradation of the GFP-ATG8e fusion protein in the GFP-ATG8e/*KIN10*-OE line was faster than in the GFP-ATG8e or GFP-ATG8e/*KIN10*-RNAi line. Consistent with this, the ratio of free GFP to GFP-ATG8e in the GFP-ATG8e/*KIN10*-OE line was higher than that of in the GFP-ATG8e or GFP-ATG8e/*KIN10*-RNAi line (Figure 4D), suggesting that overexpression of *KIN10* enhances autophagic activity.

Overexpression of *KIN10* Enhances the Phosphorylation of ATG1 Proteins

Given that AMPK phosphorylates ULK1 to activate autophagy in mammalian cells (Egan et al., 2011; Kim et al., 2011), we hypothesized that *KIN10* may be involved in autophagy by



directly or indirectly phosphorylating ATG1. To confirm this, ATG1 phosphorylation was first tested using λ protein phosphatase and phosphatase inhibitor PhosSTOP in a yellow fluorescent protein (YFP)-tagged *ATG1a* transgenic plant (*YFP-ATG1a*) (Suttangkakul et al., 2011). As shown in Figure 5A, two species of YFP-ATG1a were detected using anti-GFP antibodies by western blot. Consistent with a previous study (Suttangkakul et al., 2011), the λ phosphatase treatment of total protein extracted from the *YFP-ATG1a* transgenic plant reduced the levels of the higher molecular weight species, while PhosSTOP blocked this shift (Figure 5A). To demonstrate the role of KIN10 in the regulation of ATG1, we crossed the *YFP-ATG1a* line to the *OE-1* line to generate the *YFP-ATG1a/KIN10-OE* lines. Immunoblot analysis showed that the level of YFP-ATG1a fusion protein was significantly higher in the *YFP-ATG1a KIN10-OE* line than in the *YFP-ATG1a* line (Figure 5B). Upon carbon starvation, the phosphorylation status of ATG1 was enhanced in the *YFP-ATG1a KIN10-OE* line in comparison to the *YFP-ATG1a* line (Figures 5B,C).

To determine whether the accumulation of YFP-ATG1a was caused by the higher transcription of *YFP-ATG1a* in the

YFP-ATG1a KIN10-OE line, we analyzed the total transcript level of *ATG1a* and *YFP-ATG1a* during carbon starvation by qRT-PCR. As shown in Supplementary Figure S3, the total transcript level of *ATG1a* was enhanced in the *YFP-ATG1a KIN10-OE* line but not in the *YFP-ATG1a* line, while the *YFP-ATG1a* transcript level did not change much in either line. Interestingly, the total expression of both *ATG1a* and *YFP-ATG1a* was slightly higher in the *YFP-ATG1a KIN10-OE* line than in the *YFP-ATG1a* line.

DISCUSSION

As a mammalian ortholog of yeast ATG1, ULK1 is phosphorylated by AMPK to activate autophagy or phosphorylated by TOR to repress autophagy (Kim et al., 2011; Shang and Wang, 2011). It has been proposed that AMPK can activate autophagy by directly phosphorylating ULK1 or by suppressing the activity of mTORC1, which thereby inhibits ULK1 activity by phosphorylation (Kim et al., 2011). In this study, we present several lines of evidence to support the hypothesis that KIN10 is involved in the regulation of autophagy in *Arabidopsis*. First, the overexpression of *KIN10* (*KIN10-OE*)

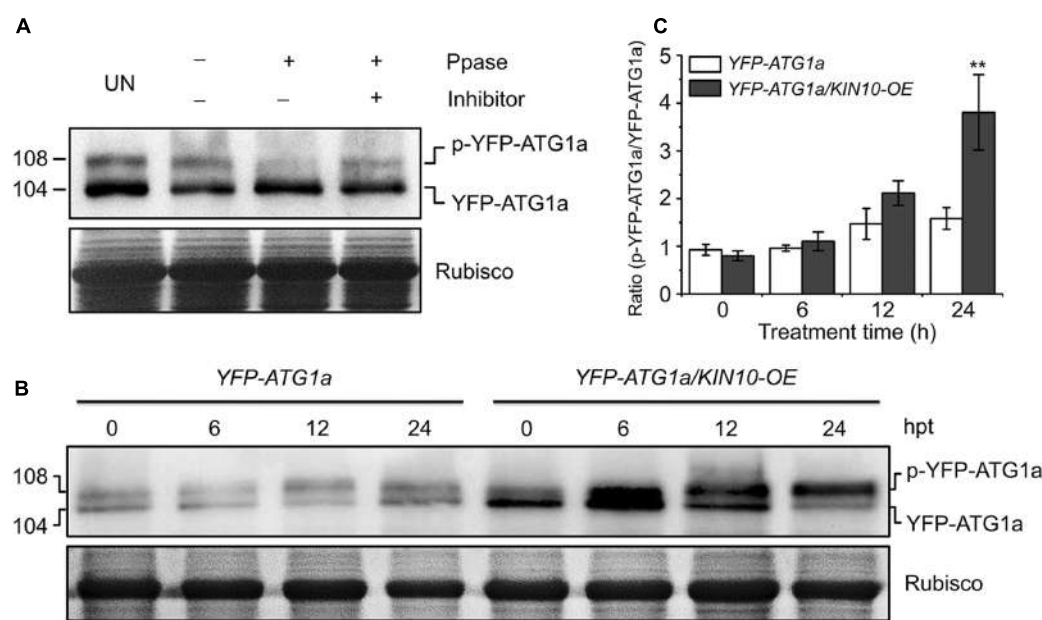


FIGURE 5 | Overexpression of *KIN10* increased the level of ATG1 phosphorylation. **(A)** Effect of λ protein phosphatase on the SDS-PAGE mobility of YFP-ATG1a. Proteins were extracted from 7-day-old YFP-ATG1a transgenic plants grown on MS medium. Extracts were treated for 1 h with λ phosphatase (Ppase) with or without the phosphatase inhibitor PhosSTOP and then subjected to immunoblot analysis with anti-GFP antibodies. UN, untreated extracts. **(B)** Immunoblot analysis of ATG1 phosphorylation in the YFP-ATG1a and YFP-ATG1a/*KIN10*-OE transgenic plants. Seven-day-old YFP-ATG1a and YFP-ATG1a/*KIN10*-OE transgenic plants were grown on MS-C medium for the indicated times prior to protein extraction. Crude extracts were subjected to SDS-PAGE and immunoblot analysis with anti-GFP antibodies. The p-YFP-ATG1a and YFP-ATG1a bands are indicated on the right. Coomassie blue-stained total proteins (Rubisco) are shown below the blots to indicate the amount of protein loaded per lane. **(C)** Quantification of the p-YFP-ATG1a/YFP-ATG1a ratio during carbon starvation by densitometric scans of the immunoblots shown in **(B)**. The data are means \pm SD ($n = 3$) calculated from three biological replicates. ** $P < 0.01$ by Student's *t*-test.

resulted in delayed leaf senescence and enhanced tolerance to nutrient deficiencies and abiotic stresses in *Arabidopsis* (Figures 1, 3). Second, the enhanced tolerance to nutrient starvation in the *KIN10*-OE lines is dependent on a functional autophagy pathway (Figure 2). Third, the expression of *ATGs* and autophagosome formation and degradation were enhanced in the *KIN10*-OE lines (Figure 4). Last, the phosphorylation of ATG1a was enhanced in the *KIN10*-OE lines in comparison to that of the wild type (Figure 5). Taken together, these results demonstrate that *KIN10* is a positive regulator of autophagy activation, possibly by enhancing the phosphorylation of ATG1, a mechanism that seems to be conserved in plants and animals.

KIN10 is an energy sensor in plants that has diverse functions in the regulation of plant metabolism, development, and stress responses (Polge and Thomas, 2007; Baena-González and Sheen, 2008; Jossier et al., 2009). *KIN10* may be essential for maintaining the cell's energy balance during nutrient starvations (Baena-González et al., 2007). For example, the overexpression of *KIN10* delays natural and nitrogen starvation-induced senescence, and the plants where *KIN10* and *KIN11* have been targeted by virus-induced gene silencing (*KIN11* is a functionally redundant homolog of *KIN10* in *Arabidopsis*) have an early senescence phenotype (Baena-González et al., 2007). Here, we investigated the autophagy-associated senescence phenotypes of the *KIN10*-OE and *KIN10*-RNAi lines and suggested that the phenotypes observed in the *KIN10*-OE lines were genetically

linked to the autophagy pathway. Though we observed significant phenotypic differences in the *KIN10*-OE lines compared to the wild type in response to the treatments, we did not observe significant differences in the autophagy-associated phenotypes, gene expression and autophagosome formation in the *KIN10*-RNAi lines after the treatments. It is not feasible to use the *kin10 kin11* virus-induced gene silencing lines in autophagy-related phenotypic analyses due to the severe growth inhibition of these silenced lines (Baena-González et al., 2007). It is still unknown whether *KIN11* plays a redundant role in the regulation of autophagy, and generation of transgenic lines with double knockdown of *KIN10* and *KIN11* expression will be useful for future investigation of the functions of *KIN10* and *KIN11* in autophagy induction.

Autophagy plays an important role in the plant's response to various stress conditions, such as oxidative stress (Xiong et al., 2007a,b), nutrient deficiency (Doelling et al., 2002), hypoxia (Chen et al., 2015), and pathogen infection (Liu et al., 2005; Wang et al., 2011). The autophagy-defective (*atg*) mutants, such as *atg2-1*, *atg5-1*, *atg7-1*, and *atg10-1*, are frequently used to study the role of autophagy in stress responses in plants. In contrast to the situation in animal systems, little is known about the effects of constitutive activation of autophagy in plants. TOR has been suggested to be a negative regulator of plant autophagy (Liu and Bassham, 2010). To circumvent the embryo lethal phenotype of *TOR* loss-of-function mutant,

RNA interference (RNAi) was used to reduce *TOR* transcript levels in the *RNAi-AtTOR* plants, which show constitutive autophagy (Liu and Bassham, 2010). Given the fundamental roles of TOR in plant growth and metabolism (Xiong and Sheen, 2014), it is difficult to distinguish whether the phenotype of the *RNAi-AtTOR* line is caused by increased autophagy or is due to the reduced expression of *TOR*. In comparison, we suggested that overexpression of *KIN10* enhances tolerance to nutrient deficiencies in *Arabidopsis* (Figure 1), and this enhanced tolerance was blocked by a deficiency in autophagy (Figure 2), which demonstrates that *KIN10* improves tolerance to nutrient starvations by directly activating the autophagy pathway. Moreover, we showed that the *KIN10-OE* lines were more tolerant to drought and submergence (Figure 3), indicating that *KIN10* is a potential candidate for genetic improvement of plant responses to nutrient deficiencies and water-related stresses. However, we cannot exclude the possibility that *KIN10* may indirectly regulate autophagy by inhibiting TOR, since the mammalian AMPK has been reported to regulate autophagy by negative modulation of mTORC1 (Kimura et al., 2003). Further investigations of the coordinated functions of *KIN10* and TOR will deepen our understanding of the upstream energy signals that regulate autophagy initiation in *Arabidopsis*.

The roles of AMPK in the regulation of autophagy have been extensively studied in animals (Gwinn et al., 2008; Lee et al., 2010; Kim et al., 2011; Alers et al., 2012; Mack et al., 2012), but the relationship between the plant AMPK and autophagy is still unknown. In our study, *KIN10* overexpression activate autophagy pathway (Figure 4). Y2H assays suggested that *KIN10* interacts with ATG1a and ATG13a *in vitro* (Supplementary Figure S4). However, we were unable to obtain further evidence of this interaction with BiFC and CoIP assays *in planta* (Supplementary Figure S5). We conclude that *KIN10* positively regulates autophagy pathway through a possible unknown mechanism bypass ATG1/ATG13 protein complex. Alternatively, the activation of autophagy pathway by *KIN10* overexpression may also be caused by inhibiting TOR activity, which is well-known to function as a negative regulator in autophagosome formation (Liu and Bassham, 2010). As suggested by Suttangkakul et al. (2011), the extent of ATG1a phosphorylation was highly regulated by the nutritional state through the action of upstream kinases and/or ATG1 autophosphorylation. Our results showed that, in response to starvation, overexpression of *KIN10* enhanced the phosphorylation of ATG1a (Figure 5) which supports the idea that autophagy may function downstream of the *KIN10* kinase by directly or indirectly targeting ATG1 proteins for phosphorylation. In conclusion, our findings demonstrated that *KIN10* is a positive regulator of autophagy in *Arabidopsis*.

AUTHOR CONTRIBUTIONS

SX and Q-FC designed the study. LC, Z-ZS, LH, F-NX, HQ, and L-JX carried out the experiments. SX, Q-FC, and LC analyzed the data. SX and LC wrote the manuscript.

FUNDING

This work was supported by the National Natural Science Foundation of China (Projects 31370298 and 31461143001), Program for New Century Excellent Talents in University (Project NCET-13-0614), the Foundation of Guangzhou Science and Technology Project (201504010021), and Sun Yat-sen University (Start-up fund to SX).

ACKNOWLEDGMENTS

We thank the ABRC for providing the T-DNA seed pools, J. Sheen (Harvard Medical School) for the *KIN10-OEs* and *KIN10-RNAi* lines, F.Q. Li (South China Agricultural University) for the *YFP-ATG1a* line, and M. L. Chye (University of Hong Kong) for the *GFP-ATG8e* line.

SUPPLEMENTARY MATERIAL

The Supplementary Material for this article can be found online at: <http://journal.frontiersin.org/article/10.3389/fpls.2017.01201/full#supplementary-material>

FIGURE S1 | Molecular identification of the *KIN10-OE* and *KIN10-RNAi* transgenic plants. **(A)** qRT-PCR analysis of *KIN10* transcript levels in 4-week-old wild type (WT), *OE-1*, *OE-2*, *RNAi-1*, and *RNAi-7* plants. Transcript levels relative to the wild type were normalized to the levels of *ACTIN2*. The data are means \pm SD ($n = 3$) calculated from three biological replicates. ** $P < 0.01$ by Student's *t*-test. **(B)** Immunoblot analysis of *KIN10* in 4-week-old WT, *OE-1*, *OE-2*, *RNAi-1*, and *RNAi-7* plants. Anti-*KIN10* antibodies were used for immunoblotting. Coomassie blue-stained total proteins (Rubisco) are shown below the blot to indicate the amount of protein loaded per lane.

FIGURE S2 | Overexpression of *KIN10* activates autophagy-related gene expression. Expression patterns of ATGs in the WT, *OE-1*, *OE-2*, *RNAi-1*, and *RNAi-7* plants. Total RNA was isolated from 4-week-old WT, *OE-1*, *OE-2*, *RNAi-1*, and *RNAi-7* plants under normal growth conditions. Transcript levels relative to the WT were normalized to that of *ACTIN2*. The data are means \pm SD ($n = 3$) calculated from three biological replicates. ** $P < 0.01$ by Student's *t*-test.

FIGURE S3 | ATG1a transcript levels in the *YFP-ATG1a* and *YFP-ATG1a/KIN10-OE* plants in response to carbon starvation. Total RNA was isolated from 7-day-old *YFP-ATG1a* and *YFP-ATG1a/KIN10-OE* transgenic plants grown on MS medium followed by carbon starvation for 0, 3, 6, 12, and 24 h. Transcript levels relative to *YFP-ATG1a* at 0 h were normalized to that of *ACTIN2*. The data are means \pm SD ($n = 3$) calculated from three biological replicates. ** $P < 0.01$ by Student's *t*-test. Light gray bars indicate gene expression in the *YFP-ATG1a*, dark gray bars indicate gene expression in the *YFP-ATG1a/KIN10-OE*.

FIGURE S4 | Yeast two-hybrid assays showing the physical interactions of *KIN10* with autophagy-related proteins (ATGs). **(A)** Y2H assay of the interaction between *KIN10* and ATG proteins (ATG1a, ATG1b, ATG1c, ATG6, ATG8e, ATG9, PI3K, ATG13a, and ATG13b). ATG1a, ATG1b, ATG1c, ATG6, ATG8e, ATG9, PI3K, ATG13a, and ATG13b bait constructs were fused to the DNA-binding domain (BD), and full-length *KIN10* was fused to the activation domain (AD). Vectors containing the AD and BD were co-expressed in yeast strain YH109. Protein interactions were determined by a growth assay in a medium lacking Trp, Leu, His, and Ade, with 30 mM 3-amino-1,2,4-triazole which was added to repress self-activation. The vector containing the AD or BD alone served as the negative control. **(B)** Y2H assay of the interaction between the functional domains of *KIN10* and ATG1a and ATG13a. ATG1a and ATG13a bait constructs were fused to the BD, and prey constructs were fused to the AD. The vector containing the BD alone served as the negative control. Full-length *KIN10* contained a protein kinase

domain (CD), a ubiquitin-associated domain (UBA) and a kinase associated domain 1 (KA1). Protein interaction was determined by a growth assay in a medium lacking Trp, Leu, His, and Ade (SD-Trp-Leu-His-Ade) supplemented with 30 mM 3-amino-1,2,4-triazole.

FIGURE S5 | *In vivo* assays showing no interaction of KIN10 with ATG1a and ATG13a. **(A)** CoIP assay of the association between KIN10 and ATG1a/ATG13a. FLAG-tagged ATG1a/ATG13a and HA-tagged KIN10 (KIN10-HA) was transiently

expressed in protoplasts from wild-type *Arabidopsis* and immunoprecipitated by FLAG affinity agarose beads. **(B)** BiFC assay of KIN10 interaction with ATG1a and ATG13a in *Arabidopsis* protoplast cells. **(C)** BiFC assay of the interaction between functional domains of KIN10 and ATG1a/ATG13a in *Arabidopsis* protoplast cells. The split nYFP and cYFP fused to KIN10 and ATG1a/ATG13 were coexpressed in leaf protoplasts. nYFP/cYFP and ATG6-nYFP/TRAF1a-cYFP vectors were similarly co-expressed as negative and positive controls. Confocal images obtained from YFP, auto-fluorescent chlorophyll, and bright-field are shown. Bars = 20 μ m.

REFERENCES

- Alers, S., Löffler, A. S., Wesselborg, S., and Stork, B. (2012). Role of AMPK-mTOR-Ulk1/2 in the regulation of autophagy: cross talk, shortcuts, and feedbacks. *Mol. Cell Biol.* 32, 2–11. doi: 10.1128/MCB.06159-11
- Baena-González, E., Rolland, F., Thevelein, J. M., and Sheen, J. (2007). A central integrator of transcription networks in plant stress and energy signalling. *Nature* 448, 938–942. doi: 10.1038/nature06069
- Baena-González, E., and Sheen, J. (2008). Convergent energy and stress signaling. *Trends Plant Sci.* 13, 474–482. doi: 10.1016/j.tplants.2008.06.006
- Chen, L., Liao, B., Qi, H., Xie, L. J., Huang, L., Tan, W. J., et al. (2015). Autophagy contributes to regulation of the hypoxia response during submergence in *Arabidopsis thaliana*. *Autophagy* 11, 2233–2246. doi: 10.1080/15548627.2015.1112483
- Doelling, J. H., Walker, J. M., Friedman, E. M., Thompson, A. R., and Vierstra, R. D. (2002). The APG8/12-activating enzyme APG7 is required for proper nutrient recycling and senescence in *Arabidopsis thaliana*. *J. Biol. Chem.* 277, 33105–33114. doi: 10.1074/jbc.M204630200
- Egan, D. F., Shackelford, D. B., Mihaylova, M. M., Gelino, S., Kohnz, R. A., Mair, W., et al. (2011). Phosphorylation of ULK1 (hATG1) by AMP-activated protein kinase connects energy sensing to mitophagy. *Science* 331, 456–461. doi: 10.1126/science.1196371
- Emanuelle, S., Hossain, M. I., Moller, I. E., Pedersen, H. L., van de Meene, A. M., Doblin, M. S., et al. (2015). SnRK1 from *Arabidopsis thaliana* is an atypical AMPK. *Plant J.* 82, 183–192. doi: 10.1111/tpj.12813
- Gwinn, D. M., Shackelford, D. B., Egan, D. F., Mihaylova, M. M., Mery, A., Vasquez, D. S., et al. (2008). AMPK phosphorylation of raptor mediates a metabolic checkpoint. *Mol. Cell* 30, 214–226. doi: 10.1016/j.molcel.2008.03.003
- Han, S., Yu, B., Wang, Y., and Liu, Y. (2011). Role of plant autophagy in stress response. *Protein Cell* 2, 784–791. doi: 10.1007/s13238-011-1104-4
- Jossier, M., Bouly, J. P., Meimoun, P., Arjmand, A., Lessard, P., Hawley, S., et al. (2009). SnRK1 (SNF1-related kinase 1) has a central role in sugar and ABA signalling in *Arabidopsis thaliana*. *Plant J.* 59, 316–328. doi: 10.1111/j.1365-313X.2009.03871.x
- Kim, J., Kundu, M., Viollet, B., and Guan, K. L. (2011). AMPK and mTOR regulate autophagy through direct phosphorylation of Ulk1. *Nat. Cell Biol.* 13, 132–141. doi: 10.1038/ncb2152
- Kimura, N., Tokunaga, C., Dalal, S., Richardson, C., Yoshino, K., Hara, K., et al. (2003). A possible linkage between AMP-activated protein kinase (AMPK) and mammalian target of rapamycin (mTOR) signalling pathway. *Genes Cells* 8, 65–79. doi: 10.1046/j.1365-2443.2003.00615.x
- Klionsky, D. J. (2007). Autophagy: from phenomenology to molecular understanding in less than a decade. *Nat. Rev. Mol. Cell Biol.* 8, 931–937. doi: 10.1038/nrm2245
- Klionsky, D. J., Abdelmohsen, K., Abe, A., Abedin, M. J., Abeliovich, H., Acevedo Arozena, A., et al. (2016). Guidelines for the use and interpretation of assays for monitoring autophagy (3rd edition). *Autophagy* 12, 1–222. doi: 10.1080/15548627.2015.1100356
- Kroemer, G., Mariño, G., and Levine, B. (2010). Autophagy and the integrated stress response. *Mol. Cell* 40, 280–293. doi: 10.1016/j.molcel.2010.09.023
- Lai, Z., Wang, F., Zheng, Z., Fan, B., and Chen, Z. (2011). A critical role of autophagy in plant resistance to necrotrophic fungal pathogens. *Plant J.* 66, 953–968. doi: 10.1111/j.1365-313X.2011.04553.x
- Lee, J. W., Park, S., Takahashi, Y., and Wang, H. G. (2010). The association of AMPK with ULK1 regulates autophagy. *PLoS ONE* 5:e15394. doi: 10.1371/journal.pone.0015394
- Li, F., Chung, T., and Vierstra, R. D. (2014). AUTOPHAGY-RELATED11 plays a critical role in general autophagy- and senescence-induced mitophagy in *Arabidopsis*. *Plant Cell* 26, 788–807. doi: 10.1105/tpc.113.120014
- Li, F., and Vierstra, R. D. (2012). Autophagy: a multifaceted intracellular system for bulk and selective recycling. *Trends Plant Sci.* 17, 526–537. doi: 10.1016/j.tplants.2012.05.006
- Liu, C. C., Lin, Y. C., Chen, Y. H., Chen, C. M., Pang, L. Y., Chen, H. A., et al. (2016). Cul3-KLHL20 ubiquitin ligase governs the turnover of ULK1 and VPS34 complexes to control autophagy termination. *Mol. Cell* 61, 84–97. doi: 10.1016/j.molcel.2015.11.001
- Liu, Y., and Bassham, D. C. (2010). TOR is a negative regulator of autophagy in *Arabidopsis thaliana*. *PLoS ONE* 5:e11883. doi: 10.1371/journal.pone.0011883
- Liu, Y., Schiff, M., Czymbek, K., Tallóczy, Z., Levine, B., and Dinesh-Kumar, S. P. (2005). Autophagy regulates programmed cell death during the plant innate immune response. *Cell* 121, 567–577. doi: 10.1016/j.cell.2005.03.007
- Liu, Y., Xiong, Y., and Bassham, D. C. (2009). Autophagy is required for tolerance of drought and salt stress in plants. *Autophagy* 5, 954–963. doi: 10.4161/auto.5.79290
- Löffler, A. S., Alers, S., Dieterle, A. M., Keppler, H., Franz-Wachtel, M., Kundu, M., et al. (2011). Ulk1-mediated phosphorylation of AMPK constitutes a negative regulatory feedback loop. *Autophagy* 7, 696–706. doi: 10.4161/auto.7.7.15451
- Mack, H. I., Zheng, B., Asara, J. M., and Thomas, S. M. (2012). AMPK-dependent phosphorylation of ULK1 regulates ATG9 localization. *Autophagy* 8, 1197–1214. doi: 10.4161/auto.20586
- Mizushima, N. (2010). The role of the Atg1/ULK1 complex in autophagy regulation. *Curr. Opin. Cell Biol.* 22, 132–139. doi: 10.1016/j.cel.2009.12.004
- Polge, C., and Thomas, M. (2007). SNF1/AMPK/SnRK1 kinases, global regulators at the heart of energy control? *Trends Plant Sci.* 12, 20–28. doi: 10.1016/j.tplants.2006.11.005
- Shang, L., and Wang, X. (2011). AMPK and mTOR coordinate the regulation of Ulk1 and mammalian autophagy initiation. *Autophagy* 7, 924–926. doi: 10.4161/auto.7.8.15860
- Suttangkakul, A., Li, F., Chung, T., and Vierstra, R. D. (2011). The ATG1/ATG13 protein kinase complex is both a regulator and a target of autophagic recycling in *Arabidopsis*. *Plant Cell* 23, 3761–3779. doi: 10.1105/tpc.111.090993
- Thompson, A. R., Doelling, J. H., Suttangkakul, A., and Vierstra, R. D. (2005). Autophagic nutrient recycling in *Arabidopsis* directed by the ATG8 and ATG12 conjugation pathways. *Plant Physiol.* 138, 2097–2110. doi: 10.1104/pp.105.060673
- Wang, Y., Nishimura, M. T., Zhao, T., and Tang, D. (2011). ATG2, an autophagy-related protein, negatively affects powdery mildew resistance and mildew-induced cell death in *Arabidopsis*. *Plant J.* 68, 74–87. doi: 10.1111/j.1365-313X.2011.04669.x
- Wirth, M., Joachim, J., and Tooze, S. A. (2013). Autophagosome formation—the role of ULK1 and Beclin1-PI3KC3 complexes in setting the stage. *Semin. Cancer Biol.* 23, 301–309. doi: 10.1016/j.semcaner.2013.05.007
- Wong, P. M., Puente, C., Ganley, I. G., and Jiang, X. (2013). The ULK1 complex: sensing nutrient signals for autophagy activation. *Autophagy* 9, 124–137. doi: 10.4161/auto.23323
- Xiao, S., Gao, W., Chen, Q. F., Chan, S. W., Zheng, S. X., Ma, J., et al. (2010). Overexpression of *Arabidopsis* acyl-CoA binding protein ACBP3

- promotes starvation-induced and age-dependent leaf senescence. *Plant Cell* 22, 1463–1482. doi: 10.1105/tpc.110.075333
- Xiong, Y., Contento, A. L., and Bassham, D. C. (2007a). Disruption of autophagy results in constitutive oxidative stress in *Arabidopsis*. *Autophagy* 3, 257–258. doi: 10.4161/auto.3847
- Xiong, Y., Contento, A. L., Nguyen, P. Q., and Bassham, D. C. (2007b). Degradation of oxidized proteins by autophagy during oxidative stress in *Arabidopsis*. *Plant Physiol.* 143, 291–299. doi: 10.1104/pp.106.092106
- Xiong, Y., and Sheen, J. (2014). The role of target of rapamycin signaling networks in plant growth and metabolism. *Plant Physiol.* 164, 499–512. doi: 10.1104/pp.113.229948

Conflict of Interest Statement: The authors declare that the research was conducted in the absence of any commercial or financial relationships that could be construed as a potential conflict of interest.

Copyright © 2017 Chen, Su, Huang, Xia, Qi, Xie, Xiao and Chen. This is an open-access article distributed under the terms of the Creative Commons Attribution License (CC BY). The use, distribution or reproduction in other forums is permitted, provided the original author(s) or licensor are credited and that the original publication in this journal is cited, in accordance with accepted academic practice. No use, distribution or reproduction is permitted which does not comply with these terms.



TOR-Dependent and -Independent Pathways Regulate Autophagy in *Arabidopsis thaliana*

Yunting Pu^{1,2}, Xinjuan Luo^{1,3} and Diane C. Bassham^{1,2,4*}

¹ Department of Genetics, Development and Cell Biology, Iowa State University, Ames, IA, United States, ² Interdepartmental Genetics Program, Iowa State University, Ames, IA, United States, ³ College of Life Sciences, Northwest A&F University, Yangling, China, ⁴ Plant Sciences Institute, Iowa State University, Ames, IA, United States

OPEN ACCESS

Edited by:

Yule Liu,
Tsinghua University, China

Reviewed by:

Shi Xiao,
Sun Yat-sen University, China
Liwen Jiang,
The Chinese University of Hong Kong,
Hong Kong

*Correspondence:

Diane C. Bassham
bassham@iastate.edu

Specialty section:

This article was submitted to
Plant Cell Biology,
a section of the journal
Frontiers in Plant Science

Received: 08 April 2017

Accepted: 26 June 2017

Published: 11 July 2017

Citation:

Pu Y, Luo X and Bassham DC (2017)
TOR-Dependent and -Independent
Pathways Regulate Autophagy
in *Arabidopsis thaliana*.
Front. Plant Sci. 8:1204.
doi: 10.3389/fpls.2017.01204

Autophagy is a critical process for recycling of cytoplasmic materials during environmental stress, senescence and cellular remodeling. It is upregulated under a wide range of abiotic stress conditions and is important for stress tolerance. Autophagy is repressed by the protein kinase target of rapamycin (TOR), which is activated in response to nutrients and in turn upregulates cell growth and translation and inhibits autophagy. Down-regulation of TOR in *Arabidopsis thaliana* leads to constitutive autophagy and to decreased growth, but the relationship to stress conditions is unclear. Here, we assess the extent to which TOR controls autophagy activation by abiotic stress. Overexpression of TOR inhibited autophagy activation by nutrient starvation, salt and osmotic stress, indicating that activation of autophagy under these conditions requires down-regulation of TOR activity. In contrast, TOR overexpression had no effect on autophagy induced by oxidative stress or ER stress, suggesting that activation of autophagy by these conditions is independent of TOR function. The plant hormone auxin has been shown previously to up-regulate TOR activity. To confirm the existence of two pathways for activation of autophagy, dependent on the stress conditions, auxin was added exogenously to activate TOR, and the effect on autophagy under different conditions was assessed. Consistent with the effect of TOR overexpression, the addition of the auxin NAA inhibited autophagy during nutrient deficiency, salt and osmotic stress, but not during oxidative or ER stress. NAA treatment was unable to block autophagy induced by a TOR inhibitor or by a mutation in the TOR complex component RAPTOR1B, indicating that auxin is upstream of TOR in the regulation of autophagy. We conclude that repression of auxin-regulated TOR activity is required for autophagy activation in response to a subset of abiotic stress conditions.

Keywords: autophagy, TOR signaling, stress responses, auxin, *Arabidopsis*

INTRODUCTION

Plants have evolved many response mechanisms to adapt to various growth conditions, including abiotic stresses. One such mechanism is autophagy, a major pathway for degradation and recycling of cytoplasmic materials in all eukaryotes (Liu and Bassham, 2012; Yang and Bassham, 2015). Autophagy is active at a low basal level even under normal conditions, and numerous human diseases are linked to autophagy defects, including cancer and various neurodegenerative diseases

such as Parkinson's, Huntington's, and Alzheimer's diseases (Cai et al., 2016; Davidson and Vander Heiden, 2017). In plants, autophagy functions in the response to both abiotic and biotic stress, and is induced during senescence and nutrient deficiency (Doelling et al., 2002; Hanaoka et al., 2002), salt and drought stresses (Liu et al., 2009), oxidative stress (Xiong et al., 2007b), endoplasmic reticulum (ER) stress (Liu et al., 2012), and pathogen infection (Liu et al., 2005).

When autophagy is activated, a double-membrane cup-shaped structure named a phagophore is formed. The phagophore expands to form a double-membrane vesicle called an autophagosome, while engulfing cellular components to be degraded. Autophagosomes are delivered to and fuse with lysosomes in mammalian cells or the vacuole in plant or yeast cells, where the cargo is degraded into small molecules by vacuolar hydrolases and recycled (Yang and Bassham, 2015). Studies in yeast have identified more than 30 autophagy-related (ATG) genes, many of which have also been found in plants (Tsukada and Ohsumi, 1993; Yang and Bassham, 2015). A key protein involved in autophagosome formation is ATG8, which can be used as a marker for autophagosomes when fused with a fluorescent protein (Yoshimoto et al., 2004; Contento et al., 2005). ATG8 is attached to the autophagosome membrane through a covalent bond to phosphatidylethanolamine (PE) via two ubiquitin-like conjugation systems that include the E1-like activating enzyme ATG7 (Ichimura et al., 2000). Knockout of ATG7 therefore prevents autophagosome formation, leading to plants being hypersensitive to both abiotic and biotic stress conditions (Doelling et al., 2002; Lenz et al., 2011; Zhou et al., 2013).

The target of rapamycin (TOR) complex is a key regulator of autophagy, and is composed of TOR itself and two binding partners, regulatory-associated protein of TOR (RAPTOR), and Lethal with Sec Thirteen 8 (LST8) (Yang et al., 2013; Dobrenel et al., 2016). TOR is a Ser/Thr protein kinase in the phosphatidylinositol-3-kinase (PI3K) – related kinase (PIKK) family (Noda and Ohsumi, 1998; Menand et al., 2002), whereas RAPTOR recruits substrates to the complex for phosphorylation by TOR (Hara et al., 2002), and LST8 stabilizes the complex (Yang et al., 2013). The TOR signaling pathway both positively regulates cell growth and metabolism and negatively regulates autophagy in yeast, mammals, and plants (Dobrenel et al., 2016). In *Arabidopsis thaliana*, a null mutation in TOR is embryo lethal (Menand et al., 2002), whereas decreased TOR expression due to RNA interference leads to autophagy induction (Liu and Bassham, 2010), and arrested plant growth and development (Deprost et al., 2007). Active-site TOR inhibitors (asTORIs) that disrupt TOR activity by competition for ATP-binding also result in plant growth defects (Montane and Menand, 2013). Consistent with this, overexpression of TOR enhances growth and osmotic stress resistance (Deprost et al., 2007; Ren et al., 2011).

Two RAPTOR genes exist in Arabidopsis, RAPTOR1A and RAPTOR1B (Anderson et al., 2005; Deprost et al., 2005). A *raptor1b* null mutant has growth defects, including delayed leaf initiation and growth, late bolting and flowering, and short roots, while *raptor1a* knock out mutants have no major developmental phenotypes, possibly due to the higher expression of RAPTOR1B

in most plant tissues (Anderson et al., 2005; Deprost et al., 2005). A *raptor1a raptor1b* double knockout mutant has minimal meristem growth, indicating that RAPTOR1A and RAPTOR1B might have some distinct functions, but is not embryo-lethal, and TOR must therefore retain some of its function in the absence of RAPTOR (Anderson et al., 2005). Two *LST8* genes have also been identified in Arabidopsis, *LST8-1* and *LST8-2*, although only *LST8-1* appears to be expressed (Moreau et al., 2012). The null mutant *lst8-1* has strong growth defects and impaired adaptation to long day conditions (Moreau et al., 2012). Mutation of *lst8-1* or *raptor1b*, or disruption of TOR activity with asTORIs, causes hypersensitivity to abscisic acid (ABA) and decreased ABA synthesis (Kravchenko et al., 2015), indicating that the TOR complex may also play a role in hormone signaling.

Target of rapamycin signals through phosphorylation of downstream substrates (Raught et al., 2001; Ren et al., 2011). Several TOR substrates have been identified in Arabidopsis, including the p70 ribosomal protein S6 kinase (S6K) (Mahfouz et al., 2006; Xiong and Sheen, 2012), the E2Fa transcription factor, which activates cell cycle genes (Xiong et al., 2013; Li et al., 2017), and TAP46, a regulatory subunit of protein phosphatase type 2A (PP2A), which was suggested to regulate plant growth and autophagy (Yorimitsu et al., 2009; Ahn et al., 2011). Arabidopsis has two S6K paralogs with 87% sequence identity, S6K1 and S6K2, both of which are phosphorylated by TOR. The activity of plant S6Ks increases in response to auxin and cytokinins (Turck et al., 2004).

Upstream regulation of TOR signaling in plants is still poorly understood. Auxin can enhance TOR activity to promote the translation reinitiation of mRNAs via S6K1, and deficiency in TOR signaling impaired auxin-mediated root gravitropism (Schepetilnikov et al., 2013). Auxin regulation is mediated by the small GTPase ROP2, which directly binds to and activates TOR (Li et al., 2017; Schepetilnikov et al., 2017). These studies indicate that auxin might regulate plant growth, development and stress responses through the TOR signaling pathway. In this study, we first confirm that the TOR complex is a negative regulator of autophagy in Arabidopsis, and demonstrate a role for RAPTOR1B in this regulation. We show that TOR regulates autophagy induced by nutrient starvation, salt or osmotic stress, but not oxidative or ER stress, indicating that TOR-dependent and -independent pathways for regulation of autophagy exist in plants. In addition, exogenous auxin has similar effects on stress-induced autophagy as TOR overexpression, suggesting a mechanism by which auxin interfaces with stress responses in plants through regulation of TOR activity.

MATERIALS AND METHODS

Plant Materials and Growth Conditions

Arabidopsis thaliana seeds of WT (Col-0) or other indicated genotypes were sterilized with 33% (v/v) bleach and 0.1% (v/v) Triton X-100 (Sigma) for 20 min, followed by five washes of 5 min each with sterile water. Sterilized seeds were stored at 4°C in darkness for at least 2 days to allow stratification before plating on solid 1/2 MS medium (2.22 g/L Murashige-Skoog vitamin and

salt mixture [Caisson Laboratory, MSP09], 1% [w/v] sucrose, 0.6% [w/v] Phytoblend agar [Caisson Laboratory], 2.4 mM 2-morpholinolino-ethanesulfonic acid [MES, Sigma], pH 5.7). Seedlings were grown under long-day conditions (16 h light) at 22°C for 7 days. Plants for transient expression in leaf protoplasts were grown in soil in a humidity-controlled growth chamber with 50% humidity at 20–23°C under long-day conditions for 4–6 weeks. T-DNA insertion mutants used in this study are: *raptor1a* (SALK_043920c), *raptor1b* (SALK_078159) (Anderson et al., 2005), S7817 (SALK_147817), G166 (GABI_166C06), G548 (GABI_548G07) (Deprost et al., 2007), and *atg7* (GABI_655B06) (Chung et al., 2010). Transgenic plants used in this study are: GFP-ATG8e (Xiong et al., 2007b), TOR-OE1 and TOR-OE2 (Ren et al., 2011).

Stress and Drug Treatments

For sucrose and nitrogen starvation, 7-day-old seedlings grown on solid 1/2 MS medium were transferred to solid 1/2 MS medium lacking sucrose or nitrogen for an additional 3 days (Doelling et al., 2002). Sucrose starvation plates were kept in the dark after transfer. For salt and mannitol treatment, 7-day-old seedlings grown on solid 1/2 MS medium were transferred to liquid 1/2 MS medium with 0.16 M NaCl or 0.35 M mannitol for 6–8 h. For oxidative and ER stress, 7-day-old seedlings grown on solid 1/2 MS medium were transferred to liquid 1/2 MS medium with 5 mM H₂O₂ (Sigma) for 2–3 h, or with 2 mM dithiothreitol (DTT, Fisher) or 5 µg/mL tunicamycin (Sigma) for 6–8 h. For AZD8055 treatment, 7-day-old seedlings grown on solid 1/2 MS medium were transferred to solid 1/2 MS medium with 2 µM AZD8055 (LC Laboratories) for 1 day, or liquid 1/2 MS medium with 1 µM AZD8055 for 2–3 h.

For auxin treatment, 7-day-old seedlings were transferred to solid 1/2 MS medium supplemented with 20 nM 1-naphthaleneacetic acid (NAA, Sigma-Aldrich, N0640) with or without starvation for an additional 3 days, or in liquid 1/2 MS medium with 20 nM NAA for 6–8 h with or without stress treatments as described above. For BTH treatment, 7-day-old seedlings were transferred to liquid 1/2 MS medium supplemented with 100 µM acibenzolar-S-methyl (BTH, Sigma-Aldrich, 32820) with or without 20 nM NAA for 8 h.

For concanamycin A treatment, 7-day-old GFP-ATG8e seedlings were transferred to liquid 1/2 MS medium with DMSO or 1 µM concanamycin A (Sigma) with or without other stress or drug treatments for 6–8 h.

Autophagy Detection by Fluorescence Microscopy

Arabidopsis seedling roots were stained with monodansylcadaverine (MDC) as described previously (Contento et al., 2005). MDC-stained seedlings were observed with a Zeiss Axio Imager.A2 upright microscope (Zeiss) equipped with Zeiss Axiocam BW/color digital cameras using a DAPI-specific filter at the Iowa State University Microscopy and Nanoimaging Facility. GFP-ATG8e transgenic seedlings were observed and photographed with the same microscope system with a GFP-specific filter. Cells within the root elongation zone

were photographed and the number of autophagosomes in each image was counted and averaged from at least 10 images per sample. Confocal microscopy images of autophagosomes in root cells and leaf protoplasts were taken using a Leica SP5 × MP confocal/multiphoton microscope system (Leica) with a 63x/1.4 oil immersion objective at the Iowa State University Roy J. Carver High Resolution Microscopy Facility (Pu and Bassham, 2016).

Transient Expression in Protoplasts

GFP-ATG8e was transiently expressed in Arabidopsis leaf protoplasts as previously described (Sheen, 2002; Liu et al., 2012). 25–30 µg of GFP-ATG8e plasmid DNA was introduced into protoplasts using 40% (w/v) polyethylene glycol (PEG, Sigma-Aldrich). Protoplasts were washed and incubated in W5 solution (154 mM NaCl, 125 mM CaCl₂, 5 mM KCl, 2 mM MES, pH 5.7). For starvation treatment, protoplasts were incubated in W5 solution without sucrose or with 0.5% (w/v) sucrose as control at room temperature in darkness for 2 days in total. For other stress treatments, protoplasts were incubated in W5 solution with treatments as described in the Stress and Auxin Treatment section. Protoplasts were observed by fluorescence microscopy (Nikon Eclipse E200) using a FITC filter, and protoplasts with more than three visible autophagosomes were counted as active for autophagy (Yang et al., 2016). A total of 100 protoplasts were observed per genotype for each condition, and the percentage of protoplasts with induced autophagy was calculated and averaged from three independent experimental replicates.

Generation of RAPTOR1B Construct

The RAPTOR1B cDNA sequence was divided into two fragments, and each fragment was amplified from Col-0 cDNA using CloneAmp HiFi PCR Premix (Takara). The 5' fragment of RAPTOR1B was amplified with forward primer 5'-CACCGAGCTCGAACATTGATGGCATTAGGAGACTTAATGGGT GTCTC-3' (inserted SacI restriction site underlined), and reverse primer 5'-GTCAAACCCAATATCAAGCAAGGTACCCA-3', digested with SacI and KpnI (within the RAPTOR1B cDNA sequence), and ligated into the pPZP212 binary vector (Hajdukiewicz et al., 1994; Li et al., 2009), which has a 35S promoter sequence at the 5' end and a MYC tag sequence at the 3' end of the insert. The 3' fragment was amplified with forward primer 5'-TG GGTACCTTGCTTGATATTGGGTTTGAC-3' and reverse primer 5'-CACCGTCGACTCTTGCTGCGAGTTGTCGTGGG TG-3' (inserted SalI restriction site underlined), digested with KpnI and SalI, and ligated into the pPZP212 vector containing the 5' fragment to complete the full sequence. The entire construct was confirmed by sequencing.

Accession Numbers

Sequence data from this article can be found in the Arabidopsis Genome Initiative under the following accession numbers: TOR, AT1G50030; RAPTOR1A, AT5G01770, RAPTOR1B, AT3G08850; ATG8e, AT2G45170; ATG7, AT5G45900.

RESULTS

Inhibition of TOR Signaling Leads to Constitutive Autophagy

We have shown previously that decreased TOR expression via RNA interference induces autophagy in *Arabidopsis*, suggesting that TOR is a negative regulator of autophagy in plants (Liu and Bassham, 2010). To confirm that autophagy is induced by inhibition of TOR kinase activity (Montane and Menand, 2013), we examined autophagy activity after application of the asTORis AZD8055 (Dong et al., 2015). WT and *atg7* seedlings, a previously characterized knockout mutant that is unable to form autophagosomes (Doelling et al., 2002), were grown under standard conditions for 7 days, followed by 1 μ M AZD8055 treatment in liquid $1/2$ MS medium for 2–3 h. Roots of seedlings were stained with monodansylcadaverine (MDC), an acidotropic dye that can stain autophagosomes (Biederick et al., 1995; Contento et al., 2005), and examined by fluorescence microscopy. Autophagosomes appear as rapidly moving fluorescent puncta, and the number of visible puncta in each image were counted for quantification. As expected, compared to the basal level of autophagy in the control, inhibition of TOR activity by AZD8055 led to a significant increase in the number of autophagosomes (Figure 1A), while no autophagosomes were detected in the *atg7* mutant. This confirmed that TOR negatively regulates autophagy in *Arabidopsis*, and that the kinase activity of TOR is critical for this regulation.

Previous studies have shown that down-regulation of TOR or its binding partners RAPTOR and LST8 leads to defects in plant growth and development (Anderson et al., 2005; Deprost et al., 2007; Moreau et al., 2012; Montane and Menand, 2013), suggesting that RAPTOR and LST8 are critical for TOR-regulated plant growth. To test whether inhibition of TOR complex activity by disruption of RAPTOR also induces autophagy, WT, *raptor1a* and *raptor1b* knockout mutant seedlings (Anderson et al., 2005) were grown on $1/2$ MS medium with sucrose for a week, and autophagy in root cells was examined by MDC staining followed by fluorescence microscopy (Figures 1B,C). Compared to the basal level of autophagy in WT seedlings, the number of autophagosomes in the *raptor1a* mutant appeared slightly higher, but this difference was not statistically significant, possibly due to the variability between seedlings. The *raptor1b* mutant had a significantly higher number of autophagosomes, suggesting that the *raptor1b* mutant has constitutive autophagy, and that RAPTOR1A and RAPTOR1B may not function equally in autophagy regulation.

To confirm that the *raptor1b* mutant has increased basal autophagy under standard conditions, the autophagosome marker GFP-ATG8e was expressed transiently in WT, *raptor1a* and *raptor1b* leaf protoplasts (Figure 1D). The GFP-ATG8e fusion protein has been used extensively as a specific marker of autophagosomes and autophagic bodies (Yoshimoto et al., 2004; Contento et al., 2005; Pu and Bassham, 2016), and active autophagy is defined as more than three visible autophagosomes in a protoplast (Yang et al., 2016). WT protoplasts maintain a basal level of autophagy with a low percentage with active

autophagy. Consistent with the MDC staining results, the percentage of *raptor1b* protoplasts with active autophagy was significantly higher than that of WT protoplasts (Figure 1E). However, *raptor1a* also had a significantly higher percentage of active autophagy in leaf protoplasts, although significantly lower than *raptor1b*. RAPTOR1A may therefore be more important for autophagy regulation in leaves than in roots.

To confirm that the constitutive autophagy in the *raptor1b* mutant is specifically due to the mutation in RAPTOR1B, the RAPTOR1B cDNA was transiently expressed under a 35S promoter together with GFP-ATG8e in *raptor1b* knock out mutant leaf protoplasts. Autophagy was assessed as described above using fluorescence microscopy (Figure 1F). Note that the number of autophagosomes in the *raptor1b* mutant is variable between experiments, depending most likely on the growth conditions and age of the plants, room temperature, etc. The percentage of protoplasts with active autophagy in the *raptor1b* mutant expressing the RAPTOR1B cDNA was substantially lower than for the mutant protoplasts alone, and was not significantly different from WT. This indicates that the increased basal autophagy observed in the *raptor1b* mutant was suppressed by expression of the RAPTOR1B cDNA, confirming that the constitutive autophagy phenotype is indeed due to the disruption of RAPTOR1B.

Overexpression of TOR Blocks Autophagy upon Starvation, Salt and Drought Stress

Previous studies and our data have shown that the TOR complex negatively regulates autophagy in *Arabidopsis* (Liu and Bassham, 2010) (Figure 1), but the conditions under which TOR is important in plants are unknown. In other organisms TOR is well-described as regulating autophagy in response to nutrients (Dobrenel et al., 2016), with a decrease in TOR activity during nutrient deficiency leading to activation of autophagy. We therefore hypothesized that overexpression of TOR might prevent activation of autophagy by nutrient deficiency, and that autophagy induction by other stresses might be TOR-independent. To test this hypothesis, we obtained several previously characterized *Arabidopsis* lines with T-DNA insertions in the TOR upstream region (S7817, G166, and G548) and two transgenic lines with TOR expressed from a 35S promotor (*TOR-OE1* and *TOR-OE2*). All lines have overexpression of TOR and enhanced growth (Deprost et al., 2007; Ren et al., 2011), with the exception of S7817, which has decreased TOR expression in leaves and overexpression of TOR in roots (Deprost et al., 2007). Seeds of WT and the five TOR overexpression lines were germinated and grown on solid $1/2$ MS medium plus sucrose for 1 week, followed by transfer to solid $1/2$ MS medium plus or minus nitrogen in the light, or minus sucrose in the dark for an additional 3 days. Autophagosomes were detected by MDC staining followed by fluorescence microscopy (Figures 2A,B). Representative images of one of the TOR overexpression lines are shown in Figure 2A. Quantification of autophagosomes indicated that both WT and the TOR overexpression lines had a low basal level of autophagy under

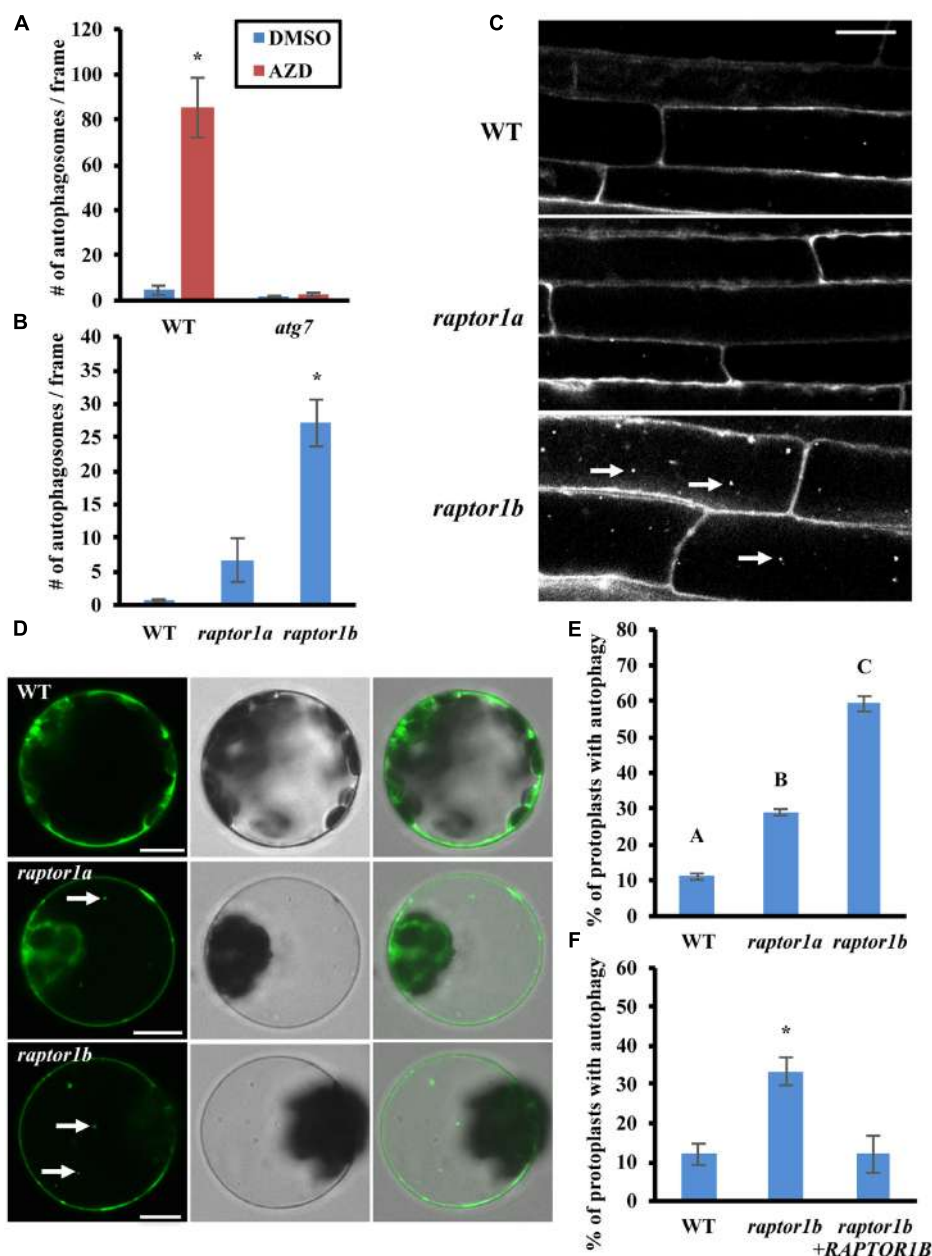


FIGURE 1 | Inhibition of TOR or RAPTOR leads to constitutive autophagy. **(A)** The TOR inhibitor AZD8055 induces autophagy. 7-day-old WT (Col-0) and *atg7* mutant seedlings were treated with DMSO or AZD8055 (AZD) for 2–3 h, stained with MDC and then observed and imaged by fluorescence microscopy. The number of puncta in each image was counted and averaged from at least 10 images per genotype for each condition. **(B,C)** Autophagy is induced in *raptor1b* mutant root cells under standard growth conditions. **(B)** 7-day-old WT, *raptor1a* and *raptor1b* knockout mutant seedlings were stained with MDC and observed by fluorescence microscopy. The number of puncta in each image was quantified as in **(A)**. **(C)** Representative confocal images of MDC-stained WT, *raptor1a* and *raptor1b* mutant seedlings. MDC-stained autophagosomes appear as white puncta within cells as indicated by white arrows. Scale bar = 20 μ m. **(D,E)** Leaf protoplasts of *raptor1a* and *raptor1b* mutants have constitutive autophagy. **(D)** Transient expression of a GFP-ATG8e fusion protein in leaf protoplasts of WT and RAPTOR mutants, observed by confocal microscopy. GFP-tagged autophagosomes appear as green puncta within leaf protoplasts in the left column as indicated by white arrows. The middle and right columns show DIC and merged images respectively. Scale bar = 10 μ m. **(E)** Quantification of **(D)**. Protoplasts were observed using epifluorescence microscopy. The percentage of protoplasts with more than three visible GFP-tagged autophagosomes was calculated, with 100 protoplasts observed per genotype for each condition. **(F)** Expression of the *RAPTOR1B* cDNA complements the *raptor1b* constitutive autophagy phenotype. A GFP-ATG8e fusion protein was transiently expressed in *raptor1b* mutant leaf protoplasts with or without full-length *RAPTOR1B*, expressed from a 35S constitutive promoter, or in WT protoplasts as a control. Protoplasts were observed using epifluorescence microscopy. The percentage of protoplasts with more than three visible GFP-tagged autophagosomes was quantified as in **(E)**. For all graphs, error bars indicate means \pm standard error (SE) from three independent replicates. Asterisks or different letters indicate statistically significant differences ($P < 0.05$) using Student's *t*-test compared with WT under control conditions.

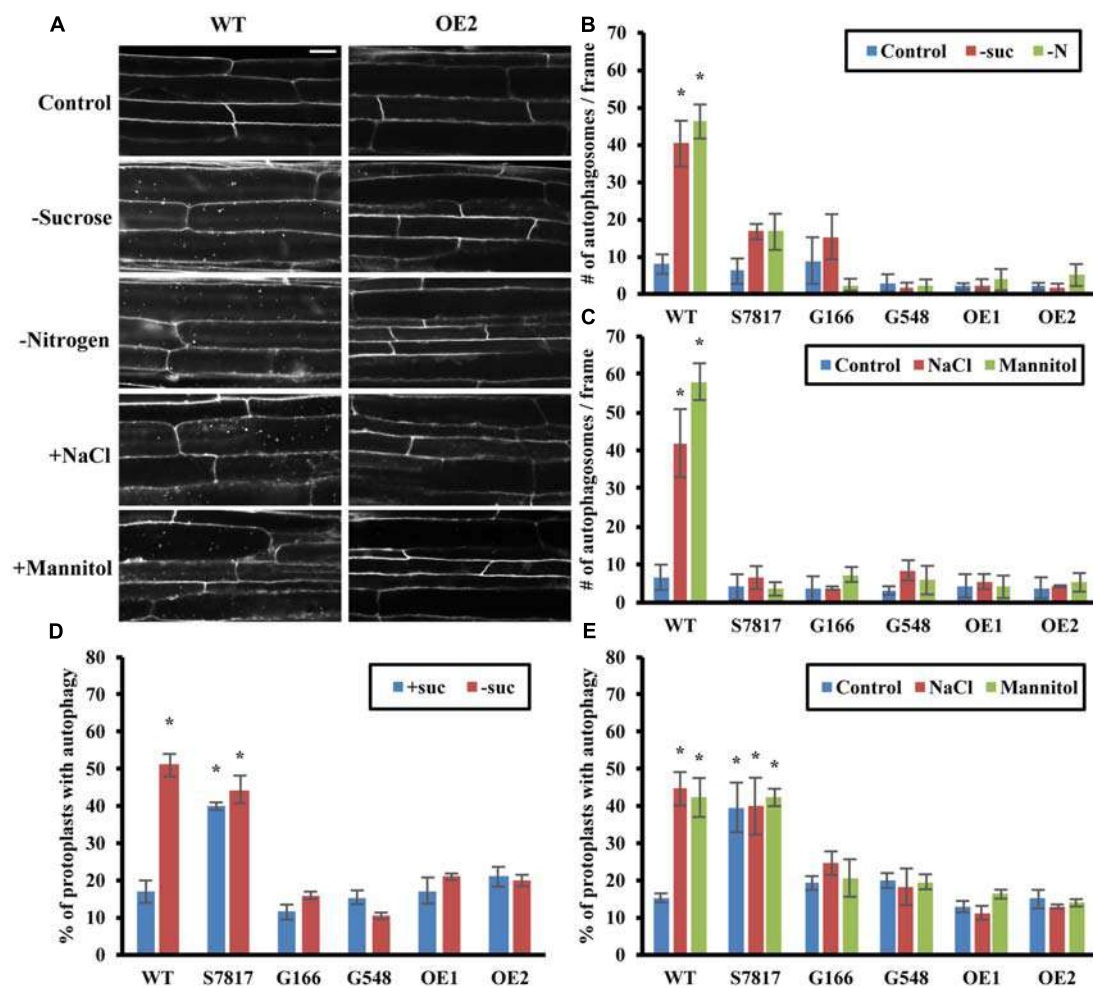


FIGURE 2 | Overexpression of TOR blocks autophagy induced by nutrient starvation, salt and osmotic stresses. **(A)** Representative confocal images of MDC-stained WT and *TOR*-OE2 seedlings after the indicated stress treatment. For nutrient starvation, 7-day-old seedlings of WT and *TOR*-OE2 transgenic lines were transferred to solid 1/2 MS medium for an additional 3 days with or without nitrogen in the light, or without sucrose in the dark. For salt and osmotic stress, 7-day-old WT and *TOR*-OE2 seedlings were transferred to liquid 1/2 MS medium plus or minus 0.16 M NaCl or 0.35 M mannitol for 6–8 h. Scale bar = 20 μ m. **(B,C)** Quantification of autophagosome number in WT and TOR overexpression lines after sucrose or nitrogen starvation **(B)**, salt, or osmotic stress **(C)**, treated as in **(A)**. MDC-stained autophagosomes were observed by fluorescence microscopy and photographed. The average number of autophagosomes was calculated from 10 images per genotype for each condition. **(D,E)** TOR overexpression lines fail to activate autophagy under sucrose starvation **(D)**, salt or osmotic stress **(E)** in leaf protoplasts. A GFP-ATG8e fusion protein was transiently expressed in leaf protoplasts of WT and TOR overexpression lines. Protoplasts were incubated in the dark plus or minus 0.5% (w/v) sucrose for 2 days **(D)**, or plus or minus 0.16 M NaCl or 0.35 M mannitol for 1 day **(E)**. Protoplasts were observed using fluorescence microscopy. The percentage of protoplasts with more than three visible GFP-tagged autophagosomes was calculated from 100 protoplasts observed per genotype for each condition. For all graphs, error bars indicate means \pm SE from three independent replicates. Asterisks indicate statistically significant differences ($P < 0.05$) using Student's *t*-test compared with WT under control conditions.

control conditions. The average number of autophagosomes in WT seedlings after sucrose or nitrogen starvation was significantly higher than in control conditions, whereas the TOR overexpression lines had no significant activation of autophagy. This indicates that overexpression of TOR can repress autophagy induced by nutrient starvation, suggesting that repression of TOR activity is required for activation of autophagy in response to nutrient depletion.

While previous studies have shown that TOR is involved in nutrient sensing (Dobrenel et al., 2016), the extent to which TOR regulates stress responses other than nutrient deficiency

is not known, although a link to osmotic stress resistance in *Arabidopsis* has been suggested (Mahfouz et al., 2006; Deprost et al., 2007). Autophagy is activated in *Arabidopsis* by salt and osmotic stresses (Liu et al., 2009). Therefore, we also tested whether overexpression of TOR affects autophagy induced by salt or osmotic stress (Figures 2A,C). WT and the TOR overexpression lines were germinated and grown on solid 1/2 MS medium for 1 week, and then transferred to liquid 1/2 MS medium containing 0.16 M NaCl or 0.35 M mannitol for 6–8 h. Autophagy in seedling roots was assayed by MDC staining followed by fluorescence microscopy (Figure 2C). Autophagy in

salt or mannitol treated WT seedlings was significantly higher than the basal level of autophagy seen under control conditions. As for nutrient deficiency, autophagy was not induced in TOR overexpression lines under salt or osmotic stress, indicating that TOR can also repress autophagy induced by these stresses.

To confirm these results, we measured autophagy by transient expression of GFP-ATG8e in leaf protoplasts from WT and TOR overexpressing plants under sucrose starvation, salt and osmotic stresses (**Figures 2D,E**). As the protoplast incubation buffer contains nitrogen, it was not possible to test nitrogen deficiency using our standard protocol. After transformation with GFP-ATG8e constructs, protoplasts were incubated with or without sucrose for 2 days (**Figure 2D**), or plus or minus 0.16 M NaCl or 0.35 M mannitol for 1 day (**Figure 2E**), after which autophagy was observed using fluorescence microscopy. The percentage of protoplasts with active autophagy was calculated, with 100 protoplasts observed per genotype for each condition. WT and TOR overexpression lines had a low level of autophagy under control conditions, except for the S7817 line which had constitutive activation of autophagy. In this line, TOR expression is decreased in leaves, potentially explaining this observation (Deprost et al., 2007). While WT protoplasts had a significantly higher level of autophagy under sucrose starvation, salt and osmotic stresses, autophagy in the TOR overexpression lines, with the exception of S7817, remained at a low basal level indistinguishable from that in control conditions. We conclude that TOR is a regulator of autophagy in response to salt and osmotic stress in addition to nutrient deficiency.

Overexpression of TOR Has No Effect on Oxidative Stress- or ER Stress-Induced Autophagy

Autophagy is also induced by oxidative stress and ER stress in plants (Xiong et al., 2007b; Liu et al., 2012; Yang et al., 2016). Oxidative stress is triggered when cells accumulate excessive reactive oxygen species (ROS), and oxidized proteins and lipids are degraded through autophagy (Xiong et al., 2007a,b). ER stress is generated when unfolded or misfolded proteins exceed the capacity of protein folding or degradation systems, causing accumulation of proteins in the ER (Howell, 2013). It can be triggered by heat stress, or experimentally by chemicals such as dithiothreitol (DTT) or tunicamycin (Howell, 2013). To determine whether TOR regulates autophagy upon oxidative or ER stress, 7-day-old WT and TOR overexpression lines were transferred to liquid $\frac{1}{2}$ MS medium plus or minus 5 mM H₂O₂ for 2–3 h to cause oxidative stress, or plus 2 mM DTT or 5 µg/mL tunicamycin for 6–8 h to cause ER stress. Autophagy in seedling roots was detected by MDC staining followed by fluorescence microscopy (**Figures 3A–C**). Representative images of one of the TOR overexpression lines are shown in **Figure 3A**. WT and TOR overexpression lines had a low level of autophagy under control conditions, and WT seedlings had significantly higher autophagy induction after oxidative or ER stress treatment. Unlike nutrient, salt or osmotic stresses, TOR overexpression had no effect on autophagy induction, as overexpression lines remained able to activate autophagy under these stresses, suggesting that

autophagy is activated via a pathway that does not require inhibition of TOR activity.

To confirm that autophagy remains induced in TOR overexpression lines under oxidative and ER stress, GFP-ATG8e was transiently expressed in leaf protoplasts of WT and TOR overexpression lines. Protoplasts were incubated with or without 5 mM H₂O₂, 2 mM DTT, or 5 µg/mL tunicamycin for 1 day, and observed using fluorescence microscopy (**Figures 3D,E**). WT protoplasts had a significantly higher level of autophagy after oxidative or ER stress treatment. In accordance with the MDC staining results, TOR overexpression lines also had a significantly higher percentage of protoplasts with active autophagy after oxidative or ER stress treatment, with no significant difference compared to WT under the same stress conditions. This demonstrates that overexpression of TOR is unable to repress autophagy induced by oxidative or ER stress, suggesting that oxidative- or ER stress-induced autophagy might be regulated through a TOR-independent pathway.

The effects of oxidative stress on autophagy can be difficult to interpret, as autophagy is also triggered by signaling ROS produced by NADPH oxidase (Liu et al., 2009). Salicylic acid (SA) has also been shown to enhance ROS signaling and induce autophagy in plants (Yoshimoto et al., 2009); we therefore tested whether SA-induced autophagy is dependent on TOR. Seven-day-old WT and TOR overexpression lines were transferred to liquid $\frac{1}{2}$ MS medium with 100 µM benzo-(1,2,3)-thiadiazole-7-carbothioic acid S-methyl ester (BTH), an SA agonist, or 80% ethanol as control for 8 h. Autophagy in seedling roots was detected by MDC staining followed by fluorescence microscopy (Supplementary Figure 1A). WT and TOR overexpression lines had a low level of autophagy under control conditions, while both WT and TOR overexpression lines had significantly increased autophagy induction upon BTH treatment, suggesting that SA-induced autophagy, as for H₂O₂-induced autophagy, is not TOR dependent.

Auxin Represses Stress-Induced Autophagy through TOR

Target of rapamycin activity in *Arabidopsis* can be enhanced by exogenous addition of the auxin 1-naphthaleneacetic acid (NAA) (Schepetilnikov et al., 2013), indicating that auxin might regulate plant growth and development via the TOR signaling pathway. We hypothesized that auxin might repress stress-induced autophagy in plants through the TOR pathway. To confirm the existence of TOR-dependent and -independent pathways for activation of autophagy, NAA was added exogenously to *GFP-ATG8e* transgenic plants to activate TOR, and the effect on autophagy under different conditions was assessed (**Figures 4A–D** and Supplementary Figure 1B). For nutrient deficiency, 7-day-old *GFP-ATG8e* transgenic seedlings were transferred to solid $\frac{1}{2}$ MS medium with or without sucrose or nitrogen and plus 20 nM NAA or DMSO for an additional 3 days. For salt, osmotic and ER stress, and BTH treatment, 7-day-old seedlings were transferred to liquid $\frac{1}{2}$ MS medium plus 0.16 M NaCl, 0.35 M mannitol, 2 mM DTT or 5 µg/mL

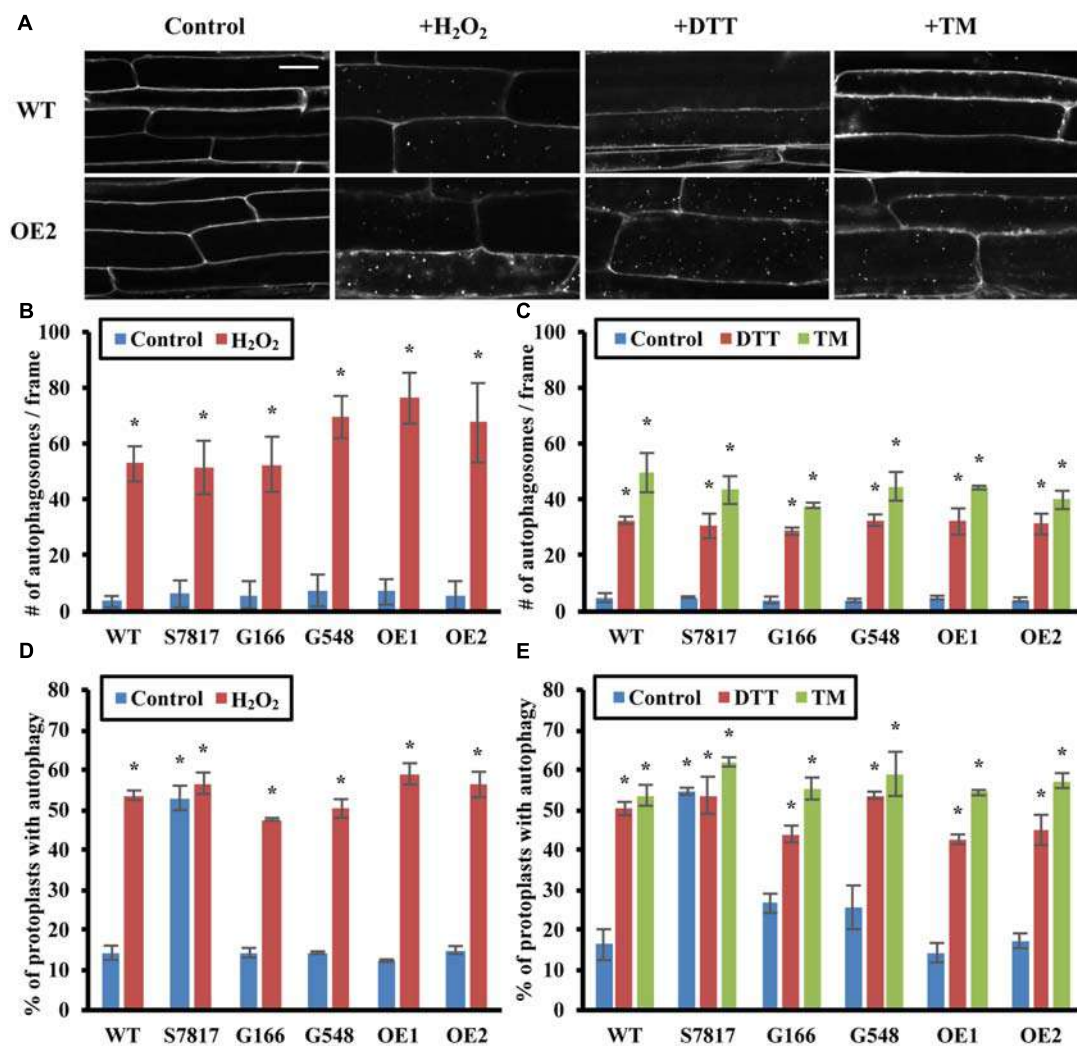
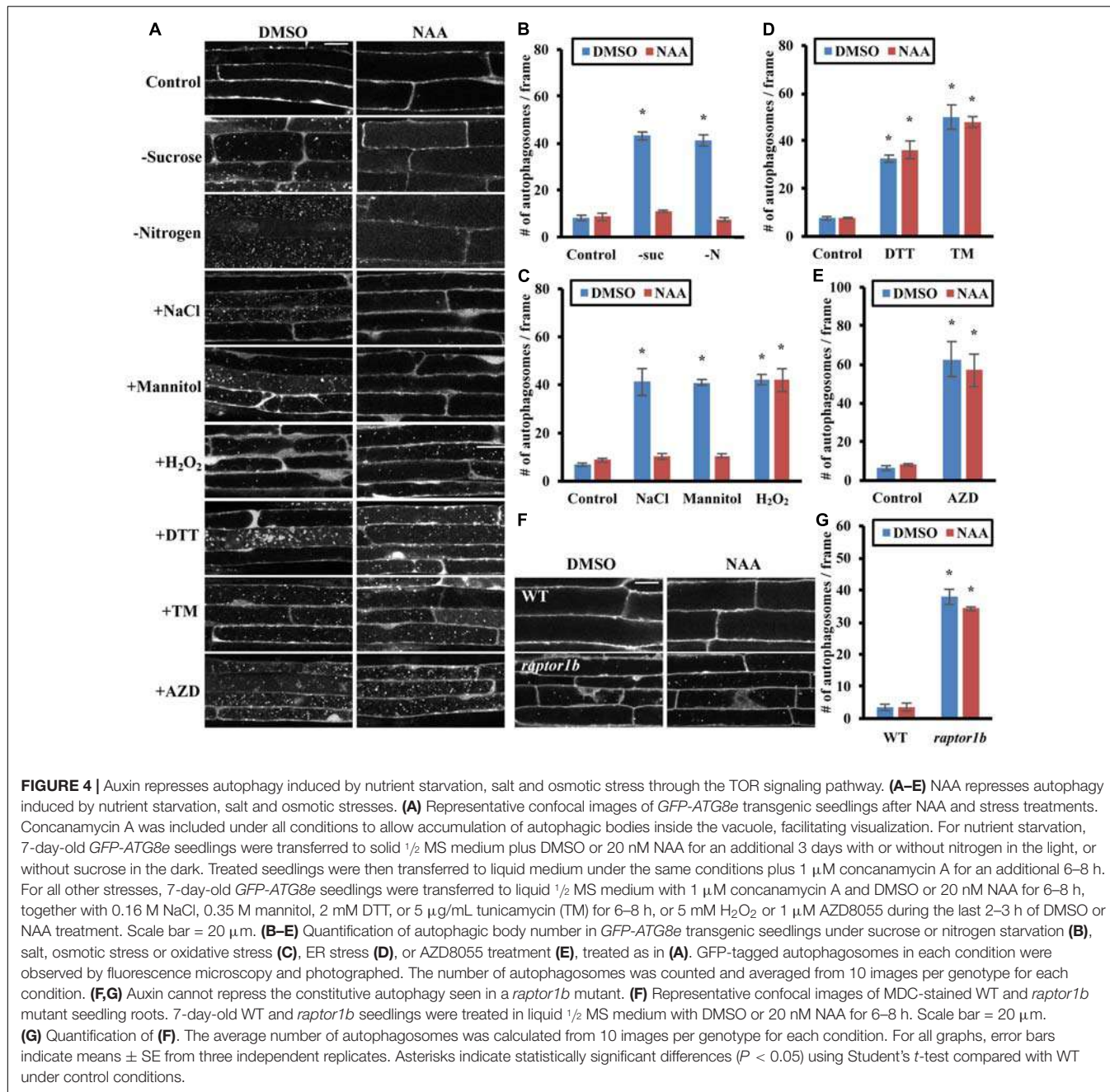


FIGURE 3 | Overexpression of TOR has no effect on oxidative stress- or ER stress- induced autophagy. **(A)** Confocal microscopy of MDC-stained WT and TOR-OE2 seedlings after the indicated stress treatment. 7-day-old WT and TOR overexpression transgenic seedlings were transferred to liquid 1/2 MS medium with or without 5 mM H₂O₂ for 2–3 h for oxidative stress, or 2 mM DTT or 5 µg/mL tunicamycin (TM) for 6–8 h for ER stress. Scale bar = 20 µm. **(B,C)** Quantification of autophagosome number in WT and TOR overexpression lines under oxidative stress **(B)** or ER stress **(C)** treated as in A. MDC-stained autophagosomes were observed by fluorescence microscopy and photographed. The average number of autophagosomes was calculated from 10 images per genotype for each condition. **(D,E)** Autophagy was induced in leaf protoplasts of TOR overexpression lines under oxidative stress **(D)** or ER stress **(E)**. A GFP-ATG8e fusion protein was transiently expressed in leaf protoplasts of WT and TOR overexpression lines. Protoplasts were incubated in the dark plus or minus 5 mM H₂O₂ for 2–3 h **(D)**, or 2 mM DTT or 5 µg/mL tunicamycin (TM) for 6–8 h **(E)**. Protoplasts were observed using fluorescence microscopy. The percentage of protoplasts with more than three visible GFP-tagged autophagosomes was calculated from 100 protoplasts observed per genotype for each condition. For all graphs, error bars indicate means ± SE from three independent replicates. Asterisks indicate statistically significant differences ($P < 0.05$) using Student's *t*-test compared with WT under control conditions.

tunicamycin, or 100 µM BTH and plus 20 nM NAA or DMSO for 6–8 h. For oxidative stress, 7-day-old seedlings were transferred to liquid 1/2 MS medium plus 20 nM NAA or DMSO for 6–8 h, with 5 mM H₂O₂ added only during the last 2–3 h to avoid cell death. To more clearly observe GFP-ATG8e-labeled autophagic bodies in the vacuoles by confocal microscopy, 1 µM concanamycin A was added to block degradation of autophagic bodies prior to imaging of the vacuoles (Dröse et al., 1993; Liu and Bassham, 2010) (Figure 4A). In control conditions, root cells had few autophagic bodies within the vacuole, whereas all stresses tested led

to accumulation of large numbers of autophagic bodies. In the presence of auxin, autophagic body accumulation was inhibited in nutrient deficiency, salt and osmotic stress, but accumulation was still observed in oxidative and ER stress and upon BTH treatment. These results also indicate that NAA reduces the number of autophagosomes observed by blocking autophagosome formation, rather than by accelerating autophagosome degradation. Autophagy was quantified by counting the number of autophagosomes under each condition, averaged from 10 images per genotype for each condition (Figures 4B–D and Supplementary Figure 1B). Compared to the



basal level of autophagy under control conditions, autophagy was significantly higher after stress treatments. In the presence of NAA, autophagy was still significantly induced by oxidative and ER stress conditions and in the presence of BTH, but no significant difference compared to control conditions was observed under nutrient starvation, salt and osmotic stresses. This suggests that NAA represses autophagy induced by sucrose and nitrogen starvation, salt and osmotic stresses, but not oxidative stress or ER stress, consistent with the results from overexpression of TOR.

To further confirm that addition of auxin represses stress-induced autophagy through activation of TOR, we

examined whether auxin can inhibit the constitutive autophagy seen upon disruption of the TOR signaling pathway by chemical inhibition or genetic mutation (Figures 4E–G). To inhibit TOR kinase activity, 7-day-old GFP-ATG8e seedlings were transferred to liquid 1/2 MS medium with or without 20 nM NAA for 6–8 h, with DMSO or 1 μM AZD8055 added during the last 2–3 h of treatment. GFP-labeled autophagic bodies in roots after concanamycin A treatment were examined using confocal microscopy (Figure 4A). AZD8055 as expected led to a high accumulation of autophagic bodies in the vacuole, and NAA had no effect on this accumulation, suggesting that NAA acts upstream of TOR in the autophagy pathway. The extent of

autophagy was quantified by counting root autophagosomes, and AZD8055 caused accumulation of autophagosomes both in the presence and absence of NAA, with no significant difference in autophagy induction (**Figure 4E**).

As an alternative approach, the effect of NAA upon inhibition of TOR complex function via knockout of *RAPTOR1B* was tested. Seven-day-old WT and *raptor1b* seedlings were transferred to liquid 1/2 MS medium with or without 20 nM NAA for 6–8 h, followed by MDC staining and autophagy detection by fluorescence microscopy (**Figures 4F,G**). NAA had no significant effect on the constitutive autophagy seen in the *raptor1b* mutant. Taken together, these results suggest that auxin acts upstream of TOR in the regulation of autophagy.

DISCUSSION

The TOR signaling pathway is a critical pathway for balancing cell growth and survival (Dobrenel et al., 2016). TOR was suggested to function as a complex with RAPTOR and LST8 based on studies in yeast and mammals (González and Hall, 2017), and previous studies in plants (Anderson et al., 2005; Deprost et al., 2005; Moreau et al., 2012). A knock out mutation in TOR is embryo-lethal in Arabidopsis (Menand et al., 2002), and down-regulation of TOR via RNA-interference arrests plant growth and induces autophagy. This suggests that TOR is a positive regulator of growth and development, and a negative regulator of autophagy in plants (Deprost et al., 2007; Liu and Bassham, 2010). To confirm that the TOR complex negatively regulates autophagy in Arabidopsis, we used a TOR inhibitor, AZD8055 (Chresta et al., 2010; Montane and Menand, 2013; Dong et al., 2015), which led to a significant induction of autophagy (**Figure 1A**). We also disrupted the TOR signaling pathway via a knockout mutant in *RAPTOR*, a binding partner of TOR. *RAPTOR1B* is the most highly expressed isoform of RAPTOR in Arabidopsis (Deprost et al., 2005), and *raptor1b* has a much more severe growth defect than *raptor1a* (Anderson et al., 2005). The *raptor1b* knockout line exhibited constitutive autophagy in both roots and leaf protoplasts, whereas a *raptor1a* mutation had only minor effects on autophagy, suggesting that *RAPTOR1B* is the primary RAPTOR isoform for repression of autophagy under our conditions.

Autophagy is induced by numerous stresses, including nutrient deficiency, salt, drought, oxidative and ER stresses (Doelling et al., 2002; Hanaoka et al., 2002; Xiong et al., 2007b; Liu et al., 2009, 2012). TOR has been well-characterized as regulating autophagy in response to nutrients in yeast and mammals, and down-regulation of TOR leads to growth defects and autophagy induction (Dobrenel et al., 2016). Therefore, we hypothesized that nutrient deficiency induces autophagy through the TOR signaling pathway in plants. As expected, overexpression of TOR repressed autophagy upon sucrose or nitrogen starvation, suggesting that TOR regulates nutrient deficiency-induced autophagy. Many upstream regulators of TOR have been identified in yeast and mammals, although many of them are not conserved in plants. One upstream kinase that is conserved throughout eukaryotes, named AMPK in mammals

and Snf1 in yeast, senses energy status and activates autophagy in response to low energy (Hulsmans et al., 2016). A homolog of AMPK and Snf1 in plants, SnRK1, has been identified, and is also activated under stress conditions (Dobrenel et al., 2016; Nukarinen et al., 2016). SnRK1 phosphorylates RAPTOR1B, potentially decreasing TOR activity, although whether this affects autophagy is as yet unknown.

Salt and drought are two major environmental stresses encountered by plants; both lead to osmotic stress, while salt stress also leads to ionic stress. Surprisingly, overexpression of TOR and activation of TOR by auxin represses autophagy in both conditions, indicating that activation of autophagy upon salt and drought stress is also dependent on TOR. A substrate of TOR, S6K, shows reduced expression and activity under salt and osmotic stress (Mizoguchi et al., 1995; Mahfouz et al., 2006), suggesting that salt and osmotic stress reduce TOR activity. However, it is unclear how salt and osmotic stresses signal to the TOR signaling pathway. Salt, osmotic stress and nutrient deficiency all increase cellular ROS levels, which might function as signaling molecules or lead to oxidative stress (Zhu, 2016). A major source of signaling ROS is generated by plasma membrane NADPH oxidases (Miller et al., 2009), and we have shown previously that NADPH oxidase inhibitors block autophagy during nutrient deficiency and salt stress, but not osmotic stress (Liu et al., 2009). Osmotic stress activation of autophagy is therefore independent of NADPH oxidase. NADPH oxidase inhibitors also fail to inhibit the constitutive autophagy caused by down-regulation of TOR by RNA interference (Liu and Bassham, 2010). TOR may therefore act downstream of NADPH oxidase in regulating autophagy, or possibly in a parallel pathway that is independent of NADPH oxidase. SA has been shown to increase ROS signaling, and autophagy is induced by the SA analog BTH (Yoshimoto et al., 2009). However, overexpression of TOR or increasing TOR activity with auxin failed to inhibit BTH-induced autophagy, suggesting that SA-induced autophagy is TOR-independent. Excessive ROS also cause oxidative stress, and increasing TOR activity by overexpression or auxin addition failed to repress autophagy induced by H₂O₂, suggesting that oxidative stress activates autophagy through a TOR-independent pathway. It is still unclear whether signaling ROS regulate autophagy through TOR, and further work is needed to identify the stress sensors that trigger activation of autophagy.

Salt, drought, and heat stresses can also cause accumulation of excessive unfolded or misfolded proteins within the ER, known as ER stress. ER stress has been shown to induce autophagy in Arabidopsis (Liu et al., 2012; Yang et al., 2016). However, our data indicate that TOR overexpression has no effect during ER stress, suggesting that ER stress-induced autophagy is independent of TOR. Upon ER stress, the plant ER stress sensor inositol-requiring enzyme-1 (IRE1) splices the mRNA encoding the transcription factor membrane-associated basic leucine zipper 60 (bZIP60) to activate the unfolded protein response (UPR). The UPR aids proper folding or degradation of unfolded and misfolded proteins via upregulation of UPR-related genes (Howell, 2013). In Arabidopsis, induction of autophagy by ER stress is triggered by unfolded and misfolded proteins (Yang et al., 2016) and is dependent on one of the IRE1 isoforms, IRE1b,

but not on IRE1a or bZIP60 (Liu et al., 2012). ER stress therefore appears to activate autophagy through IRE1b, in a pathway that is independent of TOR. However, how IRE1b regulates autophagy upon ER stress, and whether other UPR response genes are involved, requires further investigation.

Auxin has long been studied for its critical role in plant growth regulation (Enders and Strader, 2015). Auxin increases TOR activity, and auxin-mediated root gravitropism is impaired when TOR signaling is disrupted (Schepetilnikov et al., 2013). Auxin is unable to restore hypocotyl growth in estradiol-inducible *tor* mutants (Zhang et al., 2016), and many auxin response genes have reduced expression upon inhibition of TOR (Dong et al., 2015), suggesting that TOR is involved in auxin-regulated plant growth. Recent studies identified a small GTPase, ROP2, that mediates the activation of TOR by auxin (Li et al., 2017; Schepetilnikov et al., 2017). We hypothesized that enhancing TOR activity with auxin might repress stress-induced autophagy via the TOR signaling pathway. Indeed, as in the TOR overexpression lines, autophagy induced by nutrient starvation, salt or osmotic stresses was repressed by addition of NAA, whereas oxidative and ER stress-induced autophagy was not affected. NAA was unable to repress the autophagy induced by inhibition of TOR activity with the inhibitor AZD8055 or in a *raptor1b* knockout line. Exogenous application of the synthetic auxin 2, 4-D failed to restore growth of *raptor1b*, although *raptor1b* mutants can sense exogenous auxin normally (Anderson et al., 2005), supporting the conclusion that TOR signaling acts downstream of auxin.

In summary, we have demonstrated that autophagy can be regulated through TOR-dependent or -independent pathways, depending on the type of stress, and that auxin regulates plant stress responses through the TOR signaling pathway. Future

work is required to identify the upstream stress sensors that repress TOR activity to allow activation of autophagy and the components of the TOR-independent autophagy activation pathway.

AUTHOR CONTRIBUTIONS

YP and DB designed the experiments. YP and XL conducted the experiments and analyzed data. YP and DB wrote the manuscript.

FUNDING

This work was supported by grant no. 1R01GM120316-01A1 from the United States National Institutes of Health to DB and by the Iowa State University Plant Sciences Institute.

ACKNOWLEDGMENTS

We thank Drs Maureen Hanson for providing *raptor1a* and *raptor1b* mutant seeds, Raju Datla for *TOR-OE1* and *TOR-OE2* transgenic seeds, Richard Vierstra for *atg7-2* mutant seeds, Yanhai Yin for the pPZP212 vector and Margaret Carter for assistance with confocal microscopy.

SUPPLEMENTARY MATERIAL

The Supplementary Material for this article can be found online at: <http://journal.frontiersin.org/article/10.3389/fpls.2017.01204/full#supplementary-material>

REFERENCES

- Ahn, C. S., Han, J. A., Lee, H. S., Lee, S., and Pai, H. S. (2011). The PP2A regulatory subunit Tap46, a component of the TOR signaling pathway, modulates growth and metabolism in plants. *Plant Cell* 23, 185–209. doi: 10.1105/tpc.110.074005
- Anderson, G. H., Veit, B., and Hanson, M. R. (2005). The Arabidopsis *AtRaptor* genes are essential for post-embryonic plant growth. *BMC Biol.* 3:12. doi: 10.1186/1741-7007-3-12
- Biederick, A., Kern, H. F., and Elsasser, H. P. (1995). Monodansylcadaverine (MDC) is a specific in vivo marker for autophagic vacuoles. *Eur. J. Cell Biol.* 66, 3–14.
- Cai, Y., Arikkath, J., Yang, L., Guo, M. L., Periyasamy, P., and Buch, S. (2016). Interplay of endoplasmic reticulum stress and autophagy in neurodegenerative disorders. *Autophagy* 12, 225–244. doi: 10.1080/15548627.2015.1121360
- Chresta, C. M., Davies, B. R., Hickson, I., Harding, T., Cosulich, S., Critchlow, S. E., et al. (2010). AZD8055 is a potent, selective, and orally bioavailable ATP-competitive mammalian target of rapamycin kinase inhibitor with in vitro and in vivo antitumor activity. *Cancer Res.* 70, 288–298. doi: 10.1158/0008-5472.CAN-09-1751
- Chung, T., Phillips, A. R., and Vierstra, R. D. (2010). ATG8 lipidation and ATG8-mediated autophagy in Arabidopsis require ATG12 expressed from the differentially controlled *ATG12A* and *ATG12B* loci. *Plant J.* 62, 483–493. doi: 10.1111/j.1365-313X.2010.04166.x
- Contento, A. L., Xiong, Y., and Bassham, D. C. (2005). Visualization of autophagy in Arabidopsis using the fluorescent dye monodansylcadaverine and a GFP-AtATG8e fusion protein. *Plant J.* 42, 598–608. doi: 10.1111/j.1365-313X.2005.02396.x
- Davidson, S. M., and Vander Heiden, M. G. (2017). Critical functions of the lysosome in cancer biology. *Annu. Rev. Pharmacol. Toxicol.* 57, 481–507. doi: 10.1146/annurev-pharmtox-010715-103101
- Deprost, D., Truong, H. N., Robaglia, C., and Meyer, C. (2005). An Arabidopsis homolog of RAPTOR/KOG1 is essential for early embryo development. *Biochem. Biophys. Res. Commun.* 326, 844–850. doi: 10.1016/j.bbrc.2004.11.117
- Deprost, D., Yao, L., Sormani, R., Moreau, M., Leterreux, G., Nicolaï, M., et al. (2007). The *Arabidopsis* TOR kinase links plant growth, yield, stress resistance and mRNA translation. *EMBO Rep.* 8, 864–870. doi: 10.1038/sj.embo.7401043
- Dobrenel, T., Caldana, C., Hanson, J., Robaglia, C., Vincentz, M., Veit, B., et al. (2016). TOR signaling and nutrient sensing. *Annu. Rev. Plant Biol.* 67, 261–285. doi: 10.1146/annurev-arplant-043014-114648
- Doelling, J. H., Walker, J. M., Friedman, E. M., Thompson, A. R., and Vierstra, R. D. (2002). The APG8/12-activating enzyme APG7 is required for proper nutrient recycling and senescence in *Arabidopsis thaliana*. *J. Biol. Chem.* 277, 33105–33114. doi: 10.1074/jbc.M204630200
- Dong, P., Xiong, F., Que, Y., Wang, K., Yu, L., Li, Z., et al. (2015). Expression profiling and functional analysis reveals that TOR is a key player in regulating photosynthesis and phytohormone signaling pathways in *Arabidopsis*. *Front. Plant Sci.* 6:677. doi: 10.3389/fpls.2015.00677

- Dröse, S., Bindseil, K. U., Bowman, E. J., Siebers, A., Zeeck, A., and Altendorf, K. (1993). Inhibitory effect of modified baflomycins and concanamycins on P- and V-type adenosinetriphosphatases. *Biochemistry* 32, 3902–3906. doi: 10.1021/bi00066a008
- Enders, T. A., and Strader, L. C. (2015). Auxin activity: past, present, and future. *Am. J. Bot.* 102, 180–196. doi: 10.3732/ajb.1400285
- González, A., and Hall, M. N. (2017). Nutrient sensing and TOR signaling in yeast and mammals. *EMBO J.* 36, 397–408. doi: 10.15252/embj.201696010
- Hajdukiewicz, P., Svab, Z., and Maliga, P. (1994). The small, versatile pPZP family of *Agrobacterium* binary vectors for plant transformation. *Plant Mol. Biol.* 25, 989–994. doi: 10.1007/BF00014672
- Hanaoka, H., Noda, T., Shirano, Y., Kato, T., Hayashi, H., Shibata, D., et al. (2002). Leaf senescence and starvation-induced chlorosis are accelerated by the disruption of an *Arabidopsis* autophagy gene. *Plant Physiol.* 129, 1181–1193. doi: 10.1104/pp.011024
- Hara, K., Maruki, Y., Long, X., Yoshino, K., Oshiro, N., Hidayat, S., et al. (2002). Raptor, a binding partner of target of rapamycin (TOR), mediates TOR action. *Cell* 110, 177–189. doi: 10.1016/S0092-8674(02)00833-4
- Howell, S. H. (2013). Endoplasmic reticulum stress responses in plants. *Annu. Rev. Plant Biol.* 64, 477–499. doi: 10.1146/annurev-arplant-050312-120053
- Hulsmans, S., Rodriguez, M., De Coninck, B., and Rolland, F. (2016). The SnRK1 energy sensor in plant biotic interactions. *Trends Plant Sci.* 21, 648–661. doi: 10.1016/j.tplants.2016.04.008
- Ichimura, Y., Kirisako, T., Takao, T., Satomi, Y., Shimonishi, Y., Ishihara, N., et al. (2000). A ubiquitin-like system mediates protein lipidation. *Nature* 408, 488–492. doi: 10.1038/35044114
- Kravchenko, A., Citerne, S., Jehanno, I., Bersimbaev, R. I., Veit, B., Meyer, C., et al. (2015). Mutations in the *Arabidopsis* *Lst8* and *Raptor* genes encoding partners of the TOR complex, or inhibition of TOR activity decrease abscisic acid (ABA) synthesis. *Biochem. Biophys. Res. Commun.* 467, 992–997. doi: 10.1016/j.bbrc.2015.10.028
- Lenz, H. D., Haller, E., Melzer, E., Kober, K., Wurster, K., Stahl, M., et al. (2011). Autophagy differentially controls plant basal immunity to biotrophic and necrotrophic pathogens. *Plant J.* 66, 818–830. doi: 10.1111/j.1365-313X.2011.04546.x
- Li, L., Yu, X., Thompson, A., Guo, M., Yoshida, S., Asami, T., et al. (2009). *Arabidopsis* MYB30 is a direct target of BES1 and cooperates with BES1 to regulate brassinosteroid-induced gene expression. *Plant J.* 58, 275–286. doi: 10.1111/j.1365-313X.2008.03778.x
- Li, X., Cai, W., Liu, Y., Li, H., Fu, L., Liu, Z., et al. (2017). Differential TOR activation and cell proliferation in *Arabidopsis* root and shoot apexes. *Proc. Natl. Acad. Sci. U.S.A.* 114, 2765–2770. doi: 10.1073/pnas.1618782114
- Liu, Y., and Bassham, D. C. (2010). TOR is a negative regulator of autophagy in *Arabidopsis thaliana*. *PLoS ONE* 5:e11883. doi: 10.1371/journal.pone.0011883
- Liu, Y., and Bassham, D. C. (2012). Autophagy: pathways for self-eating in plant cells. *Annu. Rev. Plant Biol.* 63, 215–237. doi: 10.1146/annurev-arplant-042811-105441
- Liu, Y., Burgos, J. S., Deng, Y., Srivastava, R., Howell, S. H., and Bassham, D. C. (2012). Degradation of the endoplasmic reticulum by autophagy during endoplasmic reticulum stress in *Arabidopsis*. *Plant Cell* 24, 4635–4651. doi: 10.1105/tpc.112.101535
- Liu, Y., Schiff, M., Czymbmek, K., Tallóczy, Z., Levine, B., and Dinesh-Kumar, S. P. (2005). Autophagy regulates programmed cell death during the plant innate immune response. *Cell* 121, 567–577. doi: 10.1016/j.cell.2005.03.007
- Liu, Y., Xiong, Y., and Bassham, D. C. (2009). Autophagy is required for tolerance of drought and salt stress in plants. *Autophagy* 5, 954–963. doi: 10.4161/auto.5.79290
- Mahfouz, M. M., Kim, S., Delauney, A. J., and Verma, D. P. (2006). *Arabidopsis* TARGET OF RAPAMYCIN interacts with RAPTOR, which regulates the activity of S6 kinase in response to osmotic stress signals. *Plant Cell* 18, 477–490. doi: 10.1105/tpc.105.035931
- Menand, B., Desnos, T., Nussaume, L., Berger, F., Bouchez, D., Meyer, C., et al. (2002). Expression and disruption of the *Arabidopsis* TOR (target of rapamycin) gene. *Proc. Natl. Acad. Sci. U.S.A.* 99, 6422–6427. doi: 10.1073/pnas.092141899
- Miller, G., Schlauch, K., Tam, R., Cortes, D., Torres, M. A., Shulaev, V., et al. (2009). The plant NADPH oxidase RBOHD mediates rapid systemic signaling in response to diverse stimuli. *Sci. Signal.* 2:ra45. doi: 10.1126/scisignal.2000448
- Mizoguchi, T., Hayashida, N., Yamaguchi-Shinozaki, K., Kamada, H., and Shinozaki, K. (1995). Two genes that encode ribosomal-protein S6 kinase homologs are induced by cold or salinity stress in *Arabidopsis thaliana*. *FEBS Lett.* 358, 199–204. doi: 10.1016/0014-5793(94)01423-X
- Montane, M. H., and Menand, B. (2013). ATP-competitive mTOR kinase inhibitors delay plant growth by triggering early differentiation of meristematic cells but no developmental patterning change. *J. Exp. Bot.* 64, 4361–4374. doi: 10.1093/jxb/ert242
- Moreau, M., Azzopardi, M., Clément, G., Dobrenel, T., Marchive, C., Renne, C., et al. (2012). Mutations in the *Arabidopsis* homolog of LST8/G β L, a partner of the target of Rapamycin kinase, impair plant growth, flowering, and metabolic adaptation to long days. *Plant Cell* 24, 463–481. doi: 10.1105/tpc.111.091306
- Noda, T., and Ohsumi, Y. (1998). Tor, a phosphatidylinositol kinase homologue, controls autophagy in yeast. *J. Biol. Chem.* 273, 3963–3966. doi: 10.1074/jbc.273.7.3963
- Nukarinen, E., Nägele, T., Pedrotti, L., Wurzinger, B., Mair, A., Landgraf, R., et al. (2016). Quantitative phosphoproteomics reveals the role of the AMPK plant ortholog SnRK1 as a metabolic master regulator under energy deprivation. *Sci. Rep.* 6:31697. doi: 10.1038/srep31697
- Pu, Y., and Bassham, D. C. (2016). Detection of autophagy in plants by fluorescence microscopy. *Methods Mol. Biol.* 1450, 161–172. doi: 10.1007/978-1-4939-3759-2_13
- Raught, B., Gingras, A. C., and Sonenberg, N. (2001). The target of rapamycin (TOR) proteins. *Proc. Natl. Acad. Sci. U.S.A.* 98, 7037–7044. doi: 10.1073/pnas.121145898
- Ren, M., Qiu, S., Venglat, P., Xiang, D., Feng, L., Selvaraj, G., et al. (2011). Target of rapamycin regulates development and ribosomal RNA expression through kinase domain in *Arabidopsis*. *Plant Physiol.* 155, 1367–1382. doi: 10.1104/pp.110.169045
- Schepetilnikov, M., Dimitrova, M., Mancera-Martinez, E., Geldreich, A., Keller, M., and Ryabova, L. A. (2013). TOR and S6K1 promote translation reinitiation of uORF-containing mRNAs via phosphorylation of eIF3h. *EMBO J.* 32, 1087–1102. doi: 10.1038/embj.2013.61
- Schepetilnikov, M., Makarian, J., Sour, O., Geldreich, A., Yang, Z., Chicher, J., et al. (2017). GTPase ROP2 binds and promotes activation of target of rapamycin, TOR, in response to auxin. *EMBO J.* 36, 886–903. doi: 10.15252/embj.201694816
- Sheen, J. (2002). *A Transient Expression Assay using Arabidopsis Mesophyll Protoplasts*. Available at: http://molbio.mgh.harvard.edu/sheenweb/protocols_reg.html
- Tsukada, M., and Ohsumi, Y. (1993). Isolation and characterization of autophagy-defective mutants of *Saccharomyces cerevisiae*. *FEBS Lett.* 333, 169–174. doi: 10.1016/0014-5793(93)80398-E
- Turck, F., Zilberman, F., Kozma, S. C., Thomas, G., and Nagy, F. (2004). Phytohormones participate in an S6 kinase signal transduction pathway in *Arabidopsis*. *Plant Physiol.* 134, 1527–1535. doi: 10.1104/pp.103.035873
- Xiong, Y., Contento, A. L., and Bassham, D. C. (2007a). Disruption of autophagy results in constitutive oxidative stress in *Arabidopsis*. *Autophagy* 3, 257–258.
- Xiong, Y., Contento, A. L., Nguyen, P. Q., and Bassham, D. C. (2007b). Degradation of oxidized proteins by autophagy during oxidative stress in *Arabidopsis*. *Plant Physiol.* 143, 291–299. doi: 10.1104/pp.106.092106
- Xiong, Y., McCormack, M., Li, L., Hall, Q., Xiang, C., and Sheen, J. (2013). Glucose-TOR signalling reprograms the transcriptome and activates meristems. *Nature* 496, 181–186. doi: 10.1038/nature12030
- Xiong, Y., and Sheen, J. (2012). Rapamycin and glucose-target of rapamycin (TOR) protein signalling in plants. *J. Biol. Chem.* 287, 2836–2842. doi: 10.1074/jbc.M111.300749
- Yang, H., Rudge, D. G., Koos, J. D., Vaidialingam, B., Yang, H. J., and Pavletich, N. P. (2013). mTOR kinase structure, mechanism and regulation. *Nature* 497, 217–223. doi: 10.1038/nature12122
- Yang, X., and Bassham, D. C. (2015). “New insight into the mechanism and function of autophagy in plant cells,” in *International Review of Cell and Molecular Biology*, ed. W. Jeon Kwang (Burlington, MA: Academic Press), 1–40.
- Yang, X., Srivastava, R., Howell, S. H., and Bassham, D. C. (2016). Activation of autophagy by unfolded proteins during endoplasmic reticulum stress. *Plant J.* 85, 83–95. doi: 10.1111/tpj.13091

- Yorimitsu, T., He, C., Wang, K., and Klionsky, D. J. (2009). Tap42-associated protein phosphatase type 2A negatively regulates induction of autophagy. *Autophagy* 5, 616–624. doi: 10.4161/auto.5.5.8091
- Yoshimoto, K., Hanaoka, H., Sato, S., Kato, T., Tabata, S., Noda, T., et al. (2004). Processing of ATG8s, ubiquitin-like proteins, and their deconjugation by ATG4s are essential for plant autophagy. *Plant Cell* 16, 2967–2983. doi: 10.1105/tpc.104.025395
- Yoshimoto, K., Jikumaru, Y., Kamiya, Y., Kusano, M., Consonni, C., Panstruga, R., et al. (2009). Autophagy negatively regulates cell death by controlling NPR1-dependent salicylic acid signaling during senescence and the innate immune response in *Arabidopsis*. *Plant Cell* 21, 2914–2927. doi: 10.1105/tpc.109.068635
- Zhang, Z., Zhu, J.-Y., Roh, J., Marchive, C., Kim, S. K., Meyer, C., et al. (2016). TOR signaling promotes accumulation of BZR1 to balance growth with carbon availability in *Arabidopsis*. *Curr. Biol.* 26, 1854–1860. doi: 10.1016/j.cub.2016.05.005
- Zhou, J., Wang, J., Cheng, Y., Chi, Y. J., Fan, B., Yu, J. Q., et al. (2013). NBR1-mediated selective autophagy targets insoluble ubiquitinated protein aggregates in plant stress responses. *PLoS Genet.* 9:e1003196. doi: 10.1371/journal.pgen.1003196
- Zhu, J. K. (2016). Abiotic stress signaling and responses in plants. *Cell* 167, 313–324. doi: 10.1016/j.cell.2016.08.029

Conflict of Interest Statement: The authors declare that the research was conducted in the absence of any commercial or financial relationships that could be construed as a potential conflict of interest.

Copyright © 2017 Pu, Luo and Bassham. This is an open-access article distributed under the terms of the Creative Commons Attribution License (CC BY). The use, distribution or reproduction in other forums is permitted, provided the original author(s) or licensor are credited and that the original publication in this journal is cited, in accordance with accepted academic practice. No use, distribution or reproduction is permitted which does not comply with these terms.



Endocytosis of AtRGS1 Is Regulated by the Autophagy Pathway after D-Glucose Stimulation

Quanquan Yan¹, Jingchun Wang¹, Zheng Qing Fu² and Wenli Chen^{1*}

¹ Ministry of Education Key Laboratory of Laser Life Science and Institute of Laser Life Science, College of Biophotonics, South China Normal University, Guangzhou, China, ² Department of Biological Sciences, University of South Carolina, Columbia, SC, United States

OPEN ACCESS

Edited by:

Yule Liu,
Tsinghua University, China

Reviewed by:

Jirong Huang,
Shanghai Institutes for Biological Sciences (CAS), China
Gian Pietro Di Sansebastiano,
University of Salento, Italy

*Correspondence:

Wenli Chen
chenwl@scnu.edu.cn

Specialty section:

This article was submitted to
Plant Cell Biology,
a section of the journal
Frontiers in Plant Science

Received: 11 April 2017

Accepted: 29 June 2017

Published: 12 July 2017

Citation:

Yan Q, Wang J, Fu ZQ and Chen W (2017) Endocytosis of AtRGS1 Is Regulated by the Autophagy Pathway after D-Glucose Stimulation. *Front. Plant Sci.* 8:1229.
doi: 10.3389/fpls.2017.01229

Sugar, as a signal molecule, has significant functions in signal transduction in which the seven-transmembrane regulator of G-protein signaling (RGS1) protein participates. D-Glucose causes endocytosis of the AtRGS1, leading to the physical uncoupling of AtRGS1 from AtGPA1 and thus a release of the GAP activity and concomitant sustained activation of G-protein signaling. Autophagy involves in massive degradation and recycling of cytoplasmic components to survive environmental stresses. The function of autophagy in AtRGS1 endocytosis during D-glucose stimulation has not been elucidated. In this study, we investigate the relationship between autophagy and AtRGS1 in response to D-glucose. Our findings demonstrated that AtRGS1 mediated the activation of autophagy by affecting the activities of the five functional groups of protein complexes and promoted the formation of autophagosomes under D-glucose application. When the autophagy pathway was interrupted, AtRGS1 recovery increased and endocytosis of AtRGS1 was inhibited, indicating that autophagy pathway plays an important role in regulating the endocytosis and recovery of AtRGS1 after D-glucose stimulation.

Keywords: *Arabidopsis thaliana*, D-glucose, AtRGS1, endocytosis, autophagy

INTRODUCTION

In addition to integrating multi-faceted internal and external cues to gain nutrient homeostasis to build and fuel cells, sugars have significant hormone-like functions as primary messengers during signal transduction (Rolland et al., 2001, 2002; Ramon et al., 2008; Kang et al., 2010). In plants, a G-protein-coupled pathway is involved in sugar signaling. The *Arabidopsis thaliana* genome encodes an *Arabidopsis thaliana* regulator of G-protein signaling 1 (AtRGS1) protein that has an N-terminal seven transmembrane (7TM) domain and a catalytic RGS box at its C-terminal domain (Chen et al., 2003; Johnston et al., 2007; Urano et al., 2012; Bradford et al., 2013; Urano and Jones, 2014). In *Arabidopsis thaliana*, the heterotrimeric G-protein complex consists of one canonical G α subunit (GPA1), one G β subunit (AGB1), and three G γ subunits (Huang et al., 2015). AtRGS1 interacts with AtGPA1 and stimulates the rate-limiting GTPase activity of AtGPA1 in a D-glucose-regulated manner (Jeffrey et al., 2008). Previous studies by Urano et al. (2012) indicate that D-glucose recruits a with-no-lysine kinase (AtWNK) to phosphorylate AtRGS1 at least two C-terminal serines and that the phosphorylation of AtRGS1 is sufficient to cause endocytosis of

AtRGS1 (Fu et al., 2014). Huang lab's data reveals that deletion of the C-terminus (AtRGS¹⁻⁴¹³) has no effect on AtRGS1 localization at the plasma membrane (Hu et al., 2013). In our study, we would like to investigate whether autophagy pathway is involved in AtRGS1-mediated sugar signaling pathway.

Autophagy ('self-eating') is a highly conserved mechanism among eukaryotes for degrading and recycling intracellular materials during survival to several environmental stresses (Fujioka et al., 2008; Mizushima et al., 2011; Wang P. et al., 2016). Despite the clear role of autophagy in the innate immune system of the plant during infection by necrotrophic pathogens, recent studies have demonstrated that autophagy plays an important role in degrading and recycling intracellular molecules to regulate catabolic processes (Bassham, 2007; Li and Vierstra, 2012; Gao et al., 2016). When autophagy is induced, double-membrane vesicles (autophagosome) generate and engulf the cytoplasmic components, then transport them to the lysosome (animals) or vacuole (yeast and plants) for degradation. The degradation products of these cellular materials are released into the cytoplasm for recycling (Yang and Bassham, 2015; Wang X.D. et al., 2016). Autophagy likely has essential functions as protective mechanisms that assist plants to survive unfavorable growth conditions. Several distinct autophagic types have been defined in many species and classified as microautophagy, macroautophagy, chaperone-mediated autophagy, and organelle-specific autophagy (He and Klionsky, 2009; Liu and Bassham, 2012; Chanoca et al., 2015). Macroautophagy (hereafter, referred to as autophagy), as the most extensively studied autophagic type, is generated at the certain stage of development or upon encountering environmental stresses.

Several studies point to the relationship between RGS and autophagy pathway in animals. The Gα-interacting protein (GAIP), a member of a novel RGS family, is known to interact with the heterotrimeric G protein Gα_{i3}, to regulate inhibitory regulative G-protein (Gi) signaling pathways (Ogier-Denis et al., 1997). In human intestinal cells, GAIP/RGS19 acts as a GTPase-activating protein and inactivates the Gi protein, stimulating the lysosomal-autophagic pathway (Garcia-Marcos et al., 2011). In HT-29 cells, amino acids can mediate autophagy by inhibiting extracellular signal-regulated kinase1/2 (ERK1/2)-dependent GAIP phosphorylation (Ogier-Denis et al., 2000). Both GAIP and the Gα_{i3} protein are part of a signaling pathway that controls lysosomal autophagic catabolism. Phosphorylation of GAIP depends on the activation of the Erk1/2 MAP kinases. Activated ERK also abolishes the autophagy-inhibitory effects of the heterotrimeric Gi protein isoform Gi3 (Pattингre et al., 2003; Law et al., 2016).

Whether the AtRGS1-mediated sugar signaling pathway is related to the autophagy pathway during D-glucose stimulation remains elusive. Here, we show that autophagy is essential for regulation of the AtRGS1-mediated sugar signaling pathway in response to D-glucose in *Arabidopsis thaliana*. Furthermore, autophagy could promote the endocytosis of AtRGS1 and is involved in the recovery of AtRGS1 under D-glucose treatment.

These results provide deep insights to the mechanism of AtRGS1 endocytosis upon D-glucose stimulation.

MATERIALS AND METHODS

Plant Materials

The plants used in all experiments were *Arabidopsis thaliana* ecotype Columbia 0 (Col-0). The transgenic seeds (GFP tagged ATG8a, GFP-ATG8a adiven by 35S promoter) were provided by Dr. Li Faqiang (Biochemistry, City University of New York, New York, NY, United States). The T-DNA knockout lines *atg2* (SALK_076727), *atg5* (SALK_020601) were obtained from the *Arabidopsis* Biological Resource Center (ABRC). The 35S::AtRGS1-YFP (35S::AtRGS1 was subcloned into pEarleyGate101) *Agrobacterium* and *Atrgs1-2* (SALK_074376) mutant seeds were kindly provided by Dr. Alan Jones (University of North Carolina, Chapel Hill, NC, United States). The overexpression transgenic seeds of AtRGS1-YFP, *atg5*/AtRGS1-YFP and *atg2*/AtRGS1-YFP were created by Dr. Wenli Chen in the laboratory of Alan Jones. Homozygousities of all DNA-insertion were confirmed by PCR analysis of genomic DNA with the primer sets listed in Supplementary Table S1 and Figures S1B,C,E. The transgenic lines were screened on MS plates with Basta (10 µg·mL⁻¹) (Supplementary Figure S1A). The specific primers listed in Supplementary Table S1 were used to examine the gene expression levels of AtRGS1 described in Supplementary Figure S1D.

Growth Conditions and Treatment

Approximately, 100 seeds of *Arabidopsis thaliana* were sterilized by sequential treatments with 75% (v·v⁻¹) ethanol (1 min) and 1% (v·v⁻¹) NaClO (10 min), followed by washing with sterile distilled water six times, vernalizing in dark conditions for 3 days at 4°C for better germination, and sown in liquid Murashige and Skoog (MS, without sucrose) medium with 1% D-glucose (pH 5.8). Seedlings were incubated in a plant growth chamber under dim continuous light (25 µmol m⁻² s⁻¹) at 23°C, shaking at 100 r·min⁻¹ for another 5 days (Normal conditions). To sugar starve seedlings, the seedlings were then transferred to 500 mL flasks with 100 mL liquid MS medium without D-glucose or any other sugar and allowed to grow on a shaker (100 r·min⁻¹) in the dark for 2 h. Following sugar starvation, seedlings were removed from the sugar-free MS medium and incubated with liquid MS media containing 1% or 6% D-glucose for the indicated time periods (0, 0.5, and 2 h) on a shaker (100 r·min⁻¹) (Jeffrey et al., 2008; Urano et al., 2012).

Gene Expression Analysis

Seedlings (0.1 g) were collected and frozen in liquid nitrogen and stored at -80°C by use of the TRIzol reagent according to the manufacturer's instructions. The total isolated RNA was treated with primeScript RT Master Mix (Takara) according to the manufacturer's instructions to synthesize the cDNA (Mackey et al., 2003; Caplan et al., 2008). Then, cDNA synthesis was

performed by adding 5× PrimeScript RT Master Mix (Takara, 1× final concentration), total RNA (0–500 ng) and RNase-free dH₂O to a final volume of 10 μl, incubating the samples at 37°C for 15 min, followed by incubating at 85°C for 5 s to terminate the reactions. We amplified different autophagy-related genes to quantify transcript levels by using gene-specific primers (Supplementary Table S1) in seedlings exposed to different treatments. Real-time PCR (qRT-PCR) was performed in Applied Biosystems 7500 with the following thermocycler program: 1 min of pre-incubation at 95°C followed by 35 cycles of 15 s at 94°C, 30 s at 55°C, and 35 s at 72°C. SYBR Green dye fluorescence was used at the end of the annealing phase. To confirm the presence of single products, a melting curve from 65 to 95°C was used. The level of relative expression was analyzed by using the 2^{-ΔΔCt} analysis method (Sun et al., 2012).

Confocal Microscopy

Root cells of seedlings located approximately in the elongation region were imaged using a Zeiss LSM 710 META system (LCSM; Carl-Zeiss, Jena, Germany). Confocal microscopy with excitation at 488 nm (a multi-Ar ion laser) and emission at 505–550 nm was used to detect the GFP-ATG8a fusion protein. YFP signals were excited by a 514-nm argon laser and its emission was detected at 520–550 nm by a photomultiplier detector, and for obtaining image quantification, ImageJ plugins was used. The digital Images were captured with a 40× oil immersion objective and analyzed with Aim Image Brower Image Processing software (Carl Zeiss) (Ishida et al., 2008; Zhang and Chen, 2011; Sheng et al., 2012).

Protein Isolation and Immunoblotting

Plant samples (0.4 g) were ground in liquid nitrogen, re-suspended in ice-cold protein extraction buffer (10 mM Tris-HCl pH 7.5, 150 mM NaCl, 1 mM EDTA, 0.2% Triton X-100, 0.5% Nonidet p-40, 1 mM PMSF, 3 mM DTT, 0.5 mM CaCl₂, 1% ASB-14 [For AtRGS1-YFP protein] and inhibitors), and then incubated on ice for 20 min. Samples were centrifuged at 12000 × g at 4°C for 20 min. The supernatants were transferred to new 1.5 ml eppendorf tubes. Protein concentrations were measured by the Bradford method after the total protein was diluted 100 times. Sample buffer (5×, 25 μl) with 20 mM DTT was added to 100 μl of extracted proteins. The extracted proteins were vortexed lightly and incubated in 90°C boiling water for 2–5 min. Total proteins were then separated by SDS-polyacrylamide gel electrophoresis (PAGE) and transferred onto polyvinylidene difluoride membranes as described in earlier studies (Wang X.D. et al., 2016). The resulting membranes were blocked in TBST buffer with 5% (w/v) skim milk and incubated with the primary antibodies, followed by the corresponding secondary antibodies (Lianke®, Hangzhou, China). TBST with 5% (w/v) skim milk was used to dilute antibodies for immunoblotting. Antibodies for GFP (AG279) were purchased from the Beyotime Institute of Biotechnology (Shanghai, China); Antibodies for YFP (632381) was obtained from Clontech; Antibodies against ATG7 (ab99001) was purchased from Abcam (Shanghai, China). The levels of plant-actin were analyzed as controls for different treatments by western analysis using

plant-actin antibodies (E12-053, Enogene® Biotech, New York, NY, United States) (Yue et al., 2012). All digital images were analyzed in Image J when necessary.

Statistical Analysis

All results were repeated at least three times. Statistical analysis was performed with an ANOVA in SPSS software. Statistical significance was accepted at the level of *P < 0.05, **P < 0.01.

RESULTS

D-Glucose Activates the Autophagosomes

AtRGS1 serves as a receptor for glucose which induces its endocytosis (Grigston et al., 2008; Urano et al., 2012). Autophagy is a regulated vacuolar degradation pathway (Bassham, 2007). ATG8a protein is used as an alternative marker of autophagy. The green punctate structures, which could be labeled by GFP-ATG8a, are usually considered to be autophagosomes and their intermediates. The ATG8a protein always adheres to the autophagic vacuoles in the process of autophagic transport (Contento et al., 2005; Yoshimoto et al., 2009). To assess how the autophagy-related signaling pathway was activated in signal transduction pathways mediated by D-glucose, we examined root cells of GFP-ATG8a transgenic seedlings to see if autophagosomes were induced by D-glucose in *Arabidopsis thaliana*. Therefore, before and after D-glucose treatment, the green punctate structures were examined using laser confocal scanning microscopy. Concanamycin A (CA) is an inhibitor of the vacuolar type H⁺-ATPase (V-ATPase) that has been used to inhibit degradation by reducing the activity of vacuoles to stabilize autophagic cargoes (Kim et al., 2013; Shin et al., 2014). Before observation, the starved seedlings were treated with CA.

As observed in **Figure 1**, in the root cells of GFP-ATG8a plants, a small number of autophagosomes were detected in starved seedlings for 2 h (**Figure 1B**) and 2.5 h (**Figure 1C**). Addition of D-glucose led to dramatic changes. There was a significant increase of autophagosomes. These results indicate that D-glucose could cause AtRGS1 endocytosis by acting as a signaling factor to activate the formation of autophagosomes.

Induction of Autophagic Flux by D-Glucose

Autophagic flux was measured by western blotting using GFP antibodies in GFP-ATG8a transgenic *Arabidopsis* (Gao et al., 2016). During transport to the vacuolar lumen, GFP-ATG8, as a marker of autophagy, is often degraded to release free GFP, which was used to measure autophagic flux (Li et al., 2014). As shown in **Figure 2**, compared to the seedlings D-glucose treated for 0 h, seedlings treated for 0.5 and 2 h showed a higher level of GFP, in a time dependent manner (**Figure 2**). Our data indicate autophagic flux was induced by D-glucose in the plants of GFP-ATG8a, demonstrating that GFP-ATG8 was transported to the vacuolar lumen.

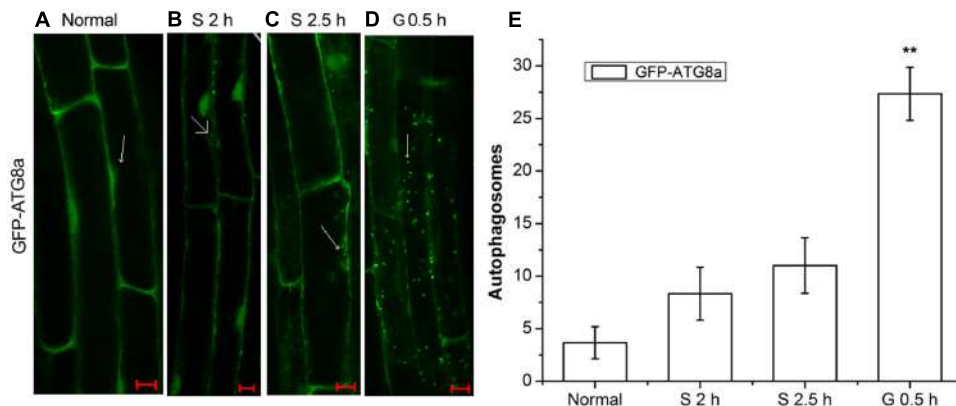


FIGURE 1 | The observation of autophagosomes. Autophagosomes labeled by GFP-ATG8a in root cells of GFP-ATG8a plants with incubation in 1 μ M CA. **(A)** Normal seedlings. **(B)** Starved seedlings for 2 h. **(C)** Starved seedlings for 2.5 h. **(D)** Starved seedlings for 2 h stimulated by 6% D-glucose for 0.5 h. **(E)** Quantification of the GFP-ATG8a-labeled autophagosomes per cell. Root cells at the indicated times was used to calculate the autophagic activity. The mean and SD values were calculated from roots of six seedlings per time point. Results in three parallel experiments were used for the quantification. The asterisks indicate significant differences from the starved seedlings treated with D-glucose for 0 h. Scale bars, 10 μ m (** P < 0.01).

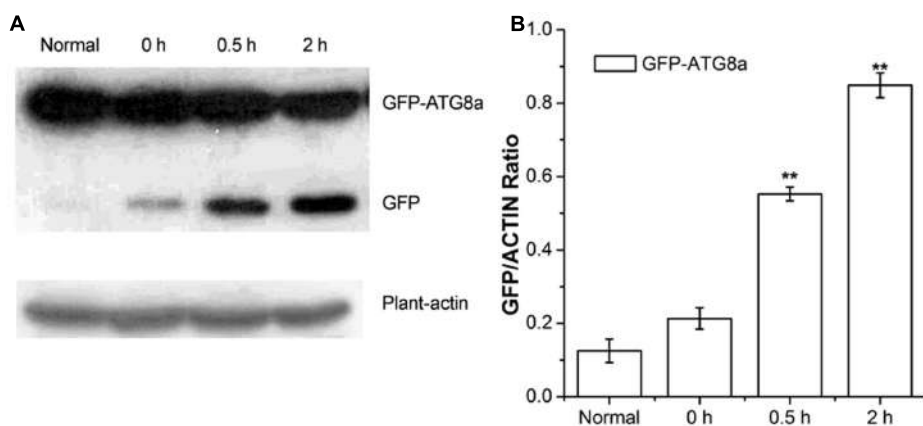


FIGURE 2 | Analysis of autophagic flux in GFP-ATG8a. Five-day-old seedlings of GFP-ATG8a were starved by liquid MS medium without sugar following stimulation by 1% D-glucose for 0, 0.5, and 2 h. **(A)** Equal amounts of protein extracted from the seedlings were used to SD-PAGE, followed by western blotting with anti-GFP and anti-plant-actin antibodies. **(B)** Quantification of changes in free GFP normalized with the expression of plant-actin. Asterisks indicate significant differences from starved seedlings treated with 1% D-glucose for 0 h at * P < 0.05 or ** P < 0.01. Error bar represent SD obtained from three independent replicates.

Autophagy-Related Genes Expressions Rise in Wild-Type after D-Glucose Treatment

Recently, several *Arabidopsis thaliana* autophagy-related (ATG) genes have been identified and their functions of them have been well-assessed (Liu and Bassham, 2012). Five functional groups, ATG1 composite enzyme complex, Beclin1-phosphatidylinositol 3-kinase (PI3K), ATG9 complex and two ubiquitination-like conjugation systems including ATG12-ATG5 and ATG8-PE, participate in the process of autophagosome formation (Hofius et al., 2011; Shpilka et al., 2015). To investigate the function of autophagy in the AtRGS1-mediated sugar signaling pathway in *Arabidopsis thaliana*, we studied the D-glucose-induced ATG gene expression in both *Atrgs1-2* mutants and wild-type (WT) plants. qRT-PCR analyses showed that after D-glucose treatment,

the transcript levels of all seven ATG genes were induced to a much higher level in WT plants than in *Atrgs1-2* null plants, indicating that AtRGS1 is required for the expression of these seven ATG genes upon D-glucose stimulation (Figure 3). In addition, the induction of ATG was slower than *Atrgs1-2* null plants than in WT plants. The expression level of ATG1, ATG4b, and ATG12a rose at 2 h in *Atrgs1-2* (Figures 3A,D,G). However, in WT, the expression level of the ATG genes reduced when treated with D-glucose for 2 h, but still higher than the expression when treated with D-glucose for 0 h except ATG4b (Figure 3D). Therefore, we believe that AtRGS1 plays an essential role in D-glucose-induced expression of autophagy genes.

In the complicated process of the autophagosome formation, five functional groups of ATG proteins are needed to form autophagosomes at the certain stage (Thompson et al., 2005;

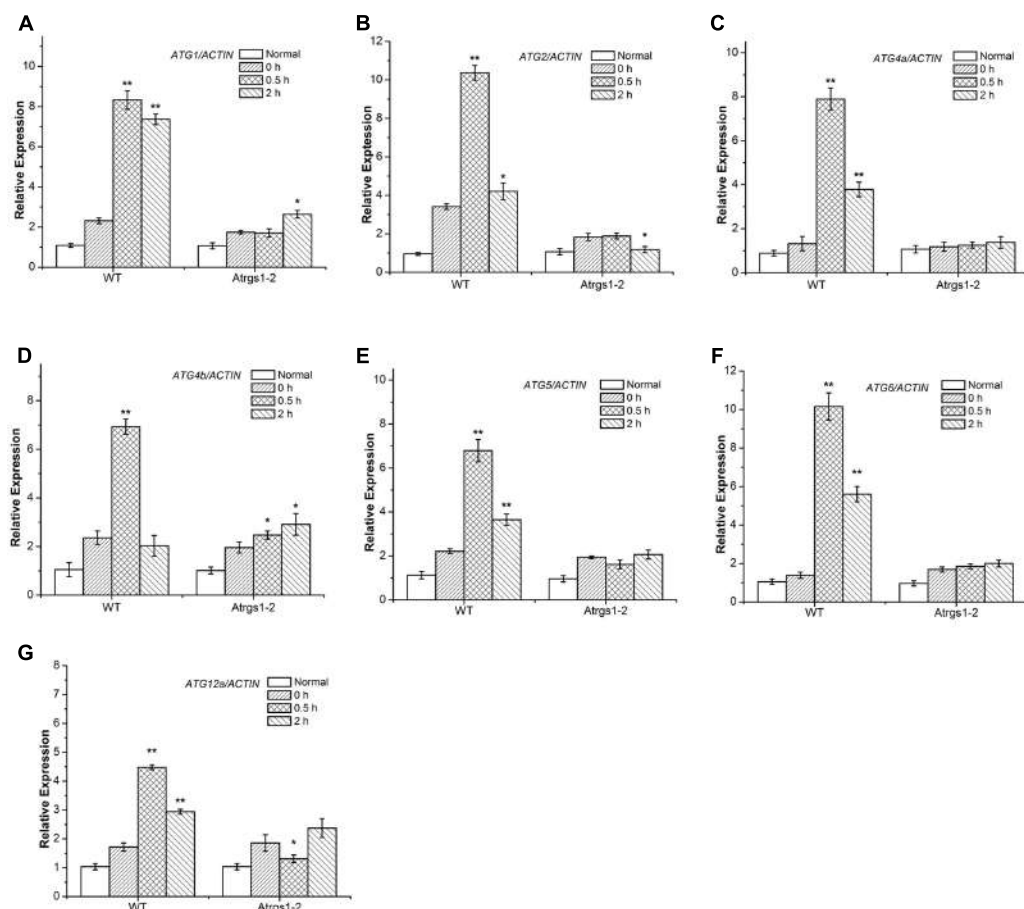


FIGURE 3 | Expression of autophagy related genes in Atrgs1-2 and wild-type (WT) in response to D-glucose. Expression of ATG1 (A), ATG2 (B), ATG5 (C), ATG4a (D), ATG4b (E), ATG6 (F), ATG12a (G) in normal conditions and D-glucose treatment for 0, 0.5, and 2 h. Total RNA isolated from Atrgs1-2 and WT was subjected to qRT-PCR using gene-specific primers. Data represent mean and SD of at least three independent experiments. The asterisk indicates a significant difference from the starved seedlings treated with 1% D-glucose for 0 h (*P < 0.05 or **P < 0.01).

Seay et al., 2006). The ATG1 which encodes a protein kinase participates in the autophagy activation and autophagosome initiation (Kamada et al., 2010; Suttangkakul et al., 2011; Noda and Fujioka, 2015), and ATG6/ PI3K is essential for the nucleation of autophagic vacuoles (Patel and Dinesh-Kumar, 2008). We found a significant increase in the transcript levels of ATG1 and ATG6 in WT after 0.5 h D-glucose induction (Figures 3A,F), suggesting that autophagy was induced and autophagic vacuoles were nucleated. The ATG9 complex was sufficient for the membrane formation of autophagosomes. ATG2 transcript level dramatically increased in response to treatment with D-glucose in WT (Figure 3B). The ATG12-ATG5 and ATG8-phosphatidylethanolamine (PE) conjugation systems are two ubiquitination-related conjugation system of autophagy, which are essential for the formation and closure of autophagic vesicles and the subsequent delivery to the vacuole (Thompson et al., 2005; Li et al., 2012; Ohsumi, 2014). As shown in Figures 3C–E,G, the increase of ATG4a, ATG4b, ATG5, and ATG12a expression after 0.5 h of stimulation suggested that the two ubiquitin-like protein-conjugating pathways were

activated. Autophagy-related gene expression increased in WT, indicating that D-glucose had an important role in the formation of the five functional groups, and promoted the formation of autophagosomes.

The Expression of ATG7 Protein Rises in Wild-Type upon D-Glucose Stimulation

The E1-like ATG7-activating enzyme is required to form ATG8-phosphatidylethanolamine (PE) and ATG12-ATG5 conjugation systems, subsequently E2-conjugating enzymes, ATG3 and ATG10 combine ATG8 and ATG12 with PE and ATG5 (Wang P. et al., 2016). To elucidate the response of autophagy to D-glucose, we examined the autophagosome generation under D-glucose; ATG7 (76 kDa) protein levels were analyzed by western blot using an anti-ATG7 antibody. In WT, the expression of ATG7 protein significantly increased in response to D-glucose (Figures 4A,B). On the contrary, in Atrgs1-2 mutants, the expression of ATG7 only slightly increased after D-glucose application (Figures 4A,B). The data obtained in the experiment

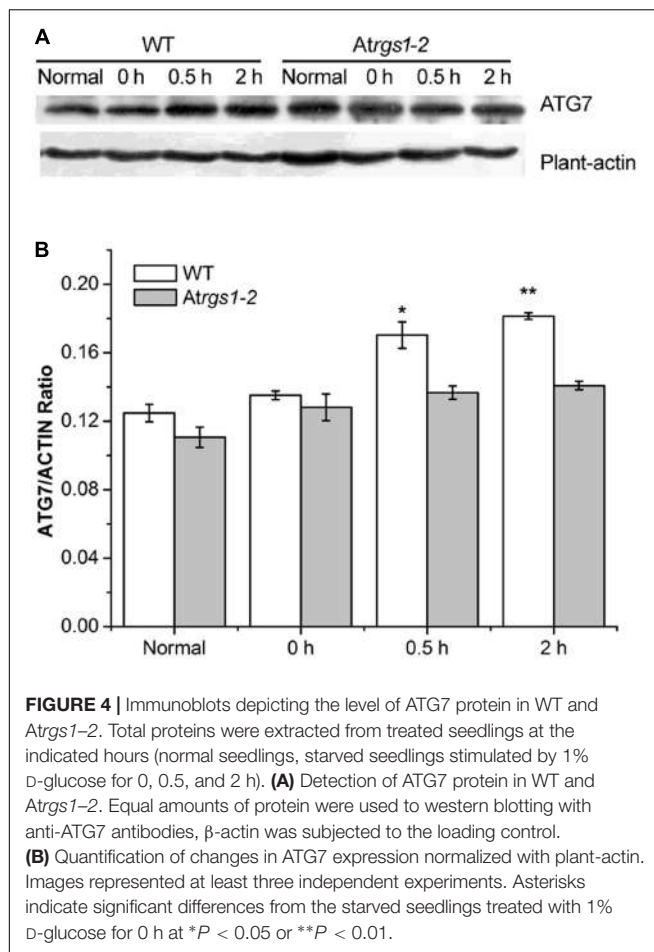


FIGURE 4 | Immunoblots depicting the level of ATG7 protein in WT and Atrgs1-2. Total proteins were extracted from treated seedlings at the indicated hours (normal seedlings, starved seedlings stimulated by 1% D-glucose for 0, 0.5, and 2 h). **(A)** Detection of ATG7 protein in WT and Atrgs1-2. Equal amounts of protein were used to western blotting with anti-ATG7 antibodies, β -actin was subjected to the loading control. **(B)** Quantification of changes in ATG7 expression normalized with plant-actin. Images represented at least three independent experiments. Asterisks indicate significant differences from the starved seedlings treated with 1% D-glucose for 0 h at $*P < 0.05$ or $**P < 0.01$.

suggested that AtRGS1 promoted the expression of ATG7 after D-glucose treatment.

ATG2 and ATG5 Inhibit the Recovery of AtRGS1 in Response to D-Glucose

Autophagy is a precise and complex machinery used to degrade and recycle intracellular molecules in plants during response and survival to environmental stresses (Kulich et al., 2013; Bassham and Crespo, 2014). The disruption of the ATG2 and ATG5 gene blocks the formation of autophagosomes (Ishida et al., 2008; Phillips et al., 2008; Lee et al., 2014). AtRGS1, as a D-glucose receptor, mediates sugar signaling pathway by endosomes. To investigate the cellular function of autophagy during the AtRGS1 response to D-glucose, the levels of AtRGS1-YFP protein were assessed by the immunoblot analysis using an anti-YFP antibody in AtRGS1-YFP, *atg2*, and *atg5* autophagy-deficient mutants.

Our data showed that AtRGS1-YFP protein expression levels were reduced after starvation, but, increased after D-glucose application in the plants of AtRGS1-YFP and the two autophagy-deficient mutants (Figures 5A–D). However, after 2 h starvation, AtRGS1-YFP protein in AtRGS1-YFP plants reduced more than that in the two mutants (Figure 5D). That means ATG2 and ATG5 promote the decrease of AtRGS1 protein under starvation treatment. After glucose application, AtRGS1-YFP

protein recovery in AtRGS1-YFP plants was slower than that in *atg2* and *atg5* mutants (Figure 5D). These results demonstrated that ATG2 and ATG5 inhibit the AtRGS1 protein recovery after D-glucose treatment.

ATG2 and ATG5 Promote the Endocytosis of AtRGS1 in Response to D-Glucose

It has been proven that D-glucose induces AtRGS1 endocytosis (Grigston et al., 2008). To determine whether autophagy functions to mediate endocytosis of AtRGS1 after D-glucose application, we analyzed the subcellular distribution of YFP fluorescence by using laser confocal scanning microscopy in AtRGS1-YFP, *atg2* and *atg5* plants. In AtRGS1-YFP plants, endocytosis occurred after D-glucose application (Figure 6A). But, in *atg2* and *atg5* mutants, AtRGS1-YFP was mainly localized to the plasma membrane, and the internalization rate increased only slightly in response to D-glucose (Figures 5B–D). The results were consistent with the movement of AtRGS1-YFP in AtRGS1-YFP, *atg2* and *atg5* plants (Supplementary Figure S2). These results revealed that under the stimulation of D-glucose, when the autophagy pathway was deficient in *atg2* and *atg5* plants, the endocytosis of AtRGS1 was inhibited. AtRGS1 is mainly localized on the plasma membrane. Our data demonstrated that means ATG2 and ATG5 promote AtRGS1 endocytosis.

DISCUSSION

AtRGS1, which is proposed to be an extracellular receptor for D-glucose, accelerates the hydrolysis of AtGPA1 to negatively regulate G-protein signaling (Urano et al., 2012). Our study indicated that D-glucose could activate autophagy and that autophagy pathway did not function well in Atrgs1-2 mutants. The rapid recovery of AtRGS1 in *atg2* and *atg5* mutants suggested that the autophagy pathway might be involved in inhibition of the recovery of AtRGS1 in response to D-glucose. AtRGS1 endocytosis was inhibited and it mainly located on the plasma membrane in plants of *atg2* and *atg5*, indicating that ATG2 and ATG5 promote the endocytosis of AtRGS1. In this study we have demonstrated that autophagy is required for regulation of the AtRGS1-mediated sugar signaling pathway in response to D-glucose.

The Autophagy Pathway Is Induced by D-Glucose

In plants, glucose as a metabolite or signaling molecule affects gene and protein expressions, and growth and developmental programs (Sheen, 2014; Huang et al., 2015). Autophagy is an intracellular degradation system conserved in eukaryotic cells that consists of the formation of double-membrane structures called autophagosomes that engulf and sequester the cytoplasmic components and then fuse them with the endosome/vacuole and finally break them down in the vacuole (Bassham, 2007; Wang P. et al., 2016).

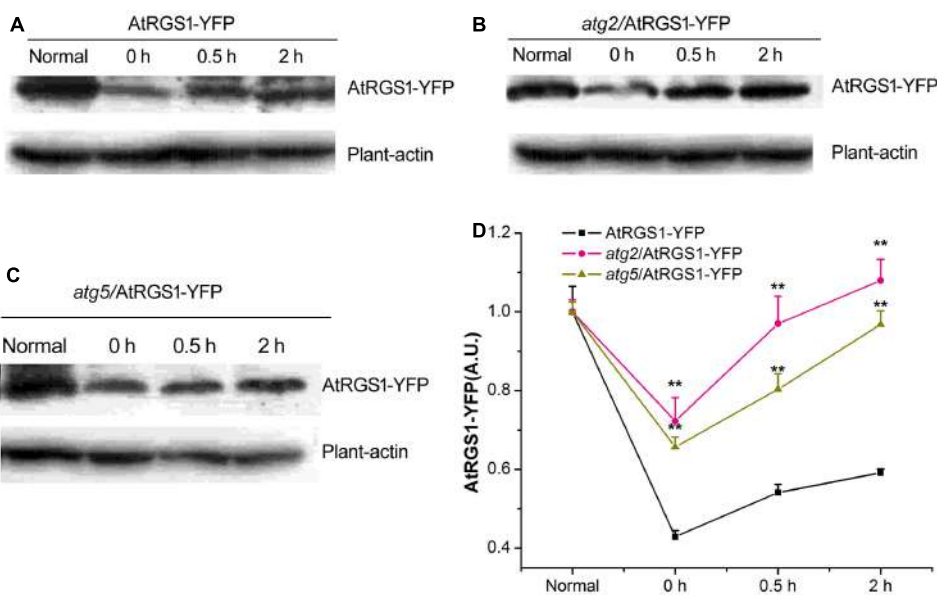


FIGURE 5 | Detection of AtRGS1-YFP protein. The seedlings of AtRGS1-YFP (**A**), *atg2*/AtRGS1-YFP (**B**), *atg5*/AtRGS1-YFP (**C**) grown in liquid MS medium, then starved for 2 h, followed by 1% D-glucose application for 0, 0.5, and 2 h. Then the expression of AtRGS1-YFP protein were analyzed with anti-YFP antibodies. Plant-actin was used as the uniform protein loading. (**D**) Quantification of the level of AtRGS1-YFP protein following normalization to the expression of plant-actin in the three seedlings. Asterisks indicated significant differences from the seedlings of AtRGS1-YFP at each time point at $*P < 0.05$ or $**P < 0.01$.

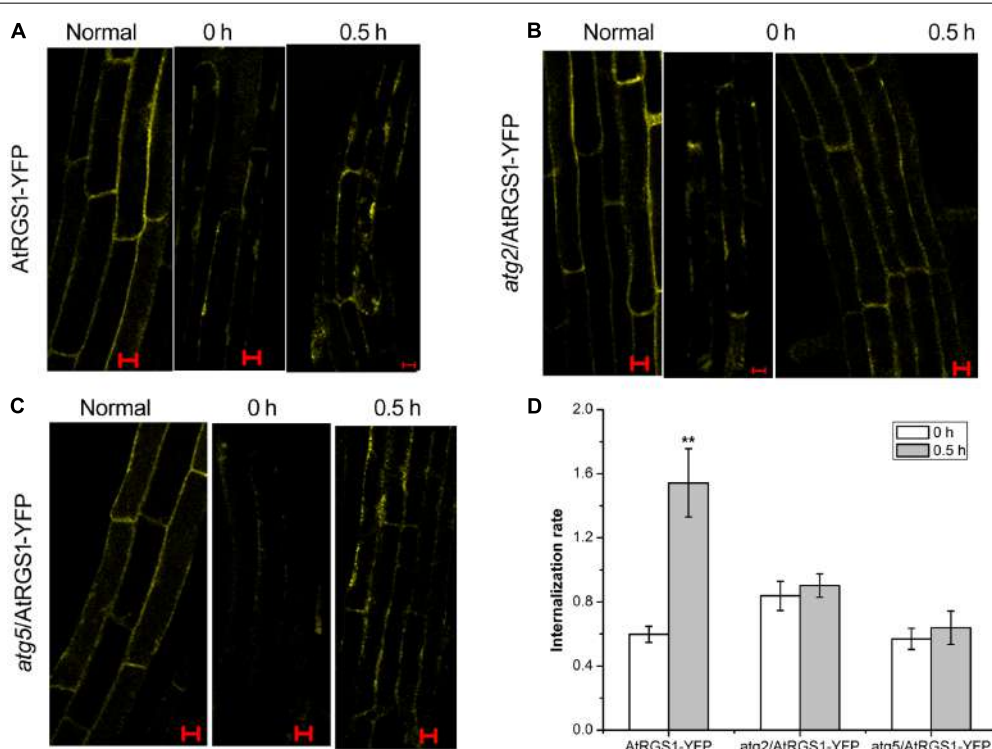


FIGURE 6 | Confocal imaging of endocytosis of AtRGS1 in the plant of AtRGS1-YFP (**A**), *atg2*/AtRGS1-YFP (**B**), *atg5*/AtRGS1-YFP (**C**) (normal seedlings, starved seedlings stimulated by 6% D-glucose for 0 and 0.5 h). Scale bars represent 10 μ m. (**D**) Quantification of AtRGS1-YFP internalization rate. Internalization rate was calculated by dividing the internalization of the starved seedlings treated with D-glucose for 0 or 0.5 h by the internalization of the normal seedlings. Experiments were performed three independent replicates with similar results. Asterisks, significant differences from the starved seedlings treated with D-glucose for 0 h, $**P < 0.01$.

Punctate-like structures labeled by GFP-ATG8a, which represent autophagosomes and their intermediates, appear in large numbers after treatment with D-glucose (**Figure 1**). Autophagic flux is often utilized to measure the degradation activity of autophagic substrates within the vesicular system (Mizushima et al., 2010; Loos et al., 2014). The increase of the accumulation of free GFP dependent on time implied that autophagic flux was induced by D-glucose in GFP-ATG8a plants (**Figure 2**), suggesting that autophagosomes were transported to the vacuole for breakdown. The assembly of five functional groups of ATG proteins is required for the formation of autophagy (Obara and Ohsumi, 2011). The increase of the expression autophagy-related gene expression in WT indicated that D-glucose promoted formation of autophagosomes (**Figure 3**). E1-like ATG7-activating enzyme is essential for the formation of ATG8-phosphatidylethanolamine (PE) and ATG12-ATG5 conjugation systems (Wang P. et al., 2016). After induction with D-glucose, the increased level of ATG7 protein in WT promotes the formation of two ubiquitination conjugation systems (**Figure 4**). Previous research has shown that the autophagic flux was inhibited in *atg7* mutants in *Arabidopsis thaliana* (Shin et al., 2014; Wang X.D. et al., 2016). In WT, the increased level of ATG7 protein induced by D-glucose will likely promote the autophagic flux (**Figure 4**). Taken together, these results indicate that D-glucose induces autophagy, which plays an important role in intracellular homeostasis.

AtRGS1 Is Required for Autophagy Pathway Induced by D-Glucose

In *Arabidopsis thaliana*, three signaling pathways that are sensitive to glucose have been analyzed. (1) The hexokinase 1 (AtHXK1) pathway: AtHXK1 is recognized as glucose sensor involving in the metabolic and physiological processes by mediating gene transcription in response to glucose (Sheen, 2014). (2) The glycolysis-dependent SNF1-RELATED KINASE1/TARGET OF RAPAMYCIN (SnRK1/TOR) pathway: the glycolysis-dependent SnRK1/TOR pathway acts as cellular energy sensors regulated growth and development (Lastdrager et al., 2014). (3) The AtRGS1-dependent G-protein-coupled signaling pathway: G-protein-coupled pathways involving AtRGS1 are involved in sugar signaling (Grigston et al., 2008). Genetic evidence suggests that D-glucose causes AtRGS1 endocytosis or a sugar metabolite regulates AtRGS1 activity toward AtGPA1 (Urano et al., 2012).

Our results demonstrate that D-glucose induces autophagy pathway in WT *Arabidopsis* plants (**Figures 1–4**). However, in *Atrgs1-2* mutants after D-glucose application, the analysis of qRT-PCR data indicate that the autophagy pathway did not function well (**Figure 3**), and the expression of ATG7 increase only slightly (**Figure 4**). The E1-like ATG7-activating enzyme is required to form the two ubiquitin-like protein-conjugating pathways (Wang P. et al., 2016), so we hypothesize that D-glucose induces the formation and activation of ATG8-phosphatidylethanolamine (PE) and ATG12-ATG5 conjugation systems, which are closely

related to AtRGS1. A lot of evidence (**Figures 3, 4**) has been provided in support of the relationship between autophagy and AtRGS1 protein. Autophagy has been shown to be involved in AtRGS1-mediated sugar signaling pathway.

ATG2 and ATG5 Regulate the Recovery and Endocytosis of AtRGS1 after D-Glucose Stimulation

Autophagy appears to be the main contributor to the maintenance of the equilibrium with different environmental stresses and the degradation and reuse of nutrients (Li et al., 2012; Liu and Bassham, 2012; Ohsumi, 2014; Wang P. et al., 2016). Endocytosis is a major route of entry for plasma membrane proteins or extracellular materials into the cell for recycling back to the plasma membrane, or degradation in the vacuole. Endocytosis plays an important role in the process of cellular responses to environmental stimuli and signaling transduction (Fan et al., 2015; Michaeli et al., 2016).

In mammalian cells, autophagosomes probably fuse with endosomes of GPCRs induced by agonists for degradation, or endosomes of GPCRs involve recycling via the endosome. In plants, the AtRGS1 interacted with some relative proteins stimulates the endocytosis of AtRGS1 and promotes downstream signaling pathway (Urano et al., 2012). AtWNK kinases recruited by D-glucose phosphorylate AtRGS1 to mediate endocytosis (Urano et al., 2012). The interactions between AtRGS1 and small GTPases molecules of RAB (Ras-like small GTP binding) and ARF (ADP-ribosylation factor) are hypothesized to regulate AtRGS1 to be endocytosed into the cytoplasm, then recycled back to the plasma membrane via recycling endosomes (Jaiswal et al., 2015).

In *Arabidopsis thaliana*, D-glucose induced the increase of the levels of AtRGS1-YFP protein expression in the plants of AtRGS1-YFP and *atg2* and *atg5* mutants (**Figures 5A–D**). After D-glucose application, AtRGS1-YFP proteins recovered more rapidly in *atg2* and *atg5* mutants than that in AtRGS1-YFP plants, indicating that ATG2 and ATG5 inhibited the AtRGS1 protein recovery after D-glucose treatment. Therefore, we conclude that autophagy pathway regulates AtRGS1 recovery (**Figure 5**).

However, in autophagy-deficient *atg2* and *atg5* mutants, the endocytosis of AtRGS1 was inhibited, indicating that ATG2 and ATG5 promote the endocytosis of AtRGS1 in response to D-glucose (**Figure 6**). Endocytosis of AtRGS1 physically uncouples the GTPase-accelerating activity of AtRGS1 from the G protein, which permits sustained activation (Urano et al., 2012). Perhaps inhibition of endocytosis of AtRGS1 leads to a physical coupling of AtRGS1 with AtGPA1 and concomitant inhibition of G-protein signaling.

In plants, endocytic and autophagic pathways interplay. Autophagosomes fuse with the endosome/vacuole, and degrade in the vacuole (Zhuang et al., 2015). So we hypothesize endocytosis of AtRGS1 and autophagic pathways interplay in *Arabidopsis thaliana*, and autophagic pathways have an effect on

the recycling back to the plasma membrane, or degradation in the vacuole of AtRGS1.

Further study aims to determine whether AtRGS1-YFP co-localized with autophagic bodies after D-glucose stimulation. This study is essential for extending our knowledge of the relationship between AtRGS1 and autophagy.

AUTHOR CONTRIBUTIONS

QY and WC conceived and designed the experiments. QY and JW performed research. QY, ZF, and WC analyzed the data. QY and ZF wrote the manuscript.

FUNDING

This research was supported by the National Natural Science Foundation of China (Grant Numbers 31570256 and 31170250), and the Natural Science Foundation of Guangdong Province, China (Grant Number, 2014A030313420).

ACKNOWLEDGMENTS

We thank Professor Alan M. Jones for providing seeds from *Atrgs1-2* mutant and the 35S::AtRGS1-YFP (35S::AtRGS1 was subcloned into pEarleyGate101) *Agrobacterium*. We also

REFERENCES

- Bassham, D. C. (2007). Plant autophagy—more than a starvation response. *Curr. Opin. Plant Biol.* 10, 587–593. doi: 10.1016/j.pbi.2007.06.006
- Bassham, D. C., and Crespo, J. L. (2014). Autophagy in plants and algae. *Front. Plant Sci.* 5:679. doi: 10.3389/fpls.2014.00679
- Bradford, W., Buckholz, A., Morton, J., Price, C., Jones, A. M., and Urano, D. (2013). Eukaryotic G protein signaling evolved to require G protein-coupled receptors for activation. *Sci. Signal.* 6, ra37. doi: 10.1126/scisignal.2003768
- Caplan, J., Padmanabhan, M., and Dinesh-Kumar, S. P. (2008). Plant NB-LRR immune receptors: from recognition to transcriptional reprogramming. *Cell Host Microbe* 3, 126–135. doi: 10.1016/j.chom.2008.02.010
- Chanoca, A., Kovinich, N., Burkell, B., Stecha, S., Bohorquez-Restrepo, A., Ueda, T., et al. (2015). Anthocyanin vacuolar inclusions form by a microautophagy mechanism. *Plant Cell* 27, 2545–2559. doi: 10.1105/tpc.15.00589
- Chen, J. G., Willard, F. S., Huang, J., Liang, J., Chasse, S. A., Jones, A. M., et al. (2003). A seven-transmembrane RGS protein that modulates plant cell proliferation. *Science* 301, 1728–1731. doi: 10.1126/science.1087790
- Contento, A. L., Xiong, Y., and Bassham, D. C. (2005). Visualization of autophagy in *Arabidopsis* using the fluorescent dye monodansylcadaverine and a GFP-AtATG8e fusion protein. *Plant J.* 42, 598–608. doi: 10.1111/j.1365-313X.2005.02396.x
- Fan, L., Li, R., Pan, J., Ding, Z., and Lin, J. (2015). Endocytosis and its regulation in plants. *Trends Plant Sci.* 20, 388–397. doi: 10.1016/j.tplants.2015.03.014
- Fu, Y., Lim, S., Urano, D., Tunc-Ozdemir, M., Phan, N. G., Elston, T. C., et al. (2014). Reciprocal encoding of signal intensity and duration in a glucose-sensing circuit. *Cell* 156, 1084–1095. doi: 10.1016/j.cell.2014.01.013
- Fujioka, Y., Noda, N. N., Fujii, K., Yoshimoto, K., Ohsumi, Y., and Inagaki, F. (2008). *In vitro* reconstitution of plant Atg8 and Atg12 conjugation systems essential for autophagy. *J. Biol. Chem.* 283, 1921–1928. doi: 10.1074/jbc.M706214200
- Gao, Y. Y., Wang, X. D., Ma, C., and Chen, W. L. (2016). EDS1-mediated activation of autophagy regulates PstDC3000 (AvrRps4)-induced programmed cell death in *Arabidopsis*. *Acta Physiol. Plant* 38, 150. doi: 10.1007/s11738-016-2160-4
- Garcia-Marcos, M., Ear, J., Farquhar, M. G., and Ghosh, P. (2011). A GDI (AGS3) and a GEF (GIV) regulate autophagy by balancing G protein activity and growth factor signals. *Mol. Biol. Cell* 22, 673–686. doi: 10.1091/mbc.E10-08-0738
- Grigston, J. C., Osuna, D., Scheible, W. R., Liu, C., Stitt, M., and Jones, A. M. (2008). D-Glucose sensing by a plasma membrane regulator of G signaling protein, AtRGS1. *FEBS Lett.* 582, 3577–3584. doi: 10.1016/j.febslet.2008.08.038
- He, C., and Klionsky, D. J. (2009). Regulation mechanisms and signaling pathways of autophagy. *Annu. Rev. Genet.* 43, 67–93. doi: 10.1146/annurev-genet-102808-114910
- Hofius, D. M., Bressendorff, S., Mundy, J., and Petersen, M. (2011). Role of autophagy in disease resistance and hypersensitive response-associated cell death. *Cell Death Differ.* 18, 1257–1262. doi: 10.1038/cdd.2011.43
- Hu, G., Suo, Y., and Huang, J. (2013). A crucial role of the RGS domain in trans-Golgi network export of AtRGS1 in the protein secretory pathway. *Mol. Plant* 6, 1933–1944. doi: 10.1093/mp/sst109
- Huang, J. P., Meral Tunc-Ozdemir, M., Chang, Y., Alan, M., and Jones, A. M. (2015). Cooperative control between AtRGS1 and AtHXR1 in a WD40-repeat protein pathway in *Arabidopsis thaliana*. *Front. Plant Sci.* 6:851. doi: 10.3389/fpls.2015.00851
- Ishida, H., Yoshimoto, K., Izumi, M., Reisen, D., Yano, Y., Makino, A., et al. (2008). Mobilization of rubisco and stroma-localized fluorescent proteins of chloroplasts to the vacuole by an ATG gene-dependent autophagic process. *Plant Physiol.* 148, 142–155. doi: 10.1104/pp.108.122770
- Jaiswal, D. K., Werth, E. G., McConnel, E. W., Hicks, L. M., and Jones, A. M. (2015). Time-dependent, glucose-regulated *Arabidopsis* regulator of G-protein signaling 1 network. *Curr. Plant Biol.* 5, 25–35. doi: 10.1093/jxb/ers399
- Jeffrey, C. G., Osuna, D., Scheible, W. R., Liu, C., Stitt, M., and Jones, A. M. (2008). D-glucose sensing by a plasma membrane regulator of G signaling protein, AtRGS1. *FEBS Lett.* 582, 3577–3584. doi: 10.1016/j.febslet.2008.08.038
- thank Dr. Li Faqiang for providing the transgenic *Arabidopsis* expressing GFP-ATG8a.

SUPPLEMENTARY MATERIAL

The Supplementary Material for this article can be found online at: <http://journal.frontiersin.org/article/10.3389/fpls.2017.01229/full#supplementary-material>

FIGURE S1 | (A) The transgenic lines (AtRGS1-YFP, *atg2*/AtRGS1-YFP and *atg5*/AtRGS1-YFP) and WT were screened on MS plates with Basta (10 µg/mL). DNA was respectively isolated from eight seedlings (1–8) of *atg2*/AtRGS1-YFP (**B**), *atg5*/AtRGS1-YFP (**C**), and *Atrgs1-2* (**E**). WT acts as a control. Homozygous for DNA-insertion were confirmed by PCR of genomic DNA with the primers. The products were electrophoresed on a 1% gel for 30 min, then detected by using UV illumination. (**D**) qRT-PCR was performed to analyze transcription level of AtRGS1 in AtRGS1-YFP, *atg2*/AtRGS1-YFP and *atg5*/AtRGS1-YFP lines grown on MS plates for 7 days. Data represent mean and SD of at least three independent experiments. The asterisk indicates a significant difference from WT (**P < 0.01).

FIGURE S2 | Movement of AtRGS1-YFP in the plant of AtRGS1-YFP (**A**), *atg2* (**B**), *atg5* (**C**). Root cells of seedlings located approximately in the elongation region were imaged using a Zeiss LSM 510 confocal laser scanning microscope (LCSM, LSM 510/ConfoCor 2, Carl-Zeiss, Jena, Germany). The normal seedlings were observation in response to D-glucose. Scale bars represent 10 µm. (**D**) Quantification of AtRGS1-YFP internalization rate. Internalization rate was calculated by dividing the internalization of the normal seedlings treated with D-glucose for 5, 10, or 15 min by the internalization of the normal seedlings treated with D-glucose for 0 min. Experiments were performed three independent replicates with similar results. Asterisks, significant differences from the starved seedlings treated with D-glucose for 0 min, *P < 0.05 or **P < 0.01.

- Johnston, C. A., Taylor, J. P., Gao, Y., Kimple, A. J., Grigston, J. C., Chen, J. G., et al. (2007). GTPase acceleration as the rate-limiting step in *Arabidopsis* G protein-coupled sugar signaling. *Proc. Natl. Acad. Sci. U.S.A.* 104, 17317–17322. doi: 10.1073/pnas.0704751104
- Kamada, Y., Yoshino, K., Kondo, C., Kawamata, T., Oshiro, N., Yonezawa, K., et al. (2010). Tor directly controls the Atg1 kinase complex to regulate autophagy. *Mol. Cell. Biol.* 30, 1049–1058.
- Kang, S. G., Price, J., Lin, P. C., Hong, J. C., and Jang, J. C. (2010). The *Arabidopsis* bZIP1 transcription factor is involved in sugar signaling, protein networking, and DNA binding. *Mol. Plant* 3, 361–373. doi: 10.1093/mp/ssp115
- Kim, J., Lee, H., Lee, H. N., Kim, S. H., Shin, K. D., and Chung, T. (2013). Autophagy-related proteins are required for degradation of peroxisomes in *Arabidopsis* hypocotyls during seedling growth. *Plant Cell* 25, 4956–4966. doi: 10.1105/tpc.113.117960
- Kulich, I., Pecenкова, T., Sekeres, J., Smetana, O., Fendrych, M., Foissner, I., et al. (2013). *Arabidopsis* exocyst subcomplex containing subunit EXO70B1 is involved in autophagy-related transport to the vacuole. *Traffic* 14, 1155–1165. doi: 10.1111/tra.12101
- Lastdrager, J., Hanson, J., and Smeekens, S. (2014). Sugar signals and the control of plant growth and development. *J. Exp. Bot.* 65, 799–807. doi: 10.1093/jxb/ert474
- Law, B. Y., Mok, S. W., Wu, A. G., Lam, C. W., Yu, M. X., and Wong, V. K. (2016). New potential pharmacological functions of Chinese herbal medicines via regulation of autophagy. *Molecules* 21:359. doi: 10.3390/molecules21030359
- Lee, H. N., Kim, J., and Chung, T. (2014). Degradation of plant peroxisomes by autophagy. *Front. Plant Sci.* 5:139. doi: 10.3389/fpls.2014.00139
- Li, F., Chung, T., and Vierstra, R. D. (2014). Autophagy-related 11 plays a critical role in general autophagy-and senescence-induced mitophagy in *Arabidopsis*. *Plant Cell* 26, 788–807. doi: 10.1105/tpc.113.120014
- Li, F., and Vierstra, R. D. (2012). Autophagy: a multifaceted intracellular system for bulk and selective recycling. *Trends Plant Sci.* 17, 526–537. doi: 10.1016/j.tplants.2012.05.006
- Li, Z., Yue, H., and Xing, D. (2012). MAP Kinase 6-mediated activation of vacuolar processing enzyme modulates heat shock-induced programmed cell death in *Arabidopsis*. *New Phytol.* 195, 85–96. doi: 10.1111/j.1469-8137.2012.04131.x
- Liu, Y., and Bassham, D. C. (2012). Autophagy: pathways for self-eating in plant cells. *Annu. Rev. Plant Biol.* 63, 215–237. doi: 10.1146/annurev-arplant-042811-105441
- Loos, B., du Toit, A., and Hofmeyr, J. H. (2014). Defining and measuring autophagosome flux—concept and reality. *Autophagy* 10, 2087–2096. doi: 10.4161/15548627.2014.973338
- Mackey, D., Belkhadir, Y., Alonso, J. M., Ecker, J. R., and Dangl, J. L. (2003). *Arabidopsis* RIN4 is a target of the type III virulence effector AvrRpt2 and modulates RPS2-mediated resistance. *Cell* 112, 379–389. doi: 10.1016/S0092-8674(03)00040-0
- Michaeli, S., Galili, G., Genschik, P., Fernie, A. R., and Avin-Wittenberg, T. (2016). Autophagy in plants—what's new on the menu? *Trends Plant Sci.* 21, 134–144. doi: 10.1016/j.tplants.2015.10.008
- Mizushima, N., Yoshimori, T., and Levine, B. (2010). Methods in mammalian autophagy research. *Cell* 140, 313–326. doi: 10.1016/j.cell.2010.01.028
- Mizushima, N., Yoshimori, T., and Ohsumi, Y. (2011). The role of Atg proteins in autophagosome formation. *Annu. Rev. Cell Dev. Biol.* 27, 107–132. doi: 10.1146/annurev-cellbio-092910-154005
- Noda, N. N., and Fujioka, Y. (2015). Atg1 family kinases in autophagy initiation. *Cell Mol. Life Sci.* 72, 3083–3096. doi: 10.1007/s0018-015-1917-z
- Obara, K., and Ohsumi, Y. (2011). PtdIns 3-kinase orchestrates autophagosome formation in yeast. *J. Lipids* 2011:498768. doi: 10.1155/2011/498768
- Ogier-Denis, E., Pattingre, S. E., Benna, J., and Codogno, P. (2000). Erk1/2-dependent phosphorylation of Ga-interacting protein stimulates its GTPase accelerating activity and autophagy in human colon cancer cells. *J. Biol. Chem.* 275, 39090–39095. doi: 10.1074/jbc.M006198200
- Ogier-Denis, E., Petiot, A., Bauvy, C., and Codogno, P. (1997). Control of the expression and activity of the Ga-interacting protein (GAIP) in Human intestinal cells. *J. Biol. Chem.* 272, 24599–24603. doi: 10.1074/jbc.272.27.24599
- Ohsumi, Y. (2014). Historical landmarks of autophagy research. *Cell Res.* 24, 9–23. doi: 10.1038/cr.2013.169
- Patel, S., and Dinesh-Kumar, S. P. (2008). *Arabidopsis* ATG6 is required to limit the pathogen-associated cell death response. *Autophagy* 4, 20–27. doi: 10.4161/auto.5056
- Pattingre, S., De Vries, L., Bauvy, C., Chantret, I., Cluzeaud, F., Ogier-Denis, E., et al. (2003). The G-protein regulator AGS3 controls an early event during macroautophagy in human intestinal HT-29 cells. *J. Biol. Chem.* 278, 20995–21002. doi: 10.1074/jbc.M300917200
- Phillips, A. R., Suttangkakul, A., and Vierstra, R. D. (2008). The ATG12 conjugating enzyme ATG10 is essential for autophagic vesicle formation in *Arabidopsis thaliana*. *Genetics* 178, 1339–1353. doi: 10.1534/genetics.107.086199
- Ramon, M., Rolland, F., and Sheen, J. (2008). *Sugar Sensing and Signaling: The Arabidopsis Book*. Rockville, MD: American Society of Plant Biologists.
- Rolland, F., Moore, B., and Sheen, J. (2002). Sugar sensing and signaling in plants. *Plant Cell* 14(Suppl.), S185–S205.
- Rolland, F., Winderickx, J., and Thevelein, J. M. (2001). Glucose-sensing mechanisms in eukaryotic cells. *Trends Biochem.* 26, 310–317. doi: 10.1016/S0968-0004(01)01805-9
- Seay, M., Patel, S., and Dinesh-Kumar, S. P. (2006). Autophagy and plant innate immunity. *Cell. Microbiol.* 8, 899–906.
- Sheen, J. (2014). Master regulators in plant glucose signaling networks. *J. Plant Biol.* 57, 67–79. doi: 10.1111/j.1462-5822.2006.00715.x
- Sheng, X., Wei, Q., Jiang, L., Li, X., Gao, Y., and Wang, L. (2012). Different degree in proteasome malfunction has various effects on root growth possibly through preventing cell division and promoting autophagic vacuolization. *PLoS ONE* 7:e45673. doi: 10.1371/journal.pone.0045673
- Shin, K. D., Lee, H. N., and Chung, T. (2014). A revised assay for monitoring autophagic flux in *Arabidopsis thaliana* reveals involvement of AUTOPHAGY-RELATED9 in autophagy. *Mol. Cells* 37, 399–405. doi: 10.14348/molcells.2014.0042
- Shipka, T., Welter, E., Borovsky, N., Amar, N., Mari, M., Reggiori, F., et al. (2015). Lipid droplets regulate autophagosome biogenesis. *Autophagy* 11, 2130–2131.
- Sun, A., Nie, S., and Xing, D. (2012). Nitric oxide-mediated maintenance of redox homeostasis contributes to NPR1-dependent plant innate immunity triggered by lipopolysaccharides. *Plant Physiol.* 160, 1081–1096. doi: 10.1104/pp.112.201798
- Suttangkakul, A., Li, F., Chung, T., and Vierstra, R. D. (2011). The ATG1/ATG13 protein kinase complex is both a regulator and a target of autophagic recycling in *Arabidopsis*. *Plant Cell* 23, 3761–3779. doi: 10.1105/tpc.111.090993
- Thompson, A. R., Doelling, J. H., Suttangkakul, A., and Vierstra, R. D. (2005). Autophagic nutrient recycling in *Arabidopsis* directed by the ATG8 and ATG12 conjugation pathways. *Plant Physiol.* 138, 2097–2110.
- Urano, D., and Jones, A. M. (2014). Heterotrimeric G protein-coupled signaling in plants. *Annu. Rev. Plant Biol.* 65, 365–384. doi: 10.1146/annurev-arplant-050213-040133
- Urano, D., Phan, N., Jones, J. C., Yang, J., Huang, J., Grigston, J., et al. (2012). Endocytosis of the seven-transmembrane RGS1 protein activates G-protein-coupled signalling in *Arabidopsis*. *Nat. Cell Biol.* 14, 1079–1088. doi: 10.1038/ncb2568
- Wang, P., Sun, X., Jia, X., Wang, N., Gong, X., and Ma, F. (2016). Characterization of an autophagy-related gene *MdATG8i* from Apple. *Front. Plant Sci.* 7:720. doi: 10.3389/fpls.2016.00720
- Wang, X. D., Gao, Y. Y., Yan, Q. Q., and Chen, W. L. (2016). Salicylic acid promotes autophagy via NPR3 and NPR4 in *Arabidopsis* senescence and innate immune response. *Acta Physiol. Plant.* 38, 241.
- Yang, X., and Bassham, D. C. (2015). Chapter one—New insights into the mechanism and function of autophagy in plant cells. *Int. Rev. Cell Mol. Biol.* 320, 1–40.
- Yoshimoto, K., Jikumaru, Y., Kamiya, Y., Kusano, M., Consonni, C., Panstruga, R., et al. (2009). Autophagy negatively regulates cell death by controlling NPR1-dependent salicylic acid signaling during senescence and the innate immune response in *Arabidopsis*. *Plant Cell* 21, 2914–2927. doi: 10.1105/tpc.109.068635
- Yue, H. Y., Nie, S. J., and Xing, D. (2012). Over-expression of *Arabidopsis* Bax inhibitor-1 delays methyl jasmonate-induced leaf senescence by suppressing the activation of MAP kinase 6. *J. Exp. Bot.* 63, 4463–4474. doi: 10.1093/jxb/ers122
- Zhang, W. N., and Chen, W. L. (2011). Role of salicylic acid in alleviating photochemical damage and autophagic cell death induction of cadmium stress in *Arabidopsis thaliana*. *Photochem. Photobiol. Sci.* 10, 947–955. doi: 10.1039/c0pp00305k

Zhuang, X. H., Cui, Y., Gao, C. J., and Jiang, L. W. (2015). Endocytic and autophagic pathways crosstalk in plants. *Curr. Opin. Plant Biol.* 28, 39–47.
doi: 10.1016/j.pbi.2015.08.010

Conflict of Interest Statement: The authors declare that the research was conducted in the absence of any commercial or financial relationships that could be construed as a potential conflict of interest.

Copyright © 2017 Yan, Wang, Fu and Chen. This is an open-access article distributed under the terms of the Creative Commons Attribution License (CC BY). The use, distribution or reproduction in other forums is permitted, provided the original author(s) or licensor are credited and that the original publication in this journal is cited, in accordance with accepted academic practice. No use, distribution or reproduction is permitted which does not comply with these terms.



Autophagy Is Rapidly Induced by Salt Stress and Is Required for Salt Tolerance in Arabidopsis

Liming Luo[†], Pingping Zhang[†], Ruihai Zhu, Jing Fu, Jing Su, Jing Zheng, Ziyue Wang, Dan Wang* and Qingqiu Gong*

Tianjin Key Laboratory of Protein Sciences, Department of Plant Biology and Ecology, College of Life Sciences, Nankai University, Tianjin, China

OPEN ACCESS

Edited by:

Minghui Lu,
Northwest A&F University, China

Reviewed by:

Caiji Gao,
South China Normal University, China
Zhaojun Ding,
Shandong University, China

*Correspondence:

Dan Wang
wangdan629@nankai.edu.cn
Qingqiu Gong
gongq@nankai.edu.cn

[†]These authors have contributed
equally to this work.

Specialty section:

This article was submitted to
Plant Cell Biology,
a section of the journal
Frontiers in Plant Science

Received: 31 December 2016

Accepted: 04 August 2017

Published: 22 August 2017

Citation:

Luo L, Zhang P, Zhu R, Fu J, Su J, Zheng J, Wang Z, Wang D and Gong Q (2017) Autophagy Is Rapidly Induced by Salt Stress and Is Required for Salt Tolerance in Arabidopsis. *Front. Plant Sci.* 8:1459.
doi: 10.3389/fpls.2017.01459

Salinity stress challenges agriculture and food security globally. Upon salt stress, plant growth slows down, nutrients are recycled, osmolytes are produced, and reallocation of Na⁺ takes place. Since autophagy is a high-throughput degradation pathway that contributes to nutrient remobilization in plants, we explored the involvement of autophagic flux in salt stress response of Arabidopsis with various approaches. Confocal microscopy of GFP-ATG8a in transgenic Arabidopsis showed that autophagosome formation is induced shortly after salt treatment. Immunoblotting of ATG8s and the autophagy receptor NBR1 confirmed that the level of autophagy peaks within 30 min of salt stress, and then settles to a new homeostasis in Arabidopsis. Such an induction is absent in mutants defective in autophagy. Within 3 h of salt treatment, accumulation of oxidized proteins is alleviated in the wild-type; however, such a reduction is not seen in *atg2* or *atg7*. Consistently, the Arabidopsis *atg* mutants are hypersensitive to both salt and osmotic stresses, and plants overexpressing ATG8 perform better than the wild-type in germination assays. Quantification of compatible osmolytes further confirmed that the autophagic flux contributes to salt stress adaptation. Imaging of intracellular Na⁺ revealed that autophagy is required for Na⁺ sequestration in the central vacuole of root cortex cells following salt treatment. These data suggest that rapid protein turnover through autophagy is a prerequisite for salt stress tolerance in Arabidopsis.

Keywords: autophagy, Arabidopsis, salt stress, autophagic flux, ATG8, NBR1, vacuoles

INTRODUCTION

Soil salinity is a major abiotic factor that limits crop yield (Flowers, 2004; Munns and Tester, 2008; Hanin et al., 2016). Globally, about 900 million hectares of land were estimated to be saline, and more than 30% of the irrigated crops were salt-affected (FAO¹) (Flowers, 2004; Schroeder et al., 2013). High concentrations of NaCl inhibits plant water uptake, and Na⁺ and Cl⁻ accumulated in the cytosol lead to ion toxicity. As results, photosynthetic rates are reduced, leading to energy depletion and accumulation of excessive reactive oxygen species (ROS) (Zhu, 2002; Deinlein et al., 2014; Golldack et al., 2014; Julkowska and Testerink, 2015). In order to alleviate the osmotic and ionic stresses, plants close their stomata to minimize water loss (Munemasa et al., 2015), reduce their growth rates (Julkowska and Testerink, 2015), and limit intracellular Na⁺ concentration by

¹www.fao.org

compartmentalization in the vacuole (Munns and Tester, 2008). Gradually, relocation of Na^+ away from young tissues takes place to exclude Na^+ from growing organs (Munns and Tester, 2008; Deinlein et al., 2014), and plants may enter a growth recovery phase to resume growth at a reduced steady rate (Munns, 2002; Julkowska and Testerink, 2015).

With engineering of salt-tolerant crops in mind, numerous studies have been carried out to elucidate salt stress response, with emphases on transcription regulation and ABA signaling (Urano et al., 2010; Osakabe et al., 2014). Enormous progress have also been made in understanding the ion transport mechanisms, such as the discovery of Salt Overly Sensitive (SOS) signaling cascade and the in-depth studies on the HKT and NHX transporters (Qiu, 2012; Ji et al., 2013; Volkov, 2015). Additionally, the molecular basis for tissue tolerance has been revealed, which includes biosynthesis of osmolytes, such as glycinebetaine, sugar alcohols, polyamines, and proline (Tarczynski et al., 1993; Szabados and Savoure, 2010; Chen and Murata, 2011).

Compared with the topics above, how salt-challenged plants manage to maintain their energy level and re-allocate the limited resources is less well understood. One pathway that may contribute to salt-elicited nutrient recycling is macroautophagy (hereafter autophagy) (Han et al., 2011; Li and Vierstra, 2012; Liu and Bassham, 2012).

Autophagy is a bulk degradation pathway that helps maintain cellular homeostasis (He and Klionsky, 2009; Mizushima et al., 2011; Liu and Bassham, 2012; Ohsumi, 2014). In this pathway, obsolete proteins and damaged organelles are enveloped by an expanding double-membranous vesicle, the isolation membrane/phagophore, which matures to a sealed autophagosome before fusing with the lytic vacuole (Li and Vierstra, 2012; Lamb et al., 2013; Shibutani and Yoshimori, 2014; Michaeli et al., 2016; Zhuang et al., 2016). The inner membrane of the autophagosome along with the cargo, termed the autophagic body, is then degraded by vacuolar hydrolases, and amino acids and other macro molecules are released back into the cytosol through transporters (Kuma and Mizushima, 2010; Shibutani and Yoshimori, 2014).

The hallmark of autophagy is the formation of the autophagosome (Xie and Klionsky, 2007; Shibutani and Yoshimori, 2014; Zhuang et al., 2016). As key players in this process, autophagy-specific ubiquitin-like proteins (UBLs) ATG8/LC3/GABARAP act as protein scaffolds to mediate phagophore expansion (Nakatogawa et al., 2007; Xie et al., 2008; Weidberg et al., 2010). Conjugation of ATG8 to the phagophore requires the activity of several other ATG proteins (Shibutani and Yoshimori, 2014). Firstly, newly synthesized ATG8 is truncated by the cysteine protease ATG4 to expose the C-terminal Glycine residue (Kirisako et al., 2000; Woo et al., 2014). The Glycine is then conjugated to the amino group of Phosphatidylethanolamine (PE) in a ubiquitin-like conjugation reaction catalyzed by ATG7 as the E1, ATG3 as the E2 (Ichimura et al., 2000), and the ATG12-ATG5-ATG16 complex as the E3 enzyme (Hanada et al., 2007). PE-conjugated ATG8 stably associates with both phagophore and completed autophagosomes, hence is commonly used as a marker for microscopic study of autophagy (Kabeya

et al., 2000; Yoshimoto et al., 2004; Contento et al., 2005). In addition, PE-conjugated ATG8 moves faster than the unconjugated ATG8 in SDS-PAGE gels, hence the amount of lipidated ATG8 is indicative of autophagic activity (Kabeya et al., 2000). Furthermore, by comparing the ATG8-PE levels in the presence and absence of vacuolar protease inhibitors, such as E-64d, or tonoplast H^+ -ATPase inhibitors, such as concanamycin A (Con A), autophagic flux can be quantified (Mizushima and Yoshimori, 2007). The selective autophagic flux can be detected by measuring Neighbor of BRCA1 (NBR1) degradation (Mizushima and Yoshimori, 2007; Svenning et al., 2011). During selective autophagy, NBR1 binds both ATG8 and mono- and (especially) polyubiquitin, linking the ubiquitinated cargoes to the autophagy machinery. Then it is transported together with the cargoes inside the autophagosome to the lytic vacuole for degradation (Mizushima and Yoshimori, 2007; Svenning et al., 2011). Hence NBR1 serves as both a receptor and a selective substrate of autophagy, and the degradation of NBR1 is indicative of selective autophagic flux (Mizushima and Yoshimori, 2007). Therefore, immunoblotting with antibodies against ATG8, NBR1, or epitope tags fused to ATG proteins provides more quantitative information for detecting autophagy (Bao et al., 2016).

To see if the level of autophagic flux correlates with salt tolerance, *Arabidopsis* mutants defective in autophagy and mutants with reduced level of autophagy, as well as transgenic plants that have increased level of autophagy were selected for further analyses (**Supplementary Figure S1**). The five ATGs belong to the core autophagy machinery (Xie and Klionsky, 2007). ATG5, ATG7, and ATG10 are required for ATG8-lipid adduct and autophagosome formation, and ATG5 have been shown to localize at the outer surface of the cortical endoplasmic reticulum (ER) to recruit ATG8 for phagophore assembly and expansion (Le Bars et al., 2014). Both *atg5* and *atg7* are autophagy-deficient mutants (Thompson et al., 2005; Inoue et al., 2006; Shin et al., 2014). ATG2 supposedly forms a complex with ATG18 to mediate the shuttle of ATG9 vesicles, which are a source of autophagosomal membranes (Yamamoto et al., 2012). Autophagic flux is known to be reduced rather than absent in *atg9* (Inoue et al., 2006; Shin et al., 2014; Zhuang et al., 2017). Transgenic *Arabidopsis* over-expressing GmATG8c (ATG8-OX) was used to represent plants with high levels of autophagy (Xia et al., 2012).

As a house-keeping pathway, autophagy is generally maintained as a basal level and can be quickly induced by nutrient deprivation and various stresses (He and Klionsky, 2009). Several lines of evidence suggest that autophagy is positively involved in plant salt stress adaptation. NaCl treatments have been shown to induce transcriptions of several *Autophagy-related* (ATG) genes, especially ATG8s and ATG18s in *Arabidopsis*, salt cress, rice, wheat, tobacco, pepper, and foxtail millet (Gong et al., 2005; Liu et al., 2009; Xia et al., 2011; Pei et al., 2014; Zhou et al., 2015; Li et al., 2016; Zhai et al., 2016). In *Arabidopsis*, *RNAi-AtATG18a* plants were hypersensitive to salt and osmotic stress in

germination and seedling growth (Liu et al., 2009). The autophagy-deficient mutants, *atg5* and *atg7*, as well as the ATG8-interacting autophagy cargo adaptor mutant *nbr1*, exhibited sensitivity toward drought and salt treatments (Zhou et al., 2013). Mutation in *ATG8-Interacting Protein 1*(*ATI1*) led to salt sensitivity during germination (Michaeli et al., 2014). Intriguingly, it was reported that over-expression of *GFP-AtAtg8f-HA* led to reduced tolerance toward mild osmotic and salt stresses, but not to stronger stresses (Slavikova et al., 2008).

Many questions remain on how autophagy contributes to salt stress tolerance in plants. When does autophagic flux peak following salt stress? Does autophagy participate in the clearance of salt-induced oxidized proteins? Does it contribute to osmolyte production? Does it have a role in Na^+ uptake or sequestration in the vacuole?

Here we show that the autophagic flux is rapidly induced by salt treatment. Then autophagy deficient (*atg5* and *atg7*, *atg10*), defective (*atg9* and possibly also *atg2*), and enhanced (*Pro35S:GmATG8c*, *ATG8-OX*) lines were selected to see if the levels of autophagy correlate with salt stress tolerance. Physiological analyses revealed that the *atg* mutants accumulated less soluble sugars and proline, whereas *ATG8-OX* plants accumulated more osmolytes. Oxidized protein is alleviated after treated with NaCl in the wild-type within 3 h. We also show that Na^+ sequestration in the lytic vacuole of salt-stressed root cortex cells is correlated with the level of autophagy. Our observations suggest that salt stress rapidly triggers autophagy to facilitate bulk protein turnover, thus providing macromolecules and energy required for plant survival.

MATERIALS AND METHODS

Accession Numbers

ATG2, At3g19190; ATG5, At5g17290; ATG7, At5g45900; ATG8a, AT4G21980; ATG9, At2g31260; ATG10, AT3G07525; NBR1, AT4G24690.

Plant Materials and Growth Conditions

Arabidopsis (ecotype Columbia-0) was grown as described (Xiong et al., 2016). Generally, seeds were surface-sterilized with 75% ethanol for 5 min, 100% ethanol for 1 min, rinsed with ddH₂O for five times, then stratified at 4°C for 2 days before plated on 1/2 Murashige and Skoog (1/2 MS) medium (Sigma-Aldrich, United States) containing 0.8% (w/v) agar (Sigma-Aldrich, United States), 1% (w/v) sucrose (Sigma-Aldrich, United States), pH5.7. Liquid 1/2 MS medium was prepared in the same way, only without agar. The plants were grown at 16 h (22°C)/8 h (18°C) with a photosynthetic photon flux density at 90 $\mu\text{E m}^{-2} \text{ sec}^{-1}$. The T-DNA insertion mutants *atg2-1* (Salk_076727), *atg5-1* (SAIL_129B07, CS806267), *atg7* (SAIL_11H07, CS862226), *atg9* (SAIL_527_A02, CS874564), and *atg10-1* (Salk_084434) were obtained from ABRC (Sessions et al., 2002; Alonso et al., 2003), and transgenic lines carrying *Pro35S:GmATG8c* were as described (Xia et al., 2012). All mutants and transgenic plants were verified by genomic PCR. Primers

used are listed in **Supplementary Table S1**. All lines have been freshly propagated to ensure wild-type level germination rates on control medium. Phenotypes were documented as described (Xiong et al., 2016). All images were analyzed with Image J², and statistical analyses (*F*-test, Student's *t*-test) were done with Microsoft Excel 2010.

Generation of an Autophagic Marker, *ProATG8a:GFP-ATG8a*

To construct *ProATG8a:GFP-ATG8a*, an 1199 bp fragment upstream of the start codon (ATG) of *ATG8a* (-1199 To 1) was PCR-amplified and inserted between *Pst* I and *Nco* I of *pCAMBIA1302*. Then a genomic fragment of *ATG8a* (942 bp) was inserted after GFP by homologous recombination with a ClonExpress II One Step Cloning Kit (Vazyme, Nanjing, China). The construct was verified by sequencing before introduced into *Agrobacterium tumefaciens* (GV3101) for floral dipping (Clough and Bent, 1998). Primary transformants were selected by antibiotic resistance and verified by PCR. The T3 homozygous marker line L5-1 was introduced into *atg10* by crossing, and *atg10/GFP-ATG8a* plants were identified by genotyping of F2 individuals.

Immunoblotting

To quantify autophagic flux, 10-day-old vertically grown seedlings (approximately 200 mg) were transferred to liquid 1/2 MS medium with 150 mM NaCl for 0, 0.5, 1, 3, and 6 h before harvested. To block autophagosome degradation in the lytic vacuole, a parallel set of seedlings were transferred to medium containing NaCl plus 0.5 μM Concanamycin A (ConA, Sigma-Aldrich, United States) and harvested at the same time points. Protein extraction, quantification, and immunoblotting were done as described (Xia et al., 2012). All SDS-PAGE gels were prepared with 6 M urea. Primary antibodies used were anti-GmATG8c (1:3000) (Xia et al., 2012), anti-NBR1 (Agrisera, 1:3000), and anti-tubulin (Uitbody, 1:5000). Each experiment was repeated for at least three times, and one representative result was shown. Quantification of immunoblots was done with Image J and statistical analyses (*F*-test, Student's *t*-test) were done with Microsoft Excel 2013.

Oxidized Protein Analysis

Oxidized protein analysis was performed following a previous report (Xiong et al., 2007). Ten-day-old seedlings grown on 1/2 MS vertical plates were transferred to liquid 1/2 MS medium with 150 mM NaCl for 0, 0.5, 1, 3, and 6 h before harvested for protein extraction. The extraction buffer contains 0.1 M Tris-HCl, pH 7.5, 0.3 M Sucrose, 1 mM EDTA, 0.1 mM phenylmethylsulphonylfluoride (PMSF), and 1% [v/v] β -mercaptoethanol. Extracts were centrifuged at 1,000 g for 10 min and supernatants were collected. Oxidized proteins were detected using an OxyBlot protein oxidation detection kit (Abcam, United Kingdom) according to the manufacturer's instructions. Dinitrophenylhydrazine (DNP) signals (entire lane)

²<http://rsb.info.nih.gov/ij/>

were quantified by densitometry in Image J and normalized to the wild-type 0 h control value, which was set as 1. Each experiment was repeated for at least three times, and one representative result was shown. Coomassie blue staining of total proteins was used as the loading control.

Quantification of Proline, Total Soluble Sugar, and Reducing Sugar content

Ten-day-old seedlings grown on 1/2 MS vertical plates were transferred to liquid 1/2 MS containing 150 mM NaCl for 0, 8, and 24 h. Harvested samples were weighed, and free proline was quantified with ninhydrin assay at A520 nm with a kit (Comin Biotech, Suzhou, China) following manufacturers' instructions. Total soluble sugar and reducing sugar contents were determined by the anthrone reagent method and dinitrosalicylic acid (DNS) method with a kit (Yuanye Biotech, Shanghai, China) following manufacturers' instructions. The sugar contents were determined against a standard curve prepared with glucose (Sigma-Aldrich, United States). Three biological replicates were done in each case with consistent results, and representative results are shown.

Amino Acid Analysis

Ten-day-old seedlings grown on 1/2 MS vertical plates were transferred to liquid 1/2 MS containing 150 mM NaCl for 0, 8, and 24 h. A parallel set of seedlings were treated with NaCl plus 10 mM Chloroquine. Harvested samples were weighed and quantified for soluble amino acid on a membraPure Amino Acid Analyzer A300 (Germany) following manufacturer's instructions.

Stress Treatments

For germination assay, stratified seeds were sown on 1/2 MS medium with or without NaCl or mannitol. Four biological replicates were done, which are consist of four seed populations obtained from self-fertilization of independent parents. More than 100 seeds were used in each seed population. Radical protrusion was scored as germination at a 4-h interval during first 3 days, then daily until day 7.

Laser Scanning Confocal Microscopy (LSCM)

To observe NaCl-induced autophagosome formation, 4- or 5-days-old vertically grown *GFP-AtATG8a* seedlings were immersed in 100 mM NaCl, or 0.5 μ M ConA, or both NaCl and ConA, for 30 min and 1 h, respectively, and scanned with a Leica SP5 (Leica, Germany) with a same set of scanning parameters. For each condition, at least 30 seedlings from three to five biological replicates were imaged, and >30 root cortex cells in the root hair zone were quantified for the numbers of autophagosomes/autophagic bodies.

For imaging of Na^+ , 5-days-old *Arabidopsis* seedlings were transferred to liquid 1/2 MS (control) or 1/2 MS containing 100 mM NaCl (salt stress) for 6 h, and then CoroNa Green AM (Thermo Fisher Scientific) was added into the medium to a final concentration of 5 μ M. Two hours later, the seedlings were stained with 5 μ M FM4-64 (Thermo Fisher Scientific) for 5 min, washed thoroughly, and scanned with a SP5 (Leica, Germany)

confocal microscope following previous reports (Meier et al., 2006; Oh et al., 2010). At least 20 seedlings from three biological replicates were imaged for each line in each condition, and >30 root cortex cells in the meristematic zone were quantified for the CoroNa Green AM fluorescent intensities in Image J.

Gene Expression Analysis

Ten-day-old seedlings were transferred to liquid 1/2 MS medium containing 150 mM NaCl for 0 (control), 30 min, and 3 h. RNA extraction, reverse transcription, RT-PCR and q-RT-PCR were performed as described (Xiong et al., 2016). *EF1a* (At5g60390) was used as an internal control. Three biological replicates consisting of three technical repeats each were done. Transcript levels of the nine salt-inducible genes following NaCl treatment in *ATG8-OX*, *atg5*, and *atg9* were compared with both WT control and with the same germplasm control using Student's *t*-test. Primers used are listed in **Supplementary Table S1**.

RESULTS

NaCl Treatment Rapidly Induces Autophagy in *Arabidopsis* Seedling Root Cortex Cells

To see if the autophagic flux is affected by salt stress, we firstly observed autophagosome formation and autophagic body turnover by looking at the autophagosome marker GFP-ATG8a in transgenic *Arabidopsis* seedlings carrying *ProATG8a:GFP-ATG8a* (**Supplementary Figure S2**). The marker line has a similar growth rate to the WT both under normal growth conditions and under nitrogen or carbon limitation, or salt and osmotic stresses (**Supplementary Figure S2**). The vacuolar proton pump inhibitor Concanamycin A (ConA) was used to preserve the autophagic bodies in the central vacuole. Under controlled conditions, GFP-ATG8a signals were mainly observed in the cytoplasm, with sporadic, relatively large (1–2 μ m in diameter) puncta representing autophagosomes also detected (**Figure 1A**, DMSO). In the presence of ConA, additional smaller puncta representing autophagic bodies were observed in the vacuole (**Figure 1A**, +ConA 0.5 h). When treated with 100 mM NaCl for 30 min, large puncta accumulated (**Figure 1A**, +NaCl 0.5 h). In the presence of ConA, the numbers of autophagosomes and autophagic bodies increased even more, indicative of induced autophagic flux (**Figure 1A**, +NaCl +ConA 0.5 h). Interestingly, the number of ATG8a puncta was slightly reduced at 1 h of salt treatment (**Figure 1A**, lower panel), suggesting that the autophagic flux peaked shortly after salt stress. Quantification of the number of autophagic bodies confirmed that the autophagic flux, represented by the difference between the numbers of autophagic bodies treated with NaCl only and that of NaCl plus ConA treatment, peaked at 0.5 h (**Figure 1C**). Imaging of an *atg10* mutant carrying *GFP-ATG8a* under the same conditions showed that few autophagosome/autophagic bodies could be detected in the mutant with or without NaCl or NaCl plus ConA (**Figure 1B**). The imaging results indicated that

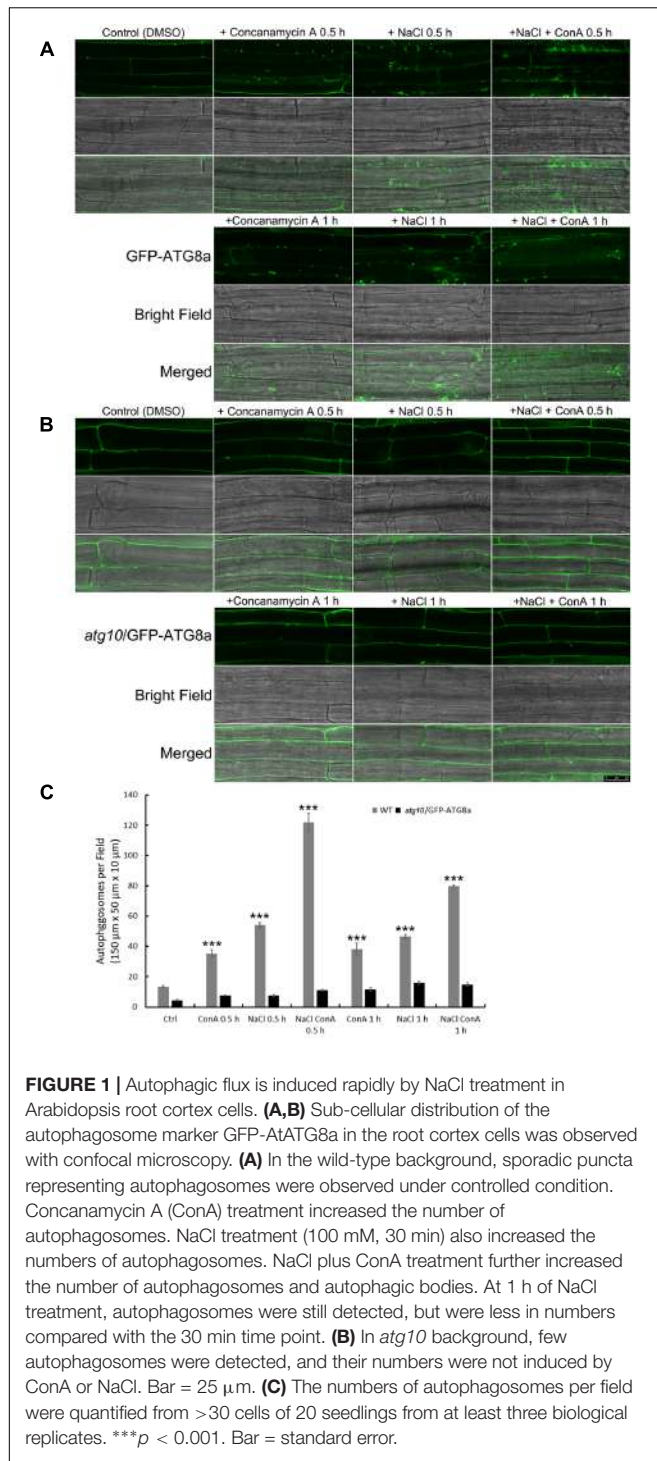


FIGURE 1 | Autophagic flux is induced rapidly by NaCl treatment in *Arabidopsis* root cortex cells. **(A,B)** Sub-cellular distribution of the autophagosome marker GFP-AtG8a in the root cortex cells was observed with confocal microscopy. **(A)** In the wild-type background, sporadic puncta representing autophagosomes were observed under controlled condition. Concanamycin A (ConA) treatment increased the number of autophagosomes. NaCl treatment (100 mM, 30 min) also increased the numbers of autophagosomes. NaCl plus ConA treatment further increased the number of autophagosomes and autophagic bodies. At 1 h of NaCl treatment, autophagosomes were still detected, but were less in numbers compared with the 30 min time point. **(B)** In *atg10* background, few autophagosomes were detected, and their numbers were not induced by ConA or NaCl. Bar = 25 μ m. **(C)** The numbers of autophagosomes per field were quantified from >30 cells of 20 seedlings from at least three biological replicates. ***p < 0.001. Bar = standard error.

autophagic flux can be rapidly induced by NaCl treatment in *Arabidopsis*.

Autophagic Flux Is Elevated Shortly after NaCl Treatment in the Wild-Type

To confirm that NaCl treatment can rapidly induce autophagy, immunoblotting of ATG8s was performed. We first examined

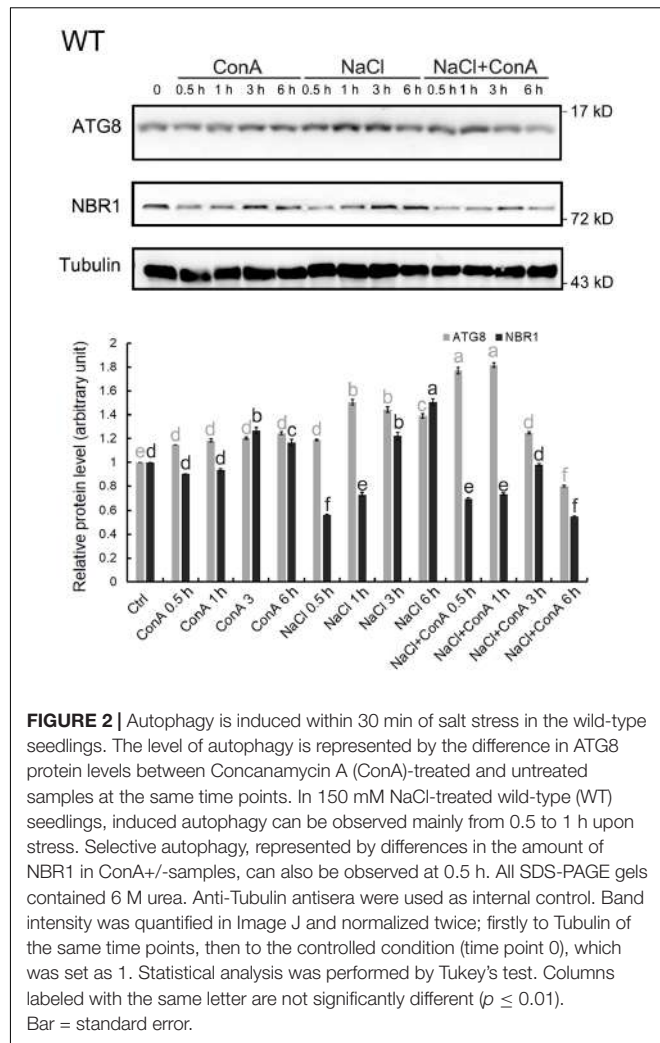


FIGURE 2 | Autophagy is induced within 30 min of salt stress in the wild-type seedlings. The level of autophagy is represented by the difference in ATG8 protein levels between Concanamycin A (ConA)-treated and untreated samples at the same time points. In 150 mM NaCl-treated wild-type (WT) seedlings, induced autophagy can be observed mainly from 0.5 to 1 h upon stress. Selective autophagy, represented by differences in the amount of NBR1 in ConA+-samples, can also be observed at 0.5 h. All SDS-PAGE gels contained 6 M urea. Anti-Tubulin antisera were used as internal control. Band intensity was quantified in Image J and normalized twice; firstly to Tubulin of the same time points, then to the controlled condition (time point 0), which was set as 1. Statistical analysis was performed by Tukey's test. Columns labeled with the same letter are not significantly different ($p \leq 0.01$). Bar = standard error.

whether the anti-GmATG8c antisera could detect both the lipidated and the non-lipidated ATG8s following a previous report (Suttangkakul et al., 2011). Total membrane fraction from the wild-type and *atg7* seedlings were collected, and the solubilized samples either treated or not with phospholipase D (PLD) were analyzed with immunoblotting. Unfortunately, the antibodies preferentially recognize un-lipidated ATG8s (**Supplementary Figure S3**). Hence the induction of autophagy was analyzed by comparing the difference in ATG8 protein levels between Concanamycin A (ConA)-treated and untreated samples at the same time points. Consistent with the imaging results (**Figure 1**), the levels of ATG8s were significantly induced at 0.5 and 1 h of NaCl plus ConA treatment (**Figure 2**).

Since the autophagic flux can also be detected by measuring NBR1 degradation (Mizushima and Yoshimori, 2007), changes in NBR1 levels following salt stress were monitored. The clear reduction in NBR1 protein level at 0.5 h of salt stress, in combination with the relative constant levels of NBR1 at the same time points in the presence of ConA (**Figure 2**), indicated that NBR1-dependent, selective autophagy peaked at 0.5 h following NaCl treatment.

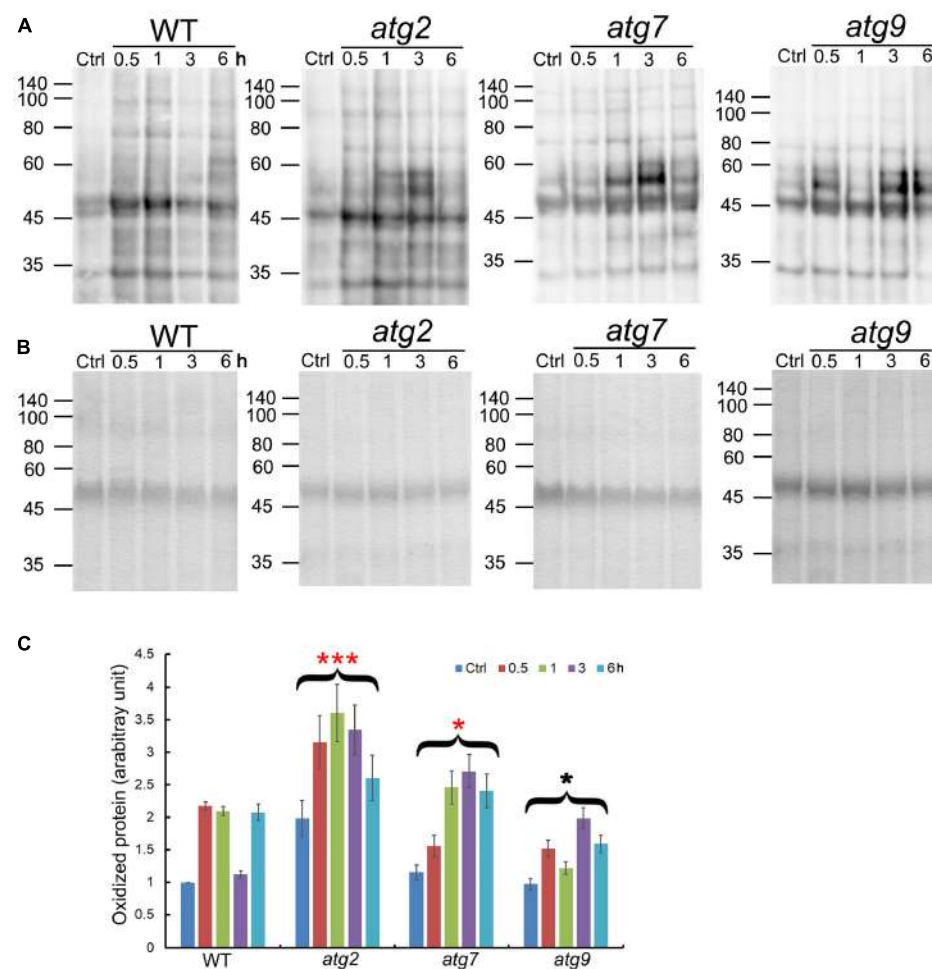


FIGURE 3 | Quantification of oxidized proteins in WT and the autophagy mutants. **(A)** Ten-day-old WT, *atg2*, *atg7*, and *atg9* seedlings were transferred to liquid 1/2 MS containing 150 mM NaCl for the indicated time. Total proteins extracted were then derivatized by DNP, followed by immunoblotting with anti-DNP antibodies. Molecular mass (kDa) are indicated at the left. **(B)** Coomassie Blue staining of total proteins (before derivatization with DNP) as the loading control. Molecular mass (kDa) are indicated at the left. **(C)** DNP signals were quantified by densitometry from three independent repeats with the WT control value set as 1; ***p < 0.001, *p < 0.05. Bar = standard error.

Salt-induced ATG8 flux, represented by an elevation in ATG8 levels following NaCl treatment and an even higher induction in NaCl plus ConA treatment, was not observed in *atg5* or *atg7* mutants (Supplementary Figure S4). ATG8 levels were induced in *atg2* and *atg9* only at 0.5 h (Supplementary Figure S4). NBR1 degradation was observed at 0.5 and 1 h in *atg9*, and at 6 h in *atg2*, however, not in *atg5* or *atg7* (Supplementary Figure S4).

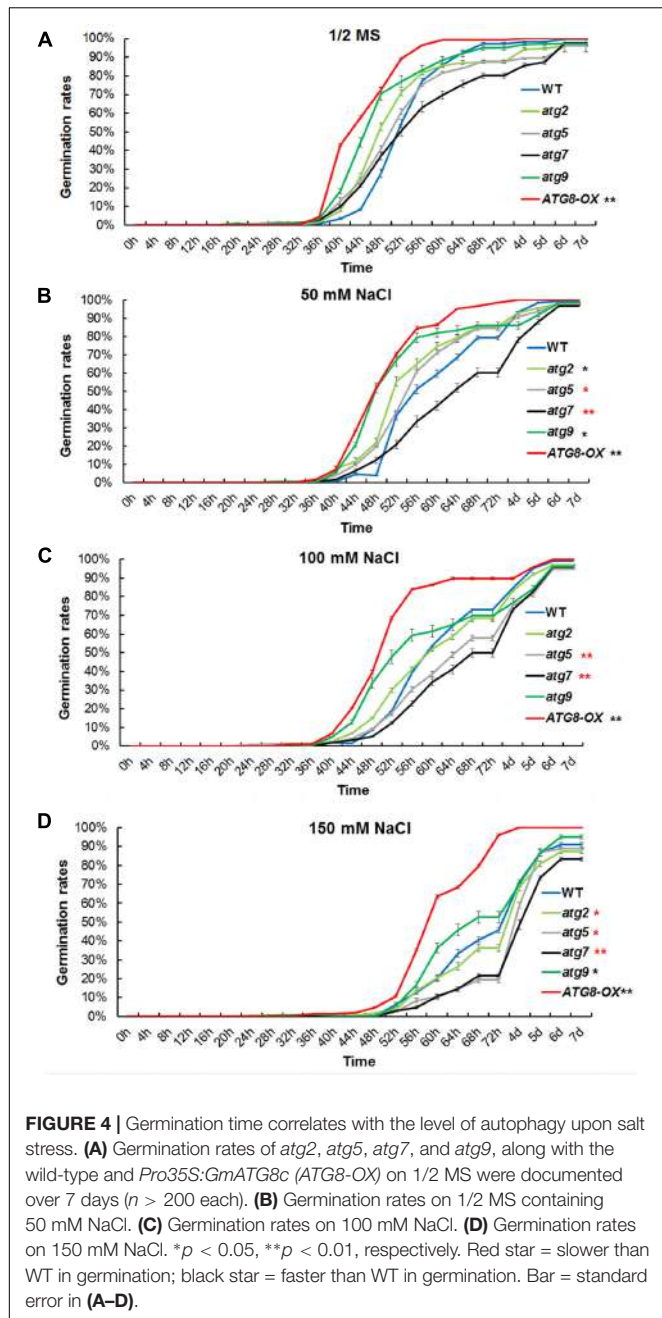
Oxidized Protein Levels Are Transiently Reduced after NaCl Treatment in the Wild-Type

Oxidized proteins induced by ROS are known substrates for autophagy (Xiong et al., 2007). To see whether autophagy may contribute to the clearance of oxidized proteins generated upon salt stress, levels of oxidized proteins were analyzed over a time-course of 6 h. In the WT, oxidized proteins accumulated significantly within 0.5 h of salt treatment, got back to the

control level at 3 h, before returning to the 0.5–1 h level by 6 h. *atg9* performed better than the WT in the clearance of oxidized proteins, with a reduction clearly observed at 1 h. *atg2* and *atg7* both had higher-than-WT levels of oxidized proteins before stress, which then got further induced by salt stress. Only at 6 h did the levels of oxidized proteins drop slightly in *atg2* and *atg7*. Overall, the results indicate that autophagy could have a positive role in transiently reducing the level of oxidized proteins generated by salt stress (Figure 3).

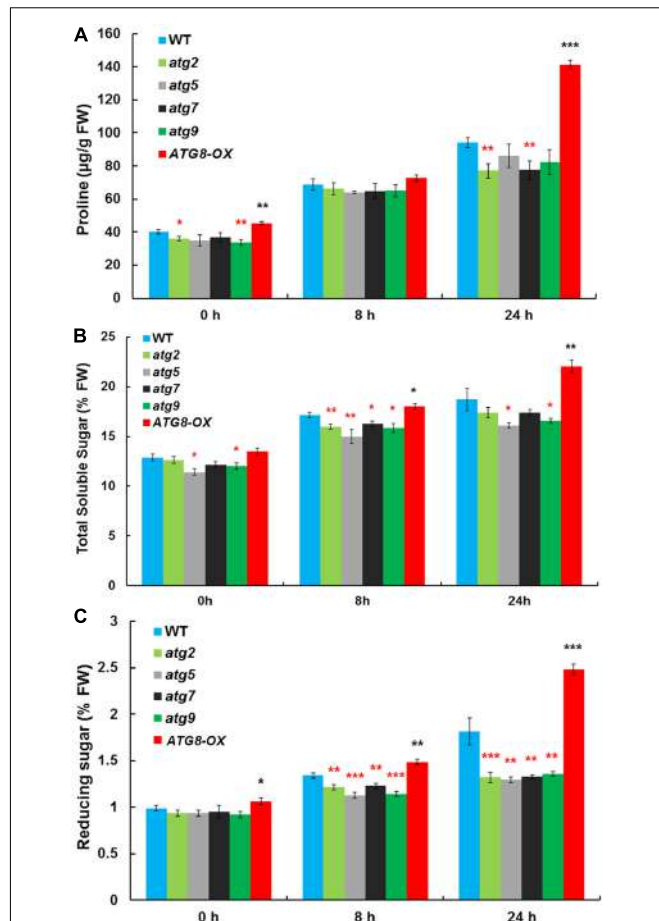
The Autophagy Mutants Are Hypersensitive to Salt Stress during Germination

To see if autophagy is positively involved in salt stress adaptation, germination percentage of the autophagy mutants and ATG8-OX plants were documented in a time course on control and NaCl-containing plates. Under controlled condition, ATG8-OX



germinated significantly faster than the wild-type ($p < 0.01$, paired student's *t*-test), whereas the autophagy mutants were statistically similar to the wild-type (Figure 4A). In the presence of NaCl, germination was slowed down in all lines, especially at higher concentrations (Figures 4B–D). The two autophagy-deficient lines, *atg5* and *atg7*, germinated significantly slower than the wild-type on all salt stress conditions (Figures 4B–D). *atg9* and *atg2* germinated faster than the wild-type on 50 mM NaCl, but not on higher concentrations (Figures 4B–D).

Similar germination curves were observed in the *atg* mutants on mannitol-containing plates (Supplementary Figure S5). These physiological data suggested that the level of autophagy



is positively correlated with the germination rate at salt- and osmotic- stress conditions.

Consistent with the germination phenotypes, root-bending assay performed on 150 mM NaCl showed that the WT and the ATG8-OX lines responded normally to gravity stimulation on vertical plates supplemented with 150 mM NaCl. In contrast, *atg5* and *atg7* had less bending in their primary roots on NaCl plates (Supplementary Figure S6). Altogether, the phenotypes confirmed that autophagy is required for the adaptation of seedlings toward salt stress.

Accumulation of Osmolytes Is Correlated with the Level of Autophagy upon Salt Stress

Autophagy may cater to the timely production of salt-induced osmolytes, such as proline and soluble sugars. The

levels of proline, soluble sugar, and reducing sugar were measured in control and salt-stressed (0, 8, and 24 h) seedlings (**Figures 5A–C**). Before salt treatment, ATG8-OX had significantly higher levels of proline and reducing sugar than the wild-type, whereas several *atg* mutants had significantly lower levels of the osmolytes compared to the wild-type. Following salt treatment, all lines accumulated more osmolytes. ATG8-OX generally had much higher levels of proline and sugars, especially at 24 h (**Figures 5A–C**). In contrast, the *atg* mutants accumulated significant less osmolytes compared with the wild-type (**Figures 5A–C**), suggesting that the production of proline and soluble sugars indeed relies on autophagy.

Expression of Salt-Inducible Genes Was Similar in Autophagy-Reduced and Autophagy-Enhanced Lines

To see if the salt-induced transcription is affected by the level of autophagy, we compared the expression patterns of salt-inducible genes in *atg5* and *atg9* mutants, ATG8-OX, and the wild-type with quantitative RT-PCR (**Figure 6**). The selected genes are known to be induced by salt stress either dependent or independent of ABA (Ma et al., 2006). Since we observed an induction of autophagic flux at 0.5 h of NaCl treatment, two relatively early time points (0.5 and 3 h) were selected for the transcript analysis. Expression of most markers was induced at 0.5 h in the wild-type, *atg9*, and ATG8-OX, and was further induced at 3 h (**Figure 6**). The expression patterns observed in the wild-type, *atg9*, and ATG8-OX indicated that autophagy may not affect salt-inducible gene expression directly. The extra high induction in gene expression observed in *atg5* (**Figure 6**), however, is unexpected, and might have resulted from a yet unknown regulatory mechanism.

Sequestration of Sodium Ions in the Vacuole of Root Cells Is Correlated with Autophagy Levels

To see whether autophagy might play a role in Na^+ compartmentation upon salt stress, sodium ions were visualized with CoroNa Green, a fluorescent dye specific for Na^+ -imaging, with a same set of scanning parameters on a confocal microscope. The lipophilic dye FM4-64 was used to stain the PM, outlining the cells. Without NaCl, the fluorescence was barely visible (**Supplementary Figures 7, 8**) as reported (Oh et al., 2010). After 8 h of 100 mM NaCl treatment, striking differences in fluorescent intensity was observed among the lines (**Figure 7** and **Supplementary Figure S7**). As described (Oh et al., 2010), Na^+ accumulated in the vacuoles of root cortex cells in all lines, however, at very different quantities. Compared with the wild-type, very weak signals were detected in *atg2*, *atg5*, and *atg7*, whereas much stronger signals were observed in ATG8-OX (**Figure 7** and **Supplementary Figure S8**). *atg9* had lower-than-WT yet clearly visible signals (**Figure 7** and **Supplementary Figure S9**). The observation suggested that sodium compartmentation in the root cortex cells positively correlates with the level of autophagy.

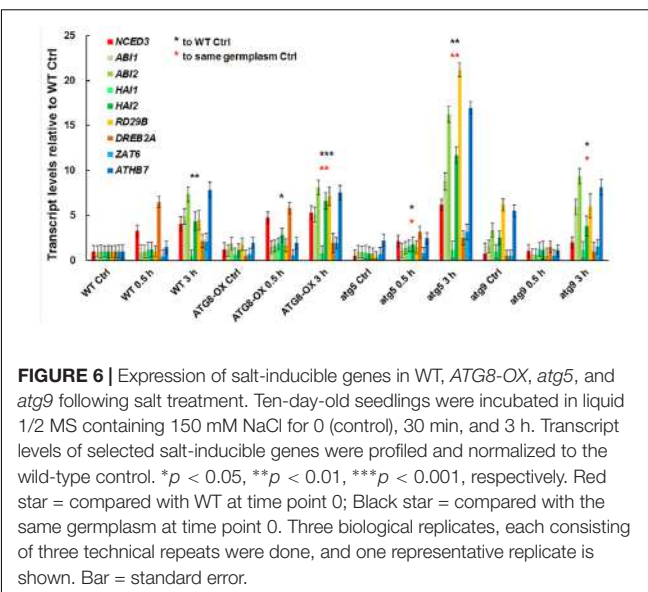


FIGURE 6 | Expression of salt-inducible genes in WT, ATG8-OX, *atg5*, and *atg9* following salt treatment. Ten-day-old seedlings were incubated in liquid 1/2 MS containing 150 mM NaCl for 0 (control), 30 min, and 3 h. Transcript levels of selected salt-inducible genes were profiled and normalized to the wild-type control. * $p < 0.05$, ** $p < 0.01$, *** $p < 0.001$, respectively. Red star = compared with WT at time point 0; Black star = compared with the same germlasm at time point 0. Three biological replicates, each consisting of three technical repeats were done, and one representative replicate is shown. Bar = standard error.

DISCUSSION

ProATG8a:GFP-ATG8a as a New Marker Line for Autophagy

In the past decade, several methods have been established for observing autophagy in plants (Klionsky et al., 2016; Pu and Bassham, 2016), including staining acidic vesicles with the fluorescent dye monodansylcadaverine (MDC), electron microscopy of cells, etc. The most widely used method is to observe the presence and distribution of *Pro35S:GFP-ATG8s* and *ProUBQ10:GFP-ATG8s* in plant cells (Yoshimoto et al., 2004; Contento et al., 2005; Suttangkakul et al., 2011; Shin et al., 2014). Studies had revealed, however, that ectopic expression of ATG8s could have measurable impact on plant development. The *Pro35S:GFP-ATG8* plants generally grow faster to larger sizes (Slavikova et al., 2008; Xia et al., 2012). In this study, we constructed *GFP-ATG8a* driven by its own promoter, and generated T3 homozygous lines. Line 5-1 had phenotypes indistinguishable from the WT under normal growth conditions, and shared the same starvation- and stress- induced phenotypes with the WT. A bonus is that the T-DNA insertion site in this line had been revealed from TAIL-PCR, so that the marker line can be easily genotyped after crossing with other lines. We also noticed that in this line, the strong nuclear ATG8 signals commonly observed in both *Pro35S:GFP-ATG8* and *ProUBQ10:GFP-ATG8* under controlled conditions (Zhou et al., 2013; Pei et al., 2014) is absent (**Figure 1** and **Supplementary Figure S2**), indicating that the ATG8a level in this line is closer to the endogenous level.

Autophagy Is Rapidly Induced by Salt Stress

An interesting finding in this study is that the autophagic flux peaks as early as 0.5 h upon salt stress in *Arabidopsis* seedlings (**Figures 1, 2**). Similarly, it has been reported that autophagic flux was induced at 30 min following hypertonic

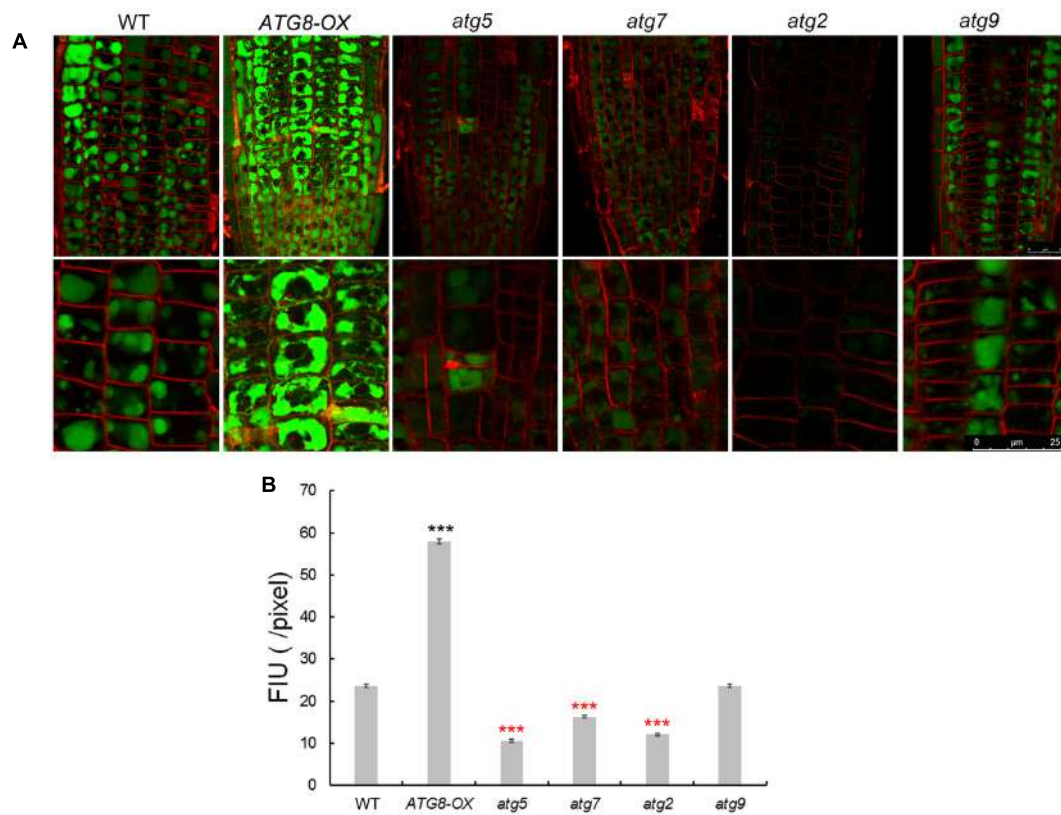
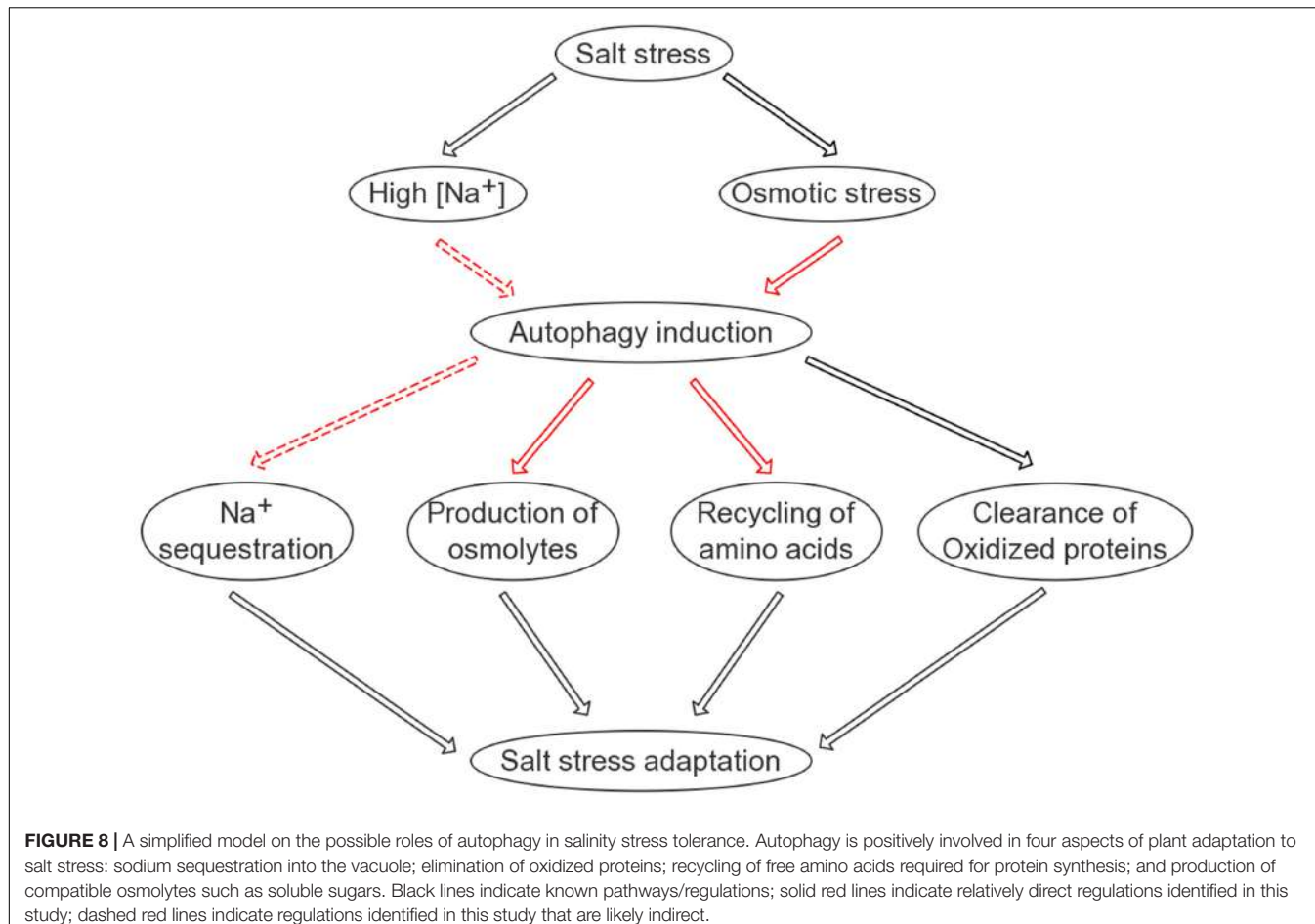


FIGURE 7 | Imaging of Na^+ in seedling roots of WT, autophagy mutants, and ATG8-OX. **(A)** Roots of 5-day-old wild-type, *atg5*, *atg7*, *atg2*, *atg9*, and ATG8-OX seedlings were incubated in liquid 1/2 MS containing 100 mM NaCl for 6 h, stained with CoroNa Green AM (5 μM) in the presence of 100 mM NaCl for 2 h, and scanned with a confocal microscope. The root tip region is shown (upper panel). Cortex cells in the meristematic region are 2.5 \times magnified (lower panel). Plasma membrane was stained with FM4-64 before scanning. **(B)** Quantification of CoroNa Green AM fluorescent intensity in **(A)**. More than 30 cells from more than 20 roots (three biological replicates), were quantified. Bar = 25 μm in **(A)**. *** $p < 0.001$. Red star = lower than WT; black star = higher than WT in **(B)**.

stress (350 and 500 mOsmol/kg NaCl, approximately 150 to 250 mM NaCl) on LLC-PK₁ renal proximal tubule-like cells (Nunes et al., 2013). Such speedy induction of autophagy is more likely based on post-translational modification rather than *de novo* synthesis of core autophagy proteins. What the possible modifications are remain to be explored. Apart from the possible regulation on ATG8 deacetylation (Huang et al., 2015), a known determinant on ATG8 activity, the redox-controlled ATG4 activity (Perez-Perez et al., 2014, 2016), might also regulate salt-induced autophagy. The ATG4 protease not only cleaves nascent ATG8 at its conserved C-terminal Glycine residue to promote conjugation of ATG8 to PE during autophagosome formation, but cleaves the amide bond between ATG8 and PE on completed autophagosome to recycle ATG8 (Yu et al., 2012). The two Arabidopsis ATG4s have been demonstrated to have different substrate preference *in vivo* and *in vitro* (Woo et al., 2014), and the activity of Chlamydomonas ATG4 has recently been shown to be inhibited by oxidation at a Cysteine residue (C400) conserved between plants and yeasts (Perez-Perez et al., 2016). It can be postulated that the oxidative stress generated during salt stress may modulate ATG8-PE formation by regulating ATG4 activity.

Autophagy Is Likely Required for the Efficient Establishment of Salt Tolerance

The germination assay clearly indicates that autophagy plays a positive role in ensuring timely germination upon salt stress treatment. There are at least two explanations for such observation. Firstly, autophagy is known to contribute to nutrient remobilization from source to sink (Guiboileau et al., 2012; Xia et al., 2012), and autophagy mutants had insufficient protein degradation in their rosette leaves (Guiboileau et al., 2013). Therefore, during seed maturation, the acquisition of seed storage proteins, free amino acids, fatty acids, and other macromolecules is likely defective in the autophagy mutants (Galili et al., 2014). When challenged by salt stress, the germinating *atg* mutants could have insufficient osmolyte production, thus exhibiting sensitivity toward osmotic challenge. In contrast, the ATG8-OX seeds could have benefited from higher levels of storage proteins and other macromolecules during germination. Such differences become clearer as the stress conditions become more severe (Figure 4 and Supplementary Figure S5), especially on the two autophagy deficient mutant, *atg5* and *atg7*. Indeed, a global analysis on etiolated (carbon starvation) autophagy mutant seedlings showed that, amino acids, organic acids, and protein



levels were significantly decreased in *atg5* (Avin-Wittenberg et al., 2015). Secondly, autophagy participates in the clearance of damaged organelles such as peroxisomes (Kim et al., 2013; Shibata et al., 2013; Yoshimoto et al., 2014), and salt stress is known to generate such damages. Salt stress also leads to accumulation of protein aggregates and oxidized proteins (Mano et al., 2014), both of which have been reported to be substrates of autophagy (Toyooka et al., 2006; Xiong et al., 2007). On the other hand, autophagy is certainly not the only degradation pathway responsible for the elimination of damaged organelles, oxidized proteins, and protein aggregates. Our observation that the level of oxidized proteins are only transiently reduced in the wild-type indicated that autophagy may not be the major pathway involved in the long-term clearance of oxidized proteins. It has been reported that proteins oxidized in salt-stressed *Arabidopsis* are versatile not only in their functions but also in their sub-cellular localizations (Mano et al., 2014). A number of them are predicted to localize to the apoplast, the plasma membrane, and the nucleus, thus are likely to be degraded by other pathways. A recent report showed that in severely salt-stressed tomato roots (250 mM NaCl, 6 h), two of the three catalytic subunits, $\beta 2$ and $\beta 5$, of the proteasome are transiently modified to generate the stress proteasome (Kovacs et al., 2017). At 24 h, a normal proteasome profile reappeared. Such a transient appearance of the

stress-induced active proteasome coincides with oxidized protein degradation (Kovacs et al., 2017) and is likely a parallel pathway to autophagy in short-term salt stress response.

Why does the autophagic flux, reflected by the turnover of both ATG8 and NBR1 in the lytic vacuole, take place at such an early time point? Considering that salt-induced transcription generally starts at a similar time point, it can be hypothesized that the efficient translation of stress-responsive proteins may rely on a reliable pool of amino acids. Indeed, the quantification of free amino acids following salt stress supported this hypothesis (**Supplementary Figure S9**). At the 8-h time point, the ATG8-OX seedlings had significantly lower levels of free amino acids, indicating that it was able to remobilize more amino acids for protein synthesis at an earlier time point. As a bulk degradation pathway, autophagy is likely a good candidate for maintaining such a pool. One may wonder which organelles or proteins are preferentially “eaten” during salt stress, since various substrates have been discovered in autophagy induced by different abiotic stresses. For instance, upon heat stress, autophagy is required for the clearance of the ubiquitinated protein aggregates (Zhou et al., 2013). Hypoxia-induced autophagy, on the other hand, may use chloroplast proteins as substrates, as the autophagy mutants die quickly following submergence and their detached leaves turn yellow faster upon ethanol treatment (Chen et al., 2015).

Interestingly, autophagy also regulates the compartmentation of sodium ions in root cells, although the underlying mechanism remains uncovered. A model summarizing our findings is presented (**Figure 8**). The interesting fact that autophagy gets induced very rapidly following salt treatment and is required for successful salt adaptation may be explored in molecular breeding of salt tolerant crops in future.

AUTHOR CONTRIBUTIONS

QG, LL, and PZ conceived and designed the study. LL, PZ, DW, and QG analyzed the data and drafted the manuscript. LL, PZ, RZ, JF, JZ, JS, and ZW carried out the experiments. All authors have read and approved the final manuscript.

FUNDING

This work was supported by the National Natural Science Foundation of China (31401179, 31671419), and in part by the Fundamental Research Funds for the Central Universities and the Funds for National basic science personnel training (J1103503).

ACKNOWLEDGMENTS

We apologize to colleagues whose works are not cited due to space limitations. We thank the Arabidopsis Biological Resource

REFERENCES

- Alonso, J. M., Stepanova, A. N., Leisse, T. J., Kim, C. J., Chen, H., Shinn, P., et al. (2003). Genome-wide insertional mutagenesis of *Arabidopsis thaliana*. *Science* 301, 653–657. doi: 10.1126/science.1086391
- Avin-Wittenberg, T., Bajdzenko, K., Wittenberg, G., Alseekh, S., Tohge, T., Bock, R., et al. (2015). Global analysis of the role of autophagy in cellular metabolism and energy homeostasis in *Arabidopsis* seedlings under carbon starvation. *Plant Cell* 27, 306–322. doi: 10.1105/tpc.114.134205
- Bao, Y., Mugume, Y., and Bassham, D. C. (2016). Biochemical methods to monitor autophagic responses in plants. *Methods Enzymol.* 588, 497–513. doi: 10.1016/bs.mie.2016.09.090
- Chen, L., Liao, B., Qi, H., Xie, L. J., Huang, L., Tan, W. J., et al. (2015). Autophagy contributes to regulation of the hypoxia response during submergence in *Arabidopsis thaliana*. *Autophagy* 11, 2233–2246. doi: 10.1080/15548627.2015.1112483
- Chen, T. H., and Murata, N. (2011). Glycinebetaine protects plants against abiotic stress: mechanisms and biotechnological applications. *Plant Cell Environ.* 34, 1–20. doi: 10.1111/j.1365-3040.2010.02232.x
- Clough, S. J., and Bent, A. F. (1998). Floral dip: a simplified method for *Agrobacterium*-mediated transformation of *Arabidopsis thaliana*. *Plant J.* 16, 735–743. doi: 10.1046/j.1365-313x.1998.00343.x
- Contento, A. L., Xiong, Y., and Bassham, D. C. (2005). Visualization of autophagy in *Arabidopsis* using the fluorescent dye monodansylcadaverine and a GFP-AtATG8e fusion protein. *Plant J.* 42, 598–608. doi: 10.1111/j.1365-313X.2005.02396.x
- Deinlein, U., Stephan, A. B., Horie, T., Luo, W., Xu, G., and Schroeder, J. I. (2014). Plant salt-tolerance mechanisms. *Trends Plant Sci.* 19, 371–379. doi: 10.1016/j.tplants.2014.02.001
- Flowers, T. J. (2004). Improving crop salt tolerance. *J. Exp. Bot.* 55, 307–319. doi: 10.1093/jxb/erh003
- Galili, G., Avin-Wittenberg, T., Angelovici, R., and Fernie, A. R. (2014). The role of photosynthesis and amino acid metabolism in the energy status during seed development. *Front. Plant Sci.* 5:447. doi: 10.3389/fpls.2014.00447
- Golldack, D., Li, C., Mohan, H., and Probst, N. (2014). Tolerance to drought and salt stress in plants: unraveling the signaling networks. *Front. Plant Sci.* 5:151. doi: 10.3389/fpls.2014.00151
- Gong, Q., Li, P., Ma, S., Indu Rupassara, S., and Bohnert, H. J. (2005). Salinity stress adaptation competence in the extremophile *Thellungiella halophila* in comparison with its relative *Arabidopsis thaliana*. *Plant J.* 44, 826–839. doi: 10.1111/j.1365-313X.2005.02587.x
- Guibouleau, A., Avila-Ospina, L., Yoshimoto, K., Soulay, F., Azzopardi, M., Marmagne, A., et al. (2013). Physiological and metabolic consequences of autophagy deficiency for the management of nitrogen and protein resources in *Arabidopsis* leaves depending on nitrate availability. *New Phytol.* 199, 683–694. doi: 10.1111/nph.12307
- Guibouleau, A., Yoshimoto, K., Soulay, F., Bataille, M. P., Avice, J. C., and Masclaux-Daubresse, C. (2012). Autophagy machinery controls nitrogen remobilization at the whole-plant level under both limiting and ample nitrate conditions in *Arabidopsis*. *New Phytol.* 194, 732–740. doi: 10.1111/j.1469-8137.2012.04084.x
- Han, S., Yu, B., Wang, Y., and Liu, Y. (2011). Role of plant autophagy in stress response. *Protein Cell* 2, 784–791. doi: 10.1007/s13238-011-1104-4
- Hanada, T., Noda, N. N., Satomi, Y., Ichimura, Y., Fujioka, Y., Takao, T., et al. (2007). The Atg12-Atg5 conjugate has a novel E3-like activity for protein lipidation in autophagy. *J. Biol. Chem.* 282, 37298–37302. doi: 10.1074/jbc.C700195200
- Hanin, M., Ebel, C., Ngom, M., Laplaze, L., and Masmoudi, K. (2016). New insights on plant salt tolerance mechanisms and their potential use for breeding. *Front. Plant Sci.* 7:1787. doi: 10.3389/fpls.2016.01787
- He, C., and Klionsky, D. J. (2009). Regulation mechanisms and signaling pathways of autophagy. *Annu. Rev. Genet.* 43, 67–93. doi: 10.1146/annurev-genet-102808-114910

Center (ABRC) for mutant lines; Dr. Fuchen Shi, Dr. Lei Chen, Ms. Ruming Liu, Ms. Lihong Zu, Mr. Jinxin Zheng, Mr. Siyuan Yan, Mr. Sheng Liu, and Mr. Wei Xu for technical assistance, and Dr. Zhiping Xie for discussions. We also thank the reviewers for their helpful suggestions.

SUPPLEMENTARY MATERIAL

The Supplementary Material for this article can be found online at: <http://journal.frontiersin.org/article/10.3389/fpls.2017.01459/full#supplementary-material>

FIGURE S1 | Illustration of materials used in this study.

FIGURE S2 | *ProATG8a:GFP-ATG8a* as a marker line for autophagy.

FIGURE S3 | The Anti-GmATG8c antisera preferentially detect the non-lipidated ATG8s.

FIGURE S4 | Autophagy is not induced by salt treatment in autophagy mutants.

FIGURE S5 | Germination of *atg* mutants, WT, and ATG8-OX on mannitol.

FIGURE S6 | Root bending assay of *atg* mutants, WT, and ATG8-OX on 150 mM NaCl.

FIGURE S7 | CoroNa Green staining of root tips of ATG8-OX lines.

FIGURE S8 | CoroNa Green staining of root tips without NaCl.

FIGURE S9 | Changes in free amino acid levels in lines with altered autophagy levels upon salt stress.

TABLE S1 | Primers used in this study.

- Huang, R., Xu, Y., Wan, W., Shou, X., Qian, J., You, Z., et al. (2015). Deacetylation of nuclear LC3 drives autophagy initiation under starvation. *Mol. Cell* 57, 456–466. doi: 10.1016/j.molcel.2014.12.013
- Ichimura, Y., Kirisako, T., Takao, T., Satomi, Y., Shimonishi, Y., Ishihara, N., et al. (2000). A ubiquitin-like system mediates protein lipidation. *Nature* 408, 488–492. doi: 10.1038/35044114
- Inoue, Y., Suzuki, T., Hattori, M., Yoshimoto, K., Ohsumi, Y., and Moriyasu, Y. (2006). AtATG genes, homologs of yeast autophagy genes, are involved in constitutive autophagy in *Arabidopsis* root tip cells. *Plant Cell Physiol.* 47, 1641–1652. doi: 10.1093/pcp/pcl031
- Ji, H., Pardo, J. M., Batelli, G., Van Oosten, M. J., Bressan, R. A., and Li, X. (2013). The salt overly sensitive (SOS) pathway: established and emerging roles. *Mol. Plant* 6, 275–286. doi: 10.1093/mp/sst017
- Julkowska, M. M., and Testerink, C. (2015). Tuning plant signaling and growth to survive salt. *Trends Plant Sci.* 20, 586–594. doi: 10.1016/j.tplants.2015.06.008
- Kabeya, Y., Mizushima, N., Ueno, T., Yamamoto, A., Kirisako, T., Noda, T., et al. (2000). LC3, a mammalian homologue of yeast Apg8p, is localized in autophagosome membranes after processing. *EMBO J.* 19, 5720–5728. doi: 10.1093/emboj/19.21.5720
- Kim, J., Lee, H., Lee, H. N., Kim, S. H., Shin, K. D., and Chung, T. (2013). Autophagy-related proteins are required for degradation of peroxisomes in *Arabidopsis* hypocotyls during seedling growth. *Plant Cell* 25, 4956–4966. doi: 10.1105/tpc.113.117960
- Kirisako, T., Ichimura, Y., Okada, H., Kabeya, Y., Mizushima, N., Yoshimori, T., et al. (2000). The reversible modification regulates the membrane-binding state of Apg8/Aut7 essential for autophagy and the cytoplasm to vacuole targeting pathway. *J. Cell Biol.* 151, 263–276. doi: 10.1083/jcb.151.2.263
- Klionsky, D. J., Abdelmohsen, K., Abe, A., Abedin, M. J., Abeliovich, H., Acevedo-Arozena, A., et al. (2016). Guidelines for the use and interpretation of assays for monitoring autophagy (3rd edition). *Autophagy* 12, 1–222. doi: 10.1080/15548627.2015.1100356
- Kovacs, J., Poor, P., Kaschani, F., Chandrasekar, B., Hong, T. N., Misas-Villamil, J. C., et al. (2017). Proteasome activity profiling uncovers alteration of catalytic beta2 and beta5 subunits of the stress-induced proteasome during salinity stress in tomato roots. *Front. Plant Sci.* 8:107. doi: 10.3389/fpls.2017.00107
- Kuma, A., and Mizushima, N. (2010). Physiological role of autophagy as an intracellular recycling system: with an emphasis on nutrient metabolism. *Semin. Cell Dev. Biol.* 21, 683–690. doi: 10.1016/j.semcd.2010.03.002
- Lamb, C. A., Yoshimori, T., and Tooze, S. A. (2013). The autophagosome: origins unknown, biogenesis complex. *Nat. Rev. Mol. Cell Biol.* 14, 759–774. doi: 10.1038/nrm3696
- Le Bars, R., Marion, J., Le Borgne, R., Satiat-Jeunemaitre, B., and Bianchi, M. W. (2014). ATG5 defines a phagophore domain connected to the endoplasmic reticulum during autophagosome formation in plants. *Nat. Commun.* 5:4121. doi: 10.1038/ncomms5121
- Li, F., and Vierstra, R. D. (2012). Autophagy: a multifaceted intracellular system for bulk and selective recycling. *Trends Plant Sci.* 17, 526–537. doi: 10.1016/j.tplants.2012.05.006
- Li, W., Chen, M., Wang, E., Hu, L., Hawkesford, M. J., Zhong, L., et al. (2016). Genome-wide analysis of autophagy-associated genes in foxtail millet (*Setaria italica* L.) and characterization of the function of SiATG8a in conferring tolerance to nitrogen starvation in rice. *BMC Genomics* 17:797. doi: 10.1186/s12864-016-3113-4
- Liu, Y., and Bassham, D. C. (2012). Autophagy: pathways for self-eating in plant cells. *Annu. Rev. Plant Biol.* 63, 215–237. doi: 10.1146/annurev-arplant-042811-105441
- Liu, Y., Xiong, Y., and Bassham, D. C. (2009). Autophagy is required for tolerance of drought and salt stress in plants. *Autophagy* 5, 954–963. doi: 10.4161/auto.5.79290
- Ma, S., Gong, Q., and Bohnert, H. J. (2006). Dissecting salt stress pathways. *J. Exp. Bot.* 57, 1097–1107. doi: 10.1093/jxb/erj098
- Mano, J., Nagata, M., Okamura, S., Shiraya, T., and Mitsui, T. (2014). Identification of oxidatively modified proteins in salt-stressed *Arabidopsis*: a carbonyl-targeted proteomics approach. *Plant Cell Physiol.* 55, 1233–1244. doi: 10.1093/pcp/pcu072
- Meier, S. D., Kovalchuk, Y., and Rose, C. R. (2006). Properties of the new fluorescent Na⁺ indicator CoroNa Green: comparison with SBFI and confocal Na⁺ imaging. *J. Neurosci. Methods* 155, 251–259. doi: 10.1016/j.jneumeth.2006.01.009
- Michaeli, S., Galili, G., Genschik, P., Fernie, A. R., and Avin-Wittenberg, T. (2016). Autophagy in plants—what's new on the menu? *Trends Plant Sci.* 21, 134–144. doi: 10.1016/j.tplants.2015.10.008
- Michaeli, S., Honig, A., Levanony, H., Peled-Zehavi, H., and Galili, G. (2014). *Arabidopsis* ATG8-INTERACTING PROTEIN1 is involved in autophagy-dependent vesicular trafficking of plastid proteins to the vacuole. *Plant Cell* 26, 4084–4101. doi: 10.1105/tpc.114.129999
- Mizushima, N., and Yoshimori, T. (2007). How to interpret LC3 immunoblotting. *Autophagy* 3, 542–545. doi: 10.4161/auto.4600
- Mizushima, N., Yoshimori, T., and Ohsumi, Y. (2011). The role of Atg proteins in autophagosome formation. *Annu. Rev. Cell Dev. Biol.* 27, 107–132. doi: 10.1146/annurev-cellbio-092910-154005
- Munemasa, S., Hauser, F., Park, J., Waadt, R., Brandt, B., and Schroeder, J. I. (2015). Mechanisms of abscisic acid-mediated control of stomatal aperture. *Curr. Opin. Plant Biol.* 28, 154–162. doi: 10.1016/j.pbi.2015.10.010
- Munnns, R. (2002). Comparative physiology of salt and water stress. *Plant Cell Environ.* 25, 239–250. doi: 10.1046/j.0016-8025.2001.00808.x
- Munnns, R., and Tester, M. (2008). Mechanisms of salinity tolerance. *Annu. Rev. Plant Biol.* 59, 651–681. doi: 10.1146/annurev.arplant.59.032607.092911
- Nakatogawa, H., Ichimura, Y., and Ohsumi, Y. (2007). Atg8, a ubiquitin-like protein required for autophagosome formation, mediates membrane tethering and hemifusion. *Cell* 130, 165–178. doi: 10.1016/j.cell.2007.05.021
- Nunes, P., Ernandez, T., Roth, I., Qiao, X., Strelbel, D., Bouley, R., et al. (2013). Hypertonic stress promotes autophagy and microtubule-dependent autophagosomal clusters. *Autophagy* 9, 550–567. doi: 10.4161/auto.23662
- Oh, D. H., Lee, S. Y., Bressan, R. A., Yun, D. J., and Bohnert, H. J. (2010). Intracellular consequences of SOS1 deficiency during salt stress. *J. Exp. Bot.* 61, 1205–1213. doi: 10.1093/jxb/erp391
- Ohsumi, Y. (2014). Historical landmarks of autophagy research. *Cell Res.* 24, 9–23. doi: 10.1038/cr.2013.169
- Osakabe, Y., Yamaguchi-Shinozaki, K., Shinozaki, K., and Tran, L. S. (2014). ABA control of plant macroelement membrane transport systems in response to water deficit and high salinity. *New Phytol.* 202, 35–49. doi: 10.1111/nph.12613
- Pei, D., Zhang, W., Sun, H., Wei, X., Yue, J., and Wang, H. (2014). Identification of autophagy-related genes ATG4 and ATG8 from wheat (*Triticum aestivum* L.) and profiling of their expression patterns responding to biotic and abiotic stresses. *Plant Cell Rep.* 33, 1697–1710. doi: 10.1007/s00299-014-1648-x
- Perez-Perez, M. E., Lemaire, S. D., and Crespo, J. L. (2016). Control of autophagy in *Chlamydomonas* is mediated through redox-dependent inactivation of the ATG4 protease. *Plant Physiol.* 172, 2219–2234. doi: 10.1104/pp.16.01582
- Perez-Perez, M. E., Zaffagnini, M., Marchand, C. H., Crespo, J. L., and Lemaire, S. D. (2014). The yeast autophagy protease Atg4 is regulated by thioredoxin. *Autophagy* 10, 1953–1964. doi: 10.4161/auto.34396
- Pu, Y., and Bassham, D. C. (2016). Detection of autophagy in plants by fluorescence microscopy. *Methods Mol. Biol.* 1450, 161–172. doi: 10.1007/978-1-4939-3759-2_13
- Qiu, Q. S. (2012). Plant and yeast NHX antiports: roles in membrane trafficking. *J. Integr. Plant Biol.* 54, 66–72. doi: 10.1111/j.1744-7909.2012.01097.x
- Schroeder, J. I., Delhaize, E., Frommer, W. B., Guerinot, M. L., Harrison, M. J., Herrera-Estrella, L., et al. (2013). Using membrane transporters to improve crops for sustainable food production. *Nature* 497, 60–66. doi: 10.1038/nature11909
- Sessions, A., Burke, E., Presting, G., Aux, G., McElver, J., Patton, D., et al. (2002). A high-throughput *Arabidopsis* reverse genetics system. *Plant Cell* 14, 2985–2994. doi: 10.1105/tpc.004630
- Shibata, M., Oikawa, K., Yoshimoto, K., Kondo, M., Mano, S., Yamada, K., et al. (2013). Highly oxidized peroxisomes are selectively degraded via autophagy in *Arabidopsis*. *Plant Cell* 25, 4967–4983. doi: 10.1105/tpc.113.116947
- Shibutani, S. T., and Yoshimori, T. (2014). A current perspective of autophagosome biogenesis. *Cell Res.* 24, 58–68. doi: 10.1038/cr.2013.159
- Shin, K. D., Lee, H. N., and Chung, T. (2014). A revised assay for monitoring autophagic flux in *Arabidopsis thaliana* reveals involvement of AUTOPHAGY-RELATED9 in autophagy. *Mol. Cells* 37, 399–405. doi: 10.14348/molcells.2014.0042
- Slavikova, S., Ufaz, S., Avin-Wittenberg, T., Levanony, H., and Galili, G. (2008). An autophagy-associated Atg8 protein is involved in the responses of *Arabidopsis*

- seedlings to hormonal controls and abiotic stresses. *J. Exp. Bot.* 59, 4029–4043. doi: 10.1093/jxb/ern244
- Suttangkakul, A., Li, F., Chung, T., and Vierstra, R. D. (2011). The ATG1/ATG13 protein kinase complex is both a regulator and a target of autophagic recycling in *Arabidopsis*. *Plant Cell* 23, 3761–3779. doi: 10.1105/tpc.111.090993
- Svenning, S., Lamark, T., Krause, K., and Johansen, T. (2011). Plant NBR1 is a selective autophagy substrate and a functional hybrid of the mammalian autophagic adapters NBR1 and p62/SQSTM1. *Autophagy* 7, 993–1010. doi: 10.4161/auto.7.9.16389
- Szabados, L., and Savoure, A. (2010). Proline: a multifunctional amino acid. *Trends Plant Sci.* 15, 89–97. doi: 10.1016/j.tplants.2009.11.009
- Tarczynski, M. C., Jensen, R. G., and Bohnert, H. J. (1993). Stress protection of transgenic tobacco by production of the osmolyte mannitol. *Science* 259, 508–510. doi: 10.1126/science.259.5094.508
- Thompson, A. R., Doelling, J. H., Suttangkakul, A., and Vierstra, R. D. (2005). Autophagic nutrient recycling in *Arabidopsis* directed by the ATG8 and ATG12 conjugation pathways. *Plant Physiol.* 138, 2097–2110. doi: 10.1104/pp.105.06073
- Toyooka, K., Moriyasu, Y., Goto, Y., Takeuchi, M., Fukuda, H., and Matsuoka, K. (2006). Protein aggregates are transported to vacuoles by a macroautophagic mechanism in nutrient-starved plant cells. *Autophagy* 2, 96–106. doi: 10.4161/auto.2.2.2366
- Urano, K., Kurihara, Y., Seki, M., and Shinozaki, K. (2010). ‘Omics’ analyses of regulatory networks in plant abiotic stress responses. *Curr. Opin. Plant Biol.* 13, 132–138. doi: 10.1016/j.pbi.2009.12.006
- Volkov, V. (2015). Salinity tolerance in plants. Quantitative approach to ion transport starting from halophytes and stepping to genetic and protein engineering for manipulating ion fluxes. *Front. Plant Sci.* 6:873. doi: 10.3389/fpls.2015.00873
- Weidberg, H., Shvets, E., Shpilka, T., Shimron, F., Shinder, V., and Elazar, Z. (2010). LC3 and GATE-16/GABARAP subfamilies are both essential yet act differently in autophagosome biogenesis. *EMBO J.* 29, 1792–1802. doi: 10.1038/emboj.2010.74
- Woo, J., Park, E., and Dinesh-Kumar, S. P. (2014). Differential processing of *Arabidopsis* ubiquitin-like Atg8 autophaoy proteins by Atg4 cysteine proteases. *Proc. Natl. Acad. Sci. U.S.A.* 111, 863–868. doi: 10.1073/pnas.1318207111
- Xia, K., Liu, T., Ouyang, J., Wang, R., Fan, T., and Zhang, M. (2011). Genome-wide identification, classification, and expression analysis of autophagy-associated gene homologues in rice (*Oryza sativa* L.). *DNA Res.* 18, 363–377. doi: 10.1093/dnares/dsr024
- Xia, T., Xiao, D., Liu, D., Chai, W., Gong, Q., and Wang, N. N. (2012). Heterologous expression of ATG8c from soybean confers tolerance to nitrogen deficiency and increases yield in *Arabidopsis*. *PLoS ONE* 7:e37217. doi: 10.1371/journal.pone.0037217
- Xie, Z., and Klionsky, D. J. (2007). Autophagosome formation: core machinery and adaptations. *Nat. Cell Biol.* 9, 1102–1109. doi: 10.1038/ncb1007-1102
- Xie, Z., Nair, U., and Klionsky, D. J. (2008). Atg8 controls phagophore expansion during autophagosome formation. *Mol. Biol. Cell* 19, 3290–3298. doi: 10.1091/mbc.E07-12-1292
- Xiong, J., Cui, X., Yuan, X., Yu, X., Sun, J., and Gong, Q. (2016). The Hippo/STE20 homolog SIK1 interacts with MOB1 to regulate cell proliferation and cell expansion in *Arabidopsis*. *J. Exp. Bot.* 67, 1461–1475. doi: 10.1093/jxb/erv538
- Xiong, Y., Contento, A. L., Nguyen, P. Q., and Bassham, D. C. (2007). Degradation of oxidized proteins by autophagy during oxidative stress in *Arabidopsis*. *Plant Physiol.* 143, 291–299. doi: 10.1104/pp.106.092106
- Yamamoto, H., Kakuta, S., Watanabe, T. M., Kitamura, A., Sekito, T., Kondo-Kakuta, C., et al. (2012). Atg9 vesicles are an important membrane source during early steps of autophagosome formation. *J. Cell Biol.* 198, 219–233. doi: 10.1083/jcb.201202061
- Yoshimoto, K., Hanaoka, H., Sato, S., Kato, T., Tabata, S., Noda, T., et al. (2004). Processing of ATG8s, ubiquitin-like proteins, and their deconjugation by ATG4s are essential for plant autophagy. *Plant Cell* 16, 2967–2983. doi: 10.1105/tpc.104.025395
- Yoshimoto, K., Shibata, M., Kondo, M., Oikawa, K., Sato, M., Toyooka, K., et al. (2014). Organ-specific quality control of plant peroxisomes is mediated by autophagy. *J. Cell Sci.* 127, 1161–1168. doi: 10.1242/jcs.139709
- Yu, Z. Q., Ni, T., Hong, B., Wang, H. Y., Jiang, F. J., Zou, S., et al. (2012). Dual roles of Atg8-PE deconjugation by Atg4 in autophagy. *Autophagy* 8, 883–892. doi: 10.4161/auto.19652
- Zhai, Y., Guo, M., Wang, H., Lu, J., Liu, J., Zhang, C., et al. (2016). Autophagy, a conserved mechanism for protein degradation, responds to heat, and other abiotic stresses in *Capsicum annuum* L. *Front. Plant Sci.* 7:131. doi: 10.3389/fpls.2016.00131
- Zhou, J., Wang, J., Cheng, Y., Chi, Y. J., Fan, B., Yu, J. Q., et al. (2013). NBR1-mediated selective autophagy targets insoluble ubiquitinated protein aggregates in plant stress responses. *PLoS Genet.* 9:e1003196. doi: 10.1371/journal.pgen.1003196
- Zhou, X. M., Zhao, P., Wang, W., Zou, J., Cheng, T. H., Peng, X. B., et al. (2015). A comprehensive genome-wide analysis of autophagy-related genes identified in tobacco suggests a central role of autophagy in plant response to various environmental cues. *DNA Res.* 22, 245–257. doi: 10.1093/dnares/dsv012
- Zhu, J. K. (2002). Salt and drought stress signal transduction in plants. *Annu. Rev. Plant Biol.* 53, 247–273. doi: 10.1146/annurev.arplant.53.091401.143329
- Zhuang, X., Chung, K. P., Cui, Y., Lin, W., Gao, C., Kang, B. H., et al. (2017). ATG9 regulates autophagosome progression from the endoplasmic reticulum in *Arabidopsis*. *Proc. Natl. Acad. Sci. U.S.A.* 114, E426–E435. doi: 10.1073/pnas.1616299114
- Zhuang, X., Chung, K. P., and Jiang, L. (2016). Origin of the autophagosomal membrane in plants. *Front. Plant Sci.* 7:1655. doi: 10.3389/fpls.2016.01655

Conflict of Interest Statement: The authors declare that the research was conducted in the absence of any commercial or financial relationships that could be construed as a potential conflict of interest.

Copyright © 2017 Luo, Zhang, Zhu, Fu, Su, Zheng, Wang, Wang and Gong. This is an open-access article distributed under the terms of the Creative Commons Attribution License (CC BY). The use, distribution or reproduction in other forums is permitted, provided the original author(s) or licensor are credited and that the original publication in this journal is cited, in accordance with accepted academic practice. No use, distribution or reproduction is permitted which does not comply with these terms.



Proteomic and Physiological Analyses Reveal Putrescine Responses in Roots of Cucumber Stressed by NaCl

Yinghui Yuan¹, Min Zhong¹, Sheng Shu¹, Nanshan Du¹, Jin Sun^{1,2} and Shirong Guo^{1,2*}

¹ Key Laboratory of Southern Vegetable Crop Genetic Improvement, Ministry of Agriculture, College of Horticulture, Nanjing Agricultural University, Nanjing, China, ² Suqian Academy of Protected Horticulture, Nanjing Agricultural University, Suqian, China

OPEN ACCESS

Edited by:

Jie Zhou,
Zhejiang University, China

Reviewed by:

Qaisar Mahmood,
COMSATS Institute of Information Technology, Pakistan
Qinghua Shi,
Shandong Agricultural University,
China

*Correspondence:

Shirong Guo
srguo@njau.edu.cn

Specialty section:

This article was submitted to
Plant Cell Biology,
a section of the journal
Frontiers in Plant Science

Received: 19 May 2016

Accepted: 01 July 2016

Published: 15 July 2016

Citation:

Yuan Y, Zhong M, Shu S, Du N, Sun J and Guo S (2016) Proteomic and Physiological Analyses Reveal Putrescine Responses in Roots of Cucumber Stressed by NaCl. *Front. Plant Sci.* 7:1035.
doi: 10.3389/fpls.2016.01035

Soil salinity is a major environmental constraint that threatens agricultural productivity. Different strategies have been developed to improve crop salt tolerance, among which the effects of polyamines have been well-reported. To gain a better understanding of the cucumber (*Cucumis sativus* L.) responses to NaCl and unravel the underlying mechanism of exogenous putrescine (Put) alleviating salt-induced damage, comparative proteomic analysis was conducted on cucumber roots treated with NaCl, and/or Put for 7 days. The results showed that exogenous Put restored the root growth inhibited by NaCl. Sixty-two differentially expressed proteins implicated in various biological processes were successfully identified by MALDI-TOF/TOF MS. The four largest categories included proteins involved in defense response (24.2%), protein metabolism (24.2%), carbohydrate metabolism (19.4%), and amino acid metabolism (14.5%). Exogenous Put up-regulated most identified proteins involved in carbohydrate metabolism, implying an enhancement in energy generation. Proteins involved in defense response and protein metabolism were differently regulated by Put, which indicated the roles of Put in stress resistance and proteome rearrangement. Put also increased the abundance of proteins involved in amino acid metabolism. Meanwhile, physiological analysis showed that Put could further up-regulated the levels of free amino acids in salt stressed-roots. In addition, Put also improved endogenous polyamines contents by regulating the transcription levels of key enzymes in polyamine metabolism. Taken together, these results suggest that Put may alleviate NaCl-induced growth inhibition through degradation of misfolded/damaged proteins, activation of stress defense, and the promotion of carbohydrate metabolism to generate more energy.

Keywords: *Cucumis sativus* L., metabolic processes, proteome, putrescine, root, salt stress

INTRODUCTION

Soil salinity is one of the most serious environmental constraints to farming production, owing to both natural reasons and inappropriate agricultural operations (Munns and Tester, 2008). Although variable strategies existed for dealing with salt stress, most crops could not grow well on saline soil. Salt tolerance is a complex trait, involved in osmotic adjustment, toxic ions exclusion, and compartmentalization, as well as morphological changes (Munns, 2005). Most studies focused

on salt-induced responses in the shoot tissues, since minimizing toxic ions accumulation in leaf is essential for plant growth and productivity (Julkowska et al., 2014). However, root is the first organ exposed to salt stress, and sometimes even shows greater growth reduction than shoot (Bernstein et al., 2004; Contreras-Cornejo et al., 2014). Root growth inhibition is the most obvious change caused by salt stress. *Arabidopsis* root exposed to NaCl exhibited a reduced meristem size and smaller mature cells, thus resulting in primary root growth inhibition (West et al., 2004). Excessive salt ions accumulating in the soil exert osmotic pressure to roots, which leads to the inhibition of water absorption capacity, over-accumulation of reactive oxygen species (ROS; Jiang et al., 2016), and interruption of membranes (Gupta and Huang, 2014). In addition, large amount of Na^+ entering into root cells is always accompanied by sustained leakage of cytosolic K^+ , resulting in severe ion imbalance and metabolic disorders (Witzel et al., 2009).

Polyamines (PAs) are biologically ubiquitous aliphatic amines in all living cells. In plants, PAs have been implicated in various processes about plant growth and development, and play essential roles in abiotic, and biotic stress responses (Alcázar et al., 2010; Gill and Tuteja, 2010). The tetraamine spermine (Spm), triamine spermidine (Spd), and their precursors, diamine putrescine (Put), are the most common PAs studied in plants. Apart from the free forms, PAs in plants also occurred as conjugates with small molecules such as hydroxycinnamic acids and phenolic, and bound to macromolecules like proteins, and nucleic acids (Quinet et al., 2010; Tiburcio et al., 2014). In most plant species, Put is synthesized either from L-Arginine or L-Ornithine by arginine decarboxylase (ADC), or ornithine decarboxylase (ODC; Dalton et al., 2016), and then converted to Spd and Spm by the action of spermidine synthase (SPDS) and spermine synthase (SPMS). S-adenosylmethionine decarboxylase (SAMDC) provides aminopropyl groups for the synthesis of Spd and Spm (Bagni and Tassoni, 2001; Fuell et al., 2010). Polyamine catabolic process is catalyzed by diamine oxidases (DAO) for Put and polyamine oxidases (PAO) for SPD/Spm. Polyamine oxidases also catalyze the back-conversion of Spm to Spd (Moschou et al., 2008). The mutual conversion among endogenous Put, Spd, and Spm makes it difficult to ascertain their individual functions (Mattoo et al., 2010).

Numerous studies using mutants, anogenic gene lines, or exogenous application demonstrated the positive role of PAs in salt tolerance (Urano et al., 2004; Wi et al., 2006; Yamaguchi et al., 2006; Kamiab et al., 2014). PAs inhibit the opening and induce closure of stomata by regulating voltage-dependent inward K^+ channel (Liu et al., 2000) or H_2O_2 signal (Konstantinos et al., 2010), thus restricting transpiration and reducing water loss. PAs also regulated ROS homeostasis during salt stress by activating antioxidant defense system and directly scavenging O_2^- and $\cdot\text{OH}$ (Li et al., 2014; Saha et al., 2015). Interactions of PAs with ion channels especially contributed to the ion homeostasis under salinity conditions (Pottosin et al., 2014). Apart from these physiological changes, PAs are also reported to interact with proteins, the final executants of life activities, to control Plant adaptations. Previous studies reported that PAs could bind to charged spots at protein interfaces and

thus regulate protein function by modulating electrostatic protein–protein interactions (Berwanger et al., 2010). PAs covalent binding with proteins by transglutaminase (TGase) helps stabilizing cell structure and function (Campos et al., 2013). Comparative proteome could provide comprehensive analysis of plant responses to environmental stresses regulated by PAs (Witzel et al., 2009). Proteomic analysis conducted on cucumber leaves revealed that increased salt tolerance by Spd was attributed to the increased levels of proteins involved in protein biosynthesis, antioxidant defense reaction, and energy metabolism (Li et al., 2013). Shi et al. (2013) found that pre-treatment of Put, Spd, and Spm enhanced salt and drought tolerance of bermudagrass by regulating carbon fixation, electron transport, energy, and defense pathways, and also activating accumulation of osmolytes. All PAs effectively depressed protein tyrosine nitration and carbonylation by eliminating reactive nitrogen and oxygen species in leaves of citrus exposed to salinity stress (Tanou et al., 2014).

Cucumber (*Cucumis sativus* L.) as world popular vegetable is sensitive to soil salinity. Studies about exogenous substances such as calcium (He et al., 2012), salicylic acid (Hao et al., 2012), 24-epibrassinolide (An et al., 2016), and Spd (Li et al., 2013) induced proteome alterations in cucumber have been well-reported. Our previous study also reported the photosynthetic associated proteins regulated by Put (Shu et al., 2015). Little information about Put regulating proteomic changes in roots of cucumber exposed to salt stress is available. In this present work, we conducted 2-dimensional gel electrophoresis to analysis the root proteins responding to Put under NaCl stress conditions. A comprehensive analysis among Put regulated proteins and related metabolic processes was then carried out to explore the mechanism of Put in alleviating the damage of salt stress.

MATERIALS AND METHODS

Plant Material and Treatment

Cucumber (*Cucumis sativus* L. cv. Jinyou No. 4) seeds were sown in quartz sand, cultured in a greenhouse, and transplanted to plastic containers at the leaf two stage as previously described (Yuan et al., 2014). After 2 days pre-culture, the seedlings were treated as follows: (a) control, seedlings grown in full-strength Hoagland nutrient solution; (b) Put, seedlings grown in full-strength Hoagland nutrient solution containing 0.8 mM Put; (c) NaCl, seedlings grown in full-strength Hoagland nutrient solution containing 75 mM NaCl; (d) NaCl + Put, seedlings grown in full-strength Hoagland nutrient solution containing 75 mM NaCl and 0.8 mM Put. The experiment was arranged in a randomized complete block design with three replicates per treatment, that is, each treatment included three containers of total 36 plants. The concentrations of NaCl and Put were selected on the basis of previous experiment (data not shown). All the nutrient solutions were renewed every 2 days.

Root Growth Determination and Viability Staining

The length of primary root was measured every day to calculate the average increment during the whole treatment period.

After 7 days of treatment, cucumber roots were cut off and photographed. Root cell viability was then assessed by fluorescein diacetate (FDA)–propidium iodide (PI) double staining method as described by Bose et al. (2014). Root segments, including the root tip (1 cm), were cut off and stained with $5 \mu\text{g mL}^{-1}$ FDA for 3 min followed by $3 \mu\text{g mL}^{-1}$ PI for 10 min. Then the stained roots were observed using a Leica DM2500 microscope (Leica Microsystems, Wetzlar, Germany). Excitation wavelengths of 488 and 594 nm were used for FDA and PI imaging, respectively. Images were acquired with a digital camera (Leica DFC495, Leica Microsystems) equipped with a LAS V3.8 (Leica Microsystems) software.

Measurement of Free Amino Acids Levels

After 7 days of treatment, root samples were harvested, oven dried, and acid hydrolyzed to analyze free amino acids by an automatic amino acid analyzer (Hitachi L-8900, Tokyo, Japan) according to Norden et al. (2004). Dried samples of root were suspended in 6 M HCl and then hydrolyzed at 110°C for 24 h. The hydrolyzed samples were centrifuged at $3000 \times g$ for 5 min,

and the supernatant was collected and evaporated to dryness. The dried samples were then redissolved in 0.1 M sodium citrate buffer (pH 2.2). The resulting amino acids solution was analyzed with 17 kinds of L-amino acid (sigma) as the standard. Results were determined as mg per 100 mg of dry samples (% DW).

Analysis of Endogenous Polyamines

Endogenous polyamines levels were analyzed by high-performance liquid chromatography (HPLC) according to Shu et al. (2015) with small modifications. After 7 days of treatment, root samples were harvested and homogenized in 5% (W/V) cold HClO_4 and incubated on ice for 1 h. After centrifugation for 20 min at $12,000 \times g$, the supernatant was used to determine free, and conjugated polyamines and the pellet was used to determine bound polyamines. For conjugated and bound polyamines, samples were hydrolyzed at 110°C for 18 h in 6 M HCl and then evaporated at 70°C . The residue was re-suspended in 5% HClO_4 and used to measure polyamines contents with the non-hydrolyzed supernatant. The resulting solutions were mixed with 2 M NaOH and benzoyl chloride, and vortexed vigorously.

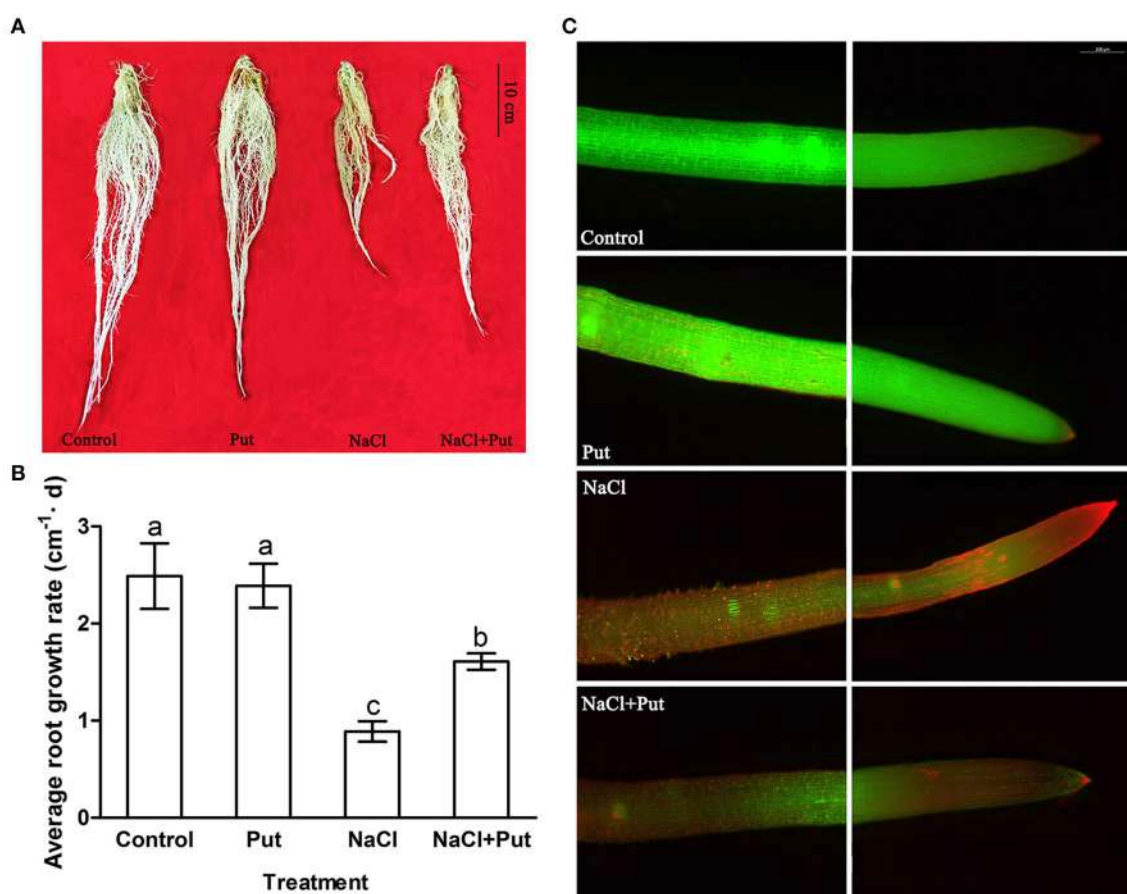


FIGURE 1 | Effects of exogenous putrescine (Put) on root morphology (A), average growth rate (B), and root viability (C) of cucumber seedlings in hydroponics with or without 75 mM NaCl for 7 d. Each histogram represents a mean \pm SE of six independent experiments ($n = 6$). Different letters indicate significant differences between treatments ($P < 0.05$) according to Duncan's multiple range tests. Control, seedlings cultured in normal nutrient solution; Put, seedlings cultured in nutrient solution with 0.8 mM Put; NaCl, seedlings cultured in nutrient solution supplemented with 75 mM NaCl; NaCl + Put: Both NaCl and Put added to the nutrient solution.

After incubation for 30 min at 37°C, saturated NaCl solution was added to terminate the reaction. The benzoyl polyamines were extracted with cold diethyl ether. Then the diethyl ether phase was evaporated to dryness and re-dissolved in 64% (v/v) cold methanol. Finally, polyamines were assayed by HPLC 1200 series system (Agilent Technologies, Santa Clara, CA) with a C18 reverse phase column (4.6 by 250 mm, 5 µm Kromasil) and a two solvent system including a methanol gradient (36–64%, v/v) at a flow rate of 0.8 mL min⁻¹. Standard Put, Spd, and Spm (Sigma) were treated in similar way.

Protein Extraction and 2-Dimensional Gel Electrophoresis (2D) Analysis

After 7 days of treatment, total root proteins were extracted using a trichloroacetic acid (TCA)-acetone precipitation method

modified from Hurkman and Tanaka (1986). Fresh root samples (2 g) were ground to fine powder with liquid nitrogen and resuspended in 6 mL of ice-cold extraction buffer which contains 20 mM Tris-HCl (pH 7.5), 1 mM ethylenebis(oxyethylenenitrilo)tetraacetic acid (EGTA), 1 mM dithiothreitol (DTT), and 1 mM phenylmethyl sulfonyl fluoride (PMSF). After standing on ice for 20 min, the homogenate was centrifuged at 15,000 × g at 4°C for 20 min. The resulting supernatant was transferred into a new centrifuge tube and precipitated with five volumes of ice-cold acetone containing 10% TCA and 0.07% β-mercaptoethanol at -20°C for at least 4 h. The resulting protein-containing suspension was centrifuged at 20,000 × g for 25 min. The protein pellet was washed three times with acetone containing 0.07% β-mercaptoethanol at -20°C for 2 h. The protein sample was air-dried and

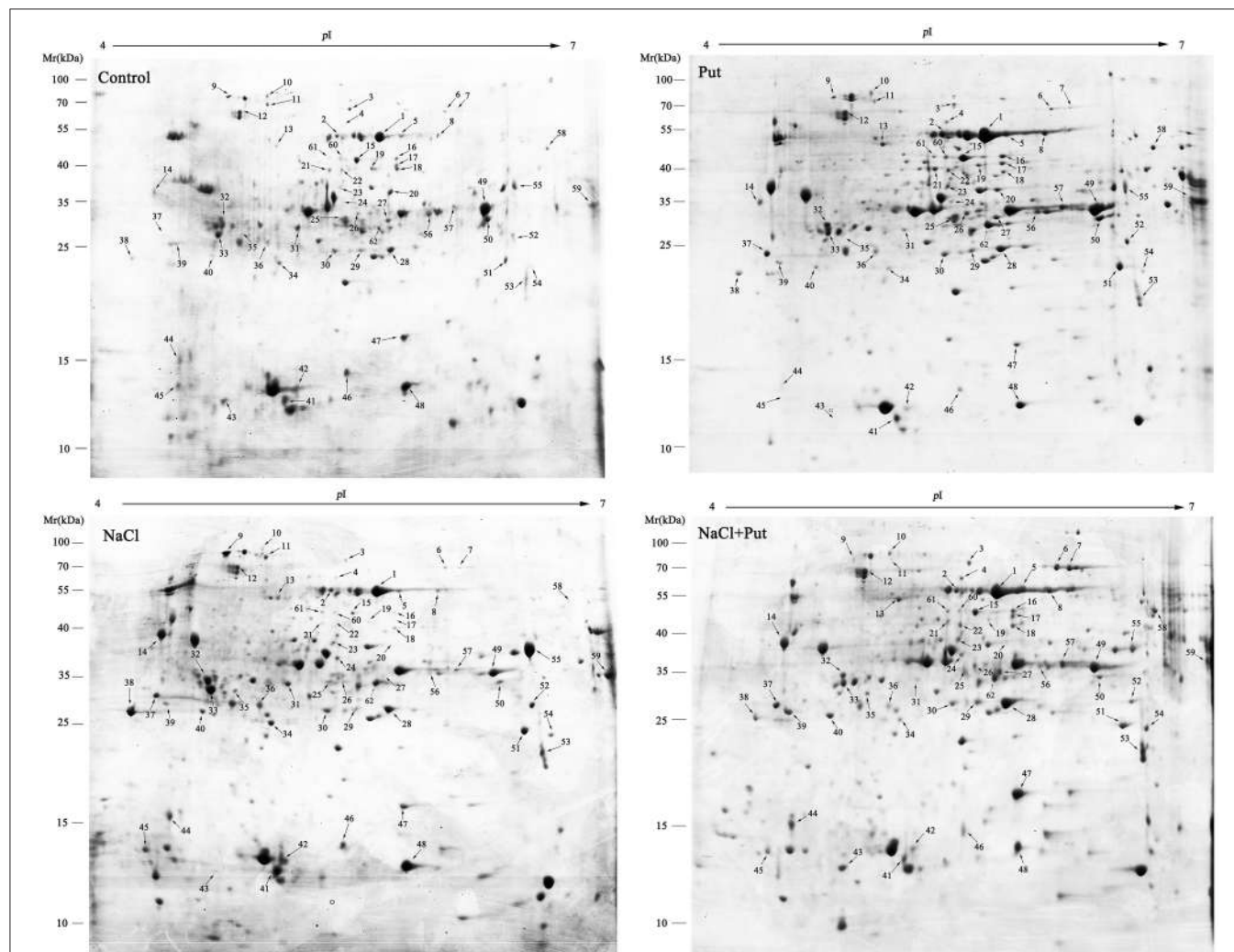


FIGURE 2 | Representative 2-DE gel images from root samples treated with NaCl and/or putrescine (Put). Total proteins were extracted and separated by IEF/SDS-PAGE then stained with Coomassie Brilliant Blue (R-250). An equal amount (800 µg) of total proteins was loaded onto 18 cm gel strip (pH 4–7, linear). The pH and molecular mass standards are indicated on the top and left side of each gel image. Sixty two differentially expressed protein spots are marked with arrows and numbers, and annotated according to the numbering in **Table 1**. Control, seedlings cultured in normal nutrient solution; Put, seedlings cultured in nutrient solution with 0.8 mM Put; NaCl, seedlings cultured in nutrient solution supplemented with 75 mM NaCl; NaCl+Put: Both NaCl and Put added to the nutrient solution.

TABLE 1 | List of differentially expressed proteins in response to NaCl and/or putrescine (Put).

Spot no. ^a	Protein name	NCBI accession no.	CARBOHYDRATE METABOLISM (12)		MP ^b	Score	Cov ^c (%)	Fold changes		
			Theoretical	Experimental				Control/Control	Put/Control	NaCl/Control
Glycolysis										
1	Enolase isoform X1	XP_004143301.1	47.94/5.48	57/5.69	15	481	18.69	1.00	2.89	1.72
2	Enolase isoform X2	XP_011657684.1	43.13/5.8	57.4/5.45	14	318	45.98	1.00	4.93	1.63
5	Enolase isoform X1	XP_004143301.1	47.94/5.48	57.4/5.82	22	1100	71.62	1.00	3.02	1.68
6	2,3-Bisphosphoglycerate-independent phosphoglycerate mutase	XP_004147519.1	61.27/5.69	74.2/6.07	34	713	84.62	1.00	2.63	1.62
7	2,3-Bisphosphoglycerate-independent phosphoglycerate mutase	XP_004147519.1	61.27/5.69	74.2/6.15	34	986	86.05	1.00	1.54	1.82
59	Fructose-bisphosphate aldolase, cytoplasmic isozyme-like	XP_004143304.1	38.73/7.57	34.5/6.95	14	224	50.00	1.00	0.94	3.99
62	Probable fructokinase-4	XP_004145029.1	35.79/5.62	31.42/5.69	14	304	51.06	1.00	4.02	1.98
Tricarboxylic Acid Cycle										
49	Malate dehydrogenase, mitochondrial	XP_004137217.1	36.41/8.52	34/6.32	11	435	47.84	1.00	1.32	0.68
50	Malate dehydrogenase, chloroplastic	XP_011660098.1	43.65/8.11	32.6/3.4	16	354	45.50	1.00	0.65	0.31
56	Malate dehydrogenase, mitochondrial	XP_004137217.1	36.41/8.52	34/5.98	13	342	45.82	1.00	0.95	0.25
Galactose Metabolism										
8	Galactokinase	XP_011651088.1	55.21/5.69	57.4/6.08	24	535	55.91	1.00	4.26	2.86
Sucrose Metabolism										
10	Acid beta-fructofuranosidase-like	XP_004143623.1	69.80/4.92	93/5.06	16	588	30.63	1.00	1.16	0.57
PROTEIN METABOLISM(15)										
Protein Folding and Assembly										
3	Heat shock 70kDa protein, mitochondrial	XP_004147511.1	73.25/5.69	79.6/5.52	32	435	60.59	1.00	0.72	0.46
4	Chaperonin CPN60-2, mitochondrial	XP_004147171.1	61.51/5.84	63.8/5.48	33	597	68.52	1.00	2.36	0.99
9	Heat shock protein 70	CAA52149.1	75.48/5.15	88.6/4.84	20	163	33.80	1.00	0.66	3.22
11	Heat shock protein 70	CAA52149.1	75.48/5.15	82/5.07	22	444	39.04	1.00	0.82	1.69
12	Protein disulfide-isomerase	KGN47715.1	57.27/4.88	70.5/4.91	27	1,080	70.39	1.00	1.55	0.57
Protein Biosynthesis										
23	Elongation factor 2	XP_011657107.1	95.03/5.97	38/5.47	19	340	27.52	1.00	3.03	1.86
35	Eukaryotic translation initiation factor 3 subunit J	XP_004140297.1	25.11/4.78	28.5/4.93	5	129	20.00	1.00	1.11	2.54
46	60S Acidic ribosomal protein P2-4	XP_004150488.1	11.42/4.53	13.5/5.52	9	631	81.58	1.00	0.34	1.09

(Continued)

TABLE 1 | Continued

Spot no. ^a	Protein name	NCBI accession no.	Experimental			Fold changes					
			Theoretical	M _r (kDa)/P _i	M _p ^b	Score	Cov ^c (%)	Control/Control	Put/Control	NaCl/Control	NaCl+Put/NaCl
Protein Degradation											
13	26S protease regulatory subunit 6A homolog	XP_004135596.1	47.81/4.96	52/5.12	17	130	46.57	1.00	3.16	1.90	2.10
36	Thiol protease aleurain-like	XP_004144033.1	39.55/6.26	26.25/5.04	10	489	43.25	1.00	1.49	2.41	0.67
40	Proteasome subunit alpha type-5	XP_0011660309.1	26.10/4.75	24.33/4.73	11	342	64.56	1.00	0.58	1.65	2.02
Protein Transport											
32	Ran-binding protein 1 homolog a-like	XP_004145252.1	24.36/4.8	31.83/4.80	5	110	37.96	1.00	0.63	0.97	0.61
33	Ran-binding protein 1 homolog a-like	XP_0011658664.1	22.41/5.06	29.5/4.78	12	551	68.02	1.00	0.82	1.66	0.56
39	Nascent polypeptide-associated complex subunit alpha-like protein 1	XP_004144316.2	21.90/4.40	25.33/4.51	11	378	75.50	1.00	1.28	1.69	4.06
Protein Modification											
42	Ubiquitin-conjugating enzyme E2 2	XP_004135191.1	17.45/5.4	12.5/5.21	2	149	17.76	1.00	0.32	1.00	0.44
DEFENSE RESPONSE (15)											
Antioxidative Reaction											
14	Peroxidase 2-like	XP_004142246.1	36.05/4.61	37.25/4.44	10	660	46.71	1.00	0.65	2.51	1.12
28	Ascorbate peroxidase, partial	AAQ88015.1	27.51/5.43	26.17/5.77	16	444	89.56	1.00	1.04	1.83	1.64
29	Ascorbate peroxidase	AGJ72850.1	27.56/5.44	25.75/5.59	11	259	52.61	1.00	1.79	1.00	1.86
30	L-ascorbate peroxidase, cytosolic-like	NP_0001267635.1	27.55/5.43	25.5/5.44	17	251	71.49	1.00	1.39	1.77	1.05
34	Ascorbate peroxidase, partial	AAQ88015.1	27.51/5.43	24.25/5.12	13	300	62.25	1.00	0.62	1.57	0.44
45	Superoxide dismutase [Cu-Zn]-like isoform X1	XP_0011658519.1	15.48/5.43	13/4.40	7	427	67.11	1.00	0.52	2.06	0.86
47	Superoxide dismutase [Cu-Zn],chloroplastic	XP_004145768.1	22.72/5.87	17/5.85	6	330	61.43	1.00	0.46	0.78	3.33
48	Peroxiredoxin-2B-like	XP_004142515.1	17.34/5.77	12.5/5.86	7	257	72.67	1.00	0.71	1.72	0.41
51	Glutathione S-transferase-like	XP_0011659352.1	23.99/5.98	23.5/6.47	10	258	69.77	1.00	3.16	2.67	0.94
52	Glutathione S-transferase DHAR2	XP_0011654937.1	23.90/6.18	27.6/6.51	13	521	63.85	1.00	1.28	1.79	0.75
55	Peroxidase 2-like	XP_004151583.1	37.68/5.64	37.25/6.51	7	227	34.01	1.00	0.92	4.92	0.23
57	Probable aldo-keto reductase 4	XP_004152112.2	37.89/5.78	35/6.13	13	319	42.61	1.00	1.57	0.55	3.38
Other defense response											
38	Chitinase	AAA33120.1	31.10/4.46	24/4.29	6	715	32.88	1.00	1.98	7.51	0.26
41	MLP-like protein 328	XP_004142283.1	17.37/5.08	12.5/5.16	10	403	82.12	1.00	0.76	1.53	0.46
43	Glycine-rich RNA-binding protein 3,mitochondrial-like	XP_004137435.1	17.25/7.82	12.25/4.81	7	278	57.31	1.00	1.32	0.22	7.36
RESPIRATION (1)											
53	Probable NAD(P)H dehydrogenase (quinone) FQR1-like 1	XP_004150766.1	21.73/6.43	21.25/5.58	9	713	51.72	1.00	1.32	1.88	1.12

(Continued)

TABLE 1 | Continued

Spot no. ^a	Protein name	NCBI accession no.	Mr(kDa)/PI		MP ^b	Score	Cov ^c (%)	Fold changes			
			Theoretical	Experimental				Control/Control	Put/Control	NaCl/Control	NaCl+Put/NaCl
AMINO ACID METABOLISM (9)											
15	S-adenosylmethionine synthase 2	XP_004153700.1	43.65/5.35	45.8/5.57	19	424	77.10	1.00	1.43	0.28	3.96
16	S-adenosylmethionine synthase 2	XP_004153700.1	43.65/5.35	45.7/5.80	13	145	40.71	1.00	2.80	0.29	5.45
17	S-adenosylmethionine synthase 2	XP_004153700.1	43.65/5.35	42.6/5.82	10	155	30.28	1.00	2.20	0.00	+
19	S-adenosylmethionine synthase 2	XP_004153700.1	43.65/5.35	42/5.65	11	119	31.30	1.00	1.24	0.32	1.41
21	S-adenosylmethionine synthase 2	XP_004153700.1	43.65/5.35	41.2/5.41	7	71	26.46	1.00	2.34	0.31	4.39
24	Arginase 1	XP_004145005.1	37.15/5.62	35.6/5.48	14	235	57.69	1.00	0.99	1.72	0.94
44	Glycine cleavage system H protein 2,mitochondrial	XP_004145438.1	6.93/4.98	14.7/5.42	4	203	47.10	1.00	3.49	1.53	1.11
60	S-adenosylmethionine synthase 2	XP_004135964.2	43.65/5.35	46.2/5.47	8	132	29.77	1.00	1.04	0.46	1.78
61	Fumarylacetoacetate	XP_004134793.1	47.60/5.21	46.4/5.40	13	88	42.33	1.00	0.96	0.54	1.72
FATTY ACID METABOLISM (2)											
25	Linoleate 13S-lipoxygenase 2-1,chloroplastic-like	XP_004142240.2	94.05/6.19	32/5.51	10	178	15.66	1.00	0.41	0.07	7.57
26	Enoyl-[acyl-carrier-protein] reductase [NADH],chloroplastic-like	XP_004142140.1	41.67/8.64	34/5.58	10	217	41.94	1.00	2.57	1.30	1.95
SECONDARY METABOLISM (3)											
20	Nitrite-specifier protein 5	XP_004139998.1	35.62/5.3	37.5/7.9	9	78	42.59	1.00	0.92	0.00	+
27	Nitrite-specifier protein 5	XP_004139998.1	35.62/5.3	32.7/5.74	13	108	43.52	1.00	2.08	0.39	4.38
54	Acetylpyruvate FAHD1,mitochondrial	XP_004134224.1	23.64/6.21	23.2/6.61	8	639	64.55	1.00	0.91	1.66	1.43
CELL RELATED PROTEIN (4)											
18	Phragmoplast orienting kinesin 2	XP_0011649250.1	158.81/5.09	40.2/5.80	30	69	26.35	1.00	0.99	0.42	3.29
22	Actin-7	XP_004147353.1	41.91/5.31	41.5/5.49	17	521	57.03	1.00	2.61	0.13	12.31
31	Tubulin beta chain-like	XP_004137743.1	50.73/4.73	30.2/5.22	9	87	28.03	1.00	0.37	0.84	0.27
58	Protein NETWORKED 1A	XP_0011650959.1	211.48/5.18	48.2/5.68	39	75	22.04	1.00	3.43	0.75	5.96
37	Uncharacterized protein A12g99795,mitochondrial-like	XP_004138451.1	28.75/4.69	26.3/4.46	5	232	27.67	1.00	2.98	2.43	1.23

^aSpot number corresponding with 2-DE gel as shown in **Figure 2**.^bNumber of identified peptides.^cPercentage of sequence coverage by matched peptides.^dThe values higher than 1.5 or lower than 0.67 indicate significant changes.

rehydrated in a rehydration buffer consisted of 7 M urea, 2 M thiourea, 4% 3-[3-cholanidopropyl] dimethylammonio]-1-propanesulfonic acid (w/v), 40 mM DTT, 0.5% (v/v) immobilized pH gradient (IPG) buffer 4–7, and 0.01% (w/v) bromophenol blue. Protein concentrations were quantified using the Bradford method (Bradford, 1976). Bovine serum albumin (BSA) was used as the standard.

Isoelectric focusing (IEF) was performed with pH 4–7, 18 cm IPG linear gradient strips (GE Healthcare, USA). IPG strips were loaded with 350 µL of protein sample containing 800 µg protein in a rehydration tray for 12–16 h at 25°C. After rehydration, IEF was accomplished at 20°C on an Ettan IPGphor 3 (GE Healthcare, USA) with the following conditions: 100 V for 1 h, followed by 200 V for 1 h, 200 V for 1 h, 500 V for 1 h, 1000 V for 1 h, 4000 V for 1 h, a gradient of 10,000 V for 1 h, and then 10,000 V rapid focus, reaching a total of 75,000 V h. The electric current during IEF was no more than 50 µA per strip.

After running the first dimension, IEF strips were equilibrated in 2D equilibrium buffer [50 mM Tris-HCl, pH 8.8, 6 M urea, 30% glycerol (v/v), 2% sodium dodecyl sulfate (SDS)] containing 1% DTT for 15 min and then in the same equilibrium buffer containing 2.5% iodoacetamide for 15 min. Then the equilibrated strips were placed directly onto 12.5% polyacrylamide-SDS slab gels and sealed with 0.5% agarose solution containing bromophenol blue dye. The second dimensional SDS-polyacrylamide gel electrophoresis (SDS-PAGE) was conducted using the EttanDaltSix electrophoresis system (GE Healthcare, USA). Electrophoresis was carried out at 15 W per gel until the bromophenol blue dye front reached about 1 cm from the bottom of the gel. The resulting gels were stained with Coomassie Brilliant Blue (CBB) R-250 to visualize protein spots.

Image and Data Analysis

After de-staining, images of CBB-stained 2-D gels were obtained using an Image scanner III (GE Healthcare, USA) and analyzed with Imagemaster 2D Platinum version 5.0 (GE Healthcare, USA). The abundance of each protein spot was estimated by the percentage volume (vol%), which was normalized as the ratio of the volume of a single spot to the whole set of spots present in the gel. Only spots with significant (Duncan's multiple range test at the $P < 0.05$ level) and reproducible changes (at least 1.5-folds change in abundance) in three replicates were used for mass spectrometry.

Protein Identification

Differentially expressed protein spots were excised from gels and in-gel protein digestion was carried out as described by He et al. (2012). The resulting peptides were used for MALDI-TOF/TOF analysis with an ABI 5800 Proteomics Analyzer MALDI-TOF/TOF analyzer (Applied Biosystems, Foster City, CA, USA). Spectral data were used to search NCBI (<http://www.ncbi.nlm.nih.gov/>) and cucumber genomics database (<http://cucumber.genomics.org.cn>) with the software MASCOT version 2.2 (Matrix Science, London, UK). MS + MS/MS spectra search criteria in the databases were: trypsin as enzyme, one missed cleavage site, carbamidomethyl set as fixed modification, methionine oxidation

allowed as dynamical modification, peptide mass tolerance within 100 ppm, the fragment tolerance set to ± 0.4 Da, and minimum ion score confidence interval for MS + MS/MS data was set to 95%.

Protein Functional Classification

The differentially expressed proteins were classified according to the biological processes in which they are involved based on UniProtKB (<http://www.uniprot.org/>) and KEGG (<http://www.genome.jp/kegg/>) databases. Hierarchical clustering of protein expression patterns was performed using Cluster software version 3.0. Input data was calculated by dividing spot abundance at NaCl and/or Put treatment by abundance of the same protein spot at control and log₂ transformed. The resulting heat map was visualized by Java Treeview.

Quantitative Real-Time PCR (qRT-PCR) Analysis

Root tissues were harvested after 1, 3, 5, and 7 days of treatment and extracted for total RNA using Trizol reagent (Takara, Otsu, Japan). A first-strand cDNA fragment was then synthesized using a SuperScript First-strand Synthesis System for qRT-PCR. qRT-PCR was performed according to the instructions provided by the SYBR® Premix Ex Taq™ II (Tli RNaseH Plus) kit (Takara). A 20 µL reaction mixture containing 2 µL of cDNA (diluted 1:5), 10 µL of SYBR® Premix ExTaq™ II (2×), 0.8 µL of each specific primer, 0.4 µL of ROX reference dye, and 6 µL of ddH₂O was run in triplicate on a StepOnePlus™ Real-Time PCR System (Applied Biosystems). Thermal cycling was initialized at 95°C for 5 min, followed by 40 cycles of 95°C for 15 s, 60°C for 1 min, and a final extension of 15 s at 95°C. Relative expression levels were calculated using the $2^{-\Delta\Delta Ct}$ method, where the Ct-values obtained from the amplification plots for tested genes were normalized against that of the housekeeping gene (actin) and compared with the control. Base sequences of these tested genes were identified by searching the NCBI and cucumber genomics database. The gene specific primers were designed using Beacon Designer 7 (Premier Biosoft International, CA, USA) and all primer sequences were listed in Supplementary Table 1.

Statistical Analysis

All data were statistically analyzed using SAS 13.0 software (SAS Institute, Inc., Cary, NC, USA) by Duncan's multiple range test at $P < 0.05$ level of significance.

RESULTS

Root Growth

The effect of exogenous Put on root growth of cucumber seedlings exposed to NaCl stress was investigated (Figure 1). Seventy-five millimolars of NaCl treatment for 7 days seriously decreased cucumber root growth, and cucumber root gradually turned flaccid, filemot, and transparent (Figure 1A). Application of exogenous Put effectively alleviated the growth inhibition induced by NaCl stress, showing a 1.8-folds up-regulation in the average growth rate, but exerted no significant effect on roots of control plants (Figure 1B). Viability staining experiments

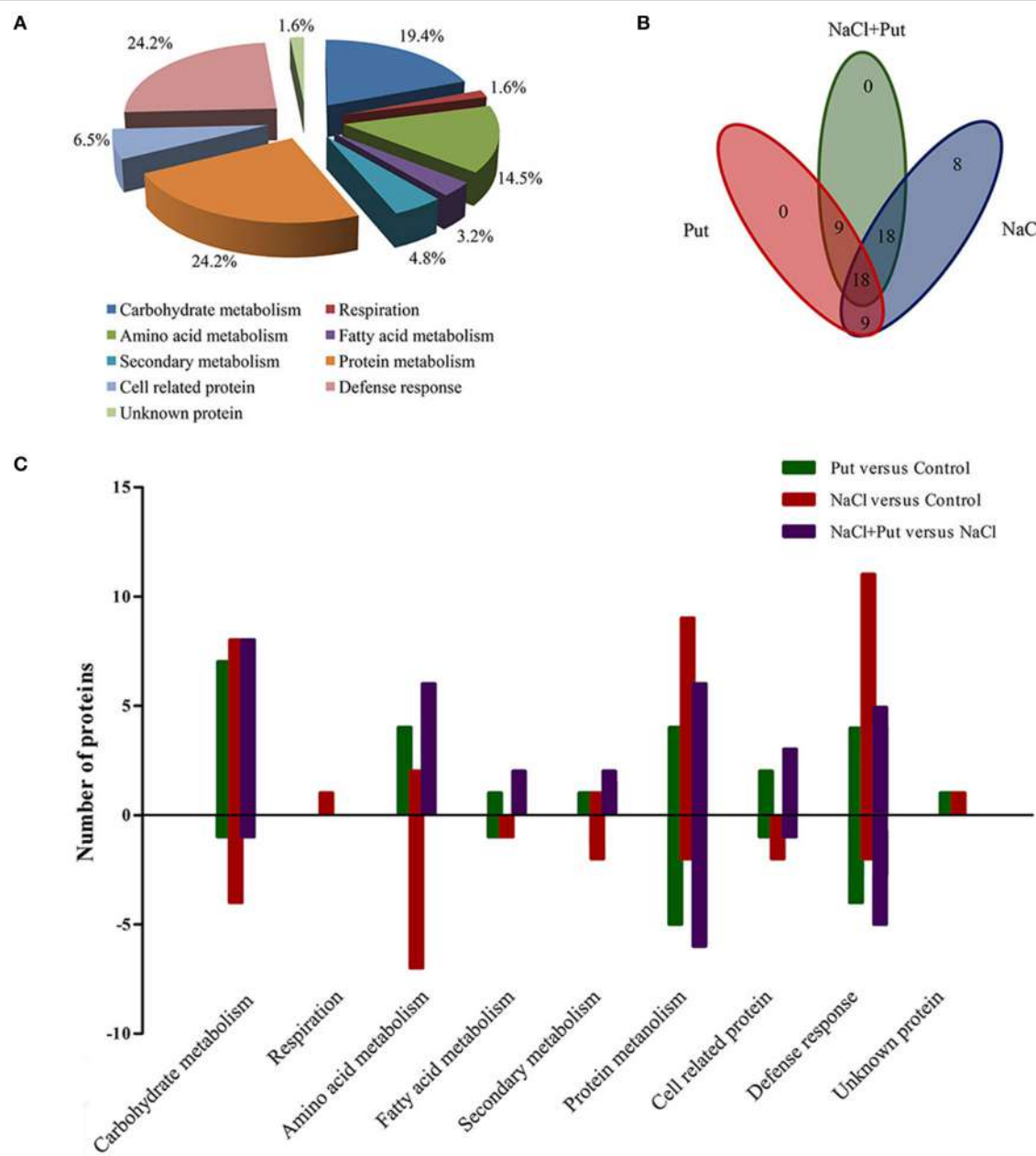


FIGURE 3 | Distribution of differentially expressed proteins by NaCl and/or putrescine (Put) in cucumber root. (A) Functional classification of 62 differentially expressed proteins. **(B)** Venn diagram showing the number of overlapping proteins that were differentially regulated by Put, NaCl, and NaCl+Put as compared with the control. **(C)** The specific number of proteins with fold changes ≥ 1.5 (up-regulated, above the horizontal axis) or fold changes ≤ 0.67 (down-regulated, below the horizontal axis) regulated by Put, NaCl, and NaCl+Put compared with the control. Control, seedlings cultured in normal nutrient solution; Put, seedlings cultured in nutrient solution with 0.8 mM Put; NaCl, seedlings cultured in nutrient solution supplemented with 75 mM NaCl; NaCl+Put: Both NaCl and Put added to the nutrient solution.

also proved that Put reduced the root cells death under NaCl stress (Figure 1C), thus maintained the absorption of water and nutrients.

Comparative Proteomic Analysis

A comparative analysis of proteome was conducted using root samples after 7 days of treatment to investigate the

profiles of NaCl and/or Put-responsive, differentially expressed proteins. Approximately 400 reproducible protein spots were detected on the 2-DE gels (Figure 2; Supplementary Figure 1), of which 62 differentially expressed protein spots (changes ≥ 1.5 folds) were successfully identified by MALDI-TOF/TOF MS. These differentially expressed proteins were listed in Table 1.

All proteins respond to Put and/or NaCl were categorized into different classes according to their biological process (**Figure 3A**), among which one protein (spot 37) had no functional annotations in the database. The categories with a high level of expression variation are those involved in protein metabolism (24.2%), defense response (24.2%), carbohydrate metabolism (19.4%), and amino acid metabolism (14.5%). The number and overlapping of differentially expressed proteins were summarized in **Figures 3B,C**. Totally, 53 protein spots were significantly regulated by NaCl when compared with control (**Figure 3B**). Of those, 33 protein spots were up-regulated in abundance, and 20 protein spots were down-regulated. Most identified proteins involved in carbohydrate metabolism, protein metabolism, and defense response were up-regulated and most identified proteins involved in amino acid metabolism, fatty acid metabolism, and secondary metabolism were down-regulated (**Figure 3C**). However, 54 protein spots were significantly regulated by Put under control or NaCl stress conditions, of which 27 protein spots were regulated by Put under both control and NaCl stress conditions (**Figure 3B**). Put up-regulated the expression of most identified proteins involved in different biological processes, while also decreased the abundance of several proteins involved in defense response and protein metabolism (**Figure 3C**).

In order to identify proteins with similar expression patterns, hierarchical clustering was performed (**Figure 4**). Cluster A was composed of 13 proteins that were up-regulated under both NaCl and NaCl+Put treatment as compared with those of the control. Most of these proteins were involved in defense response. Cluster B involved 15 proteins that were down-regulated by Put both under the control and NaCl stress conditions, and most of these proteins were corresponding to defense response and protein metabolism. Cluster C included 19 proteins that were down-regulated by NaCl, but recovered by the application of Put. Most identified proteins participating in amino acid metabolism were included in this cluster. Proteins involved in carbohydrate metabolism, especially tricarboxylic acid cycle, were also present in this cluster. Cluster D contained 15 proteins with increased abundance by Put under both the control and NaCl stress conditions. Most identified proteins functional in glycolysis (part of carbohydrate metabolism) were included in this cluster.

Free Amino Acids Contents

Many proteins related to protein and amino acid metabolism were identified in this study. Considering that amino acid is the raw material for protein synthesis, we measured the free amino acid levels under different treatment (**Table 2**). Glutamic acid (Glu) was the most abundant amino acid in cucumber root, occupied over 2% of dry weight, while cysteine, the least amino acid identified, occupied <0.1% of root dry weight. Except for proline, all the other amino acids contents were increased by NaCl stress, leading to 15.2% increase in total amino acids level as compared with that of the control. Exogenous Put increased all amino acids levels in control plants, and total amino acids level was 1.23-fold higher than the control. Put applied to NaCl stressed plants further increased amino acids levels except for cysteine. Exogenous Put caused a higher increase in amino acids

levels than NaCl, which reflected a promotion in amino acid metabolism and protein hydrolysis.

Endogenous Polyamines Metabolism

In response to NaCl stress, free, conjugated, and bound Put and Spm contents in cucumber roots were increased in comparison with those of the control (**Table 3**). Free Spd level was also increased by NaCl, whereas conjugated and bound forms of Spd were decreased significantly. Treatment with Put under NaCl stress condition caused increase in almost all kinds of PAs when compared with NaCl-only treatment, except for the bound Spm, which was decreased by Put. Exogenous Put also increased free PAs levels in control plants. Generally, NaCl stress caused increase in total Put and Spm levels, but decreased Spd level. Put treatment increased total Put and Spd contents both under control and stressed conditions, but decrease total Spm level stressed by NaCl.

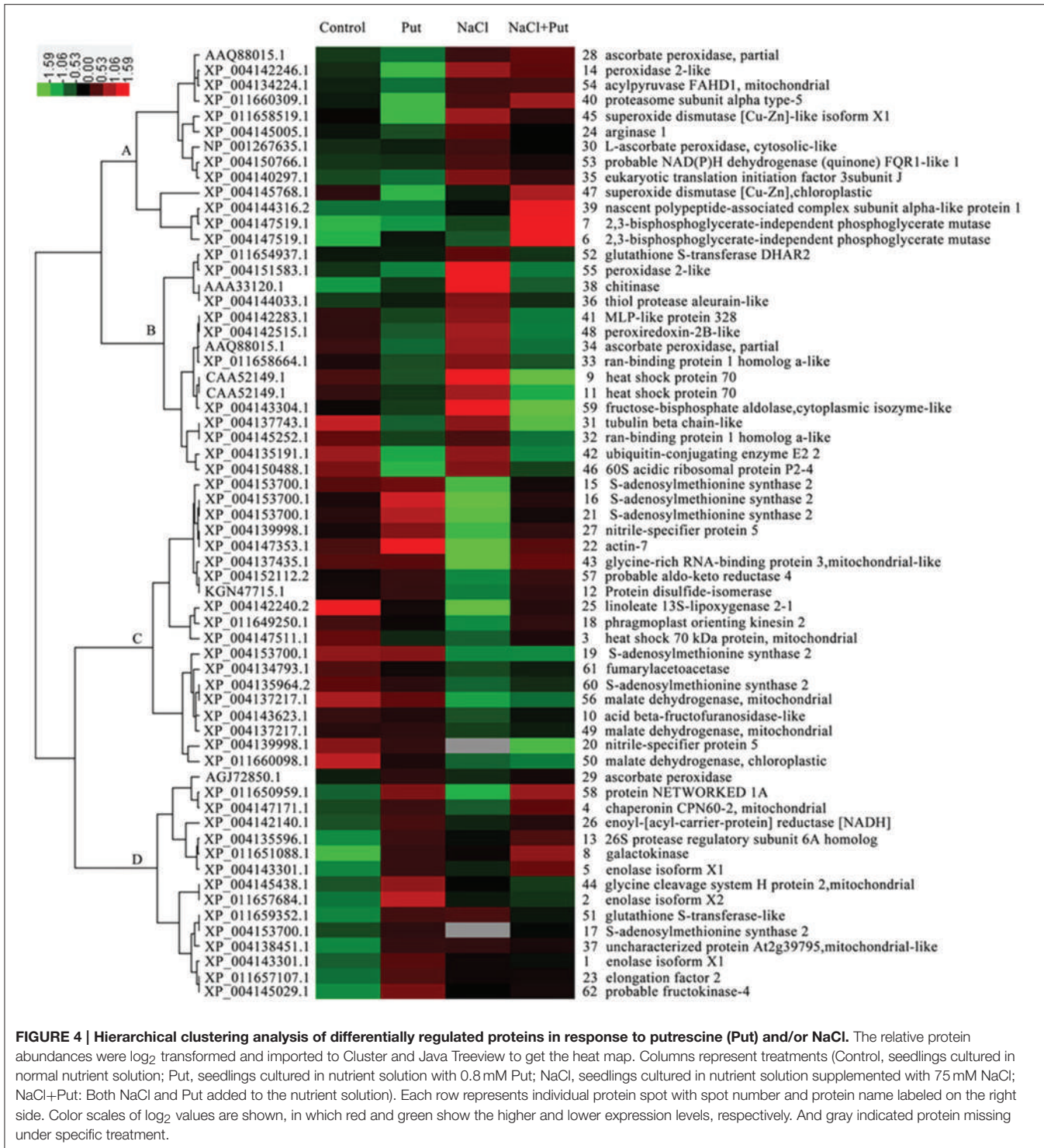
Expressions of seven genes encoding enzymes involved in PAs metabolism were then analyzed after 1, 3, 5, and 7 days of treatment. NaCl stress up-regulated all tested genes involved in PAs biosynthesis (**Figures 5A–E**). PAO expression was also increased by NaCl (**Figure 5G**), while DAO was first increased and then decreased after 5 days of NaCl treatment (**Figure 5F**). Put applied to NaCl-stressed plants down-regulated the expression of *ADC*, *ODC*, *SAMDC*, *SPDS*, and *SPMS* induced by NaCl, but increased *DAO* expression. After 1 day of treatment, Put up-regulated the expression of *ADC*, *SAMDC*, *SPDS*, and *DAO*, but down-regulated *SPMS* and *PAO* expression in the control plants. In fact, Put decreased the expression of *SPMS* and increased *DAO* expression in the control plants during the whole treatment period.

DISCUSSION

Multiple publications showed that polyamines can increase plants tolerance to various environmental stresses (Urano et al., 2004; Yamaguchi et al., 2006). In the present study, Put was found to restore cucumber root growth and root cell vitality decreased by NaCl stress (**Figure 1**). 2-DE analysis was conducted to obtain the profiling of the total proteins in cucumber roots responding to Put under NaCl stress conditions (**Figure 2, Table 1**). After quantitative and MALDI-TOF/TOF MS analysis, 62 differentially regulated protein spots were successfully identified. Proteins involved in protein metabolism, and defense response took up the highest percentage of differentially expressed proteins. Twelve carbohydrate metabolism related proteins and nine amino acid metabolism related proteins made the third and fourth group of identified proteins. In addition, several proteins participated in other metabolic processes were also identified. The regulation of Put and NaCl to these metabolic processes is discussed below.

Putrescine Regulates Protein Metabolism

Previous studies in bacteria provided direct evidence for the function of polyamines in protein synthesis (Algranati et al., 1977). Eukaryotic translation initiation factor 3 subunit J (eIF3J, spot 35) and elongation factor 2 (EF2, spot 23) are involved



in the initiation and elongation stage of mRNA translation and protein synthesis (Kanhema et al., 2006). Put maintained the high level of eIF3J abundance induced by NaCl, and further increased EF2 expression in NaCl stressed conditions (Table 1, Figure 2), which proved the role of Put in protein synthesis. However, Put decreased the abundance of 60S acidic ribosomal protein P2-4

(RPP2D, spot 46), which is part of large subunit of ribosomes. This may be related to the function of Put in balancing ribosomal particles and protein synthesis, which was reported in *E. coli* by Algranati et al. (1977). Stimulating the synthesis of specific proteins by Put might play an important role in coping with salt stress.

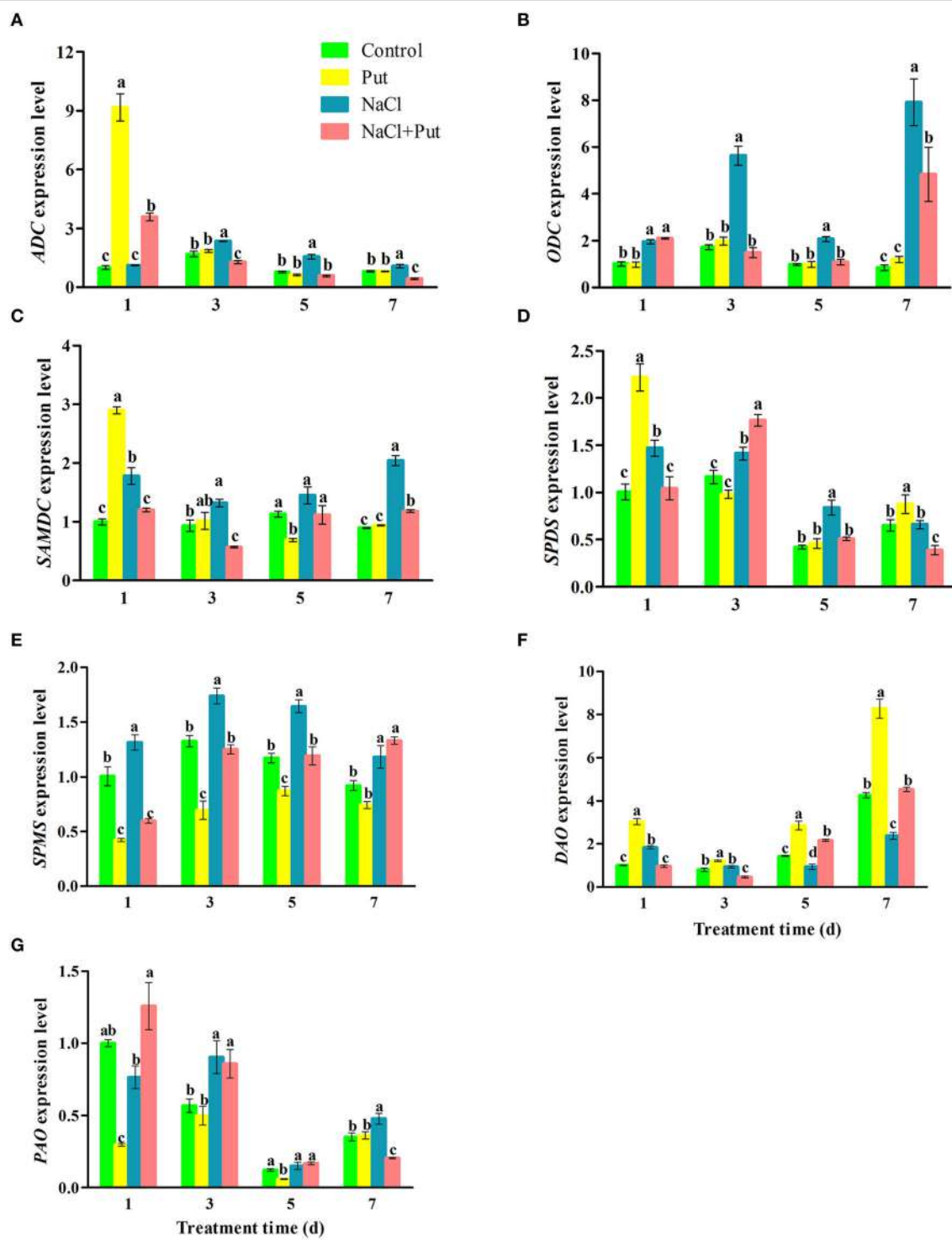


FIGURE 5 | Effects of exogenous putrescine (Put) on the expression of *ADC* (A), *ODC* (B), *SAMDC* (C), *SPDS* (D), *SPMS* (E), *DAO* (F), and *PAO* (G) in roots of cucumber seedlings exposed to 75 mM NaCl for 1, 3, 5, and 7 d. Each histogram represents a mean \pm SE of three independent experiments ($n = 3$). Different letters indicate significant differences between treatments ($P < 0.05$) according to Duncan's multiple range tests. Control, seedlings cultured in normal nutrient solution; Put, seedlings cultured in nutrient solution with 0.8 mM Put; NaCl, seedlings cultured in nutrient solution supplemented with 75 mM NaCl; NaCl+Put: Both NaCl and Put added to the nutrient solution.

TABLE 2 | Effect of exogenous putrescine (Put) on free amino acid contents (%DW) in roots of cucumber seedlings exposed to 75 mM NaCl for 7 d.

Amino acid name	Treatment			
	Control	Put	NaCl	NaCl+Put
Alanine	1.213 ± 0.012d	1.373 ± 0.007b	1.321 ± 0.005c	1.544 ± 0.004a
Arginine	0.992 ± 0.007c	1.232 ± 0.016a	1.125 ± 0.007b	1.232 ± 0.006a
Aspartic acid	1.645 ± 0.023d	2.070 ± 0.014a	1.917 ± 0.009c	1.995 ± 0.003b
Cysteine	0.064 ± 0.003c	0.078 ± 0.001b	0.089 ± 0.003a	0.079 ± 0.001b
Glutamic acid	2.262 ± 0.011d	2.623 ± 0.017b	2.532 ± 0.009c	2.793 ± 0.004a
Glycine	1.036 ± 0.008d	1.157 ± 0.008b	1.134 ± 0.004c	1.246 ± 0.002a
Histidine	0.367 ± 0.004c	0.433 ± 0.005a	0.404 ± 0.004b	0.436 ± 0.001a
Isoleucine	0.965 ± 0.008d	1.126 ± 0.005a	1.005 ± 0.005c	1.072 ± 0.001b
Leucine	1.605 ± 0.017d	1.847 ± 0.009a	1.681 ± 0.007c	1.774 ± 0.003b
Lysine	1.409 ± 0.015d	1.689 ± 0.011a	1.490 ± 0.006c	1.635 ± 0.004b
Methionine	0.274 ± 0.015b	0.283 ± 0.002ab	0.307 ± 0.002a	0.302 ± 0.002a
Phenylalanine	1.014 ± 0.008d	1.222 ± 0.010a	1.114 ± 0.004c	1.177 ± 0.003b
Proline	0.921 ± 0.009b	0.986 ± 0.007a	0.919 ± 0.003b	0.977 ± 0.005a
Serine	0.784 ± 0.007d	1.293 ± 0.016a	1.211 ± 0.004c	1.249 ± 0.003b
Threonine	0.453 ± 0.012c	0.921 ± 0.013ab	0.894 ± 0.005b	0.929 ± 0.002a
Tyrosine	0.305 ± 0.016b	0.614 ± 0.008a	0.605 ± 0.004a	0.614 ± 0.003a
Valine	1.238 ± 0.013d	1.437 ± 0.008a	1.320 ± 0.007c	1.409 ± 0.001b
Total amino acids	16.547 ± 0.134c	20.384 ± 0.154a	19.068 ± 0.073b	20.464 ± 0.035a

Each value is the mean ± SE of three independent experiments ($n = 3$). Different letters indicate significant differences between treatments ($P < 0.05$) according to Duncan's multiple range tests. Control, seedlings cultured in normal nutrient solution; Put, seedlings cultured in nutrient solution with 0.8 mM Put; NaCl, seedlings cultured in nutrient solution supplemented with 75 mM NaCl; NaCl+Put: Both NaCl and Put added to the nutrient solution.

Salt stress leads to protein unfolding or misfolding, which affects protein conformation and function, and causes metabolic disruption (Kumari et al., 2015). In this study, five spots were identified as protein chaperones (Table 1). Three out of the five spots represented heat shock 70 kDa protein (HSP70, spots 3, 9, and 11). HSP70 can be induced by various environmental stresses (Tomanek and Sanford, 2003), and this was further demonstrated in our study by 3.22- and 1.69-folds increases in abundance (spots 9 and 11) under NaCl stress as compared with that of the control. However, Put significantly decreased HSP70 (spots 9 and 11) expression both under control and NaCl stress conditions (Table 1). This result was consistent with Li et al. (2013), who found that Spd could down-regulated the expression of HSP70. Polyamines were reported to influence the DNA binding capacity of heat shock transcriptional factor HSF in rat cells and thus affecting the accumulation of HSP70 mRNA (Desiderio et al., 1999). Königshofer and Lechner (2002) reported that under heat stress conditions, polyamine metabolic status in tobacco, or alfalfa cells influence the HSP synthesis by affecting cell membranes integrity and properties. Mitochondrial chaperonin CPN60-2 (spot 4) belongs to HSP60 family, implicated in mitochondrial protein import, and macromolecular assembly (Tsugeki et al., 1992). In cucumber leaf, CPN60-2 was not affect by NaCl stress, but down-regulated by exogenous Spd (Li et al., 2013). In the present study, CPN60-2 in cucumber root was not changed under NaCl stress condition either, but significantly up-regulated by Put. Put also increased the abundance of protein disulfide-isomerase (PDI, spot 12), which

catalyzes the formation, breakage or rearrangement of disulfide bonds during proteins folding (Gruber et al., 2006). Hence, Put may regulate chaperones to facilitate protein folding and prevent unfolding/misfolding-induced protein aggregation, thus reestablishing normal protein conformation and maintaining cellular metabolism when exposed to salt stress.

Votyakova et al. (1999) reported that proteins covalently attached with PAs became more resistant to proteolysis. Wajnberg and Fagan (1989) demonstrated that polyamines inhibited the ATP-dependent degradation of ubiquitinated proteins. Ubiquitin-conjugating enzyme E2 2 (UBC2, spot 42) participates in protein modification by catalyzing covalent attachment of ubiquitin to proteins. This process is involved in ubiquitin-mediated protein degradation by the 26S proteasome (Cui et al., 2012). In accordance, Put decreased the abundance of UBC2 under control and NaCl stress conditions (Table 1). This result suggested that Put not only targeting energy consumption (Wajnberg and Fagan, 1989) but also the ubiquitinated processes to inhibit protein degradation. However, Put further up-regulated the NaCl-induced increase in 26S protease regulatory subunit 6A homolog (RPT5A, spot 13) and proteasome subunit alpha type-5 (PSMA5, spot 4), which were also involved in the degradation of ubiquitinated proteins. Combination with the response in chaperones, Put may accelerate the degradation of misfolded/damaged proteins caused by NaCl to alleviate salt stress induced-damage. In addition, Put regulated protein metabolism may reprogram proteome of cucumber roots in response to salt stress, which is supported by Tanou et al. (2014), thus maintaining cell homeostasis.

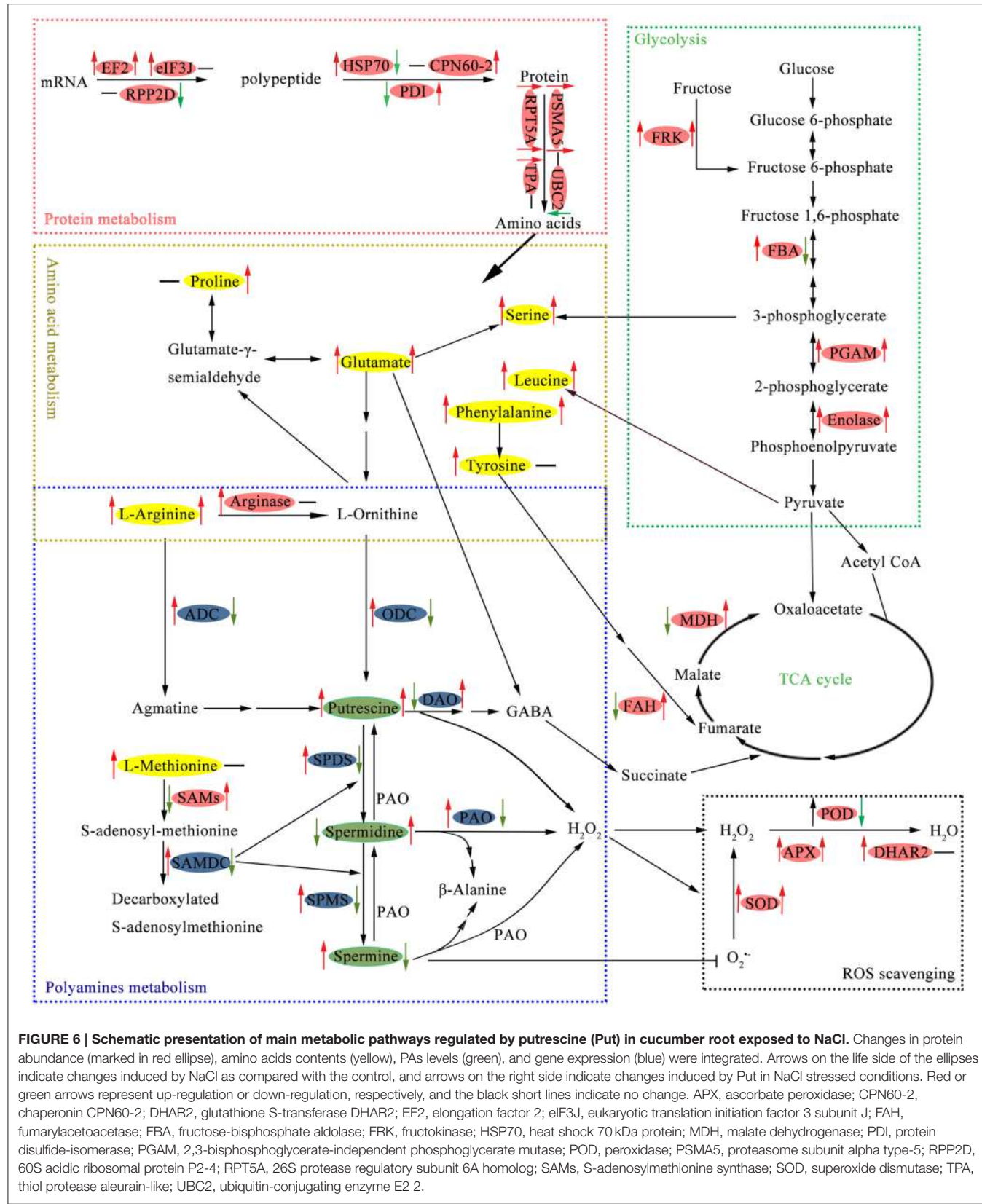


FIGURE 6 | Schematic presentation of main metabolic pathways regulated by putrescine (Put) in cucumber root exposed to NaCl. Changes in protein abundance (marked in red ellipse), amino acids contents (yellow), PAs levels (green), and gene expression (blue) were integrated. Arrows on the life side of the ellipses indicate changes induced by NaCl as compared with the control, and arrows on the right side indicate changes induced by Put in NaCl stressed conditions. Red or green arrows represent up-regulation or down-regulation, respectively, and the black short lines indicate no change. APX, ascorbate peroxidase; CPN60-2, chaperonin CPN60-2; DHAR2, glutathione S-transferase DHAR2; EF2, elongation factor 2; eIF3J, eukaryotic translation initiation factor 3 subunit J; FAH, fumarylacetoacetate; FBA, fructose-bisphosphate aldolase; FRK, fructokinase; HSP70, heat shock 70 kDa protein; MDH, malate dehydrogenase; PDI, protein disulfide-isomerase; PGAM, 2,3-bisphosphoglycerate-independent phosphoglycerate mutase; POD, peroxidase; PSMA5, proteasome subunit alpha type-5; RPP2D, 60S acidic ribosomal protein P2-4; RPT5A, 26S protease regulatory subunit 6A homolog; SAMs, S-adenosylmethionine synthase; SOD, superoxide dismutase; TPA, thiol protease aleurain-like; UBC2, ubiquitin-conjugating enzyme E2 2.

TABLE 3 | Effect of exogenous putrescine (Put) on contents of endogenous free, conjugated, and bound PAs in roots of cucumber seedlings exposed to 75 mM NaCl for 7d.

Chemical forms	Treatments	Put (nmol·g ⁻¹ FW)	Spd (nmol·g ⁻¹ FW)	Spm (nmol·g ⁻¹ FW)	Put+Spd+Spm (nmol·g ⁻¹ FW)
Free	Control	51.8 ± 4.08c	286.6 ± 24.17d	27.1 ± 1.49c	365.4 ± 21.89c
	Put	88.1 ± 4.17c	792.9 ± 20.95b	33.6 ± 2.88c	914.5 ± 16.91b
	NaCl	219.0 ± 18.29b	566.6 ± 25.77c	55.2 ± 6.31b	840.8 ± 7.67b
	NaCl+Put	301.4 ± 21.66a	1110.61 ± 53.79a	74.6 ± 6.04a	1486.6 ± 46.17a
Conjugated	Control	89.5 ± 7.82c	678.4 ± 18.30a	57.8 ± 7.92b	825.7 ± 16.88a
	Put	113.7 ± 7.10c	666.1 ± 54.01a	59.3 ± 8.35b	839.1 ± 62.34a
	NaCl	204.4 ± 8.50b	154.1 ± 12.69c	86.3 ± 3.51a	444.8 ± 18.68c
	NaCl+Put	300.2 ± 32.19a	270.4 ± 15.09b	102.2 ± 6.18a	672.8 ± 38.29b
Bound	Control	172.9 ± 14.32d	215.0 ± 7.67a	93.8 ± 3.90c	481.7 ± 19.68d
	Put	260.2 ± 10.89c	202.9 ± 10.94a	109.9 ± 9.91c	573.0 ± 19.71c
	NaCl	338.3 ± 12.60b	71.5 ± 3.97c	278.1 ± 7.96a	687.9 ± 7.48b
	NaCl+Put	419.9 ± 20.25a	120.8 ± 8.81b	201.5 ± 15.96b	742.2 ± 7.24a
Total	Control	314.1 ± 20.88d	1179.9 ± 45.18c	178.7 ± 10.88c	1672.8 ± 35.31d
	Put	461.9 ± 15.25c	1661.9 ± 33.30a	202.8 ± 6.12c	2326.6 ± 28.31b
	NaCl	761.7 ± 29.54b	792.2 ± 32.37d	419.7 ± 9.70a	1973.6 ± 24.95c
	NaCl+Put	1021.6 ± 36.37a	1501.9 ± 61.34b	378.3 ± 7.28b	2901.7 ± 60.51a

Each value represents a mean ± SE of three independent experiments ($n = 3$). Different letters indicate significant differences between treatments ($P < 0.05$) according to Duncan's multiple range tests. Control, seedlings cultured in normal nutrient solution; Put, seedlings cultured in nutrient solution with 0.8 mM Put; NaCl, seedlings cultured in nutrient solution supplemented with 75 mM NaCl; NaCl+Put: Both NaCl and Put added to the nutrient solution.

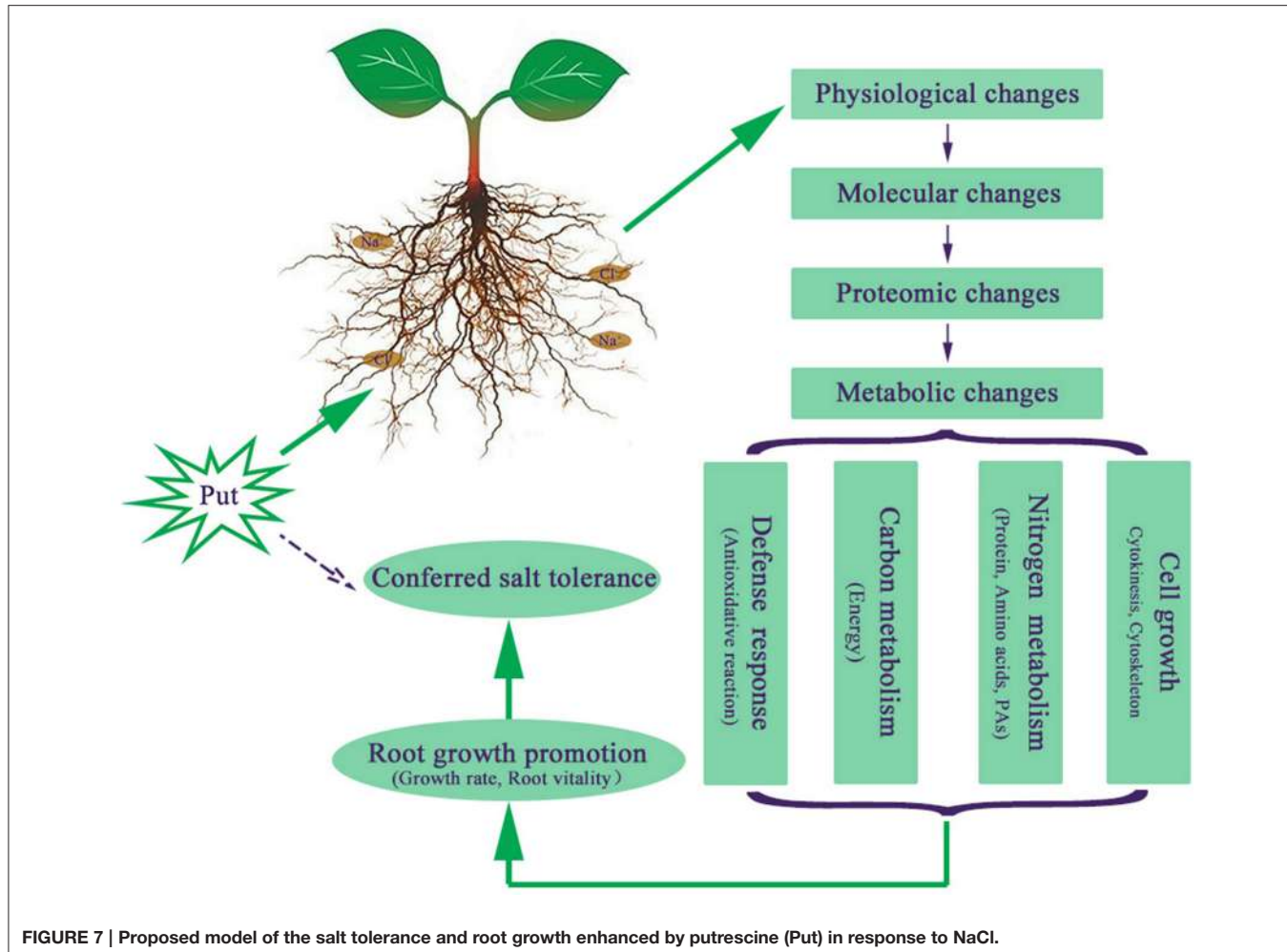
Putrescine Activates Stress Defense Responses to Alleviate Salt Induced Damage

Plants activate a broad array of defense responses to protect themselves from stress induced injuries. Chitinases are usually considered as pathogenesis-related proteins, and widely distributed in plants. Despite of their role against pathogen stress, chitinases are also implicated in various abiotic stresses (Grover, 2012). In the present work, Put increased chitinase (spot 38) abundance under control conditions (Table 1), indicated a promotion in plant defense. Glycine-rich RNA-binding protein (GR-RBP) has a role in RNA transcription or processing during stress by acting as RNA chaperone. GR-RBP7 was also reported to be involved in plant innate immunity (Lee et al., 2012). The increase in GR-RBP3 (spot 43) abundance induced by Put further proved the involvement of PAs in plant immunity. Apart from the plant immunity, redox regulation also represents essential defense response. In the current study, a total of 12 spots (spots 14, 28, 29, 30, 34, 45, 47, 48, 51, 52, 55, and 57) were identified as antioxidant related proteins and mostly showed up-regulated expression when exposed to NaCl stress (Table 1). The ability of Put in increasing the activities of antioxidant enzymes, such as superoxide dismutase (SOD), peroxidase (POD), and ascorbate peroxidase (APX), to alleviate oxidative damage caused by environmental stresses has been widely studied (Verma and Mishra, 2005). In this study, Put application to NaCl-stressed seedlings further improved the abundance of SOD (spots 45 and

47), POD (spot 14), APX (spots 28, 29 and 30), and glutathione S-transferases (GST, spot 51), which implied that Put regulated both abundance and activities of antioxidant enzymes to mitigate oxidative damage induced by salt stress. Aldo-keto reductase 4 (AKR, spot 57) belongs to AKR superfamily, which play central roles in response to oxidative stress by detoxifying toxic aldehydes, and ketones to the appropriate alcohol (Hyndman et al., 2003). AKR was also up-regulated by Put (Table 1). These results indicated that Put could enhance plant defense responses to reduce stress injuries and gain better growth in NaCl stress conditions.

Putrescine Promotes Energy Metabolism

Plants struggled in stress conditions need a substantial amount of energy to maintain their growth and development. Mitochondrial respiratory chain, the main provider of energy needed for cellular metabolism, has been reported to be activated by salt stress (Fry et al., 1986). Consistently, the abundance of NAD(P)H dehydrogenase (spot 53) was induced by NaCl in the present study, indicating an activation of respiratory electron transport systems. Carbohydrates metabolism, especially glycolysis (EMP), and tricarboxylic acid (TCA) cycle is also a primary source of energy for plant metabolism (Kumari et al., 2015). In the present study, seven differentially expressed spots were identified as enzymes participated in glycolysis (Table 1). Fructokinase-4 (FRK, spot 62), fructose-bisphosphate aldolase (FBA, spot 59), 2,3-bisphosphoglycerate-independent



phosphoglycerate mutase (PGAM, spots 6 and 7), and enolase (spots 1, 2, and 5) were all up-regulated by NaCl, suggesting that roots attempted to generate more energy to cope with salt stress. However, NaCl stress decreased the abundance of malate dehydrogenase (MDH, spots 49, 50, and 56) involved in TCA cycle.

Several studies reported the involvement of PAs in adjusting EMP-TCA metabolism under stressed environment. Jia et al. (2010) found that exogenous Spd enhanced hypoxia stress tolerance by up-regulating activities of enzymes functioning in TCA cycle. Put sprayed to leaves partly reserved the NaCl-reduced activities of phosphofructokinase (PFK), pyruvate kinase (PK), and phosphoenolpyruvate pyruvate kinase (PEPC) involved in glycolysis metabolism, as well as activities of succinate dehydrogenase (SDH), isocitrate dehydrogenase (IDH), and MDH in TCA cycle (Zhong et al., 2015). Here we found that despite of decreased FBA abundance, exogenous Put increased the abundance of FRK, PGAM, and FBA both under control and NaCl stress conditions. What's more, Put partly reserved the MDH expression decreased by NaCl. All of these changes suggested that exogenous Put could promote

EMP-TCA pathway activity. In addition to directly regulating these enzymes, Put may also affect TCA cycle through its metabolite, γ -aminobutyric acid (GABA; Gill and Tuteja, 2010). Adjusting EMP-TCA pathway to produce more energy may be an important mechanism for Put to alleviate salt stress induced damage.

Polyamines and Amino Acid Metabolism Play Key Roles in Salt Tolerance

Amino acid metabolic pathways as well as the protective metabolites produced constitute integral parts of the plant immune system (Zeier, 2013). In this study, nine spots were identified as proteins participated in amino acid metabolism (**Table 1**), while seven of these also related to PAs biosynthesis. Polyamines and amino acid metabolism play key roles in connecting C and N metabolism and several secondary metabolism pathways (Majumdar et al., 2016). We summarized the crossed metabolism connecting PAs, amino acids, and EMP-TCA cycle in **Figure 6**.

NaCl stress increased the soluble amino acid levels, which were further improved by Put (**Table 2**). Free amino acids

can serve as osmolytes to regulate osmotic stress caused by salt, and their increases in response to NaCl and/or Put is largely attributed to protein hydrolysis (Yuan et al., 2012). This is further proved by the simultaneous up-regulation of glycine content (**Table 2**) and glycine cleavage system H protein 2 (spot 44) abundance (**Table 1**). Glu is the most abundant amino acid in cucumber root (**Table 2**), and is considered as the center of N metabolism in plants. Glu can be converted into ornithine (Orn), a non-protein amino acid present in low concentration in plants, which is an important precursor for Put (Majumdar et al., 2016). The increase in arginine (Arg) level, another precursor for Put, provided sufficient substrates for the synthesis of Put. In addition, Arg can be converted to Orn and urea via arginase (spot 24), which showed increased abundance under NaCl stress condition but did not respond to Put (**Table 1**). This result indicated that Put production through *ODC* might be enhanced by NaCl stress. The up-regulated expression of *ODC* also proved this assumption. Glu and Orn contribute to proline (Pro) synthesis by different routes. Salt stress induced Pro accumulation is an important mechanism for osmotic regulation. However, NaCl stress exerted no significant influence on Pro level in this study (**Table 2**). The most probable reason for this result was the substantial synthesis of Put consumed Arg and Orn thus limiting Glu and Orn flow into Pro. External Put inhibited the synthesis of more Put by regulating *ADC* and *ODC* expression, and consequently more N was available for Pro production. In this situation, the direct absorption of Put from nutrient solution may contribute large part of the increase in endogenous Put level (Shu et al., 2015).

Methionine (Met) is also related to PAs synthesis through conversion into S-adenosylmethionine (SAM). S-adenosylmethionine synthase (SAMs, spots 15, 16, 17, 19, 21, and 60) catalyzes the biosynthesis of SAM from Met and ATP, and serves as a common precursor for PAs and ethylene (Gong et al., 2014). Transgenic experiments proved that SAMs contributed to stress tolerance by increasing PAs accumulation (Qi et al., 2010; Gong et al., 2014). Put up-regulated SAMs abundance both under control and NaCl stress conditions (**Table 1**), and Spd showed the similar effect (Li et al., 2013). The increase in SAMs was partly responsible for the elevation in endogenous PAs levels (**Table 3**). Although SAMs was significantly reduced by NaCl, PAs levels were still increased due to the transcriptional activation of PAs biosynthesis (**Figure 5**).

The protective roles of PAs are partly attributed to their association with low molecular weight compounds and macromolecules, therefore the conjugated and bound PAs are essential for plant stress tolerance. Quinet et al. (2010) observed that the conjugated PAs pool was positively linked with rice salt tolerance. The conjugated PAs pool was reduced by NaCl in the present study due to a large decrease in conjugated Spd level (**Table 3**). Put application increased the conjugated and bound PAs levels, thus stabilizing the intercellular small molecules and macromolecules to resist salt stress. Exogenous Put induced the accumulation of endogenous Put, also elevated the expression of *DAO* (**Figure 5F**), which proved the transcriptional activation reported by Quinet et al.

(2010). Interestingly, the oxidation of Put is accompanied by the production of H₂O₂, and GABA, and the latter is key component connecting PAs and amino acid metabolism (Majumdar et al., 2016). Another protein, fumarylacetoacetate (FAH, spot 61), is involved in the multiple steps synthesis of acetoacetate and fumarate from L-phenylalanine or L-tyrosine (Herrera et al., 2010). Fumarate happened to be an intermediate of TCA cycle (**Figure 6**). Put reversed NaCl reduced FAH abundance is an indirect evidence for its regulation to TCA cycle.

Apart from the proteins mentioned above, Put was also found to regulate proteins involved in other metabolic pathways like lipid metabolism (spots 25 and 26) and nitrile formation (spots 20 and 27), indicating Put regulated various metabolic pathways to counteract salt stress-induced changes. Moreover, the identification of proteins related to cell division (spot 18) and cell cytoskeleton (spots 22, 31, and 58) proved the ability of Put to improve plant growth. We proposed a model of the NaCl stress tolerance conferred by external Put in cucumber seedlings (**Figure 7**). The application of Put to NaCl-stressed seedlings results in a series of responses from physiological level to metabolic level. Put enhanced stress defense capacity, regulated carbon and nitrogen metabolism to supply substrates and energy for various metabolic processes, and affected cell growth. All these changes contribute to the Put induced root growth promotion and salt tolerance.

CONCLUSION

In conclusion, this work demonstrated that Put improving cucumber root growth and salt tolerance could be associated with the following points: (1) stimulating protein synthesis and degrading misfolded/damaged proteins induced by NaCl; (2) activation of stress defense response to alleviate salt induced injuries; and (3) providing more energy for various metabolic processes by up-regulating proteins involved in carbohydrate metabolism. This study provides comprehensive insights into the cell metabolism regulated by NaCl and/or Put, and would be able to better enrich our understanding of the mechanism by which Put improves the salt tolerance of cucumber seedlings.

AUTHOR CONTRIBUTIONS

SG designed the study and guided the research. YY wrote the main manuscript text and performed the experiments. MZ and ND prepared all the figures and performed some of the experiments. SS and JS modified this manuscript. All authors reviewed and approved the manuscript.

FUNDING

This work was supported financially by the National Natural Science Foundation of China (31401919, 31471869, and 31272209), the China Earmarked Fund for Modern Agro-

industry Technology Research System (CARS-25-C-03), the Priority Academic Program Development (PAPD) of Jiangsu Higher Education Institutions, and the Research Fund for the Doctoral Program of Higher Education (20130097120015).

REFERENCES

- Alcázar, R., Altabella, T., Marco, F., Bortolotti, C., Reymond, M., Koncz, C., et al. (2010). Polyamines: molecules with regulatory functions in plant abiotic stress tolerance. *Planta* 231, 1237–1249. doi: 10.1007/s00425-010-1130-0
- Algranati, I. D., Echandi, G., García-Patrone, M., Gonzalez, N. S., and Goldemberg, S. H. (1977). Polyamines, equilibrium between ribosomal particles and protein synthesis in bacteria. *Arch. Biol. Med. Exp.* 10, 49–60.
- An, Y., Zhou, H., Zhong, M., Sun, J., Shu, S., Shao, Q., et al. (2016). Root proteomics reveals cucumber 24-epibrassinolide responses under Ca(NO₃)₂ stress. *Plant Cell Rep.* 35, 1081–1101. doi: 10.1007/s00299-016-1940-z
- Bagni, N., and Tassoni, A. (2001). Biosynthesis, oxidation and conjugation of aliphatic polyamines in higher plants. *Amino Acids* 20, 301–317. doi: 10.1007/s007260170046
- Bernstein, N., Meiri, A., and Zilberman, M. (2004). Root growth of avocado is more sensitive to salinity than shoot growth. *J. Am. Soc. Hortic. Sci.* 129, 188–192. Available online at: <http://journal.ashpublications.org/content/129/2/188.full.pdf+html>
- Berwanger, A., Eyrisch, S., Schuster, I., Helms, V., and Bernhardt, R. (2010). Polyamines: naturally occurring small molecule modulators of electrostatic protein-protein interactions. *J. Inorg. Biochem.* 104, 118–125. doi: 10.1016/j.jinorgbio.2009.10.007
- Bose, J., Shabala, L., Pottosin, I., Zeng, F., Velarde-Buendía, A., Massart, A., et al. (2014). Kinetics of xylem loading, membrane potential maintenance, and sensitivity of K⁺-permeable channels to reactive oxygen species: physiological traits that differentiate salinity tolerance between pea and barley. *Plant Cell Environ.* 37, 589–600. doi: 10.1111/pce.12180
- Bradford, M. M. (1976). A rapid and sensitive method for the quantitation of microgram quantities of protein utilizing the principle of protein-dye binding. *Anal. Biochem.* 72, 248–254. doi: 10.1016/0003-2697(76)90527-3
- Campos, N., Castañón, S., Urreta, I., Santos, M., and Torné, J. M. (2013). Rice transglutaminase gene: Identification, protein expression, functionality, light dependence and specific cell location. *Plant Sci.* 205–206, 97–110. doi: 10.1016/j.plantsci.2013.01.014
- Contreras-Corral, H. A., Macías-Rodríguez, L., Alfaro-Cuevas, R., and López-Bucio, J. (2014). *Trichoderma* spp. Improve growth of *Arabidopsis* seedlings under salt stress through enhanced root development, osmolite production, and Na⁺ elimination through root exudates. *Mol. Plant Microbe Interact.* 27, 503–514. doi: 10.1094/MPMI-09-13-0265-R
- Cui, F., Liu, L., Zhao, Q., Zhang, Z., Li, Q., Lin, Q., et al. (2012). Arabidopsis ubiquitin conjugase UBC32 is an ERAD component that functions in brassinosteroid-mediated salt stress tolerance. *Plant Cell* 24, 233–244. doi: 10.1105/tpc.111.093062
- Dalton, H. L., Blomstedt, C. K., Neale, A. D., Gleadow, R., DeBoer, K. D., and Hamill, J. D. (2016). Effects of down-regulating ornithine decarboxylase upon putrescine-associated metabolism and growth in *Nicotiana tabacum* L. *J. Exp. Bot.* 67, 3367–3381. doi: 10.1093/jxb/erw166
- Desiderio, M. A., Dansi, P., Tacchini, L., and Bernelli-Zazzera, A. (1999). Influence of polyamines on DNA binding of heat shock and activator protein 1 transcription factors induced by heat shock. *FEBS Lett.* 455, 149–153. doi: 10.1016/S0014-5793(99)00873-X
- Fry, I. V., Huflejt, M., Erber, W. W., Peschek, G. A., and Packer, L. (1986). The role of respiration during adaptation of the freshwater cyanobacterium *Synechococcus* 6311 to salinity. *Arch. Biochem. Biophys.* 244, 686–691. doi: 10.1016/0003-9861(86)90637-5
- Fuell, C., Elliott, K. A., Hanfrey, C. C., Franceschetti, M., and Michael, A. J. (2010). Polyamine biosynthetic diversity in plants and algae. *Plant Physiol. Biochem.* 48, 513–520. doi: 10.1016/j.plaphy.2010.02.008
- Gong, B., Li, X., VandenLangenberg, K. M., Wen, D., Sun, S., Wei, M., et al. (2014). Overexpression of S-adenosyl-L-methionine synthetase increased tomato tolerance to alkali stress through polyamine metabolism. *Plant Biotechnol. J.* 12, 694–708. doi: 10.1111/pbi.12173
- Gill, S. S., and Tuteja, N. (2010). Polyamines and abiotic stress tolerance in plants. *Plant Signal. Behav.* 5, 26–33. doi: 10.4161/psb.5.1.10291
- Grover, A. (2012). Plant chitinases: genetic diversity and physiological roles. *Crit. Rev. Plant Sci.* 31, 57–73. doi: 10.1080/07352689.2011.616043
- Gruber, C. W., Čemažar, M., Heras, B., Martin, J. L., and Craik, D. J. (2006). Protein disulfide isomerase: the structure of oxidative folding. *Trends Biochem. Sci.* 31, 455–464. doi: 10.1016/j.tibs.2006.06.001
- Gupta, B., and Huang, B. (2014). Mechanism of salinity tolerance in plants: physiological, biochemical, and molecular characterization. *Int. J. Genomics* 6, 727–740. doi: 10.1155/2014/701596
- Hao, J. H., Dong, C. J., Zhang, Z. G., Wang, X. L., and Shang, Q. M. (2012). Insights into salicylic acid responses in cucumber (*Cucumis sativus* L.) cotyledons based on a comparative proteomic analysis. *Plant Sci.* 187, 69–82. doi: 10.1016/j.plantsci.2012.01.001
- He, L., Lu, X., Tian, J., Yang, Y., Li, B., Li, J., et al. (2012). Proteomic analysis of the effects of exogenous calcium on hypoxic-responsive proteins in cucumber roots. *Proteome Sci.* 10:42. doi: 10.1186/1477-5956-10-42
- Herrera, M. C., Duque, E., Rodríguez-Herva, J. J., Fernández-Escamilla, A. M., and Ramos, J. L. (2010). Identification and characterization of the PhhR regulon in *Pseudomonas putida*. *Environ. Microbiol.* 12, 1427–1438. doi: 10.1111/j.1462-2920.2009.02124.x
- Hurkman, W. J., and Tanaka, C. K. (1986). Solubilization of plant membrane proteins for analysis by two-dimensional gel electrophoresis. *Plant Physiol.* 81, 802–806. doi: 10.1104/pp.81.3.802
- Hyndman, D., Bauman, D. R., Heredia, V. V., and Penning, T. M. (2003). The aldoketo reductase superfamily homepage. *Chem. Biol. Interact.* 143–144, 621–631. doi: 10.1016/S0009-2779(02)00193-X
- Jia, Y. X., Sun, J., Guo, S. R., Li, J., Hu, X. H., and Wang, S. P. (2010). Effect of root-applied spermidine on growth and respiratory metabolism in roots of cucumber (*Cucumis sativus*) seedlings under hypoxia. *Russ. J. Plant Physiol.* 57, 648–655. doi: 10.1134/S1021443710050079
- Jiang, K., Moe-Lange, J., Hennet, L., and Feldman, L. (2016). Salt stress affects the redox status of *Arabidopsis* root meristems. *Front. Plant Sci.* 7:8. doi: 10.3389/fpls.2016.000081
- Julkowska, M. M., Hoefsloot, H. C. J., Selena, M., Richard, F., Gert-Jan, D. B., Haring, M. A., et al. (2014). Capturing *Arabidopsis* root architecture dynamics with ROOT-FIT reveals diversity in responses to salinity. *Plant Physiol.* 166, 1387–1402. doi: 10.1104/pp.114.248963
- Kamiab, F., Talaie, A., Khezri, M., and Javanshah, A. (2014). Exogenous application of free polyamines enhance salt tolerance of pistachio (*Pistacia vera* L.) seedlings. *Plant Growth Regul.* 72, 257–268. doi: 10.1007/s10725-013-9857-9
- Kanhema, T., Dagestad, G., Panja, D., Tiron, A., Messaoudi, E., Håvik, B., et al. (2006). Dual regulation of translation initiation and peptide chain elongation during BDNF-induced LTP *in vivo*: evidence for compartment-specific translation control. *J. Neurochem.* 99, 1328–1337. doi: 10.1111/j.1471-4159.2006.04158.x
- Königshofer, H., and Lechner, S. (2002). Are polyamines involved in the synthesis of heat-shock proteins in cell suspension cultures of tobacco and alfalfa in response to high-temperature stress? *Plant Physiol. Biochem.* 40, 51–59. doi: 10.1016/S0981-9428(01)01347-X
- Konstantinos, P. A., Toumi, I., Panagiotis, M. N., and Roubelakis-Angelakis, K. A. (2010). ABA-dependent amine oxidases-derived H₂O₂ affects stomata conductance. *Plant Signal. Behav.* 5, 1153–1156. doi: 10.4161/psb.5.9.12679
- Kumari, A., Das, P., Parida, A. K., and Agarwal, P. K. (2015). Proteomics, metabolomics, and ionomics perspectives of salinity tolerance in halophytes. *Front. Plant Sci.* 6:537. doi: 10.3389/fpls.2015.00537

SUPPLEMENTARY MATERIAL

The Supplementary Material for this article can be found online at: <http://journal.frontiersin.org/article/10.3389/fpls.2016.01035>

- Lee, H. J., Jin, S. K., Yoo, S. J., Kang, E. Y., Song, H. H., Yang, K. Y., et al. (2012). Different roles of glycine-rich RNA-binding protein7 in plant defense against *Pectobacterium carotovorum*, *Botrytis cinerea*, and tobacco mosaic viruses. *Plant Physiol. Biochem.* 60, 46–52. doi: 10.1016/j.plaphy.2012.07.020
- Li, B., He, L., Guo, S., Li, J., Yang, Y., Yan, B., et al. (2013). Proteomics reveal cucumber Spd-responses under normal condition and salt stress. *Plant Physiol. Biochem.* 67, 7–14. doi: 10.1016/j.plaphy.2013.02.016
- Li, Z., Zhang, Y., Peng, D., Wang, X., Peng, Y., He, X., et al. (2014). Polyamine regulates tolerance to water stress in leaves of white clover associated with antioxidant defense and dehydrin genes via involvement in calcium messenger system and hydrogen peroxide signaling. *Front. Physiol.* 6:280. doi: 10.3389/fphys.2015.00280
- Liu, K., Fu, H., Bei, Q., and Luan, S. (2000). Inward potassium channel in guard cells as a target for polyamine regulation of stomatal movements. *Plant Physiol.* 124, 1315–1325. doi: 10.1104/pp.124.3.1315
- Majumdar, R., Barchi, B., Turlapati, S. A., Gagne, M., Minocha, R., Long, S., et al. (2016). Glutamate, ornithine, arginine, proline, and polyamine metabolic interactions: the pathway is regulated at the post-transcriptional level. *Front. Plant Sci.* 7:78. doi: 10.3389/fpls.2016.00078
- Mattoo, A. K., Minocha, S. C., Minocha, R., and Handa, A. K. (2010). Polyamines and cellular metabolism in plants: transgenic approaches reveal different responses to diamine putrescine versus higher polyamines spermidine and spermine. *Amino Acids* 38, 405–413. doi: 10.1007/s00726-009-0399-4
- Moschou, P. N., Paschalidis, K. A., Delis, I. D., Andriopoulou, A. H., Lagiotis, G. D., Yakoumakis, D. I., et al. (2008). Spermidine exodus and oxidation in the apoplast induced by abiotic stress is responsible for H₂O₂ signatures that direct tolerance responses in tobacco. *Plant Cell* 20, 1708–1724. doi: 10.1101/tpc.108.059733
- Munns, R. (2005). Genes and salt tolerance: bringing them together. *New Phytol.* 167, 645–663. doi: 10.1111/j.1469-8137.2005.01487.x
- Munns, R., and Tester, M. (2008). Mechanisms of salinity tolerance. *Annu. Rev. Plant Biol.* 59, 651–681. doi: 10.1146/annurev.arplant.59.032607.092911
- Norden, A. G. W., Peter, S., Cutillas, P. R., Rainer, C., Gardner, S. C., and Unwin, R. J. (2004). Quantitative amino acid and proteomic analysis: very low excretion of polypeptides >750 Da in normal urine. *Prog. Polym. Sci.* 25, 1215–1260. doi: 10.1111/j.1523-1755.2004.00970.x
- Pottosin, I., Velarde-Buendia, A. M., Bose, J., Zepeda-Jazo, I., Shabala, S., and Dobrovinskaya, O. (2014). Cross-talk between reactive oxygen species and polyamines in regulation of ion transport across the plasma membrane: implications for plant adaptive responses. *J. Exp. Bot.* 65, 1271–1283. doi: 10.1093/jxb/er423
- Qi, Y. C., Wang, F. F., Hui, Z., and Liu, W. Q. (2010). Overexpression of suadea salsa S-adenosylmethionine synthetase gene promotes salt tolerance in transgenic tobacco. *Acta Physiol. Plant.* 32, 263–269. doi: 10.1007/s11738-009-0403-3
- Quinet, M., Ndayiragije, A., Lefèvre, I., Lambillotte, B., Dupont-Gillain, C. C., and Lutts, S. (2010). Putrescine differently influences the effect of salt stress on polyamine metabolism and ethylene synthesis in rice cultivars differing in salt resistance. *J. Exp. Bot.* 61, 2719–2733. doi: 10.1093/jxb/erq118
- Saha, J., Brauer, E. K., Sengupta, A., Popescu, S. C., Gupta, K., and Gupta, B. (2015). Polyamines as redox homeostasis regulators during salt stress in plants. *Front. Environ. Sci.* 3:21. doi: 10.3389/fenvs.2015.00021
- Shi, H., Ye, T., and Chan, Z. (2013). Comparative proteomic and physiological analyses reveal the protective effect of exogenous polyamines in the bermudagrass (*Cynodon dactylon*) response to salt and drought stresses. *J. Proteome Res.* 12, 4951–4964. doi: 10.1021/pr000479k
- Shu, S., Yuan, Y., Chen, J., Sun, J., Zhang, W., Tang, Y., et al. (2015). The role of putrescine in the regulation of proteins and fatty acids of thylakoid membranes under salt stress. *Sci. Rep.* 5:14390. doi: 10.1038/srep14390
- Tanou, G., Ziogas, V., Belghazi, M., Christou, A., Filippou, P., Job, D., et al. (2014). Polyamines reprogram oxidative and nitrosative status and the proteome of citrus plants exposed to salinity stress. *Plant Cell Environ.* 37, 864–885. doi: 10.1111/pce.12204
- Tiburcio, A. F., Altabella, T., Bitrián, M., and Alcázar, R. (2014). The roles of polyamines during the lifespan of plants: from development to stress. *Planta* 240, 1–18. doi: 10.1007/s00425-014-2055-9
- Tomanek, L., and Sanford, E. (2003). Heat-shock protein 70 (Hsp70) as a biochemical stress indicator: an experimental field test in two congeneric intertidal gastropods (genus: *Tegula*). *Biol. Bull.* 205, 276–284. doi: 10.2307/1543291
- Tsugeki, R., Mori, H., and Nishimura, M. (1992). Purification, cDNA cloning and Northern-blot analysis of mitochondrial chaperonin 60 from pumpkin cotyledons. *Eur. J. Biochem.* 209, 453–458. doi: 10.1111/j.1432-1033.1992.tb17309.x
- Urano, K., Yoshioka, Y., Nanjo, T., Ito, T., Yamaguchi-Shinozaki, K., and Shinozaki, K. (2004). *Arabidopsis* stress-inducible gene for arginine decarboxylase *AtADC2* is required for accumulation of putrescine in salt tolerance. *Biochem. Biophys. Res. Commun.* 313, 369–375. doi: 10.1016/j.bbrc.2003.11.119
- Verma, S., and Mishra, S. N. (2005). Putrescine alleviation of growth in salt stressed *Brassica juncea* by inducing antioxidant defense system. *J. Plant Physiol.* 162, 669–677. doi: 10.1016/j.jplph.2004.08.008
- Votyakova, T. V., Wallace, H. M., Dunbar, B., and Wilson, S. B. (1999). The covalent attachment of polyamines to proteins in plant mitochondria. *Eur. J. Biochem.* 260, 250–257. doi: 10.1046/j.1432-1327.1999.00147.x
- Wajnberg, E. F., and Fagan, J. M. (1989). Polyamines inhibit the ATP-dependent proteolytic pathway in rabbit reticulocyte lysates. *FEBS Lett.* 243, 141–144. doi: 10.1016/0014-5793(89)80116-4
- West, G., Inzé, D., and Beemster, G. T. (2004). Cell cycle modulation in the response of the primary root of *Arabidopsis* to salt stress. *Plant Physiol.* 135, 1050–1058. doi: 10.1104/pp.104.040022
- Wi, S. J., Kim, W. T., and Park, K. Y. (2006). Overexpression of carnation S-adenosylmethionine decarboxylase gene generates a broad-spectrum tolerance to abiotic stresses in transgenic tobacco plants. *Plant Cell Rep.* 25, 1111–1121. doi: 10.1007/s00299-006-0160-3
- Witzel, K., Weidner, A., Surabhi, G. K., Börner, A., and Mock, H. P. (2009). Salt stress-induced alterations in the root proteome of barley genotypes with contrasting response towards salinity. *J. Exp. Bot.* 60, 3545–3557. doi: 10.1093/jxb/erp198
- Yamaguchi, K., Takahashi, Y., Berberich, T., Imai, A., Miyazaki, A., Takahashi, T., et al. (2006). The polyamine spermine protects against high salt stress in *Arabidopsis thaliana*. *FEBS Lett.* 580, 6783–6788. doi: 10.1016/j.febslet.2006.10.078
- Yuan, L., Yuan, Y., Du, J., Sun, J., and Guo, S. (2012). Effects of 24-epibrassinolide on nitrogen metabolism in cucumber seedlings under Ca(NO₃)₂ stress. *Plant Physiol. Biochem.* 61, 29–35. doi: 10.1016/j.plaphy.2012.09.004
- Yuan, Y., Shu, S., Li, S., He, L., Li, H., Du, N., et al. (2014). Effects of exogenous putrescine on chlorophyll fluorescence imaging and heat dissipation capacity in cucumber (*Cucumis sativus* L.) under salt stress. *J. Plant Growth Regul.* 33, 798–808. doi: 10.1007/s00344-014-9427-z
- Zeier, J. (2013). New insights into the regulation of plant immunity by amino acid metabolic pathways. *Plant Cell Environ.* 36, 2085–2103. doi: 10.1111/pce.12122
- Zhong, M., Yuan, Y., Shu, S., Sun, J., Guo, S., Yuan, R., et al. (2015). Effects of exogenous putrescine on glycolysis and Krebs cycle metabolism in cucumber leaves subjected to salt stress. *Plant Growth Regul.* 79, 319–330. doi: 10.1007/s10725-015-0136-9

Conflict of Interest Statement: The authors declare that the research was conducted in the absence of any commercial or financial relationships that could be construed as a potential conflict of interest.

Copyright © 2016 Yuan, Zhong, Shu, Du, Sun and Guo. This is an open-access article distributed under the terms of the Creative Commons Attribution License (CC BY). The use, distribution or reproduction in other forums is permitted, provided the original author(s) or licensor are credited and that the original publication in this journal is cited, in accordance with accepted academic practice. No use, distribution or reproduction is permitted which does not comply with these terms.



Comparative Proteomic Analysis Provides Insight into the Key Proteins Involved in Cucumber (*Cucumis sativus* L.) Adventitious Root Emergence under Waterlogging Stress

Xuewen Xu, Jing Ji, Xiaotian Ma, Qiang Xu, Xiaohua Qi and Xuehao Chen ^{*}

Department of Horticulture, School of Horticulture and Plant Protection, Yangzhou University, Yangzhou, China

OPEN ACCESS

Edited by:

Wei Wang,

Henan Agricultural University, China

Reviewed by:

Abu Hena Mostafa Kamal,

University of Texas at Arlington, USA

GuoJun Yu,

National Cancer Institute, USA

***Correspondence:**

Xuehao Chen

xhchen@yzu.edu.cn

Specialty section:

This article was submitted to

Plant Cell Biology,

a section of the journal

Frontiers in Plant Science

Received: 12 August 2016

Accepted: 26 September 2016

Published: 13 October 2016

Citation:

Xu X, Ji J, Ma X, Xu Q, Qi X and Chen X (2016) Comparative Proteomic Analysis Provides Insight into the Key Proteins Involved in Cucumber (*Cucumis sativus* L.) Adventitious Root Emergence under Waterlogging Stress. *Front. Plant Sci.* 7:1515.
doi: 10.3389/fpls.2016.01515

Waterlogging is a common abiotic stress in both natural and agricultural systems, and it primarily affects plant growth by the slow oxygen diffusion in water. To sustain root function in the hypoxic environment, a key adaptation for waterlogging tolerant plants is the formation of adventitious roots (ARs). We found that cucumber waterlogging tolerant line Zaoer-N seedlings adapt to waterlogging stress by developing a larger number of ARs in hypocotyls, while almost no AR is generated in sensitive line Pepino. To understand the molecular mechanisms underlying AR emergence, the iTRAQ-based quantitative proteomics approach was employed to map the proteomes of hypocotyls cells of the Zaoer-N and Pepino under control and waterlogging conditions. A total of 5508 proteins were identified and 146 were differentially regulated proteins (DRPs), of which 47 and 56 DRPs were specific to tolerant and sensitive line, respectively. In the waterlogged Zaoer-N hypocotyls, DRPs related to alcohol dehydrogenases (ADH), 1-aminocyclopropane-1-carboxylicacid oxidases, peroxidases, 60S ribosomal proteins, GSDL esterases/lipases, histone deacetylases, and histone H5 and were strongly overrepresented to manage the energy crisis, promote ethylene release, minimize oxidative damage, mobilize storage lipids, and stimulate cell division, differentiation and growth. The evaluations of ethylene production, ADH activity, pyruvate decarboxylase (PDC) activity and ethanol production were in good agreement with the proteomic results. qRT-PCR analysis of the corresponding 146 genes further confirmed the accuracy of the observed protein abundance. These findings shed light on the mechanisms underlying waterlogging triggered cucumber ARs emergence, and provided valuable information for the breeding of cucumber with enhanced tolerance to waterlogging.

Keywords: cucumber, waterlogging, hypocotyls, adventitious root, iTRAQ

INTRODUCTION

Waterlogging is described as the saturation of the soil with water around the plant roots, and constitutes one of the most severe abiotic stresses for plant growth and development (Sairam et al., 2009). Nearly 16% of the fertile areas of our globe annually undergo waterlogging due to excessive rainfall, lack of soil drainage, and irregular topography, which resulting in severe economic loss (Ahsan et al., 2007; Xu et al., 2014). In particular, the availability of oxygen for respiration is blocked in waterlogged organs because of gas diffusion in water is about 10^3 times slower than that in the air (van Veen et al., 2014). To sustain energy supply, it is essential for the waterlogged organs to switch over to anaerobic mode for energy production (Jackson and Colmer, 2005; Xu et al., 2014). However, it is obviously inefficient to provide enough energy via glycolysis and fermentation when waterlogging is prolonged (Bailey-Serres and Voesenek, 2008; van Veen et al., 2014). To survive from long-term waterlogging stress, aerobic respiration for plants must be maintained via oxygen transport to enhance internal oxygen diffusion (Shimamura et al., 2014). Some species adapted to waterlogging stress by faster stem/hypocotyls elongation that enable the shoot to regain contact with the open atmosphere, such as *Rumex* and rice (Evans, 2004; Jiang et al., 2010).

Another key adaptation to waterlogging is the formation of ARs, which minimize the distance for oxygen diffusion and improve gas diffusivity (Sauter, 2013). ARs usually originated from the waterlogged part of hypocotyls or basal stem region, and such adaptation can replace the deteriorating primary roots (Bailey-Serres et al., 2012; Sauter, 2013). Therefore, the adaptive responses of ARs formation to waterlogging might be more important than those of primary roots for survival in waterlogged soil (Li et al., 2009; Yamauchi et al., 2014). Genetic, molecular, and physiological approaches have confirmed that auxin, ethylene and carbohydrate status can affect ARs formation (Changdee et al., 2009). A transgenic *Arabidopsis* line overexpressing the *auxin response factor (ARF)* 17 developed fewer ARs than wild-type plants, confirming the potential role of ARF genes in the regulation of ARs development by auxin (Sorin et al., 2005). Taramino et al. (2007) reported that the defective initiation of maize ARs in the *rootless concerning crown and seminal roots* mutant was caused by a mutation in the gene encoding the Lateral Oaternal Boundaries (LOB) domain protein. Expression of the *LOB* gene was rapidly induced by the application of auxin, and the *LOB* protein is thought to be the direct targets of *ARF* transcription factor in the auxin signaling pathway. Rigal et al. (2012) have showed that overexpression of *AINTEGUMENTA LIKE 1 (PtAIL1)*, a transcription factor belongs to APETALA2/ETHYLENE RESPONSE FACTOR family, increased number of ARs in *Populus*, while RNA interference lines with a reduced level of *PtAIL1* transcripts had fewer ARs. However, the underlying mechanisms by which ARs formation is affected have not fully understood, and the reported findings have been contradictory. For examples, in flood-induced ARs of rice stem nodes, it is ethylene but not auxin that signals activation of the cell cycle (Lorbicke and Sauter, 1999), which is followed by generation

of ROS as measured with electron paramagnetic resonance spectroscopy (Voesenek and Bailey-Serres, 2015). Vidoz et al. (2010) found that there may be interaction between ethylene and auxin with respect to AR production in flooded tomato hypocotyls using ethylene- and auxin-insensitive mutants. These contradictory findings may be due to variation in the different plant species, growth conditions, and methods of quantifying ARs.

Cucumber is an economically important vegetable crop and is widely grown in the world with total harvest of more than two million hectares in 2016, ranking 4th in quantity of world vegetable production (FAO STAT 2016, <http://faostat3.fao.org>). Cucumber is also known for its sensitivity to waterlogging and easily affected by heavy rain or soil waterlogging due to its shallow root system and strict oxygen requirement (Qi et al., 2012; Xu et al., 2014, 2016). The relative tolerance of different cucumber accessions to waterlogging stress has been evaluated in our previous study (Qi et al., 2011). In greenhouse waterlogging experiment, we found that the waterlogging tolerant line Zaoer-N adapt to waterlogging treatment by developing numerous ARs in hypocotyls, while almost no ARs were generated in the sensitive line Pepino. As we known, proteomic applications provide a powerful tool for understanding plant proteome changes in response to abiotic and biotic stress (Chen and Harmon, 2006; Yang et al., 2013; Cui et al., 2015). In recent years, the iTRAQ-based quantitative proteomic approach has been widely used for the comparative analyses of proteome changes because it allows for the simultaneous identification and quantification of peptides by measuring the peak intensities of reporter ions with MS/MS (Yu et al., 2015). In the present study, an iTRAQ-based quantitative proteomics approach was employed to elucidate the detail effects of waterlogging stress on the protein expression levels in hypocotyls of the two contrasting cucumber lines differing in waterlogging tolerance ability and the capacity of ARs formation. The results will provide new insights into the physiological and molecular mechanisms associated with waterlogging stress in hypocotyls cells of cucumber seedling. To the best of knowledge, this is the first frame work that reveals the molecular mechanisms underlying AR emergence upon waterlogging on cucumber lines. Our findings provide a list of potential candidates for further elucidating waterlogging tolerance in plants.

MATERIALS AND METHODS

Plant Growth and Treatments

Waterlogging tolerant line Zaoer-N and sensitive line Pepino were grown in 8-cm-wide pots containing peat, vermiculite, and perlite (3:1:1, v/v/v) in a greenhouse at 28/20°C (14/10 h) day/night temperature and a relative humidity ranging from 70 to 85%. Cucumber seedlings at the three-leaf stage (21 days after germination) were placed in plastic cups filled with water (pH 7.03, 25°C, electrical conductivity 0.34 dS m^{-1} , dissolved oxygen level 7.17 mg/L) to the base of the first true leaves ($\sim 4 \text{ cm}$ above the soil surface, soil redox potentials $Eh 272 \pm 4.5 \text{ mV}$). Water was maintained at this level for the duration

of the treatment. For control treatments, plants were watered daily and allowed to drain freely. Hypocotyls (below the water surface) were collected from the Zaoer-N and Pepino seedlings after 2 days of waterlogging and control for physiological assay. Thirty seedling hypocotyls from the three replicate were pooled, immediately frozen in liquid nitrogen, and then stored at -80°C for iTRAQ analysis and RNA extraction.

Protein Extraction and iTRAQ Analysis

Cucumber hypocotyls were grinded to a fine powder in liquid nitrogen and then transferred to 700 μl extraction solution (8 M urea, 4% CHAPS, 2 M thiourea, 40 mM Tris/HCl, pH 8.5, 2 mM EDTA, 1 mM PMSF, 10 mM dithiothreitol). The mix was sonicated for 15 min, and then at 4°C centrifuged 25,000 g for 20 min. The supernatants were removed to a new tube and mixed well with 5 volumes of pre-chilled acetone incubated at -20°C for 2 h. After centrifugation, the resulting pellet was washed three times with cold acetone. The air-dried pellet was dissolved in the 250 μl of 0.5 M TEAB (Applied Biosystems, Milan, Italy), and sonicated for 15 min. The centrifugation step was repeated, and the supernatant was transferred to a new tube and protein concentration was quantified by the 2-D Quant kit (GE Healthcare) according to the manufacturer's protocol.

Hundred microliter of proteins for each sample were incubated with trypsin (Promega, Madison, WI, USA) at a ratio of protein: Trypsin = 20:1 overnight at 37°C . After digestion, the peptides were dried by vacuum centrifugation, reconstituted in 0.5 M TEAB. Labeling was performed according to the manufacturer's manual for the iTRAQ (Applied Biosystems, Foster City, CA USA) (113 tags for Zaoer-N control, 114 tags for Zaoer-N waterlogging treatment, 117 tags for Pepino control, 118 tags for Pepino waterlogging treatment). One unit of iTRAQ reagent (defined as the amount of reagent required to label 100 μg of protein) was thawed and reconstituted in 70 μL isopropanol. The labeled peptide mixtures were incubated for 2 h at room temperature and then dried by vacuum centrifugation. Peptides were purified using an SCX chromatography (LC-20AB HPLC pump system, Shimadzu Corporation, Kyoto, Japan). The fractions were then loaded into a Shimadzu LC-20AD nano HPLC by the auto sampler onto a 2 cm C18 trap column. Peptides were eluted at a flow rate of 300 $\mu\text{L}/\text{min}$ with a linear gradient of 5–30% buffer B (95% ACN, 0.1% formic acid) over 60 min followed by ramping up to 100% buffer B over 5 min and holding for 20 min. The collected peptides were subjected to 5600 TripleTOF Analyzer (AB Sciex).

The charge states of peptides were set to +2, +3, and +4. The mass spectrometer was maintained in positive ion mode, and MS spectra were acquired over a range of 300–1800 m/z. The resolving powers of the MS/MS and MS scan at 200 m/z for the Q-Exactive were set as 17,500 and 70,000, respectively. For the acquired MS spectra, the top ten most intense signals were collected for MS/MS analysis. Ions were fragmented through higher energy collisional dissociation with normalized collision energies of 30 eV, and the isolation window was 2 m/z. The maximum ion injection times were set at 10 ms for the survey scan and 60 ms for the MS/MS scans. The automatic gain control target values for both scan modes were set to 3.0×10^6 . The

dynamic exclusion duration was 25 s. The chromatograms were recorded at 214 nm. The underfill ratio was defined as 0.1% on the Q-Exactive.

Peptide and Protein Identification and Proteomic Data Analysis

The raw mass files were analyzed by the Proteome Discoverer 1.4 software (Thermo Fisher Scientific). Search for the fragmentation spectra was performed by the MASCOT 2.3.02 software search engine embedded in Proteome Discoverer against the cucumber 9930 reference genome database version 2 (<http://www.icugi.org/cgi-bin/ICuGI/index.cgi>). The following search parameters were used: The initial precursor mass tolerance was set to ± 20 ppm, and the fragment ion mass tolerance was set to ± 20 mmu, trypsin as the cleavage enzyme. The protein identification was calculated by at least two unique peptides, minimum peptides for protein quantification was set to one, the normalization method and protein change ratio type (upregulated or downregulated) were both set as median. The results were filtered based on a false discovery rate (FDR) of no more than 1% to guarantee the result's confidence and a Mascot probability of 95%.

Total RNA Extraction and qRT-PCR

Total RNA from each sample was isolated by RNAiso Plus (Takara, China), then dissolved in water-DEPC and kept at a final concentration of 1000 $\mu\text{g}/\text{mL}$ using Biophotometer Plus (Expander, Germany). Total RNA was reverse-transcribed by a Takara PrimeScript[®] RT reagent kit with gDNA eraser according to the manufacturer's manual (Takara, China). Primer sequences for qRT-PCR were designed using Primer Premier 5.0 (Premier Biosoft International, Palo Alto, CA, USA). qRT-PCR was performed using a Takara SYBR[®] PrimeScript[™] RT-PCR kit (Takara, China). SYBR Green PCR cycling was performed on an iQ[™] 5 Multicolor real-time PCR detection system (Bio-RAD, USA) using 20 μL samples with the following temperature program: 95°C for 10 s, followed by 40 cycles of 95°C for 15 s, and then annealing at 52°C for 30 s. The relative quantization of gene expressions were calculated and normalized to *Actin*. Three replicates were used for qRT-PCR.

Physiological Determination

The chlorophyll concentration was measured by a SPAD (soil and plant analysis development) meter (SPAD-502Plus, Konica Minolta, Tokyo, Japan). 7 days after removing waterlogging treatment, cucumber plants were visually compared with well-watered control and scored for tolerance rating (TOR) using a scale of 0–5 (Navazio and Staub, 1994), where 0 = dead plants, 1 = 75 ~100% of wilt, 2 = 50~74% wilt, 3 = leaves undulating and recurved, 4 = recurved leave margins and 5 = green plant with no sign of stress. The lower scale stood for waterlogging susceptibility while the higher scale stood for tolerance. Ethylene production after 48 h of waterlogging treatment was measured by a gas chromatograph device equipped with a TRB-5 capillary column (0.32 mm id, 30 m length, 0.25 lm df) and a flame ionization detector. Temperature, injection, detector and heat clamber 150, 150, and 100°C were set. Nitrogen was employed

as the carrier gas. PDC (EC 4.1.1.1) and ADH (EC 1.1.1.1) activities were detected by spectrophotometer (Spectrum SP-752, Shanghai, China) metrically at 340 nm, following the methods described by Xu et al. (2014). Crude enzymes extracts of hypocotyls were prepared by macerating 1.0 g of the tissue in 5.0 cm³ of 0.1 M cold Tris-HCl buffer (pH 8.0) as described by Mustroph and Albrecht (2003). ADH and PDC activity was determined spectrophotometrically by measuring the rate of reduction of NAD⁺ (Waters et al., 1991). The reaction mixture contained 30 mM ethanol, 65 mM Tris-HCl buffer (pH 9.5), 1 mM NAD+, and 0.1 cm³ of crude enzyme extracts. Increase in absorbance due to production of NADH was recorded at room temperature. 1 U of PDC and ADH was defined as the amount of enzyme required to decompose 1 mol of substrate per g protein per minute. For ethanol production experiment, fresh hypocotyls were harvested and frozen rapidly in liquid nitrogen and ground to a powder. 500 mg root material was homogenized with 50 Mm cold 0.1 M HCl in a Teflon-sealed test tube. After 20 min incubation at 70°C, a 1 mL sample of headspace was injected into a gas chromatograph (Thermo Trace GC Ultra) equipped with a supelcowax 10 column (30 m × 0.32 mm × 0.25 μm) and a flame ionization detector following the instructions of Kato-Noguchi and Watada (1997). Ethanol evaporation under these conditions was negligible.

RESULTS

Phenotype Differences of Zaoer-N and Pepino in Responding to Waterlogging Treatment

To evaluate the phenotype differences of waterlogging stress on the tolerant Zaoer-N and the sensitive Pepino, seven representative phenotypes after 7 days of waterlogging were recorded. As is shown in Table 1, the tolerance rating, SPAD value, leaf flesh weight, ARs number, and flesh weight for Zaoer-N were considerably greater than those for Pepino, indicating that Zaoer-N was significantly more tolerant than Pepino ($p < 0.05$). However, the differences between Zaoer-N and Pepino for primary root flesh weight and hypocotyls length were not significant which suggesting the primary root injury and hypocotyls elongation may

not contribute to waterlogging tolerance between the two lines.

Transferring Zaoer-N seedlings to waterlogging stress resulted in ARs primordia emergence and visible on the hypocotyls surface 2 days after waterlogging, in comparing with control plants and waterlogged Pepino (Figure 1). Seven days after treatment, the average AR numbers protruded at the basal part of the hypocotyls were 30.4 (Figure S1). To elucidate the response mechanisms related to morphological differences between the two genotypes in responding to waterlogging, an iTRAQ proteomic approach was thus applied to the hypocotyls of the two-day-waterlogged Zaoer-N and Pepino seedlings.

Inventory of Hypocotyls Proteins Identified by iTRAQ

Using the Mascot software, a total of 52,053 spectra matched to known spectra, 46,773 spectra matched to unique peptides, and 23,533 peptides, 22,066 unique peptides, and 5508 proteins were identified (Table 2). All the mass spectrometry data have been deposited into the ProteomeXchange Consortium via the PRIDE partner repository with the dataset identifier PXD004023. Among these proteins, 1048 were between 20 to 60 kDa, 129

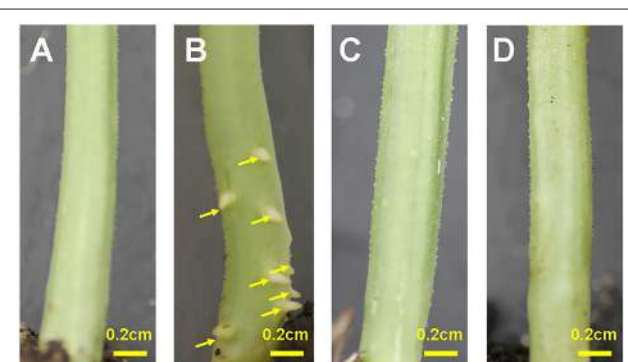


FIGURE 1 | Adventitious root formation on hypocotyls of cucumber seedlings. (A) Zaoer-N control; (B) Zaoer-N waterlogging; (C) Pepino control; (D) Pepino waterlogging. The yellow arrows in the picture indicated the location of adventitious roots. The water level was kept at about 2 cm above the soil for 2 days and then removed for photography.

TABLE 1 | Response of waterlogging tolerant line Zaoer-N and sensitive line Pepino after 7 days of waterlogging treatment.

Trait	Zaoer-N control	Zaoer-N waterlogged	Pepino control	Pepino waterlogged
TOR	5 ± 0a	4.67 ± 0.33a	5 ± 0a	1.09 ± 0.16b
SPAD	41.89 ± 1.24a	39.71 ± 2.41a	43.03 ± 0.56a	21.50 ± 1.34b
ARN	0 ± 0bc	29.43 ± 2.5a	0 ± 0bc	2.17 ± 1.43b
HLH	5.12 ± 0.27a	5.23 ± 0.22a	5.26 ± 0.77a	5.35 ± 0.67a
LFW	0.48 ± 0.14a	0.36 ± 0.09a	0.56 ± 0.17a	0.19 ± 0.1ab
HFW	0.92 ± 0.11b	1.6 ± 0.36a	0.8 ± 0.03a	0.4 ± 0.23b
PRFW	0.36 ± 0.05a	0.13 ± 0.11b	0.42 ± 0.1a	0.12 ± 0.07b

TOR, tolerance rating = 0 (dead plants)–5 (green plants with no sign of symptom); SPAD, soil plant analysis development; ARN, adventitious root numbers; HLH, hypocotyls length; LFW, leaf flesh weight; HFW, hypocotyls flesh weight; PRFW, primary root flesh weight. Means within trait followed by the same letter(s) are not significant difference at p -value < 0.05 .

between 0 to 20 kDa, 379 between 60 to 100 kDa, and 175 over 100 kDa (**Figure 2A**). 1792 proteins had one identified peptide, 1027 had two, 417 had more than 11, and the left had 3–10 (**Figure 2B**). The peptide sequence coverage was primarily less than 20% (**Figure 2C**). Ratio distributions for the identified proteins in Zaoer-N and D8 were shown in **Figures S2A,B**, respectively. Because iTRAQ quantification underestimated the amount of real fold change between two samples, protein with a fold-change >2 or <0.5 in abundance were regarded as DRPs.

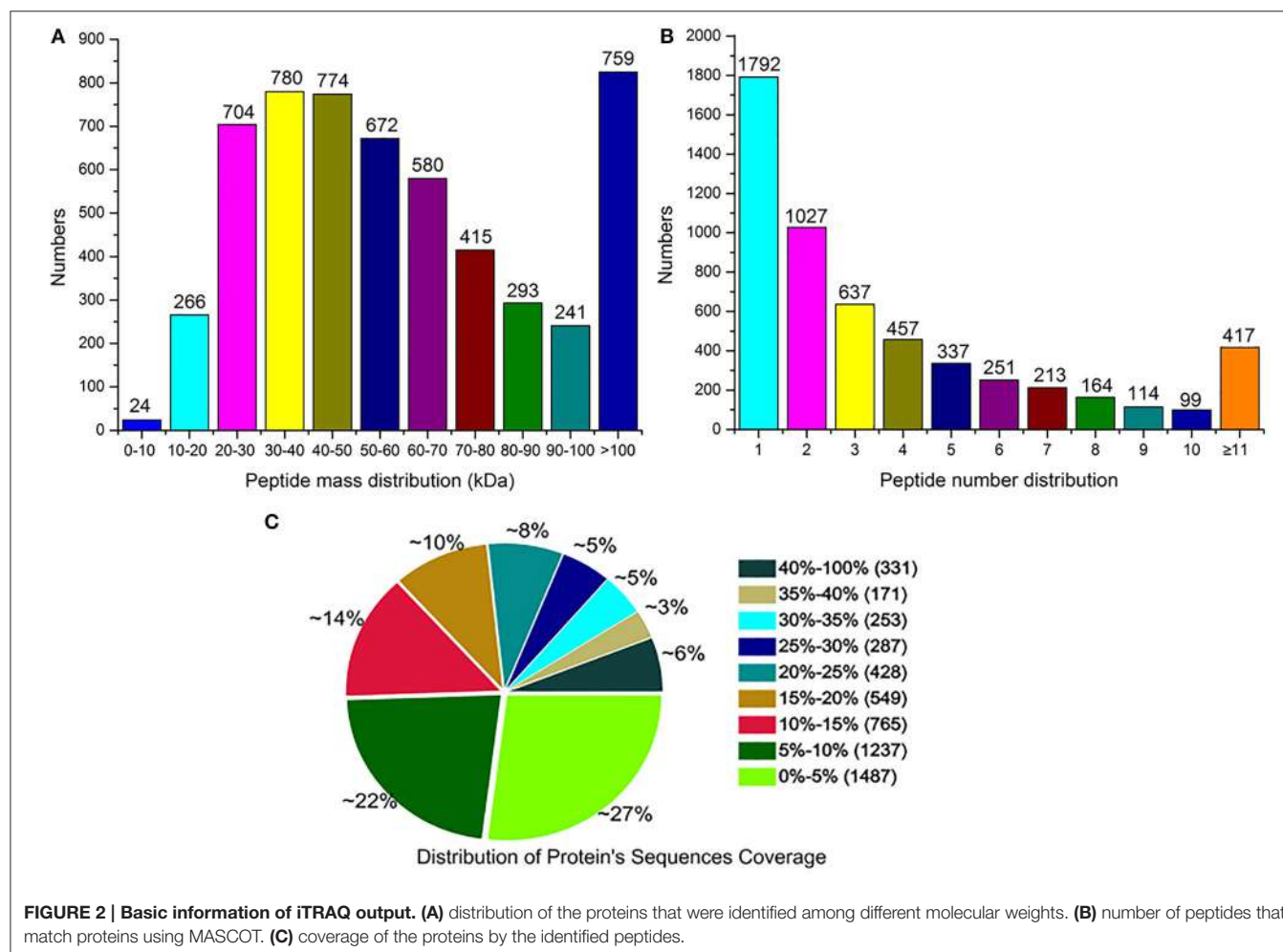
TABLE 2 | Spectra, peptides, and proteins that were identified from iTRAQ proteomics by searching against the cucumber reference genome 9930 version 2 database.

#	Category	Number
1	Total spectra	331,676
2	Spectra	52,053
3	Unique spectra	46,773
4	Peptide	23,533
5	Unique peptide	22,066
6	Protein	5508

Based on this criteria, 146 DRPs in the Zaoer-N and/or Pepino were selected for further analysis. Of these, 90 DRPs (62 increased and 28 decreased in abundance) changed significantly in the tolerant Zaoer-N and 99 DRPs (62 increased and 37 decreased in abundance) in the sensitive Pepino (**Table S1**). Only 43 DRPs (34 increased and 9 decreased in abundance) were shared between the two lines, while 47 DRPs were only identified in Zaoer-N, and 56 DRPs were only identified in Pepino.

Classification of Waterlogging Responsive DRPs

Of the 146 DRPs, 131 DRPs can be assigned to 21 categories using the COG database. The largest group was general function prediction only (18.3%) followed by posttranslational modification, protein turnover, chaperones (9.9%), carbohydrate transport and metabolism (9.2%), amino acid transport and metabolism (9.2%) and Translation, ribosomal structure and biogenesis (6.1%) (**Figure 3**). To further characterize these identified waterlogging responsive proteins, the DRPs identified in Zaoer-N and Pepino were respectively passed through GO enrichment analysis using the agriGO (<http://bioinfo.cau.edu.cn/agriGO>). A GO term was considered



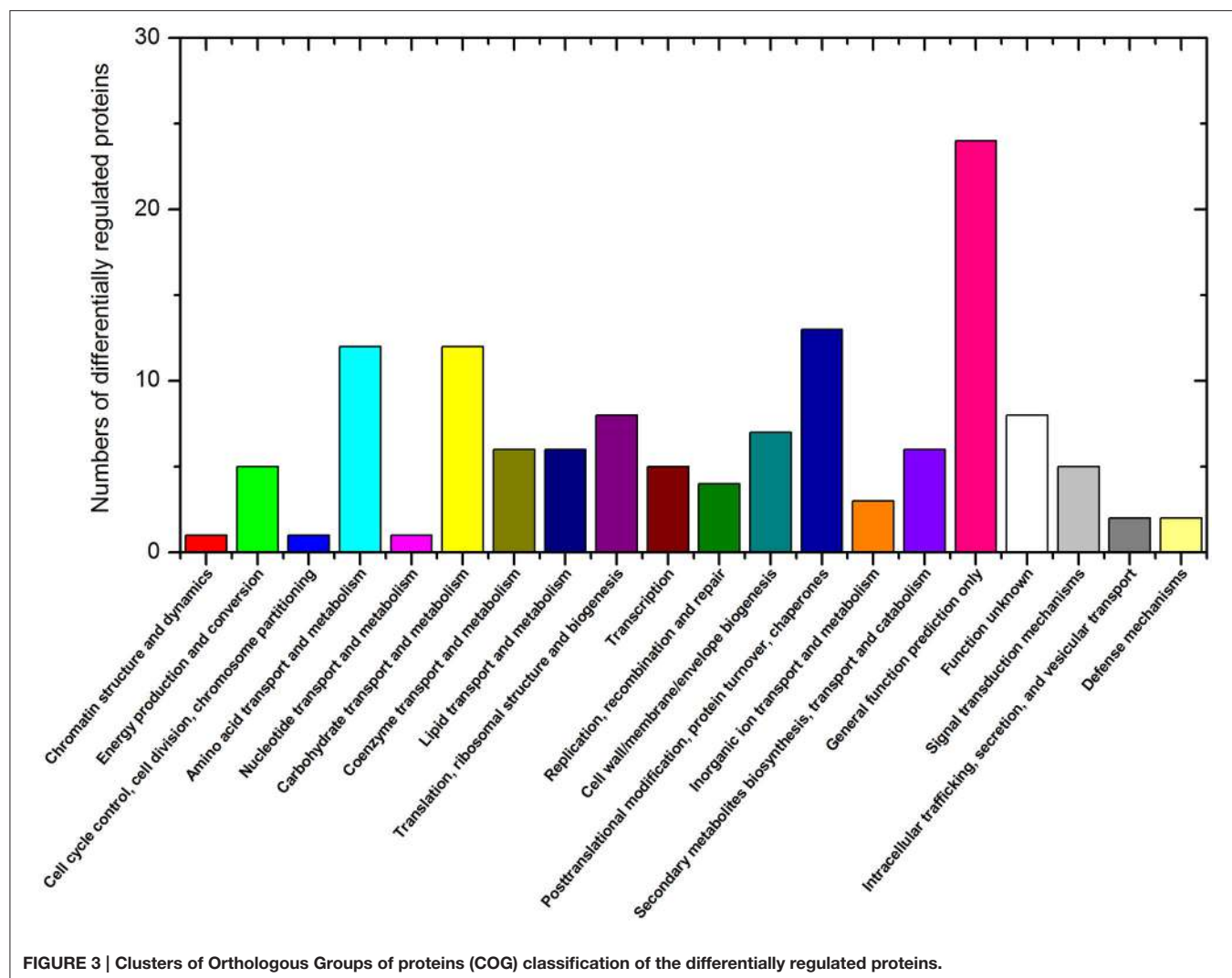


FIGURE 3 | Clusters of Orthologous Groups of proteins (COG) classification of the differentially regulated proteins.

to be significantly enriched if the false discovery rate was below 0.05. Enrichment analysis of GO functions revealed that 12 GO terms were found shared between Zaoer-N and Pepino, such as oxidoreductase activity (GO:0016491), response to stress (GO:0006950) and heme binding (GO:0020037). Four GO terms were unique to Zaoer-N, including response to oxidative stress (GO:0006979), response to chemical stimulus (GO:0042221), peroxidase activity (GO:0004601), and antioxidant activity (GO:0016209). On the contrary, GO terms related to carbohydrate metabolic process (GO:0005975), hydrolase activity (GO:0016798), and cofactor binding (GO:0048037) were specially enriched in Pepino (**Figure 4**).

To characterize the functional consequences of the DRPs associate with waterlogging stress and subsequent AR formation, KEEG pathway mapping based on KEGG orthology terms for assignment was also carried out. Only significantly enriched pathway categories that had a *p-value* lower than 0.05 were selected. The results indicated that waterlogging could affect phenylpropanoid biosynthesis and alpha-Linolenic acid metabolism in both of the two lines. KEEG terms

"glycolysis/gluconeogenesis" and "biosynthesis of secondary metabolites" were the highly enriched in the DRPs that were specifically up-regulated in the Zaoer-N, but "arginine biosynthesis," "alanine, aspartate, and glutamate metabolism," and "biosynthesis of amino acids" were dramatically enriched in DRPs in Pepino (**Table 3**). All of the DRPs in KEGG categories were shown in **Tables S2, S3**.

Protein–Protein Interaction Analysis

Plant proteins play interrelated roles together in the context of networks. To investigate how the cucumber hypocotyls transmit waterlogging stress signaling through protein–protein interactions, the identified DRPs in Zaoer-N and Pepino were analyzed respectively using the String database (<http://string-db.org>). The abbreviations of the protein names in the networks were shown in **Table S4**. Eight separate interaction networks were predicted in Zaoer-N (**Figure 5A**). The ribosomal proteins, including 40S ribosomal protein (AT5G39850), 60S ribosomal proteins (RPL16A, AT5G02870, AT1G57660, AT2G19730, AT4G29410), ribosomal protein L5 (AT3G25520),

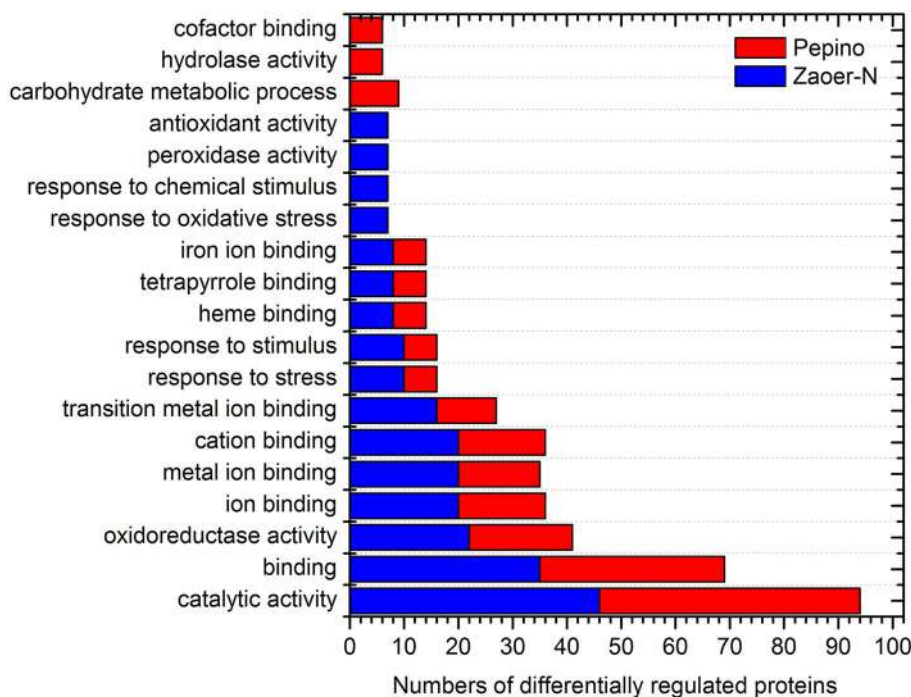


FIGURE 4 | Functional classification of differentially regulated proteins identified in this study. AgriGO web-based program was used to analyze GO categories (<http://bioinfo.cau.edu.cn/agriGO/>). The X-axis is the numbers of differentially regulated proteins. The Y-axis is categories of GO term.

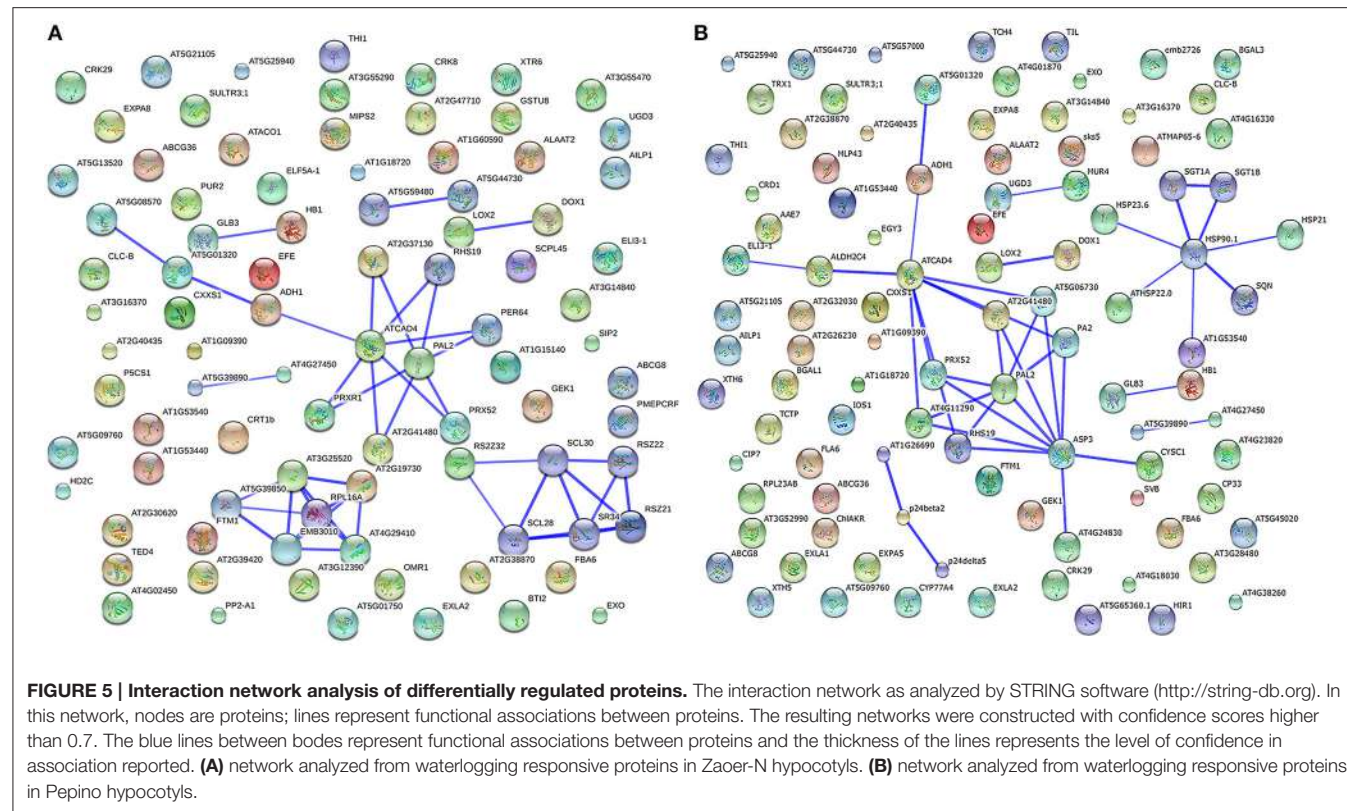
TABLE 3 | KEGG pathway enrichment analysis of differentially regulated proteins (DRPs).

#	KEEG term	Pathway ID	DRPs in Zaoer-N	P-value	DRPs in Pepino	P-value
1	Phenylpropanoid biosynthesis	csv00940	9	2.94 E-04	7	0.005
2	alpha-Linolenic acid metabolism	csv00592	4	0.005	3	0.031
3	Biosynthesis of secondary metabolites	csv01110	20	0.0176	0	—
4	Glycolysis / Gluconeogenesis	csv00010	5	0.016	0	—
5	Biosynthesis of amino acids	csv01230	0	—	6	0.046
6	Arginine biosynthesis	csv00220	0	—	3	0.012
7	Alanine, aspartate and glutamate metabolism	csv00250	0	—	3	0.028

KOBAS2.0 web-based program was used for KEEG mapping (<http://kobas.cbi.pku.edu.cn/>).

were found to be actively interacted with embryo defective 3031 (EMB3031). Another notable interacted protein group is composed of pyruvate kinase (AT5G08570), PDC (AT5G01320), ADH1, cinnamyl alcohol dehydrogenase 1 (ATCAD4), Prxs (PRXR1, AT2G41480, PRX52, PER64, RHS19, and AT2G37130), and phenylalanine ammonia-lyase 2 (PAL2). Argine-serine-rich zinc knuckle-containing protein 33 (RS2Z33) was a key protein in another network and interacted with pre-mRNA-splicing factor SR34, serine/arginine-rich protein RSZ22, zinc finger protein RSZ21, SC35-like splicing factors (SCL30A, SCL30, and SCL28). Furthermore, there were five pairs of interactive protein-species in this network. The main two pairs were hemoglobin 3 (GLB3) and hemoglobin 1 (HB1), deoxyhypusine synthase (DHS) and eukaryotic elongation factor (ELF5A-1), lipoxygenase 2

(LOX2) and alpha-dioxygenase (DOX1), haloacid dehalogenase-like hydrolase domain-containing protein (AT5G59480) and haloacid dehalogenase-like hydrolase domain-containing protein (AT5G44730), uncharacterized protein (AT5G39890) and aluminum induced protein (AT4G27450), respectively. Seven separate interaction networks were predicted in Pepino, and some of them were overlapped with the prediction in Zaoer-N (Figure 5B). However, the network made up of heat shock proteins (HSP90.1, HSP23.6, ATHSP22.0, AT1G53540, and HSP21), phosphatases (SGT1A and SGT1B) and SQUINT were only found in Pepino. Although these predicted interaction networks need to be verified, they have provided a narrow pool of protein–protein interactions in cucumber hypocotyls in responding to waterlogging for our further investigations.



Correlation of iTRAQ Data with mRNA Expression Data

The correlation of iTRAQ data and mRNA expression levels were carried out to further investigate protein expression profiles under waterlogging stress. The mRNA expression levels were obtained by qRT-PCR analysis of the corresponding 146 genes with the same experimental design. In the correlation analysis, we calculated the Pearson's correlation coefficients (PCC-value). The PCC-values of the DRPs and mRNA pairs were 0.26 in Zaoer-N (Figure 6A), while PCC-values were 0.18 for groups in Pepino, respectively (Figure 6B). As expected, significant correlations existed in both of the two groups at the 0.05 level (2-tailed). The positive correlation of iTRAQ data and mRNA expression levels suggested that the regulation of these proteins likely resulted from the transcriptional inductions of the corresponding genes in the waterlogged hypocotyls cells. However, the results also showed that some proteins and corresponding gene relative expression levels were not well correlated. The discrepancy of these protein and mRNA expression levels also has been found in other iTRAQ studies, and may be ascribed to translational and posttranslational regulatory processes or feedback loops between the processes of mRNA translation and protein degradation (Vogel and Marcotte, 2012).

Physiological Responses of Zaoer-N and Pepino to Waterlogging

To investigate whether these identified DRPs can result in physiological changes, we also evaluated the ethylene release,

ADH and PDC activities and production of ethanol (Figure 7). Two days of waterlogging treatment led to a significant increase in ADH and PDC activities ($p < 0.05$) and both of them were higher in Zaoer-N than that in Pepino (Figures 7A,B). As we known, the production of ethanol closely correlated with ADH activity. Compared with non-waterlogged cucumber hypocotyls, the ethanol concentrations after 2 days of waterlogging increased significantly ($p < 0.05$) in both lines but to a greater degree in Zaoer-N than in Pepino (Figure 7C). A 7.3-fold and 4.1-fold increase in ethylene release after 2 days of waterlogging was observed in hypocotyls of Zaoer-N and Pepino, respectively (Figure 7D).

DISCUSSION

ARs formation as a result of flooding or waterlogging stress were reported for tomato (Vidoz et al., 2010), bittersweet (Dawood et al., 2014, 2016), wheat (Barrett-Lennard et al., 1988), barley (Pang et al., 2007), rice (Bleecker et al., 1986), and maize (Mano et al., 2005). In deep-water rice cultivar *Pin Gaew56*, AR primordia emerged from the stem node within 8 ~ 10 h of partial submergence (Lorbicke and Sauter, 1999). The present study showed that ARs primordia emergence and visible on the cucumber hypocotyls surface 2 days after waterlogging, the number of ARs significantly increased in Zaoer-N compared with Pepino 7 days after waterlogging, and the SPAD value in the leaves was significantly higher in Zaoer-N than in Pepino (Table 1). These observations indicated that Zaoer-N adapted

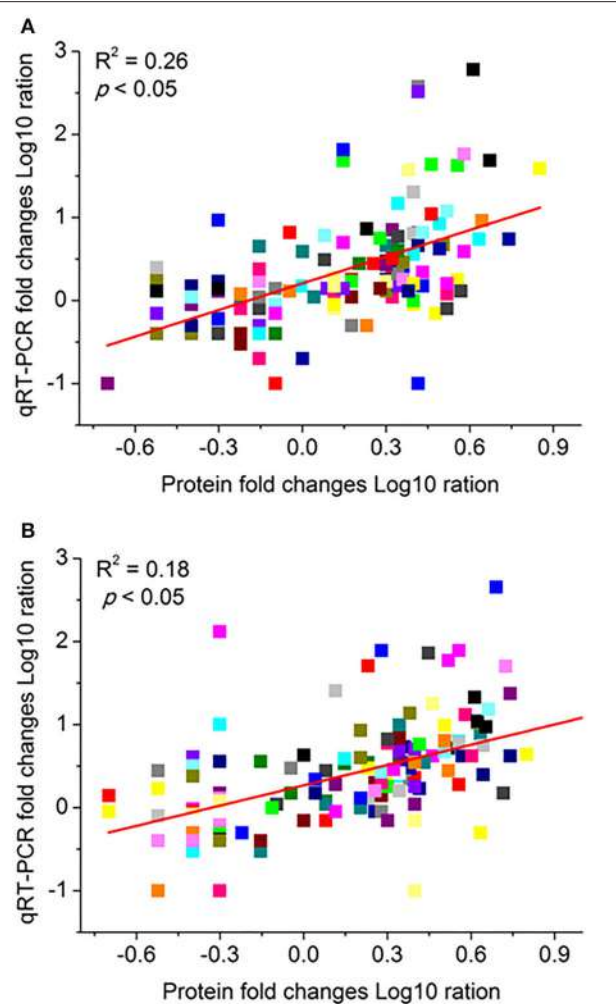


FIGURE 6 | Comparison of protein folds change levels measured by iTRAQ and quantitative real-time reverse transcription-PCR (qRT-PCR) assays in Zaoer-N (A) and Pepino (B). The gene expression values were transformed to the log10 scale. The protein fold changes log10-values (X-axis) were plotted against the qRT-PCR fold changes log2-values (Y-axis). The cucumber β -actin gene (GenBank AB010922) was used as an internal control to normalize the expression data. Each value denotes the mean relative level of expression of three biological replicates.

better to waterlogging stress than Pepino. ARs facilitate oxygen diffusion in Zaoer-N to accelerate aerobic metabolism, and maintaining a sufficient energy supply to meet the demands of the long-term survival (Bailey-Serres and Voesenek, 2008). The process of activation of AR emergence under waterlogging, however, has been studied to a much lesser extent. To further our understanding about the molecular and physiological reprogramming that enable AR primordia to resume growth upon an abiotic trigger, we thus analyzed the proteomic response to waterlogging in cucumber at the initial stage of ARs growth.

Management of the Energy Crisis

Energy crisis is a major factor affecting waterlogged organs survival because only 2 ~ 4 mol ATP per mol hexose were

produced by glycolysis and fermentation when compared with 30 ~ 36 mol ATP produced by aerobic respiration (Bailey-Serres and Voesenek, 2008). Previous studies have confirmed that both sensitive and tolerant plants are able to maintain their ATP production by inducing glycolytic and fermentative enzymes at the early adaptive response to waterlogging treatment (Yu et al., 2015). As expected, we also found that several enzymes, such as UDP-glucose 6-dehydrogenase (Csa1M012150.1) in hemicellulose synthesis, fructose-bisphosphate aldolase (Csa3M750920.1), and pyruvate kinase (Csa5M580610.1 and Csa6M449830.1) involved in glycolysis, and ADH (Csa7M320050.1) and PDC (Csa6M518930.1) in ethanol fermentation were significantly accumulated in both of Zaoer-N and Pepino, suggesting the common regulation of energy generation in waterlogged cucumber hypocotyls. However, our data showed that ADH (Csa7M322060.1) accumulated only in Zaoer-N (Table 4, Table S1), in accordance with the observation of ADH activity and ethanol concentrations (Figures 7A,C). As we known, ADH plays an essential role in the recycling of NADH to NAD^+ , which is pivotal for the continuation of glycolysis pathway (Ismond et al., 2013), and is the only energy source under oxygen deprivation condition. Interestingly, aldehyde dehydrogenase (ALDH, Csa1M372010.1), which converts the acetaldehyde into acetate, was accumulated only in Pepino. As postulated by Nakazono et al. (2000), the conversion of acetaldehyde to acetate by ALDH also consumes NAD^+ , which could potentially further block glycolysis and ATP supply. Together, these results suggested that the two lines exhibit a similar enzymes cascade as other plants species in responding to waterlogging stress, but the more efficient of regenerate ATP and NAD^+ and continuation of the glycolysis pathway in tolerant Zaoer-N than sensitive Pepino to cope with energy crises imposed by waterlogging. Nevertheless, high rates of glycolysis and alcohol fermentation will unavoidably lead to the fast depletion of sugar stores and carbon crisis, and the products of alcohol fermentation (acetaldehyde and ethanol) may have damaging consequences on cell integrity (Limami et al., 2008). Thus, escape from the damaging consequences appears an important issue in survival strategy, especially for those tolerant lines if waterlogging stress prolonged.

Ethylene Production and ROS Production in Responses to Waterlogging

Among several internal changes in the waterlogged plants, it is the pervasive and rapid accumulation of ethylene that makes it an early and reliable waterlogging-triggered signal (Sasidharan and Voesenek, 2015). In our previous study, we found that the ARN in Zaoer-N hypocotyls 3 days after waterlogging was significantly inhibited when pretreated with 100 mg/L 1-methylcyclopropene as an inhibitor of ethylene action (Xu et al., 2016), suggesting the importance of ethylene in waterlogging-triggered cucumber AR production. Ethylene production was observed in both of Zaoer-N and Pepino 2 days after treatment (Figure 7D). As is known to all, the gaseous phytohormone ethylene is biosynthesized from methionine, and it is produced by the activation of 1-aminocyclopropane-1-carboxylic acid (ACC)

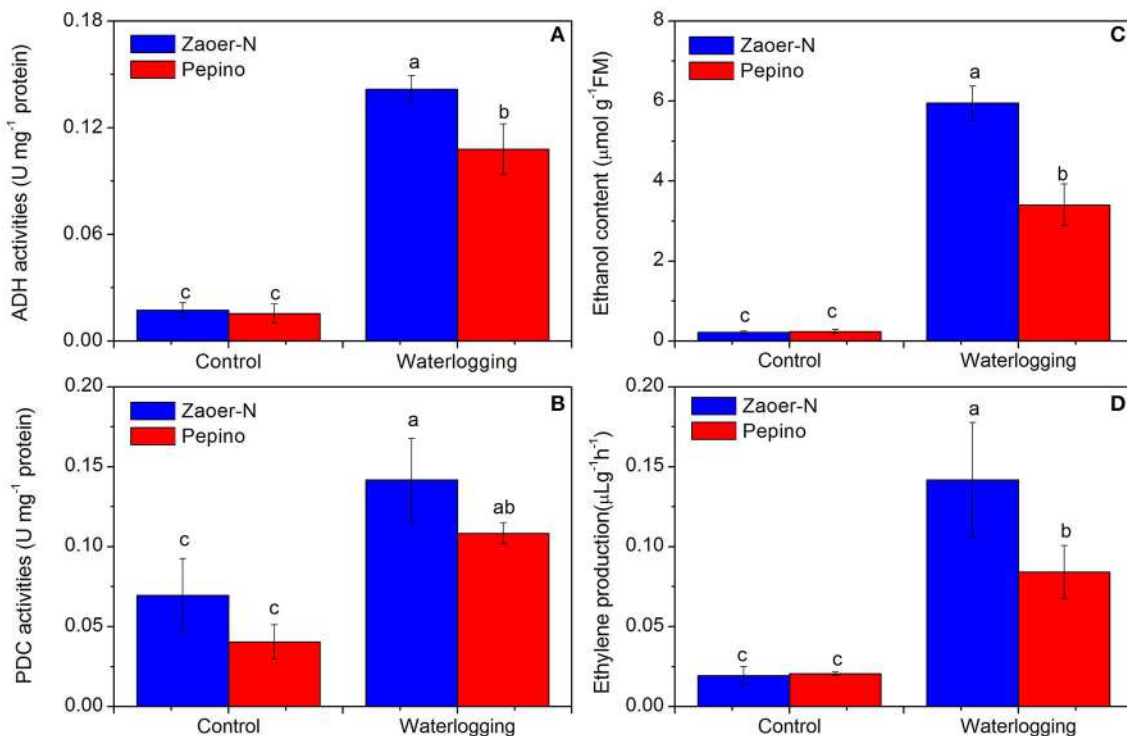


FIGURE 7 | Physiological responses of Zaoer-N and Pepino hypocotyls to waterlogging stress. Hypocotyls of control and treated plants were harvested as described in Materials and methods. Four physiological parameters, including alcohol dehydrogenase (ADH) activity (**A**), pyruvate decarboxylase (PDC) activity (**B**), ethanol production (**C**), and ethylene production (**D**) were measured. Data represents the average values \pm SE of three independent experiments. Letters above the bars indicate a statistically significant difference ($p < 0.05$) according to Duncan's multiple range test.

TABLE 4 | Information of differentially regulated proteins related to alcohol dehydrogenase, pyruvate decarboxylase, and 1-aminocyclopropane-1-carboxylate oxidase.

Protein name	Function	Coverage (%)	No. of unique peptides	Fold changes (waterlogging vs. controls)	
				Zaoer-N	Pepino
Csa7M320050.1	alcohol dehydrogenase	49.2	9	3.333	4.484
Csa7M322060.1	alcohol dehydrogenase	60.7	11	3.788	—
Csa6M518930.1	pyruvate decarboxylase	22.8	7	2.628	2.075
Csa2M000520.1	1-aminocyclopropane-1-carboxylate oxidase	27	7	4.651	—
Csa4M056660.1	1-aminocyclopropane-1-carboxylate oxidase	8.8	3	2.050	2.062
Csa6M511860.1	1-aminocyclopropane-1-carboxylate oxidase	27.2	5	2.500	2.32

synthase and ACC oxidase (ACO) (Yang and Oetiker, 1994). We identified three ACOs (Csa2M000520.1, Csa4M056660.1, and Csa6M511860.1), and two of these proteins were accumulated in both lines, whereas Csa2M000520.1 accumulated only in Zaoer-N, indicating that a higher quantity of ethylene production in waterlogged Zaoer-N than those in Pepino may caused by accumulation of this protein (Table 4, Table S1). It should be pointed out that S-adenosyl-L-methionine synthetase (SAM, Csa3M016410.1) was decreased following exposure to 2 days of treatment. SAM is the key enzyme in the synthesis of S-adenosyl-L-methionine, which is an important metabolic component in the ethylene biosynthesis pathway (Yang and Hofman, 1984). The decrease of SAM in the proteome from waterlogging-treated

tomato root has also been reported (Ahsan et al., 2007). The decrease of SAM observed in the current study indicated that ethylene production in cucumber hypocotyls would be reduced after 2 days of treatment. In deep-water rice, the enhanced formation of epidermal cell death at sites where ARs primordia emerge is dependent on the presence of ethylene (Mergemann and Sauter, 2000; Steffens et al., 2011). The growing ARs exert a mechanical force on the epidermal cells overlying them in a process that also requires ethylene-mediated ROS generation (Steffens et al., 2006). Despite of ROS at lower concentrations may act as signaling molecules involved in acclimation to environmental stress, a high level of these compounds are also harm to the plant cell. Heat shock proteins (HSPs) are the

most recurrent of ROS related proteins that not only respond to heat stress, but also in respond to other stress, such as waterlogging, and has been proven to be associated with the presence of hydrogen peroxide (Pucciariello et al., 2012; Banti et al., 2013). Five HSPs were identified in present study, and all of them (Csa3M113300.1, Csa3M020080.1, Csa3M183950.1, Csa5M138480.1, and Csa5M591720.1) were accumulated only in Pepinos. Increase of HSPs has been proposed to be specific H_2O_2 sensors in plants, suggesting the higher H_2O_2 production in Pepino.

Proteins Involved in Cell Division and Cell Growth

The process of AR primordia emergence is accompanied with extensive cell division and cell growth. Regulation of cell division and cell growth-related proteins were also apparent. The DRPs list contained 14 cell wall remolding proteins, including expansins, pectinesterase, proteinase inhibitor, xyloglucan endotransglucosylase/hydrolases, polygalacturonase, and some structural constituent of cell wall. Most of these proteins had higher fold changes in Zaoer-N than Pepino, suggesting the AR primordia emergence in Zaoer-N could not be separated with cell wall extensibility. Interestingly, nine peroxidase (Prxs), which involved in many development processes such as cell growth and differentiation (Dunand et al., 2007), were also differentially regulated. Five of them (Csa6M495000.1, Csa7M049140.1, Csa7M061710.1, Csa2M346020.1, and Csa3M736970.1) were accumulated only in the waterlogged hypocotyls of Zaoer-N. Passardi et al. (2006) found that Arabidopsis seedlings lacking *Prx33* transcripts have shorter roots than the wild-type controls and roots are still shorter in the double mutant, while seedlings overexpressing *AtPrx34* exhibit significantly longer roots. Studies have also provided evidences that Prxs activities play an protective role in the ROS scavenging process upon waterlogging stress (Qi et al., 2012). Thus, accumulation of Prxs in Zaoer-N will help consumption of ROS and promote cell elongation around the AR primordia. Additionally, our iTRAQ data also showed that two histone deacetylases (Csa3M748810.1 and Csa6M150540.1) were decreased in Zaoer-N specially, which might results in decondensation of the chromatin structure around the promoter regions of embryonic genes and help stimulating cell differentiation (Yoo et al., 2006). The Arabidopsis histone deacetylases HDA6 and HDA19 redundantly regulate embryonic genes and negatively affect callus formation from the hypocotyls (Tanaka et al., 2008). Thus, decrease of these histone deacetylases may also help promoting the emergence of AR primordia in Zaoer-N hypocotyls. Although we did not detect cyclin or cyclin dependent kinase in the hypocotyls of Zaoer-N at the 2 days time point, there were already a specific induction of many proteins controlling cell size and cell proliferation in Zaoer-N hypocotyls, such as 60S ribosomal proteins, which are absolutely required for protein synthesis (Bailey-Serres and Freeling, 1990), and histone H5 (Csa6M407650.1) in cell division (Bailey-Serres and Voesenek, 2008). In contrast to the situation in the primordia, a large group of cell wall modifying- and cell cycle-related proteins were decreased in the hypocotyls of Pepino. These findings

suggest that cell division and growth are suppressed in Pepino hypocotyls upon waterlogging, such that these hypocotyls might enters a state of endurance.

Proteins Related to Jasmonic Acid (JA) Content

The threonine dehydratase (TD, Csa6M448730.1) was the highest decreased (~ 0.048 fold than control) protein that specifically regulated in waterlogged Zaoer-N. TD catalyzes the formation of α -keto butyrate from Thr, the first step in the biosynthesis of Ile (Kang et al., 2006). For more than a decade, TD has been recognized as a reliable marker for JA elicitation in potato and tomato (Dammann et al., 1997). This information prompted us to investigate the JA concentration during AR emergence on cucumber hypocotyls. As expected, JA concentrations in 2-day waterlogged Zaoer-N hypocotyls were significantly decreased (~ 0.33 fold) than control. On the contrary, JA concentrations in Pepino hypocotyls were significantly increased (~ 1.99 fold) than control after 2 days of waterlogging (Table S5). Sanders et al. (2000) and von Malek et al. (2002) found that JA deficient mutants *opr3/dde1* and *dde2-2* produced more ARs than the wild type, Gutierrez et al. (2012) showed that *Arabidopsis gh3* triple mutant accumulated twice as much JA but inhibited the AR initiation compared with the wild type. It is tempting to speculate that JA is an inhibitor of cucumber adventitious rooting. The accumulation of JA in waterlogged Pepino might be caused by the higher fold changes of lipoxygenase (Csa4M286960.1, ~ 6.29 fold than control, Table S1), which is a key enzyme in JA biosynthesis. However, due to the oxygen requirement of lipoxygenase (Arbona and Gómez-Cadenas, 2008), the increased JA biosynthesis via lipoxygenase pathway will unavoidably lead to higher risk of being injured by oxygen deprivation under waterlogging condition.

Proteins Related to Phenylpropanoid Metabolism and Lipid Catabolism

A feature of plant responses to waterlogging is the activation of phenylpropanoid metabolism, which is also supported by our KEEG pathway mapping (Table 3). We found that DRPs enriched in KEEG term “phenylpropanoid metabolism” (Table S3) were all Prxs (as described in Proteins Involved in Cell Division and Cell Growth Section) except for a phenylalanine ammonia-lyase (PAL, 4.3.1.5). PAL catalyzes the first committed step of the core pathway of general phenylpropanoid metabolism (Gómez-Vásquez et al., 2004), and is one of the most extensively studied enzymes with respect to plant responses to abiotic stress. Higher levels of PAL activity or mRNA accumulation in response to waterlogging have been found in tomato roots, *Vigna sinensis* and *Zea mays* (Alla et al., 2002). However, in current investigation, we found that PAL (Csa6M147460.1) decreased in cucumber hypocotyls after 2 days of waterlogging treatment, and to a greater degree in Zaoer-N (0.071) than in Pepino (0.456). Politycka (1998) found that the upregulation of PAL activity resulted in cucumber root growth decreasing. The highly inhibition of PAL enzyme could result from accumulation of its intermediate product in phenylpropanoid metabolism i.e., the

trans-cinnamic acid, and we thus speculated that the decrease of PAL in waterlogged Zaoer-N could benefit to waterlogging triggered AR growth.

In plants, lipid catabolism is known to be an active process that can mobilize storage lipids and can detoxify deleterious membrane lipids caused by abiotic stresses (Kim et al., 2016). Except for the lipoxygenase discussed above, our iTRAQ study also found that three GDSL esterases/lipases, Csa1M058140.1, Csa3M669600.1, and Csa3M434970.1, were differentially regulated by waterlogging stress. GDSL esterases/lipases are a newly discovered subclass of lipolytic enzymes that can break down lipids and hydrolyze triglycerides into glycerol and free fatty acids (Chepyshko et al., 2012). Thus, far, little data have apparently been published on the detailed role of GDSL esterase/lipase activity in waterlogging tolerance or AR formation. Interestingly, Csa3M669600.1 was the highest accumulated (~7.029 fold than control) protein in waterlogged Zaoer-N, and Csa1M058140.1 was induced only in Zaoer-N. These indicated enhanced lipid catabolism, possibly via elevated glycerol to provide additional carbon and energy sources for AR primordia growth or free fatty acids for membrane constituents of those newly developed cells (Li et al., 2016).

Together, this study reveals the proteomic difference of the tolerant line Zaoer-N and the sensitive line Pepino upon exposure to waterlogging stress. Our iTRAQ-based proteomic data showed that the more efficient of regenerate ATP and NAD⁺ and continuation of the glycolysis pathway in tolerant line Zaoer-N appears to be an important way to maintain the level of available carbohydrate and energy to prevent intracellular energy shortage resulting from the waterlogging-caused oxygen deprivation. Moreover, the phytohormone ethylene and ROS production might act as the response signaling in activating the apical meristem in AR primordial, whereas the JA might play an opposite role. Compare with Pepino, proteins cell division, cell growth, phenylpropanoid metabolism, and lipid catabolism are also important to facilitate protrusion of the AR primordia to the outside in Zaoer-N hypocotyls. These results indicated that proteomics with bioinformatics analysis is a good starting point for understanding the overall molecular response of cucumber hypocotyls to waterlogging. A deep and broad understanding of the DRPs identified is ongoing to make clear their specific role in ARs emergence upon waterlogging.

REFERENCES

- Ahsan, N., Lee, D. G., Lee, S. H., Lee, K. W., Bahk, J. D., and Lee, B. H. (2007). A proteomic screen and identification of waterlogging-regulated proteins in tomato roots. *Plant Soil* 295, 37–51. doi: 10.1007/s11104-007-9258-9
- Alla, M. N., Younis, M. E., El-Shihaby, O. A., and El-Bastawisy, Z. M. (2002). Kinetin regulation of growth and secondary metabolism in waterlogging and salinity treated *Vigna sinensis* and *Zea mays*. *Acta Physiol. Plant* 24, 19–27. doi: 10.1007/s11738-002-0017-5
- Arbona, V., and Gómez-Cadenas, A. (2008). Hormonal modulation of citrus responses to flooding. *J. Plant Growth Regul.* 27, 241–250. doi: 10.1007/s00344-008-9051-x
- Bailey-Serres, J., and Freeling, M. (1990). Hypoxic stress-induced changes in ribosomes of maize seedling roots. *Plant Physiol.* 94, 1237–1243. doi: 10.1104/pp.94.3.1237

AUTHOR CONTRIBUTIONS

XC conceived the experiment. XX and JJ performed the research. XX, JJ, and XM collected data. XX, QX, and XQ analyzed the data and wrote the manuscript.

ACKNOWLEDGMENTS

This research was funded by the National Natural Science Foundation of China (31372087). The funder had no role in study design, data collection and analysis, decision to publish, or preparation of the manuscript. The authors gratefully acknowledge financial support from China scholarship council and foundation of excellent doctoral dissertation of Yangzhou University.

SUPPLEMENTARY MATERIAL

The Supplementary Material for this article can be found online at: <http://journal.frontiersin.org/article/10.3389/fpls.2016.01515>

Table S1 | Detailed information of the differentially regulated proteins identified by iTRAQ.

Table S2 | KEEG pathway enrichment analysis of differentially regulated proteins in Zaoer-N.

Table S3 | KEEG pathway enrichment analysis of differentially regulated proteins in Pepino.

Table S4 | The abbreviations of the protein names showed in the networks of Figure 5.

Table S5 | Endogenous jasmonic acid concentrations in hypocotyls of Zaoer-N and Pepino after 2 days of waterlogging.

Figure S1 | Morphology of 7-day waterlogged Zaoer-N and Pepino. The water level was kept at about 2 cm above the soil for 7 days and then removed for photography.

Figure S2 | Ratio distributions for the identified proteins. The changes of protein contents in Zaoer-N (**A**) and Pepino (**B**) 48 h after waterlogging treatment were analyzed. The horizontal axis displays the base Log2-transformed ratios. The red point indicates that the ratio was greater than 1.5, and the green point indicates that the ratio was less than 0.67. The differentially regulated proteins with a fold-change >2 (red points on the right of red lines) or <0.5 (green points on the left of green lines) in abundance were further analyzed in the present study.

Bailey-Serres, J., and Voesenek, L. A. (2008). Flooding stress: acclimations and genetic diversity. *Annu. Rev. Plant Biol.* 59, 313–339. doi: 10.1146/annurev.arplant.59.032607.092752

Bailey-Serres, J., Fukao, T., Gibbs, D. J., Holdsworth, M. J., Lee, S. C., Licausi, F., et al. (2012). Making sense of low oxygen sensing. *Trends Plant Sci.* 17, 129–138. doi: 10.1016/j.tplants.2011.12.004

Banti, V., Giuntoli, B., Gonzali, S., Loreti, E., Magneschi, L., Novi, G., et al. (2013). Low oxygen response mechanisms in green organisms. *Int. J. Mol. Sci.* 14, 4734–4761. doi: 10.3390/ijms14034734

Barrett-Lennard, E. G., Leighton, P. D., Buwalda, F., Gibbs, J., Armstrong, W., Thomson, C. J., et al. (1988). Effects of growing wheat in hypoxic nutrient solution and of subsequent transfer to aerated solutions. I. Growth and carbohydrate status of shoots and roots. *Funct. Plant Biol.* 15, 585–598. doi: 10.1071/PP9880585

- Bleeker, A. B., Schuette, J. L., and Kende, H. (1986). Anatomical analysis of growth and development patterns in the internode of deepwater rice. *Planta* 169, 490–497. doi: 10.1007/BF00392097
- Changdee, T., Polthanee, A., Akkasaeng, C., and Morita, S. (2009). Effect of different waterlogging regimes on growth, some yield and roots development parameters in three fiber crops (*Hibiscus cannabinus* L., *Hibiscus sabdariffa* L. and *Cochruss olitorius* L.). *Asian J. Plant Sci.* 8, 515. doi: 10.3923/ajps.2009.515.525
- Chen, S., and Harmon, A. C. (2006). Advances in plant proteomics. *Proteomics* 6, 5504–5516. doi: 10.1002/pmic.200600143
- Chepyskho, H., Lai, C. P., Huang, L. M., Liu, J. H., and Shaw, J. F. (2012). Multifunctionality and diversity of GDSL esterase/lipase gene family in rice (*Oryza sativa* L. japonica) genome: new insights from bioinformatics analysis. *BMC Genomics* 13:309. doi: 10.1186/1471-2164-13-309
- Cui, D., Wu, D., Liu, J., Li, D., Xu, C., Li, S., et al. (2015). Proteomic analysis of seedling roots of two maize inbred lines that differ significantly in the salt stress response. *PLoS ONE* 10:e0116697. doi: 10.1371/journal.pone.0116697
- Dammann, C., Rojo, E., and Sánchez-Serrano, J. J. (1997). Abscisic acid and jasmonic acid activate wound-inducible genes in potato through separate, organ-specific signal transduction pathways. *Plant J.* 11, 773–782. doi: 10.1046/j.1365-313X.1997.11040773.x
- Dawood, T., Rieu, I., Wolters-Arts, M., Derkens, E. B., Mariani, C., and Visser, E. J. W. (2014). Rapid flooding-induced adventitious root development from preformed primordia in *Solanum dulcamara*. *AoB Plants* 6:plt058. doi: 10.1093/aobpla/plt058
- Dawood, T., Yang, X., Visser, E. J. W., Te Beek, T. A. H., Kensche, P. R., Cristescu, S. M., et al. (2016). A co-opted hormonal cascade activates dormant adventitious root primordia upon flooding in *Solanum dulcamara*. *Plant Physiol.* 170, 2351–2364. doi: 10.1104/pp.15.00773
- Dunand, C., Crèvecœur, M., and Penel, C. (2007). Distribution of superoxide and hydrogen peroxide in *Arabidopsis* root and their influence on root development: possible interaction with peroxidases. *New Phytol.* 174, 332–341. doi: 10.1111/j.1469-8137.2007.01995.x
- Evans, D. E. (2004). Aerenchyma formation. *New Phytol.* 161, 35–49. doi: 10.1046/j.1469-8137.2003.00907.x
- Gutierrez, L., Mongelard, G., Floková, K., Păcurar, D. I., Novák, O., Staswick, P., et al. (2012). Auxin controls *Arabidopsis* adventitious root initiation by regulating jasmonic acid homeostasis. *Plant Cell* 24, 2515–2527. doi: 10.1105/tpc.112.099119
- Gómez-Vásquez, R., Day, R., Buschmann, H., Randles, S., Beeching, J. R., and Cooper, R. M. (2004). Phenylpropanoids, phenylalanine ammonia lyase and peroxidases in elicitor-challenged cassava (*Manihot esculenta*) suspension cells and leaves. *Ann. Bot.* 94, 87–97. doi: 10.1093/aob/mch107
- Ismond, K. P., Dolferus, R., de Pauw, M., Dennis, E. S., and Good, A. G. (2013). Enhanced low oxygen survival in *Arabidopsis* through increased metabolic flux in the fermentative pathway. *Plant Physiol.* 132, 1292–1302. doi: 10.1104/pp.103.022244
- Jackson, M. B., and Colmer, T. D. (2005). Response and adaptation by plants to flooding stress. *Ann. Bot.* 96, 501–505. doi: 10.1093/aob/mci205
- Jiang, Z., Song, X. F., Zhou, Z. Q., Wang, L. K., Li, J. W., Deng, X. Y., et al. (2010). Aerenchyma formation: programmed cell death in adventitious roots of winter wheat (*Triticum aestivum*) under waterlogging. *Funct. Plant Biol.* 37, 748–755. doi: 10.1071/FP09252
- Kang, J. H., Wang, L., Giri, A., and Baldwin, I. T. (2006). Silencing threonine deaminase and JAR4 in *Nicotiana attenuata* impairs jasmonic acid-isoleucine-mediated defenses against *Manduca sexta*. *Plant Cell* 18, 3303–3320. doi: 10.1105/tpc.106.041103
- Kato-Noguchi, H., and Watada, A. E. (1997). Effects of low-oxygen atmosphere on ethanolic fermentation in fresh-cut carrots. *J. Am. Soc. Hortic. Sci.* 122, 107–111.
- Kim, R. J., Kim, H. J., Shim, D., and Suh, M. C. (2016). Molecular and biochemical characterizations of monoacylglycerol lipase gene family of *Arabidopsis thaliana*. *Plant J.* 85, 758–771. doi: 10.1111/tpj.13146
- Li, N., Xu, C., Li-Beisson, Y., and Philipp, K. (2016). Fatty acid and lipid transport in plant cells. *Trends Plant Sci.* 21, 145–158. doi: 10.1016/j.tplants.2015.10.011
- Li, S. W., Xue, L., Xu, S., Feng, H., and An, L. (2009). Hydrogen peroxide acts as a signal molecule in the adventitious root formation of mung bean seedlings. *Environ. Exp. Bot.* 65, 63–71. doi: 10.1016/j.envexpbot.2008.06.004
- Limami, A. M., Glévarec, G., Ricoult, C., Cliquet, J.-B., and Planchet, E. (2008). Concerted modulation of alanine and glutamate metabolism in young *Medicago truncatula* seedlings under hypoxic stress. *J. Exp. Bot.* 59, 2325–2335. doi: 10.1093/jxb/ern102
- Lorbiecke, R., and Sauter, M. (1999). Adventitious root growth and cell-cycle induction in deepwater rice. *Plant Physiol.* 119, 21–30. doi: 10.1104/pp.11.9.1.21
- Mano, Y., Muraki, M., Fujimori, M., Takamizo, T., and Kindiger, B. (2005). Identification of QTL controlling adventitious root formation during flooding conditions in teosinte (*Zea mays* ssp. *huehuetenangensis*) seedlings. *Euphytica* 142, 33–42. doi: 10.1007/s10681-005-0449-2
- Mergemann, H., and Sauter, M. (2000). Ethylene induces epidermal cell death at the site of adventitious root emergence in rice. *Plant Physiol.* 124, 609–614. doi: 10.1104/pp.124.2.609
- Mustroph, A., and Albrecht, G. (2003). Tolerance of crop plants to oxygen deficiency stress: Fermentative activity and photosynthetic capacity of entire seedlings under hypoxia and anoxia. *Physiol. Plant.* 117, 508–520. doi: 10.1034/j.1399-3054.2003.00051.x
- Nakazono, M., Tsuji, H., Li, Y., Saisho, D., Arimura, S.-I., Tsutsumi, N., et al. (2000). Expression of a gene encoding mitochondrial aldehyde dehydrogenase in rice increases under submerged conditions. *Plant Physiol.* 124, 587–598. doi: 10.1104/pp.124.2.587
- Navazio, J. P., and Staub, J. E. (1994). Effects of soil moisture, cultivar, and postharvest handling on pillow fruit disorder in cucumber. *J. Am. Soc. Hortic. Sci.* 119, 1234–1242.
- Pang, J., Cuin, T., Shabala, L., Zhou, M., Mendham, N., and Shabala, S. (2007). Effect of secondary metabolites associated with anaerobic soil conditions on ion fluxes and electrophysiology in barley roots. *Plant Physiol.* 145, 266–276. doi: 10.1104/pp.107.102624
- Passardi, F., Tognoli, M., De Meyer, M., Penel, C., and Dunand, C. (2006). Two cell wall associated peroxidases from *Arabidopsis* influence root elongation. *Planta* 223, 965–974. doi: 10.1007/s00425-005-0153-4
- Politycka, B. (1998). Phenolics and the activities of phenylalanine ammonia-lyase, phenol- β -glucosyltransferase and β -glucosidase in cucumber roots as affected by phenolic allelochemicals. *Acta Physiol. Plant.* 20, 405–410. doi: 10.1007/s11738-998-0027-z
- Pucciariello, C., Parlanti, S., Banti, V., Novi, G., and Perata, P. (2012). Reactive oxygen species-driven transcription in *Arabidopsis* under oxygen deprivation. *Plant Physiol.* 159, 184–196. doi: 10.1104/pp.111.191122
- Qi, X. H., Xu, X. W., Lin, X. J., Zhang, W. J., and Chen, X. H. (2012). Identification of differentially expressed genes in cucumber (*Cucumis sativus* L.) root under waterlogging stress by digital gene expression profile. *Genomics* 99, 160–168. doi: 10.1016/j.ygeno.2011.12.008
- Qi, X., Chen, R., Xu, Q., and Chen, X. (2011). Preliminary analysis of cucumber submergence tolerance at seedling stage. *China Vegetables* 4, 7.
- Rigal, A., Yordanov, Y. S., Perrone, I., Karlberg, A., Tisserant, E., Bellini, C., et al. (2012). The AINTEGUMENTA LIKE1 homeotic transcription factor PtAIL1 controls the formation of adventitious root primordia in poplar. *Plant Physiol.* 160, 1996–2006. doi: 10.1104/pp.112.204453
- Sairam, R. K., Dharmar, K., Chinnusamy, V., and Meena, R. C. (2009). Waterlogging-induced increase in sugar mobilization, fermentation, and related gene expression in the roots of mung bean (*Vigna radiata*). *J. Plant Physiol.* 166, 602–616. doi: 10.1016/j.jplph.2008.09.005
- Sanders, P. M., Lee, P. Y., Biesgen, C., Boone, J. D., Beals, T. P., Weiler, E. W., et al. (2000). The *Arabidopsis* DE-LAYED DEHISCENCE1 gene encodes an enzyme in the jasmonic acid synthesis pathway. *Plant Cell* 12, 1041–1061. doi: 10.1105/tpc.12.7.1041
- Sasidharan, R., and Voesenek, L. A. (2015). Ethylene-mediated acclimations to flooding stress. *Plant Physiol.* 169, 3–12. doi: 10.1104/pp.15.00387
- Sauter, M. (2013). Root responses to flooding. *Curr. Opin. Plant Biol.* 16, 282–286. doi: 10.1016/j.pbi.2013.03.013
- Shimamura, S., Yoshioka, T., Yamamoto, R., Hiraga, S., Nakamura, T., Shimada, S., et al. (2014). Role of abscisic acid in flood-induced secondary aerenchyma formation in soybean (*Glycine max*) hypocotyls. *Plant Prod. Sci.* 17, 131–137. doi: 10.1626/pps.17.131
- Steffens, B., Geske, T., and Sauter, M. (2011). Aerenchyma formation in the rice stem and its promotion by H_2O_2 . *New Phytol.* 190, 369–378. doi: 10.1111/j.1469-8137.2010.03496.x

- Steffens, B., Wang, J., and Sauter, M. (2006). Interactions between ethylene, gibberellin and abscisic acid regulate emergence and growth rate of adventitious roots in deepwater rice. *Planta* 223, 604–612. doi: 10.1007/s00425-005-0111-1
- Sorin, C., Bussell, J. D., Camus, I., Ljung, K., Kowalczyk, M., Geiss, G., et al. (2005). Auxin and light control of adventitious rooting in *Arabidopsis* require ARGONAUTE1. *Plant Cell* 17, 1343–1359. doi: 10.1105/tpc.105.031625
- Tanaka, M., Kikuchi, A., and Kamada, H. (2008). The *Arabidopsis* histone deacetylases HDA6 and HDA19 contribute to the repression of embryonic properties after germination. *Plant Physiol.* 146, 149–161. doi: 10.1104/pp.107.111674
- Taramino, G., Sauer, M., Stauffer, J. L., Multani, D., Niu, X., Sakai, H. et al. (2007). The maize (*Zea mays* L.) RTCS gene encodes a LOB domain protein that is a key regulator of embryonic seminal and post-embryonic shoot-borne root initiation. *Plant J.* 50, 649–659. doi: 10.1111/j.1365-313X.2007.03075.x
- van Veen, H., Akman, M., Jamar, D. C. L., Vreugdenhil, D., Kooiker, M., van Tienderen, P., et al. (2014). Group VII ethylene response factor diversification and regulation in four species from flood-prone environments. *Plant Cell Environ.* 37, 2421–2432. doi: 10.1111/pce.12302
- Vidoz, M. L., Loreti, E., Mensuali, A., Alpi, A., and Perata, P. (2010). Hormonal interplay during adventitious root formation in flooded tomato plants. *Plant J.* 63, 551–562. doi: 10.1111/j.1365-313X.2010.04262.x
- Voesenek, L. A., and Bailey-Serres, J. (2015). Flood adaptive traits and processes: an overview. *New Phytol.* 206, 57–73. doi: 10.1111/nph.13209
- Vogel, C., and Marcotte, E. M. (2012). Insights into the regulation of protein abundance from proteomic and transcriptomic analyses. *Nat. Rev. Genet.* 13, 227–232. doi: 10.1038/nrg3185
- von Malek, B., van der Graaff, E., Schneitz, K., and Keller, B. (2002). The *Arabidopsis* male-sterile mutant dde2-2 is defective in the ALLENE OXIDE SYNTHASE gene encoding one of the key enzymes of the jasmonic acid biosynthesis pathway. *Planta* 216, 187–192. doi: 10.1007/s00425-002-0906-2
- Waters, I., Morell, S., Greenway, H., and Colmer, T. D. (1991). Effects of anoxia on wheat seedlings. Influence of O₂ supply prior to anoxia on tolerance to anoxia, alcoholic fermentation, and sugar levels. *J. Exp. Bot.* 42, 1437–1447. doi: 10.1093/jxb/42.11.1437
- Xu, X., Wang, H., Qi, X., Xu, Q., and Chen, X. (2014). Waterlogging-induced increase in fermentation and related gene expression in the root of cucumber (*Cucumis sativus* L.). *Sci. Hortic.* 179, 388–395. doi: 10.1016/j.scienta.2014.10.001
- Xu, X. W., Ji, J., Lu, L., Qi, X. H., and Chen, X. H. (2016). Cloning and expression analysis of *Cucumis sativus* calcium-dependent protein kinase 5 gene (*CsCDPK5*) under waterlogging stress. *Acta Hortic. Sin.* 43, 704–714. doi: 10.16420/j.issn.0513-353x.2015-0851
- Yamauchi, T., Abe, F., Kawaguchi, K., Oyanagi, A., and Nakazono, M. (2014). Adventitious roots of wheat seedlings that emerge in oxygen-deficient conditions have increased root diameters with highly developed lysigenous aerenchyma. *Plant Signal. Behav.* 9:e28506. doi: 10.4161/psb.28506
- Yang, L.-T., Qi, Y.-P., Lu, Y.-B., Guo, P., Sang, W., Feng, H., et al. (2013). iTRAQ protein profile analysis of *Citrus sinensis* roots in response to long-term boron-deficiency. *J. Proteomics* 93, 179–206. doi: 10.1016/j.jprot.2013.04.025
- Yang, S. F., and Hofman, N. E. (1984). Ethylene biosynthesis and its regulation in higher plants. *Annu. Rev. Plant Physiol.* 35, 155–189. doi: 10.1146/annurev.pp.35.060184.001103
- Yang, S. F., and Oetiker, J. H. (1994). The role of ethylene in fruit ripening. *Postharvest Physiol. Fruits* 398, 167–178. doi: 10.17660/ActaHortic.1995.398.17
- Yoo, E. J., Chung, J. J., Choe, S. S., Kim, K. H., and Kim, J. B. (2006). Down-regulation of histone deacetylases stimulates adipocyte differentiation. *J. Biol. Chem.* 281, 6608–6615. doi: 10.1074/jbc.M508982200
- Yu, F., Han, X., Geng, C., Zhao, Y., Zhang, Z., and Qiu, F. (2015). Comparative proteomic analysis revealing the complex network associated with waterlogging stress in maize (*Zea mays* L.) seedling root cells. *Proteomics* 15, 135–147. doi: 10.1002/pmic.201400156

Conflict of Interest Statement: The authors declare that the research was conducted in the absence of any commercial or financial relationships that could be construed as a potential conflict of interest.

Copyright © 2016 Xu, Ji, Ma, Xu, Qi and Chen. This is an open-access article distributed under the terms of the Creative Commons Attribution License (CC BY). The use, distribution or reproduction in other forums is permitted, provided the original author(s) or licensor are credited and that the original publication in this journal is cited, in accordance with accepted academic practice. No use, distribution or reproduction is permitted which does not comply with these terms.



Proteomic Analysis Reveals the Positive Roles of the Plant-Growth-Promoting Rhizobacterium NSY50 in the Response of Cucumber Roots to *Fusarium oxysporum* f. sp. *cucumerinum* Inoculation

OPEN ACCESS

Edited by:

Jie Zhou,

Zhejiang University, China

Reviewed by:

Yuan Huang,

Huazhong Agricultural University,
China

***Correspondence:**

Shirong Guo

srguo@njau.edu.cn

[†]These authors have contributed
equally to this work.

Specialty section:

This article was submitted to

Plant Biotic Interactions,

a section of the journal

Frontiers in Plant Science

Received: 26 September 2016

Accepted: 25 November 2016

Published: 14 December 2016

Citation:

Du N, Shi L, Yuan Y, Li B, Shu S, Sun J and Guo S (2016) Proteomic Analysis Reveals the Positive Roles of the Plant-Growth-Promoting Rhizobacterium NSY50 in the Response of Cucumber Roots to *Fusarium oxysporum* f. sp. *cucumerinum* Inoculation. *Front. Plant Sci.* 7:1859.
doi: 10.3389/fpls.2016.01859

Nanshan Du^{1†}, Lu Shi^{1†}, Yinghui Yuan¹, Bin Li², Sheng Shu^{1,3}, Jin Sun^{1,3} and Shirong Guo^{1,3*}

¹ Key Laboratory of Southern Vegetable Crop Genetic Improvement in Ministry of Agriculture, College of Horticulture, Nanjing Agricultural University, Nanjing, China, ² Department of Horticulture, Shanxi Agricultural University, Taigu, China, ³ Suqian Academy of Protected Horticulture, Nanjing Agricultural University, Suqian, China

Plant-growth-promoting rhizobacteria (PGPR) can both improve plant growth and enhance plant resistance against a variety of environmental stresses. To investigate the mechanisms that PGPR use to protect plants under pathogenic attack, transmission electron microscopy analysis and a proteomic approach were designed to test the effects of the new potential PGPR strain *Paenibacillus polymyxa* NSY50 on cucumber seedling roots after they were inoculated with the destructive phytopathogen *Fusarium oxysporum* f. sp. *cucumerinum* (FOC). NSY50 could apparently mitigate the injury caused by the FOC infection and maintain the stability of cell structures. The two-dimensional electrophoresis (2-DE) approach in conjunction with MALDI-TOF/TOF analysis revealed a total of 56 proteins that were differentially expressed in response to NSY50 and/or FOC. The application of NSY50 up-regulated most of the identified proteins that were involved in carbohydrate metabolism and amino acid metabolism under normal conditions, which implied that both energy generation and the production of amino acids were enhanced, thereby ensuring an adequate supply of amino acids for the synthesis of new proteins in cucumber seedlings to promote plant growth. Inoculation with FOC inhibited most of the proteins related to carbohydrate and energy metabolism and to protein metabolism. The combined inoculation treatment (NSY50+FOC) accumulated abundant proteins involved in defense mechanisms against oxidation and detoxification as well as carbohydrate metabolism, which might play important roles in preventing pathogens from attacking. Meanwhile, western blotting was used to analyze the accumulation of enolase (ENO) and S-adenosylmethionine synthase (SAMs). NSY50 further increased the expression of

ENO and SAMs under FOC stress. In addition, NSY50 adjusted the transcription levels of genes related to those proteins. Taken together, these results suggest that *P. polymyxa* NSY50 may promote plant growth and alleviate FOC-induced damage by improving the metabolism and activation of defense-related proteins in cucumber roots.

Keywords: cucumber, *Fusarium oxysporum* f. sp. *cucumerinum*, plant-growth-promoting rhizobacteria, proteomics, root

INTRODUCTION

Cucumber (*Cucumis sativus* L.) is an important and popular vegetable cash crop that is consumed worldwide. However, the production of this plant is severely threatened by cucumber *Fusarium* wilt, which is caused by the soilborne fungal pathogen *Fusarium oxysporum* f. sp. *cucumerinum* (FOC), a destructive vascular disease that can cause plant death and serious economic loss (Ahn et al., 1998; Huang et al., 2012). Because there are no available effective chemical products or resistant varieties and because grafting is time consuming (Chung et al., 2008; Cao et al., 2012), other effective, economical, and environmentally friendly cultivation methods have been developed and tested.

To date, alternative methods, such as biological control agents, have been shown to be effective and have been increasingly applied in the field (Yang et al., 2010; Li et al., 2012; Lin et al., 2014; Xu et al., 2014). Among these methods, some beneficial bacteria inhabiting the plant rhizosphere, called plant growth-promoting rhizobacteria (PGPR), are directly or indirectly involved in promoting plant growth and the biological control of plant diseases (Klopper and Metting, 1992). A variety of mechanisms have been confirmed to improve plant health and increase crop productivity for those strains, such as synthesizing different antimicrobial compounds (Tamehiro et al., 2002; Ongena et al., 2007; Chen et al., 2014), various hormones (Bottini et al., 2004; Martínez-Viveros et al., 2010; Kocher et al., 2011), increasing the availability of plant nutrients in the rhizosphere (Idriss et al., 2002; Palacios et al., 2014), and inducing systemic resistance in host plants (Niu et al., 2011; Jiang et al., 2015).

Numerous technical methods, such as DNA microarray technology and proteomic analysis, have been applied to improve our understanding of plant-PGPR interactions. A study in the *Arabidopsis* root transcriptome showed that extensive changes were induced in hormone- and defense-related genes after exposure to *Azospirillum brasilense* Sp245 (Spaepen et al., 2014). In another study, the ISR- and iron acquisition-related transcription factors in *Arabidopsis* roots were activated by *Pseudomonas fluorescens* WCS417 and its volatiles (Zamioudis et al., 2015). A dynamic protein network was designed to explain the mechanism of *P. putida* UW4 to release hypoxic stress and promote cucumber growth (Li et al., 2013b). Proteins involved in growth promotion and defense reactions were significantly induced in *Arabidopsis* following inoculation with *Paenibacillus polymyxa* E681 (Kwon et al., 2016). In addition, many other researchers have used proteomics to investigate plant-pathogen interactions. Wang et al. (2011) found that a switch from glycolysis to the pentose phosphate pathway may be an active response of the cotton plant against *V. dahliae* infection to

enhance wilt tolerance or resistance. Total root protein was isolated from infected cucumber roots of the susceptible bulk and resistant bulk of cucumber generation F2, and the result showed that jasmonic acid and redox signaling components occurred in response to *F. oxysporum* infection in resistant plants (Zhang et al., 2016). Eighty-six differentially expressed proteins were identified from the leaves of resistant tomato cultivar "Zheza-301" and susceptible cultivar "Jinpeng-1" after TYLCV infection, which demonstrated that an interaction network between tomato leaves and TYLCV infection was established (Huang et al., 2016). To date, although several papers have addressed the use of proteomics to investigate the interactions of plants and pathogens (Konishi et al., 2001; Wang et al., 2011; Carrillo et al., 2014) or plants and PGPR (Kandasamy et al., 2009; Wang et al., 2013), little research is available on the effects of PGPB on cucumber plants under pathogenic attack.

In this present study, a promising bio-control agent *Paenibacillus polymyxa*-NSY50, which was originally isolated from the high suppression capacity of compost (Du et al., 2015; Shi et al., 2016), was used to better understand direct or indirect interactions among *P. polymyxa* NSY50, the pathogen FOC and cucumber roots. A total of 56 proteins were identified that were up- or down-regulated by the inoculation of *P. polymyxa* NSY50 and/or FOC, and the proteins could be classified into multiple biological functions. This work provides key insights into the promotion mechanisms of *P. polymyxa* NSY50 action to determine the optimal use of this beneficial PGPR in sustainable agricultural practices.

MATERIAL AND METHODS

Plant Material, Microbial Culture Conditions, and Treatments

Cucumber (*Cucumis sativus* L. cv. Jinchun No. 2) seeds were sown in quartz sand and cultivated in a greenhouse. *Paenibacillus polymyxa*-NSY50 was grown on LB medium at 28°C for 3 days, and the cucumber Fusarium wilt pathogen *F. oxysporum* f. sp. *cucumerinum* (FOC) was incubated in PDA liquid culture for 7 days.

At the two true leaves stage, the cucumber seedlings were transplanted to tanks containing half-strength Hoagland nutrient solution (He et al., 2015). After 3 days of pre-culture, the seedlings were treated as follows: (1) control, control plants were grown in Hoagland's solution; (2) NSY50, seedlings grown in Hoagland nutrient solution containing 500-mL 1.0×10^8 NSY50 cell suspension; (3) FOC: 500 mL of a cell suspension of FOC at 1×10^7 conidia/mL was poured into the tanks after 6 days

of culture; and (4) NSY50+FOC: plants were inoculated with 500 mL of NSY50 (1×10^8 CFU/mL) after 3 days of culture, and 3 days later, the plants were challenge-inoculated with 500 mL of a cell suspension of FOC (1×10^7 conidia/mL). The experiment was arranged in a randomized complete block design with three replicates for each treatment, which resulted in a total of 36 seedlings per treatment. Seedlings were reared in a greenhouse at 25–30°C in the daytime and at 15–18°C at night under natural lighting at 60–75% relative humidity.

Plant Growth Analysis

After 9 days of FOC treatment, shoot, and root were separated from one another and measured after being washed with sterile distilled water. The plant height, biomass, and volume of root in each treatment were measured as previously described (Shi et al., 2016). Each data point was the average of measurements collected in triplicate.

TEM Analysis

For transmission electron microscopy, roots of seedlings from different treatments were excised and immediately cut into small segments (1~2 mm, including the tip); The samples were then fixed with 2.5% glutaraldehyde in 0.1 M phosphate buffer (pH 7.4) for 24 h (primary fixation) and immersed in 2% osmic acid in the same buffer for 2 h (second fixation). After dehydration in acetone and embedding in Durcupan ACM (Fluka), the resulting roots were cut to obtain ultra-thin sections, stained with uranium acetate and lead citrate in series and examined using a HITACHI transmission electron microscope (Carl Zeiss, Göttingen, Germany) at an accelerating voltage of 80 kV.

Protein Extraction

The cucumber roots were prepared for protein fractionation 3 days post-inoculation of FOC. Total protein extraction was performed using a trichloroacetic acid, i.e., the acetone precipitation method modified described by Hurkman and Tanaka (1986). Fresh root samples (2 g) were milled with liquid nitrogen and suspended in extraction buffer as described by An et al. (2016). The homogenate was centrifuged at 15,000 g at 4°C for 20 min. An aliquot (1 mL) of the resulting supernatant was transferred to a new tube and precipitated with ice-cold acetone (10% TCA and 0.07% β-mercaptoethanol) overnight at –20°C, and then the resulting protein sample was centrifuged at 20,000 g for 25 min. The pellet was washed three times with cold acetone (0.07% β-mercaptoethanol) and allowed to stand at –20°C for 2 h. Finally, the protein pellet was air-dried and used for 2-DE.

2-DE and Image Analysis

Isoelectric focusing (IEF) was performed using an 18-cm IPG linear gradient strip, pH 4–7 (GE Healthcare, San Francisco, USA). The dried protein pellet was rehydrated in a rehydration buffer that contained 7 M urea, 2 M thiourea, 4% 3-[*(3-cholamidopropyl) dimethylammonio]-1-propanesulfonic acid (w/v), 40 mM DTT, 0.5% (v/v) IPG buffer 4–7 and 0.01% (w/v) bromophenol blue. The protein levels were quantified using the Bradford method (Bradford, 1976). The 350 μL protein samples*

were loaded on IPG strips containing 800 μg of protein and rehydrated for 12–16 h at 25°C. After rehydration, the IPG strips were run on an Ettan IPGphor 3 (GE Healthcare, San Francisco, USA) using the following protocol: the voltage for IEF was set at 100 V for 1 h, followed by 200 V for 1 h, 200 V for 1 h, 500 V for 1 h, 1000 V for 1 h, 4000 V for 1 h, a gradient of 10,000 V for 1 h, and then a 10,000 V rapid focus, which reached a total of 75,000 V h with a maximum electric current of 50 μA per strip. After accomplishing the first dimension, IEF strips were equilibrated for 15 min in a 2D equilibrium buffer that consisted of 6 M urea, 30% glycerol (v/v), 50 mM Tris-HCl (pH 8.8), and 2% sodium dodecyl sulfate (SDS) containing 1% DTT (w/v); the strips were then incubated in 2.5% (w/v) iodoacetamide instead of DTT for 15 min. Then, the strips were placed directly onto 12.5% polyacrylamide-SDS slab gels and sealed using 1% molten agarose solution. The second dimensional separation was conducted using the EttanDalySix electrophoresis system (GE Healthcare, USA). At 15 mA per gel, the electrophoresis was not stopped until the bromophenol blue dye reached approximately 1 cm from the bottom of the gel. Protein spots were visualized using Coomassie Brilliant Blue (CBB) R-250.

The CBB-stained 2-DE gels were scanned using an Image scanner III (GE Healthcare, USA). The digitized images of three independent experiments were analyzed with Imagemaster 2D Platinum version 5.0 (GE Healthcare, USA). The abundance of each protein spot was estimated by the percentage volume (vol.%), and the spot volumes were normalized as the ratio of the total volume for all of the spots that were present. Spots with a vol.% that represented at least a 1.5-fold change and was significant at the $P < 0.05$ level (Duncan's multiple range tests) were used for identification.

Protein Identification and Functional Classification

The differentially expressed protein spots were extracted from CBB-stained preparative polyacrylamide gels and then identified using an ABI 5800 Proteomics Analyzer MALDI-TOF/TOF (Applied Biosystems, Foster City, CA, USA). The data lists were used as a query to search in the NCBI (<http://www.ncbi.nlm.nih.gov/>) and cucumber genomics databases (<http://cucumber.genomics.org.cn>) using the software MASCOT version 2.2 (Matrix Science, London, UK). The following search parameter criteria were used: trypsin cleavage, one missed cleavage site allowed; carbamidomethyl set as a fixed modification; oxidation of methionines allowed as a variable modification; a peptide mass tolerance within 100 ppm; fragment tolerance set to ± 0.4 Da; and a minimum ion score confidence interval for MS/MS data set to 95%.

Identified proteins were categorized according to the biological processes with which they were involved based on Gene Ontology (GO) (<http://www.geneontology.org/>) and the Uniprot Protein Knowledgebase (<http://www.uniprot.org/>). Hierarchical clustering of the protein expression patterns was performed on the log-transformed (using log base 2) spot abundance ratios using the software Cluster version 3.0. A heat map was created using Java Treeview.

Western Blot Analysis

Root tissues were milled in a mortar with ice-cold extraction buffer containing 30 mM Tris-HCl (pH 8.7), 1 mM MgCl₂, 0.7 M sucrose, 1 mM EDTA, 1 mM DTT, 1 mM PMSF, and 1 mM ascorbic acid. The extracted protein was quantified using the Bradford method (1976), denatured at 95°C for 3–5 min and then stored at –20°C until analysis.

For western blot analysis, SDS-polyacrylamide gel electrophoresis (SDS-PAGE) was conducted using the methods of Laemmli (1970). Briefly, 11 µg protein samples were transferred to a 0.45 µm PVDF membrane at 10 V for 1.5 h and were washed with TBST three times; then, the PVDF membrane was blocked with 5% nonfat dry milk for 2 h, washed with TBST three times, and incubated with monoclonal antibodies against S-adenosylmethionine synthase and enolase (produced in rabbit; Univ-bio, Shanghai, China) for 2 h. The membrane was washed with TBST and incubated at room temperature for 1 h with a Goat Anti-Rabbit IgG HRP-conjugate. The membrane was then washed with TBST three times and developed using diaminobenzidine (DAB) and H₂O₂ (He et al., 2012).

Total RNA Extraction and Quantitative Real-Time PCR (qRT-PCR) Analysis

Root tissues were harvested at 1, 3, 9 days after inoculation with FOC. The total RNA was extracted according to the TRI reagent protocol (Takara Bio Inc.) and then converted into cDNA following the manufacturer's instructions. Primers were designed based on the sequences obtained from NCBI using Beacon Designer 7.90 (Supplementary Table 1). qRT-PCR was performed using the SYBR PrimeScript™ RT-PCR Kit (Takara Bio Inc.) in accordance with the manufacturer's instructions and run on a StepOne™ real-time PCR system (Applied Biosystems, Singapore). The relative gene expression was calculated using the 2^{–ΔΔCt} method (Livak and Schmittgen, 2001), and the methods were based on a previously described protocol (Shi et al., 2016). All reactions were conducted with three biological replicates.

Statistical Analysis

All data were statistically analyzed using SPSS 20.0 for Windows, and significance was assigned at the $P < 0.05$ level using Duncan's multiple comparisons test.

RESULTS

Plant Growth

The biomass of the cucumber seedlings was measured 9 days post-inoculation (dpi) with the pathogen. The plant height, shoot freshness and dry mass of NSY50-treated seedlings were significantly greater than those of plants grown under control conditions (Table 1). However, pathogen inoculation (treatment FOC) seriously decreased the growth of the cucumber seedlings, the plant height, shoot fresh weight, dry weight and root volume and the root fresh weight and dry weight, which were significantly suppressed compared to the control. Moreover, under pathogen stress, plant biomass

was significantly higher in *P. polymyxa* NSY50 pre-treated cucumber plants, which showed a 1.2–1.5-fold up-regulation in plant growth compared to untreated plants. Thus, the results clearly indicated that the pathogen inoculation inhibited growth in cucumber seedlings and that *P. polymyxa* NSY50 can release at least a portion of the stress and promote plant growth.

Ultrastructure of the Roots

Under control conditions, the vacuoles had small sizes, and many nuclei and mitochondria could be seen clearly under the microscope (Figure 1). The cellular ultrastructure of cucumber roots seemed to show no difference between the control plants and plants treated with NSY50 alone (NSY50). However, the inoculation of FOC (FOC) caused remarkable structural changes. Specifically, the karyotheca appeared to have contracted, and the number of the mitochondria decreased compared to the control. Furthermore, the number of central vacuoles and autophagosomes appeared to indicate that the pathogen attack advanced the cell aging and death process. Pre-treatment with NSY50 (NSY50+FOC) apparently enhanced the stability of the cell structure.

Identification and Functional Classification of Proteins

Approximately 350 reproducible protein spots were detected on the 2-DE gels, and 56 differentially expressed protein spots (changes ≥ 1.5 -fold) were successfully identified by MALDI-TOF/TOF MS (Figure 2; Supplementary Figure 1). These differentially expressed proteins are listed in Table 2.

The identified proteins were grouped into seven different categories on the basis of biological processes to which they were related according to the Gene Ontology and Uniprot Protein Knowledgebase (Figure 3A). The categories with a high level of expression variation included the defense response (28.6%), protein metabolism (25.0%), carbohydrate and energy metabolism (19.6%) and amino acid metabolism (17.9%). Among the 56 differentially expressed spots, 44 protein spots were significantly regulated by the pathogen FOC compared to the control (Figure 3B), and there were 16 up-regulated spots and 28 down-regulated spots (Figure 3C). The defense-response-related proteins had the highest up-regulation rate, and the decreased proteins were involved in protein metabolism (10 spots), carbohydrate, and energy metabolism (7 spots), and amino acid metabolism (7 spots). Additionally, 32 protein spots were significantly induced by NSY50 inoculation compared to the control (Figure 3B). Of those spots, 25 were up-regulated, and seven were down-regulated. The defense-response-related proteins (10 spots) and amino acid metabolism (5 spots) were the most highly enriched categories (Figure 3C). However, compared to FOC, 33 proteins had changes, including 24 proteins that increased and 9 proteins that decreased after pre-treatment with NSY50 (NSY50+FOC). The category of carbohydrate and energy metabolism had the highest up-regulation rate, whereas the decreased proteins were distributed among the defense response,

TABLE 1 | Effects of plant-growth-promoting bacteria on the growth of cucumber seedlings under Fusarium wilt stress.

Treatment	Plant height (cm)	Shoot fresh mass (g/plant)	Shoot dry mass (g/plant)	Root fresh mass (g/plant)	Root dry mass (g/plant)	Root volume (cm ³)
Control	20.97 ± 1.87b	10.08 ± 0.40b	0.77 ± 0.07b	2.82 ± 0.10a	0.15 ± 0.009a	2.14 ± 0.20a
NSY50	26.07 ± 1.01a	14.23 ± 0.47a	0.96 ± 0.02a	2.78 ± 0.15a	0.13 ± 0.006ab	2.05 ± 0.09a
FOC	16.53 ± 1.26c	7.16 ± 0.96c	0.45 ± 0.05c	1.53 ± 0.12c	0.08 ± 0.013c	1.17 ± 0.09c
NSY50+FOC	19.07 ± 1.07b	9.37 ± 0.94b	0.63 ± 0.05b	2.28 ± 0.18b	0.11 ± 0.009b	1.59 ± 0.10bc

Each value is the mean ± SE of three replicates. Different letters indicate significant differences at $P < 0.05$ according to Duncan's multiple range tests. Control, seedlings cultured in normal nutrient solution; NSY50, control+ *P. polymyxa* NSY50 (2.5×10^6 CFU/mL); FOC, control+ FOC (2.5×10^5 conidia/mL); NSY50+FOC, pre-treated with NSY50 (2.5×10^6 CFU/mL) for 3 days, then challenged with FOC (2.5×10^5 conidia/mL).

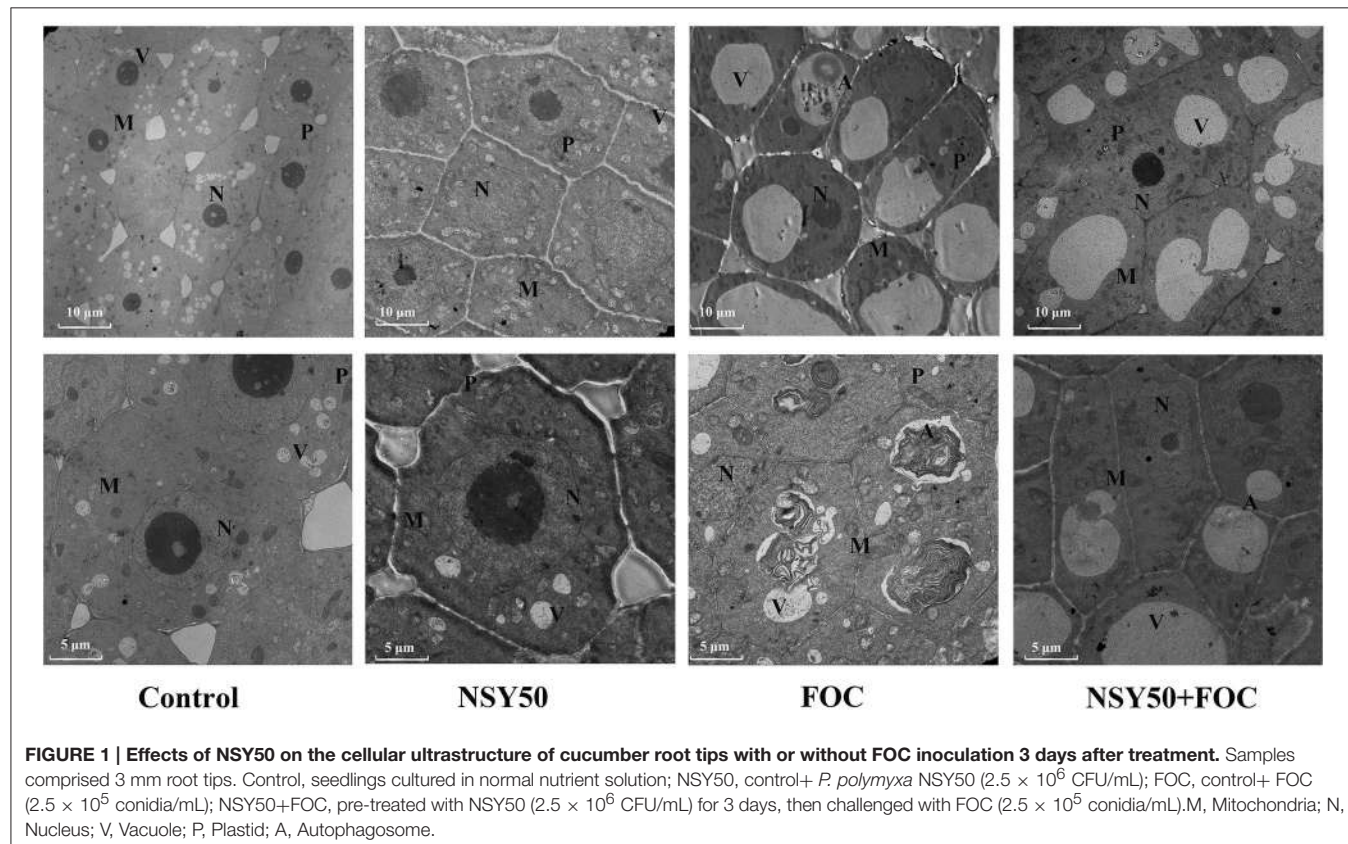


FIGURE 1 | Effects of NSY50 on the cellular ultrastructure of cucumber root tips with or without FOC inoculation 3 days after treatment. Samples comprised 3 mm root tips. Control, seedlings cultured in normal nutrient solution; NSY50, control+ *P. polymyxa* NSY50 (2.5×10^6 CFU/mL); FOC, control+ FOC (2.5×10^5 conidia/mL); NSY50+FOC, pre-treated with NSY50 (2.5×10^6 CFU/mL) for 3 days, then challenged with FOC (2.5×10^5 conidia/mL). M, Mitochondria; N, Nucleus; V, Vacuole; P, Plastid; A, Autophagosome.

protein metabolism, secondary metabolism and cell-related protein categories (Figure 3C).

Clustering Analysis of Differentially Expressed Proteins

To acquire a comprehensive overview of the differentially expressed proteins that were affected by NSY50 under control conditions and FOC stress, hierarchical clustering was performed, and proteins with similar expression patterns were grouped together (Figure 4). Cluster A consisted of 4 proteins (spots 9, 6, 13, and 10) that were up-regulated by NSY50, down-regulated after inoculation with FOC compared to the control, but recovered by the application of NSY50 (NSY50+FOC). Cluster B was composed of 23 proteins that decreased considerably under FOC stress

with/without NSY50 inoculation. Most of the identified proteins in this cluster were involved in protein metabolism, carbohydrate and energy metabolism. Cluster C involved 7 proteins that were up-regulated by NSY50 under both control conditions and FOC stress conditions, and these proteins corresponded to defense responses, carbohydrate and energy metabolism, amino acid metabolism, and protein metabolism. Cluster D included 10 proteins that were down-regulated by NSY50 but up-regulated by the inoculation of FOC. Most of these proteins were involved in defense responses. Cluster E contained 4 proteins that were down-regulated by NSY50 but up-regulated by the inoculation of FOC, regardless of whether they were pre-inoculated with NSY50. Cluster F included 8 proteins that increased in abundance when inoculated with NSY50 or FOC alone

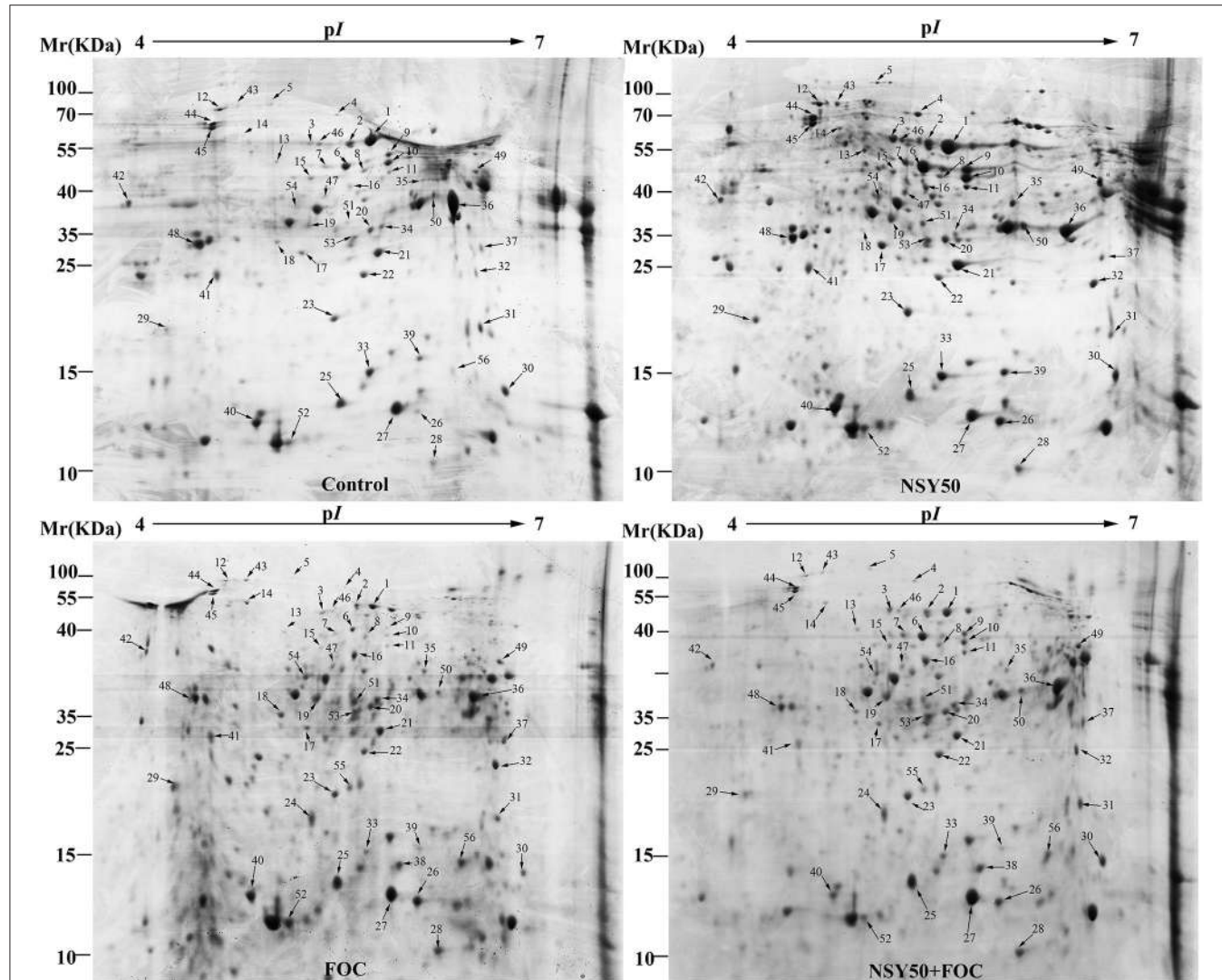


FIGURE 2 | Representative 2-DE gel images of total protein extracts from root samples inoculated with NSY50 and/or FOC. An equal amount ($800\text{ }\mu\text{g}$) of total proteins were separated by IEF/SDS-PAGE and then stained with Coomassie Brilliant Blue (R-250) and loaded on each 18 cm gel strip (pH 4–7, linear). The numbers for the 56 differentially expressed proteins are marked and annotated according to the numbering in **Table 2**. Control, seedlings cultured in normal nutrient solution; NSY50, control+ *P. polymyxa* NSY50 (2.5×10^6 CFU/mL); FOC, control+ FOC (2.5×10^5 conidia/mL); NSY50+FOC, pre-treated with NSY50 (2.5×10^6 CFU/mL) for 3 days then challenged with FOC (2.5×10^5 conidia/mL).

but were down-regulated in combined inoculation treatment (NSY50+FOC).

Validation of Differentially Expressed Proteins

As shown in **Table 2**, five differentially expressed protein spots belonging to ENO and eight SAMs protein spots were successfully identified by MALDI-TOF/TOF MS, and they were all significantly regulated by inoculation with NSY50 and/or FOC. This outcome indicated that ENO and SAMs were considered important plant proteins for coping with pathogen invasion. Therefore, ENO and SAMs were analyzed by western blotting to verify the proteomic data. The result showed a similar tendency, in that the expression of ENO and SAMs

were slightly more highly regulated by the inoculation of NSY50 but significantly down-regulated by FOC infection compared to the control. However, the expression of both of these proteins was recovered by pre-treatment with NSY50 (NSY50+FOC) compared to FOC, regardless of whether measurements were taken 1, 3, or 9 days post-inoculation with FOC (**Figures 5A,C**; Supplementary Figures 2–5). Additionally, the level of SAMs was seriously decreased by FOC inoculation on the first day after inoculation (**Figure 5C**).

Expression Analysis of Several Identified Protein-Related Genes

The ENO and SAMs gene expression levels were then analyzed 1, 3, and 9 days post-inoculation. FOC up-regulated both proteins

TABLE 2 | Root proteins responsive to NSY50 and/or FOC identified by MALDI-TOF/TOF MS.

Spot no. ^a	Protein name	NCBI Accession no.	Mr(kDa)/PI		MP ^b	Score	Cov ^c (%)	Ratio ^d							
			Theoretical	Experimental				Control/Control	NSY50/Control	FOC/Control	NSY50+/FOC/FOC				
CARBOHYDRATE AND ENERGY METABOLISM (11)															
Glycolysis															
1	Enolase isoform X2	gi 778717375	43.13/5.80	60.0/5.78	6	202	26.13	1.00	0.94	0.18	1.55				
2	Enolase isoform X2	gi 778717375	43.13/5.80	61.25/5.67	15	326	59.30	1.00	0.70	0.37	1.51				
13	Protein DJ-1 homolog D	gi 449469102	42.40/5.12	53.0/5.30	10	187	37.95	1.00	2.28	0.21	4.25				
17	Enolase isoform X1	gi 449451102	47.84/5.48	33.0/5.42	17	427	34.91	1.00	0.94	0.18	4.05				
18	Enolase isoform X1	gi 449451102	47.94/5.48	33.0/5.42	2	137	5.18	1.00	0.57	1.27	0.45				
20	Probable fructokinase-4	gi 449454574	35.79/5.62	36.75/5.48	21	531	61.63	1.00	1.18	0.60	1.36				
46	Enolase isoform X2	gi 778717375	43.13/5.80	60.75/5.51	14	292	49.50	1.00	2.58	0.86	1.66				
55	Fructose-bisphosphate aldolase, cytoplasmic isozyme-like	gi 449451108	38.73/7.57	23.50/6.65	18	293	51.96	0.00	0.00	0.15	0.62				
Tricarboxylic Acid Cycle															
36	Malate dehydrogenase, mitochondrial	gi 449438883	36.41/8.52	37.25/6.33	7	201	32.28	1.00	0.52	0.24	2.34				
Sucrose Metabolism															
43	Acid beta-fructofuranosidase-like	gi 449451749	69.80/4.92	90.25/5.11	9	17	15.56	1.00	3.25	2.57	0.61				
Energy Metabolism															
3	ATP synthase subunit beta, mitochondrial-like	gi 449465916	60.18/5.90	61.40/5.48	30	662	70.89	1.00	5.56	0.60	3.44				
PROTEIN METABOLISM (14)															
Protein Folding and Assembly															
14	Protein disulfide-isomerase	gi 449464162	57.27/4.88	65.0/5.13	19	209	53.92	1.00	1.90	2.42	0.45				
23	20 kDa chaperonin, chloroplastic	gi 778663199	26.87/7.85	27.8/5.73	9	183	43.36	1.00	1.04	0.56	1.26				
42	Protein disulfide-isomerase	gi 449464162	57.27/4.88	41.75/4.53	18	122	52.94	1.00	0.80	0.37	0.72				
44	Protein disulfide-isomerase	gi 449464162	57.27/4.88	72.0/4.97	29	622	64.12	1.00	0.75	0.42	0.87				
45	Protein disulfide-isomerase	gi 449464162	57.27/4.88	69.25/4.97	33	911	72.35	1.00	1.13	0.60	0.94				
Protein Biosynthesis															
33	Eukaryotic translation initiation factor 5A	gi 449455523	17.64/5.60	18.00/5.67	8	82	61.64	1.00	0.85	0.13	2.58				
38	Eukaryotic translation initiation factor 5A	gi 449455523	17.64/5.60	17.0/5.92	10	185	54.72	0.00	0.00	0.12	1.88				
39	Eukaryotic translation initiation factor 5A	gi 449455523	17.64/5.60	18.67/6.07	13	191	73.58	1.00	1.18	0.15	1.28				
47	Elongation factor 2	gi 778713730	95.03/5.97	41.25/5.55	13	113	19.69	1.00	2.70	1.35	0.65				
56	Eukaryotic translation initiation factor 5A-2	gi 700210064	17.77/5.59	18.0/6.28	4	104	22.50	1.00	0.00	4.26	1.36				
Protein Degradation															
22	Proteasome subunit alpha type-2-A	gi 449455401	25.63/5.51	31.0/5.83	3	74	13.44	1.00	1.48	0.44	1.54				
41	Thiol protease aleurain-like	gi 449452572	39.55/6.26	29.0/4.97	11	423	49.44	1.00	1.58	0.59	0.89				
Protein Transport															
28	Nuclear transport factor 2-like	gi 778689955	13.67/6.00	12.25/6.15	7	351	95.93	1.00	5.13	4.58	1.14				
Protein Modification															
30	Ubiquitin-conjugating enzyme E2 variant 1C	gi 449437446	16.68/6.20	17.0/6.59	16	319	85.62	1.00	1.19	0.37	2.03				

(Continued)

TABLE 2 | Continued

Spot no. ^a	Protein name	NCBI Accession no.	Mr(kDa)/PI		MP ^b	Score	Cov ^c (%)	Ratio ^d							
			Theoretical	Experimental				Control/ Control	NSY50/ Control	FOC/ Control	NSY50+ FOC/FOC				
DEFENSE RESPONSE (16)															
Antioxidant Reaction															
19	Peroxidase 2-like	gi 778693042	35.94/5.51	35.0/5.29	8	106	26.06	1.00	4.81	3.95	1.61				
21	L-ascorbate peroxidase, cytosolic-like	gi 525507192	27.55/5.43	35.25/5.77	14	318	67.87	1.00	1.55	0.57	1.01				
24	Peroxidase 2-like	gi 778693034	37.17/5.51	21.0/5.45	8	365	23.37	0.00	0.00	0.13	1.58				
25	Superoxide dismutase [Cu-Zn], chloroplastic	gi 449456060	22.72/5.87	16.0/5.59	8	557	73.09	1.00	0.59	0.63	1.51				
27	Superoxide dismutase [Cu-Zn]-like isoform X1	gi 778655163	15.48/5.43	15.4/5.90	1	137	13.82	1.00	0.69	0.89	2.01				
32	Glutathione S-transferase-like	gi 778727975	24.00/5.98	27.60/6.46	12	156	68.37	1.00	2.33	1.34	0.82				
37	Glutathione S-transferase DHAR2	gi 778700922	23.90/6.18	32.4/6.50	5	105	32.86	1.00	1.04	0.56	1.66				
50	Probable aldo-keto reductase 4	gi 778689965	37.89/5.78	37.75/6.15	21	223	61.70	1.00	2.14	0.68	2.81				
52	Thioredoxin H-type 1 isoform X2	gi 778671470	13.74/5.91	14.0/5.33	6	119	36.59	1.00	1.67	2.72	0.82				
53	Probable L-ascorbate peroxidase 6, chloroplastic isoform X2	gi 778715658	45.03/7.09	34.75/5.68	13	189	40.44	1.00	1.67	2.17	0.43				
54	Peroxidase 2-like	gi 778693034	37.17/5.51	39.74/5.40	12	273	47.04	0.00	0.03	0.11	0.78				
Other Defense Response															
4	Heat shock 70 kDa protein, mitochondrial	gi 449459554	73.25/5.69	78.5/5.61	25	269	44.12	1.00	3.31	0.37	1.45				
12	Heat shock protein 70	gi 1143427	75.48/5.15	87.75/5.02	24	300	39.04	1.00	1.26	0.75	0.52				
26	MLP-like protein 328	gi 449449064	17.66/5.65	15.0/6.04	12	347	87.42	1.00	3.23	3.68	0.85				
31	Glycine-rich protein 2	gi 778722923	20.01/6.29	21.75/6.48	5	64	45.28	1.00	0.50	0.70	0.95				
40	Major allergen Pru ar 1-like	gi 778714676	17.27/4.98	15.25/5.16	15	704	84.28	1.00	1.77	0.93	0.41				
AMINO ACID METABOLISM (10)															
6	S-adenosylmethionine synthase 2	gi 778728392	43.65/5.35	51.25/5.65	23	260	86.01	1.00	1.98	0.22	4.15				
7	S-adenosylmethionine synthase 2-like	gi 449472803	44.67/5.29	51.50/5.55	18	301	71.07	1.00	0.94	0.29	1.92				
8	S-adenosylmethionine synthase 2	gi 778728392	43.65/5.35	48.75/5.74	18	470	63.36	1.00	0.76	0.37	1.29				
9	S-adenosylmethionine synthase 4	gi 449451048	43.03/6.07	53.25/5.87	13	301	36.15	1.00	2.21	0.08	9.54				
10	S-adenosylmethionine synthase 4	gi 449451048	43.03/6.07	49.75/5.87	15	329	48.72	1.00	1.55	0.15	3.61				
11	Glutamine synthetase leaf isozyme, chloroplastic	gi 778678626	48.03/7.62	46.25/5.87	18	146	51.85	1.00	2.05	0.80	1.88				
15	S-adenosylmethionine synthase 2-like	gi 449472803	44.67/5.29	47.25/5.48	18	277	56.61	1.00	0.99	0.29	2.51				
16	S-adenosylmethionine synthase 2	gi 778728392	43.65/5.35	43.25/5.67	16	314	58.27	1.00	1.01	1.72	1.26				
35	Glutamine synthetase cytosolic isozyme-like	gi 525507210	39.42/5.82	42.5/6.07	9	71	32.02	1.00	5.96	2.27	1.24				
48	S-adenosylmethionine synthase 2-like	gi 449472803	44.67/5.29	35.20/4.88	11	137	45.14	1.00	0.65	0.47	0.74				

(Continued)

TABLE 2 | Continued

Spot no. ^a	Protein name	NCBI Accession no.	Mr(kDa)/PI		MP ^b	Score	Cov ^c (%)	Ratio ^d			
			Theoretical	Experimental				Control/ Control	NSY50/ Control	FOC/ Control	NSY50+ FOC/FOC
FATTY ACID METABOLIS (2)											
49	12-oxophytodienoate reductase 1	gi 778672814	42.31/6.17	45.80/6.47	21	252	56.12	1.00	2.68	1.33	0.96
51	Enoyl-[acyl-carrier-protein] reductase [NADH], chloroplastic-like	gi 449448774	41.67/8.64	36.50/5.66	13	446	52.94	1.00	1.10	3.08	0.99
SECONDARY METABOLISM (1)											
34	Nitrile-specifier protein 5	gi 449444472	35.62/5.30	36.25/5.82	19	206	48.46	1.00	0.54	1.43	0.64
CELL RELATED PROTEIN (2)											
5	Cell division control protein 48 homolog E	gi 449440119	90.09/5.06	102/5.30	32	274	49.75	1.00	0.72	0.20	0.92
29	Translationally-controlled tumor protein homolog	gi 449432858	18.76/4.56	22.50/4.71	9	176	67.26	1.00	1.73	4.19	0.20

^aSpot number corresponding with 2-DE gel as shown in **Figure 2**.

^bNumber of identified peptides.

^cPercentage of sequence coverage by matched peptides.

^dThe values higher than 1.5 or lower than 0.67 indicate significant changes.

at all time points compared to the control (**Figures 5B,D**). The gene expression of *ENO* after NSY50 treatment was significantly lower compared to the FOC treatment. However, SAMs showed a contrary tendency in the early stages of inoculation (**Figure 5D**), and the transcript levels in NSY50+FOC were higher and increased more rapidly compared to those of plants that were inoculated with only FOC (FO C) from 1 to 3 days post-inoculation.

Seven other genes related to the identified proteins, including *GST*, *SAMDC*, *ACS*, *ACO1*, *ACO2*, *HSP70*, and *OPR1*, were selected and subjected to expression pattern analysis. NSY50 up-regulated almost all of these genes (except *ACS* and *ACO1*) compared to the control (**Figure 6**). FOC stress up-regulated the expression of *GST*, *SAMDC* and *ACO1* but decreased the *ACS* and *ACO2* expression. The combined inoculation (NSY50+FOC) treatments up-regulated expression of almost all of these genes (except *SAMDC* and *ACS*) compared with the FOC treatment. We summarize the metabolism pathways that connect the expression of these genes, the proteins related to an antioxidant response, amino acid metabolism, and the EMP-TCA cycle in **Figure 7**.

DISCUSSION

Biological control is one of the most beneficial methods because it is both efficient and environmentally friendly for plant protection (Bargabus et al., 2003; Tjamos et al., 2005). Currently, the commercialization of bio-control agents is still limited (Szewczyk et al., 2006) due to complicated mechanisms of bio-control that have yet to be clarified (Niu et al., 2011). *Paenibacillus polymyxa* has been considered a bio-control agent for a wide range of plant pathogens (Dijksterhuis et al., 1999; Ling et al., 2011; Hong

et al., 2016). It is an important *Bacillus* species because of its ability to produce different bioactive compounds with a broad spectrum of activities or induce systemic resistance against a variety of environmental stresses (Kim et al., 2015; Zhou et al., 2016). With the goal of commercializing *P. polymyxa* NSY50 in the future, we analyzed the proteins in cucumber roots that responded to NSY50 under FOC stress conditions to investigate the promotion and protection mechanisms of NSY50. The results of our proteome analysis are discussed below.

Proteins Related to Defense

Reactive oxygen species (ROS) have been demonstrated to be involved in symbiotic interactions between plants and microorganisms (Scheler et al., 2013). During pathogen invasion, plants have always suffered from ROS and reactive aldehyde bursts, which often lead to cellular damage (Niu et al., 2011; Gupta et al., 2014; Sengupta et al., 2015; Camejo et al., 2016). Fortunately, plants have developed an antioxidant enzymatic system to scavenge for and collect these toxic compounds. In the present study, a total of 16 spots were identified as defense-related proteins, and most of them were regulated by the inoculation of NSY50 and/or FOC (**Table 2**, **Figure 3C**).

Two superoxide dismutases (SOD, spots 25, and 27) were identified and were significantly up-regulated by pre-treatment with NSY50 (NSY50+FOC) compared to FOC treatment. Three peroxidases (POD, spots 19, 24, and 54) with different subunits were identified and showed different accumulation patterns. Regardless of whether they were inoculated with NSY50 or FOC, the expression levels were both up-regulated compared to the control. Additionally, spots 19 and 24 showed expression levels in NSY50+FOC that were higher than the proteins inoculated with FOC alone. Ascorbate peroxidase (APX, spot 21) was also

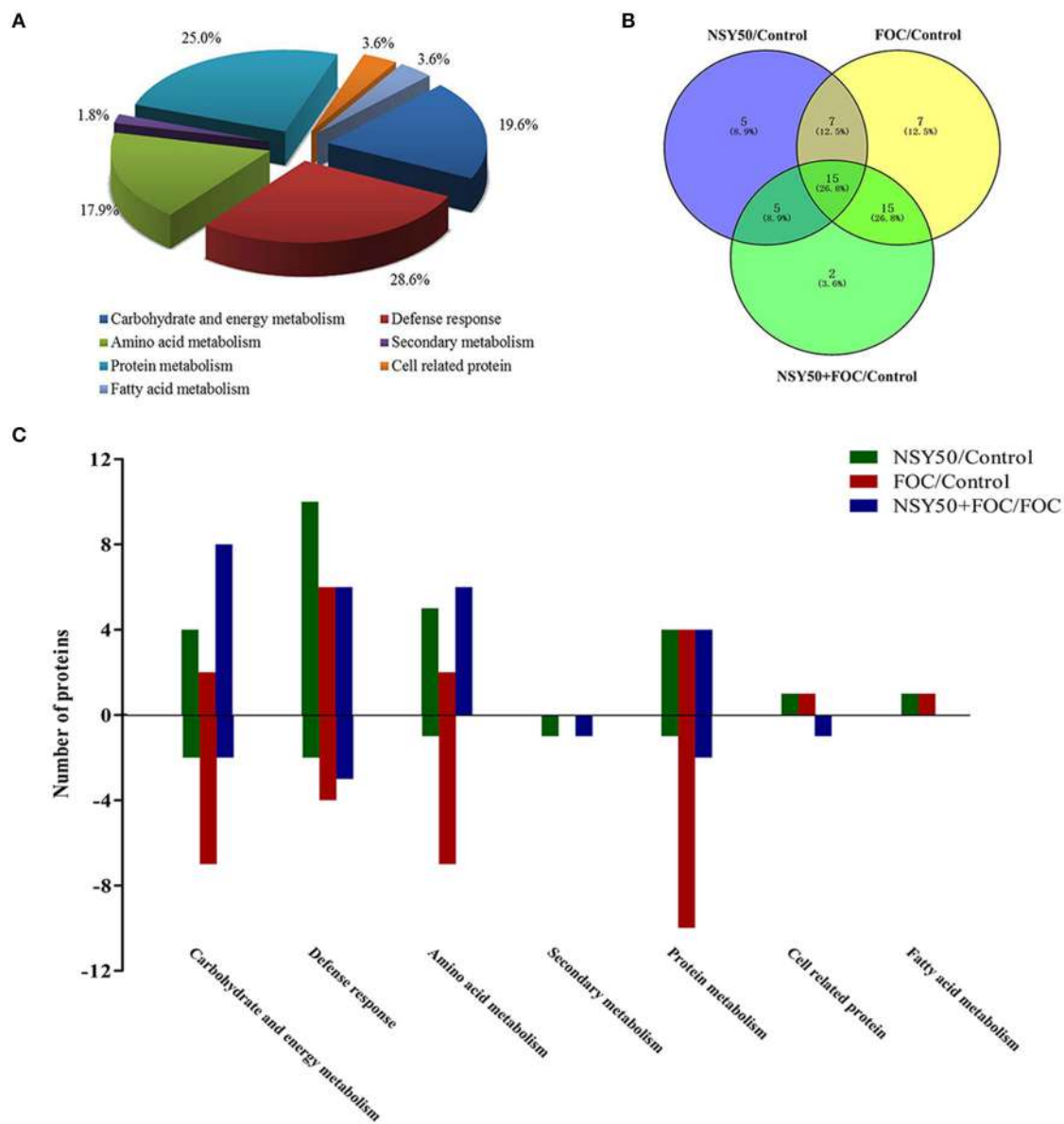
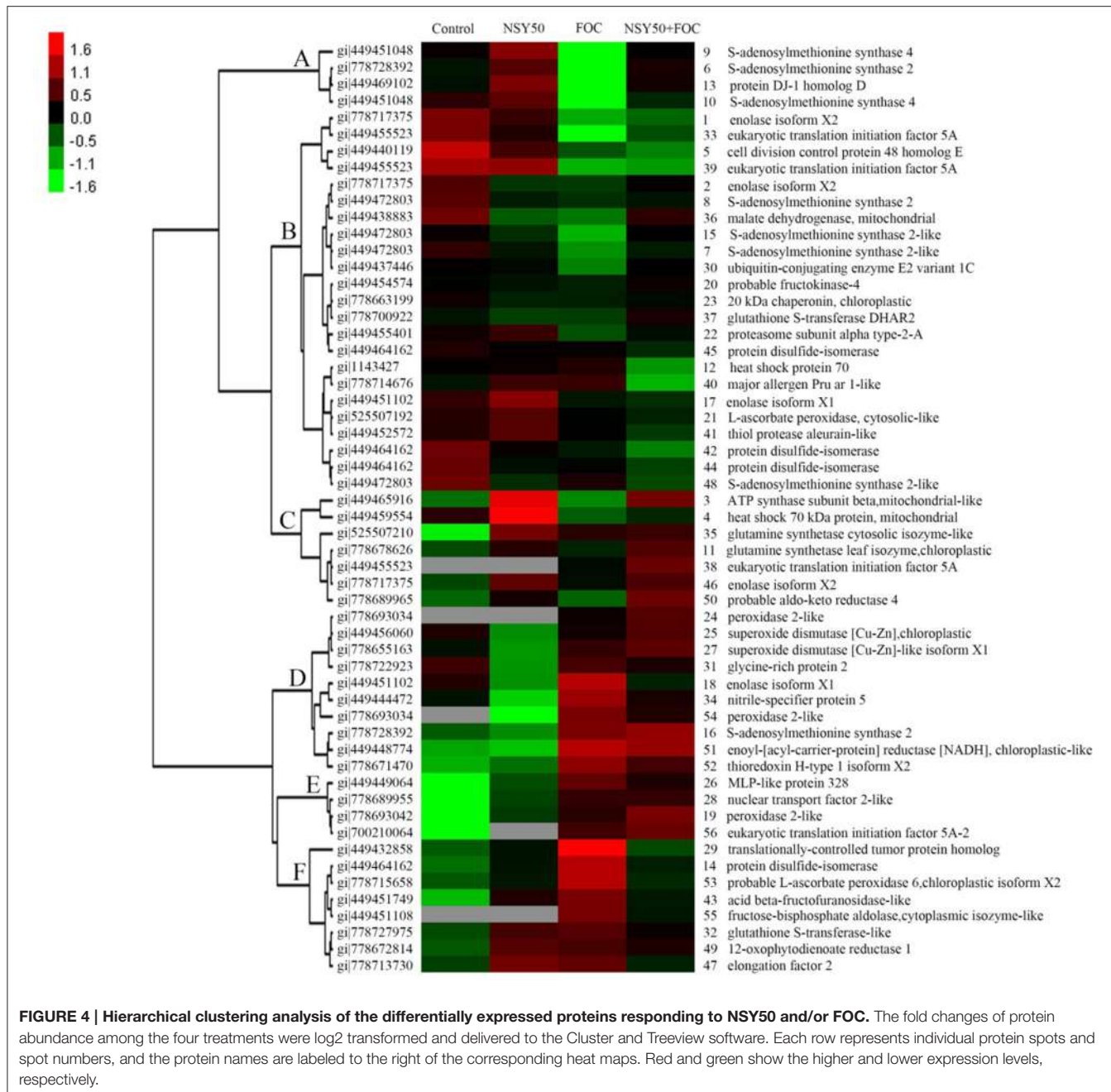


FIGURE 3 | Distribution of differentially expressed proteins by NSY50 and/or FOC in cucumber roots. (A) Functional classification and distribution of all 56 differentially expressed proteins. **(B)** Venn diagram showing the number of overlapping proteins that were differentially regulated by NSY50, FOC, and NSY50+FOC compared to the control. **(C)** Functional protein distribution in the compared groups (changes ≥ 1.5 -fold or ≤ 0.67 -fold).

up-regulated by NSY50 (NSY50) compared to the control. It is known that the activation of antioxidant enzymes is a major plant cell method for protection (Youssef et al., 2016). Several studies confirmed the ability of bio-control agents to mitigate the effects of oxidative bursts by increasing the activity of antioxidant enzymes (Israr et al., 2016; Youssef et al., 2016). Thus, the results of the present study indicated that application of NSY50 played an active role in determining the abundance of antioxidant enzymes.

GSTs belong to a family of multifunctional enzymes that play critical roles in protecting tissues from oxidative damage

by quenching reactive molecules (An et al., 2016). Previous studies have reported that GSTs can enhance resistance to the virulent bacterial pathogen *Pseudomonas syringae* pv. tomato DC3000 in *Arabidopsis* (Jones et al., 2006) and were increased in response to various hormones, such as salicylic acid, ethylene, methyl jasmonate, and auxin, and to biotic and abiotic stress (Lieberherr et al., 2003; Faltin et al., 2010). Additionally, Kwon et al. (2016) found that four glutathione S-transferases were significantly up-regulated by plant-growth-promoting rhizobacterium *P. polymyxa* E681 in *Arabidopsis* and suggested that the activation of defense-related proteins may be



reason for resistance to the fungal pathogen. It was reported that the overexpression of GSTs induced by another PGPR, *P. fluorescens*, had an essential role in the ISR by priming rice plants and protecting cells from oxidative damage (Kandasamy et al., 2009). In the present study, two glutathione S-transferases (GST, spots 32, and 37) were identified. One of them (spot 32) was significantly up-regulated in NSY50, and the other (spot 37) showed expression levels in NSY50+FOC that were much higher than those in FOC. The qRT-PCR analysis also showed that the application of NSY50 significantly up-regulated this gene expression, regardless of whether the plants were inoculated with

FOC (Figure 6). This result indicated that NSY50 could increase GST content to remove toxins in cucumber seedlings.

Plant thioredoxins appear to play a fundamental role in plant tolerance of oxidative stress by supplying power to reductases detoxifying lipid hydroperoxides or repairing oxidized proteins (Vieira Dos Santos and Rey, 2006). Thioredoxin H-type 1 isoform X2 (TRX, spot 52) belongs to the thioredoxins family and was up-regulated by the inoculation of NSY50 and/or FOC. This result was consistent with the results of Laloi et al. (2004), who reported that the *Arabidopsis* cytosolic thioredoxin h5 gene was induced by oxidative stress and its response to a

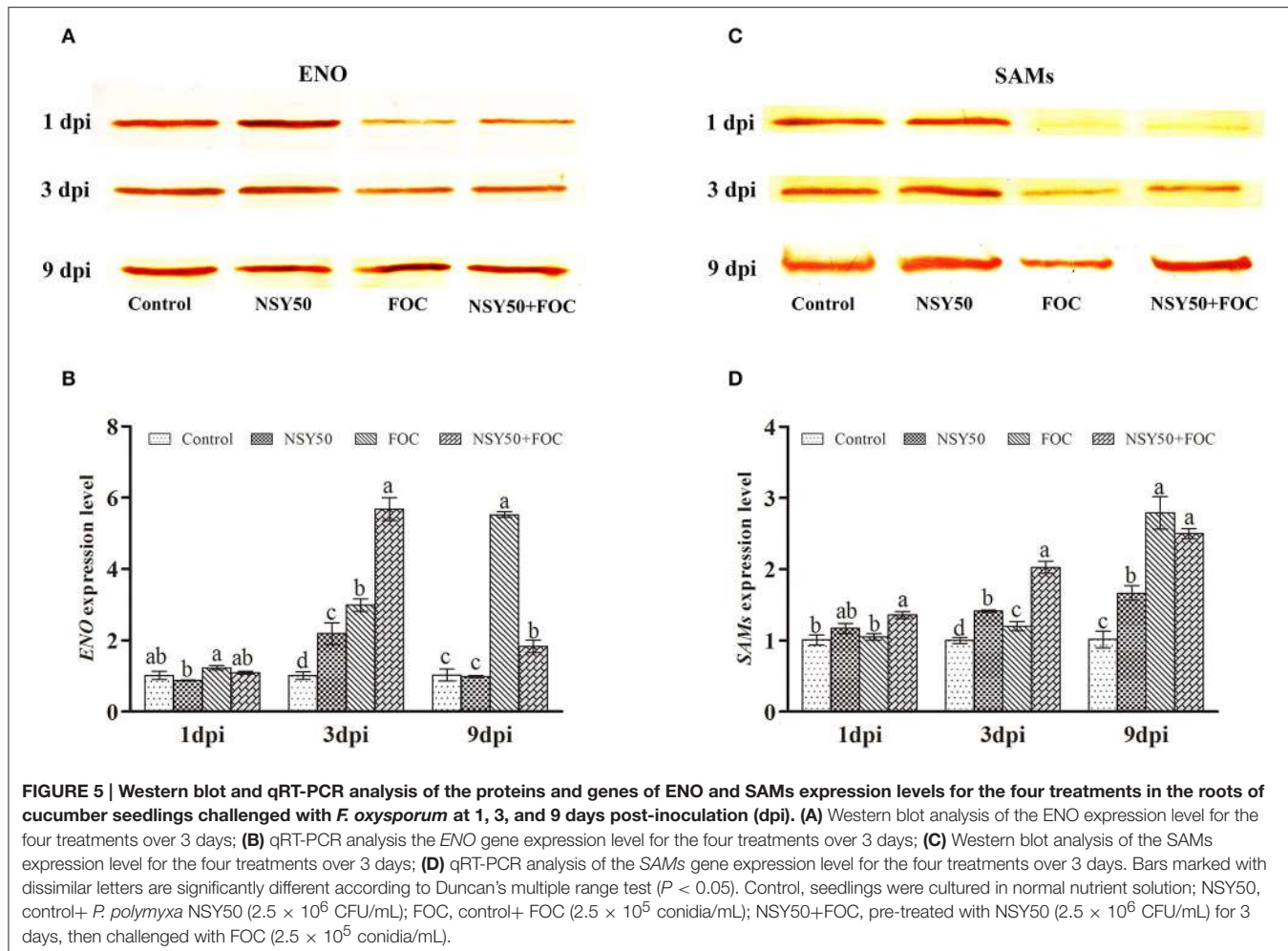


FIGURE 5 | Western blot and qRT-PCR analysis of the proteins and genes of ENO and SAMs expression levels for the four treatments in the roots of cucumber seedlings challenged with *F. oxysporum* at 1, 3, and 9 days post-inoculation (dpi). **(A)** Western blot analysis of the ENO expression level for the four treatments over 3 days; **(B)** qRT-PCR analysis the ENO gene expression level for the four treatments over 3 days; **(C)** Western blot analysis of the SAMs expression level for the four treatments over 3 days; **(D)** qRT-PCR analysis of the SAMs gene expression level for the four treatments over 3 days. Bars marked with dissimilar letters are significantly different according to Duncan's multiple range test ($P < 0.05$). Control, seedlings were cultured in normal nutrient solution; NSY50, control+ *P. polymyxa* NSY50 (2.5×10^6 CFU/mL); FOC, control+ FOC (2.5×10^5 conidia/mL); NSY50+FOC, pre-treated with NSY50 (2.5×10^6 CFU/mL) for 3 days, then challenged with FOC (2.5×10^5 conidia/mL).

pathogen elicitor. In addition, Sun et al. (2010) found that the overexpression of NtTRXh3 (An h-type thioredoxin in tobacco) conferred resistance to Tobacco mosaic virus and Cucumber mosaic virus, both of which had reduced multiplication and pathogenicity in NtTRXh3- overexpressing plants compared to controls. These reductions indicated that TRX participated in defense mechanisms linked to the oxidative bursts resulting from pathogen attack.

In this study, a probable aldo-keto reductase 4 (AKRs, spots 50) was successfully identified, which showed that inoculation with NSY50 significantly up-regulated the expression of aldo-keto reductase (AKRs), with or without FOC. The AKRs superfamily comprises a large number of primarily monomeric protein members that reduce a broad spectrum of substrates, which range from simple sugars to potentially toxic aldehydes (Sengupta et al., 2015). There are a number of interesting reports on the active involvement of plant AKRs in detoxification of stress-induced reactive carbonyls as plant defense systems against biotic stress factors, such as pathogenic attack (Tremblay et al., 2010; Santos et al., 2012; Xu et al., 2013). This may be the first report on a type of protein induced by the PGPR that actively contributes to defense against biotic stressors.

Other defense response proteins, such as heat shock protein 70 (HSP70, spots 4 and 12) and MLP-like protein 328 (MLP328, spot 26), were also identified in this study. HSP70 can be induced by various environmental stresses, such as cold, salt, high temperature, and hypoxic stress, and this protein often acts as a molecular chaperone (Xu et al., 2011; Li et al., 2013b; Yuan et al., 2016) to prevent the irreversible aggregation of other proteins and regulate the folding and accumulation of proteins (Feder and Hofmann, 1999). In this study, it was observed that NSY50 enhances the expression of HSP70 (spot 4) by 3.31-fold compared to the control. Whereas, FOC significantly decreased HSP70 expression both under control conditions and pre-treatment with NSY50 (Table 2), the combined inoculation (NSY50+FOC) showed much higher up-regulation than FOC, although there was no significant difference. The transcription of HSP70 showed a significant increase in NSY50+FOC compared to inoculation with FOC alone (Figure 6). This result indicates that the PGPR are capable of enhancing the expression of this important protein. This result was consistent with the research of Li et al. (2013b), who reported that PGPR *P. putida* UW4 significantly enhanced the level of plant heat shock proteins under hypoxic stress to improve stress resistance. The role of

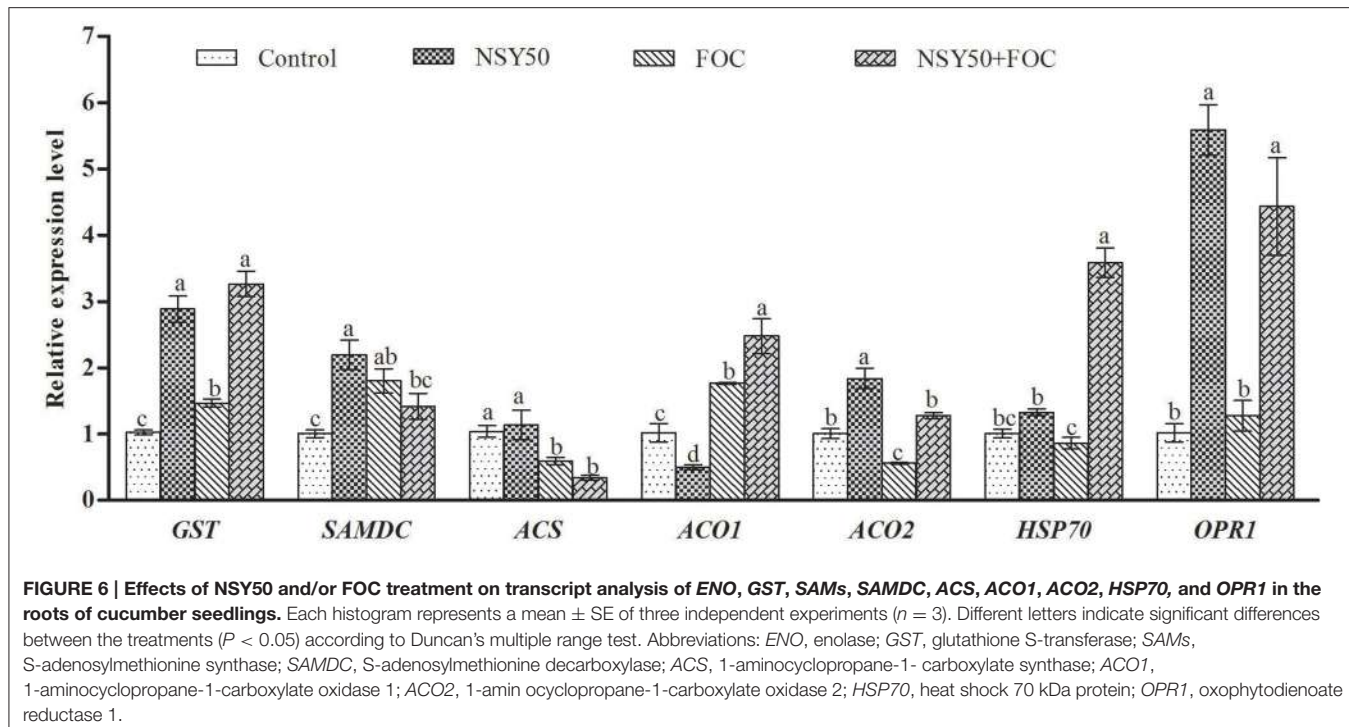


FIGURE 6 | Effects of NSY50 and/or FOC treatment on transcript analysis of ENO, GST, SAMs, SAMDC, ACS, ACO1, ACO2, HSP70, and OPR1 in the roots of cucumber seedlings. Each histogram represents a mean \pm SE of three independent experiments ($n = 3$). Different letters indicate significant differences between the treatments ($P < 0.05$) according to Duncan's multiple range test. Abbreviations: ENO, enolase; GST, glutathione S-transferase; SAMs, S-adenosylmethionine synthase; SAMDC, S-adenosylmethionine decarboxylase; ACS, 1-aminocyclopropane-1-carboxylate synthase; ACO1, 1-aminocyclopropane-1-carboxylate oxidase 1; ACO2, 1-aminocyclopropane-1-carboxylate oxidase 2; HSP70, heat shock 70 kDa protein; OPR1, oxophytodienoate reductase 1.

the MLP-like protein was unclear, and it was hypothesized to be a physiological defense protein that responded to stress (Fukao et al., 2009; An et al., 2016). However, in this study, MLP328 was significantly up-regulated, with a 3.13–3.68-fold increase following the inoculation of NSY50 and/or FOC compared to the control. The mechanism of this type of physiological defense protein needs further study.

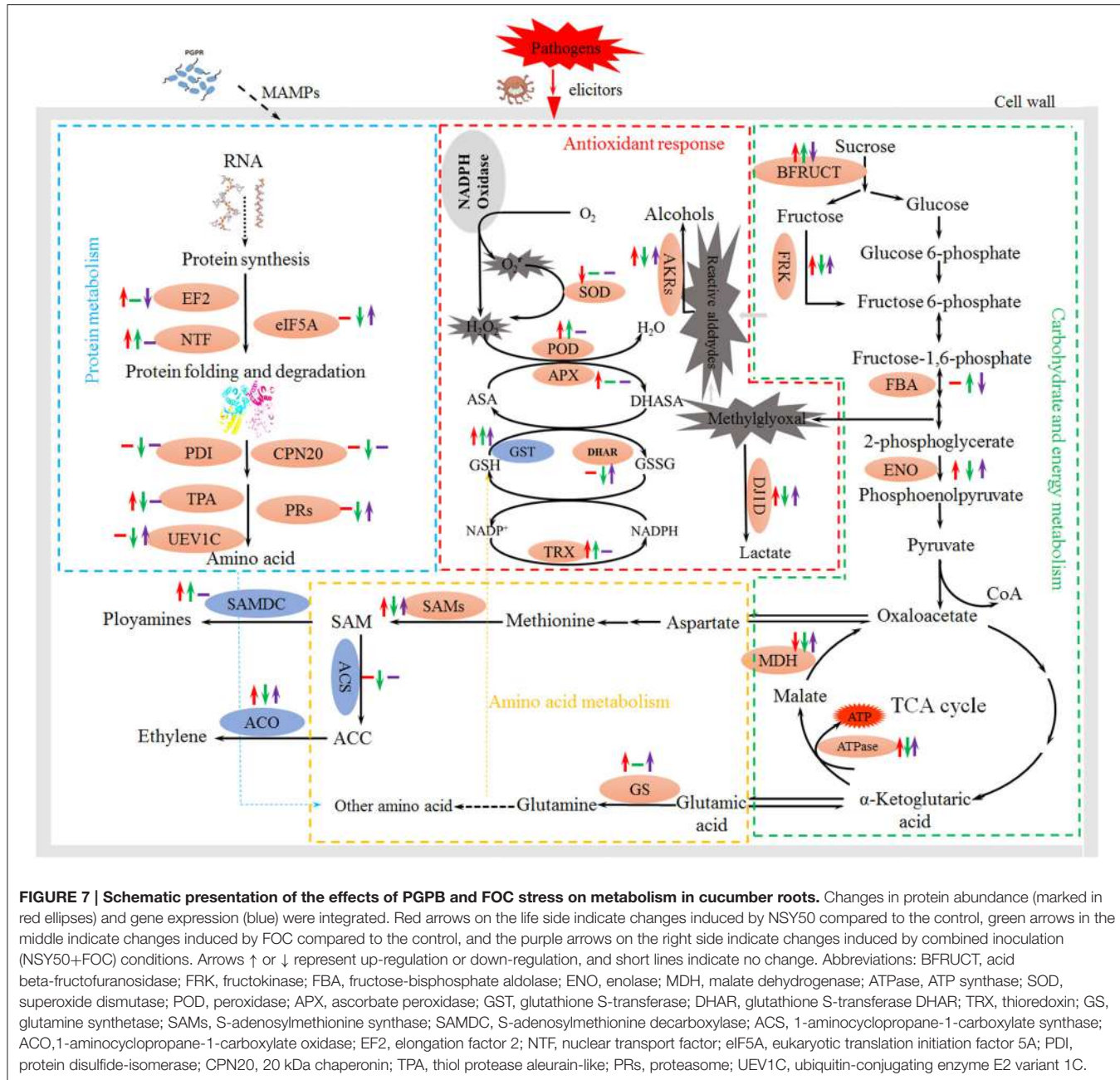
Protein Metabolism

Of the differentially accumulated proteins, 14 were identified as responding to FOC and/or NSY50 treatments; these responses were attributed to protein metabolism, and the proteins could be divided into five functional groups (Table 2). The first group includes those involved in protein folding and assembly, including four protein disulfide-isomerase (PDI, spots 14, 42, 44, and 45) and a 20 kDa chaperonin (CPN20, spot 23). Both the NSY50 and FOC treatments enhanced the expression of PDI (spot 14) by 1.90–2.42-fold compared to the control. Several studies have shown that the overexpression of PDI in plants that are challenged with pathogens has been thought to be related to the correct folding of defense proteins (Gruber et al., 2007; Palomares-Rius et al., 2011; Cipriano et al., 2015). However, the remaining three PDI proteins (spots 42, 44, and 45) were significantly decreased by pathogen attack (inoculated with FOC). This effect may be due to the stresses that were inhibited expression of this type of protein, which was consistent with previous reports (Yuan et al., 2016). However, another report showed that the application of PGPR recovered the expression level of this protein under stress conditions (Li et al., 2013b). The CPN20 (spot 23), which was among the most-represented proteins that emphasize the impact of stress on

post-translation modification/ modification machinery (Zhang et al., 2015) showed similar results when inoculated with FOC.

The second group included three spots of eukaryotic translation initiation factor 5A (eIF-5A, spots 33, 38, and 39), one eukaryotic translation initiation factor 5A-2 (eIF-5A2, spot 56) and one elongation factor 2 (EF2, spot 47), which are involved in the initiation and elongation stage of mRNA translation and protein synthesis (Thompson et al., 2004; Yuan et al., 2016). Overall, the FOC inoculation significantly decreased the eIF-5A expression levels in cucumber seedling roots, whereas pre-treatment with NSY50 (NSY50+FOC) enhanced the expression of eIF-5A. However, the eIF-5A2 protein had a higher accumulation after FOC inoculation conditions both with and without NSY50 compared to non-stress conditions. The protein eIF-5A2 was reported to likely be involved in the regulation of apoptotic cell death (Feng et al., 2007). EF2 was significantly up-regulated, with a 2.70-fold increase after inoculation with NSY50 compared to the control, whereas inoculation with FOC showed only a slight increase. These results indicated that the PGPR could balance ribosomal particles and protein synthesis, which was consistent with previous reports (Li et al., 2013b).

The third group included proteasome subunit alpha type-2-A (PRs, spot 22) and thiol protease aleurain-like (TPA, spot 41), which are involved in protein degradation. The proteasome was assigned a precise role in the degradation of the oxidized proteins generated by many stresses, which avoided the inhibition of the plant's metabolic pathway (Polge et al., 2009). In this study, infection with FOC down-regulated the expression level of TPA, and the plants metabolic pathway may have been damaged by this destructive fungal pathogen, which was consistent with the TEM result. The PRs significantly



decreased under FOC stress but were remarkably up-regulated by inoculation with NSY50, which indicated that the degradation of proteins with oxidative damage was enhanced (An et al., 2016). The fourth group was protein transport and included one protein called nuclear transport factor 2-like (NTF2, spot 28). The NTF2 facilitated protein transport into the nucleus (Zhao et al., 2006). Both inoculation with NSY50 and FOC were significantly up-regulated the expression of this protein. The ubiquitin-conjugating enzyme E2 variant 1C (UEV1C, spot 30) belonged to the fifth group, protein modification, and it participates in protein modification by catalyzing the covalent attachment of ubiquitin to proteins (Yuan et al., 2016). In this

study, FOC significantly decreased the expression of UEV1C, whereas pre-treatment with NSY50 (NSY50+FOC) enhanced its expression. These results suggest that the application of NSY50 alleviated the damage to protein metabolism that was induced by *F. oxysporum*.

Carbohydrate and Energy Metabolism

The proteins related to carbohydrate and energy metabolism, particularly the proteins involved in the glycolysis (EMP) and tricarboxylic acid (TCA) cycle were significantly changed and are shown in Table 2. A total of 11 identified proteins in response to two strains were found and were divided into four functional

groups. The first group focused on glycolysis and included five spots with enolase isoform (ENO, spots 1, 2, 17, 18, and 46), protein DJ-1 homolog D (DJ1D, spot 13), probable fructokinase-4 (FRK, spot 20) and fructose-bisphosphate aldolase (FBA, spot 55). The others were involved with the tricarboxylic acid cycle, including malate dehydrogenase (MDH, spot 36), sucrose metabolism protein acid beta-fructofuranosidase-like (BFRUCT, spot 43), and energy metabolism protein ATP synthase (ATPase, spot 3). Almost all of them were down-regulated by FOC and recovered by treatment with NSY50 (NSY50+FOC), except FBA and BFRUCT.

Enolases, known as 2-phospho-D-glycerate hydrolases, are one of the most important enzymes in glycolysis. They catalyze the dehydration of 2-phosphoglycerate into phosphoenolpyruvate. Five spots were identified as enolases in this study, and western blotting was used to verify proteomic data (**Table 2**, **Figure 5A**; Supplementary Figures 2, 3) and showed a similar tendency, regardless of whether measurements were taken 1, 3, or 9 days post-inoculation with the pathogen FOC. The gene expression showed a reverse trend, and inoculation with FOC significantly up-regulated its gene expression (**Figure 5B**). Interestingly, protein abundance significantly recovered along with inoculation time (**Figure 5A**). Several studies reported that both the ENO protein and the gene expression increased under salt stress and attempted to generate more energy to cope with the stress (Ndimba et al., 2005; Zhong et al., 2015; An et al., 2016; Yuan et al., 2016).

The DJ-1D protein (DJ1D, spot 13), which was reported to have several functions, including functioning as an antioxidant (Taira et al., 2004), is a redox-dependent chaperone (Krebiehl et al., 2010) and can convert glyoxals to carboxylic acids (Kwon et al., 2013). Glyoxals are reactive 2-oxoaldehydes that are found in cells under various stress conditions (Thornalley, 1996). In this study, DJ1D was significantly up-regulated, with 4.25- and 2.28-fold increases after inoculation with NSY50 and/or FOC, respectively.

Li et al. (2013b) reported that the application of PGPR *P. putida* UW4 adjusted the EMP-TCA metabolism under hypoxic stress. In contrast, Kwon et al. (2016) found that some of the proteins related to the glycolysis pathway, such as FBA and pyruvate dehydrogenase complex component E2, were significantly up-regulated by the PGPR strain *P. polymyxa* E681 in *Arabidopsis* roots. Carbohydrate metabolism provides the plant with required carbon, which is critical for the production of new tissues, and also can have profound effects on plant growth through modulation of cell division and expansion (Eveland and Jackson, 2012; Kwon et al., 2016). In this study, we found that the application of *P. polymyxa* NSY50 increased the abundance of FRK, ENO, BFRUCT, and ATPase compared to control conditions. Additionally, NSY50 partially recovered the ENO, FRK, DJ1D, MDH, and ATPase expression, which had been decreased by FOC. These results suggested that the application of NSY50 could promote EMP-TCA pathway activity. Presumably, these results imply there was an enhancement in energy generation and carbohydrate production to promote plant growth and resist stress damage.

Amino Acid Metabolism

Ten spots were identified as proteins involved in amino acid metabolism. Eight S-adenosylmethionine synthases (SAMs, spots 6, 7, 8, 9, 10, 15, 16, and 48) comprising different subunits were identified and markedly decreased (except spot 16) in response to FOC infection. SAMs catalyze the biosynthesis of S-adenosylmethionine (SAM) from methionine and ATP, and they are active in the biosynthesis of lignin, glycine betaine and polyamines (Fontecave et al., 2004). These proteins can be induced by various environmental stresses, such as cold, salt, drought stress and even pathogen infection (Li et al., 2013a; Huang et al., 2016), and most of them were down-regulated by stress (Wang et al., 2016; Yuan et al., 2016). This outcome was consistent with the results showing that the inoculation of FOC significantly decreased SAMs expression (**Table 2**, **Figure 5C**; Supplementary Figures 4, 5). However, pre-treatment with NSY50 up-regulated SAMs abundance both under control and pathogen infection conditions. The accumulation of SAMs in plants has been shown to be related to the enhance tolerance to various kinds of environmental stresses. Overexpression of *suadea salsa* SAMs gene promoted salt tolerance in transgenic tobacco (Qi et al., 2010). An increase in production of SAMs was observed in cold stressed rice (Cui et al., 2005), mechanically wounded *Phaseolus lunatus* (Arimura et al., 2002), salt-stressed barley (Witzel et al., 2009), and in response to cotton worm feeding in soybean (Fan et al., 2012). Hence, the remarkable expression of SAMs by NSY50 suggested that plant might promote SAM-dependant metabolism through synthesize more SAM to further enhance the synthesis of new proteins and stress tolerance.

Glutamine synthetase (GS) is a key enzyme in plant N assimilation that catalyzes the combination of ammonia and glutamate into glutamine (Nam et al., 2011; Rogić et al., 2015). Two types of GS (spots 11 and 35) were identified and showed different accumulation patterns. However, they were both up-regulated by NSY50, regardless of whether the plants were inoculated with FOC. This result suggested that the application of NSY50 could lead to a high accumulation of amino acid metabolism, and this was probably one way in which NSY50 promoted plant growth and intensified resistance to pathogen infection for cucumber seedlings.

Fatty Acid Metabolism Proteins

Jasmonic acid is a signaling compound that influences multiple cellular functions and plays crucial roles in the signaling network regulating the development of induced resistance, including systemic acquired resistance (SAR) and induced systemic resistance (Glazebrook, 2001). Niu et al. (2011) found that PGPR *Bacillus cereus* AR156 induced ISR to *Pseudomonas syringae* pv. *tomato* DC3000 in *Arabidopsis* via the simultaneous activation of salicylic acid-, jasmonic acid-, and ethylene-dependent signaling pathways. In the present study, 12-oxophytodienoate reductase 1 (spot 49), which is involved in jasmonate biosynthesis, was identified to be induced by both NSY50 and FOC inoculation. Additionally, NSY50 treatment showed a 2.02-fold increase in abundance compared to FOC. A good correlation was observed between this protein and transcript abundance, as

etermined by qPCR analysis (**Figure 6**). This outcome indicated that *P. polymyxa* NSY50 may stimulate the jasmonate signal transduction network.

Enoyl-[acyl-carrier-protein] reductase [NADH] (ACP, spot 51), which is a subunit of the fatty acid synthase complex that catalyzes the *de novo* synthesis of fatty acids (Mou et al., 2000), was significantly up-regulated by inoculation with FOC. It was recently reported that ACP was sensitive to the diphenyl ether cyperin produced by certain pathogenic fungi in the tissues of infected plants, which likely contributed to the virulence of these disease agents (Dayan et al., 2008). The role of the ACP during pathogen infection remains unclear, and further study is required.

Secondary Metabolism and Cell-Related Proteins

The NSY50 was also found to regulate proteins involved in other metabolic pathways, such as secondary metabolism (spot 34) and cell-related protein (spots 5 and 29), which indicated that NSY50 regulated various metabolic pathways to counteract FOC infection. The mechanism of action will need to be studied in future investigations.

CONCLUSION

To the best of our knowledge, this is the first proteomic-based research to focus on the interactions between cucumber plants, the pathogen *F. oxysporum*, and PGPR strain *P. polymyxa* NSY50. A total of 56 protein spots were identified with a change more than 1.5-fold or less than the 0.67-fold in the protein abundance ratio in cucumber seedling roots after inoculation with *P. polymyxa* NSY50 and/or FOC. The majority of these proteins were related to defense responses, protein metabolism, carbohydrate and energy metabolism and amino acid metabolism. These proteins might work cooperatively to enhance resistance to FOC attack and keep plant growth on a mostly even keel. Our results showed that the improved plant

growth and defenses by *P. polymyxa* NSY50 might be associated with the following processes: (i) activation of stress defense-related proteins by stress injuries that are alleviated by NSY50; (ii) NSY50 stimulating protein synthesis and degrading damaged proteins induced by FOC; (iii) up-regulation of proteins in the EMP-TCA route to provide more carbohydrates and energy to promote plant growth and resist debilitation; or (iv) adjusting the plant amino acid metabolism to increase biomass of the plant and regulate other metabolic pathways, such as jasmonic acid, to enhance resistance to FOC. This research enriched our understanding of the mechanisms of how PGPR mediates the stress response in plants and promotes protection from pathogen infection.

AUTHOR CONTRIBUTIONS

We thank the numerous individuals who participated in this research. SG designed the study and guided the research. ND and LS wrote the main manuscript text and performed the experiments. YY prepared all the figures and performed some of the experiments. BL contributed new reagents and analytical tools. SS and JS edited this manuscript. All authors reviewed and approved the manuscript.

FUNDING

This work was financially supported by the National Natural Science Foundation of China (No. 31672199, No. 31471869, and No. 31401919), the China Agriculture Research System (CARS-25-C-03), and the Priority Academic Program Development of Jiangsu Higher Education Institutions (PAPD).

SUPPLEMENTARY MATERIAL

The Supplementary Material for this article can be found online at: <http://journal.frontiersin.org/article/10.3389/fpls.2016.01859/full#supplementary-material>

REFERENCES

- Ahn, I. P., Chung, H. S., and Lee, Y. H. (1998). Vegetative compatibility groups and pathogenicity among isolates of *Fusarium oxysporum* f. sp. *cucumerinum*. *Plant Dis.* 82, 244–246. doi: 10.1094/PDIS.1998.82.2.244
- An, Y., Zhou, H., Zhong, M., Sun, J., Shu, S., Shao, Q., et al. (2016). Root proteomics reveals cucumber 24-epibrassinolide responses under Ca(NO₃)₂ stress. *Plant Cell Rep.* 35, 1081–1101. doi: 10.1007/s00299-016-1940-z
- Arimura, G., Ozawa, R., Nishioka, T., Boland, W., Koch, T., Kühnemann, F., et al. (2002). Herbivore-induced volatiles induce the emission of ethylene in neighboring lima bean plants. *Plant J.* 29, 87–98. doi: 10.1046/j.1365-313x.2002.01198.x
- Bargabus, R. L., Zidack, N. K., and Sherwood Jacobsen, B. J. (2003). Oxidative burst elicited by *Bacillus mycoides* isolate Bac J., a biological control agent, occurs independently of hypersensitive cell death in sugar beet. *Mol. Plant Microbe Interact.* 16, 1145–1153. doi: 10.1094/MPMI.2003.16.12.1145
- Bottini, R., Cassán, F., and Piccoli, P. (2004). Gibberellin production by bacteria and its involvement in plant growth promotion and yield increase. *Appl. Microbiol. Biotechnol.* 65, 497–503. doi: 10.1007/s00253-004-1696-1
- Bradford, M. M. (1976). A rapid and sensitive method for the quantitation of microgram quantities of protein utilizing the principle of protein-dye binding. *Anal. Biochem.* 72, 248–254. doi: 10.1016/0003-2697(76)90527-3
- Camejo, D., Guzmán-Cedeño, Á., and Moreno, A. (2016). Reactive oxygen species, essential molecules, during plant-pathogen interactions. *Plant Physiol. Biochem.* 103, 10–23. doi: 10.1016/j.plaphy.2016.02.035
- Cao, Y., Xu, Z., Ling, N., Yuan, Y., Yang, X., Chen, L., et al. (2012). Isolation and identification of lipopeptides produced by *B. subtilis* SQR 9 for suppressing Fusarium wilt of cucumber. *Sci. Hortic.* 135, 32–39. doi: 10.1016/j.scienta.2011.12.002
- Carrillo, E., Rubiales, D., and Castillejo, M. (2014). Proteomic analysis of pea (*Pisum sativum* L.) response during compatible and incompatible interactions with the pea aphid (*Acyrthosiphon pisum* H.). *Plant Mol. Biol. Rep.* 32, 697–718. doi: 10.1007/s11105-013-0677-x
- Chen, D., Liu, X., Li, C., Tian, W., Shen, Q., and Shen, B. (2014). Isolation of *Bacillus amyloliquefaciens* S20 and its application in control of eggplant bacterial wilt. *J. Environ. Manag.* 137, 120–127. doi: 10.1016/j.jenvman.2014.01.043
- Chung, S., Kong, H., Buyer, J. S., Lakshman, D. K., Lydon, J., Kim, S. D., et al. (2008). Isolation and partial characterization of *Bacillus subtilis* ME488 for

- suppression of soilborne pathogens of cucumber and pepper. *Appl. Microbiol. Biotechnol.* 80, 115–123. doi: 10.1007/s00253-008-1520-4
- Cipriano, A. K., Gondim, D. M., Vasconcelos, I. M., Martins, J. A., Moura, A. A., Moreno, F. B., et al. (2015). Proteomic analysis of responsive stem proteins of resistant and susceptible cashew plants after *Lasiodiplodia theobromae* infection. *J. Proteomics* 113, 90–109. doi: 10.1016/j.jprot.2014.09.022
- Cui, S., Huang, F., Wang, J., Ma, X., Cheng, Y., and Liu, J. (2005). A proteomic analysis of cold stress responses in rice seedlings. *Proteomics* 5, 3162–3172. doi: 10.1002/pmic.200401148
- Dayan, F. E., Ferreira, D., Wang, Y. H., Khan, I. A., McInroy, J. A., and Pan, Z. (2008). A pathogenic fungi diphenyl ether phytotoxin targets plant enoyl (acyl carrier protein) reductase. *Plant Physiol.* 147, 1062–1071. doi: 10.1104/pp.108.118372
- Dijksterhuis, J., Sanders, M., Gorris, L. G., and Smid, E. J. (1999). Antibiosis plays a role in the context of direct interaction during antagonism of *Paenibacillus polymyxa* towards *Fusarium oxysporum*. *J. Appl. Microbiol.* 86, 13–21. doi: 10.1046/j.1365-2672.1999.t01-1-00600.x
- Du, N., Shi, L., Du, L., Yuan, Y., Li, B., Sang, T., et al. (2015). Effect of vinegar residue compost amendments on cucumber growth and Fusarium wilt. *Environ. Sci. Pollut. Res. Int.* 22, 19133–19141. doi: 10.1007/s11356-015-4816-9
- Eveland, A. L., and Jackson, D. P. (2012). Sugars, signalling, and plant development. *J. Exp. Bot.* 63, 3367–3377. doi: 10.1093/jxb/err379
- Faltin, Z., Holland, D., Velcheva, M., Tsapovetsky, M., RoeckelDrevet, P., Handa, A. K., et al. (2010). Glutathione peroxidase regulation of reactive oxygen species level is crucial for *in vitro* plant differentiation. *Plant Cell Physiol.* 51, 1151–1162. doi: 10.1093/pcp/pcq082
- Fan, R., Wang, H., Wang, Y., and Yu, D. (2012). Proteomic analysis of soybean defense response induced by cotton worm (*prodenia litura*, *fabricius*) feeding. *Proteome Sci.* 10, 338–348. doi: 10.1186/1477-5956-10-16
- Feder, M. E., and Hofmann, G. E. (1999). Heat-shock proteins, molecular chaperones, and the stress response: evolutionary and ecological physiology. *Annu. Rev. Physiol.* 61, 243–282.
- Feng, H., Chen, Q., Feng, J., Zhang, J., Yang, X., and Zuo, J. (2007). Functional characterization of the *Arabidopsis* eukaryotic translation initiation factor 5A-2 that plays a crucial role in plant growth and development by regulating cell division, cell growth, and cell death. *Plant Physiol.* 144, 1531–1545. doi: 10.1104/pp.107.098079
- Fontecave, M., Atta, M., and Mulliez, E. (2004). S-adenosylmethionine: nothing goes to waste. *Trends Biochem. Sci.* 29, 243–249. doi: 10.1016/j.tibs.2004.03.007
- Fukao, Y., Ferjani, A., Fujiwara, M., Nishimori, Y., and Ohtsu, I. (2009). Identification of zinc-responsive proteins in the roots of *Arabidopsis thaliana* using a highly improved method of two-dimensional electrophoresis. *Plant Cell Physiol.* 50, 2234–2239. doi: 10.1093/pcp/pcp154
- Glazebrook, J. (2001). Genes controlling expression of defense responses in *Arabidopsis*-2001 status. *Curr. Opin. Plant Biol.* 4, 301–308. doi: 10.1016/s1369-5266(00)00177-1
- Gruber, C. W., Cemazar, M., Clark, R. J., Horibe, T., Renda, R. F., Anderson, M. A., et al. (2007). A novel plant protein-disulfide isomerase involved in the oxidative folding of cystine knot defense proteins. *J. Biol. Chem.* 282, 20435–20446. doi: 10.1074/jbc.M700018200
- Gupta, K. J., Mur, L. A., and Brotman, Y. (2014). Trichoderma asperelloides suppresses nitric oxide generation elicited by *Fusarium oxysporum* in *Arabidopsis* roots. *Mol. Plant Microbe Interact.* 27, 307–314. doi: 10.1094/MPMI-06-13-0160-R
- He, L., Li, B., Lu, X., Yuan, L., Yang, Y., Yuan, Y., et al. (2015). The effect of exogenous calcium on mitochondria, respiratory metabolism enzymes and ion transport in cucumber roots under hypoxia. *Sci. Rep.* 5:11391. doi: 10.1038/srep11391
- He, L., Lu, X., Tian, J., Yang, Y., Li, B., Li, J., et al. (2012). Proteomic analysis of the effects of exogenous calcium on hypoxic-responsive proteins in cucumber roots. *Proteome Sci.* 10, 1–15. doi: 10.1186/1477-5956-10-42
- Hong, C. E., Kwon, S. Y., and Park, J. M. (2016). Biocontrol activity of *Paenibacillus polymyxa* AC-1 against *Pseudomonas syringae* and its interaction with *Arabidopsis thaliana*. *Microbiol. Res.* 185, 13–21. doi: 10.1016/j.micres.2016.01.004
- Huang, X., Shi, D., Sun, F., Lu, H., Liu, J., and Wu, W. (2012). Efficacy of sludge and manure compost amendments against *Fusarium* wilt of cucumber. *Environ. Sci. Pollut. Res. Int.* 19, 3895–3905. doi: 10.1007/s11356-012-1025-7
- Huang, Y., Ma, H. Y., Huang, W., Wang, F., Xu, Z. S., and Xiong, A. S. (2016). Comparative proteomic analysis provides novel insight into the interaction between resistant vs susceptible tomato cultivars and TYLCV infection. *BMC Plant Biol.* 16:162. doi: 10.1186/s12870-016-0819-z
- Hurkman, W. J., and Tanaka, C. K. (1986). Solubilization of plant membrane proteins for analysis by two-dimensional gel electrophoresis. *Plant Physiol.* 81, 802–806.
- Idriss, E. E., Makarewicz, O., Farouk, A., Rosner, K., Greiner, R., Bochow, H., et al. (2002). Extracellular phytase activity of *Bacillus amyloliquefaciens* FZB45 contributes to its plant-growth-promoting effect. *Microbiology* 148(Pt 7), 2097–2109. doi: 10.1099/00221287-148-7-2097
- Israr, D., Mustafa, G., Khan, K. S., Shahzad, M., Ahmad, N., and Masood, S. (2016). Interactive effects of phosphorus and *Pseudomonas putida* on chickpea (*Cicer arietinum* L.) growth, nutrient uptake, antioxidant enzymes and organic acids exudation. *Plant Physiol. Biochem.* 108, 304–312. doi: 10.1016/j.plaphy.2016.07.023
- Jiang, C. H., Wu, F., Yu, Z. Y., Xie, P., Ke, H. J., Li, H. W., et al. (2015). Study on screening and antagonistic mechanisms of *Bacillus amyloliquefaciens* 54 against bacterial fruit blotch (BFB) caused by *Acidovorax avenae* subsp. *citrulli*. *Microbiol. Res.* 170, 95–104. doi: 10.1016/j.micres.2014.08.009
- Jones, A. M. E., Thomas, V., Bennett, M. H., Mansfield, J., and Grant, M. (2006). Modifications to the *Arabidopsis* defense proteome occur prior to significant transcriptional change in response to inoculation with *Pseudomonas syringae*. *Plant Physiol.* 142, 1603–1620. doi: 10.1104/pp.106.086231
- Kandasamy, S., Loganathan, K., Muthuraj, R., Duraisamy, S., Seetharaman, S., Thiruvengadam, R., et al. (2009). Understanding the molecular basis of plant growth promotional effect of *Pseudomonas fluorescens* on rice through protein profiling. *Proteome Sci.* 7, 9143–9148. doi: 10.1186/1477-5956-7-47
- Kim, Y. S., Kotnala, B., Kim, Y. H., and Jeon, Y. (2015). Biological characteristics of *Paenibacillus polymyxa* GBR-1 involved in root rot of stored Korean ginseng. *J. Ginseng Res.* 40, 453–461. doi: 10.1016/j.jgr.2015.09.003
- Kloepper, J., and Metting F. Jr. (1992). "Plant growth-promoting rhizobacteria as biological control agents," in *Soil Microbial Ecology: Applications in Agricultural and Environmental Management*, ed F. B. Metting (New York, NY: Marcel Dekker), 255–274.
- Kochar, M., Upadhyay, A., and Srivastava, S. (2011). Indole-3-acetic acid biosynthesis in the biocontrol strain *Pseudomonas fluorescens* Psd and plant growth regulation by hormone overexpression. *Res. Microbiol.* 162, 426–435. doi: 10.1016/j.resmic.2011.03.006
- Konishi, H., Ishiguro, K., and Komatsu, S. (2001). A proteomics approach towards understanding blast fungus infection of rice grown under different levels of nitrogen fertilization. *Proteomics* 1, 1162–1171. doi: 10.1002/1615-9861(200109)1:9<1162::AID-PROT1162>3.0.CO;2-S
- Krebbehl, G., Ruckerbauer, S., Burbulla, L. F., Kieper, N., Maurer, B., Waak, J., et al. (2010). Reduced basal autophagy and impaired mitochondrial dynamics due to loss of Parkinson's disease-associated protein DJ-1. *PLoS ONE* 5:e9367. doi: 10.1371/journal.pone.0009367
- Kwon, K., Choi, D., Hyun, J. K., Jung, H. S., Baek, K., and Park, C. (2013). Novel glyoxalases from *Arabidopsis thaliana*. *FEBS J.* 280, 3328–3339. doi: 10.1111/febs.12321
- Kwon, Y. S., Lee, D. Y., Rakwal, R., Baek, S.-B., Lee, J. H., Kwak, Y.-S., et al. (2016). Proteomic analyses of the interaction between the plant-growth promoting rhizobacterium *Paenibacillus polymyxa* E681 and *Arabidopsis thaliana*. *Proteomics* 16, 122–135. doi: 10.1002/pmic.201500196
- Laemmli, U. K. (1970). Cleavage of structural proteins during the assembly of the head of bacteriophage T4. *Nature* 227, 680–685. doi: 10.1038/227680a0
- Laloi, C., Mestresortega, D., Marco, Y., Meyer, Y., and Reichheld, J. P. (2004). The *Arabidopsis* cytosolic thioredoxin h5 gene induction by oxidative stress and its W-box-mediated response to pathogen elicitor. *Plant Physiol.* 134, 1006–1016. doi: 10.1104/pp.103.035782
- Li, B., He, L., Guo, S., Li, J., Yang, Y., Yan, B., et al. (2013a). Proteomics reveal cucumber Spd-responses under normal condition and salt stress. *Plant Physiol. Biochem.* 67, 7–14. doi: 10.1016/j.plaphy.2013.02.016
- Li, J., McConkey, B. J., Cheng, Z., Guo, S., and Glick, B. R. (2013b). Identification of plant growth-promoting bacteria-responsive proteins in cucumber roots under hypoxic stress using a proteomic approach. *J. Proteomics* 84, 119–131. doi: 10.1016/j.jprot.2013.03.011

- Li, L., Ma, J., Li, Y., Wang, Z., Gao, T., and Wang, Q. (2012). Screening and partial characterization of *Bacillus* with potential applications in biocontrol of cucumber *Fusarium* wilt. *Crop Protect.* 35, 29–35. doi: 10.1016/j.cropro.2011.12.004
- Lieberherr, D., Wagner, U., Dubuis, P. H., Métraux, J. P., and Mauch, F. (2003). The rapid induction of glutathione S-transferases AtGSTF2 and AtGSTF6 by avirulent *Pseudomonas syringae* is the result of combined salicylic acid and ethylene signaling. *Plant Cell Physiol.* 44, 750–757. doi: 10.1093/pcp/pcg093
- Lin, Y., Du, D., Si, C., Zhao, Q., Li, Z., and Li, P. (2014). Potential biocontrol *Bacillus* sp. strains isolated by an improved method from vinegar waste compost exhibit antibiosis against fungal pathogens and promote growth of cucumbers. *Biol. Control* 71, 7–15. doi: 10.1016/j.biocontrol.2013.12.010
- Ling, N., Huang, Q., Guo, S., and Shen, Q. (2011). *Paenibacillus polymyxa* SQR-21 systemically affects root exudates of watermelon to decrease the conidial germination of *Fusarium oxysporum* f. sp. *niveum*. *Plant Soil* 341, 485–493. doi: 10.1007/s11104-010-0660-3
- Livak, K. J., and Schmittgen, T. D. (2001). Analysis of relative gene expression data using real-time quantitative PCR and the $2^{-\Delta\Delta CT}$ Method. *Methods* 25, 402–408. doi: 10.1006/mpmeth.2001.1262
- Martínez-Viveros, O., Jorquera, M. A., Crowley, D. E., Gajardo, G., and Mora, M. L. (2010). Mechanisms and practical considerations involved in plant growth promotion by rhizobacteria. *J. Soil Sci. Plant Nutr.* 10, 293–319. doi: 10.4067/s0718-95162010000100006
- Mou, Z., He, Y., Dai, Y., Liu, X., and Li, J. (2000). Deficiency in fatty acid synthase leads to premature cell death and dramatic alterations in plant morphology. *Plant Cell* 12, 405–418. doi: 10.1105/tpc.12.3.405
- Nam, M. H., Sun, M. H., Kim, K. M., Park, W. J., Seo, J. B., Cho, K., et al. (2011). Comparative proteomic analysis of early salt stress-responsive proteins in roots of SnRK2 transgenic rice. *Proteome Sci.* 10, 1–19. doi: 10.1186/1477-5956-10-25
- Ndimba, B. K., Chivasa, S., Simon, W. J., and Slabas, A. R. (2005). Identification of *Arabidopsis* salt and osmotic stress responsive proteins using two-dimensional difference gel electrophoresis and mass spectrometry. *Proteomics* 5, 4185–4196. doi: 10.1002/pmic.200401282
- Niu, D. D., Liu, H. X., Jiang, C. H., Wang, Y. P., Wang, Q. Y., Jin, H. L., et al. (2011). The plant growth-promoting rhizobacterium *Bacillus cereus* AR156 induces systemic resistance in *Arabidopsis thaliana* by simultaneously activating salicylate- and jasmonate/ethylene-dependent signaling pathways. *Mol. Plant Microbe Interact.* 24, 533–542. doi: 10.1094/MPMI-09-10-0213
- Onsga, M., Jourdan, E., Adam, A., Paquot, M., Brans, A., Joris, B., et al. (2007). Surfactin and fengycin lipopeptides of *Bacillus subtilis* as elicitors of induced systemic resistance in plants. *Environ. Microbiol.* 9, 1084–1090. doi: 10.1111/j.1462-2920.2006.01202.x
- Palacios, O. A., Bashan, Y., and De-Bashan, L. E. (2014). Proven and potential involvement of vitamins in interactions of plants with plant growth-promoting bacteria—an overview. *Biol. Fertil. Soils* 50, 415–432. doi: 10.1007/s00374-013-0894-3
- Palomares-Rius, J. E., Castillo, P., Navas-Cortés, J. A., Jiménez-Díaz, R. M., and Tena, M. (2011). A proteomic study of in-root interactions between chickpea pathogens: the root-knot nematode *Meloidogyne artiellia* and the soil-borne fungus *Fusarium oxysporum* f. sp. *ciceris* race 5. *J. Proteomics* 74, 2034–2051. doi: 10.1016/j.jprot.2011.05.026
- Polge, C., Jaquinod, M., Holzer, F., Bourguignon, J., Walling, L., and Brouquisse, R. (2009). Evidence for the existence in *Arabidopsis thaliana* of the proteasome proteolytic pathway: activation in response to cadmium. *J. Biol. Chem.* 284, 35412–35424. doi: 10.1074/jbc.M109.035394
- Qi, Y. C., Wang, F. F., Hui, Z., and Liu, W. Q. (2010). Overexpression of *suadea salsa* S-adenosylmethionine synthetase gene promotes salt tolerance in transgenic tobacco. *Acta Physiol. Plant.* 32, 263–269. doi: 10.1007/s11738-009-0403-3
- Rogić, T., Horvatić, A., Tkalec, M., Cindrić, M., and Balen, B. (2015). Proteomic analysis of *Mammillaria gracilis* Pfeiff. *in vitro*-grown cultures exposed to iso-osmotic NaCl and mannitol. *Plant Cell Tissue Organ Cult.* 122, 127–146. doi: 10.1007/s11240-015-0756-9
- Santos, C. S., Pinheiro, M., Silva, A. I., Egas, C., and Vasconcelos, M. W. (2012). Searching for resistance genes to *Bursaphelenchus xylophilus* using high throughput screening. *BMC Genomics* 13, 1–16. doi: 10.1186/1471-2164-13-599
- Scheler, C., Durner, J., and Astier, J. (2013). Nitric oxide and reactive oxygen species in plant biotic interactions. *Curr. Opin. Plant Biol.* 16, 534–539. doi: 10.1016/j.pbi.2013.06.020
- Sengupta, D., Naik, D., and Reddy, A. R. (2015). Plant aldo-keto reductases (AKRs) as multi-tasking soldiers involved in diverse plant metabolic processes and stress defense: a structure-function update. *J. Plant Physiol.* 179, 40–55. doi: 10.1016/j.jplph.2015.03.004
- Shi, L., Du, N., Yuan, Y., Shu, S., Sun, J., and Guo, S. (2016). Vinegar residue compost as a growth substrate enhances cucumber resistance against the *Fusarium* wilt pathogen *Fusarium oxysporum* by regulating physiological and biochemical responses. *Environ. Sci. Pollut. Res. Int.* 23, 18277–18287. doi: 10.1007/s11356-016-6798-7
- Spaepen, S., Bossuyt, S., Engelen, K., Marchal, K., and Vanderleyden, J. (2014). Phenotypic and molecular responses of *Arabidopsis thaliana* roots as a result of inoculation with the auxin-producing bacterium *Azospirillum brasiliense*. *New Phytol.* 201, 850–861. doi: 10.1111/nph.12590
- Sun, L., Ren, H., Liu, R., Li, B., Wu, T., Sun, F., et al. (2010). An h-type thioredoxin functions in tobacco defense responses to two species of viruses and an abiotic oxidative stress. *Mol. Plant Microbe Interact.* 23, 1470–1485. doi: 10.1094/MPMI-01-10-0029
- Szewczyk, B., Hoyos-Carvajal, L., Paluszek, M., Skrzecz, I., and Lobo de Souza, M. (2006). Baculoviruses—re-emerging biopesticides. *Biotechnol. Adv.* 24, 143–160. doi: 10.1016/j.biotechadv.2005.09.001
- Taira, T., Saito, Y., Niki, T., Iguchi-Ariga, S. M., Takahashi, K., and Ariga, H. (2004). DJ-1 has a role in antioxidative stress to prevent cell death. *EMBO Rep.* 5, 213–218. doi: 10.1038/sj.emboj.7400074
- Tamehiro, N., Okamoto-Hosoya, Y., Okamoto, S., Ubukata, M., Hamada, M., Naganawa, H., et al. (2002). Bacilysocin, a novel phospholipid antibiotic produced by *Bacillus subtilis* 168. *Antimicrob. Agents Chemother.* 46, 315–320. doi: 10.1128/AAC.46.2.315-320.2002
- Thompson, J. E., Hopkins, M. T., Taylor, C., and Wang, T. W. (2004). Regulation of senescence by eukaryotic translation initiation factor 5A: implications for plant growth and development. *Trends Plant Sci.* 9, 174–179. doi: 10.1016/j.tplants.2004.02.008
- Thornalley, P. J. (1996). Pharmacology of methylglyoxal: formation, modification of proteins and nucleic acids, and enzymatic detoxification—A role in pathogenesis and antiproliferative chemotherapy. *Gen. Pharmacol.* 27, 565–573. doi: 10.1016/0306-3623(95)02054-3
- Tjamos, S. E., Flemetakis, E., Paplomatas, E. J., and Katinakis, P. (2005). Induction of resistance to *Verticillium dahliae* in *Arabidopsis thaliana* by the biocontrol agent K-165 and pathogenesis-related proteins gene expression. *Mol. Plant Microbe Interact.* 18, 555–561. doi: 10.1094/MPMI-18-0555
- Tremblay, A., Hosseini, P., Alkharrout, N. W., Li, S., and Matthews, B. F. (2010). Transcriptome analysis of a compatible response by Glycine max to *Phakopsora pachyrhizi* infection. *Plant Sci.* 179, 183–193. doi: 10.1016/j.plantsci.2010.04.011
- Vieira Dos Santos, C., and Rey, P. (2006). Plant thioredoxins are key actors in the oxidative stress response. *Trends Plant Sci.* 11, 329–334. doi: 10.1016/j.tplants.2006.05.005
- Wang, F. X., Ma, Y. P., Yang, C. L., Zhao, P. M., Yuan, Y., Jian, G. L., et al. (2011). Proteomic analysis of the sea-island cotton roots infected by wilt pathogen *Verticillium dahliae*. *Proteomics* 11, 4296–4309. doi: 10.1002/pmic.201100062
- Wang, W., Chen, L. N., Wu, H., Zang, H., Gao, S., Yang, Y., et al. (2013). Comparative proteomic analysis of rice seedlings in response to inoculation with *Bacillus cereus*. *Lett. Appl. Microbiol.* 56, 208–215. doi: 10.1111/lam.12035
- Wang, X., Oh, M. W., and Komatsu, S. (2016). Characterization of S-adenosylmethionine synthetases in soybean under flooding and drought stresses. *Biol. Plant* 60, 269–278. doi: 10.1007/s10535-016-0586-6
- Witzel, K., Weidner, A., Surabhi, G. K., Börner, A., and Mock, H. P. (2009). Salt stress-induced alterations in the root proteome of barley genotypes with contrasting response towards salinity. *J. Exp. Bot.* 60, 3545–3557. doi: 10.1093/jxb/erp198
- Xu, L., Liu, Z. Y., Zhang, K., Lu, Q., Liang, J., and Zhang, X. Y. (2013). Characterization of the *Pinus massoniana* transcriptional response to *Bursaphelenchus xylophilus* infection using suppression subtractive hybridization. *Int. J. Mol. Sci.* 14, 11356–11375. doi: 10.3390/ijms14061356

- Xu, Q., Zou, Q., Zheng, H., Zhang, F., Tang, B., and Wang, S. (2011). Three heat shock proteins from *Spodoptera exigua*: gene cloning, characterization and comparative stress response during heat and cold shocks. *Comp. Biochem. Physiol. B Biochem. Mol. Biol.* 159, 92–102. doi: 10.1016/j.cbpb.2011.02.005
- Xu, Z., Zhang, R., Wang, D., Qiu, M., Feng, H., Zhang, N., et al. (2014). Enhanced control of cucumber wilt disease by *Bacillus amyloliquefaciens* SQR9 by altering the regulation of its degu phosphorylation. *Appl. Environ. Microbiol.* 80, 2941–2950. doi: 10.1128/AEM.03943-13
- Yang, X., Chen, L., Yong, X., and Shen, Q. (2010). Formulations can affect rhizosphere colonization and biocontrol efficiency of *Trichoderma harzianum* SQR-T037 against *Fusarium* wilt of cucumbers. *Biol. Fertil. Soils* 47, 239–248. doi: 10.1007/s00374-010-0527-z
- Youssef, S. A., Tartoura, K. A., and Abdelraouf, G. A. (2016). Evaluation of *Trichoderma harzianum* and *Serratia proteamaculans* effect on disease suppression, stimulation of ROS-scavenging enzymes and improving tomato growth infected by *Rhizoctonia solani*. *Biol. Control.* 100, 79–86. doi: 10.1016/j.bioccontrol.2016.06.001
- Yuan, Y., Zhong, M., Shu, S., Du, N., Sun, J., and Guo, S. (2016). Proteomic and physiological analyses reveal putrescine responses in roots of cucumber stressed by NaCl. *Front. Plant Sci.* 7:1035. doi: 10.3389/fpls.2016.01035
- Zamioudis, C., Korteland, J., Van Pelt, J. A., van Hamersveld, M., Dombrowski, N., Bai, Y., et al. (2015). Rhizobacterial volatiles and photosynthesis-related signals coordinate MYB72 expression in *Arabidopsis* roots during onset of induced systemic resistance and iron-deficiency responses. *Plant J.* 84, 309–322. doi: 10.1111/tpj.12995
- Zhang, D., Meng, K. X., Hao, Y. H., Fan, H. Y., Cui, N., Wang, S. S., et al. (2016). Comparative proteomic analysis of cucumber roots infected by *Fusarium oxysporum* f. sp. *Cucumerium* Owen. *Physiol. Mol. Plant Pathol.* 96, 77–84. doi: 10.1016/j.pmp.2016.09.002
- Zhang, H., Wang, W. Q., Liu, S. J., Moller, I. M., and Song, S. Q. (2015). Proteome analysis of poplar seed vigor. *PLoS ONE* 10:e0132509. doi: 10.1371/journal.pone.0132509
- Zhao, Q., Leung, S., Corbett, A. H., and Meier, I. (2006). Identification and characterization of the *Arabidopsis* orthologs of nuclear transport factor 2, the nuclear import factor of ran. *Plant Physiol.* 140, 869–878. doi: 10.1104/pp.105.075499
- Zhong, M., Yuan, Y., Shu, S., Sun, J., Guo, S., Yuan, R., et al. (2015). Effects of exogenous putrescine on glycolysis and Krebs cycle metabolism in cucumber leaves subjected to salt stress. *Plant Growth Regul.* 79, 319–330. doi: 10.1007/s10725-015-0136-9
- Zhou, C., Guo, J., Zhu, L., Xiao, X., Xie, Y., Zhu, J., et al. (2016). *Paenibacillus polymyxa* BFKC01 enhances plant iron absorption via improved root systems and activated iron acquisition mechanisms. *Plant Physiol. Biochem.* 105, 162–173. doi: 10.1016/j.plaphy.2016.04.025

Conflict of Interest Statement: The authors declare that the research was conducted in the absence of any commercial or financial relationships that could be construed as a potential conflict of interest.

Copyright © 2016 Du, Shi, Yuan, Li, Shu, Sun and Guo. This is an open-access article distributed under the terms of the Creative Commons Attribution License (CC BY). The use, distribution or reproduction in other forums is permitted, provided the original author(s) or licensor are credited and that the original publication in this journal is cited, in accordance with accepted academic practice. No use, distribution or reproduction is permitted which does not comply with these terms.



Proteomic Analysis Reveals the Positive Effect of Exogenous Spermidine in Tomato Seedlings' Response to High-Temperature Stress

Qinqin Sang¹, Xi Shan¹, Yahong An¹, Sheng Shu¹, Jin Sun^{1,2} and Shirong Guo^{1,2*}

¹ Key Laboratory of Southern Vegetable Crop Genetic Improvement in Ministry of Agriculture, College of Horticulture, Nanjing Agricultural University, Nanjing, China, ² Nanjing Agricultural University (Suqian), Academy of Protected Horticulture, Suqian, China

OPEN ACCESS

Edited by:

Jie Zhou,
Zhejiang University, China

Reviewed by:

Caiji Gao,
South China Normal University, China
Hao Wang,
South China Agricultural University,
China

***Correspondence:**

Shirong Guo
srguo@njau.edu.cn

Specialty section:

This article was submitted to
Plant Cell Biology,
a section of the journal
Frontiers in Plant Science

Received: 18 October 2016

Accepted: 20 January 2017

Published: 06 February 2017

Citation:

Sang Q, Shan X, An Y, Shu S, Sun J and Guo S (2017) Proteomic Analysis Reveals the Positive Effect of Exogenous Spermidine in Tomato Seedlings' Response to High-Temperature Stress. *Front. Plant Sci.* 8:120.
doi: 10.3389/fpls.2017.00120

Polyamines are phytohormones that regulate plant growth and development as well as the response to environmental stresses. To evaluate their functions in high-temperature stress responses, the effects of exogenous spermidine (Spd) were determined in tomato leaves using two-dimensional electrophoresis and MALDI-TOF/TOF MS. A total of 67 differentially expressed proteins were identified in response to high-temperature stress and/or exogenous Spd, which were grouped into different categories according to biological processes. The four largest categories included proteins involved in photosynthesis (27%), cell rescue, and defense (24%), protein synthesis, folding and degradation (22%), and energy and metabolism (13%). Exogenous Spd up-regulated most identified proteins involved in photosynthesis, implying an enhancement in photosynthetic capacity. Meanwhile, physiological analysis showed that Spd could improve net photosynthetic rate and the biomass accumulation. Moreover, an increased high-temperature stress tolerance by exogenous Spd would contribute to the higher expressions of proteins involved in cell rescue and defense, and Spd regulated the antioxidant enzymes activities and related genes expression in tomato seedlings exposed to high temperature. Taken together, these findings provide a better understanding of the Spd-induced high-temperature resistance by proteomic approaches, providing valuable insight into improving the high-temperature stress tolerance in the global warming epoch.

Keywords: antioxidant, high-temperature stress, proteomics, spermidine, tomato

INTRODUCTION

High-temperature stress represents one of the most frequent abiotic stresses worldwide, inducing several physiological and biochemical processes in cells, and limiting the growth and productivity of plants (Bita and Gerats, 2013). Plants respond to high temperature by reprogramming their proteome, metabolome and transcriptome to establish a new steady-state balance of metabolic processes (Kosová et al., 2011; Lin H. H. et al., 2015; Sruthi et al., 2016).

Polyamines (PAs) are ubiquitous low-molecular-weight aliphatic amines, and include putrescine (Put), spermidine (Spd), and spermine (Spm). PAs are known to participate in the regulation

of physiological and developmental processes (Liu et al., 2007; Gupta et al., 2013), and they are also involved in the defense reaction of plants against various environmental stresses (Todorova et al., 2007; Berberich et al., 2015; Pál et al., 2015). The integration of environmental stimuli, signal transduction and the stress response is mediated, at least partially, by intensive cross-talk among plant hormones (Wahid et al., 2007). Recent studies indicated that polyamines act as cellular signals in the intricate cross talk with different metabolic routes and complex hormonal pathways (Pál et al., 2015). The exogenous Spd enhancement of high-temperature stress tolerance via the involvement of antioxidant ability and photosynthetic efficiency had been described (Tian et al., 2012; Mostofa et al., 2014), but little information about Spd regulating proteomic changes under the high-temperature stress is available.

As mRNA abundance is not enough to provide information about the proteins, proteomic analysis has become a powerful tool to elucidate the mechanisms of plant stress tolerance (Skalák et al., 2016). Previous studies reported that PAs could bind to charged spots at protein interfaces and modulate electrostatic protein–protein interactions to regulate the protein functions (Berwanger et al., 2010). Exogenous polyamines had been found to activate multiple pathways that conferred increased salt and drought tolerances in bermudagrass by reprogramming the proteome (Shi et al., 2013). Li et al. (2013) and Yuan et al. (2016) showed that application of Spd/Put changed the expression of proteins and contributed to counteract the damage induced by salt stress in cucumber seedlings. Igarashi and Kashiwagi (2015) reported that polyamines could stimulate the synthesis of proteins at the translation level due to the formation of a polyamine-RNA complex.

The tomato (*Lycopersicon esculentum*) is one of the most important vegetables from both the nutritional and economic points of view. The effects of exogenous Spd in enhancing the stress tolerance had been described in cucumber (Tian et al., 2012) and in rice (Mostofa et al., 2014). However, little information is available to explain the specific mechanisms by which PAs regulate the high-temperature stress responses through a proteomic approach. In this study, we investigated the differentially expressed proteins in tomato leaves through 2-dimensional gel electrophoresis to better understand the underlying mechanisms of Spd application in high-temperature stress resistance.

MATERIALS AND METHODS

Plant Materials and Treatments

Tomato (*Lycopersicon esculentum* Mill. cv. Puhong 968) seeds were obtained from the Shanghai Academy of Agricultural Sciences, China. Seeds were germinated and grown in plastic nutrition pots filled with growth media (Zhenjiang Peilei Co., Ltd., China). The germinated seedlings were grown under controlled condition (light intensity, $600 \mu\text{mol m}^{-2}\text{s}^{-1}$; day/night temperature, $25/18^\circ\text{C}$; light/dark photoperiod, 14 h/10 h; relative humidity, 55–65%) in growth chambers (Ningbo Jiangnan Instrument Factory, Ningbo, China).

After the third true leaf developed, the seedlings were subjected to high-temperature (day/night temperature, $38/28^\circ\text{C}$; light/dark photoperiod, 14/10 h; relative humidity, 55–65%). The experimental plots included four different treatments: (1) Cont; (2) Spd (1 mM); (3) HT; (4) HT + Spd (1 mM). The concentration of Spd was selected on the basis of previous experiment (data not shown). One millimole Spd was sprayed to leaves at 17:00 every day, and the control plants were sprayed with distilled water. After 7 days of treatment, the third fully expanded tomato leaves of each treatment were stored at -80°C for physiological and proteomic analysis. The experiment was arranged in a randomized complete block design and biological replicates were independently carried out three times.

Measurement of Dry Weight, Chlorophyll Content, and Net Photosynthetic Rate (Pn)

The tomato seedlings were washed with sterile distilled water. After wiped with gauze, samples were dried in an oven at 105°C for 15 min followed by 75°C for 72 h, until reaching a constant weight, and then weighed for dry weight. Chlorophyll was extracted with a mixture of acetone, ethanol and water (4.5: 4.5: 1 by volume) and its content was estimated using the method of Arnon (1949). Pn was measured using a portable photosynthesis system (LI-6400, LI-COR Inc, USA).

Protein Extraction

Protein extraction was performed according to a modified version of the trichloroacetic acid (TCA) acetone precipitation method described by Hurkman and Tanaka (1986). Frozen leaf tissues were ground in liquid nitrogen and suspended in ice-cold extraction buffer (8 M urea, 1% (w/v) dithiothreitol (DTT), 4% (w/v) CHAPS and 40 mM Tris). Then the homogenates were centrifuged at $15,000 \times g$ for 20 min at 4°C , and the supernatants were precipitated overnight with ice-cold acetone containing 10% (w/v) TCA and 0.07% (v/v) β -mercaptoethanol. The resulting protein-containing suspensions were centrifuged at $20,000 \times g$ for 30 min at 4°C , and then the protein pellets were washed three times with cold acetone containing 0.07% (v/v) β -mercaptoethanol. Finally, the protein pellets were air-dried at room temperature and dissolved in rehydration buffer (8 M urea, 1 M thiourea, 2% w/v CHAPS). The protein concentrations were determined by the methods of Bradford (1976) using bovine serum albumin as the standard, and then the protein was stored at -80°C until being subjected to two-dimensional gel electrophoresis (2-DE).

2-DE

For first dimensional isoelectric focusing (IEF), IPG strips (GE Healthcare, San Francisco, CA, USA, 17 cm, pH 4–7 linear gradient) were used according to the methods of Li et al. (2013). The dry IPG strips were rehydrated at room temperature for 12–16 h in $350 \mu\text{L}$ rehydration solution [8 M (w/v) urea, 1 M (w/v) thiourea, 2% (w/v) CHAPS, 65 mM DTT, 0.8% (v/v) IPG buffer 4–7, and 1% (w/v) bromophenol blue]. Following rehydration, the IPG strips were run on an Ettan IPGphor 3 (GE Healthcare, USA) with a gradient of 100 V (1 h), 200 V (1 h), 200 V (1 h), 500 V (1 h), 1000 V (1 h), 4000 V (1 h), and 10,000 V (1 h), finally

reaching a value of 75,000 V h. The working temperature was maintained at 20°C with a maximum current of 50 mA per strip. After the first dimension, the IEF strips were equilibrated for 15 min in equilibration solution I [1% (w/v) DTT, 6 M urea, 30% (v/v) glycerol, 2% (w/v) SDS, and 50 mM Tris-HCl (pH 8.8)], and then in equilibration solution II [2.5% (w/v) iodoacetamide, 6 M urea, 30% (v/v) glycerol, 2% (w/v) SDS, and 50 mM Tris-HCl (pH 8.8)] for 15 min.

The second dimensional SDS-polyacrylamide gel electrophoresis was performed on running gels (Hoefer SE600 Ruby Standard Vertical System, GE Healthcare; 12.5% polyacrylamide) as described by Laemmli (1970). The strips were embedded on the top of the SDS gel and then sealed with 1% molten agarose solution. Electrophoresis was carried out at 15 mA per gel until the bromophenol blue dye reached the bottom of the gel. After the 2-DE, the gels were stained overnight with Coomassie Brilliant Blue (CBB) R-250 solution (0.1% (w/v) of CBB R-250 in 1:4:5 (v/v) methanol: acetic acid: deionized water) and destained with a 1:1:8 (v/v) methanol: acetic acid: deionized water solution with several changes, until a colorless background was achieved.

Image and Data Analysis

The 2-D gels were scanned with an Image Scanner III (GE Healthcare, San Francisco, USA). Spot detection, quantification and matching were performed with Imagemaster™ 2D Platinum software (version 6.0, GE Healthcare, San Francisco, USA). The intensity of each spot on the 2-D gels was quantified based on the volumes percentage (vol. %). Only spots with significant changes (at least 1.5-fold quantitative changes, $P < 0.05$) were considered to be differentially expressed.

Protein Identification

The protein spots were excised from the polyacrylamide gels, and identified using MALDI-TOF/TOF MS by an Ultraflex II mass spectrometer (Applied Biosystems, Foster City, CA, USA). The resulting peptide mass lists were searched in NCBI (<http://www.ncbi.nlm.nih.gov>) using the software MASCOT version 2.1 (Matrix Science, London, UK). The parameter criteria were as follows: trypsin cleavage, one missed cleavage allowed; carbamidomethyl (C) set as a fixed modification; oxidation of methionines allowed as a variable modification; peptide mass tolerance within 100 ppm; fragment tolerance set to ± 0.4 Da; and minimum ion score confidence interval for MS/MS data set to 95%.

The classification of the identified proteins was performed by searching in the UniProt Knowledgebase (UniProtKB, <http://www.uniprot.org>).

Hierarchical Cluster Analysis and Interaction Network

The hierarchical clustering of the protein expression patterns was performed on the \log_2 transformed vol. % of each protein spot using Cluster software (version 3.0). The complete linkage algorithm was enabled, and the results were plotted using Treeview software (version 1.60).

Mapping of the interaction network was performed using the STRING database (<http://string.embl.de>) based on conformed and predicted interactions.

Enzyme Activity Analysis

Ascorbate peroxidase (APX, EC 1.11.1.11) activity was determined according to Nakano and Asada (1981) by measuring the rate of ascorbate oxidation at 290 nm ($\epsilon = 2.8 \text{ mM}^{-1} \text{ cm}^{-1}$). Dehydroascorbate reductase (DHAR, EC 1.8.5.1) activity was calculated from the change in absorbance at 265 nm and the extinction coefficient of $14 \text{ mM}^{-1} \text{ cm}^{-1}$, as described by Nakano and Asada (1981). Superoxide dismutase (SOD, EC 1.15.1.1) activity was calculated by inhibiting the photochemical reduction of NBT at 560 nm. One unit of SOD activity was defined as the amount of enzyme that caused 50% inhibition of NBT reduction rate (Becana et al., 1986).

Total RNA Extraction and Quantitative Real-Time PCR (qRT-PCR) Analysis

The total RNA was extracted from the tomato leaf tissues as described in the TRI reagent protocol (Takara Bio Inc.). The total RNA and cDNA syntheses were performed according to the manufacturer's instructions. The primers were designed according to the NCBI (Supplementary Table 1). qRT-PCR was performed with the SYBR PrimeScript™ RT-PCR Kit (Takara Bio Inc.) according to the manufacturer's instructions. All experiments were repeated three times and the relative gene expression was calculated by the $2^{-\Delta\Delta Ct}$ method.

Statistical Analysis

All biochemical analyses were conducted at least three times. Data were statistically analyzed with statistical software SPSS 17.0 (SPSS Inc., Chicago, IL, USA) using Duncan's multiple range test at the $P < 0.05$ level of significance.

RESULTS

Morphological and Physiological Responses

After 7 days' treatment with exogenous Spd, no significant differences were observed in the tomato leaves under non-stressful conditions. Phenotypic observations showed that the untreated high-temperature stressed seedlings exhibited chlorosis and yellowing, whereas the Spd-treated seedlings had a better visual appearance (Figure 1A). Under the high-temperature stress, the dry weight, chlorophyll content and net photosynthetic rate (Pn) decreased by 33.0, 16.4, and 58.9%, respectively. However, exogenous Spd application resulted in improvements in these parameters (Figure 1).

Proteomic Analysis

To reveal the protective effect of exogenous Spd on the tomato under high-temperature stress, a total of 67 differentially expressed spots were identified using 2-DE and MALDI-TOF-MS (Figure 2, Table 1, Supplementary Figure 1). To better understand which physiological process was regulated by Spd under the high-temperature stress, the identified proteins

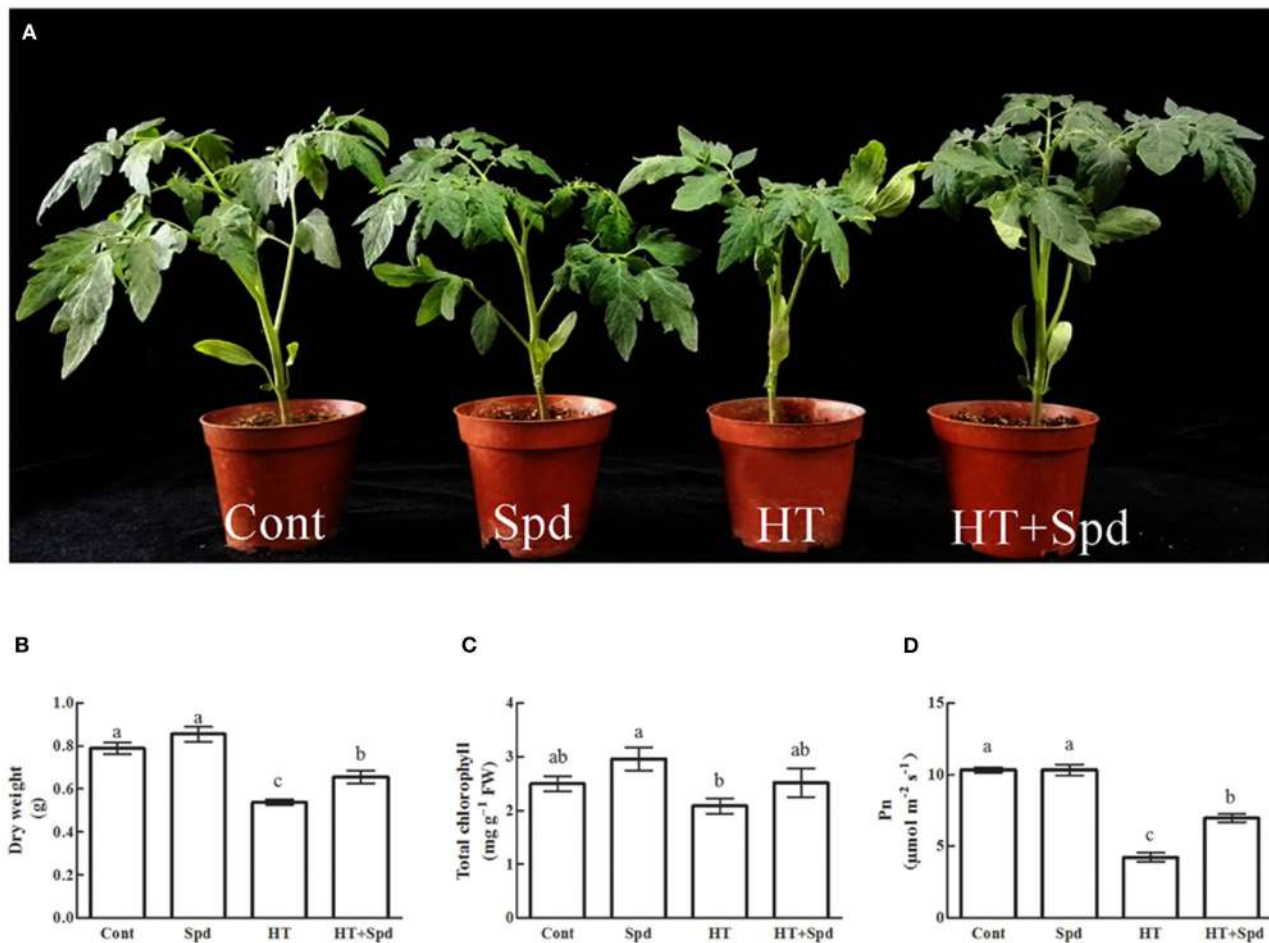


FIGURE 1 | Effects of Spd on plant morphology (A), dry weight (B), chlorophyll content (C), and Pn (D) in leaves of tomato exposed to high temperature stress. Cont, control plants under 25/18°C (day/night); Spd, plants under 25/18°C with 1 mM Spd foliar spraying; HT, plants under 38/28°C; HT+Spd, plants under 38/28°C with 1 mM Spd foliar spraying. Each histogram represents a mean \pm SE of three independent experiments ($n = 3$). Different letters indicate significant differences between treatments ($P < 0.05$) according to Duncan's multiple range tests.

were grouped into 7 categories based on their biological functions according to Gene Ontology (Figure 3). Among the 67 proteins, the majority were sorted into photosynthesis (27%), followed by cell rescue and defense (24%), protein synthesis, folding, and degradation (22%), energy and metabolism (13%), amino acid metabolism (5%), signal transduction (5%), and unknown (4%).

Compared with the control, there were 33 up-regulated spots and 32 down-regulated spots in response to the high-temperature stress (Figure 4A). For the high-temperature stress induced proteins, the most highly enriched category was cell rescue and defense. However, exogenous Spd up-regulated 35 spots and down-regulated 26 spots compared with the untreated seedlings subjected to high-temperature stress, and of these proteins, the most prevalent category was photosynthesis (Figure 4B).

To obtain a comprehensive overview of the differentially expressed proteins, hierarchical cluster analysis was conducted

to categorize the proteins that showed differential expression profiles affected by Spd under the normal and high-temperature stress conditions (Figure 5).

Antioxidant Enzymes and Related Genes Expression Analysis

The proteomic results revealed that the abundances of some antioxidant enzymes (spots 25, 29, 35, 36) were changed (Figure 6A), so we further analyzed the associated antioxidant enzyme activities (APX, DHAR, SOD) and related gene expressions (APX 2, APX 6, DHAR 1, DHAR 2, Fe SOD, Cu/Zn SOD). The activities of the enzymes showed significant decreases under high-temperature stress. However, exogenous Spd remarkably increased their activity compared with the high-temperature stress alone (Figure 6B). A similar trend was observed for the expression levels of most of the antioxidant enzyme related genes (Figure 6C).

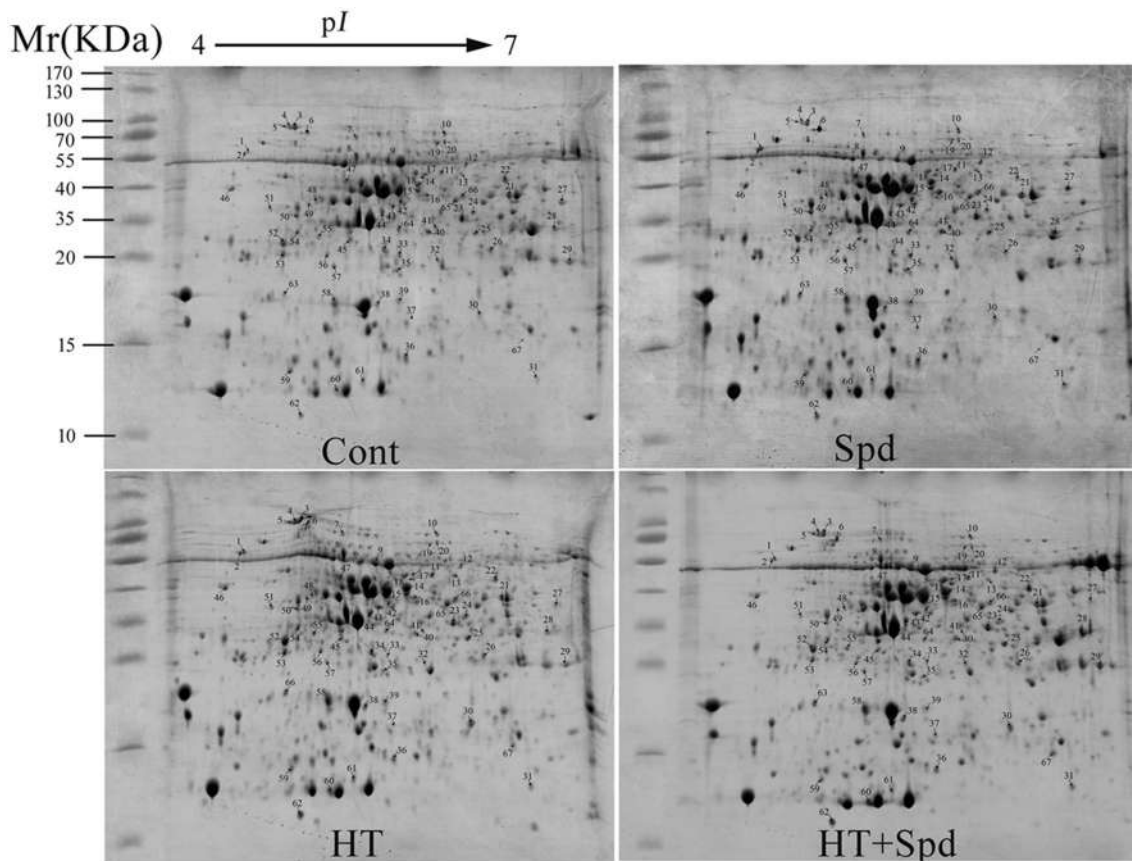


FIGURE 2 | Coomassie Brilliant blue (R-250)-stained 2-DE gels. Spot numbers indicate the 67 identified differentially expressed proteins. The range of the molecular mass of protein markers was from 10 to 170 kDa.

Interaction Network Analysis

The proteins act together in the context of networks in cells, rather than performing their functions in an isolated manner (Bian et al., 2015). The STRING database provides a critical assessment and integration of protein–protein interactions, including direct (physical) as well as indirect (functional) associations. A network was used to show the interactions of the identified proteins and revealed the potential information at the protein level (Figure 7). Most energy metabolism related proteins (86.7%) and cell rescue and defense (68.8%) were involved in the protein–protein interaction network. Among the interaction proteins, the energy metabolism related proteins represented the highest proportion (35.1%). More importantly, GAPDH (spot 22) and phosphoglycerate kinase (spot 18) were the important junctions of interacting proteins in the network, suggesting that energy was of the utmost importance for the response to high temperature stress with exogenous Spd treatment.

DISCUSSION

Polyamines are known to effectively alleviate the plant growth inhibition by abiotic stress. In this study, exogenous Spd was shown to promote the growth and improve the photosynthetic

capacity of the tomato under high-temperature stress (Figure 1), which is consistent with a previous finding in rice (Mostofa et al., 2014). 2-DE analysis was conducted, and 67 differentially regulated proteins were identified in response to high temperature and/or exogenous Spd (Figure 2, Table 1). The regulation of the metabolic processes by Spd and high temperature is discussed below.

Photosynthesis-Related Proteins

Photosynthesis is highly sensitive to high-temperature stress and is often inhibited before other cell functions are impaired (Mathur et al., 2014). Importantly, Rubisco and Rubisco activase (RCA) are the primary limiting factors of net photosynthesis under stress (Ahsan et al., 2007; Hu et al., 2015). In this study, we found that proteins related to Rubisco (spots 6, 28, 49) and RCA (spots 16, 64) markedly decreased in response to high-temperature stress, similar to other proteomic studies (Han et al., 2009; Lin K. H. et al., 2015). High temperature can reduce the activation state of Rubisco (Law and Crafts-Brandner, 1999), which is often attributed to the thermostability and loss of activity of RCA under high-temperature stress (Salvucci and Crafts-Brandner, 2004; Sharkey, 2005). However, exogenous Spd had positive effects on Rubisco and RCA in tomato leaves, suggesting

TABLE 1 | Leaf proteins responsive to high temperature stress and/or Spd identified by MALDI-TOF/TOF MS.

^a Spot No.	Protein name	Accession No.	^b Tpi/Epi	^c TMr/EMr (kDa)	Score	^d MP	^e Cov (%)	Fold changes			
								Cont/Cont	Spd/Cont	HT/Cont	HT+Spd/HT
PHOTOSYNTHESIS											
6	ruBisCO large subunit-binding protein subunit alpha	gi 460411525	5.21/4.90	62.03/69	313	17	37.24	1.00	2.02	0.28	2.92
11	glutamate 1-semialdehyde 2,1-aminomutase	gi 642911	6.54/5.84	51.72/46	858	18	56.13	1.00	0.90	1.51	0.62
13	glutamate 1-semialdehyde 2,1-aminomutase	gi 642911	6.54/5.99	51.72/45	361	15	47.61	1.00	1.12	1.68	0.65
14	ribulose bisphosphate carboxylase/oxygenase activase 1, chloroplastic isoform X1	gi 460401823	8.15/5.68	49.05/40	1070	26	70.52	1.00	1.54	2.96	0.88
15	ribulose bisphosphate carboxylase/oxygenase activase 1, chloroplastic isoform X1	gi 460401823	8.15/5.69	49.05/39	1120	28	73.92	1.00	1.07	1.89	0.74
16	Ribulose bisphosphate carboxylase/oxygenase activase, chloroplastic-like	gi 723739979	8.76/5.74	50.97/38	481	16	38.56	1.00	1.06	0.65	1.31
23	ferredoxin-NADP reductase, leaf-type isozyme, chloroplastic	gi 460373374	8.37/5.99	40.77/34	617	18	55.25	1.00	0.90	0.67	1.23
26	carbonic anhydrase	gi 56562177	6.67/6.21	34.84/25	563	16	63.55	1.00	0.72	0.80	1.29
28	ribulose 1,5-bisphosphate carboxylase/oxygenase large subunit (chloroplast)	gi 779776586	6.55/6.67	53.43/33	623	24	54.30	1.00	0.81	0.60	1.65
32	oxygen-evolving enhancer protein 1, chloroplastic	gi 823630968	5.91/5.83	35.15/25	582	13	52.89	1.00	1.20	0.00	+
39	oxygen-evolving enhancer protein 2, chloroplastic	gi 929045135	7.63/5.54	27.86/19	352	8	42.25	1.00	0.85	0.47	1.85
43	coproporphyrinogen-III oxidase 1, chloroplastic	gi 460405900	5.92/5.48	45.24/37	744	21	58.40	1.00	1.21	1.59	0.87
49	ribulose 1,5-bisphosphate carboxylase, partial (chloroplast)	gi 488453392	6.99/4.90	48.29/37	189	8	28.24	1.00	1.05	0.55	1.94
57	oxygen-evolving enhancer protein 1, chloroplastic	gi 823630968	5.91/5.09	35.15/24	692	14	56.53	1.00	1.32	0.52	1.61
60	ribulose-1,5-bisphosphate carboxylase/oxygenase small subunit	gi 170500	3.67/5.13	20.45/12	319	9	55.00	1.00	0.59	1.36	1.31
61	photosystem II reaction center Psb28 protein	gi 460403300	9.42/5.30	20.25/13	121	5	31.67	1.00	1.67	2.51	0.61
62	ribulose-1,5-bisphosphate carboxylase/oxygenase large subunit, partial (chloroplast)	gi 778481335	6.18/4.86	5.68/11	84	3	58.82	1.00	1.42	2.69	0.83
64	ribulose bisphosphate carboxylase/oxygenase activase, chloroplastic-like	gi 723739979	8.76/5.53	50.97/31	771	21	39.65	1.00	0.69	0.48	1.23
CELL RESCUE AND DEFENSE											
3	heat shock protein 70	gi 158635118	5.41/4.80	74.41/78	388	22	33.67	1.00	0.86	1.43	0.60
4	stromal 70 kDa heat shock-related protein, chloroplastic	gi 460369188	5.20/4.77	74.96/75	1230	33	54.48	1.00	0.76	1.86	0.49
5	stromal 70 kDa heat shock-related protein, chloroplastic	gi 460369188	5.20/4.74	74.96/77	1090	27	47.08	1.00	0.99	1.90	0.41
25	stromal ascorbate peroxidase	gi 807201017	8.48/6.11	38.07/29	945	23	76.81	1.00	1.13	1.56	0.94
29	dehydroascorbate reductase	gi 929524249	6.32/6.79	23.71/24	578	17	83.33	1.00	1.02	0.58	1.86
30	temperature-induced lipocalin'	gi 77744859	5.96/6.15	21.30/17	436	10	60.00	1.00	0.87	3.16	0.78
35	superoxide dismutase [Fe] (plastid)	gi 33413303	6.60/5.52	27.89/23	131	5	20.08	1.00	0.93	0.50	1.54
36	superoxide dismutase [Cu-Zn], chloroplastic	gi 915409259	6.02/5.62	22.38/14	760	6	58.53	1.00	1.08	0.64	1.06

(Continued)

TABLE 1 | Continued

^a Spot No.	Protein name	Accession No.	^b Tpi/Epi	^c TMr/EMr (kDa)	Score	^d MP	^e Cov (%)	Fold changes			
								Cont/Cont	Spd/Cont	HT/Cont	HT+Spd/HT
37	class I small heat shock protein	gi 349591296	5.57/5.59	17.62/16	551	12	73.38	0.00	0.00	+	1.74
41	thioredoxin-like protein CDSP32, chloroplastic	gi 460385401	7.57/5.81	33.78/32	175	12	39.19	1.00	1.15	0.49	1.73
44	2-oxoglutarate-dependent dioxygenase homolog, partial	gi 717140	6.82/5.40	25.86/36	518	11	43.61	1.00	0.65	1.36	0.79
45	plasma membrane-associated cation-binding protein 1	gi 460405902	5.03/5.20	21.98/28	275	12	73.63	1.00	1.22	2.55	0.57
58	23 kda heat-induced protein (N-terminal)	gi 1835994	3.75/5.10	27.86/19	134	1	87.50	1.00	1.19	1.77	0.67
59	inducible plastid-lipid associated protein	gi 75266304	5.81/4.79	18.30/13	391	8	70.69	1.00	0.98	1.41	0.65
63	2-Cys peroxiredoxin BAS1, chloroplastic	gi 460407951	6.00/4.74	29.73/20	87	3	10.11	1.00	1.92	1.96	0.48
67	class II small heat shock protein Le-HSP17.6	gi 1773291	6.32/6.46	17.67/15	191	7	53.80	0.00	0.00	+	1.41
AMINO ACID METABOLISM											
47	glutamine synthetase, chloroplastic	gi 460367196	6.29/5.16	47.85/41	552	17	40.74	1.00	1.15	0.48	1.42
48	cysteine synthase, chloroplastic/chromoplastic	gi 460398434	5.41/4.96	41.26/37	900	12	46.89	1.00	0.38	0.26	1.94
50	serine carboxypeptidase-like 20	gi 460393680	5.43/4.83	56.46/36	211	4	11.04	1.00	1.08	0.55	1.63
PROTEIN SYNTHESIS, FOLDING AND DEGRADATION											
7	ATP-dependent zinc metalloprotease FTSH 2, chloroplastic	gi 460395390	6.00/5.22	74.42/69	770	25	51.37	1.00	0.91	0.60	1.44
17	elongation factor TuB, chloroplastic-like	gi 460391817	6.69/5.72	56.29/46	98	10	22.97	1.00	0.74	0.58	1.18
20	putative inosine monophosphate cyclohydrolase	gi 260528216	6.21/5.87	66.20/66	269	16	31.67	1.00	0.81	0.69	1.49
33	proteasome subunit alpha type-2-A-like	gi 460405457	5.39/5.54	25.66/26	524	12	71.06	1.00	1.07	0.34	1.72
38	peptidyl-prolyl cis-trans isomerase FKBP16-3, chloroplastic	gi 460381848	6.75/5.37	25.76/18	324	8	30.64	1.00	1.25	1.59	0.80
46	ankyrin repeat domain-containing protein 2	gi 460369292	4.43/4.33	37.35/39	745	16	56.73	1.00	1.02	1.43	0.82
52	cysteine proteinase 3-like	gi 460396286	5.33/4.73	39.63/28	297	9	43.18	1.00	0.89	1.89	0.63
54	haloacid dehalogenase-like hydrolase domain-containing protein At3g48420	gi 460381143	5.67/4.83	34.50/31	697	17	58.04	1.00	0.92	1.34	0.73
66	mRNA binding protein precursor	gi 936975812	7.1/6.00	44.06/38	650	16	47.42	1.00	1.21	0.80	1.41
ENERGY AND METABOLISM											
8	ATP synthase CF1 alpha subunit (chloroplast)	gi 779776563	5.14/5.22	55.43/56	843	20	45.96	1.00	0.93	1.45	0.63
9	ATP synthase CF1 beta subunit (chloroplast)	gi 779776585	5.28/5.43	53.49/51	1560	26	75.30	1.00	1.08	1.93	0.66
10	transketolase, chloroplastic	gi 460406209	5.97/5.87	80.27/70	421	23	39.35	1.00	0.77	0.55	1.53
18	phosphoglycerate kinase, chloroplastic	gi 460396820	7.66/5.73	50.59/43	808	27	74.90	1.00	0.94	1.00	1.56
19	2,3-bisphosphoglycerate-independent phosphoglycerate mutase	gi 460396104	5.59/5.83	61.28/65	535	29	64.94	1.00	0.83	0.53	1.60
21	mitochondrial malate dehydrogenase	gi 927442679	8.73/6.34	36.29/38	642	12	50.58	1.00	0.94	0.68	1.28
22	glyceraldehyde-3-phosphate dehydrogenase B, chloroplastic-like	gi 460415552	6.72/6.28	48.54/41	459	16	37.33	1.00	0.84	0.49	2.05
24	fructose-bisphosphate aldolase 1, chloroplastic	gi 808175957	8.15/6.09	42.66/36	684	15	51.79	1.00	0.80	1.58	0.52
27	fructose-bisphosphate aldolase, cytoplasmic isozyme 1	gi 840084522	6.86/6.73	38.41/38	755	13	52.66	1.00	1.05	0.53	1.96
31	nucleoside diphosphate kinase	gi 575953	6.84/6.60	15.47/13	608	8	46.48	1.00	1.15	1.79	1.05
34	triosephosphate isomerase, chloroplastic	gi 460370086	6.45/5.45	35.04/25	769	19	70.55	1.00	1.09	1.71	0.88
42	fructose-bisphosphate aldolase 1, chloroplastic-like	gi 460375513	6.07/5.55	42.87/37	816	15	47.59	1.00	0.97	0.48	1.22

(Continued)

TABLE 1 | Continued

^a Spot No.	Protein name	Accession No.	^b Tpl/Epl	^c TMr/EMr (kDa)	Score	^d MP	^e Cov (%)	Fold changes			
								Cont/Cont	Spd/Cont	HT/Cont	HT+Spd/HT
53	ATP synthase beta subunit, partial (chloroplast)	gi 159227612	5.18/4.73	35.93/26	102	8	35.71	1.00	0.76	1.31	0.50
55	ribose-5-phosphate isomerase 3, chloroplastic	gi 460368501	6.00/4.95	31.19/31	458	6	28.33	1.00	1.11	0.65	0.99
65	malate dehydrogenase	gi 460404529	5.91/5.94	35.70/38	128	8	25.00	1.00	0.80	1.51	0.95
SIGNAL TRANSDUCTION											
1	calreticulin	gi 460368893	4.50/4.45	47.80/56	412	21	42.69	1.00	1.46	2.66	0.64
2	calreticulin	gi 460368893	4.50/4.42	47.80/56	439	20	52.28	1.00	2.38	1.97	0.53
56	harpin binding protein 1	gi 38679319	6.25/5.04	30.29/25	643	13	55.43	1.00	0.81	0.66	0.99
UNKNOWN											
12	Hop-interacting protein THI113	gi 365222922	5.82/6.04	37.34/50	507	13	69.14	1.00	1.26	0.82	2.47
40	unnamed protein product	gi 939066554	5.64/5.76	21.84/31	151	10	46.94	1.00	1.09	0.73	1.32
51	uncharacterized protein LOC101260160	gi 460398472	4.66/4.64	35.10/36	164	15	52.85	1.00	0.92	1.27	0.60

^aSpot numbers corresponding to spots in **Figure 1**.^bTpl and Epl are the theoretical isoelectric point and experimental isoelectric point, respectively.^cTMr and EMr are the theoretical molecular mass and experimental molecular mass, respectively.^dThe total number of identified peptides.^ePercentage of sequence coverage by matched peptides.

that the Calvin cycle and photosynthetic carbon assimilation were maintained at high levels, contributing to the biomass accumulation under high-temperature stress.

Ferredoxin-NADP reductase (spot 23) is the last enzyme in the transfer of electrons during photosynthesis from PS I to NADPH, producing NADPH for CO₂ assimilation (Fukuyama, 2004; Tian et al., 2015). Oxygen-evolving enhancer proteins (spots 32, 39, 57) are also involved in the light reaction of PS II, and are the most heat-susceptible part of the PS II apparatus (Vani et al., 2001). The abundances of ferredoxin-NADP reductase and the oxygen-evolving enhancer (OEE) decreased in response to high-temperature stress, but the expression significantly increased with the application of Spd compared with the stress alone, suggesting that Spd played an active role in the photosynthetic chain, resulted in a higher stability of PS II and an enhancement of oxygen evolving complex capacity, and then subsequently led to an enhancement of the photosynthetic capacity (Shi et al., 2013; Su et al., 2013).

Three spots were identified as proteins implicated in chlorophyll biosynthesis. Glutamate-1-semialdehyde 2,1-aminomutase (spots 11, 13) is an important enzyme to catalyze the formation of 5-aminolevulinic acid (ALA), a vital precursor of chlorophyll (Zhu et al., 2013). Coproporphyrinogen III oxidase 1 (spot 43) catalyzes the oxidative decarboxylation of coproporphyrinogen III to protoporphyrinogen IX in the chlorophyll biosynthesis pathways (Tian et al., 2015). Interestingly, the expression of chlorophyll biosynthesis proteins was increased under high-temperature stress, whereas the chlorophyll content was decreased (**Figure 1C**). One plausible explanation of this observation is that chlorophyll biosynthesis in plants is very complicated and co-regulated by many factors, but the temperature-related inhibition of the enzyme activity could

be an important reason for the inhibition of the chlorophyll biosynthesis.

Cell Rescue and Defense

Plants have evolved a complex sensory mechanism to monitor and adapt to prevailing environmental conditions (Ahsan et al., 2007). Heat shock proteins (HSPs) are typically induced when cells are exposed to high-temperature stress, and are closely related to the acquired thermo-tolerance (Charng et al., 2006). In our study, three forms of HSP70 (spots 3, 4, 5) were identified and significantly up-regulated under high-temperature stress, which is a key part of the high-temperature response (Liao et al., 2014). In addition, two small heat shock proteins (sHSPs, spots 37, 67) were found to be newly induced by high-temperature stress, and were both found to be absent under normal conditions. The sHSPs were further up-regulated by exogenous Spd, suggesting that Spd played a crucial role in maintaining proper folding, facilitating the refolding and preventing the aggregation of the denatured proteins under high-temperature stress (Shi et al., 2013). In this experiment, the stimulation of the heat shock protein with the application of Spd may be relevant to the influence of polyamines on the DNA-binding capacity of heat shock transcriptional factor HSF (Desiderio et al., 1999).

Reactive oxygen species (ROS) metabolism is a universal response to environmental stresses. The stress-induced accumulation of ROS seriously damages the cellular membrane and internal function components, and plants have developed an antioxidant system to regulate the ROS level (Li et al., 2015). In the present study, five proteins were found to have antioxidant-related functions. Among them, Spd increased the abundances of stromal ascorbate peroxidase (APX, spot 25) and dehydroascorbate reductase (DHAR, spot 29) under high-temperature stress (**Figure 6A**). Further analysis revealed that

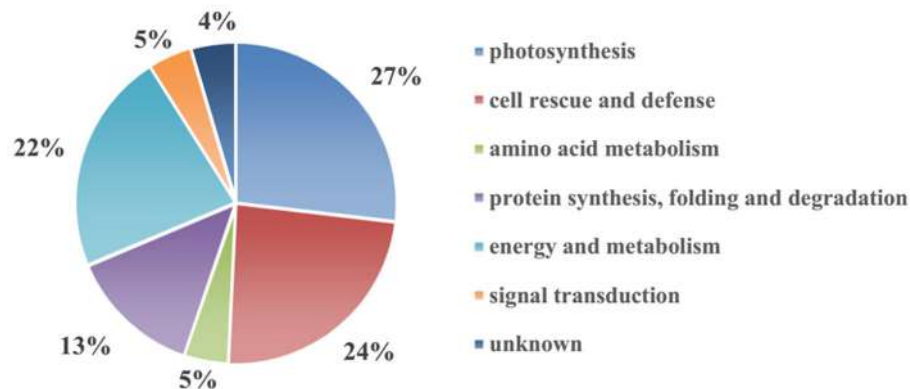


FIGURE 3 | Functional classification of the 67 identified differentially expressed proteins in tomato leaves.

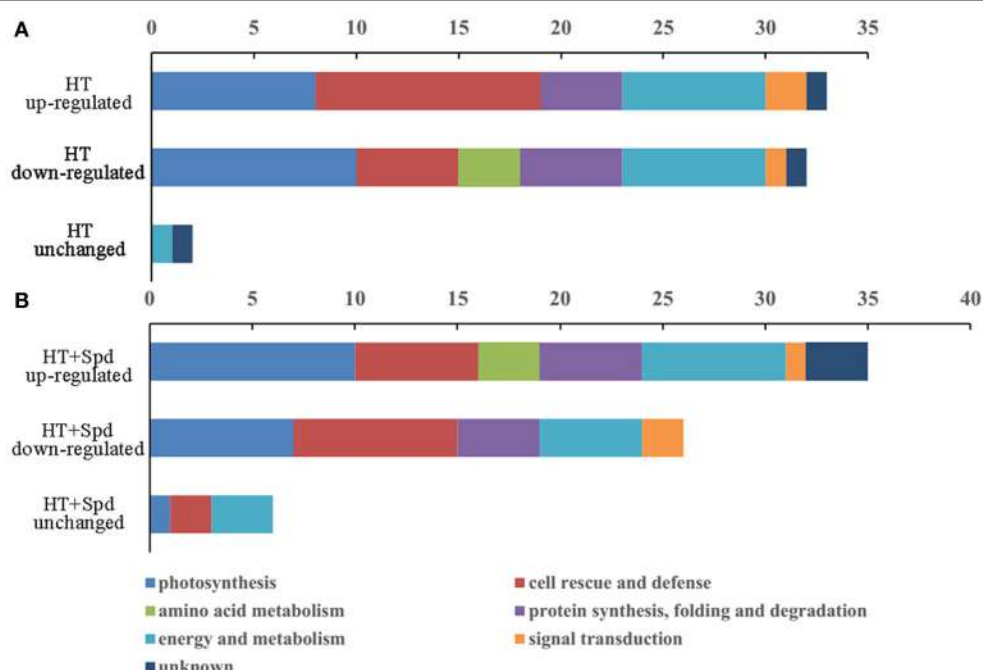


FIGURE 4 | The number and functional classification of identified proteins changed in abundance in tomato leaves. (A) Differentially expression proteins responded to high temperature (HT) stress compare with the control. (B) Differentially expression proteins responded to Spd under high temperature stress (HT+Spd) compare with high temperature stress alone.

the activities of APX and DHAR were increased significantly with the application of Spd under high-temperature stress (**Figure 6B**). The enhanced activities could be largely explained by the up-regulated mRNA levels of *APX2*, *APX6*, *DHARI*, and *DHAR2* (**Figure 6C**). Interestingly, the expression of superoxide dismutases [Fe] (Fe SOD, spot 35) in the plastid was not in accordance with the superoxide dismutase [Cu-Zn] (Cu/Zn SOD, spot 36) in the chloroplast. Moreover, the protein expression, activities of enzymes and related mRNA levels also showed different change patterns in response to high-temperature and/or Spd treatment. The variance might be due to the post-transcriptional regulation and post-translational

modification of SOD through complex mechanisms, which needs further study. Taken together, the exogenous Spd is involved in antioxidant and detoxification defense mechanisms, mitigating oxidative damage and intensifying the resistance to high-temperature stress (Mostofa et al., 2014; Sang et al., 2016).

Protein Synthesis, Folding and Degradation

Generally, abiotic stress causes a transient suppression of *de novo* protein synthesis (Capriotti et al., 2014). In this study, proteomic analysis identified two spots related to protein synthesis, including elongation factor TuB (spot 17)

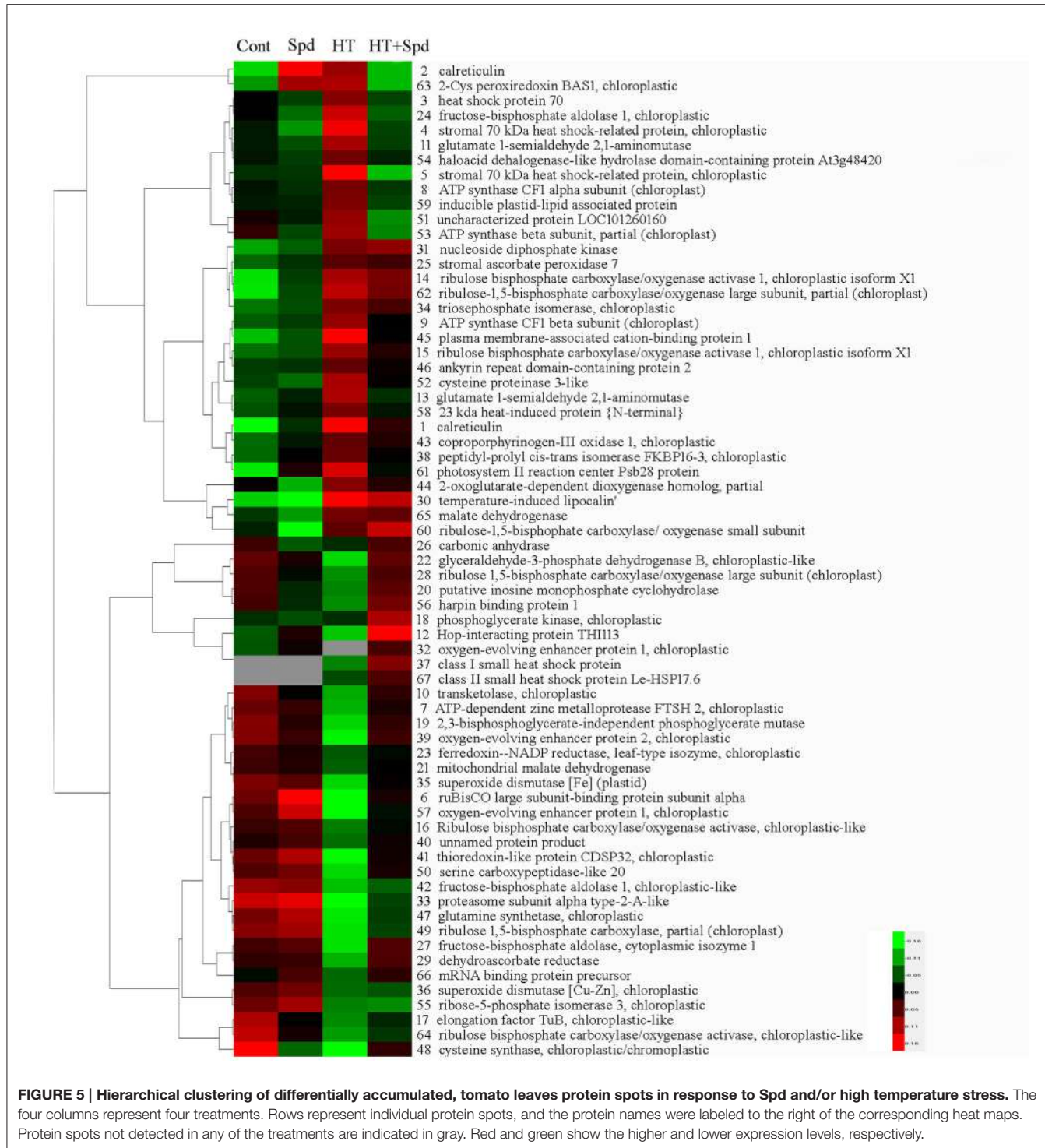
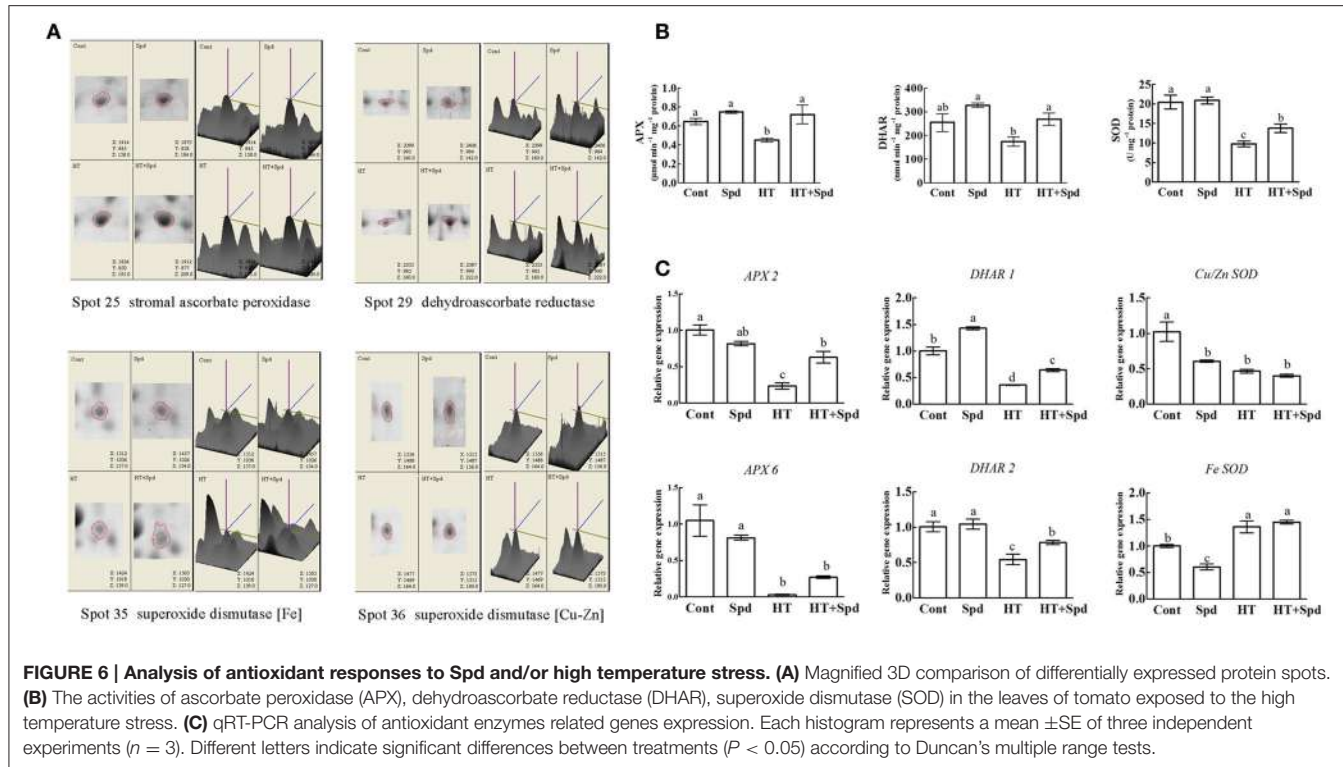


FIGURE 5 | Hierarchical clustering of differentially accumulated, tomato leaves protein spots in response to Spd and/or high temperature stress. The four columns represent four treatments. Rows represent individual protein spots, and the protein names were labeled to the right of the corresponding heat maps. Protein spots not detected in any of the treatments are indicated in gray. Red and green show the higher and lower expression levels, respectively.

and mRNA binding protein precursor (spot 66), which were markedly decreased under the high-temperature stress. However, the expression was enhanced after the application of Spd. According to previous data (Li et al., 2012), it can be hypothesized that stimulating the synthesis of specific proteins by exogenous Spd may play important roles in regulating the proteins synthesis and translational machinery,

which are important components of the stress response in plants.

Two proteins (spots 38, 46) that induce proper protein folding and/or prevent the aggregation of stress-damaged proteins were preferentially upregulated under high-temperature stress. In agreement with this observation, the upregulation of peptidyl-propyl *cis-trans* isomerase FKBP 16-3 (spot 38) had been



reported in *Arabidopsis* and rice in response to high-temperature stress (Palmlad et al., 2008; Gammula et al., 2011). The two proteins showed a decreasing pattern under the stress with Spd, indicating that exogenous Spd might regulate protein folding and assembly, participating in the high-temperature stress tolerance.

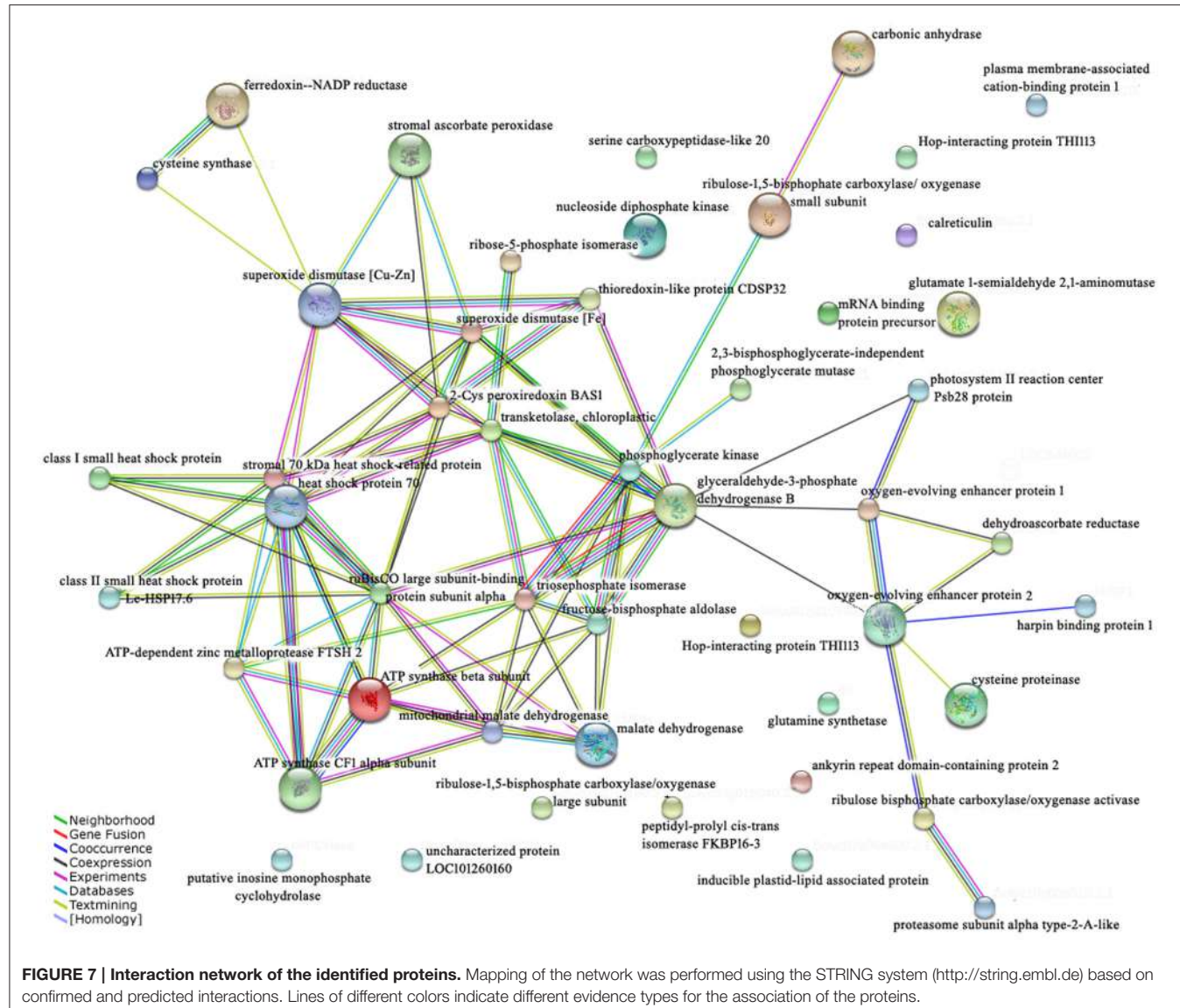
Proteolysis is a complex process involving many enzymes and pathways in various cellular compartments. Proteases play a central role in metabolism under abiotic stress as they are involved in protein inactivation and the degradation of damaged proteins (Capriotti et al., 2014). In our study, the cysteine proteinase 3-like (spot 52) was up-regulated under high-temperature stress, in agreement with previous studies (Koizumi et al., 1993; Callls, 1995). Interestingly, the expression of ATP-dependent zinc metalloprotease (spot 7) and proteasome subunit alpha type-2-A-like (spot 33) were decreased under high-temperature stress but increased significantly with the application of exogenous Spd. Stimulating the proteolysis of specific proteins by Spd accelerated the degradation of misfolded/damaged proteins, and made tissues more stable by covalently attaching with proteins (Li et al., 2013). Furthermore, the PAs regulated the protein metabolism and may reprogram the proteome in response to abiotic stress (Yuan et al., 2016), which may also account for the resistance to high-temperature stress of the tomato seedlings.

Energy and Metabolism

It is well-known that sufficient ATP is necessary in response to abiotic stress in plants (Hu et al., 2014). Three proteins associated with ATP synthase (spots 8, 9, and 53) were significantly

upregulated under the high-temperature stress, suggesting a higher energy demand for the degradation and biosynthesis of proteins (Das et al., 2015). However, the ATP synthase proteins were down-regulated by the exogenous application of Spd under high-temperature stress, stabilizing the process of ATP synthesis, and energy metabolism.

ATP is mainly produced by carbohydrate metabolism, such as glycolysis, the tricarboxylic acid cycle and the pentose phosphate pathway (Hu et al., 2015). The first group included 7 proteins involved in glycolysis pathway. Among them, our results showed that fructose-bisphosphate (FBP) aldolase in the cytoplasm (spot 27), and chloroplastic (spot 42) decreased significantly under high temperature. Moreover, glyceraldehyde-3-phosphate dehydrogenase (GAPDH, spot 22), and 2,3-bisphosphoglycerate-independent phosphoglycerate mutase (spot 19) also decreased under the stress, which would inhibit the glycolysis pathway and glycolysis associated with intermediate metabolism. However, exogenous Spd up-regulated these proteins, allowing more carbohydrates to enter the glycolic pathway and maintain the normal physiological metabolism of the tomato seedlings, thereby supporting the high-temperature resistance (Shan et al., 2016). The second group included malate dehydrogenase (MDH, spots 21, 65), involved in the tricarboxylic acid cycle. In this study, MDH showed different accumulation patterns in response to high temperature, whereas exogenous Spd sprayed on the leaves maintained the MDH expression at a high level. The third group was protein participating in the pentose phosphate pathway. Under high-temperature stress, the abundance of transketolase (TK, spot 10) and ribose-5-phosphate



isomerase (spot 55) decreased. Spd application further improved the abundance of TK, whereas it affected ribose-5-phosphate isomerase unremarkably. Adjusting the EMP-TCA-PPP pathway to produce more energy may be an important mechanism for Spd to alleviate stress induced damage (Li et al., 2015).

Signal Transduction

Signal transduction pathways play an important role in abiotic stress at the cellular level, leading to changes in metabolic pathways and cellular processes. After the perception of the stress, a signal would be transferred from the cell surface to the nucleus, and then the responsive proteins would be translated (Guo et al., 2013). Within this functional category, we identified calreticulin (spots 1, 2) and harpin binding protein 1 (spot 56). Calreticulin, a major endoplasmic reticulum Ca^{2+} -binding chaperone, is involved in a variety of cellular signaling pathways. Calreticulin also plays a crucial role in regulating

Ca^{2+} intracellular homeostasis (Nakamura et al., 2001). In our study, calreticulin was significantly up-regulated under the high-temperature stress, but was down-regulated by Spd. These observations suggested that Spd has a relationship with the stress-induced Ca^{2+} signal transduction, probably allowing the release of free Ca^{2+} to relieve stress. Interestingly, harpin binding protein 1 was significantly down-regulated in the tomato leaves under the high-temperature stress, which was concordant with the finding in spring soybean under cold stress (Tian et al., 2015). However, the protein level recovered the controlled level after Spd treatment, and the regulatory mechanism remains unclear.

CONCLUSION

In conclusion, our results demonstrated that exogenous Spd improving tomato seedlings growth and high temperature

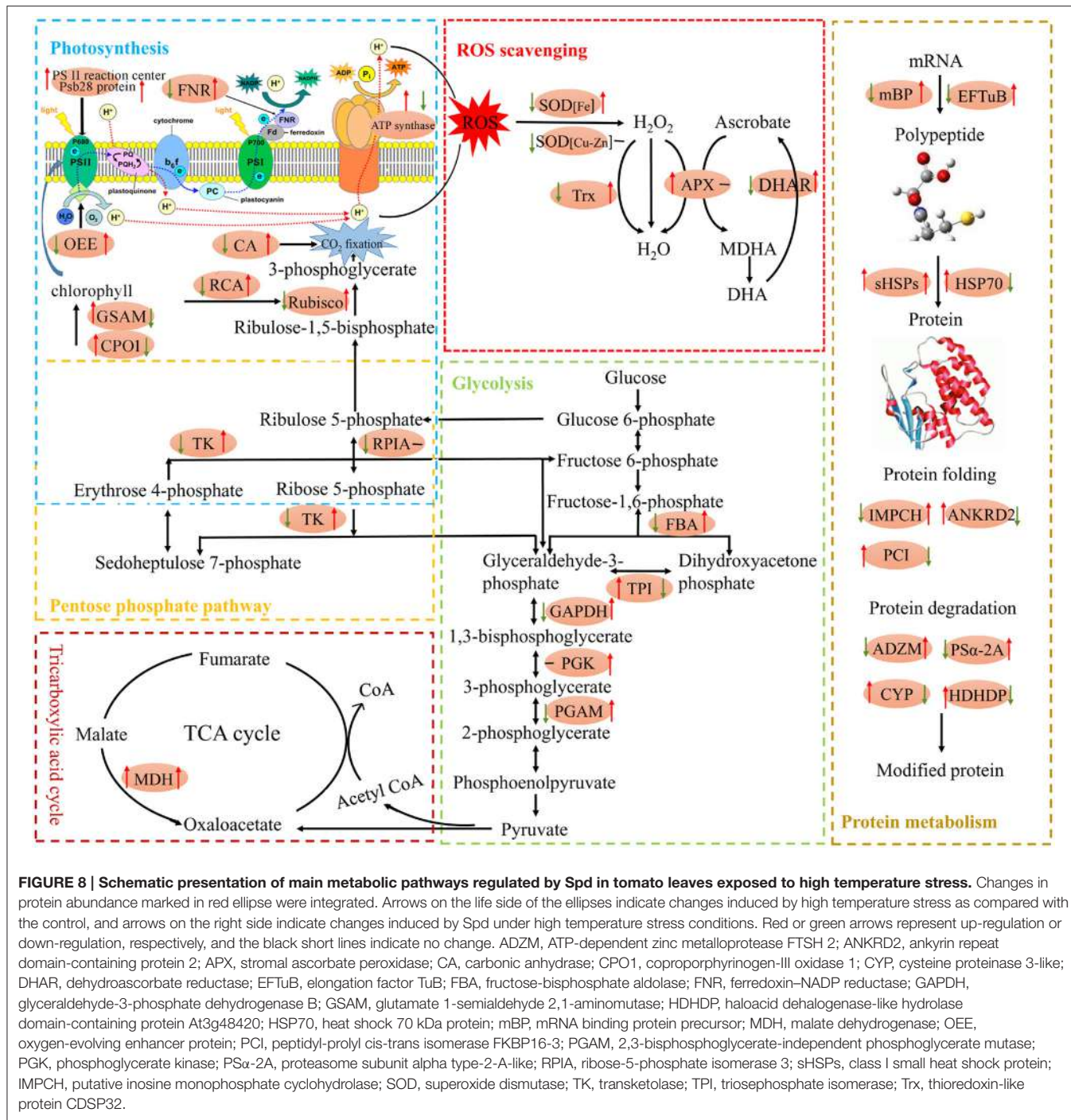


FIGURE 8 | Schematic presentation of main metabolic pathways regulated by Spd in tomato leaves exposed to high temperature stress. Changes in protein abundance marked in red ellipses were integrated. Arrows on the life side of the ellipses indicate changes induced by high temperature stress as compared with the control, and arrows on the right side indicate changes induced by Spd under high temperature stress conditions. Red or green arrows represent up-regulation or down-regulation, respectively, and the black short lines indicate no change. ADZM, ATP-dependent zinc metalloprotease FTSH 2; ANKRD2, ankyrin repeat domain-containing protein 2; APX, stromal ascorbate peroxidase; CA, carbonic anhydrase; CPO1, coproporphyrinogen-III oxidase 1; CYP, cysteine proteinase 3-like; DHAR, dehydroascorbate reductase; EFTuB, elongation factor TuB; FBA, fructose-bisphosphate aldolase; FNR, ferredoxin-NADP reductase; GSAM, glutamate 1-semialdehyde 2,1-aminomutase; HDHDP, haloacid dehalogenase-like hydrolase domain-containing protein At3g48420; HSP70, heat shock 70 kDa protein; mBP, mRNA binding protein precursor; MDH, malate dehydrogenase; OEE, oxygen-evolving enhancer protein; PCI, peptidyl-prolyl cis-trans isomerase FKBP16-3; PGAM, 2,3-bisphosphoglycerate-independent phosphoglycerate mutase; PGK, phosphoglycerate kinase; PSα-2A, proteasome subunit alpha type-2-A-like; RPIA, ribose-5-phosphate isomerase 3; sHSPs, class I small heat shock protein; IMPCH, putative inosine monophosphate cyclohydrolase; SOD, superoxide dismutase; TK, transketolase; TPI, triosephosphate isomerase; Trx, thioredoxin-like protein CDSP32.

tolerance, could be associated with the following processes: (1) stimulating protein related to photosynthesis and energy metabolism, enhancing photosynthetic capacity, providing higher energy for various metabolic processes to cope with high-temperature stress; (2) activation of cell rescue and defense response to alleviate stress induced injuries, activating the antioxidant system; (3) stimulating protein synthesis and degrading misfolded/damaged

proteins induced by high temperature stress. Schematics (Figure 8) was formed to illustrate the detailed mechanism to reveal cell metabolism regulated by high temperature and/or Spd. This study provides comprehensive insights through comparative proteomics, and would be able to better enrich our understanding of the mechanism of Spd improves the tolerance of under the high-temperature stress.

AUTHOR CONTRIBUTIONS

SG designed the research and proposed the research proceeding. QS wrote the main manuscript text. XS and YA prepared all figures and modified this manuscript until submitted. SS and JS improved the manuscript. All authors reviewed and approved the manuscript.

FUNDING

This work was supported by the National Natural Science Foundation of China (No. 31471869, No. 31401919 and No.

31272209), the Jiangsu Province Scientific and Technological Achievements into Special Fund (BA2014147), the China Earmarked Fund for Modern Agro-industry Technology Research System (CARS-25-C-03), and the Priority Academic Program Development of Jiangsu Higher Education Institutions (PAPD).

SUPPLEMENTARY MATERIAL

The Supplementary Material for this article can be found online at: <http://journal.frontiersin.org/article/10.3389/fpls.2017.00120/full#supplementary-material>

REFERENCES

- Ahsan, N., Lee, D. G., Lee, S. H., Kang, K. Y., Bahk, J. D., Choi, M. S., et al. (2007). A comparative proteomic analysis of tomato leaves in response to waterlogging stress. *Physiol. Plant.* 131, 555–570. doi: 10.1111/j.1399-3054.2007.00980.x
- Arnon, D. T. (1949). Copper enzymes in isolated chloroplasts polyphenol oxidase in *Beta vulgaris*. *Plant Physiol.* 24, 1–15. doi: 10.1104/pp.24.1.1
- Becana, M., Aparicio-Tejo, P., Irigoyan, J. J., and Sanchez-Diaz, M. (1986). Some enzymes of hydrogen peroxide metabolism in leaves and root nodules of *Medicago sativa*. *Plant Physiol.* 82, 1169–1171. doi: 10.1104/pp.82.4.1169
- Berberich, T., Sagor, G. H. M. and Kusano, T. (2015). “Polyamines in plant stress response,” in *Polyamines*, eds T. Kusano and H. Suzuki (Springer: Japan), 155–168. doi: 10.1007/978-4-431-55212-3_13
- Berwanger, A., Eyrisch, S., Schuster, I., Helms, V., and Bernhardt, R. (2010). Polyamines: naturally occurring small molecule modulators of electrostatic protein-protein interactions. *J. Inorg. Biochem.* 104, 118–125. doi: 10.1016/j.jinorgbio.2009.10.007
- Bian, Y. W., Lv, D. W., Cheng, Z. W., Gu, A. Q., and Yan, Y. M. (2015). Integrative proteome analysis of *Brachypodium distachyon* roots and leaves reveals a synergetic responsive network under H₂O₂ stress. *J. Proteome Res.* 128, 388–402. doi: 10.1016/j.jprot.2015.08.020
- Bita, C. E., and Gerats, T. (2013). Plant tolerance to high temperature in a changing environment: scientific fundamentals and production of heat stress-tolerant crops. *Front. Plant Sci.* 4:273. doi: 10.3389/fpls.2013.00273
- Bradford, M. M. (1976). A rapid and sensitive method for the quantitation of microgram quantities of protein utilizing the principle of protein-dye binding. *Anal. Biochem.* 72, 248–254. doi: 10.1016/0003-2697(76)90527-3
- Callls, J. (1995). Regulation of protein degradation. *Plant Cell* 7, 845–857. doi: 10.1105/tpc.7.7.845
- Capriotti, A. L., Borrelli, G. M., Colacicchoni, V., Papa, R., Piovesana, S., Samperi, R., et al. (2014). Proteomic study of tolerant genotype of durum wheat under salt-stress conditions. *Anal. Bioanal. Chem.* 406, 1423–1435. doi: 10.1007/s00216-013-7549-y
- Charng, Y. Y., Liu, H. C., Liu, N. Y., Hsu, F. C., and Ko, S. S. (2006). Arabidopsis Hsa32, a novel heat shock protein, is essential for acquired thermos tolerance during long recovery after acclimation. *Plant Physiol.* 140, 1297–1305. doi: 10.1104/pp.105.074898
- Das, S., Krishnan, P., Mishra, V., Kumar, R., Ramakrishnan, B., and Singh, N. K. (2015). Proteomic changes in rice leaves grown under open field high temperature stress conditions. *Mol. Biol. Rep.* 42, 1545–1558. doi: 10.1007/s11033-015-3923-5
- Desiderio, M. A., Dansi, P., Tacchini, L., and Bernelli-Zazzera, A. (1999). Influence of polyamines on DNA binding of heat shock and activator protein 1 transcription factors induced by heat shock. *FEBS Lett.* 455, 149–153. doi: 10.1016/S0014-5793(99)00873-X
- Fukuyama, K. (2004). Structure and function of plant type ferredoxins. *Photosynth. Res.* 81, 289–301. doi: 10.1023/b:pres.0000036882.19322.0a
- Gammula, C. G., Pascoiu, D., Atwell, B. J., and Haynes, P. A. (2011). Differential proteomic response of rice (*Oryza sativa*) leaves exposed to high- and low-temperature stress. *Proteomics* 11, 2839–2850. doi: 10.1002/pmic.201100068
- Guo, M. L., Gao, W. X., Li, L., Li, H., Xu, Y. L., and Zhou, C. X. (2013). Proteomic and phosphoproteomic analyses of NaCl stress-responsive proteins in *Arabidopsis* roots. *J. Plant Interact.* 9, 396–401. doi: 10.1080/17429145.2013.845262
- Gupta, K., Dey, A., and Gupta, B. (2013). Plant polyamines in abiotic stress responses. *Acta Physiol. Plant.* 35, 2015–2036. doi: 10.1007/s11738-013-1239-4
- Han, F., Chen, H., Li, X., J., Yang, M. F., Liu, G. S., and Shen, S. H. (2009). A comparative proteomic analysis of rice seedlings under various high-temperature stresses. *Biochim. Biophys. Acta* 1794, 1625–1634. doi: 10.1016/j.bbapap.2009.07.013
- Hu, W. J., Chen, J., Liu, T. W., Wu, Q., Wang, W. H., Liu, X., et al. (2014). Proteome and calcium-related gene expression in *Pinus massoniana* needles in response to acid rain under different calcium levels. *Plant Soil* 380, 285–303. doi: 10.1007/s11104-014-2086-9
- Hu, W. J., Wu, Q., Liu, X., Shen, Z. J., Chen, J., Zhu, C. Q., et al. (2015). Comparative proteomic analysis reveals the effects of exogenous calcium against acid rain stress in *Liquidambar formosana* Hance leaves. *J. Proteome Res.* 15, 216–228. doi: 10.1021/acs.jproteome.5b00771
- Hurkman, W. J., and Tanaka, C. K. (1986). Solubilization of plant membrane proteins for analysis by two-dimensional gel electrophoresis. *Plant Physiol.* 81, 802–806. doi: 10.1104/pp.81.3.802
- Igarashi, K., and Kashiwagi, K. (2015). Modulation of protein synthesis by polyamines. *IUBMB Life* 67, 160–169. doi: 10.1002/iub.1363
- Koizumi, M., Yamaguchi-Shinozaki, K., Tsuji, H., and Shinozaki, K. (1993). Structures and expression of two genes that encode distinct drought-inducible cysteine proteinases in *Arabidopsis thaliana*. *Gene* 129, 175–182. doi: 10.1016/0378-1119(93)90266-6
- Kosová, K., Vítámvás, P., Prášil, I. T., and Renaut, J. (2011). Plant proteome changes under abiotic stress—contribution of proteomics studies to understanding plant stress response. *J. Proteomics* 74, 1301–1322. doi: 10.1016/j.jprot.2011.02.006
- Laemmli, U. K. (1970). Cleavage of structural proteins during the assembly of the head of bacteriophage T4. *Nature* 227, 680–685. doi: 10.1038/227680a0
- Law, R. D., and Crafts-Brandner, S. J. (1999). Inhibition and acclimation of photosynthesis to heat stress is closely correlated with activation of ribulose-1,5-bisphosphate carboxylase/oxygenase. *Plant Physiol.* 120, 173–182. doi: 10.1104/pp.120.1.173
- Li, B., He, L., Guo, S., Li, J., Yang, Y., Yan, B., et al. (2013). Proteomics reveal cucumber Spd-responses under normal condition and salt stress. *Plant Physiol. Biochem.* 67, 7–14. doi: 10.1016/j.plaphy.2013.02.016
- Li, J., Sun, J., Yang, Y., Guo, S., and Glick, B. (2012). Identification of hypoxic- responsive proteins in cucumber roots using a proteomic approach. *Plant Physiol. Biochem.* 51, 74–80. doi: 10.1016/j.plaphy.2011.10.011
- Li, X., Hao, C., Zhong, J., Liu, F., Cai, J., Wang, X., et al. (2015). Mechanostimulated modifications in the chloroplast antioxidant system and proteome changes are associated with cold response in wheat. *BMC Plant Biol.* 15:219. doi: 10.1186/s12870-015-0610-6
- Liao, J. L., Zhou, H. W., Zhang, H. Y., Zhong, P. A., and Huang, Y. J. (2014). Comparative proteomic analysis of differentially expressed proteins in the early

- milky stage of rice grains during high temperature stress. *J. Exp. Bot.* 65, 655–671. doi: 10.1093/jxb/ert435
- Lin, H. H., Lin, K. H., Syu, J. Y., Tang, S. Y., and Lo, H. F. (2015). Physiological and proteomic analysis in two wild tomato lines under waterlogging and high temperature stress. *J. Plant Biochem. Biotechnol.* 25, 87–96. doi: 10.1007/s13562-015-0314-x
- Lin, K. H., Chen, L. F. O., Li, S. D., and Lo, H. D. (2015). Comparative proteomic analysis of cauliflower under high temperature and flooding stresses. *Sci. Hortic.* 183, 118–129. doi: 10.1016/j.scientia.2014.12.013
- Liu, J. H., Kitashiba, H., Wang, J., Ban, Y., and Moriguchi, T. (2007). Polyamines and their ability to provide environmental stress tolerance to plants. *Plant Biotechnol.* 24, 117–126. doi: 10.5511/plantbiotechnology.24.117
- Mathur, S., Agrawal, D., and Jajoo, A. (2014). Photosynthesis: response to high temperature stress. *J. Photochem. Photobiol. B* 137, 116–126. doi: 10.1016/j.jphotobiol.2014.01.010
- Mostofa, M. G., Yoshida, N., and Fujita, M. (2014). Spermidine pretreatment enhances heat tolerance in rice seedlings through modulating antioxidative and glyoxalase systems. *Plant Growth Regul.* 73, 31–44. doi: 10.1007/s10725-013-9865-9
- Nakamura, K., Zuppini, A., Arnaudeau, S., Lynch, J., Ahsan, I., Krause, R., et al. (2001). Functional specialization of calreticulin domains. *J. Cell Biol.* 154, 961–972. doi: 10.1083/jcb.200102073
- Nakano, Y., and Asada, K. (1981). Hydrogen peroxide is scavenged by ascorbate-specific peroxidase in spinach chloroplasts. *Plant Cell Physiol.* 22, 867–880.
- Palmbald, M., Mills, D. J., and Bindschedler, L. V. (2008). Heat-shock response in *Arabidopsis thaliana* explored by multiplexed quantitative proteomics using differential metabolic labeling. *J. Proteome Res.* 7, 780–785. doi: 10.1021/pr0705340
- Pál, M., Szalai, G., and Janda, T. (2015). Speculation: polyamines are important in abiotic stress signaling. *Plant Sci.* 237, 16–23. doi: 10.1016/j.plantsci.2015.05.003
- Skalák, J., Černý, M., Jedelský, P., Dobrá, J., Ge, E., Novák, J., et al. (2016). Stimulation of *ipt* overexpression as a tool to elucidate the role of cytokinins in high temperature responses of *Arabidopsis thaliana*. *J. Exp. Bot.* 67, 2861–2873. doi: 10.1093/jxb/erw129
- Salvucci, M. E., and Crafts-Brandner, S. J. (2004). Inhibition of photosynthesis by heat stress: the activation state of Rubisco as a limiting factor in photosynthesis. *Physiol. Plant.* 120, 179–186. doi: 10.1111/j.0031-9317.2004.0173.x
- Sang, Q. Q., Shu, S., Shan, X., Guo, S. R., and Sun, J. (2016). Effects of exogenous spermidine on antioxidant system of tomato seedlings exposed to high temperature stress. *Russ. J. Plant Physiol.* 63, 645–655. doi: 10.7868/s005330316050110
- Shan, X., Zhou, H., Sang, T., Shu, S., Sun, J., and Guo, S. R. (2016). Effects of exogenous spermidine on carbon and nitrogen metabolism in tomato seedlings under high temperature. *J. Am. Soc. Hortic. Sci.* 141, 381–388.
- Sharkey, T. D. (2005). Effects of moderate heat stress on photosynthesis: importance of thylakoid reactions, Rubisco deactivation, reactive oxygen species, and thermos tolerance provided by isoprene. *Plant Cell Environ.* 28, 269–277. doi: 10.1111/j.1365-3040.2005.01324.x
- Shi, H., Ye, T., and Chan, Z. (2013). Comparative proteomic and physiological analyses reveal the protective effect of exogenous polyamines in the Bermudagrass (*Cynodon dactylon*) response to salt and drought stresses. *J. Proteome Res.* 12, 4951–4964. doi: 10.1021/pr400479k
- Sruthi, N., Tamura, P. J., Roth, M. R., Vara, P. P. V., and Ruth, W. (2016). Wheat leaf lipids during heat stress: I. High day and night temperatures result in major lipid alterations. *Plant Cell Environ.* 39, 787–803. doi: 10.1111/pce.12649
- Su, X. Q., Wang, M. Y., Shu, S., Sun, J., and Guo, S. R. (2013). Effects of exogenous spermidine on the fast Chlorophyll fluorescence induction dynamics in tomato seedlings under high temperature stress. *Chin. J. Hort.* 40, 2409–2418. doi: 10.16420/j.issn.0513-353x.2013.12.011
- Tian, J., Wang, L. P., Yang, Y. J., Sun, J., and Guo, S. R. (2012). Exogenous spermidine alleviates the oxidative damage in cucumber seedlings subjected to high temperatures. *J. Am. Soc. Hortic. Sci.* 137, 11–19.
- Tian, X., Liu, Y., Huang, Z., Duan, H., Tong, J., He, X., et al. (2015). Comparative proteomic analysis of seedling leaves of cold-tolerant and -sensitive spring soybean cultivars. *Mol. Biol. Rep.* 42, 581–601. doi: 10.1007/s11033-014-3803-4
- Todorova, D., Sergiev, I., Alexieva, V., Karanov, E., Smith, A., and Hall, M. (2007). Polyamine content in *Arabidopsis thaliana* (L.) Heynh during recovery after low and high temperature treatments. *Plant Growth Regul.* 51, 185–191. doi: 10.1007/s10725-006-9143-1
- Vani, B., Saradhi, P. P., and Mohanty, P. (2001). Alteration in chloroplast structure and thylakoid membrane composition due to *in vivo* heat treatment of rice seedlings: correlation with the functional changes. *J. Plant Physiol.* 158, 583–592. doi: 10.1078/0176-1617-00260
- Wahid, A., Gelani, S., Ashraf, M., and Foolad, M. R. (2007). Heat tolerance in plants: an overview. *Environ. Exp. Bot.* 61, 199–223. doi: 10.1016/j.envexpbot.2007.05.011
- Yuan, Y., Zhong, M., Shu, S., Du, N., Sun, J., and Guo, S. (2016). Proteomic and physiological analyses reveal putrescine responses in roots of cucumber stressed by NaCl. *Front. Plant Sci.* 7:1035. doi: 10.3389/fpls.2016.01035
- Zhu, Y., Zhu, G., Guo, Q., Zhu, Z., Wang, C., and Liu, Z. (2013). A comparative proteomic analysis of *Pinellia ternata* leaves exposed to heat stress. *Int. J. Mol. Sci.* 14, 20614–20634. doi: 10.3390/ijms141020614

Conflict of Interest Statement: The authors declare that the research was conducted in the absence of any commercial or financial relationships that could be construed as a potential conflict of interest.

Copyright © 2017 Sang, Shan, An, Shu, Sun and Guo. This is an open-access article distributed under the terms of the Creative Commons Attribution License (CC BY). The use, distribution or reproduction in other forums is permitted, provided the original author(s) or licensor are credited and that the original publication in this journal is cited, in accordance with accepted academic practice. No use, distribution or reproduction is permitted which does not comply with these terms.

Advantages of publishing in Frontiers



OPEN ACCESS

Articles are free to read for greatest visibility and readership



FAST PUBLICATION

Around 90 days from submission to decision



HIGH QUALITY PEER-REVIEW

Rigorous, collaborative, and constructive peer-review



TRANSPARENT PEER-REVIEW

Editors and reviewers acknowledged by name on published articles



REPRODUCIBILITY OF RESEARCH

Support open data and methods to enhance research reproducibility



DIGITAL PUBLISHING

Articles designed for optimal readership across devices



FOLLOW US
@frontiersin



IMPACT METRICS
Advanced article metrics track visibility across digital media



EXTENSIVE PROMOTION
Marketing and promotion of impactful research



LOOP RESEARCH NETWORK
Our network increases your article's readership

Frontiers

Avenue du Tribunal-Fédéral 34
1005 Lausanne | Switzerland

Visit us: www.frontiersin.org

Contact us: info@frontiersin.org | +41 21 510 17 00